THE UNIVERSITY OF MICHIGAN

COLLEGE OF ENGINEERING
Department of Chemical Engineering

Technical Report

THE MEASUREMENT AND PREDICTION OF THERMAL PROPERTIES OF SELECTED MIXTURES OF METHANE, ETHANE AND PROPANE

André W. Furtado

Project 345330

supported by:

NATURAL GAS PROCESSORS ASSOCIATION
TULSA, OKLAHOMA

administered through:

DIVISION OF RESEARCH DEVELOPMENT AND ADMINISTRATION ANN ARBOR

January 1974

To Professor J. J. Martin

(The person most responsible for
making the study of thermodynamics
a religious experience for me)

Pater, dimitte illis; non enim sciunt quid faciunt.

St. Luke

To

Two Important Women
in My Life
Annette, my mother
Carol, my wife.

PREFACE

It is admittedly a difficult task to coax anyone to even approach a dissertation of this size and weight without some trepidation and it is, therefore, hoped that the following commentary will induce potential readers to seek out areas of specific interest with greater facility.

Chapter I summarizes the important thermodynamic relations relevant to the calculation of enthalpies from various types of measurements, with particular emphasis on flow calorimetry. Chapter II essentially involves a review of the existing thermodynamic data on the systems investigated in this work.

Chapter III and IV are concerned with methods for correlating and predicting thermodynamic properties. Many theoretical and empirical techniques are examined in an effort to impart a more eclectic flavor to the review, and to broaden the author's perspective of this very fascinating field. But, the reader is warned that the sections devoted to theoretical methods are perhaps more imbued with a neophyte's fervor than with the wisdom that comes with enlightenment. One asks the reader's indulgence if these sections seem, at first, unintelligible. If it is any consolation at all, the literature on the subject is, in this author's experience, considerably more formidable. The material is best digested if the references alluded to in these sections are examined along with the review. Chapter IV highlights some interesting theoretical developments with respect to the Van der Waal mixing rules.

Chapter V concentrates on the development of a new approach for representing mixture enthalpies as a function of composition in a corresponding states framework. Much attention has been paid to ancillary work on the development of reduced correlations for the second virial coefficient, a quantity whose accurate estimation is of pivotal importance to the success of the proposed enthalpy prediction technique. Chapters VI and VII describe the equipment, the experimental procedure, and data reduction techniques in considerable depth in order that Chapter VIII may be concisely devoted to the presentation of smoothed experimental calorimetric data. Although perhaps the most "unfun" part of this work, it is a matter of paramount interest to the sponsors of the Enthalpy Project and also to salivating enthalpy

correlators all over the country. Comparisons with compilations and other data in the literature are also included.

Chapter IX focuses on the evaluation of various mixing rules for the pseudo-critical parameters (previously discussed in Chapters IV and V) for their ability to represent the enthalpy data for the various mixtures of this work in the Powers Generalized Correlation. This chapter should perhaps be read more slowly than others as the author admits to an inexplicable lapse of communicability. Chapter X contains suggestions for further research and offers valuable hindsight into how this research should have been really conducted for maximum effectiveness.

In a departure from normal practice, aspects of this research that were either unsuccessful, or which were reluctantly, and abruptly terminated (sometimes tantalizingly near fruition) because of the pressing weight of the experimental commitment, are included in the thesis in the hope firstly, that past sins may not be repeated, and secondly, that promising areas will be eagerly attacked by other investigators, particularly should this author's association with the field end.

In the interests of economy, the computer programs used in this work will be placed on file at the Thermal Properties of Fluids Laboratory at the University of Michigan.

Acknowledgements are in order: To Professor John E. Powers, Chairman of the Doctoral Committee for permitting the author the luxury of an occasional disagreement, and also for having provided an unforgettable and devastating introduction to manual labor.

To Professor Gene E. Smith, Donald L. Katz, James O. Wilkes and James H. Hand for consenting to serve on the Doctoral Committee.

To Joseph C. Golba Sr., and to Victor Yesavage for administering the Initiation Rites to the Enthalpy Project which would be the envy of any and all fraternal organizations.

To Joseph Boisseneault for valuable assistance in the capacity of laboratory technician during the early stages of this work.

To John Dziuba and Vijay Khanna for assistance in operating the calorimetric facility in times of crucial need, and to Takaya Miyazaki and Kwan Kim for stimulating discussions related to this research.

To Lillian Toney, for offering very accomodating service with regard to the reproduction of the material in this work.

To Harry Willsher and his convivial crew: The Sallys, Marty and Curry and Eugene "Pink Floyd" Leppanen, for their help with what seemed like an interminable number of illustrations, and for their good fellowship.

To Edward Rupke and Herbert "Hot Hands" Senecal for their assistance in fashioning various pieces of equipment. The fabrication of the modified heater capsule to the isobaric calorimeter was, in particular, excellent enough to make fabrication of the data unnecessary.

To Judy Arms for doing an outstanding job in preparing many computer programs relating to the Powers Generalized Correlation.

To Kathleen Speer, a veritable angel of deliverance, who cheerfully plunged into the awesome task of typing the manuscript, braving the formidable equations with remarkable equanimity.

To the entire chemical engineering department, and particularly the faculty, for having improved immensely my perception of human nature, during my thirteen year stay.

To all previous graduate students at the Enthalpy Project, whose relentless toil at the "pit" has not been in vain.

To the Natural Gas Processors' Associations who supported this research and provided fellowship money for a period of three years, and who, perhaps, have since then justifiably wondered where their money went. It is hoped that they may someday feel that their patience has not gone unrewarded.

To the American Petroleum Institute for secondary financial support.

To the Southern California Gas Company for the supply of methane used in this work.

To the National Bureau of Standards for the calibration of thermocouples, a standard cell, and a platinum resistance thermometer.

On a more personal level the author is indebted to: one-time fellow student, Vasant Bhirud for his sustained empathy with my many frustrations.

To my close friend Arun Vasudev Hejmadi for cheerfully lending a

very patient and discriminating ear to a constant barrage of sundry ideas involving this research.

To my many friends so very anxious to see the end of the student-existentialist phase of my life, for their concern.

To my in-laws, Mr. and Mrs. Howard M. Kieft, for providing, on many a weekend, a haven "far from the madding crowds' ignoble strife."

To my wife Carol for her infinite patience.

To my true friend, the late Professor Lars Thomassen, a man of tremendous warmth, whose keen interest in my academic progress, and whose constant encouragement, particularly in the darkest hours during the early stages of this work, will always be gratefully remembered.

To my Maker, for the prospect of an imminent rebirth that awaits only an impending primal scream.

"The time has come, the walrus said,
To think of other things
Of ships and sails and sealing wax
Of cabbages and kings."

- A famous mathematician more renowned for his fantasy trips -

TABLE OF CONTENTS

LIST OF TABLES

LIST OF TABLES (contd.)

LIST OF TABLES (contd.)

LIST OF TABLES (contd.)

LIST OF TABLES (contd.)

LIST OF TABLES (contd.)

LIST OF TABLES (contd.)

LIST OF TABLES (contd.)

LIST OF FIGURES

LIST OF FIGURES (contd.)

LIST OF FIGURES (contd.)

LIST OF FIGURES (contd.)

LIST OF FIGURES (contd.)

LIST OF APPENDICES

LIST OF APPENDICES (contd.)

NOMENCLATURE

a	Spherical core parameter for Kihara potential
a,b	Constants in the Van der Waal Equation of State
a,b,c,d	Constants for a flowmeter calibration equation
a,b,c,d	Constants for the Starling Modified BWR Equation
a,b,c,d,e,f,g	Constants for the least squares regression equation for Cp and $(dH/dP)_T$
a',b',c',d'	Constants for a flowmeter calibration equation
a",b",c",d"	Constants for a flowmeter calibration equation
a_h,b_h,c_h,d_h	Constants for the low pressure transducer calibration equation
a_l,b_l,c_l,d_l	Constants for the low pressure transducer calibration equation
a_n,b_n,c_n,d_n	Constants for the null output of the differential pressure transducer as a function of pressure
A	Constant in the Sutherland equation for zero pressure viscosity
A	Area
A	Helmholtz free energy
A_o,B_o,C_o,D_o,E_o	Constants for the Starling Modified BWR Equation
b,c,d,e	Constants for the polynomial regression of Yesavage, expressing Cp as a function of temperature
b_d,c_d,d_d	Constants for the differential pressure transducer calibration
B	Second Virial Coefficient
B'	dB/dT
B_{ij}	Second virial coefficient for the i-j intermolecular interaction
B_M	Maximum value of the second virial coefficient
Br	Reduced second virial coefficient
c	Coefficient of London attractive dispersion forces
c(r)	Direct correlation function
C	Third virial coefficient

C'	dC/dT
Cp	Isobaric heat capacity
Cs	(dQ/dT) for the pure saturated fluid along the vapor pressure curve
Cv	Isochoric heat capacity
d	Diameter
d	Chueh-Prausnitz correlating parameter for the third virial coefficient.
d_{ij}	Hard sphere diameter for the i-j interaction
D	Fourth virial coefficient
E	Total energy
E	Young's modulus
E	Voltage
EMF	Electromotive Force
f	Symbol for a functional relationship
$\overline{f}$	Partial molal fugacity
f	Friction factor
F	Mass flowrate
F	Symbol for a functional relationship
g	Symbol for a functional relationship
g	Gravitational acceleration
g	Radial distribution function
G	Symbol for a functional relationship
G	Free energy
h	Planck's symbol
h	Symbol for a functional relationship
h	Heat transfer coefficient
h	Height
H	Enthalpy
$\underline{H}$	Specific enthalpy
$\overline{H}$	Partial molal enthalpy
$\tilde{H}$	Configurational enthalpy
$\mathcal{H}$	Modified reduced enthalpy due to Powers

Hc	Enthalpy at the critical point
I	Current
I	The configurational energy integral expressed as a function of dimensionless distance
k	BWR equation parameter in Equation (IV-52)
k	Boltzmann Constant
k_{ij}	Correction factor to the geometric mean rule for the unlike i-j pair interaction.
K	Symbol for a functional relationship
L	Well width for the square well potential
m	Mass
$\dot{m}$	Mass flowrate
m,n	Exponents for the Lennard-Jones bireciprocal intermolecular potential
M	Molecular weight
n	Number of carbon atoms in an n-alkane molecule
N	Number of molecules
N_o	Avogadro number
NBP	Normal boiling point
P	Pressure
PGC	Power's generalized correlation
Pc	Critical pressure
Pc_x	Critical pressure of a mixture
P_k	Pressure corresponding to the peak or maximum value of any given thermodynamic property
Pr	Reduced pressure, P/Pc
Ps	Saturation pressure for the liquid-vapor transition
PY	Percus-Yevick
p,q	Indices for mixing rules

$\dot{q}$	Rate of heat transfer
Q	Heat input
$\vec{r}$	Coordinate vector
r	Distance
R	Gas constant
R	Resistance
Re	Reynolds number, ($\rho vd/\mu$)
S	Constant in the Sutherland equation for zero pressure viscosity
SCFM	Standard cubic feet per minute
T	Temperature
T_b	Bath temperature
TPFL	Thermal Properties of Fluids laboratory
Tb	Boyle temperature
Tc	Critical temperature
T_o	Reference temperature
Tc_x	Critical temperature for a mixture
T_M	Temperature at which the second virial coefficient attains its maximum value
Tr	Reduced temperature (T/Tc)
Tr_{oo}	Modified reduced temperature
Ts	Temperature of calorimetric shield
Ts	Saturation temperature
u(r)	Intermolecular potential function
$\tilde{U}$	Configurational energy
U	Internal energy
	Internal energy of calorimeter
v	Velocity
V	Volume
Vb	Boyle volume, $-(TdB/dT)_{T=Tb}$
Vc	Critical volume

Vr	Reduced volume, V/Vc
$\underline{V}$	Specific Volume
w	Mass fraction
w	Weighting factor
w	Work input
$\dot{w}$	Rate of transfer of work
W	Molecular weight
x	Mole fraction
[x]	Composition array
y	Mole fraction (usually gas phase)
z	Mole fraction (usually for two phase mixtures)
z	Elevation
z	Compressibility factor
zc	Critical compressibility factor
α	Constant in Leland-Mueller mixing rule
α	Inverse steepness parameter for Barker-Henderson perturbation theory
$\alpha,\beta,\gamma,\delta$	Constants in the differential pressure transducer calibration equation
α,γ	Constants in the BWR equation
$\alpha',\beta',\gamma',\delta$	Constants in the differential pressure transducer calibration equation
$\overline{\alpha}$	Average polarizability
αc	The slope d(lnPr)/d(lnTr) of the vapor pressure curve at the critical point
$\beta-\beta_{oo}$	Perturbation parameter for three parameter corresponding states theories
δ	Perturbation parameter of Cook and Rowlinson
δ	Third parameter expressing departure from two parameter corresponding states theory

Δ	Difference
ΔH^{ν}	Enthalpy of vaporization
ε	Molecular energy parameter
η	$(\varepsilon_{jj} - \varepsilon_{ii})/2\varepsilon_{oo}$
θ	Shape factor in corresponding states theory
θ	Time
μ	Joule-Thomson coefficient, $(dT/dP)_H$
μ	Dipole moment
ν	Index on energy parameter for generalized Van der Waal mixing rules
ξ	Volume density ..... $\frac{1}{6}\pi \sum_{i=1}^{n} \rho_i N \sigma_i^3$
ρ	Density
ρr	Reduced density, $\rho N\sigma^3$
σ	Molecular size parameter
τ	Powers corresponding states parameter
Φ	Symbol for a functional form
ϕ	Isothermal throttling coefficient, $(dH/dP)_T$
ϕ	$(\sigma_{jj}^3 - \sigma_{ii}^3)/2\sigma_{oo}^3$
$\overline{\phi}$	Mean value of $(dH/dP)_T$ over some pressure internal
χ	Diagmagnetic susceptibility
Ψ	..... $\frac{d}{dT}\left(\frac{dH}{dP}\right)_T$, or $\left(\frac{dCp}{dP}\right)_T$ or $-T\left(\frac{d^2V}{dT^2}\right)_P$
Ψ	Shape factor in corresponding states theory
Ψ	$1 - (\varepsilon_{ii}\varepsilon_{jj})^{1/2}/\varepsilon_{ij}$

Subscripts

A	Pertaining to point A
b	Calorimeter bath conditions
bp	Bubble point condition
B	Pertaining to point B
C	Critical point property
dp	Dew point condition
f	Final state
f	Outlet condition
h	Pertaining to the high pressure side

HS	Hard sphere property
i	Inlet condition
ij	Pertaining to the interaction between molecules of species i and species j
i,j,k	Component in a mixture
k	Pertaining to a peak in some specified property
l	Pertaining to the low pressure side
m	Total mixture property
M	Pertaining to the condition where the second virial coefficient is a maximum
p	Constant pressure
s	Property at saturation
T	Constant temperature
v	Constant volume
x	Mixture property
o	Reference substance property
o	Outlet condition
oo	Reference property (for the o-o interaction)

Superscript

o	Zero pressure property
E	Excess property
l	Liquid phase property
g	Vapor phase property
HS	Hard sphere property
L	Property of the liquid phase
V	Property of the vapor phase

Conversion Factors for Units Used in this Work

1 atm	=	14.696 psia = 101325 Newtons/sq. meter
1 btu	=	1055.87 Joules
1 cu ft	=	28317 ml

1 dyne/cm^2	=	1.45038×10^{-5} psi
g_c	=	980.665 gm-cm/gmf-sec^2
in	=	0.0254005 meters
lb	=	0.453592 kg
°R	=	°F + 459.67 = (°K)•1.8
R	=	10.73147 psi ft^3/(°R)(lb mole)

ABSTRACT

THE MEASUREMENT AND PREDICTION OF THERMAL PROPERTIES OF SELECTED MIXTURES OF METHANE, ETHANE, AND PROPANE

by
André Wilkinson Furtado

Chairman: John E. Powers

The major goal of this work is to predict the enthalpy behaviour of a ternary methane-ethane-propane mixture from constituent pure component and binary enthalpy data as part of a broad effort to improve the estimation of the thermodynamic properties of multi-component fluid mixtures of hydrocarbons and other non-polar substances of industrial interest. The objectives of this research are: 1) To improve the overall operation of the calorimetric facility at the Thermal Properties of Fluids Laboratory at the University of Michigan. 2) To review the literature to determine the most practical and efficient procedure for estimating multi-component enthalpies from constituent binary data and to develop new procedures if necessary. 3) To obtain wide ranging enthalpy data on one ternary methane-ethane-propane mixture and on those of its constituent pure component and binary systems that are thus far inadequately characterized in the literature. 4) To use the basic measurements on the individual systems to generate smoothed enthalpies as a function of temperature and pressure at regular intervals. 5) To evaluate the selected prediction techniques for their ability to codify the pure component and binary data and to predict the enthalpy behaviour of the ternary mixture.

Major modifications include the installation of strain gage transducers for measuring pressure and differential pressure at the calorimeter, the construction of a differential mercury manometer for the calibration of differential pressures upto 200 psid at line pressures upto 2000 psia, and the fabrication of a new heater capsule for the isobaric calorimeter.

Measurements involving discrete enthalpy changes along isobars and isotherms were obtained for ethane, three ethane-propane mixtures containing 0.76, 0.50, and 0.27 mole fraction ethane, respectively, and for a ternary mixture (0.369 CH_4, 0.305 C_2H_6, 0.326 C_3H_8) over the

range -250°F to +300°F and from 100 psia to 2000 psia including the liquid, two phase, critical and gaseous regions using both isobaric and throttling direct flow calorimeters. Some isenthalpic data was also obtained. Cp and $(dH/dP)_T$ were obtained from the basic data by graphical equal area smoothing. Computer aided integration yielded smoothed enthalpies over the entire measurement range and down to 0 psia using additional data in the literature. The examination of closed enthalpy paths established that the data were internally self consistent to about $\pm$ 0.3%. Comprehensive enthalpy diagrams were constructed for ethane and for the ternary mixture. The tabulated enthalpies for all systems investigated are believed to be accurate to within 1 Btu/lb.

A comprehensive review of prediction techniques from the standpoint of both theory and practice recommended the use of the pseudo-critical method in conjunction with the three parameter Powers Generalized Correlation (PGC). The enthalpies for the individual systems examined were adequately (1% or better on the average) encoded in the PGC framework for an optimum choice of pseudo-parameters for each specific case. A test was also developed to examine the consistency between the pseudo-parameters for all mixtures belonging to a given binary system based on the composition independence of the second interaction virial coefficient B_{ij}.

Next, ten sets of mixing rules for calculating the pseudo-critical parameters as a function of composition were investigated. Four of these were developed in this work and were based on the exact relationship:

$$B_m = \sum_{i=1}^{n} \sum_{j=1}^{n} x_i x_j B_{ij}$$

in the dilute gas region. A pair of reduced three parameter second virial coefficient correlations extending over the ranges $0.5 \leq Tr \leq 3.26$ and $9.0 \leq Tr \leq 30$, respectively, were also developed as part of the effort. For eight of the ten rules, the binary interaction constants were all empirically adjusted to fit the available binary enthalpy data. All these rules were found to predict the enthalpy behaviour of the ternary mixture within engineering accuracy (2% or better).

INTRODUCTION

Some form of energy transfer to or from a fluid is a common occurence in most chemical processes. In such situations, the characterization of process streams and the sizing of equipment such as heat exchangers, heaters, and refrigerators requires the accurate estimation of the thermal properties of the fluids involved over the range of operating conditions. One solution is to obtain laboratory measurements on the desired system at the conditions of interest. This approach has, in fact, been used to characterize the thermodynamic properties of many industrially important pure fluids and some binary mixtures. However, the systematic acquisition of thermal property data for systems of interest with a greater number of components is too time consuming, experimentally difficult, and financially prohibitive to be considered as a feasible approach to the problem.

Early workers in the field were aware of the situation, and sought to predict the thermodynamic properties of a multicomponent mixture solely from those of its pure components by assuming oversimplified solution models with limited success. By the early sixties, a sizable body of binary mixture data confined primarily to volumetric measurements was accumulated. The calculation of mixture enthalpies from such information requires the volumetric data to be differentiated, and consequently yields results of limited accuracy.

As the enthalpy prediction techniques improved, the American Petroleum Institute (API) [7] found that mixture data of the range and accuracy necessary to discriminate between the various correlations could scarcely be met by existing sources of data, particularly in the critical region, and recommended that extensive high accuracy calorimetric measurements were desirable. Very little work was reported in this area before 1955, primarily because the direct determination of the enthalpies of fluid mixtures turned out to be a surprisingly difficult experimental problem. The experimental difficulty was further compounded for measurements obtained at high pressures.

The established need for reliable mixture enthalpy data led the National Science Foundation (NSF) and The Petroleum Research Fund (PRF)

to sponsor the development of the Thermal Properties of Fluids Laboratory (TPFL). Support for adapting the facility to handle mixtures was generously provided by the Natural Gas Processors Association. Since the early sixties, the facility has been involved in the measurement of the enthalpies of pure and binary mixed fluids involving helium, nitrogen, methane, and propane over a wide range of operating conditions using direct flow calorimetry. These systems are of direct interest to the petroleum industry, where trends towards lower temperatures in gas processing to allow recovery of light hydrocarbons, without absorption in oil, require that the enthalpy be very accurately estimated in order to ensure the reliability of design calculations under such conditions. More importantly, such measurements have long range value because they can serve as standards for the evaluation of continually evolving thermodynamic property prediction methods for some time to come.

The research at the TPFL has also contributed significantly to the interpretation of the basic experimental calorimetric measurements to yield useful and readily accessible smoothed wide ranging thermal property charts and tables with little loss in accuracy. In particular, the construction of a temperature-entropy diagram for a methane-propane mixture containing 0.946 mole fraction methane, including both the single and two phase region [22], has been found to be particularly valuable in the design of natural gas turbo-expander processes. Nevertheless, the acquisition and interpretation of the basic data obtained at the TPFL has at best been a difficult and tedious problem with heavy manpower requirements. Even so, it is the commitment to continuous improvement of the facility that has been primarily responsible for the success obtained in the past. For the present, it appears that equipment modifications that permit the reduction of operating personnel, and the increased use of computer techniques in sensing human error at various stages are both highly desirable if the efficiency of the operation is to be further improved.

Having accumulated a fair amount of enthalpy measurements, the research at the TPFL has, in the past few years, been increasingly associated with the evaluation of existing correlations and the development of new techniques for the prediction of mixture enthalpies. The application of such techniques to binary systems investigated at

the TPFL has confirmed the need for incorporating empirically determined binary interaction parameters into such correlation schemes. A logical, interesting, and industrially valuable extension of this approach would be to determine if the properties of the multicomponent mixture can be predicted if all the pair interactions in the mixture are thus characterized. A systematic experimental investigation that will allow this approach to be more concretely explored is, therefore, desirable. The investigation of the methane-ethane-propane system is highly suited to this end as explained below.

The methane-propane system including the pure components has already been investigated in depth at the TPFL. Correlated enthalpy values for the methane-ethane system are available in the literature. It would appear that the investigation of the ethane-propane system and at least one ternary mixture of methane, ethane, and propane could satisfy the minimum requirements of the proposed research. Surprisingly, reliable enthalpy data for ethane in the subcooled liquid and the critical regions are scarce, and therefore, its examination is also desirable. Such a study would not only serve industrial interests, where the increased demand for ethane both as a fuel and as a petrochemical feedstock has led to cryogenic processing techniques, but would also permit pure component enthalpy prediction techniques to be examined in the rarely investigated subcooled liquid and critical regions.

Although thermodynamic property prediction techniques in common use are primarily empirical in nature, recent advances in the application of statistical mechanical techniques to the prediction of mixture properties have, in some cases, suggested the equivalent theoretical approximations at the microscopic level, contributing immensely in the process to a much more fundamental understanding of the problem. These results, coupled with the increasingly successful use of the hard sphere equation of state as a starting point for the calculation of the thermodynamic properties of pure components and mixtures, seem to indicate that a new generation of sophisticated prediction techniques is in the offing. A discussion of such techniques would serve the useful purpose of helping the design engineer keep abreast of the more recent developments in the area.

Accordingly, the objectives of this research are as follows:

(1) To improve as necessary, the overall operation of the calorimetric facility.

(2) To undertake calorimetric measurements on ethane, on selected ethane-propane mixtures, and one, preferably, approximately equimolar methane-ethane-propane mixture over the approximate range $-240°F \leq T \leq 300°F$, 100 psia $\leq P \leq$ 2000 psia.

(3) To interpret the basic calorimetric measurements so as to yield smoothed tables or diagrams that illustrate the effect of temperature and pressure on the enthalpy and its appropriate derivatives for each system over the region of investigation.

(4) To review the present state of enthalpy prediction techniques with special emphasis on theoretical developments that throw new light on long used empirical methods.

(5) To select the most suitable framework for the codification of the enthalpy data for the pure component and binary systems that constitute the ternary mixture.

(6) To evaluate the prediction of the enthalpy behaviour of the ternary mixture from constituent pure component and binary data within the confines of the framework selected in Step 5.

(7) To comment on future directions for both theoretical and experimental investigation as suggested by the acquisition, interpretation, and correlation of the measurements obtained in this work, and also from related investigations.

Chapter I

PRELIMINARY CONSIDERATIONS

In the past, the thermal properties of pure and mixed fluids have been primarily calculated from PVT data using appropriate thermodynamic relationships instead of attempting to measure them directly by calorimetry, because it is experimentally easier to investigate and control a static system than a dynamic one. Although such relationships are rigorously true in theory, practical difficulties in their application can offset the experimental advantages to be obtained. Some of the more useful of these thermodynamic identities are noted in this chapter and the limitations of such approaches are discussed briefly. Next, various calorimetric techniques are outlined, and the thermodynamics of a flow calorimeter with heat shield, typical of those used in this work, is developed to illustrate how thermal properties may be directly specified from such measurements.

Thermal Properties from Volumetric and Phase Equilibria Data

Miyazaki, Furtado and Powers [179] used the thermodynamic relations

$$\Psi = \left(\frac{\partial Cp}{\partial P}\right)_T = \frac{\partial}{\partial T}\left[\left(\frac{\partial H}{\partial P}\right)_T\right]_P = -T\left(\frac{\partial^2 V}{\partial T^2}\right)_P = -\frac{RT}{P}\left[\left(T\frac{\partial^2 z}{\partial T^2}\right)_P + 2\left(\frac{\partial z}{\partial T}\right)_P\right] \qquad (I\text{-}1)$$

to calculate the isothermal differences in Cp, and the isobaric differences in $(\partial H/\partial P)_T$ using a two dimensional interpolation of volumetric data on propane. On integration, Equation (I-1) yields the isothermal throttling coefficient ϕ as

$$\phi = \left(\frac{\partial H}{\partial P}\right)_T = V - T\left(\frac{\partial V}{\partial T}\right)_P = -T^2\left[\frac{\partial (V/T)}{\partial T}\right]_P = -\frac{RT^2}{P}\left(\frac{dz}{dT}\right)_P \qquad (I\text{-}2)$$

On further integration, we obtain the result

$$(H - H^\circ)_{T,P} = \int_0^P \left[V - T\left(\frac{\partial V}{\partial T}\right)_P\right]_T dP \qquad (I\text{-}3)$$

where $(H-H^\circ)$ is the isothermal enthalpy departure at pressure P from the ideal gas state at temperature T, and is equivalent to the

configurational enthalpy $\tilde{H}$.

If we wish to calculate the enthalpy at any T and P for any given substance relative to that in the ideal gas state, H°_{To}, for the same substance at some specified temperature To, then it is necessary to invoke the thermodynamic relation

$$H_{T,P} = H^\circ_{To} + \int_{To}^{T} Cp^\circ(T)\,dT + \int_{0}^{P} \left[V - T \left(\frac{\partial V}{\partial T} \right)_P \right]_T dP \qquad \text{(I-3a)}$$

where Cp° is the heat capacity at zero pressure. In effect, the enthalpy difference between any two points in the P-T plane may be calculated given sufficient volumetric data, and the behaviour of the zero pressure heat capacity as a function of temperature. If the volumetric data are specified along isochores instead of isotherms, then it is practically easier to obtain the enthalpy departure with T and V as the independent variables as given by the thermodynamic identity

$$H(T,\infty) - H(T,V) = RT - PV - \int_{\infty}^{V} \left[P - T \left(\frac{\partial P}{\partial T} \right)_V \right]_T dV \qquad \text{(I-4)}$$

Equations (I-3) and (I-4) are also applicable to total mixture properties in a mixture of fixed overall composition even within the two phase region. For pure components, however, $(dV/dT)_P$ is discontinuous across the saturation boundary. In such cases it is necessary to use an expanded version of Equation (I-3a) which yields

$$H_{T,P} = H^\circ_{To} + \int_{To}^{T} Cp^\circ(T)\,dT + \int_{0}^{Ps} \left[V - T \left(\frac{dV}{dT} \right)_P \right] dP + \Delta H^\nu + \int_{Ps}^{P} \left[V - T \left(\frac{dV}{dT} \right)_P \right] dP \qquad \text{(I-5)}$$

where ΔH^ν is the enthalpy change for any first order transition occuring at Ps and T. If ΔH^ν corresponds to the enthalpy change on vaporization, then it may also be calculated from a knowledge of the saturation properties at the same temperature using the familiar Clapeyron equation

$$\left(\frac{dP}{dT} \right)_{T=Ts} = \frac{\Delta H^\nu}{T(V^V - V^L)} \qquad \text{(I-6)}$$

where the left hand side represents the slope of the vapor pressure curve at T=Ts, and V^V, V^L are are the saturated vapor and liquid

volumes at the same temperature. If such computations are made at a series of temperatures, then the difference between the saturated liquid and vapor heat capacities along the vapor pressure curve may be obtained by the relation

$$Cs^V - Cs^L = \frac{d}{dT}[\Delta H^\nu] - \frac{\Delta H^\nu}{T} \tag{I-7}$$

where the saturated heat capacity Cs for a given phase can be defined in terms of Cp for the same phase by the relation

$$(Cs)_{Ts,Ps} = (Cp)_{Ts,Ps} - T\left(\frac{\partial V}{\partial T}\right)_{Ps}\left(\frac{dP}{dT}\right)_{Ts,Ps} \tag{I-8}$$

Equations (I-1) through (I-4) are useful for calculating thermal properties of a mixture, only if the volumetric data are obtained on a system of fixed composition. If such data are instead available at a series of compositions, then the enthalpy departure for example, at any composition may be obtained from the relation

$$-\frac{[H_m - H_m^\circ]}{RT^2} = \sum_i y_i \frac{\partial \ln f_i/y_i P}{\partial T} \tag{I-9}$$

where the fugacity coefficient $f_i/y_i P$ is defined from the relation

$$\ln(f_i/y_i P) = \frac{1}{RT}\int_0^P \left[\left(\frac{\partial V_m}{\partial n_i}\right)_{T,P,n_j} - \frac{RT}{P}\right] dP \tag{I-10}$$

where the subscript m stands for the total mixture property in any given phase. These relations can also be used within the two phase region, as demonstrated by Edmister [68] with respect to the helium-hydrogen system, to calculate the enthalpy departures of coexisting liquid and vapor phases along isotherms.

Unlike a pure fluid, the value of the enthalpy of vaporization at constant pressure for a saturated liquid mixture differs from that obtained at constant temperature. This happens because the location of the saturated vapor phase corresponding to a saturated liquid mixture depends additionally upon the path selected.
As most industrial processes are conducted at constant pressure conditions, the estimation of $(\Delta H^\nu)_P$ is therefore more important. If the

dew and bubble point temperatures T_{dp}, and T_{bp} respectively are measured at some constant pressure P, for a given mixture, and if the heat capacities at zero pressure, Cp°_i are known for each component i over the interval T_{bp} to T_{dp}, then, as Tao [262] has recently determined, $(\Delta H^v)_p$ may be calculated strictly from vapor phase volumetric data as a function of pressure and composition at the two temperatures T_{dp}, and T_{bp} using the relation

$$(\Delta H^v)_p = RT^2_{bp} \sum_{i=1}^{n} z_i \left(\frac{\partial \ln \bar{f}_i^V}{\partial T} \right)_{T_{bp}} - RT^2_{dp} \sum_{i=1}^{n} z_i \left(\frac{\partial \ln \bar{f}_i^V}{\partial T} \right)_{T_{dp}} + \sum_{i=1}^{n} z_i \int_{T_{bp}}^{T_{dp}} Cp^\circ_i \, dT \qquad \text{(I-11)}$$

where z_i is the mole fraction of component i in the mixture. The second term on the right hand side of the above equation may also be obtained from volumetric data in the gaseous phase as a function of pressure alone along the dew point isotherm using Equation (I-3) instead if the composition corresponds to that of the total mixture.

Inadequacies of Volumetric Data and Equations of State in Calculating Thermal Properties

Although the thermodynamic relations (I-1) through (I-9) are rigorous, errors in specifying the desired volumetric properties in these relations can cause proportionally larger errors in the calculated values of the thermal properties. The right hand side of Equation (I-3) for example, involves a difference of two terms that are usually both positive and of about equal magnitude. Consequently, the calculated enthalpy departure is at least an order of magnitude less precise than the specified values of V and $T(\partial V/\partial T)_p$ along any isotherm.

Volumetric data are usually not abundant enough to provide measured values of the integrands in Equations (I-3a) and (I-4) for calculating the enthalpy departures for all conditions of interest, and in practice, it is necessary to either interpolate the data, or to fit it to a PVT equation of state. Consequently, the errors introcuded in the calculation of the enthalpy departure stem not only from errors in the basic volumetric measurements, but also from inaccuracies that are inherent in approximate representations of the true P-V-T surface.

The fact that P-V-T data are, for engineering purposes, satisfactorily represented by such approximations may at first lead to the deceptively simple conclusion that all other thermodynamic properties may then be calculated to the same degree of accuracy. The deficiencies of some of these formulations with respect to the calculation of thermal properties have been amply illustrated in the literature [24, 182]. The Benedict-Webb-Rubin (BWR) equation of state (20) given by

$$P = RT\rho + (B_oRT - A_o - \frac{C_o}{T^2})\rho^2 + (bRT - a)\rho^3 + a\alpha\rho^6 + \frac{c\rho^3}{T^2}[(1+\gamma\rho^2)e^{-\gamma\rho^2}] \qquad (I\text{-}12)$$

has been extensively used in representing the P-V-T surface of pure non-polar fluids.

Morsy (182) used both the original and a modified BWR equation of state with 8 and 11 constants respectively to fit the volumetric data for CF_4 between 0°C and 350°C and upto 1.6 times the critical density. Tables of derived thermodynamic properties were independently computed over the same range by Harrison and Douslin (97) using their own precise, unsmoothed experimental compressibility data by a combination of analytic and graphical methods. The absolute average deviation in the fit to the compressibility data was obtained as 0.55% and 0.13% respectively for the two empirical equations as monitored by the difference between the calculated and tabulated pressures. Although comparable deviations were also obtained for the configurational free energy, and the entropy, the agreement with the tabulated enthalpy departures were significantly poorer at 11.18% and 2.18%, respectively.

In another study involving the origianl BWR equation, Bishnoi [24] determined that both the values of the empirical constants and the goodness of fit with respect to experimental measurements were sensitive to the specific optimization technique employed, the best results being obtained by multiple non-linear regression analysis. It was again noted that even though the compressibility of CO_2 from 100°F to 400°F, and up to 4000 psia was represented to better than 0.4%, the fit to experimental heat capacity measurements in the same range using volumetrically derived constants was no better than 6.7%. Simultaneous regression on both properties resulted in only a minor improvement in the

representation of heat capacities. These studies suggest that the original BWR equation, widely used for the concise codification of thermodynamic properties, is probably unsuitable for the precise representation of thermal data in the critical and dense fluid regions. Attempts to improve the performance of the equation have involved the addition of a few extra terms [251,254], or the specification of separate constants for the liquid, critical and gaseous regions with the added constraint of smoothness in the thermodynamic properties across the interfaces [76,82].

Other recent attempts to improve the representation of thermal properties with a PVT equation of state have required a rather drastic increase in the number of empirical constants used. Jacobsen [115], for example, fitted a 31 constant equation of state to critically selected thermodynamic data for nitrogen with generally good (0.5% or better) results over the entire fluid phase. Nevertheless, the behaviour of the PVT surface in the critical region still appears to be unsatisfactory as deviations of over 60% were obtained with respect to the heat capacity data of Jones [119].

Miyazaki, Furtado, and Powers [179] determined Ψ in the critical and supercritical region by interpolating the smoothed calorimetric data of Yesavage [284] and from the volumetric data of Reamer, Sage and Lacey [210] using Equation (I-1). The discrepancy between the Ψ values so calculated averaged to about 28%, with some differences as high as 200%. These differences are particularly significant because the analysis did not require the data in either case to be subjected to the additional constraint of an empirical PVT equation of state. In spite of this precaution, the Ψ values derived from volumetric data were nevertheless found to be sensitive even to the specific interpolation scheme used. An average Ψ variation of 6% was traced to differences in the interpolated values for $(\partial^2 z/\partial T^2)_p$ in Equation (I-1) for a given set of z vs T data at some fixed pressure. It was concluded that for the techniques of data interpretation employed in the study, the estimation of volumetric properties from calorimetric data yielded better results than vice-versa.

An examination of Equations (I-9) and (I-10) suggest that the calculation of the enthalpy departure as a function of composition,

given P-V-T-x data for any system, requires the data to be differentiated not only with respect to temperature, but also with respect to composition. Ellington and Eakin [69] indicate that the interpretation of such data to yield thermal properties could involve a ten to hundred-fold reduction in accuracy, and in conclusion, the authors plead for the acquisition of volumetric data of high (better than 0.02% accuracy) over wide ranges of temperatures and pressures to permit a reliable calculation of PVT derived thermodynamic properties.

Thermal Properties from Direct Calorimetric Measurements

The arguments so far suggest that thermal properties of fluids, particularly in the critical region, may be more fruitfully obtained by considering other techniques that do not involve the interpretation of volumetric data. Partington and Shilling [190] for example, have reviewed early methods of obtaining the heat capacity both directly and indirectly from a wide variety of measurements involving both static and flow systems including 1) Direct flow calorimetry, 2) Constant volume calorimetry, 3) Heat exchange with the same fluid, 4)Heat exchange with a different fluid, 5) Explosion, 6) Isentropic expansion, 7) Velocity of sound, 8) Resonance, 9) Self-sustained oscillations, 10) Flow comparison, and 11) Molecular spectroscopy. Since then, Rowlinson [222] has outlined methods used in the past half century, and more recently, McCullough and Scott [158] have published an authoritative compilation of experimental techniques involved in the calorimetry of non-reacting systems in all phases, including the pure saturated fluids. Other reviews on the subject are due to Masi [166], Faulkner [79], Barieau [11], Sturtevant [258], and Yesavage, et al. [286]. These works together encompass a significant body of literature on the subject to which the reader is referred for further information.

An examination of the literature suggests that steady state flow calorimetry is to be preferred over static closed system calorimetric techniques for measurements on gases and vapors, because inescapable corrections in the latter case involving the thermal properties of the containing vessel are significant when compared with the relatively low heat capacity of the gas phase. Perhaps the most

straightforward technique of flow calorimetry for a system of fixed composition involves adding a known amount of energy to a flowing stream, and monitoring the change in some specified intensive property of the stream, be it temperature or pressure.

In the case of fluid mixtures, the technique of flow calorimetry may also be utilized to measure the enthalpy change on mixing the constituent pure components at some specified T and P. If the enthalpy H_i of each of the constituent pure components is also known at the same T and P, then the mixture enthalpy H_m may be calculated from the thermodynamic relation

$$H_m = \sum_{i=1}^{n} x_i H_i + H^E \qquad \text{(I-13)}$$

where x_i is the mole fraction of component i, and H^E is the heat of mixing. This technique has two notable advantages. Firstly, if the pure component enthalpies can be accurately specified at the given T and P, then even relatively crude measurements (5-10%) on H^E can serve to provide fairly accurate estimates of H_m, because the mixing effect, H^E, with the notable exception of the critical and the two phase region, is usually a small fraction of the total contribution of the right hand side of Equation (I-13). Secondly, relative adjustment of the flow rates of the constituent pure components is easily accomplished so that the technique provides for the rapid specification of H_m as a function of composition at any given T and P, unlike flow calorimetry at fixed composition.

There are, however, two important limitations. Firstly, the application of the technique to exothermic mixing situations also requires the heat capacity of the mixture to be known over the interval of the temperature rise [100], unless the heat generated can be removed isothermally. Secondly, such calorimeters are usually operated in the single pass mode, in view of the impracticability of regenerating the pure components on a continuous basis. The rapid consumption of feed materials is a significant drawback, and has served to limit such investigations to relatively inexpensive systems. These considerations suggest that if thermal property measurements on mixtures are to cover a wide range of conditions, they may be more economically

accomplished using a flow calorimeter in a recycle system at fixed composition.

Thermodynamics of a Shielded Flow Calorimeter

We now discuss the thermodynamics of a flow calorimeter with a heat shield typical of that used in this work to illustrate exactly how thermal properties may be specified from such measurements for a system at constant composition. A schematic of the calorimeter is shown in Figure (I-1) below

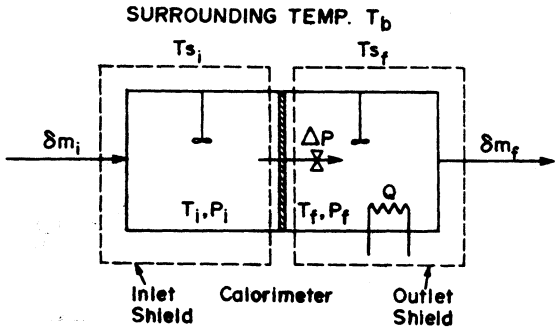

Figure I-1. Direct Flow Calorimeter - Schematic.

If δm_i and δm_f are the quantities of mass transferred across the inlet and the outlet of the calorimeter respectively, in some time period $\delta\theta$, an energy balance across the calorimeter in the absence of specially impressed force fields yields

$$(\underline{U}_i + P\underline{V}_i + \tfrac{1}{2} v_i^2 + gz_i)\,\delta m_i - (\underline{U}_f + P\underline{V}_f + \tfrac{1}{2} v_f^2 + gz_f)\,\delta m_f + \delta Q - \delta W = \mathcal{U}_F - \mathcal{U}_I \qquad \text{(I-14)}$$

where $\underline{U}$ is the specific internal energy of the flowing stream

$\underline{V}$ is the specific volume of the flowing stream

v is the velocity of the flowing stream

z is the elevation

δQ is the net heat transferred to the calorimeter in time $\delta\theta$

δW is the work obtained from the calorimeter in time $\delta\theta$

$(\mathcal{U}_F - \mathcal{U}_I)$ is the net change in the total energy of the calorimeter in time $\delta\theta$.

Converting (I-14) into a rate equation, and substituting $(\underline{U} + P\underline{V})$ by $\underline{H}$, we obtain

$$(\underline{H}_i + \tfrac{1}{2} v_i^2 + gz_i)\dot{m}_i - (\underline{H}_f + \tfrac{1}{2} v_f^2 + gz_f)\dot{m}_f + \dot{q} - \dot{w} = \left(\frac{d\mathcal{U}}{d\theta}\right)_{system} \tag{I-15}$$

For steady state mass flow

$$\dot{m}_i = \dot{m}_f = \dot{m} \tag{I-16}$$

Furthermore, neglecting changes in velocity and elevation between the measurement points, we obtain the simplification

$$\underline{H}_f - \underline{H}_i = [\dot{q} - \dot{w} - \left(\frac{d\mathcal{U}}{d\theta}\right)_{system}]/\dot{m} \tag{I-17}$$

The simplification of Equation (I-17) is valid for the calorimeters of Faulkner [79], and of Mather [168] that are used in this work. In each case, the difference in elevation between inlet and outlet conditions is less than 6 inches, and the resultant head effect is less than 10^{-7} Btu/lb. Variations in velocity arise from density changes caused by a pressure drop or a change in phase across the calorimeters. The upper limit of this effect is of the order of 0.002 Btu/lb., and occurs in the case of a liquid inlet and vapor outlet. Referring to the model schematically presented in Figure (I-1), the calorimeter is permitted to exchange heat with the surrounding bath at temperature T_b. The calorimeter is divided into two isothermal components at T_i and T_f respectively, each provided with a separate heat shield at temperature Ts_i and Ts_f respectively. The shield is in each case interposed between the calorimeter and the bath. The net rate of heat transfer to such a shielded calorimeter is given by

$$\dot{q} = h_i A_i (Ts_i - T_i) + h_f A_f (Ts_f - T_f) \tag{I-18}$$

where h and A represent the average heat transfer coefficient and the interfacial area for heat transfer respectively. If electrical energy is supplied at the rate EI to the outlet section of the calorimeter, where E is the voltage, and I is the current, then

$$\dot{w} = -EI \tag{I-19}$$

As the bath temperature T_b for the calorimeters of this work is essentially maintained at the inlet temperature T_i, there is no need for a shield at the inlet section. For non-isothermal operation, the shield at the outlet section is wrapped with heating wire, the power to which is adjusted until a differential thermocouple between the shield at the outlet section, as monitored by a lamp and scale mirror galvanometer, indicates zero temperature difference. In such cases, the energy generated at the "guard heater" is in theory completely transferred to the bath and $\dot{q}$ is essentially zero. If a sufficient time period is allowed to elapse after the input of power to the outlet section, the calorimeter will reach its final energy state for any steady state process occurring within. Thus, at steady state

$$d\mathcal{U}/d\theta = 0 \tag{I-20}$$

Under the above restrictions, Equation (I-17) reduces to the form

$$\underline{H}_{T_f,P_f,[x]} - \underline{H}_{T_i,P_i,[x]} = \frac{E\,I}{\dot{m}} \tag{I-21}$$

where T_i, P_i, T_f, P_f, [x], EI, and $\dot{m}$ are all experimentally accessible quantities.

Determination of Enthalpy Derivatives by Flow Calorimetry

It is possible to obtain specific information on the enthalpy derivatives with respect to temperature or pressure by controlling the operating path of the flow process in the calorimeter. As $\underline{H}$ is a point function of state, Equation (I-17) may be rewritten as

$$\left[\underline{H}_{P_f,[x]} - \underline{H}_{P_i,[x]}\right]_{T_i} + \left[\underline{H}_{T_f,[x]} - \underline{H}_{T_i,[x]}\right]_{P_f} = \frac{E\,I}{\dot{m}} \tag{I-22}$$

In the absence of unnusual force fields, the differential enthalpy change $d\underline{H}$ may be given by the exact differential equation

$$d\underline{H} = \left(\frac{\partial \underline{H}}{\partial P}\right)_{T,[x]} dP + \left(\frac{\partial \underline{H}}{\partial T}\right)_{P,[x]} dT + \sum_{i=1}^{n} \left(\frac{\partial \underline{H}}{\partial w_i}\right)_{T,P,w_{j\neq i}} dw_i \tag{I-23}$$

where dw_i is a change in the mass of component i. For a system

at constant composition Equation (I-23) may be rewritten as

$$d\underline{H} = \phi \, dP + Cp \, dT \tag{I-24}$$

By combining Equations (I-22) and (I-24) we obtain

$$\int_{P_i}^{P_f} (\phi)_{T_i} \, dP + \int_{T_i}^{T_f} (Cp)_{P_f} \, dT = EI/\dot{m} \tag{I-25}$$

Equation (I-23) and hence (I-25) are valid only when all the enthalpy derivatives in the equations are continuous. This condition is not met for measurements across the saturation boundary in a pure component. In such a case it is necessary to use the more general form

$$\int_{P_i}^{P_s} (\phi)^{L}_{T_i} \, dP + \int_{T_i}^{T_s} (Cp)^{L}_{P_f} \, dT + \Delta\underline{H}^{v} + \int_{P_s}^{P_f} (\phi)^{V}_{T_i} \, dP + \int_{T_s}^{T_f} (Cp)^{V}_{P_f} \, dT = EI/\dot{m} \tag{I-26}$$

where $\Delta\underline{H}^{v}$ is the enthalpy of vaporization at Ts and Ps.

In examining Equation (I-25) we observe that the operation of the calorimeter may be specified so as to enhance the contribution of one term with respect to the other. In isobaric operation, for example, the pressure drop across the calorimeter is made as small as possible so that the electrical energy input is used mainly to raise the temperature of the fluid, and provides us with an integral average of Cp over the temperature range T_i through T_f.

In the calorimeter developed by Mather [168], a sizable pressure drop is induced by directing the fluid through a capillary coil of fixed length and diameter. An insulated heating wire coaxial with, and inside the capillary supplies an adjustable quantity of heat to maintain the outlet temperature T_f as near as possible to that of the inlet at temperature T_i. Thus, no heat shields or guard heaters are necessary.

In cases where a pressure drop causes a rise in temperature in the fluid, the removal of energy required for isothermal operation cannot be accomplished by the above technique. It is then necessary to operate the calorimeter in the isenthalpic mode. In this case, no electrical energy is added to the calorimeter, and the guard heater is activated to compensate for the heat leak at the outlet section of

the calorimeter. Equation (I-21) simplifies to yield

$$\underline{H}_{T_f,P_f,[x]} = \underline{H}_{T_i,P_i,[x]} \tag{I-27}$$

For this case, Equation (I-25) also simplifies to

$$\int_{T_i}^{T_f} (Cp)_{P_f} \, dT = -\int_{P_i}^{P_f} (\phi)_{T_i} \, dP \tag{I-28}$$

or

$$(\bar{C}p)_{P_f} \, (T_f - T_i) = -(\bar{\phi})_{T_i} \, (P_f - P_i) \tag{I-29}$$

where $\bar{C}p$ and $\bar{\phi}$ are the equal area mean values of the derivatives Cp, and ϕ over the appropriate intervals. Therefore,

$$\frac{T_f - T_i}{P_f - P_i} = -(\bar{\phi})_{T_i} / (\bar{C}p)_{P_f} = \bar{\mu} \tag{I-30}$$

Thus, the measurement of the temperature and pressure at the inlet and the outlet of the calorimeter defines $\bar{\mu}$, the mean adiabatic Joule-Thomson coefficient for the fluid, for the specific isenthalp generated across the calorimeter.

Chapter II

LITERATURE REVIEW OF EXPERIMENTAL AND CORRELATED DATA

Chapter I was concerned with illustrating how classical thermodynamics may be utilized in specifying the thermal properties of substances from experimental measurements. This section is devoted to the examination of the literature for information that is relevant to the description of the thermal properties of those systems which are to be experimentally investigated in this work. These include pure ethane, ethane-propane, and the methane-ethane-propane system. As a major goal of this work involves the use of constituent pure component and binary data to predict the enthalpy of the ternary mixture, the experimental measurements for other subsystems of the methane-ethane-propane system are also reviewed. A brief account of recent calorimetric measurements on other systems of interest is also added.

a) General Reviews

Masi [166] has reviewed heat capacity measurements upto 1954 for ten industrially important gases. Mage [161], Mather [168], and Yesavage et al. [286] have since then summarized available heat capacity, isothermal and adiabatic Joule-Thomson coefficient, and enthalpy of vaporization data on both pure and mixed systems. Excess enthalpy measurements on binary mixtures have been tabulated by Hejmadi [100]. Katz and Rzasa [124] have prepared a bibliography that provides general information on the experimental and correlated thermodynamic properties of hydrocarbons upto 1945. This work has been extended to cover the literature upto 1960 by Muckleroy [183]. The American Petroleum Institute [5,6] has since then compiled thermodynamic data sources for pure and mixed hydrocarbons. More recently, Clark et al. [48] have reviewed the volumetric, thermal and transport property measurements for systems of industrial interest that liquefy at cryogenic temperatures.

b) Methane

A compilation of thermodynamic properties including a comprehensive

literature search is presented by Tester et al. [264]. A bibliography that includes the thermophysical properties of methane in all phases has recently been prepared by the Cryogenics Data Center of the National Bureau of Standards [52]. The comprehensive isobaric enthalpy measurements of Jones [119] extending from -240°F to 50 °F and from 150 to 2000 psia, and the volumetric data of Vennix [273] and Douslin et al. [67] deserve special mention for their excellence.

c) Ethane

i) Compilation of Thermodynamic Properties. Compilations on the thermodynamic properties of ethane have appeared since 1935, when Plank and Kambeitz [199] prepared a Mollier diagram in the range -100°C to 32°C, and from 0.5 to 50 kg/cm^2. In 1937, Sage, Webster, and Lacey [234] prepared V, f, H, and S tables for ethane ranging from 70°F to 250°F, and upto 3500 psia. These tables were later extended to 460°F and upto 10,000 psia [209,232]. Similar tabulations covering the range from -220°F to 700°F and upto 1500 psia, but excluding the compressed liquid region were later prepared by Barkelew, Valentine and Hurd [12], in which the thermodynamic properties of the superheated gas were calculated by fitting the volumetric data upto 1947 by the BWR equation of state. The compilation of Tester [264] contains, in addition, a comprehensive and critical discussion of the measurements obtained upto 1957. Since then, Canjar et al. [39] have published thermodynamic property tables derived from the BWR equation of state and covering the range 180K to 1500K and upto 500 atm. [38]. Joffe and Delaney [116] have calculated Cp values from volumetric data in the range 313K to 973K and from 33 atm. to 680 atm. also using the same equation of state. A comprehensive bibliography of the thermophysical properties of ethane upto 1968, covering both experimental measurements and compilations has been prepared by the Cryogenics Data Center [51].

The most recent compilation (1971) is due to Eubank [75], in which the configurational properties of ethane including the enthalpy and heat capacity departures are computed principally from volumetric data using separate sets of BWR constants to fit the liquid, critical and gaseous regions. The compilation covers the range 180K to 540K

with pressures upto 500 atm. Significantly, the tabulated compressibility factors reproduce the apparently superior data of Michels and co-workers [171,172,174] to within 0.1% except near the critical region [82]. The compressibility factors and the enthalpy departures were also compared with those of Barkelew et al. [12], Canjar [39], and Tester [264], at 300K, 400K, and 500K, and upto 500 atm. The agreement in z between all sources was exceptionally good with rare discrepancies beyond 1%. The agreement in H - H° was found to be less satisfactory. The span of the tabulated values at any given T and P was rarely below 1%, and rose to about 4% in the critical region with the magnitude of Tester's and Eubanks' values lying consistently above and below the mean, respectively.

ii) Direct Thermal Property Measurements. Some direct measurements of the thermal properties of ethane are available in the literature. Tsaturyants [269] obtained adiabatic Joule-Thomson data on ethane from 10-400 atm. and from 320K to 450K. Similar measurements have been reported by Sage, Webster and Lacey [254] from 70°F to 220°F with an estimated accuracy of 2%, and by Stockett and Wenzel [255] from -40°F to +45°F, at pressures extending upto 600 psia in each case. The measurements in the first case also include Cv data in the vicinity of the critical isochore from 60°F to 140°F, the accuracy of which is estimated at 2%.

Other direct measurements of the heat capacity in the fluid phase have been primarily confined to the liquid along the saturation curve, and the gas phase at and below 1 atm. The data of Eucken and Hauk [77] from 80K to 300K, of Wiebe, Hubbard, and Brevoort [277], from 67.4K upto the critical point, and of Witt and Kemp [280] from 90K to the normal boiling point of 184.1K lie in the first category. The results of Eucken and Hauk are suspected to be poor as they are between 9 and 25% higher than the results from the other two investigations which are mutually consistent to 0.8%.

Flow calorimetric measurements on the heat capacity in the gas phase at or below 1 atm. have been obtained by Scheele and Heuse [236] from 193K to 298K, by Thayer and Stegeman [265] from 273K to 338K, and by Dailey and Felsing [56] from 340K to 700K. The

spectroscopic data of Smith [267], the thermal conductivity apparatus of Kistiakowski and co-workers [129,130], and the velocity of sound measurements of Dixon, Campbell and Parker [64], have all been used in the calculation of zero pressure heat capacities. Nevertheless, Tester [264] has suggested that the statistical calculations of C_p° by Rossini [220] are to be considered superior to the values derived from experimental data.

Apart from the relatively imprecise data (4%) of Dana, et al. [57] from 233.5K to 271.7K, and the single but reliable value of Witt and Kemp [280] at the normal boiling point, direct measurements on the enthalpy of vaporization are scarce. Barkelew et al. [12] and Eubank [74] have tabulated enthalpy of vaporization values as a function of temperature by making use of a closed enthalpy cycle involving the single experimental value of ΔH^ν at the normal boiling point, the enthalpy change for both the ideal gas and the liquid along the saturation curve between the normal boiling point and the temperature of interest, and the enthalpy departure for the saturated vapor at the two temperatures, as shown in Figure (II-1) below:

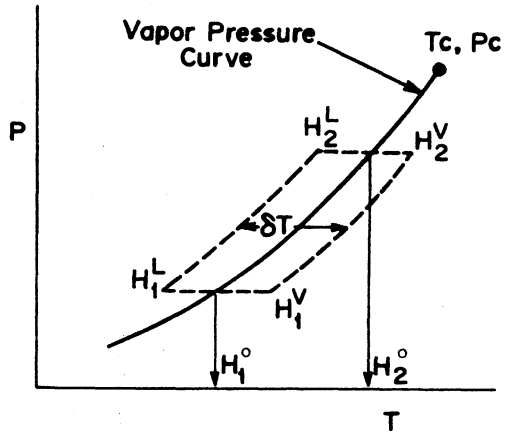

$$(H_2^V - H_2^L) = (H_1^V - H_1^L) + (H_2^V - H_1^V) - (H_2^L - H_1^L)$$

As $\delta T \to 0$

$$\Delta H^\nu(T_2,P_2) = \Delta H^\nu(T_1,P_1) + (H_2^V - H_2^\circ) + (H_2^\circ - H_1^\circ) + (H_1^\circ - H_1^V) - (H_2^L - H_1^L)$$

Figure II-1. Enthalpy Cycle for the Calculation of ΔH^ν as a Function of Pressure.

An independent calculation of ΔH^ν at the normal boiling point by Porter [201] using vapor pressure and saturated volume measurements in conjunction with Equation (I-6) yielded a value that was about 5% lower than the measured result of Witt and Kemp [280].

iii) Additional Measurements. Recent investigations on ethane not included in the earlier bibliographies consist of the second and third virial coefficient measurements of Pope [200] from 206K to 307K, the vapor pressure measurements of Carruth [42] from 91.3K to 144.1K, and the saturated liquid density data of Shana'a and Canfield [239] at -165°F, and of Sliwinski [246] between 283.15K and the critical point.

iv) Conclusions. An examination of the literature reveals that the thermal properties of ethane in the critical region are not as yet adequately defined from existing measurements. Ultrasonic velocity measurements in the critical region have been obtained by Noury and co-workers [186,187] and by Tannenberger [261]. In the latter case, the results were used to calculate Cv from 31.5°C to 40°C and from 100 to 200 amagats using the relation

$$C_v = \frac{T}{\rho^2 \left[\omega^2 + \left(\frac{\partial P}{\partial \rho} \right)_T \right]} \left(\partial P / \partial T \right)_\rho^2 \qquad \text{(II-1)}$$

where ω is the velocity of ultrasound. The accuracy of these calculated results have not yet been established, and await comparison with direct measurements.

The absence of thermodynamic property tabulations for the subcooled liquid region is also noted. The measurement of the enthalpy change as a function of temperature and pressure in this area would be very useful in filling the gaps in existing compilations. Accurate enthalpy of vaporization measurements at higher pressures, and particularly in the vicinity of the critical point are also seen to be necessary.

d) Propane

A compilation of the thermodynamic properties of propane including an extensive bibliography has been presented by Kuloor et al. [135]. A temperature-pressure-enthalpy table has since been prepared by Yesavage [284] making extensive use of his own excellent calorimetric data from -240°F to +300°F and upto 2000 psia. Ernst et al. [72,73] have also reported low pressure Cp measurements upto 14 kg/cm^3. The

estimated accuracy of the data is better than 0.5% in each case.

e) Methane-Ethane

i) Bibliographies and Experimental Data. A bibliography of the thermophysical properties of mixtures containing methane, prepared by the Cryogenics Data Center [53], contains a list of the data sources relevant to this system. Clark et al. [48] have defined existing sources of experimental and correlated thermodynamic data on a series of P-T plots. Michels and Nederbragt [173] have obtained excellent volumetric data on four mixtures ranging from 20 to 80 mole percent ethane from 0°C to 50°C and upto 60 atm., including some data in the two phase region. Sage and Lacey [231] have also reported volumetric measurements on several mixtures extending from 70°F to 460°F and upto 3000 psia. Morlet [181] has measured liquid densities at -183°C and 1 atm. throughout the composition range, and concluded that there was negligible volume change on mixing under these conditions. Interaction second virial coefficient data extending from 298.15 to 373.15K have recently been obtained by Dantzler et al. [59].

In what must be considered as the most extensive investigation of this system, Bloomer and co-workers [25] have obtained P-V-T-x data for mixtures ranging from 15 to 70 mole % ethane between 140K and 300K, and from saturation conditions upto 300 atm. The critical locus, and the dew and bubble point temperatures above 100 psia were also determined for mixtures containing between 2.5 and 95% ethane. Phase equilibria data were also obtained by Price and Kobayashi [207] from -200°F to +50°F at pressures above 100 psia, by Ruhemann [229] from 5 to 20 atm. between 143K and 236K, and by Levitskaya [156] from 30 to 40 atm., and between 177K and 188K. The agreement between the data of Price et al. and Bloomer et al. is good. The data of Ruhemann are, however, seriously inconsistent with the results of Bloomer et al. particularly near the critical region [70]. Wichterle and Kobayashi [276] have recently obtained additional phase equilibria measurements to supplement the earlier work of Price and Kobayashi.

Adiabatic Joule-Thomson data accurate to $\pm$ 3% were obtained by Budenholzer, Sage, and Lacey [34] for mixtures containing between 23 and 76 mole percent ethane over the range 70°F to 300°F, and

upto 100 atm. More recently, the variation in the enthalpy of the gaseous phase as a function of pressure was investigated for three well spaced mixtures containing from 26 to 77 mole percent ethane by Alkasab [4], over the temperature range from -59°F to +35°F and for pressures upto 950 psia by isothermal and adiabatic flow calorimetry. The estimated accuracy of the results is better than 1.5%.

ii) Compilations of Thermodynamic Properties. Sage and Lacey [232] have derived thermodynamic properties including the enthalpy departures for the methane-ethane system using principally their own volumetric measurements. The tabulated compressibility factors at 70°F were since found by Berry and Sage [21] to be inconsistent with the more accurate results of Bloomer et al. [25] by as much as 10%, in some cases. Houser and Weber [109] have prepared an enthalpy composition diagram for saturated liquid mixtures using the data of Bloomer et al. [25] in conjunction with the BWR equation of state and a graphical procedure for differentiating mixture enthalpies. The authors have indicated some of the deficiencies of their technique which suggest that an appreciable loss of accuracy occurs in the transformation. Alkasab [4] has prepared an enthalpy diagram over the limited range of the measurements obtained for each mixture investigated.

iii) Conclusions. The existing data and the correlated enthalpies for this system have been closely examined, as it was originally intended to use these results to define the binary interaction parameters for the methane-ethane system for later use in predicting the enthalpy of the ternary methane-ethane-propane mixture. It was concluded that the existing compilations, with the possible exception of the results of Alkasab, cannot provide enthalpy values that are comparable either in accuracy or extent to those obtained from direct calorimetric measurements at the TPFL at the University of Michigan.

f) Ethane-Propane

The experimental measurements for this system upto 1963 are

summarized in a bibliography by the American Petroleum Institute [5,6]. Considerable effort has been directed towards the determination of the phase equilibria. Price and Kobayashi [207] have reported measurements at 0°F and 50°F respectively. Matschke and Thodos [169] have obtained data at higher temperatures along isotherms between 100°F and 200°F and from 200 psia upto the critical pressure. Special emphasis was placed in specifying the vapor-liquid equilibria in the critical region. These measurements are complemented by the low temperature data of Djordjevich [63] extending from -230°F to 0°F, and from 0.1 mm Hg to 218 psia. The reported equilibrium compositions at 0°F and 100 psia are in agreement with the results of Price and Kobayashi to within 2%.

Volumetric measurements on this system are scarce, and are limited to the saturated liquid density data of Shana'a and Canfield [239] at -165°F, for mixtures containing 27% to 81% ethane, and to the gas phase second interaction virial coefficient determinations of Dantzler et al. [59] from 298.15K to 373.15K. Direct calorimetric measurements have not as yet been attempted. The absence of experimental or correlated enthalpy data for the system suggests that its investigation at the present facility would be necessary to establish the required binary interaction parameters for the prediction of the enthalpy behaviour of the ternary mixture.

g) Methane-Propane

The thermodynamic properties of this system have been extensively reviewed by Mather [168] and later by Yesavage [284], with special emphasis on thermal properties and phase behaviour. Of particular interest to this work is the vast body of isobaric, isothermal, and isenthalpic flow calorimetric measurements on five mixtures containing 94.9, 88.3, 72.0, 49.4 and 23.4 mole percent methane respectively, over the temperature range from -240°F upto 300°F and from 100 psia to 2000 psia obtained in a series of investigations [162,168,284] at this facility. In each case, P-T-H diagrams were constructed for the individual mixtures over the range of the data, and including the two phase region. Smoothed values of Cp, ϕ and μ are also reported at conditions appropriate to the operating mode of the calorimeters

at the facility. In addition, a temperature-enthalpy diagram was constructed for the 94.9% mixture [22] as already explained in the Introduction.

Recent measurements not covered by previous reviews include the phase equilibria data of Wichterle and Kobayashi [276] from -225°F to 75°F and between 500 psia and the cricondenbar, the saturated liquid density data of Shana'a and Canfield [239] at -165°F, and the second interaction virial coefficient measurements of Dantzler et al. [59] from 298.15K to 373.15K.

It appears that the interpretation of the existing enthalpy data may be sufficient to define the necessary methane-propane binary interaction parameters. Consequently, no further investigation of this system is planned in this work.

h) Methane-Ethane-Propane

The phase equilibria for the system have been investigated in depth by Price and Kobayashi [207] to cover the range from -200°F to 50°F and upwards of 100 psia. Recently Wichterle and Kobayashi [276] have obtained additional measurements from -59.5°F to 115°F and upto 725 psia. Rutherford [230] has determined the location of the liquid-vapor phase boundaries for the system as a function of composition and pressure at 110°F. Adler et al. [1] and Chueh and Prausnitz [47] have correlated the data of Price and Kobayashi using the Redlich-Kwong equation, the interaction constants for which were defined from constituent binary vapor-liquid equilibria data. The correlations differ primarily in the algebraic form of the function used to represent the activity coefficients in the liquid phase as a function of composition.

Liquid density measurements at -161°C and -182°C have been reported by Morlet [181] for mixtures containing 5 and 10 mole percent propane, and varying amounts of other components. It was noted that while the three components were completely miscible at these temperatures, the further addition of butane could lead to the formation of two liquid phases. Very accurate measurements were also reported for two ternary mixtures at -165°C by Shana'a and Canfield [239]. Both investigations confirm that the assumption of ideal mixing at the indicated

temperature can provide better estimates of ternary mixture densities than the principle of congruence. Direct thermal property measurements are virtually unknown with the exception of some unpublished data obtained at CB & I [138] using a boil off calorimeter. The investigation was concentrated in the range - 240°F to +125°F and upto 50 psia, although some measurements were obtained at higher pressures upto 500 psia.

i) Recent Calorimetric Measurements on Other Systems of Interest

A wide variety of calorimetric measurements on many classes of substances have been presented at the First International Conference on Calorimetry and Thermodynamics at Warsaw (1969) and suggests that the use of flow calorimetry for the direct determination of thermal properties is becoming increasingly popular. Balaban [9,10] has used the heat exchanger method for the determination of Cp ratios for nitrogen in the range -20°C to +60°C and upto 2000 psia, for trifluoromethane from 22°C to 60°C upto and slightly beyond the critical density, and also for two mixtures composed of these components. Bishnoi [24] has used a similar technique for nitrogen in the range 60 to 150°C and upto 2250 psia, and for two binary mixtures of methane and carbon dioxide containing 14.5% and 42.5% methane respectively from 40°C to 150°C with an estimated accuracy of better than 1%. Jacobsen and Barieau [114] have developed a double heat exchanger method to determine the heat capacity of a single phase helium-nitrogen mixture at room temperature and upto 300 atm. in terms of the heat capacity of the pure components at the same conditions. A heat exchange flow calorimeter that measures the energy used to cool natural gases by monitoring the rate of vaporization of liquid nitrogen has been designed by Laverman and Selkukoglu [139]. The device operates at temperatures from 100°F to -310°F and upto 2800 psia and measures isobaric enthalpy changes within $\pm$ 1%.

Francis, McGlashan and Wormald [83] have developed a vapor flow calorimeter with adjustable throttle for the measurement of $(dH/dP)_T$. The authors report experimental results for benzene below 1 atm. over the range 330K to 403K. These low pressure measurements were processed to yield values of the temperature derivative of the second virial

coefficient using the thermodynamic relation

$$\left(\frac{dH}{dP}\right)_{T,\ P\to o} = \frac{d(B/T)}{dT} \qquad \text{(II-1)}$$

where B is the second virial coefficient.

The recent resurgence of interest in the heat of mixing can, in part, be ascribed to the need for measurements that are particularly sensitive to mixture theories. A complete review of such data is beyond the scope of this work. An important contribution is due to Monk and Wadso [180] who constructed a flow calorimeter for the measurement of both exothermic and endothermic heats of mixing, which was improved later by Goodwin and Newsham [90] to permit rapid measurements. Hejmadi [100] has recently developed and tested an outstanding flow calorimetric facility for measurements in the gaseous phase upto 1000 psia. The systems investigated include nitrogen-carbon dioxide, nitrogen-ethane, and nitrogen-oxygen with a reported accuracy of better than 2%. The flow calorimeter of McGlashan and Stoeckli [160] and the isothermal displacement calorimeter of Marsh, Stokes and co-workers [78], which directly measures the partial molal enthalpy of mixing of infinite dilution are some of the other noteworthy developments.

Other measurements from existing facilities include the Cp data of Ernst and Busser [73] at pressures upto 14 kg/cm^3 for propane, i-butane, and a number of fluoro and chloro substituted methanes from 20°C to 80°C. Maurer [170] has added a throttling calorimeter to the facility at Karlsruhe and obtained Cp and μ data on propylene to accuracies of 0.1% and 0.5% respectively from 25 to 125°C and upto 120 bars including the critical region. These results are in good agreement with the tabulations of Michels et al. [175] derived from P-V-T data. Subramanian, Kao, and Lee [259] have made a number of thermodynamic and transport property measurements on natural gas mixtures including phase equilibria, isobaric, and isothermal calorimetric determinations over the range -240°F to +200°F.

Chapter III

SELECTION OF A METHOD FOR REPRESENTING AND PREDICTING PURE COMPONENT ENTHALPIES

The first step in attempting to predict multicomponent enthalpies from constituent pure component and binary data is to select a framework for representing the constituent pure component data which has in large measure the desirable attributes of being concise, accurate, wide ranging, and universal. This section evaluates several schemes of both theoretical and empirical origin with special emphasis on the principle of corresponding states. The theoretical counterparts of empirical corresponding states schemes are stressed to enhance our insight into such techniques.

A) Equations of State - Theoretical

Although classical thermodynamics is a powerful tool in establishing the connection between different equilibrium properties, it cannot of itself determine why a particular property should have a certain numerical value at some fixed temperature and pressure, or how equilibrium property measurements on one fluid can be used to calculate those of another. If the dynamics of a real system can be accurately described at the microscopic level by molecular physics, then, statistical thermodynamics permits this information to be scaled up to yield a macroscopic description of the same system. In the initial stages, the engineering applications of statistical thermodynamics were primarily restricted to the prediction of intramolecular properties, i.e., the properties of isolated non-interacting molecules. More recently, the discipline is being actively applied towards the calculation of configurational properties, i.e., the properties that depend only on the interaction between two or more molecules. Some of these developments are discussed below.

i) The Gas Phase. One of the earliest, and perhaps the best known applications of statistical mechanics to the calculation of configurational properties is provided by the virial equation of state which expresses the compressibility z as a power series expansion

in inverse volume about the ideal gas

$$z = \frac{PV}{NkT} = 1 + \frac{B(T)}{V} + \frac{C(T)}{V^2} + \frac{D(T)}{V^3} + \ldots. \qquad \text{(III-1)}$$

where k is the Boltzman constant; and the coefficients B,C,D etc. of the expansion terms are only functions of temperature. Thermal properties may be calculated from Equation (III-1) using the equilibrium property interrelationships of classical thermodynamics. The isothermal throttling coefficient, and the heat capacity departure have been expressed to the first and second order terms respectively in inverse volume [158,167] as

$$\left(\frac{dH}{dP}\right)_T = -(B-TB')+[2B^2-2TBB'-2C+TC'-\frac{RT^2}{Cp^\circ}B''(B-TB')]\frac{1}{V} \qquad \text{(III-1a)}$$

$$Cp-Cp^\circ = \left(\frac{-RT^2B''}{V}\right) + R[(B-TB')^2-C+TC'-\frac{1}{2}T^2C'']\frac{1}{(V^2+2BV)} \qquad \text{(III-1b)}$$

where $B' = dB/dT$, $B'' = d^2B/dT^2$

$C' = dC/dT$, $C'' = d^2C/dT^2$

The statistical mechanical derivation of the virial equation [167] establishes its applicability to any non-ionized gas, polar or nonpolar. Essentially, the interaction between N bodies is expressed as a series of interactions involving a progressively increasing number of molecules. The second and third virial coefficients B and C, for example, represent deviations from ideality for two and three body interactions, respectively. The virial coefficients can be empirically obtained using wide ranging compressibility data on a given substance, or else, they may, in principle, be calculated from statistical mechanics if the intermolecular forces can be specified. Thus, the second virial coefficient for interactions between spherically symmetric molecules can be rigorously obtained [167] as

$$B = -\frac{N}{2}\int_0^\infty \left[1 - \exp(-u_{ij}(r)/kT)\right] 4\pi r^2 dr \qquad \text{(III-2)}$$

where $u_{ij}(r)$ is the intermolecular pair potential between molecules i and j, separated by a distance r. The calculation of higher order

virial coefficients is obtained in similar fashion [167], but requires the intermolecular potential between three and more molecules to be first specified. This is a difficult problem, and mathematically tractable results in such cases are obtained by making the assumption of pairwise additivity, which requires the intermolecular energy of any arbitrary configuration to be further simplified so as to be expressed as a sum of pair potentials

$$u(\vec{r}_1 \ldots \vec{r}_N) = \sum_{i>j} u_{ij}(r) \qquad \text{(III-3)}$$

ii) Determination of the Pair-Potential Function. From a purely phenomenological standpoint, the fact that gases condense to liquids suggests that intermolecular forces must be attractive at large separations, at least in the average sense. On the other hand, the fact that liquids resist compression indicates that forces at small separation must be repulsive and probably steeply so. In spite of considerable advances with respect to the nature of intermolecular forces in real substances [107,111], the stipulation of the pair potential function from a priori quantum mechanical calculations of the interactions between the electron shells of a given molecular pair is again an intractable problem for all but the simplest molecules such as hydrogen.

Mason and Spurling [167] discuss efforts to obtain $u_{ij}(r)$ from second virial coefficient data by inversion of Equation (III-2), and have also found them to be unsuccessful. The failure of such direct approaches have led to the common procedure of specifying a microscopic model, i.e., a mathematical expression for the potential energy as a function of interaction distance with undetermined constants, then calculating some macroscopic property (usually the second virial coefficient) in terms of these constants, and lastly specifying these constants by optimizing the agreement with experimental measurements on the same macroscopic property. The model thus determined can then be tested for its ability to predict other properties such as:
1) Second virial coefficients in a different temperature range

2) Third virial coefficients
3) Transport coefficients of dilute gases (coefficients of viscosity, thermal conductivity, diffusion, and thermal diffusion)
4) Crystal properties (such as lattice spacing, heat of sublimation, mechanical constants).

Perhaps the simplest model which attributes both a size and an attractive force to molecules is the square well potential shown in Figure III-1a. This consists of a hard core of diameter σ surrounded by an attractive potential well of depth ε, which specifies the minimum energy corresponding to the equilibrium separation, and extends from σ to g σ:

$$\begin{aligned} u(r) &= \infty && r < \sigma \\ u(r) &= -\varepsilon && \sigma < r < g\,\sigma \\ u(r) &= 0 && r > g\,\sigma \end{aligned} \qquad \text{(III-4)}$$

For this simple case, the second virial coefficient is obtained from Equation (III-2) as

$$B(T) = \frac{2\pi N}{3}\sigma^3[1 - (g^3 - 1)(e^{\varepsilon/kT} - 1)] \qquad \text{(III-4a)}$$

A more generally useful model which includes the effect of repulsive forces is the Mie potential (Figure III-1b) given by

$$u(r) = \frac{m}{m-n}\left(\frac{m}{n}\right)^{\frac{n}{m-n}} \varepsilon\left[\left(\frac{\sigma}{r}\right)^m - \left(\frac{\sigma}{r}\right)^n\right] \qquad \text{(III-5)}$$

where m and n are the exponents on the repulsive and attractive terms, respectively. Here σ is the distance parameter corresponding to the intermolecular separation when the potential energy is zero as sketched in Figure (III-1b). Quantum mechanical calculations lead to the value n=6 for the principle attractive Van der Waal potential contribution for non-polar spherical molecules [153]. For the repulsion, it is found empirically that m=12 corresponds reasonably well with the actual molecular repulsion for rare gas atoms [167]. For this special case, Equation (III-5) reduces to the well known Lennard-Jones 6-12 potential function. The second virial coefficient for this potential function is known to reproduce the principal

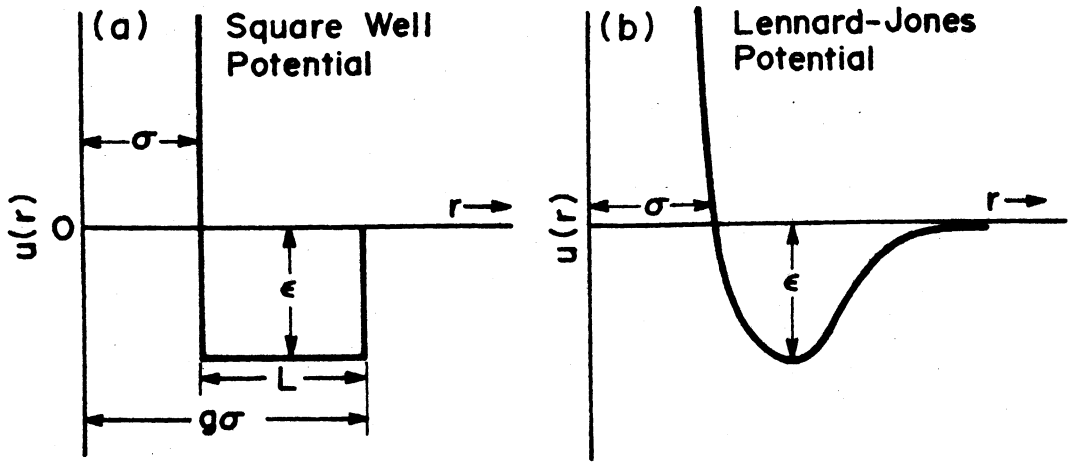

Figure III-1. Simple Models for Representing Intermolecular Forces Between Real Fluids.

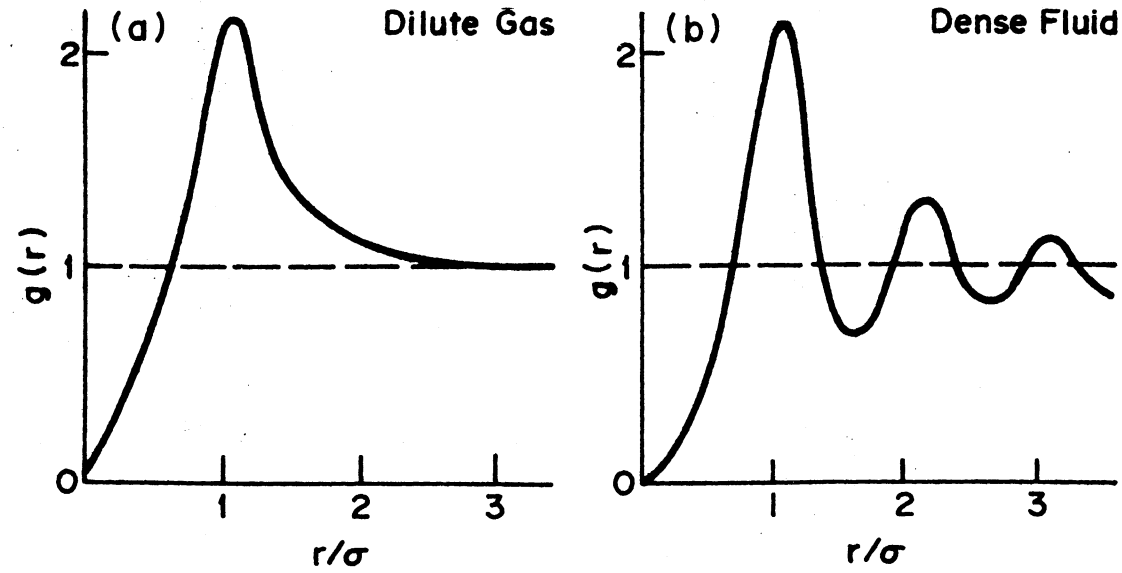

Figure III-2. The Radial Distribution Function for Real Fluids - Schematic.

features of experimental data for non-polar molecules over a wide temperature range, and accounts for its popularity. Computations on higher order virial coefficients upto the fifth are available, but the calculations even with high speed computing machines become progressively more difficult [167].

iii) Dense Fluid Theories. The poor convergence of the virial equation in the dense fluid region and its inability to account for the liquid-vapor phase transition has led to an alternative approach that uses the precise description of the spatial distribution of molecules for the purpose of constructing a statistical theory of matter. An important quantity in this connection is the pair distribution function which is defined as the deviation from randomness in the probability of finding two molecules simultaneously in two specified volume elements. The deviation from randomness is, of course, caused by the potential field between the molecules themselves. For spherically symmetric systems it is more convenient to use the radial distribution function $g(r)$ which is the factor by which the "local density" $\rho g(r)$ at r deviates from the bulk density ρ.

Figure III-2 shows the typical behaviour of $g(r)$ as a function of the distance r from a central molecule in the dilute gas and the liquid region for the potential specified. At large separations, the interaction between molecules is feeble, and consequently $g(r)$ approaches unity.
approaches unity. For non-interacting molecules, i.e., for an ideal gas $g(r)$ is unity everywhere. If a molecule of diameter σ is impenetrable, then no other molecules would be observed at $r < \sigma$ and consequently $g(r)$ approaches zero in this range. We can also expect $g(r)$ to rise as $u(r)$ becomes negative, reaching a maximum at the position of minimum energy, i.e., at the base of the potential well which is the position of maximum stability. For close packed impenetrable molecules in the liquid phase, $g(r)$ can be expected to show damped oscillations about one molecular diameter apart. Unlike the potential function $u(r)$, $g(r)$ varies also with temperature and density.

Although the radial distribution function is a measure of fluid

structure, it is primarily of interest in statistical mechanics because the thermodynamic functions of the fluid can be expressed in terms of it. In particular, the configurational energy $\tilde{U}$, the configurational heat capacity at constant volume $\tilde{C}v$, and the equation of state for spherically symmetric molecules are respectively given by

$$\tilde{U} = \frac{1}{2}\frac{N^2}{V}\int_0^\infty u(r)\, g(r,\rho,T)\, 4\pi r^2 dr \qquad \text{(III-6)}$$

$$\tilde{C}v = \frac{1}{2}\frac{N^2}{V}\int_0^\infty u(r)\, \frac{\partial[g(r,\rho,T)]}{\partial T}\, 4\pi r^2 dr \qquad \text{(III-7)}$$

$$\frac{PV}{NkT} = 1 - \frac{1}{6}\frac{N}{kTV}\int_0^\infty r\, \frac{d[u(r)]}{dr}\, g(r,\rho,T)\, 4\pi r^2 dr \qquad \text{(III-8)}$$

The proofs of Equations (III-6) and (III-8) are lucidly derived by Hill [105], and Reed and Gubbins [212] and are exact for spherical molecules with pairwise additivity. More general expressions including orientation effects are also indicated by Hill, but their complexity has prohibited their use in practical calculations. In addition to Equation (III-8), there is another independent equation which relates the equation of state to the pair distribution function and is given by [212]

$$kT\left[\frac{d(1/V)}{dP}\right] - 1 = \frac{N^2}{V}\int_0^\infty [g(r,\rho,T) - 1]\, 4\pi r^2 dr \qquad \text{(III-9)}$$

This equation is termed the "compressibility" equation. Given the assumption of pariwise additivity, the consistency between the results obtained from the two equations is a measure of the correctness of the estimated value of $g(r,\rho,T)$ for the specified potential function. If $g(r)$ is characterized by short range order, as in liquids, then we can expect the integrals in the above equations to converge rapidly, in contrast to convergence problems exhibited in the application of the virial equation to dense fluids.

iv) Determination of the Radial Distribution Function. Even if the constants ε and σ for some specified potential function $u(r)$ have been obtained, for example, from second virial coefficient data, the calculation of thermodynamic properties in the dense fluid requires

an accurate estimate of the radial distribution function; a quantity that itself varies with distance, density and temperature. Although this is a task of prohibitive difficulty, there are basically three techniques used for estimating g(r).

1) Computer Techniques: If the pair potential is specified precisely, then g(r) can be obtained by a computer simulation of a model assembly. In the molecular dynamics technique prescribed by Alder and co-workers [2,3], the detailed trajectories of an artificial system of a small number of particles, usually from 30 to 500, are calculated by the numerical solution of the equations of motion for each particle. The molecular distribution is followed with time until a state of equilibrium with respect to both position and velocity is achieved. Thermodynamic properties such as U,T and P are found by computing mean values of the potential energy, kinetic energy and the mean momentum carried across a plane per unit time. The Monte Carlo technique is similar but instead involves an ensemble averaging process [222].

Extensive calculations of this kind have been made for hard spheres and for Lennard-Jones 6-12 molecules [2,3]. The reliability of such procedures is established by their excellent agreement (within 2%) with independently calculated virial coefficients for the hard sphere case [215]. The accuracy of the calculations for Lennard-Jones molecules are, at present, not sufficient to permit good estimates of the vapor pressure to be obtained [227]. Nevertheless, such calculations are valuable in assessing the validity of various approximations that must be made in order to compute macroscopic properties from microscopic situations using statistical mechanical techniques without encountering the inevitable uncertainty involved in applying such calculations to real systems for which the potential function is usually only approximately defined.

2) Experimental Measurements: X-rays or neutrons can be scattered in their passage through a fluid specimen creating a diffraction pattern which is the sum of interference effects from molecular pairs. The intensity of the scattering pattern is a function of the difference between the actual spatial ordering and a random distribution. The

quantitative relationships between the two have been summarized by Rowlinson [226]. An interesting feature of this approach is that it provides information on $g(r,\rho,T)$ for real systems, given pairwise additivity, without specifying $u(r)$, and in principle could suggest an alternate route for the evaluation of intermolecular potential parameters if some thermodynamic properties at the scattering conditions are also known. Mikolaj and Pings [176] have applied the technique to calculate $g(r)$ for argon in the liquid region. The extremes of the scattering angle range which contain the most information of fluid structure are difficult to explore quantitatively. Consequently, the accuracy of the scattering measurements is as yet not sufficient to provide reliable estimates of thermodynamic properties using this technique.

3) Approximation Techniques: In these techniques, the deviation from randomness between the positions of a central molecule A and another specified molecule B due to the action of a potential field is further divided into two parts, a direct influence $c(r,\rho,T)$ of A on B, and an indirect influence whereby molecule A influences the distribution of other molecules which in turn exert their influence on molecule B. The functions $c(r,\rho,T)$ and $g(r,\rho,T)$ can be defined in terms of one another by an integral identity whose discussion is beyond the scope of this work. The approximations involve the specification of an additional independent relationship between $c(r,\rho,T)$ and $g(r,\rho,T)$ in order that the distribution function may be evaluated. The accuracy of the approximations are judged by the consistency of the results obtained from Equations (III-8) and (III-9), respectively. The subject is examined in more detail by Rowlinson [225].

The most successful of these approximations from the standpoint of internal consistency and agreement with hard sphere machine calculations is the Percus-Yevick (PY) [191] approximation given by

$$\frac{c(r,\rho,T)}{g(r,\rho,T)} = \frac{[e^{-u(r)/kT} - 1]}{e^{-u(r)/kT}} \qquad \text{(III-10)}$$

Although the PY approximation yields an analytic solution for a system of hard spheres, its application to more realistic potentials cannot be accomplished without recourse to numerical methods. Furthermore, Rowlinson [227] indicates that at temperatures below the critical, there are densities for which no solution is obtained. O'Connell and Prausnitz [188] have reviewed thermodynamic property calculations on argon from several approximation techniques using the L-J 6-12 potential with parameters derived from second virial coefficient data and concluded that the PY results, though consistent, are not accurate. Furthermore, the uncertainty in the calculations themselves are reported to be as high as $\pm$ 4%. Such techniques are clearly not yet ready to serve as useable frameworks for the representation of the thermodynamic properties of real substances governed by complex intermolecular forces.

v) Perturbation Models. Computer simulation results now provide us with a good understanding of the behaviour of a hard sphere fluid. These results, in turn, have stimulated efforts to obtain accurate analytical formulations for the hard sphere equation of state. The best current approximation due to Carnahan and Starling [41] valid only for the fluid branch, is given by

$$z^{HS} = \frac{1 + \xi + \xi^2 - \xi^3}{(1 - \xi)^3} \qquad \text{(III-11)}$$

where ξ is the volume density given by $\frac{1}{6} \pi \rho N \sigma^3$, and serves as a measure of the reduced density. Recent efforts to overcome the calculation problems associated with more complex potentials have lead to the development of perturbation theories where a complicated potential is written as a sum of a simple potential (e.g. a hard sphere) for which g(r) and z are fairly well known, and a weak perturbing potential. The effects of the latter are approximated by averaging the perturbation over the known distribution function of the unperturbed assembly. For a first order perturbation about the hard sphere case, we can express this concept mathematically as [287]

$$\frac{A}{NkT} = \frac{A^{HS}}{NkT} + \frac{\pi\rho}{2kT} \int_{\sigma^{HS}}^{\infty} [u(r) - u^{HS}(r)]\, g^{HS}(r)\, 4\pi r^2 dr \qquad \text{(III-12)}$$

where A is the Helmholtz free energy for the given potential function, and the superscript HS applies to hard sphere properties. If for example, the perturbation potential has the form

$$u(r) - u^{HS}(r) = -\frac{3}{4\pi}\frac{a}{\gamma^3}\exp\left[\frac{\sigma^3 - r^3}{\gamma^3}\right] \qquad \text{(III-13)}$$

then the equation of state and the configurational energy are given by [120]

$$\frac{PV}{NkT} = \left(\frac{PV}{NkT}\right)^{HS} - a\frac{N}{VkT} \qquad \text{(III-14)}$$

$$U = \frac{N^2 a}{V} \qquad \text{(III-15)}$$

where $\left(\frac{PV}{NkT}\right)^{HS}$ can be obtained from Equation (III-11). If instead we express the hard sphere equation of state by the less accurate form

$$\left(\frac{PV}{NkT}\right)^{HS} = \frac{1}{1 - b\frac{N}{V}} \qquad \text{(III-16)}$$

then, Equation (III-14) realizes the well known Van der Waal equation of state where the excluded volume b equals $4\xi/N\rho$. In the hard sphere fluid, there is no distinction between liquid and vapor. The power of this technique is seen in the fact that if the hard spheres are placed in an attractive potential field of infinite range and infinitesmal depth as given by Equation (III-13), the resultant equation of state predicts, at least qualitatively, the behaviour of real fluids, Even more interesting is the fact that g(r) still remains only a function of density [120].

More complex schemes involving both repulsive and attractive perturbations, and including higher order expansion terms have been excellently reviewed by Mansoori and Canfield [163] and will not be pursued here. The most successful of these is due to Barker and Henderson [13,14]. Recognizing that a more accurate representation of the equation of state of real fluids would require a temperature dependence to be imposed on the distribution function, they ingeniously chose a reference system of hard spheres with temperature varying

diameters, and were able by this artifice to obtain rapid convergence of the perturbation series in the liquid phase.

Calculation of Thermodynamic Properties from Perturbation Models

Rogers and Prausnitz [219] investigated the ability of the Barker and Henderson perturbation model to represent the thermodynamic properties of spherically symmetric molecules such as methane, argon and neo-pentane. The three parameter Kihara pair potential

$$u(r) = 4\varepsilon \left[\left(\frac{\sigma-2a}{r-2a} \right)^{12} - \left(\frac{\sigma-2a}{r-2a} \right)^{6} \right] \quad r > 2a \qquad \text{(III-17)}$$

$$u(r) = \infty \qquad r \leq 2a \qquad \text{(III-17a)}$$

was chosen to represent the fluids on a microscopic level. The parameters ε, σ and a were obtained from the best fit to a broad spectrum of P,ρ,T data encompassing the saturated vapor, saturated liquid, critical, and supercritical regions. The pressures in all cases were fitted to an accuracy of 2% or better. Interestingly, the pure fluid Kihara parameters that produced the best fit to the thermodynamic data used by Rogers and Prausnitz in the perturbation framework were significantly different from those obtained by fitting wide ranging second virial coefficient data. In particular, the ε/k value used for methane varied accordingly from 204.15K to 227.13K. Consequently, it is highly unlikely that the perturbation model will yield accurate values of the second virial coefficient at reduced temperatures below 0.7, where the computed value of B becomes very sensitive to the precise value of ε/k.

A modified perturbation approach was used by Orentlicher and Prausnitz [189] to calculate the volumes and enthalpy departures for the cryogenic fluids A, CH_4, N_2, C_2H_6, CO_2, and C_3H_8. The pair interactions were governed by the L-J 6-12 potential with a hard sphere core of radius R. The distribution function for the potential was approximated as

$$g(r,\rho,T) = g^{HS}(r,\rho) \qquad r < R \qquad \text{(III-18)}$$

$$g(r,\rho,T) = [e^{-u(r)/kT}]\,[g^{HS}(r,\rho)] \quad r \geq R \qquad \text{(III-18a)}$$

A separation of the temperature and density dependance of g(r) was achieved in this manner. Furthermore, Equation (III-18a) gives the correct distribution functions for a hard core molecule in the limit of high temperature and in the limit of zero density. The functional form of the equation also provides a better approximation to the distribution functions of real liquids. To simplify computations, an analytic approximation for $g^{HS}(r,\rho)$ was made which was found to preclude the application of the technique to liquids at densities larger than those of saturated liquids at reduced temperatures below 0.8. Enthalpy and volumetric data in the liquid phase from 0.86 to 1.3Tr were simultaneously used to specify the potential parameters. The goodness of fit with respect to the enthalpy departure varied from 2 to 6%.

vi) Conclusions: The independent specification of the potential function is, and will continue to be, the chief stumbling block in making a priori calculations of thermodynamic properties. Although the application of theoretically based perturbation treatments to real spherically symmetric systems has made recent spectacular gains, it is clear that the best representation is obtained only by sacrificing some or all of the thermodynamic data in defining the potential parameters. From a practical engineering standpoint, these approaches should then be judged by their ability to compete with empirical equations of state with the same number of adjustable parameters. Even if such approaches were to be found superior for some spherically symmetric systems, more empirical methods will continue to be favored until such treatments can be extended to include more complex molecules with orientation dependent or polar intermolecular forces.

B) Equations of State - Empirical

The restriction of the theoretically attractive virial equation of state to the gas phase has led to many empirical efforts to obtain functional forms that ensure the concise representation of thermodynamic properties over the entire fluid region. The earliest

of these contained few adjustable parameters, and like the two parameter Van der Waal equation, are now beginning to find theoretical meaning which speaks well for the remarkable intuition of early workers in the field. More recent formulations involve an increased number of empirical parameters that serve mainly to improve the goodness of fit. If our goal is to choose a general framework for the representation of thermodynamic properties, our choice is confined to those equations that have been extensively used in correlating thermodynamic data.

The most popular form used in design calculations involving hydrocarbons is the eight parameter BWR equation of state [Equation (I-12)]. A compilation of the BWR parameters for 58 compounds has been tabulated by Cooper and Goldfranck [50]. The constants for most equations of state including the BWR are usually derived from volumetric data. If our primary concern is the representation of pure component enthalpies, then for reasons already discussed in Chapter I, we must further restrict ourselves to the examination of equations which represent the PVT surface very precisely. Comparisons made by Yesavage [284] on light hydrocarbons, including propane, have established the inadequacy of the original BWR for representing enthalpies in the liquid phase at low reduced temperatures.

A recent modification of the BWR equation by Starling [251,254] expressed in the form

$$P = RT\rho + \left(B_o RT - A_o - \frac{C_o}{T^2} + \frac{D_o}{T^3} - \frac{E_o}{T^4}\right)\rho^2 + \left(bRT - a - \frac{d}{T}\right)\rho^3 + \left(a + \frac{d}{T}\right)\alpha\rho^6 + \frac{c\rho^3}{T^2}\left[(1+\gamma\rho^2)e^{-\gamma\rho^2}\right] \qquad \text{(III-19)}$$

has been successful in overcoming some of the deficiencies of the original version. The terms involving D_o and E_o in the coefficient of ρ^2 serve to improve the prediction of the second virial coefficient at low temperature. The other extra constant d improves the performance of the equation in the critical region. The expressions for thermal properties as derived from the above equation are presented in Appendix H-1. Simultaneous regression on volumetric and enthalpy data for methane and propane over the liquid, gaseous and dense fluid regions yielded a fit of about 0.9 Btu/lb in the enthalpy departure and 0.44% in the density, upto a reduced density of 2.0. At very low reduced

temperatures, the error in the prediction of the enthalpy departure can, however, be as high as 4%.

In a recent review of the state of the art, Martin [165] offers the sobering opinion that only limited objectives may be accomplished with complex empirical equations of state. Even the best of these wide ranging equations can rarely if ever be applied beyond 2.3 times the critical density. Even though more extensively applicable formulations can be expected to appear in the near future, the necessity for recalculating the equation of state constants for all substances of interest to obtain the maximum advantage of new developments as they occur would be an unavoidably cumbersome task.

C) The Principle of Corresponding States.

i) Theoretical Basis - Two Parameter Theory: Difficulties in the a priori calculation of thermodynamic properties and the time consuming effort required to incorporate thermodynamic measurements into equations of state suggest that it might be easier to attempt to deduce the thermodynamic properties of a given species from the experimental results obtained on another similar substance. Pitzer [193] showed from statistical mechanical considerations that if a class of substances were to satisfy the following requirements:

1) The Hamiltonian of the system, i.e., the sum of the potential and kinetic energy of any arbitrary molecular configuration, is separable into a contribution from the internal degrees of freedom of the molecules, (e.g., the vibration in the case of nitrogen,) depending only on their internal coordinates and momenta, and a configurational contribution depending only on the coordinates and momenta of the centres of mass of the molecules.
2) The configurational contribution above can be treated by the methods of classical statistical mechanics.
3) The intermolecular potentials for all substances are conformal, i.e., the potentials for all substances in the class can be expressed in the form

$$u(\vec{r}_1,\vec{r}_2,\vec{r}_3 \ldots \vec{r}_n) = \varepsilon f\left(\frac{r_{12}}{\sigma},\frac{r_{13}}{\sigma}, \ldots \frac{r_{23}}{\sigma},\frac{r_{24}}{\sigma}, \ldots\ldots \frac{r_{nn}}{\sigma}\right) \qquad \text{(III-20)}$$

where f is a universal function whose exact nature need not be explicitly specified and n is the number of molecules involved. Then, the equation of state for all substances in the class can be expressed as

$$z = h\left(\frac{kT}{\varepsilon}, \frac{V}{N\sigma^3}\right) \qquad \text{(III-21)}$$

where h is a universal function.

If the state of a reference substance in the class is represented by a PVT surface, then the states of all other conformal substances are represented by geometrically similar surfaces in which the axes of volume and temperature are multiplied by the ratios $\frac{\sigma^3}{\sigma_{oo}}_3$ and $\frac{\varepsilon}{\varepsilon_{oo}}$ respectively, where the subscript oo applies to the properties of the reference substance. It follows that all characteristic points on the surface such as the solid, liquid and gas at the triple point and the fluid at the critical point have values of P,V, and T in the ratio of these scale factors. Consequently, ε/k and $N\sigma^3$ may be substituted by the macroscopically determined parameters Tc and Vc to yield [212]

$$z = h\left(\frac{T}{Tc}, \frac{V}{Vc}\right) \qquad \text{(III-22)}$$

$$\text{or} \quad z = h'\left(\frac{T}{Tc}, \frac{P}{Pc}\right) \qquad \text{(III-22a)}$$

if Pc is instead used as the reducing parameter. The equations are an expression of the principle of corresponding states and have been widely used by engineers in predicting thermodynamic properties of a reference fluid.

ii) Extended Corresponding States Theory: Experimental verification of the two parameter principle is spectacular for the rare gases argon, xenon and krypton [188,226]. The principle is applicable to a somewhat lesser degree of accuracy if nitrogen, carbon monoxide, oxygen and methane are included in the family [195,198]. In the case of n-alkanes, for example, as one departs from the critical point, the reduced vapor pressure curve shifts away from that for the

simple fluids. At a given reduced temperature, the reduced vapor pressure for a chain molecule such as n-heptane is less than that for a spherical molecule like methane. (See Figure III-3). Such departures from strict two parameter theory have also been observed for other configurational properties [195,226].

Cook and Rowlinson [49] have attempted to explain such departures for both non-spherical and polar molecules from theoretical considerations. In order to define the magnitude of such effects relative to the spherically symmetric case, they were forced to further restrict the development to a specific molecular model chosen, for convenience, to be the Lennard-Jones 6-12 potential. The effect of orientation, for example, was incorporated into the potential function now defined in terms of additional angular coordinates $\vec{\theta}$ to yield

$$u(r,\vec{\theta}) = 4\varepsilon[(\frac{\sigma}{r})^{12} - (\frac{\sigma}{r})^{6}(1 + af(\vec{\theta}))] \qquad \text{(III-23)}$$

where a is a constant for each species with a value of zero for the unperturbed spherically symmetric case, and $f(\vec{\theta})$ represents the orientation dependence of the attractive forces. For simplicity, the repulsive forces were kept unchanged. The potential function was then integrated over all orientations yielding the expression

$$u(r,T) = 4\varepsilon[(\frac{\sigma}{r})^{12}(1-2a^2\overline{f}^2\frac{\varepsilon}{kT}) - (\frac{\sigma}{r})^{6}] \qquad \text{(III-24)}$$

where $\overline{f}^2$ is the weighted average value of $f(\vec{\theta})$ over all angles. If a parameter δ is now defined such that

$$\delta(T) = a^2\overline{f}^2\varepsilon/kT \qquad \text{(III-25)}$$

then we obtain

$$u(r,T) = 4\varepsilon[(\frac{\sigma}{r})^{12}(1 - 2\delta(T)) - (\frac{\sigma}{r})^{6}] \qquad \text{(III-25a)}$$

The net effect of orientation forces is such that the resultant potential is still conformal with the original potential for symmetric molecules but is now also a function of temperature. The maximum

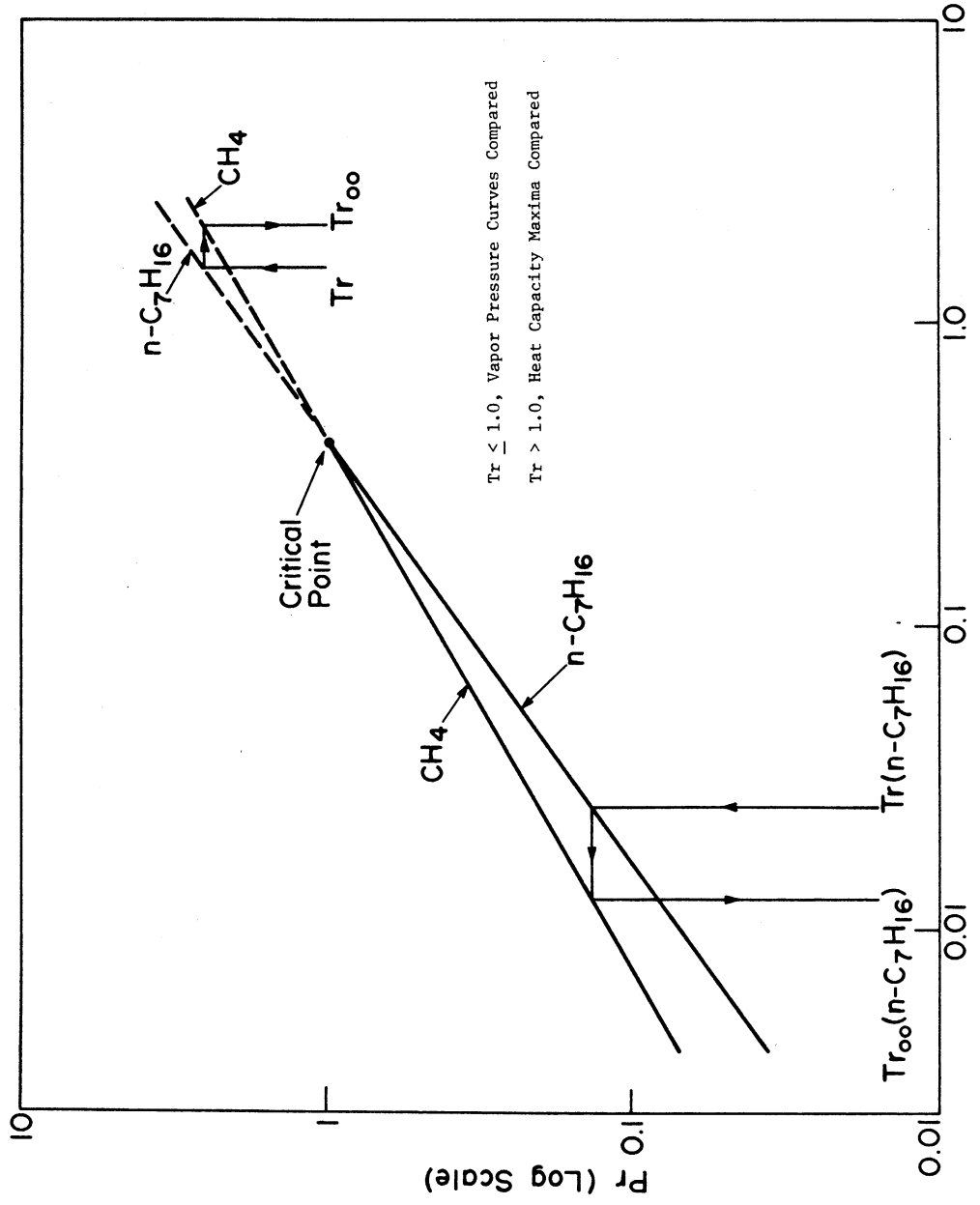

Figure III-3. Effect of Non-Central Forces on the Reduced Vapor Pressure Curve.

depth ε_e, and the collison diameter σ_e were found to be given by

$$\varepsilon_e/\varepsilon_{oo} = 1 + 2\delta(T) \qquad \text{(III-26)}$$

$$\sigma_e/\sigma_{oo} = 1 - \delta(T) \qquad \text{(III-27)}$$

where the subscript oo denotes a molecule whose potential is obtained from Equation (III-23) by putting a=0. The equation of state was then given by

$$\Phi\,[P(1+3\delta),\ V(1-\delta),\ T(1+2\delta)] = \Phi_{oo}[P,V,T] \qquad \text{(III-28)}$$

The equation of state of the asymmetric species was later [223] expressed as a first order perturbation about that of the reference symmetric species by the relation

$$z(Tr,\rho r) = z_{oo}(Tr,\rho r) - \delta c\,[\,\frac{1 - Tr}{Tr}\,][2Tr\,(\,\frac{\partial z_{oo}}{\partial Tr}\,)_{\rho r} + \rho r(\,\frac{\partial z_{oo}}{\partial \rho r}\,)_{Tr}\,] \qquad \text{(III-28a)}$$

where δc is the value of δ at the critical point. It may be noted that the perturbation term is required to change sign at Tr=1 regardless of the reduced density ρr.

The most important consequence of this approach is that the thermodynamic properties of asymmetric molecules can, for some limiting cases, be obtained from those of symmetric molecules by using temperature dependent scale factors. Similar conclusions were reached for dipolar molecules. A significant drawback of this approach is that it still requires the critical compressibility factor zc to remain unchanged, unlike the situation for real fluids. In fact, zc varies from 0.291 for methane to 0.269 for hexane. Brown [32] has suggested that such changes could be predicted by the theory if non-central repulsive forces were also considered. Nevertheless, the theory in its original form has been tested for a variety of substances including the n-alkanes upto n-butane using $\delta(Tc)$ as the correlating the parameter [226]. The calculated value of $\delta(Tc)$ from a variety of measurements, including the reduced vapor pressure, liquid density, entropy of vaporization, and the configurational heat capacity

was fairly constant. The parameter $\delta(Tc)$ was found to be related to the slope of the reduced vapor pressure curve, or the Riedel [216] parameter αc by the expression

$$\alpha c = \left(\frac{d \ln Pr}{d \ln Tr}\right)_{Tr \to 1} = \alpha c_{oo} + 11.8\, \delta(Tc) \qquad \text{(III-29)}$$

where αc_{oo} is the corresponding value for the spherically symmetric system.

It would be presumptuous to expect that such simplified perturbation models are applicable to all systems of interest. A more general approach would require the introduction of additional dimensionless groups involving dipolar moments, quadruple moments, non-isotropic polarizabilities which encompass the orientation effects due to dispersion forces, quantum corrections, and molecular association into the equation of state given by Equation (III-21). The specific contribution of each additional term could then, at least in principle, be ascertained from experimental measurements on the thermodynamic properties and the dimensionless perturbation variables for groups of substances where such effects are separately present. As indicated by Leland et al. [144] in an excellent review of the corresponding states principle, the current state of the extent and accuracy of such measurements precludes the semi-empirical formulation of such an universal approach. Even if such measurements were available, it is not clear whether the predictions would be successful for molecules where two or more of these perturbation effects are coupled.

iii) Empirical Extensions of the Corresponding States Principle:

1) The Pitzer-Riedel Three Parameter Principle: Empirical efforts to universalize the two parameter principle have centered around the use of macroscopically determined parameters to serve as a measure of the deviation from the principle. From a physical standpoint, such parameters represent the lumped contribution of non-central forces relative to those in symmetric molecules such as argon and krypton. Considerable success has been obtained by both Pitzer and co-workers [195,198] and Riedel [217] in representing a

a class of substances called "normal fluids" by this approach. Included in this category are the spherically symmetric molecules Ar, Kr, etc., the n-alkanes, and other hydrocarbons. If β and β_{oo} are the values of the third parameter for the actual and reference substance, respectively, then the reduced configurational properties of "normal" fluids are expressed in terms of those for a simple fluid using the perturbation parameter $(\beta - \beta_{oo})$ as the expansion variable. For the reduced enthalpy departure, one obtains

$$\frac{H-H^\circ}{RTc}(Tr,Pr) = \left[\frac{H-H^\circ}{RTc}(Tr,Pr)\right]_{oo} + (\beta-\beta_{oo})\left\{\frac{d\left[\frac{H-H^\circ}{RTc}(Tr,Pr)\right]}{d\beta}\right\}_{oo} + \ldots \qquad \text{(III-30)}$$

Pitzer relied on the differences in the reduced vapor pressure curve for pure substances at 0.7Tc to define the third parameter ω given by

$$\omega = [-1 - \log_{10} Pr]_{Tr = 0.7} \qquad \text{(III-31)}$$

As ω is approximately zero for the spherically symmetric inert gases, it was justifiably called the "acentric factor." Riedel worked with the parameter αc instead, defined from measured values of the slope of the reduced vapor pressure curve at the critical point. The two parameters are related through the reduced empirical three parameter vapor pressure equation of Riedel [216], which yields [226]

$$\omega = 0.203\,(\alpha c - 7.00) + 0.242 \qquad \text{(III-32)}$$

The linear relationship between ω and αc implies that the two procedures are essentially interchangeable. The excellent intuition behind these empirical approaches is seen from the fact that the value of Rowlinson's perturbation parameter defined from a consideration of orientation effects is, at the critical point, linearly related to the empirical parameter $(\alpha c - \alpha c_{oo})$ as indicated in Equation (III-29).

One important difference between the theoretical approach of Cook and Rowlinson and the above empirical efforts is that the reduction or scale factors used in the latter case do not vary with

temperature. In the region between the reduced saturation curves for two substances differing significantly in αc values, (e.g. methane and n-heptane as shown schematically in Figure III-3) serious errors occur in the calculated values of the thermodynamic properties of the asymmetric molecule as its phase differs from that of the symmetric reference under the same reduced conditions. Pitzer and co-workers [195] recognized the problem, and extrapolated the reference fluid properties in each phase, so that once the phase of the asymmetric fluid was correctly identified by an independently obtained reduced three parameter vapor pressure equation, major calculation errors could be avoided. In a broader sense, the conformal mapping of two points, i.e. the critical points, in a corresponding states correlation does not ensure that other characteristic locii in the fluid, such as the vapor pressure curve, the Joule-Thomson inversion curve, $[(\partial H/\partial P)_T = 0]$, the Boyle curve $[(\partial z/\partial P)_T = 0]$, the Amagat curve $[(\partial z/\partial V)_P = 0]$, or the heat capacity maxima

$$\left[\left\{ \frac{\partial (Cp - Cp^\circ)}{\partial T} \right\}_P = 0, \text{ or } \left(\frac{\partial Cp}{\partial P} \right)_T = 0 \right]$$

will be simultaneously matched.

2) The Shape Factor Approach of Leland: Leland and co-workers [140] formulated an alternate empirical approach that closely follows the theoretical treatment of Rowlinson. There is no deviation term as in Equation (III-29) which incorporates differences in the reduced dependent variable or configurational property at the same Tr and Pr. Instead, the critical parameters are modified by multiplicative temperature and density dependent "shape factor" corrections to generate the desired configurational properties from the unperturbed framework alone. If at least two or more measured configurational properties of a given fluid are compared with that of the reference fluid, and the corresponding reduced temperatures and pressures which yield identical values of the reduced properties so examined, are obtained, then the "shape" modifiers to Tc and Vc for the given fluid may be uniquely determined as functions of temperature and volume relative to the reference fluid case. Such

factors were determined for selected fluids by the process just described and then used to develop empirical correlations that defined these factors for other fluids as functions of reduced temperature and pressure in terms of additional parameters such as the acentric factor ω. A drawback of this approach is that the physical correspondence between characteristic points in the PVT surface for any two fluids is lost. For example, at the critical point, the reduced enthalpy departure for propane is greater than that for a symmetric molecule such as methane [284]. Consequently, the shape factors for propane relative to methane will be different from unity if a methane reference table is used.

3) The Powers Generalized Correlation (PGC): The Powers Generalized Correlation [204] has the attractive attributes of both of the above approaches. Firstly, it involves a modification to the independent variable Tr somewhat like the route taken by Leland and coworkers, and secondly, the dependent variable i.e. the reduced configurational property of the fluid, is expressed in terms of the corresponding reduced property of the reference fluid and a perturbation term much like the approaches of Pitzer and Riedel. More importantly, the method seeks to maintain conformality at a singular point, i.e. the critical point, and along other selected locii.

The technique was originally devised explicity for the calculation of thermal properties. Consequently, the most desirable locus for conformal mapping is one across which thermal property variations are most severe. The vapor pressure curve upto the critical temperature, and the locus of the heat capacity maxima, $(\partial Cp/\partial P)_T=0$, in the supercritical region admirably meet this criterion. In practice, the locus of $(\partial Cp/\partial T)_P = 0$ was used instead, as there are considerably more experimental determinations of the latter obtained principally at the Thermal Properties of Fluids Laboratory at the University of Michigan [49,161,162,168,284]. However, unlike the locus of the maxima at constant temperature, the locus of $(\partial Cp/\partial T)_P = 0$ is not a true configurational property characteristic of the fluid if Cp° also varies with temperature. It does, however, serve as a good approximation to another true configurational locus, $\left[\frac{d(Cp-Cp^\circ)}{dT}\right]_P=0$, for some distance beyond the

critical temperature [245] and may be used as an acceptable replacement until more precise measurements permit the true configurational locii to be defined. The reduced coordinates used in the technique are given by (τ, Pr) where

$$\tau = \ln Pr_s(Tr,\alpha c\ldots) \quad Tr \leq 1.0 \tag{III-33}$$

$$\tau = \ln Pr_M(Tr,\alpha c\ldots) \quad Tr > 1.0 \tag{III-33a}$$

where the subscript s stands for the vapor pressure curve, and the subscript M applies to the locus of $(\partial Cp/\partial T)_p=0$. Defined in another way, the actual reduced temperature Tr of a substance is modified to another value designated as Tr_{oo}, such that the reduced saturation pressure Pr_s $(Tr \leq 1)$, or the reduced pressure at the heat capacity maximum Pr_M $(Tr > 1)$ for the given fluid at Tr is the same as that for an archetypical reference fluid at Tr_{oo} (See Figure III-3).

The reduced enthalpy departure for any substance is expressed in terms of that for a reference fluid by the relation

$$(Tr,Pr,\alpha c) = \mathcal{H}_{oo}\,(Tr,Pr,\alpha c_{oo}) + \left[\frac{\partial \mathcal{H}}{\partial \alpha c}\,(Tr,Pr,\alpha c_{oo})\right]\left[\alpha c - \alpha c_{oo}\right] \tag{III-34}$$

where the subscript oo applies to the properties of the reference fluid, and $\mathcal{H}$ is defined as

$$\mathcal{H} = \frac{H - H^\circ + \Delta H^\nu}{(Hc - H^\circ)_{Tr=1,\ Pr=1}}, \quad \Delta H^\nu = 0 \text{ in the vapor phase} \tag{III-35}$$

where $(Hc - H^\circ)$ is the enthalpy departure at the critical point and ΔH^ν is the enthalpy of vaporization at τ or Tr_{oo}. The incorporation of the enthalpy of vaporization permits a more accurate correlation of the relatively small effect involved in the isothermal variation of enthalpy with pressure in the liquid phase without having to contend with the large masking effect associated with a phase change. A special feature of the technique lies in the fact that the dependent variable $\mathcal{H}$ is also defined to be unity at the critical point.

A potential disadvantage of the procedure is that it requires the vapor pressure, the locus of heat capacity maxima along isobars, and

the enthalpy departure at the critical point to be first established for the fluid in question. However, if the value of the Riedel parameter αc is known, then excellent approximations to the desired information may be obtained. The vapor pressure curve may be adequately expressed by the empirical equation of Riedel [175] as

$$\log Pr_s = -\Phi(Tr) - (\alpha c - 7)\,\Psi(Tr) \qquad \text{(III-36)}$$

where

$$\Phi(Tr) = 0.118\,\Theta(Tr) - 7 \log Tr \qquad \text{(III-36a)}$$
$$\Psi(Tr) = 0.0364\,\Theta(Tr) - \log Tr \qquad \text{(III-36b)}$$
$$\Theta(Tr) = 36/Tr + 42 \log Tr - 35 - Tr^6 \qquad \text{(III-36c)}$$

The locus of the desired heat capacity maxima can be expressed as

$$\ln Pr_M = \alpha c \ln Tr \qquad Tr > 1.0 \qquad \text{(III-37)}$$

and the value of $(Hc - H°)$ may be described by the relation

$$\frac{Hc - H°}{RTc} = 1.5113 + 0.5081\,(\alpha c - 3.750) \qquad \text{(III-38)}$$

The empirical relations expressed by Equations (III-37) and (III-38) were obtained principally from an examination of the accumulated measurements at the calorimetric facility of the University of Michigan [202].

4) The Representation of the Reference Functions in Corresponding States Correlations: A major factor that determines the success of such techniques is the accuracy with which the equation of state for the reference substance can be specified, and it is here that the techniques differ in their original implementation. Pitzer and Curl [195] determined enthalpy departures for the reference fluid and the slope term by graphical processing of smoothed compressibilities, whereas Leland and coworkers [80,81,144] used as their reference, an empirical equation of state for methane based on precise volumetric

data. Powers [204], however, made direct use of smoothed precise calorimetric data to establish the reference function and the slope term in tabular form. The calorimetric measurements on methane and propane obtained by Jones [119] and Yesavage [284], respectively, were weighted heavily in defining these functions. Propane was also particularly attractive as the enthalpy values in the liquid phase were obtained down to a Tr value of about 0.3, which is lower than the reduced triple point temperature for most substances. Recent extensions of the acentric factor approach by Greenkorn and Chao [91], and the shape factor approach by Fisher and Leland [81] to low reduced temperatures have also featured enthalpy tabulations in the liquid phase obtained from the calorimetric measurements at the University of Michigan. Johnson and Colver [118] directly fitted the Starling BWR equation to the methane and propane enthalpy data and used these results to define the two reduced enthalpy functions [Equation (III-30] in the Pitzer framework. The approach follows that of Yesavage [284], but replaces his reference tables with equations of state.

5) The Reduced Virial Equation of State: If we set for ourselves the more limited objective of restricting our predictions to the gas phase alone, then the reduced virial equation represented by

$$z = 1 + \frac{B/Vc}{Vr} + \frac{C/Vc^2}{Vr^2} \ldots. \qquad \text{(III-39)}$$

must be considered as an attractive vehicle for the corresponding state principle in view of its theoretical roots. If this equation is to be implemented, then generalized correlations for the reduced virial coefficients B/Vc, C/Vc^2, etc., as a function of Tr, and a third parameter to account for asymmetric effects if necessary, must be developed.

The most popular reduced second virial coefficient correlations are those of Pitzer and Curl [196] and McGlashan and Potter [159]. In the former case, the correlation uses the acentric factor and is expressed as

$$Br = \frac{B}{RTc/Pc} = Br_{oo} + Br_1\omega \qquad \text{(III-40)}$$

where

$$Br_{oo} = 0.1445 - 0.330/Tr - 0.1385/Tr^2 - 0.0121/Tr^3 \qquad \text{(III-41)}$$

$$Br_1 = 0.073 + 46/Tr - 0.5/Tr^2 - 0.097/Tr^3 - 0.073/Tr^8 \qquad \text{(III-42)}$$

and is restricted to "normal" fluids over the range $0.5 \leq Tr \leq 6.0$. Although the equation is generally considered to be very reliable, the predictions are about 8% too negative for ethane at 215K when compared with the apparently precise measurements of Hoover et al. [108], and about 5% too negative at 110.83K for methane when compared with the precise measurement of Byrne et al. [35].

The correlation of McGlashan and Potter [159] developed specifically for n-alkanes is given by

$$\frac{B}{Vc} = 0.430 - \frac{0.886}{Tr} - \frac{0.694}{Tr^2} - \frac{0.0375\ (n-1)}{Tr^{4.5}} \qquad \text{(III-43)}$$

where n is the number of carbon atoms in the molecule. The value of n has been related to αc by the empirical expression [202]

$$n = 23.257 - 9.763\ \alpha c + 1.0203\ \alpha c^2 \qquad \text{(III-43a)}$$

The authors suggest that the equation is valid over the range $0.5 \leq Tr \leq 6.0$. An analysis of the methane and propane data by Hecht and Donth [99] indicates that the B/Vc curves for the two substances cross each other at a Tr value slightly higher than unity. A similar result can also be seen in Figure (V-1) if the solid curve for methane is compared with the dashed line for propane. This behaviour is also in substantial agreement with Rowlinson's [222,223] theory which requires the differences between the reduced configurational properties of the reference and perturbed system to change sign at a Tr value of 1.0. A glance at Equation (III-43) indicates that B/Vc for propane will always be more negative than that for methane, and suggests that its functional form is not optimally suited to the representation of wide ranging measurements. The apparent deficiences of these equations underscore, at least for the present, the necessity of developing improved correlations for the reduced second virial coefficient.

Chueh and Prausnitz [45] have correlated the third virial coefficient for a number of substances including argon, ethane, neo-pentane, n-octane and benzene over the region $0.8 \leq Tr \leq 4.0$ using the relation

$$\frac{C}{Vc^2} = \left[\frac{0.232}{Tr^{0.25}} + \frac{0.468}{Tr^5}\right]\left[1 - e^{(1-1.89Tr^2)}\right] + de^{-(2.49 + 2.30Tr + 2.70Tr^2)} \qquad \text{(III-44)}$$

where C is the third virial coefficient and d is an empirically determined parameter that has a value of zero for argon. It may be expressed in terms of αc by the approximate relation

$$d = 2.2\,(\alpha c - 5.78) \qquad \text{(III-44a)}$$

as empirically noted in this work.

Generalized empirical correlations for higher order virial coefficients are unavailable as the accuracy of the volumetric measurements necessary for the precise calculation of such quantities is beyond the range of most previous investigations. However, truncation at the third virial coefficient will permit reliable calculations of the compressibility and the enthalpy departure upto 0.8 and 0.5 times the critical density, respectively. The range of applicability increases somewhat beyond the critical temperature. Gunn et al. [96] have recently added dimensionless coefficients to the cubic and quartic terms in the virial equation but have cautioned that these are not true higher order virial coefficients.

D) Comparison Studies of Enthalpy Prediction Methods for Pure Non-polar Fluids: Comparison studies of various correlations against accurate smoothed enthalpy measurements can serve as an invaluable aid in assessing their performance relative to one another. Such techniques are constantly being refined as new data become available, and consequently only the latest comparisons present an accurate picture of their abilities. Starling et al. [253] have recently made comprehensive investigation of eight correlations used in the natural gas industry against the accurate wide ranging enthalpy data for the pure components investigated at the TPFL. The correlations were also

compared with enthalpy measurements for n-pentane, n-hexene and n-octane from other sources [149,150]. All but two of the methods investigated involve the corresponding states principle in some form, and include most of the techniques discussed in this section with the notable exception of the reduced virial equation. The Powers Generalized Correlation (PGC) was unquestionably superior to the rest for the case of light hydrocarbons upto propane and nitrogen, producing a fit of better than 0.5 Btu/lb with respect to the enthalpy departure. This result is not surprising because these data were heavily involved in the development of the correlation itself. For the systems n-pentane through n-octane, the lowest mean deviation of 1.95 Btu/lb was obtained for the Rice Properties III correlation of Fisher and Leland [81], perhaps, because they use n-pentane as their reference for compounds that are heavier than n-butane. The PGC deviations were only slightly worse at 2.13 Btu/lb. The authors of the comparison study suggested that inaccuracies in the measurements could be responsible for the higher deviations obtained for the heavier systems.

F) Conclusion

The considerations in this chapter lead us to conclude that the PGC is the most accurate practical framework that we could use to represent the enthalpies of the pure substances methane, ethane, and propane that constitute the ternary mixture whose enthalpies we seek to predict in this work.

Chapter IV
SELECTION OF A METHOD FOR REPRESENTING AND PREDICTING MIXTURE ENTHALPIES

In Chapter III, the PGC was selected as the most desirable framework for representing pure component enthalpies for non-polar compounds that fall under the category of "normal" fluids as specified by Pitzer [195,198]. The next step in predicting multicomponent mixture enthalpies from constitutent pure component and binary data, is to select a framework that permits the concise and accurate representation of the enthalpies of mixtures of "normal" fluids over the entire fluid phase. The discussion in this section parallels the approach of the previous chapter. First, the specific benefits obtained by applying the virial equation of state to mixtures in the gas phase are summarized. The extension of pure component dense fluid theories, discussed in Chapter III, to mixtures is then examined.

Because the PGC is eminently suitable and convenient for representing the thermodynamic properties of pure non-polar substances over a wide range of conditions, one is immediately tempted to use it as a starting point for the representation of mixtures of such substances. Before accepting the empirical extension of the framework to mixtures, it is desirable to establish, at least in theory, the precise circumstances that permit the application of the pure component corresponding states principle to mixtures.

The theory of conformal solutions is first briefly discussed. Next, procedures for estimating the unlike pair interaction parameters for conformal molecules are briefly described. Various corresponding states models that issue from the basic theory are noted. Several prescriptions or "mixing rules" for calculating the pseudoparameters of any given mixture as a function of the conformal pair interaction parameters and the composition are outlined. In particular, the theoretical restrictions peculiar to the empirically popular Van der Waal mixing rules are examined. The performance of various mixing rules are compared against the results obtained for a variety of thermodynamic data on both real and artificial systems to determine which of the approximations is the most realistic. The entire

presentation upto this point is primarily restricted to the two parameter theory because the theoretical studies in the literature have been confined mainly to this case alone.

The discussion then proceeds to the examination of the three parameter corresponding states principle. Empirical justification for applying the theory to non-polar mixtures is first presented, and the macroscopic equivalents of some theoretical mixing rules discussed earlier in the chapter are noted. Additional empirically successful rules including one for the third parameter are also discussed. Finally, the results of comparison studies on various enthalpy prediction techniques using mixture enthalpy data are used to select the best framework for representing mixture enthalpies.

The Application of the Virial Equation of State to Mixtures in the Gas Phase

The prediction of the thermodynamic properties of multicomponent systems from pure component and constituent binary data is most rigorously accomplished for the special case of the virial equation of state but is restricted to mixtures in the gaseous phase only. It can be shown from statistical mechanics [167] that the mixture virial coefficients can be expressed as a function of the constituent pure component and unlike multi-body interaction terms. In particular, the second and third mixture virial coefficients B_m and C_m are respectively given by

$$(B_m)_T = \sum_{i=1}^{n} \sum_{j=1}^{n} x_i x_j (B_{ij})_T \qquad \text{(IV-1)}$$

$$(C_m)_T = \sum_{i=1}^{n} \sum_{j=1}^{n} \sum_{k=1}^{n} x_i x_j x_k (C_{ijk})_T \qquad \text{(IV-2)}$$

where B_{ij} and C_{ijk} are the second and third virial coefficients for the i-j and the i-j-k interactions, respectively. If B_{ii} and B_{jj} are known at any given temperature for a mixture of two components i and j of known composition, and if B_m is measured at the same temperature for the same mixture, then Equation (IV-1) permits B_{ij} to be calculated at the same temperature. This result in turn characterizes the value of B_m for all binary mixtures of i and j at that temperature. If the interaction virial coefficients are so determined for all binary pairs of a multicomponent mixture at temperature T, then Equation (IV-1) permits the rigorous calculation of B_m for the multicomponent mixture

from binary data alone. Similarly, the characterization of the nth virial coefficient as a function of composition at a fixed temperature for a given binary mixture requires experimental measurements of the nth virial coefficient for the two pure components and for (n-1) mixtures at the same temperature. This technique has been applied by Douslin [65] to characterize the second, third and fourth virial coefficients of methane-tetrafluoromethane mixtures, but such precise comprehensive measurements are rare.

If the potential function for all pair interactions in a mixture can somehow be adequately specified, then the interactions parameters for all pair interactions, including the like and unlike pairs, may be obtained by fitting Equation (III-2) to experimental B_{ij} data for all i,j. Once all constituent pair parameters are thus specified, it is possible to calculate higher order virial coefficients with the usual assumption of pairwise additivity [167]. The importance of the interaction second virial coefficient must not be under-estimated, as the dilute gas is the only region in the entire fluid phase where the theoretically rigorous definition of the parameters for any specified unlike pair potential function is possible.

Dense Fluid Theoretical Results

The unsuitability of the virial equation for the dense fluid makes it desirable to use the mixture analogues of Equations (III-6) and (III-8) instead in such cases. With the usual assumption of pairwise additivity, the configurational energy $\tilde{U}_m$, and the equation of state for a mixture of spherically symmetric molecules are respectively expressed as [212]

$$\tilde{U}_m = \frac{N^2}{2V_m} \sum_{i=1}^{n} \sum_{j=1}^{n} x_i x_j \int_0^{\infty} u_{ij}(r,\rho,T,[\varepsilon],[\sigma],[x])\, 4\pi r^2 dr \qquad \text{(IV-3)}$$

$$\left(1 - \frac{PV_m}{NkT}\right) = 1 - \frac{1}{6}\frac{N}{kTV} \sum_{i=1}^{n} \sum_{j=1}^{n} x_i x_j \int_0^{\infty} u_{ij}(r) g_{ij}(r,\rho,T,[\varepsilon],[\sigma],[x])\, 4\pi r^2 dr \qquad \text{(IV-4)}$$

where $u_{ij}(r)$ and $g_{ij}(r)$ are the pair potential and the radial distribution function, respectively, for the i-j interaction, and $[\varepsilon]$ and $[\sigma]$ are pair energy and volume parameter arrays, respectively, and [x] is the composition array for the mixture.

The first requirement in the application of Equations (IV-3) and (IV-4) to real fluid mixtures is the specification of a reasonable model for all possible pair potentials in the given mixture. This may be difficultly accomplished for unlike pair interactions in complex mixtures if the constituent like pair interactions are found to subscribe to different molecular models. Nevertheless, assuming all $u_{ij}(r)$ can be specified, all $g_{ij}(r)$ must be next determined. The statistical mechanical problem involving the evaluation of $g_{ij}(r)$ in mixtures is much more formidable than in the pure component case, because it is now not only a function of r and ε_{ij}/kT, but also of the number density ρ_i of each component (or equivalently, the overall mixture density and the mole fraction of each species), and the relative magnitudes of the size and energy parameters for the various molecular species in the given mixture. One simplifying approach, parallel to that used for real pure components, is the express real fluid mixture properties as perturbations about simpler artificial mixed systems which can be more tractably treated.

Perturbation Techniques

Most efforts in correlating the thermodynamic properties of real fluid mixtures using perturbation approaches have centered around the description of the equation of state and the distribution function of a mixture of hard spheres. Many of these attempts have been discussed by Reed and Gubbins [212], and Mansoori and Canfield [163]. The perturbation approach for pure components exemplified by Equation (III-12) may now be extended to the calculation of thermodynamic properties using the hard sphere mixture as the reference fluid. One of the simplest of such models involves the extension of Equation (III-14) to mixtures to yield

$$z = z_m^{HS} - \frac{a_m N}{kTV_m} \qquad \text{(IV-5)}$$

Lebowitz [141] has obtained an analytic solution of the P-Y equation for hard sphere mixtures. The P-Y compressibility equation result is given by

$$z_m^{HS} = \frac{1}{\gamma_o}\left[\frac{\gamma_o}{1-\xi} + \frac{3\gamma_1\gamma_2}{(1-\xi)^2} + \frac{3\gamma_2^3}{(1-\xi)^3}\right] \qquad \text{(IV-6)}$$

where $\gamma_i = \frac{1}{6}\pi \sum_{k=1}^{n} \rho_k \sigma_k^i$

An improved analytic form for z_m^{HS} obtained by combining the P-Y pressure and compressibility equation results has been recently developed by Mansoori and Leland [164]. Their results were in good agreement with the molecular dynamics calculation of Alder [2,3] for mixtures of hard spheres with diameters in the ratio 3:1. The mixture perturbation constant a_m is given by the relation

$$a_m = \sum_i \sum_j x_i x_j a_{ij} \qquad \text{(IV-7)}$$

Recent work [98] has suggested that any single component that subscribes to the equation of state given by Equation (III-14), will yield Equation (IV-7) for multicomponent systems if the model is generalized in a consistent manner.

Equation (IV-7) is, however, an empirical equation of long standing first suggested by Van der Waals. In fact, if in Equation (IV-5), we substitute z_m^{HS} by the relatively crude approximation

$$z_m^{HS} = \frac{1}{1 - \sum_i \sum_j x_i x_j b_{ij} \frac{N}{V_m}} \qquad \text{(IV-8)}$$

where b_{ij} is the covolume encountered before in Equation (III-16), then we obtain the original multicomponent Van der Waal equation of state.

Snider and Herrington [248] have used the equation of state expressed by Equations (IV-5), (IV-6) and (IV-7) to correlate the excess properties of mixtures of spherically symmetric non-polar substances in the liquid phase with considerable success. Their results are analyzed in greater detail at a later stage. Rogers and Prausnitz [219] extended their perturbation model representation of the thermodynamic properties of argon, methane and neo-pentane as discussed in Chapter III to the representation of the vapor-liquid equilibria, critical properties and saturated liquid and vapor densities for the system argon-neopentane at 50°C from 40 to 253 atm., and for the system methane-neopentane

at 25°C from 20 to 156 atm. The calculated results were found to give excellent (within 2%) agreement with experimental data. It must, however, be noted that the energy parameter ε_{ij} for the unlike pair interaction was in each case adjusted to provide the best fit to the data. These results are significant, because they establish for the first time that highly non-random mixtures, i.e, with pure component critical temperature and volume ratios as high as 2.8 and 4.0 respectively, can be successfully treated by theoretically based approaches. These methods are all the more attractive because such calculations can be extended to multicomponent mixtures using only constituent binary data to establish the appropriate unlike pair interaction parameters. There are, however, three important disadvantages to such approaches. Firstly, the theories are at present restricted in application to systems consisting of spherically symmetric molecules. Secondly, even in such cases, the applicability of the method to the entire fluid phase has not yet been demonstrated, and thirdly, as Rogers and Prausnitz [219] indicate, the calculations are very demanding of computer time.

Conformal Solutions

Before the recent breakthrough in describing the hard sphere equation of state, solution theories were developed which concentrated on the properties of pure real fluids as their starting point in an attempt to avoid the direct statistical mechanical calculation of mixture properties. Most of these theories assume as their first premise that the intermolecular pair potentials for all i-j interactions including those for the unlike species can be expressed in the form

$$u_{ij}(r) = \varepsilon_{ij} F\left(\frac{r}{\sigma_{ij}}\right) \qquad \text{(IV-9)}$$

where F is a universal dimensionless function applicable to all constituent pair interactions and ε_{ij} and σ_{ij} are the energy and size parameter, respectively, for the i-j pair interaction. Such mixtures were given the name "conformal solutions" by Longuet-Higgins [153].

In principle, it is easy to determine if the like pair interactions for real fluids subscribe to Equation (IV-9), by examining the

correspondence between their experimentally determined configurational properties using suitable experimentally determined reduction factors such as the critical temperature and the critical volume. The acquisition of similar experimental evidence for the unlike pair interaction is almost impossible as it requires the effect of the i-j interactions to be isolated from the unavoidable simultaneous effects of the i-i and j-j interactions. The equivalent critical parameter $Tc_{ij}(i\neq j)$, for example, cannot be defined from direct experimental critical measurements on mixtures. Fortunately, as indicated earlier in this chapter, the unlike pair interaction effect may be isolated from experimental measurements on mixture second virial coefficients alone, through Equation (IV-1).

If Equation (IV-9) is substituted into Equation (III-2), then one can construct the dimensionless relation

$$\frac{B_{ij}}{N_o\sigma_{ij}^3} = f_B\left(\frac{kT}{\varepsilon_{ij}}\right) \qquad \text{(IV-10)}$$

where

$$f_B = \int_0^\infty \{1 - \exp[-F(\tfrac{r}{\sigma})\tfrac{\varepsilon_{ij}}{kT}]\}\, 4\pi(\tfrac{r}{\sigma})^2\, d(\tfrac{r}{\sigma}) \qquad \text{(IV-10a)}$$

Consequently, one can examine the correspondence between reduced second virial coefficients $\frac{B}{N_o\sigma^3}$ in all cases as a function of $\frac{\varepsilon}{kT}$ to determine if the theory applies. A difficulty arises from the fact that ε_{ij} and σ_{ij} for the unlike pair must themselves be obtained from B_{ij} measurements.

If two substances are strictly conformal in a two parameter framework, then the ratio of their temperature and pressure coordinates for all uniquely identifiable characteristic conditions in the P-T plane will be invariant. In particular, the reduction factors for the configurational properties may be equivalently defined from any other characteristic condition besides the critical point. The Boyle point located along the zero pressure axis and defined to be the point where the second virial coefficient has a zero value is one alternative where experimentally accessible parameters may be defined for the unlike pair interaction. Douslin [65] used the parameters Tb and Vb, where Tb is the Boyle temperature, and Vb is the Boyle volume defined by

$$Vb = \left(-T\frac{dB}{dT}\right)_{T=Tb} \qquad \text{(IV-11)}$$

to reduce the second virial coefficients of CH_4 and CF_4.

In practice, such specifically located measurements are rarely available, even for pure components, and consequently this technique has not found widespread use.

Approximation Techniques for Estimating Unlike Pair Interaction Parameters for Conformal Substances

In the absence of Boyle point data, it is necessary to use approximation techniques for the estimation of unlike pair parameters. The most commonly used combination rule for size is the arithmetic mean rule given by

$$\sigma_{ij} = (\sigma_{ii} + \sigma_{jj})/2 \qquad \text{(IV-12)}$$

The justification for the σ rule is simply by analogy with rigid spheres. The rules for ε_{ij} have a more complicated origin. The leading term in the London formula [152] for attractive dispersion forces is given by c'_{ij}/r^6 where c'_{ij} can be approximated by the relation

$$c'_{ij} = (c'_{ii}\, c'_{jj})^{1/2} \cdot \frac{2(I_{ii}I_{jj})^{1/2}}{I_{ii} + I_{jj}} \qquad \text{(IV-13)}$$

for spherically symmetric molecules [167]. I_{ii} and I_{jj} are the first ionization potentials for molecules i and j, and c'_{ii}, c'_{jj} are the corresponding pure component constants. The attractive part of any (n-6) potential is given by $\varepsilon_{ij}\left(\frac{\sigma_{ij}}{r}\right)^6$. If we equate this quantity to c'_{ij}, we obtain

$$\varepsilon_{ij} = (\varepsilon_{ii}\varepsilon_{jj})^{1/2} \left[\frac{\sigma_{ii}\,\sigma_{jj}}{\sigma_{ij}^2}\right]^3 \frac{2(I_{ii}I_{jj})^{1/2}}{I_{ii} + I_{jj}} \qquad \text{(IV-14)}$$

If the arithmetic mean rule [Equation (IV-12)] holds for σ_{ij}, then Equation (IV-14) requires that

$$\varepsilon_{ij} = k_{ij}(\varepsilon_{ii}\,\varepsilon_{jj})^{1/2}, \qquad k_{ij} \leq 1 \qquad \text{(IV-14a)}$$

This results from the fact that a geometric mean is always less than an arithmetic mean and the other factors in Equation (IV-14) are the ratio of geometric to arithmetic means. Leland [213] developed

the equation

$$\varepsilon_{ij} = (\varepsilon_{ii}\varepsilon_{jj})^{1/2} \frac{(\sigma_{ii}^3\sigma_{jj}^3)^{1/2}}{\sigma_{ij}^6} \qquad \text{(IV-15)}$$

as a simplification of Equation (IV-14). Mason and Spurling [167] have shown that if one starts with the Kirkwood-Mueller formula for c', one may obtain the rule

$$\varepsilon_{ij} = \left(\frac{2\varepsilon_{ii}\varepsilon_{jj}}{\varepsilon_{ii}+\varepsilon_{jj}}\right)\left(\frac{\sigma_{ii}\sigma_{jj}}{\sigma_{ij}}\right)^6 \left[\frac{(\varepsilon_{ii}+\varepsilon_{jj})\sigma_{ij}^6/\chi_{ii}\chi_{jj}}{\varepsilon_{ii}\sigma_{ii}^6/\chi_{ii}^2 + \varepsilon_{jj}\sigma_{jj}^6/\chi_{jj}^2}\right] \qquad \text{(IV-16)}$$

where χ is the diagmagnetic susceptibility. Procedures for calculating I and χ for pure components for use in Equations (IV-14) and (IV-16), respectively, have been demonstrated by Hirschfelder, Curtiss and Bird [107]. Pitzer [194] has tabulated the values of these constants for selected pure components. For molecules with similar values of σ and χ, Equation (IV-16) reduces to

$$\varepsilon_{ij} = \frac{2\,\varepsilon_{ii}\,\varepsilon_{jj}}{\varepsilon_{ii}+\varepsilon_{jj}} \qquad \text{(IV-16a)}$$

Although theory has suggested the form of these combination rules, the approximations made in obtaining usable recipes are so drastic that the rules may be considered semi-empirical at best.

In a two parameter framework, Equations (IV-12) may be expressed in terms of the equivalent macroscopic parameters Vc or RTc/Pc by the relations

$$Vc_{ij}^{1/3} = [Vc_{ii}^{1/3} + Vc_{jj}^{1/3}]/2 \qquad \text{(IV-17)}$$

or

$$\left(\frac{RTc_{ij}}{Pc_{ij}}\right)^{1/3} = \left[\left(\frac{RTc_{ii}}{Pc_{ii}}\right)^{1/3} + \left(\frac{RTc_{jj}}{Pc_{jj}}\right)^{1/3}\right]/2 \qquad \text{(IV-18)}$$

if one recognizes the proportionality between σ^3 and Vc or RTc/Pc. Similarly Equations (IV-14a),(IV-15) and (IV-16a) may be expressed in the forms

$$Tc_{ij} = k_{ij}(Tc_{ii}\,Tc_{jj})^{1/2}, \quad k_{ij} \leq 1 \qquad \text{(IV-19)}$$

$$Tc_{ij} = (Tc_{ii}\, Tc_{jj})^{1/2} \left(\frac{Vc_{ii}\, V_{jj}}{Vc_{ij}}\right)^{1/2} \qquad \text{(IV-19a)}$$

$$Tc_{ij} = 2\,\frac{Tc_{ii}\, Tc_{jj}}{Tc_{ii} + Tc_{jj}} \qquad \text{(IV-20)}$$

respectively. The advantage in using the macroscopic parameters Tc, and Vc instead of ε/k and σ^3 lies in the fact that they can be unequivocally defined for each pure component from experimental measurements without having to assign a specific molecular model for the conformal pair interactions.

If we assume that the i-i, the i-j, and the j-j interactions are mutually conformal, then we can, from the like pair second virial coefficient data, establish an empirical reduced function

$$\frac{B}{Vc} = f_B\left(\frac{T}{Tc}\right) \qquad \text{(IV-21)}$$

to fit the pure component results. If then, some B_{ij} data are available for $i \neq j$, the parameters Tc_{ij} and Vc_{ij} can be obtained by determining the best fit to the pure component function f_B. To ensure some degree of specificity in obtaining the parameters in this fashion, it is necessary to have accurate and wide ranging B_{ij} measurements. Nevertheless, this technique allows the extraction of two parameters from experimental measurements without requiring the potential function to be explicitly specified.

Corresponding States Formulations for Mixtures

Having investigated various means for specifying the parameters for all conformal pair interactions in a mixture, we are now in a position to examine the macroscopic consequences of these assumptions. First, a model for expressing the thermodynamic properties of a mixture in terms of the appropriate reduced pure component thermodynamic functions must be proposed, and next, a recipe for specifying the potential parameters for a mixture, if at all necessary, must be established in terms of the constituent pure component and interaction parameters so as to yield the best representation of the mixture properties in the specified framework.

All the developments described in this section require the same assumptions used in establishing the pure component corresponding states

model as described in Chapter III. The treatment of conformal solutions is, however, further restricted to pairwise additive interactions. The dimensionless argument used to derive the corresponding states principle for pure substances cannot be used for mixtures since the energy of an arbitrary molecular configuration will depend not only on the positions of the molecules, but also upon which chemical species is in each position. Therefore, unlike the pure component case, a variety of models can be proposed each of which makes a specific statement in regard to the distribution of molecules by species in a mixture.

The detailed examination in this work of the theoretical results for mixtures conformal in only two parameters requires some justification especially since the pure components for which we seek to apply such techniques require at least three parameters for an acceptable degree of correspondence. The problem lies in the fact that very little theoretical work has been accomplished for the three parameter framework. Furthermore, the current state of the art is such that the mixing rules for the two parameters common to both frameworks are the same. The one, two and three fluid corresponding state models are examined below. These models derive their names from the number of separate reduced conditions at which the dimensionless reference fluid configurational property function must be evaluated in order to specify completely the appropriate configurational property for a binary mixture.

a) The One Fluid Model

In this case, the mixture is assumed to be equivalent to a hypothetical pure component with temperature and density independent potential parameters ε_m and σ_m which yield the mixture configurational properties when used in some reference pure fluid configurational property framework. If the reference fluid parameters are ε_{oo} and σ_{oo}, respectively, then the configurational enthalpy $\tilde{H}_m$ of the mixture is given in terms of the reference fluid configurational enthalpy $\tilde{H}_{oo}$ by the relation

$$\tilde{H}_m(T,P,[x]) = \frac{\varepsilon_m}{\varepsilon_{oo}} \tilde{H}_{oo}\left(kT \frac{\varepsilon_{oo}}{\varepsilon_m}, P \frac{\varepsilon_{oo}}{\varepsilon_m} \frac{\sigma_m^3}{\sigma_{oo}^3}\right) \qquad \text{(IV-22)}$$

where $\tilde{H}_m(T,P,[x])$ is identical to the enthalpy departure with respect

to the ideal gas state. The excess thermodynamic properties of the mixture may also be expressed in terms of the configurational properties of the reference fluid. The excess enthalpy, for instance, is given by

$$H^E(T,P,[x]) = \frac{\varepsilon_m}{\varepsilon_{oo}} \bar{H}_{oo}\left(kT \frac{\varepsilon_{oo}}{\varepsilon_m}, P \frac{\varepsilon_{oo}\sigma_m^3}{\varepsilon_m \sigma_{oo}^3}\right) - \sum_{i=1}^{n} x_i \frac{\varepsilon_{ii}}{\varepsilon_{oo}} \bar{H}_{oo}\left(kT \frac{\varepsilon_{oo}}{\varepsilon_{ii}}, P \frac{\varepsilon_{oo}}{\varepsilon_{ii}} \frac{\sigma_{ii}^3}{\sigma_{oo}^3}\right) \qquad \text{(IV-23)}$$

and is obtained by combining Equations (IV-22) and (I-13) given the knowledge that H^E is zero in the ideal gas state.

This model represents the direct extension of the one fluid pure component corresponding states principle to mixtures. In independent investigations, Wojtowicz, Salsburg and Kirkwood [281], and Brown [31] determined from statistical mechanical considerations that the model was rigorously true only for solutions of conformal molecules in a condition of random mixing defined to occur when the potential energy of a mixture for each spatial configuration of molecules is the average over all assignments of the different species to all positions in proportion to the mole fraction. Mathematically

$$u_m(r) = \sum_{i}^{n} \sum_{j}^{n} x_i x_j \, u_{ij}(r) \qquad \text{(IV-24)}$$

where $u_{ij}(r)$ is the potential function for each i-j pair. It was also shown that if the molecules were of unequal size, the condition of random mixing required the conformal potentials to be further restricted to the Lennard-Jones p-q form with the mixture parameters ε_m and σ_m given by

$$\varepsilon_m \sigma_m^{\,p} = \sum_{i}^{n} \sum_{j}^{n} x_i x_j \, \varepsilon_{ij} \, \sigma_{ij}^{\,p} \qquad \text{(IV-25)}$$

$$\varepsilon_m \sigma_m^{\,q} = \sum_{i} \sum_{j} x_i x_j \, \varepsilon_{ij} \, \sigma_{ij}^{\,q}, \qquad q \neq p \qquad \text{(IV-26)}$$

The most commonly used values of p and q are 6 and 12 respectively. If we apply the model to a case where all ε_{ij}'s are approximately equal and q approaches infinity, then on dividing Equation (IV-26) by the size parameter for the largest molecule in the mixture, we obtain in the limiting case of infinitely hard repulsion ($q \to \infty$), the absurd

result that σ_m is equal to the size of the size of the largest molecule in the mixture even for vanishingly small concentrations of the largest species. This occurs because it is in fact unrealistic to assume that all configurations of a reference pure fluid are equally open to a mixture of small and large molecules. In particular, the replacement of a small molecule by a large one in an already close-packed configuration must lead to an overlapping of such molecules. If the repulsion between such molecules is assumed to be infinitely hard, then an infinite value will be obtained for the configurational energy of that assembly [226,227].

One Fluid Model - Generalized Van der Waal Mixing Rules

Leland, Rowlinson and Sather [147] proposed an alternate set of rules that were notably free from any explicit dependence on the potential function. The rules are given by the equations

$$\varepsilon_m \sigma_m^3 = \sum_i^n \sum_j^n x_i x_j \varepsilon_{ij} \sigma_{ij}^3 \qquad \text{(IV-27)}$$

$$\varepsilon_m^{1+\nu} \sigma_m^3 = \sum_i^n \sum_j^n x_i x_j \varepsilon_{ij}^{1+\nu} \sigma_{ij}^3 \qquad \text{(IV-28)}$$

where ν is a variable. For $\nu = 0$, the rules yield the simple results

$$\sigma_m^3 = \sum_i \sum_j x_i x_j \sigma_{ij}^3 \qquad \text{(IV-29)}$$

$$\varepsilon_m \sigma_m^3 = \sum_i \sum_j x_i x_j \varepsilon_{ij} \sigma_{ij}^3 \qquad \text{(IV-30)}$$

and are essentially those empirically deduced by Van der Waal in extending his equation of state to multicomponent systems. Hence, they are called the Van der Waal mixing rules.

We will now attempt to examine the specific restrictions imposed by these rules on the distribution of molecules by species. The application of the one fluid corresponding state theory to mixtures involves the additional assumption that the mixture can be replaced by a hypothetical pure component. The molecular interactions between these hypothetical molecules are also assumed to be conformal with potential fields for each i-j pair interaction. Thus

$$u_m(r) = \varepsilon_m F\left(\frac{r}{\sigma_m}\right) \tag{IV-31}$$

where ε_m and σ_m are the molecular parameters for the hypothetical pure components. We may then express the configurational energy for the mixture using the pure component energy equation [Equation (III-6)] expressed in terms of dimensionless distance. Thus

$$\tilde{U}_m = \frac{N^2}{2V} \varepsilon_m \sigma_m^3 \int_0^\infty F\left(\frac{r}{\sigma_m}\right) G^*_{oo}\left(\frac{r}{\sigma_m}, \frac{\varepsilon_m}{kT}, \xi_m\right) 4\pi\left(\frac{r}{\sigma_m}\right)^2 d\left(\frac{r}{\sigma_m}\right) \tag{IV-32}$$

where G^*_{oo} is the distribution function for the pure reference fluid expressed in terms of dimensionless distance, and ξ_m is the pseudo volume density $\frac{1}{6}\pi\rho_m N\sigma_m^3$ for the hypothetical fluid.

If the right hand side of Equation (IV-4) is also expressed in dimensionless form, and equated to Equation (IV-32), we obtain the result

$$\varepsilon_m\sigma_m^3 \int_0^\infty F\left(\frac{r}{\sigma_m}\right) G^*_{oo}\left(\frac{r}{\sigma_m}, \frac{\varepsilon_m}{kT}, \xi_m\right) 4\pi\left(\frac{r}{\sigma_m}\right)^2 d\left(\frac{r}{\sigma_m}\right) = \sum_{i=1}^{n}\sum_{j=1}^{n} x_i x_j \varepsilon_{ij}\sigma_{ij}^3 \int_0^\infty F\left(\frac{r}{\sigma_{ij}}\right) g^*_{ij}\left(\frac{r}{\sigma_{ij}}, \rho, T, [\varepsilon], [\sigma], [x]\right) 4\pi\left(\frac{r}{\sigma_{ij}}\right)^2 d\left(\frac{r}{\sigma_{ij}}\right) \tag{IV-33}$$

If we define the integral on the left hand side by $I_{oo}\left(\frac{\varepsilon_m}{kT}, \xi_m\right)$ and each of the integrals on the right hand side by $I_{ij}\ (\rho, T, [\varepsilon], [\sigma], [x])$, we obtain

$$\varepsilon_m\sigma_m^3 I_{oo}\left(\frac{\varepsilon_m}{kT}, \xi_m\right) = \sum_{i}^{n}\sum_{j}^{n} x_i x_j \varepsilon_{ij} \sigma_{ij}^3 I_{ij}(\rho, T, [\varepsilon], [\sigma], [x]) \tag{IV-34}$$

If for convenience we define K_{ij} such that

$$K_{ij}(\rho, T, [\varepsilon], [\sigma], [x]) = \frac{I_{ij}}{I_{oo}} \tag{IV-35}$$

then Equation (IV-34) can be rewritten in the form

$$\varepsilon_m\sigma_m^3 = \sum_{i=1}^{n}\sum_{j=1}^{n} x_i x_j K_{ij}\varepsilon_{ij}\sigma_{ij}^3 \tag{IV-36}$$

where $K_{ii} \to 1.0$ as $x_i \to 1.0$ at all temperatures and pressures because the mixture parameters must approach those of the pure fluid i as the

mole fraction of i approaches unity.

Equation (IV-36) is seen to result in the Van der Waal mixing rule given by Equation (IV-30) if

$$K_{ij} = 1 \tag{IV-37}$$

at every temperature and pressure for all i,j. This assumption in turn implies that

$$g^*_{ii}\left(\frac{r}{\sigma_{ii}}\right)_{T,\rho,[x]} = g^*_{ij}\left(\frac{r}{\sigma_{ij}}\right)_{T,\rho,[x]} = g^*_{jj}\left(\frac{r}{\sigma_{jj}}\right)_{T,\rho,[x]} = G^*_{oo}\left(\frac{r}{\sigma_m}, \frac{\epsilon_m}{kT}, \xi_m\right) \tag{IV-38}$$

Physically, the above constraint requires the distribution function for all pair interactions in the mixture to be expressed as a single universal function of dimensionless distance at the specified temperature, density, and composition. Furthermore, this dimensionless function is that obtained from the distribution function of the pure reference fluid at the reduced condition ϵ_m/kT, ξ_m.

In contrast, when the conformal molecules i and j are in their respective pure component states, their distribution functions can be expressed in terms of the reference fluid distribution functions by the relations

$$g^*_{ii}\left(\frac{r}{\sigma_{ii}}\right)_{T,\rho,x_i=1} = G^*_{oo}\left(\frac{r}{\sigma_{ii}}, \frac{\epsilon_{ii}}{kT}, \xi_{ii}\right) \tag{IV-39}$$

$$g^*_{jj}\left(\frac{r}{\sigma_{jj}}\right)_{T,\rho,x_j=1} = G^*_{oo}\left(\frac{r}{\sigma_{jj}}, \frac{\epsilon_{jj}}{kT}, \xi_{jj}\right) \tag{IV-40}$$

Therefore, the distribution functions for the i-i and j-j interactions expressed as a function of dimensionless distance in their respective pure fluids are equivalent only at the same reduced temperature and reduced density.

The Van der Waal rule for σ_m^3 can be similarly obtained if we work instead with the multicomponent equivalent of the equation of state given by Equation (III-8), expand each radial distribution function about the hard sphere case, and equate the corresponding temperature independent hard sphere terms. A detailed proof of the rule is provided by Leland and Chappelear. [144]. A proof of Equation

(IV-30) is also provided by the same authors but is less rigorous than the approach used in this work. The generalized Van der Waal equations expressed by Equations (IV-27) and (IV-28) can be obtained if we instead assume the distribution functions in the mixture to be described by the relation

$$g^{*}_{ij}\left(\frac{r}{\sigma},\rho,T,[\varepsilon],[\sigma],[x]\right) = \left(\frac{\varepsilon_{ij}}{kT}\right)^{\nu} G^{*}_{oo}\left(\frac{r}{\sigma_m}, \frac{\varepsilon_m}{kT}, \xi_m\right) \qquad \text{(IV-41)}$$

for all i, j. For non zero values of ν, the distribution function for the i-j interaction in the mixture is now also a function of the reduced temperature ε_{ij}/kT as specified in the above equation.

As the distribution functions are well defined for the real dilute gas, we can in fact examine the validity of the Van der Waal rule for this particular case. If we express each term in Equation (IV-1) using the reduced form suggested by Equations (IV-10) and (IV-11) we obtain the result

$$\sigma_m^3 \int_0^\infty \{1 - \exp[-\frac{\varepsilon_m}{kT} F(\frac{r}{\sigma_m})]\} (\frac{r}{\sigma_m})^2 d(\frac{r}{\sigma_m}) = \sum_i^n \sum_j^n x_i x_j \sigma_{ij}^3 \int_0^\infty \{1 - \exp[-\frac{\varepsilon_{ij}}{kT} F(\frac{r}{\sigma_{ij}})]\}(\frac{r}{\sigma_{ij}})^2 d(\frac{r}{\sigma_{ij}})$$

(IV-42)

If the ratio of the integral for the i-j interaction to that for the mixture in the above equation is denoted by L_{ij}, then the above equation may be rewritten as

$$\sigma_m^3 = \sum_{i=1}^n \sum_{j=1}^n x_i x_j L_{ij}\left(\varepsilon_{ij}/kT, \varepsilon_m/kT\right) \sigma_{ij}^3 \qquad \text{(IV-43)}$$

We see from Equation (IV-42) that the Van der Waal rule for σ_m^3 ($L_{ij} = 1$, all i,j) is exact either if all the ε values are identical, or if the temperature is high enough so that all exponential terms are significantly less than unity. For other situations, particularly at lower temperatures, it may be possible to define some optimum non-zero value of ν in Equation (IV-27) to yield the best approximation to Equation (IV-42) at any given temperature. The optimum value of ν will, of course, increase as the temperature decreases, because the distribution function in this case exhibits a stronger dependence on temperature as the temperature is lowered. Furthermore, we see that L_{ij} also varies with composition at a given temperature because

ε_m varies with the mixture composition.

If we were to differentiate Equation (IV-1) with respect to temperature and repeat the process we would obtain similar results with respect to the Van der Waal rule for $\varepsilon_m \sigma_m^3$. Leland and colleagues [147,148] have expressed the opinion that the Van der Waal rules are not necessarily restricted to the Van der Waal equation of state, and may be applied to all mixtures with conformal potentials. The above considerations suggest that their opinion should be accepted with considerable caution for mixtures of substances with large differences in their ε parameters in regions where the distribution functions are strongly dependent on temperature.

b) Two Fluid Model

The "two fluid" model attempts to relax the too rigid specification of a single average set of parameters for all interactions in the mixture. In this case the actual mixture of n components is replaced by an ideal mixture of n equivalent hypothetical components. Each of these n hypothetical fluids are assigned pseudoparameter values ε_i and σ_i which characterize the separate average environments of each species in the actual mixture. Thus, the configurational enthalpy and the heat of mixing can be expressed in terms of the pure reference fluid properties by the relations

$$\tilde{H}_m(T,P,[x]) = \sum_{i=1}^{n} x_i \tilde{H}_{oo}\left(T \frac{\varepsilon_{oo}}{\varepsilon_i}, P \frac{\varepsilon_{oo}}{\varepsilon_i} \frac{\sigma_i^3}{\sigma_{oo}^3}\right) \qquad \text{(IV-44)}$$

$$H^E(T,P,[x]) = \sum_i x_i \left[\frac{\varepsilon_i}{\varepsilon_{oo}} \tilde{H}_{oo}\left(T \frac{\varepsilon_{oo}}{\varepsilon_i}, P \frac{\varepsilon_{oo}}{\varepsilon_i} \frac{\sigma_i^3}{\sigma_{oo}^3}\right) - \frac{\varepsilon_{ii}}{\varepsilon_{oo}} \tilde{H}_{oo}\left(T \frac{\varepsilon_{oo}}{\varepsilon_{ii}}, P \frac{\varepsilon_{oo}}{\varepsilon_{ii}} \frac{\sigma_{ii}^3}{\sigma_{oo}^3}\right) \right] \qquad \text{(IV-45)}$$

1) Semi-Random Mixing Rules. The above model was derived from statistical mechanical considerations by Brown [31,33] given the assumption that all molecules were individually located in cells. It was also assumed that the cell size in each case was proportional to the volume of the molecule contained, and the number of nearest neighbours were allowed to approach infinity. Now, given the premise that the local distribution of molecules around each cell is random, the potential energy for the interaction of a molecule of species i with one of its neighbours is given by [31,33]

$$u_i(r) = \sum_{j=1}^{n} x_j u_{ij}(r) \qquad \text{(IV-46)}$$

Brown further noted that the pseudopotential $u_i(r)$ was conformal with each pair interaction potential $u_{ij}(r)$, only if they were all represented by the Lennard-Jones p-q form. Under these restricted conditions the pseudopotential parameters ε_i and σ_i, were related to the pair potential parameters by the expressions

$$\varepsilon_i \sigma_i^{\,p} = \sum_{j=1}^{n} x_j \varepsilon_{ij} \sigma_{ij}^{\,p} \qquad \text{(IV-47)}$$

$$\varepsilon_i \sigma_i^{\,q} = \sum_{j=1}^{n} x_j \varepsilon_{ij} \sigma_{ij}^{\,q} \quad (q \neq p) \qquad \text{(IV-48)}$$

These prescriptions coupled with the averaging procedure of Equation (IV-44) together define the "average potential" or the "semi-random mixing" model. This model still provides the same absurd results for hard sphere mixtures that were obtained with the random mixing rule defined by Equation (IV-26), but is superior for softer potentials [19,147].

2) Van der Waal Mixing Rules. Again, Leland and co-workers [148] provided an alternative prescription for the two fluid model that was independent of the potential function. They proposed the two fluid Van der Waal mixing rules given by

$$\varepsilon_i \sigma_i^{\,3} = \sum_{j=1}^{n} x_j \varepsilon_{ij} \sigma_{ij}^{\,3} \qquad \text{(IV-49)}$$

$$\sigma_i^{\,3} = \sum_{j=1}^{n} x_j \sigma_{ij}^{\,3} \qquad \text{(IV-50)}$$

If as before, we start with Equation (IV-3), substitute Equation (IV-49) into it, and express it in dimensionless form assuming that the hypothetical potentials $u_i(r)$ are conformal with the actual like and unlike pair potentials, we may obtain the averaging procedure for the two fluid model expressed by Equation (IV-44) if the distribution functions for the i-j interactions in the mixture satisfy the constraints [101,102]

$$\overset{*}{g}_{ij}\left(\frac{r}{\sigma_{ij}}\right)_{T,\rho,[x]} = \frac{1}{2}\left[\overset{*}{g}_{ii}\left(\frac{r}{\sigma_{ii}}\right)_{T,\rho,[x]} + \overset{*}{g}_{ii}\left(\frac{r}{\sigma_{jj}}\right)_{T,\rho,[x]}\right] \qquad \text{(IV-51)}$$

This statement implies that the distribution function for any unlike pair interaction in the mixture expressed as a function of dimensionless distance is the average of those for the pertinent like pair interactions in the mixture at a fixed temperature, pressure and composition. This condition is less restrictive than obtained for the corresponding one fluid Van der Waal model, where all three were required to be expressed by the same function of dimensionless distance. The Van der Waal rule given by Equations (IV-46) may then be similarly derived under the additional constraints

$$\overset{*}{g}_{ii}\left(\frac{r}{\sigma_{ii}}\right)_{T,\rho,[x]} = G^{*}_{oo}\left(\frac{r}{\sigma_i}, \frac{\varepsilon_i}{kT}, \xi_i\right) \qquad \text{(IV-52)}$$

$$\overset{*}{g}_{jj}\left(\frac{r}{\sigma_{ij}}\right)_{T,\rho,[x]} = G^{*}_{oo}\left(\frac{r}{\sigma_j}, \frac{\varepsilon_j}{kT}, \xi_j\right) \qquad \text{(IV-53)}$$

The rule given by Equation (IV-47) may be derived from the multicomponent pressure equation of state [Equation (IV-4)] if the distribution functions are expressed as perturbations about the hard sphere case, and the temperature independent hard sphere terms are treated as outlined above [101,102].

c) The Three Fluid Model

In this case, unlike the one and two fluid models, there is no correlation between the distribution functions for the different kinds of pairs in the mixture. For this particular model, the configurational properties of an n component system are averaged over n(n+1)/2 equivalent pure fluids, one for each i-j interaction and characterized by the parameters ε_{ij} and σ_{ij}. The configurational enthalpy for instance is given by

$$\tilde{H}_m(T,P,[x]) = \sum_{i=1}^{n}\sum_{j=1}^{n} x_i x_j \tilde{H}_{ij}(T,P) \qquad \text{(IV-54)}$$

where $\tilde{H}_{ij}$ is the configurational enthalpy in the pure i-j fluid. For conformal molecules we obtain the further restriction

$$\tilde{H}_m(T,P,[x]) = \sum_{i=1}^{n}\sum_{j=1}^{n} x_i x_j \frac{\varepsilon_{oo}}{\varepsilon_{ij}} \tilde{H}_{oo}\left(kT\frac{\varepsilon_{oo}}{\varepsilon_{ij}}, P\frac{\varepsilon_{oo}}{\varepsilon_{ij}}\frac{\sigma_{ij}^3}{\sigma_{oo}^3}\right) \qquad \text{(IV-55)}$$

The model differs from the other two, in that it does not require additional hypothetical fluid parameters to be defined, and may be obtained with Equation (IV-3) as the starting point under the constraint [101,102].

$$g_{ii}(r)_{T,P,[x]} = g_{ii}(r)_{T,P,x_i\to 1.0} = g_{oo}\left(r\frac{\sigma_{oo}}{\sigma_{ii}}, kT\frac{\varepsilon_{oo}}{\varepsilon_{ii}}, \frac{\xi_{ii}}{\xi_{oo}}\right) \qquad \text{(IV-56)}$$

for all like pair interactions in the mixture, and with the additional restriction

$$g_{ij}(r)_{T,P,[x]} = g_{oo}\left(r\frac{\sigma_{oo}}{\sigma_{ij}}, kT\frac{\varepsilon_{oo}}{\varepsilon_{ij}}, \frac{\xi_{ij}}{\xi_{oo}}\right) \qquad \text{(IV-57)}$$

In essence, the model implies that the like pair distribution functions in the mixture are the same as those in the corresponding pure fluids at the same temperature and pressure, irrespective of the mixture composition. These like pair fluid distribution functions may in turn be obtained from the pure reference fluid at the same reduced state. The unlike pair distribution function in the mixture is obtained from the same pure reference fluid using the parameters ε_{ij} and σ_{ij} instead.

Comparison Between the Corresponding States Models for Mixtures

a) Functional Differences. Each of the models examined permits the characterization of the configurational properties of a binary mixture using six interaction parameters ε_{ii}, σ_{ii}, ε_{ij}, σ_{ij}, ε_{jj}, σ_{jj}. They differ primarily in the order of averaging. The one fluid model averages the molecular parameters, while the three fluid model averages the thermodynamic properties. The intermediate two fluid model does some of both. An important feature common to all these models is their ability to predict the configurational properties of any multicomponent mixture purely from a knowledge of all the constituent binary interaction parameters and the configurational properties of the pure reference fluid. The examination of such models is therefore very relevant to the main objective of this work: the prediction of the enthalpies of the ternary methane-ethane-propane mixture.

Our next objective is to review the literature to determine how these models and their associated mixing rules have performed in representing and predicting the configurational properties of mixtures. Although we are, in this work, mainly concerned with the prediction of mixture enthalpies, comparison studies on other thermodynamic properties can also provide useful information in regard to these rules.

b) Prediction of Excess Properties of Real Systems. Excess property measurements for liquid mixtures of six "simple" fluids such as argon, krypton, xenon, methane, nitrogen, oxygen and carbon monoxide have been extensively used as a testing ground for such theories at low temperatures [19,36,37,147,148,177,248]. We note from Equations (IV-23) and (IV-45) that an excess property is calculated as a small difference in large numbers of the same sign, particularly if all the potential parameter ratios $\varepsilon_{ij}/\varepsilon_{oo}$ and σ_{ij}/σ_{oo} approach unity. Consequently, any uncertainty in the value of the pure reference fluid properties at each of the reduced conditions required to establish the excess enthalpy may cause serious errors in the estimation of the latter.

Most investigators have, therefore, eschewed the use of the forms examplified by Equations (IV-23) and (IV-45) for calculating excess properties in favor of expanding each term on the right hand side of these equations as a power series involving the pure reference fluid parameters. Brown [31] and Leland et al. [147] have, in fact, developed such expansions for the excess configurational free energy of binary mixtures upto the second order for the one fluid random mixing and Van der Waal models respectively, in terms of variables that involve only the pair interaction parameters, by substituting the appropriate mixing rule for expansion terms involving ε_m and σ_m. The coefficients of these expansion variables now involve thermodynamic properties of the reference substance at the temperature and pressure of measurement only, in contrast to the exact form of Equation (IV-23), where $\tilde{H}_{oo}$, for example, must be evaluated at three separate reduced conditions.

These expansions are cumbersome, but we include here, for simplicity, the result for H^E upto the first order terms as obtained

earlier by Longuet-Higgins [153] given by

$$H^E = \sum_{i=1}^{n}\sum_{j=1}^{n} x_i x_j \{ [\tilde{U} - T\frac{d\tilde{U}}{dT}] [2\frac{\epsilon_{ij}}{\epsilon_{oo}} - \frac{\epsilon_{ii}}{\epsilon_{oo}} - \frac{\epsilon_{jj}}{\epsilon_{oo}}] + [(3RT-PV) - \frac{Td(3RT-PV)}{dT}] [2\frac{\sigma_{oo}}{\sigma_{ij}} - \frac{\sigma_{oo}}{\sigma_{ii}} - \frac{\sigma_{oo}}{\sigma_{jj}}] \} \quad \text{(IV-58)}$$

where $\tilde{U}$ and V are the configurational energy and the volume for the reference fluid at a given T and P. The first order expansion is seen to be symmetrical in composition and independent of the specific mixing rule utilized. The properties V^E, G^E, H^E and S^E are all required to have the same sign for this particular case [153]. In fact, later efforts to include second order terms were motivated by the observation that measurements on certain systems violated the above restrictions [31].

For liquids at low pressure, $\tilde{U}$ is large relative to PV, and is opposite in sign to $d\tilde{U}/dT$. In such cases Equation (IV-58) may be simplified to include the one term involving the energy parameters only. Table (IV-1) lists similar simplified expansion results, including additional terms upto the second order for the excess free energy of a binary mixture in the liquid phase at low pressure as calculated by Scott and Fenby [238] using argon at 87K as the reference fluid.

Table IV-1

Power Series Expansions for the Excess Free Energy in the Liquid Phase for Varions Corresponding States Models [238]

G^E/x_1x_2RT	
$16.1\Psi + 15.2\eta^2 - 2.0\eta\phi + 58.0\,\phi^2$	One Fluid Random Mixing, Eq. (IV-25,26) p=6, q=12
$16.1\Psi + 15.2\eta^2 - 16.1\eta\phi - 1.3\,\phi^2$	One Fluid Van der Waal, Eq. (IV-29,30)
$16.1\Psi + 13.4\eta^2 - 1.0\eta\phi + 28.9\,\phi^2$	Two Fluid Average Potential, Eq. (IV-47,48) p=6, q=12
$16.1\Psi + 13.4\eta^2 - 8.05\eta\phi - 0.6\,\phi^2$	Two Fluid Van der Waal, Eq. (IV-49,50)
$16.1\Psi + 11.6\eta^2 - 0.3\,\phi^2$	Three Fluid, Eq. (IV-54)

Notation: $(1-\Psi) = (\epsilon_{11}\epsilon_{22})^{1/2}/\epsilon_{12}$

$2\eta = (\epsilon_{22} - \epsilon_{11})/\epsilon_{oo}$

$2\phi = (\sigma_{22}^3 - \sigma_{11}^3)/\sigma_{oo}^3$

The random mixing and average potential model results reported in Table (IV-1) are obtained for the specific case of the Lennard-Jones

6-12 potential function. It is immediately obvious that the rules differ primarily in the second order size contribution ϕ^2 to the excess free energy. The terms in ϕ^2 are considerably higher for the random mixing and average potential models though the size contribution in the two fluid models is about half of that for the corresponding one fluid case.

The excess property calculations for these models require the various pair interaction parameters to be first determined. The like parameters were obtained from critical data on the pure fluids [19,147, 148]. Initially, the unlike pair energy parameter was approximated by the geometric mean rule of Equation (IV-19) with k_{ij} equal to unity and the corresponding size parameter was approximated by the arithmetic mean rule of Equation (IV-17). These popular assumptions are collectively known as the Lorentz-Berthlot approximations. The values of G^E, H^E, and V^E for several equimolar mixtures of simple liquids as obtained from such calculations have been summarized by Rowlinson [226]. These results are reported as part of Table IV-2a. The appropriate parameter ratios $\varepsilon/\varepsilon_{oo}$ and σ^3/σ_{oo}^3 relative to Argon are shown in Table IV-2b. In general, the random mixing (not shown in the table) and semi-random mixing models realize G^E and H^E values that are algebraically larger than the experimental data. The Van der Waal one and two fluid models on the other hand yield excess property values that are algebraically smaller in that order.

In making such calculations for the one fluid random mixing model, Brown [31] observed that slight departures from two parameter corresponding states theory could complicate the interpretation of the results. For example, the calculated value of H^E for the equimolar CO-CH_4 mixture at 90.7°K varied from 70 to 105 Joules/gm mole as the reference fluid was changed from CH_4 to CO. This emphasized the necessity for restricting the analysis to substances that are strictly conformal in two parameters. The sensitivity of such calculations to the precise choice of the potential parameter ratios $\varepsilon_{11}/\varepsilon_{oo}$ and $\varepsilon_{22}/\varepsilon_{oo}$ and to the selected indices for the potential function for the particular case of the two fluid average potential model given by Equations (IV-47) and (IV-48) was examined by Calado and Staveley [36], using the data on the CH_4-Kr system. Three independent sets of Lennard-Jones 6-12 potential

TABLE IV-2a

Excess Property Predictions for Real Binary Mixtures According to Various Models

System	η^+	ϕ	Excess Property	Value of Ex. Prop. (Equimolar Mixture) Exptl. I	Average Pot. L-J 6-12 Two Fluid	Three Fluid	Van der Waal One Fluid	Van der Waal Two Fluid	Van der Waal Adjusted One Fluid	Van der Waal Adjusted Two Fluid	FLHW Adjusted One Fluid (Hard Sphere)	FLHW Adjusted One Fluid (Dilute Gas)	Gas Phase k_{ij} Staveley et al. [35]
					Lorentz-Berthelot Rules [226]				[147]	[148]	[248]	[117]	
				I	II	III	IV	V	VI	VII	VIII	IX	X
Ar-Kr 116K	.14	.34	G^E	+84	+110	+68	+38	+53	(+84)*	(+84)	(+84)	+97	
			V^E	-0.53	-0.44	-0.28	-0.78	-0.54	-0.66	-0.44	-0.79	-0.78	
			k_{ij}		1.00	1.00	1.00	1.00	0.986	0.990	0.990	0.994	0.994
Ar-N_2 84K[2]	.08	-0.30	G^E	+34	+80	+15	+40	+27	+46	(+34)	(+34)	+34	
			H^E	+51	+105	+13	+42	+27	(+51)	+38	+46	+48	
			V^E	-0.18	-0.07	-0.20	-0.32	-0.26	-0.31	-0.23	-0.21	-0.21	
			k_{ij}		1.00	1.00	1.00	1.00	0.998	0.997	0.999	0.999	
Ar-O_2 84K[2]	.01	-0.02	G^E	+37	+1	0	+1	0	+42	(+37)	(+37)	+33	
			H^E	+60	+2	0	+1	0	(+60)	+52	+59	+50	
			V^E	+0.14	+0.01	0.00	0.00	0.00	+0.06	+0.05	0.08	+0.07	
			k_{ij}		1.00	1.00	1.00	1.00	0.986	0.988	0.988	0.990	
Ar-CO 91K	.06	-0.42	G^E	+57	+70	+8	+26	+16	(+57)	(+57)	(+57)	+55	
			V^E	+0.1	+0.1	-0.14	-0.20	0.17	-0.13	-0.07	+0.07	+0.06	
			k_{ij}		1.00	1.00	1.00	1.00	0.989	0.985	0.985	0.986	
Ar-CH_4 91K	.11	+.29	G^E	+74	+170	+5	-19	+6	+92	(+74)	(+74)	+61	
			H^E	+103	+240	-8	-52	-11	(+103)	+85	104	+75	
			V^E	+0.72	-0.15	-0.15	-0.23	-0.23	-0.16	-0.13	+0.07	+0.02*	
			k_{ij}		1.00	1.00	1.00	1.00	0.967	0.979	0.976	0.98	0.988
Kr-CH_4 116K[4]	.07	-0.13	G^E	+29	+38		+21	+15	(+29)	(+29)	(+29)		
			H^E	+55	+56		+25	+17	36.3	35.7	36.8		
			V^E	-0.03	+0.01		-0.14	-0.11	0.13	-0.09	-0.02		
			k_{ij}		1.00		1.00	1.00	0.998	0.995	0.998	1.00	0.994
Kr-Xe 161K	.14	+.27	G^E	+114.5	+265		+5	+44	(+114.5)	(+114.5)	(+114.5)		
			V^E	-0.70	+0.97		-0.91	-0.62	-0.61	-0.41	-0.23		
			k_{ij}		1.00		1.00	1.00	0.974	0.929	0.989		
N_2-O_2 78K	.09	-0.38	G^E	+43	+65	+19	+19	+35	+45	(+43)	(+43)	+46	
			H^E	+46	+85	+17	+17	+35	(+46)	+45	+46	+60	
			V^E	-0.2	-0.11	-0.19	-0.32	-0.25	+0.33	-0.24		-0.33	
			k_{ij}	-0.2	1.00	1.00	1.00	1.00	1.002	0.997	1.004	1.001	
N_2- CO 84K	.03	.03	G^E	+23	+2	+1	+1	+1	(+23)	(+23)	(+23)	+22	
			V^E	0.1	-0.01	-0.01	-0.02	-0.01	+0.06	+0.10	0.06	0.09	
			k_{ij}		1.00	1.00	1.00	1.00	0.991	0.992	0.990	0.990	
N_2-CH_4	.16	.13	G^E	+135			+94			(+135)			
			V^E	-0.21			-0.82			-0.72			
			k_{ij}				1.00			0.986			
CO-CH_4 91K	.14	.10	G^E	+115	+105	+74	+75	+74	+131	(+115)	(+115)	+65	
			H^E	+105	+80	+64	+23	+43	(+105)	+106	+125	+41	
			V^E	-0.32	-0.50	-0.35	-0.84	-0.60	-0.72	-0.44	-0.36	-0.54	
			k_{ij}		1.00	1.00	1.00	1.00	0.982	0.987	0.982	0.998	
CH_4-CF_4 111K	.01	3.0	G^E	+360					+280	+350			
			V^E	+0.88					+0.90	1.07			
			k_{ij}						0.908	0.908			

+ η and ϕ are defined in Table IV-1. The reference substance for each mixture is taken to be the component with the larger value of ϵ.

* Bracketed term is an adjusted property

++ See References, 36, 147, 148 for sources of data

TABLE IV-2b

Energy and Volume Parameters Relative to Argon for Substances Examined in Table IV-2a

Substances	ϵ/ϵ_{Ar}	σ^3/σ^3_{Ar}
Argon	1.000	1.000
Krypton	1.387	1.225
Xenon	1.916	1.580
Nitrogen	0.836	1.198
Oxygen	1.022	0.988
Carbon Monoxide	0.881	1.225
Methane	1.226	1.327
Carbon Tetrafluoride	1.245	2.540

parameters obtained from the literature were used to characterize each of the pure fluids. The calculated value of G^E in the liquid phase was found to vary from 11.3 to 38.1 Joules/gm mole for the average potential model depending on the choice of potential parameters. If the L-J 18-6 potential was used instead with appropriately defined parameters, the calculated G^E value rose to 100.7 Joules/gm mole in marked disagreement with the experimental value of 28.7 Joules/gm mole. This result is all the more disconcerting because the 18-6 potential was found to be considerably superior to the 12-6 in representing the second virial coefficient data for each of the pure components of the mixture [35].

We note from Equation (IV-58), and the expansions in Table IV-1, that the H^E and G^E values are both sensitive to the precise choice of ε_{12}. Therefore, it appears doubtful whether calculations made with real test data using the Lorentz-Berthelot assumptions are really significant in discriminating between these various theories. The next phase in the examination of these models involves the adjustment of ε_{12}, or the correction term k_{12} to the geometric mean approximation, by fitting one excess property measurement (usually G^E) exactly for each mixture. The models are then evaluated for their ability to predict other excess properties for the same mixture at the same temperature. The agreement in all cases was significantly improved, [19,147,148,226,248], but the comparison between the rules remains obscure because ε_{12} or k_{12} is now specific to each mixing rule instead of being a fixed independently defined quantity as it should be.

The results for the one and two fluid VDW models [147,148] after such adjustments are indicated in Columns VI and VII of Table IV-2a. The specific excess property adjusted is enclosed in brackets. The adjusted results obtained by Snider and Herrington [248] with the Longuet-Higgins-Widom (LHW) perturbation model described by Equations (IV-5), (IV-6) and (IV-7) were also included because of the theoretical superiority of the hard sphere mixing rule for the size parameter. Although the LHW model calculates the excess properties using the exact one fluid model result instead of a series expansion, each of the pure component configurational property terms [in Equation (IV-23) for example] are calculated from the best fit LHW equation of state. Therefore errors

incurred in representing the pure components may decrease the precision of the excess property calculations. We note, however, that since G^E and H^E are relatively insensitive to the mixing rule for the size parameter in the dense fluid, and since the mixing rule for the parameter a_m in the Snider and Herrington model is equivalent to that for $\varepsilon_m\sigma_m^3$ in the one fluid Van der Waal model, the calculated results for these two models should be, and are, in general agreement. The two fluid VDW model results are seen to be slightly superior to both of these. The sensitivity of excess properties to the precise value of k_{12} is indicated by the fact that the calculated value of H^E for the $CO-CH_4$ system changes from 23 to 106 Joules/gm mole, as the value of k_{12} for the one fluid VDW model varies from 1.000 to 0.982.

Miller [117] repeated the calculations of Snider and Herrington [248], but instead used k_{12} values determined independently from second virial coefficient data. These results are also indicated in Table (IV-2a), column IX, and are seen to be in reasonable agreement with the experimental measurements (except for the system $CO-CH_4$ where the k_{12} value was obtained from the examination of a single B_{12} measurement). Even such calculations are not definitive as the temperature range of available B_{12} data is almost never sufficient to define k_{12} values precisely. Furthermore, the k_{12} values used by Miller were derived primarily from the data of Brewer [28], and are somewhat different from those obtained by Staveley and co-workers [35] from their own second virial coefficient measurements for the systems $Kr-CH_4$, Ar-Kr, and $Ar-CH_4$. Nevertheless, these results, within the limits of accuracy of the k_{12} determinations, make a case for the one fluid VDW rule for $\varepsilon_m\sigma_m^3$.

Leland et al. [147,148] noted that the k_{12} values adjusted with respect to the liquid phase excess properties for the one and two fluid VDW models were almost always below unity in keeping with the restriction imposed by the simple London calculation for the unlike pair dispersion energy [See Equation (IV-19)]. In contrast, the k_{12} values for the one and two fluid potential dependent models were above unity in several cases [19,36,37]. It was also noted that the adjusted k_{12} values for both VDW models were in better agreement with the values independently derived from second virial coefficient data.

Although such arguments are persuasive, it is difficult to make a definitive statement about these rules from comparisons that are restricted to a single condition in the liquid phase for each system examined.

The excess enthalpy data of van Eijnsbergen [270,271] on the systems CH_4-Ar, CH_4-N_2, CH_4-H_2, He-CH_4, and He-Ar as a function of pressure upto 160 atmospheres at selected temperatures, and including the gaseous, critical and dense fluid regions should serve as an excellent source for evaluating the various theories for conformal mixtures. Unfortunately, the analysis of the various models with respect to these results have not been as exhaustive or as critical as for the liquid mixtures described above. Although van Eijnsbergen and Beenakker [272] tested the one, two and three fluid models using the exact expressions for the excess enthalpy in each case, their analysis did not include the VDW rules. Furthermore, no attempt was made to empirically define k_{12} values using either part of the excess enthalpy data for each mixture, or independent second virial coefficient measurements. Quantum effects in mixtures containing hydrogen and helium also complicate the evaluation of models which assume classical fluid behaviour. They did, however, make the interesting observation that a single set of scale factors could not be found that would match the reduced configurational enthalpies of the three pure components N_2, Ar, and CH_4 taken two by two over the entire fluid region. It was suspected that deviations from strict two parameter theory and errors in the tabulated enthalpy values in the literature were jointly responsible for this situation.

Figure (IV-1) typifies some of their calculation results on a CH_4-N_2 mixture for the three models considered. The Lorentz-Berthelot approximations were used in each case. The 12-6 indices were assumed for the one and two fluid models. As the figure and the rest of their calculations show, the calculated value of H^E decreases in going from the one to the three fluid model.

c) Prediction of Phase Equilibria for Real Conformal Mixtures. Watson and Rowlinson [275] applied the one and two fluid Van der Waal models to the calculation of the phase equilibria for the

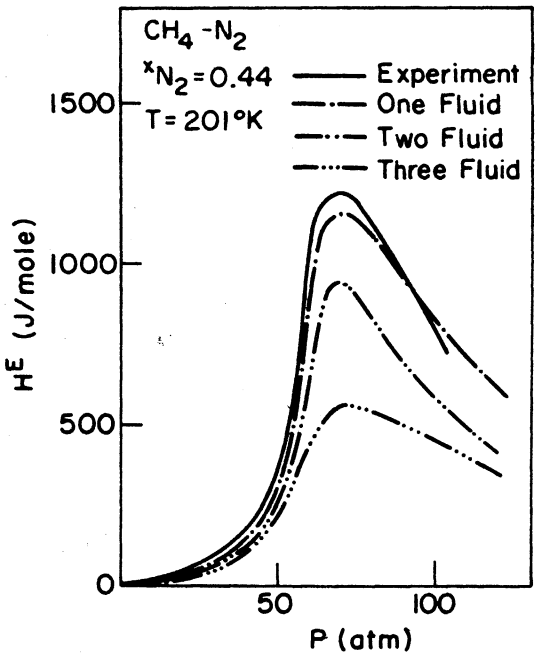

Figure IV-1. The Performance of Various Corresponding States Models in Predicting H^E for the Methane-Nitrogen System Using the Lorentz-Berthelot Rules [272].

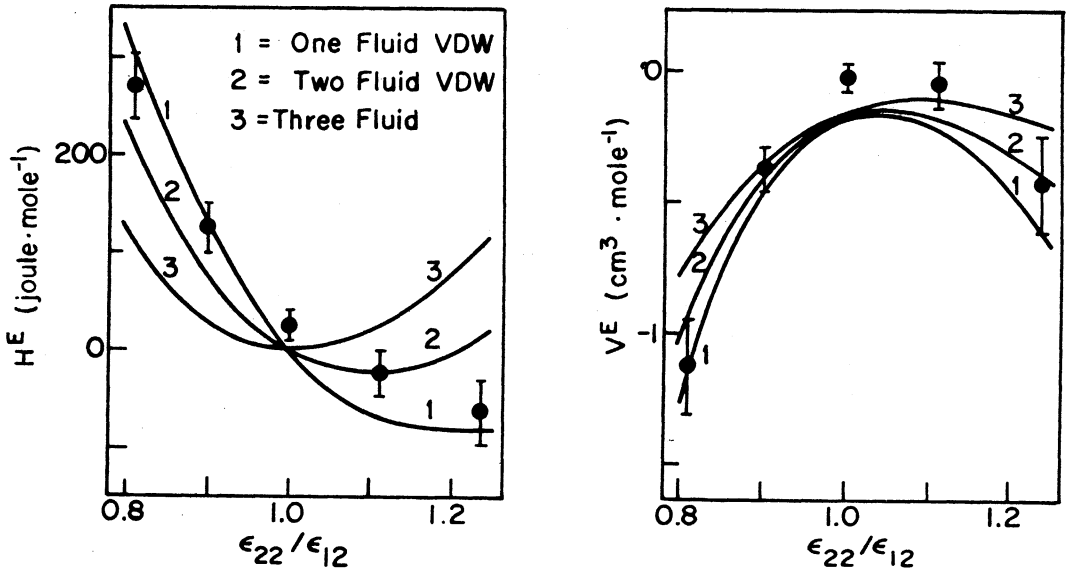

Figure IV-2. The Performance of Some Models in Predicting G^E and H^E for a Mixture of Lennard-Jones Molecules [102].

constituent binaries of the Ar-N_2-O_2 system upto 26 atmospheres using k_{ij} parameters derived in each case from binary liquid phase G^E data at low temperatures. The arithmetic mean rule was used to define the unlike pair size parameter in each case. The predictions were generally excellent (within 2%) for both models. The technique used by the authors in making these calculations was presented in a companion paper [228]. The prediction of the phase behaviour of the ternary mixture without the use of additional adjustable parameters was comparable to that obtained for the constituent binary systems. Although it is tempting to conclude that these results speak well for the extension of the corresponding states principle to mixtures of conformal substances, it must be remembered that the critical temperatures and volumes for the pure components of the particular ternary system investigated do not differ by more than 20%, and such results cannot therefore serve as the critical test we are looking for.

d) Problems in Verifying the Corresponding States Principle Using Real Data. In summarizing the evidence examined so far, it appears that the accurate assessment of a theory of mixtures by virtue of its ability to predict the thermodynamic properties of real systems is probably more difficultly accomplished than the formulation of the theory itself. The calculation of macroscopic properties from conformal solution theories depends on:

1) The judicious selection of the reference fluid and the accurate specification of its thermodynamic properties.

2) The validity of the assumption of conformal pair interactions for all i-j pairs in the mixture.

3) The accurate determination of the reduction parameters for each pure component in the mixture.

4) The assigned values for the unlike pair interaction parameters, and

5) The mixing rule.

As uncertainties associated with the first three steps, and particularly the third step, are unavoidable in application of such theories to real systems, it becomes difficult to establish the superiority of one mixing rule over another. Quasi-experimental

computer simulation results or thermodynamic property calculations from statistical mechanical considerations on systems that are simple enough to yield accurate results may serve as a desirable alternative to real data. In such cases the microscopic situation is rigidly and unequivocally fixed and under the complete control of the investigator. By fixing the conformal potential functions and the pair parameters for the like and unlike interactions, the macroscopic consequences are more impartially dependent on the mixing rule.

e) Performance of Corresponding States Models for Soft Sphere Mixtures. Although the hard sphere is the simplest model suitable for comparison, it has been previously established in this chapter that the random mixing and average potential models lead to absurd results for this particular case. Consequently, Leland et al. [147] chose to test the theories for the next simplest system; a mixture of soft spheres. The PY equation for the free energy of a mixture of hard spheres [141] was extended to the soft sphere case by replacing the hard sphere diameter σ_{oo} by the temperature dependent function $c\sigma_{oo}$ where

$$c = \left(\frac{\varepsilon_{oo}}{kT}\right)^{1/n}\left[1 + \frac{0.577}{n}\right] + 0(n^{-2}) \qquad \text{(IV-59)}$$

and n is a variable measure of softness. The value of A^E was obtained as a power series expansion for both one fluid models and the P-Y case upto the second order term ϕ^2 in size difference as defined in Table (IV-3) using the arithmetic mean diameter for the unlike pair. The coefficients of the second order term ϕ^2, expressed in each expansion as a function of the reference soft sphere volume density ξ_{oo}, were then compared. The results are summarized in Table (IV-3).

If $n \sim 12$, A^E is seen to be large and positive for the random mixing model, and becomes positive infinite as n approaches infinity. The coefficient of ϕ^2 for the P-Y and VDW models are essentially small and negative. The authors also expressed the ϕ^2 coefficients in terms of the virial expansion truncated at the third virial coefficient. These results are shown in Table (IV-4) where B_{oo} and C_{oo} are the virial coefficients for the soft sphere reference. This particular

TABLE (IV-3)

The Coefficient of the Second Order Size Term ϕ^2 in the Expansion of A^E for Soft Sphere Mixtures [147].

Model	Coefficient
Percus-Yevick	$4[\frac{5}{6}\frac{(1+\xi_{oo}+\frac{8}{5}\xi^2_{oo})}{(1-\xi_{oo})^3}-\frac{1}{3}-\frac{(1+2\xi_{oo})^2}{(1-\xi_{oo})^4}]$
Random Mixing (One Fluid)	$4[\frac{n+7}{12}\frac{(1+\xi_{oo}+\xi^2_{oo})}{(1-\xi_{oo})^3}-\frac{(n+1)}{12}-\frac{1}{2}-\frac{(1+2\xi_{oo})^2}{(1-\xi_{oo})^4}]$
Van der Waal (One Fluid)	$4[\frac{5}{6}\frac{(1+\xi_{oo}+\xi^2_{oo})}{(1-\xi_{oo})^3}-\frac{1}{3}-\frac{1}{2}\frac{(1+2\xi_{oo})^2}{(1-\xi_{oo})^4}]$

TABLE (IV-4)

The Coefficient of the Second Order Size Term ϕ^2 in the Virial Expansion A^E for Soft Sphere Mixtures [147]

Model	Coefficient
Percus-Yevick	$4[-\frac{1}{6}(\frac{B_{oo}}{V})-\frac{37}{60}(\frac{C_{oo}}{V^2})]$
Random Mixing (One Fluid)	$4[+(\frac{n-5}{12})(\frac{B_{oo}}{V})+(\frac{n-11}{12})(\frac{C_{oo}}{V^2})]$
Van der Waal (One Fluid)	$4[-\frac{1}{6}(\frac{B_{oo}}{V})-\frac{2}{3}(\frac{C_{oo}}{V^2})]$
Average Potential (Two Fluid)	$4[+(\frac{n-7}{24})(\frac{B_{oo}}{V})+(\frac{n-16}{24})(\frac{C_{oo}}{V^2})]$
Van der Waal (Two Fluid)	$4[-\frac{1}{6}(\frac{B_{oo}}{V})-\frac{13}{24}(\frac{C_{oo}}{V^2})]$
Three Fluid Model	$4[-\frac{1}{6}(\frac{B_{oo}}{V})-\frac{5}{12}(\frac{C_{oo}}{V^2})]$

TABLE (IV-5)

Comparison of the Coefficients for the Second Order Size Term ϕ^2 in the Free Energy Expansion with Computer Simulation Results [227]

	J/mole
Monte-Carlo Experiment [243]	$4(-200 \pm 100)$
Random Mixing (One Fluid, 6-12 Model)	4(+ 9900)
Van der Waal (One Fluid Model)	4(- 270)
Average Potential (Two Fluid 6-12 Model)	4(+ 4900)
Van der Waal (Two Fluid Model)	4(- 170)
Three Fluid Model	4(- 85)*

Simulation Conditions: Lennard-Jones 6-12 Potential

$T = 97K$

$\varepsilon_{11} = \varepsilon_{12} = \varepsilon_{22} = 133.5K$

$\sigma_{12} = 3.596\ A^\circ = (\sigma_{11} + \sigma_{22})/2$

$\sigma_{22}^3/\sigma_{11}^3 = 2.0$

* Approximate estimate

comparison was made because the P-Y result is exact upto the term C_{oo} [147,148] and provides a simple standard for judging the other theories. The one and two fluid Van der Waal models are seen to be superior to the rest in that order for n > 3.

f) Performance of Corresponding States Models for Mixtures of Lennard-Jones Molecules. An additional comparison study for the more complicated case of the Lennard-Jones 6-12 potential has been made by Rowlinson [227] using the Monte Carlo simulation results of Singer [243] on a binary mixture in the liquid phase with $\varepsilon_{11} = \varepsilon_{12} = \varepsilon_{22}$. The arithmetic mean rule was assumed for σ_{12}, and the volume ratio for the pure species was set at 2.0. These conditions were chosen to isolate the effect of size, as the leading term in the expansion for G^E (See Table IV-1) is now of the order of ϕ^2. The results are tabulated in Table IV-5. These results again establish the superiority of the Van der Waal mixing recipes.

The comparison studies of Leland et al. [147] and Rowlinson [227] have both made a pointed attempt to evaluate the effect of size while ignoring the contributions due to differences in the energy parameters, precisely because it is the size effects that maximize the differences between the potential dependent and the VDW mixing rules for both the one and two fluid models, respectively. For molecules of the same size, we see by comparing Equations (IV-26) and (IV-30) that the random mixing and VDW one fluid models yield the same mixing rule for ε_m. Both two fluid models are also seen to be equivalent for this limiting case. Our next objective then, is to compare the behaviour of the one and two fluid models for the case where the energy parameters are significantly different.

g) Inadequacies of Comparison Studies Based Strictly on the Coefficient of the Second Order Size Term. In referring to Table (IV-1), we note that both the one and two fluid VDW models have significantly higher values for the coefficients of the term $\eta\phi$ than each of the corresponding potential dependent cases. The term $\eta\phi$ which involves the simultaneous coupling of size and energy effects is seen to be absent for the three fluid model, but considerably complicates

the analysis of the energy and/or size effects for the VDW models. This point is inadequately treated in the literature, and merits further discussion here.

The contribution of the energy-size effect may be illustrated with respect to the liquid phase G^E expansions presented in Table (IV-1) by calculating the variation of G^E/x_1x_2RT as a function of η^2 or ϕ^2 for various values of η/ϕ for each model. We observe that the coefficient of Ψ is the same for all models, and for simplicity assume the geometric mean rule for ε_{ij} (Ψ=0) in order to enhance the relative contribution of the other terms in the series. The results are shown in Table (IV-6). The bracketed quantities indicate the % contribution of the coupling term $\eta\phi$ to the total value of G^E/x_1x_2RT.

Several observations may be made from the results presented in Table (IV-6). Firstly, we note that irrespective of the value and sign of $\eta\phi$, the value of G^E/x_1x_2RT is always positive for the random mixing and average potential models. The differences between these models and the equivalent Van der Waal formulations are seen to increase as η/ϕ decreases, i.e. as the size differences get larger. In general, we also observe that the percentage contribution of the coefficient of the coupled term $\eta\phi$ is very significant for the one and two fluid Van der Waal models particularly in the ranges $2.5 \leq \frac{\eta}{\phi} \leq 0.16$, and $-0.16 \leq \frac{\eta}{\phi} \leq -0.5$. In the former case, the molecule with the larger ε also has the larger size. In the latter case, the sizes of the two species considered are interchanged. Each condition is seen to discriminate between the various models. Furthermore, even though the coefficient of the second order size term ϕ^2 is small for both VDW models, we may, by changing the sign of ϕ for a given η, induce drastic changes in G^E including that of sign in both cases.

For most of the real liquid mixtures of Table (IV-2a), η/ϕ lies in the ranges $2.5 \leq \frac{\eta}{\phi} \leq 0.5$, $-0.5 \leq \frac{\eta}{\phi} \leq -2.5$, where the coupling term is seen to be of significant importance for the two Van der Waal models. Therefore, we are forced to conclude that theoretical evaluations based on the examination of the coefficient of the second order expansion term ϕ^2 alone are not wholly adequate in providing us with an accurate estimate of the behaviour of the Van der Waal models

TABLE (IV-6)

The Contribution of the Coupling Term $\eta\phi$ as a Function of η/ϕ to G^E/RT in the Liquid Phase as Derived from the Results of Table IV-1*

Model	$\eta/\phi = \infty$	$\eta/\phi = 5$	$\eta/\phi = 2.5$	$\eta/\phi = 1.0$	$\eta/\phi = 0.5$	$\eta/\phi = 0.16$	$\eta/\phi = 0$
VDW (One Fluid)	$15.2\eta^2$,(0%)	$11.9\eta^2$,(-32%)	$8.6\eta^2$,(-74%)	$-2.2\eta^2$,(800%)	$-22.2\eta^2$,(145%)	$-135.4\eta^2$,(74%)	$-1.3\phi^2$,(0%)
VDW (Two Fluid)	$13.4\eta^2$,(0%)	$11.8\eta^2$,(-16%)	$10.1\eta^2$,(-170%)	$4.7\eta^2$,(-170%)	$-5.3\eta^2$,(300%)	$-52.4\eta^2$,(97%)	$-0.65\phi^2$,(0%)
(Three Fluid)	$11.6\eta^2$,(0%)	$11.6\eta^2$,(0%)	$11.5\eta^2$,(0%)	$10.4\eta^2$,(0%)	$10.4\eta^2$,(0%)	$-0.1\eta^2$,(0%)	$-0.3\phi^2$,(0%)
Random Mixi g (One Fluid)	$15.2\eta^2$,(0%)	$17.1\eta^2$,(-2%)	$23.7\eta^2$,(-3%)	$71.2\eta^2$,(-3%)	243 η^2,(-2%)	2268 η^2,(0.6%)	$+58.0\phi^2$,(0%)
Average Potential (Two Fluid)	$13.4\eta^2$,(0%)	$14.3\eta^2$,(-1%)	$17.6\eta^2$,(-2%)	$40.3\eta^2$,(-2%)	127 η^2,(-2%)	1136 η^2,(0.6%)	$+28.9\phi^2$,(0%)

Model	$\eta/\phi = -5$	$\eta/\phi = -2.5$	$\eta/\phi = -1.0$	$\eta/\phi = -0.5$	$\eta/\phi = -0.16$
VDW (One Fluid)	$17.4\eta^2$,(18.5%)	$21.5\eta^2$,(30%)	$30.0\eta^2$,(54%)	$42.2\eta^2$,(77%)	$+65\eta^2$,(154%)
VDW (Two Fluid)	$16.8\eta^2$,(10%)	$16.5\eta^2$,(20%)	$20.8\eta^2$,(39%)	$26.9\eta^2$,(60%)	$+38\eta^2$,(132%)
(Three Fluid)	$11.6\eta^2$,(0%)	$11.5\eta^2$,(0%)	$11.3\eta^2$,(0%)	$11.3\eta^2$,(0%)	$0.3\eta^2$,(0%)
Random Mixing (One Fluid)	$17.9\eta^2$,(2%)	$25.3\eta^2$,(3%)	$75.2\eta^2$,(3%)	$251\eta^2$,(-2%)	$2293\eta^2$,(0.6%)
Average Potential (Two Fluid)	$14.8\eta^2$,(1%)	$18.4\eta^2$,(2%)	$42.3\eta^2$,(2%)	$131\eta^2$,(-2%)	$1148\eta^2$,(0.6%)

*For Definition of η and ϕ, See Table IV-1.

for real or artificial conformal mixtures whose pure components have significantly different values of ε.

A more relevant comparison of the first three models of Table (IV-6) was made by Henderson and Leonard [102] using the quasi-experimental G^E, H^E and V^E data of Singer et al. [242,243] for a binary Lorentz-Berthelot mixture of Lennard-Jones 6-12 molecules at 97K for $\varepsilon_{22}/\varepsilon_{12}$ values varying from 0.8 to 1.2, with σ_{22}/σ_{12} fixed at 1.06. The results of these comparisons should be significant with respect to the application of such models to real systems because they extend over the range $1.3 \leq n/\phi \leq -1.3$. The results for V^E and H^E are indicated in Figure IV-2. It was concluded that the one fluid Van der Waal model was superior to the other two for the particular case examined.

h) The Role of the Distribution Function in Evaluating Corresponding States Models for Mixtures. Earlier in this chapter, we examined various corresponding states models from the standpoint of the constraints that they imposed on the dimensionless radial distribution functions for all pair interactions in the mixture. Therefore, if we are independently able to specify $g_{ij}(\frac{r}{\sigma})$ in a mixture for all i, j, then we may also evaluate such models by determining how realistic such constraints actually are. In effect, this approach evaluates various models by subjecting the microscopic structure of mixtures to close scrutiny in contrast to the more traditional procedure of rating the same models for their ability to predict the macroscopic properties. Such information has not yet been determined from the direct interpretation of experimental data on real mixtures. Some useful results have, however, been obtained as a byproduct of thermodynamic property calculations on simpler artificially specified systems using either computer simulation or statistical mechanical methods.

In a definitive study, Throop and Bearman [267] examined the variation of the radial distribution function for both like and unlike interactions in various binary mixtures as a function of density, composition, and the size and energy parameter ratios for the constituent pure components using both the hard sphere and the Lennard-Jones 6-12 models. The study was primarily confined to the dense fluid

region at supercritical temperatures because of difficulties experienced with obtaining a numerical solution of the multi-component P-Y equation for the Lennard-Jones potential at other conditions.

We will now attempt to briefly show how their results could be used to examine the applicability of the two parameter corresponding states principle to mixtures. For illustrative purposes we confine our interpretation to the calculated values of $g_{ij}(r)$, for all constituent i-j pairs of the Ne-Kr system at three compositions with the volume density ξ and temperature fixed at 0.3 and 260K, respectively. (For reference, the critical temperature and density for krypton occur approximately at $\varepsilon/kT = 0.8$ and $\xi = 0.167$, respectively). The results are plotted in Figure IV-3 b, c, and d as a function of the dimensionless distance r/σ_{ij} for all i, j, instead of the distance r/σ_{jj} used in the original work, where σ_{jj} is the size parameter of the largest species in the mixture. The change in variable makes it easier to visually relate the results to the various corresponding states models. All pair interactions were assumed to be conformal and of the Lennard-Jones 6-12 type as indicated in Figure IV-3a. The unlike pair parameters were arbitrarily chosen to satisfy the Lorentz-Berthelot rules as indicated by Equations (IV-12) and (IV-14a), respectively, with k_{ij} equal to 1.0. As the volume and energy parameter ratios for the pure components of the mixture are significantly different from unity ($\sigma_{jj}^3/\sigma_{ii}^3 = 2.2$, $\varepsilon_{jj}/\varepsilon_{ii} = 4.7$, where the subscript jj stands for the Kr-Kr interaction), we can expect $g_{ij}(r/\sigma_{ij})$ for each i-j pair to be influenced by both size and energy effects.

In examining each of the Figures IV-3 b, c, and d separately, we observe that although the general shape of $g_{ij}(r/\sigma_{ij})$ is the same for all pair interactions in the mixture, particularly with respect to the location of the extrema, there are some differences in the magnitude of the radial distribution function for the various i-j pairs at any fixed value of r/σ especially near the first peak. Therefore, the constraint of Equation (IV-38) which requires all $g_{ij}(r/\sigma)$ in the mixture to be equivalent at all values of r/σ and which is implied by the one fluid Van der Waal model of Equation (IV-30) with $\nu=0$ is not optimally suited to this particular case.

If we ascribe the differences in the magnitude of $g_{ij}(r/\sigma)$ mainly

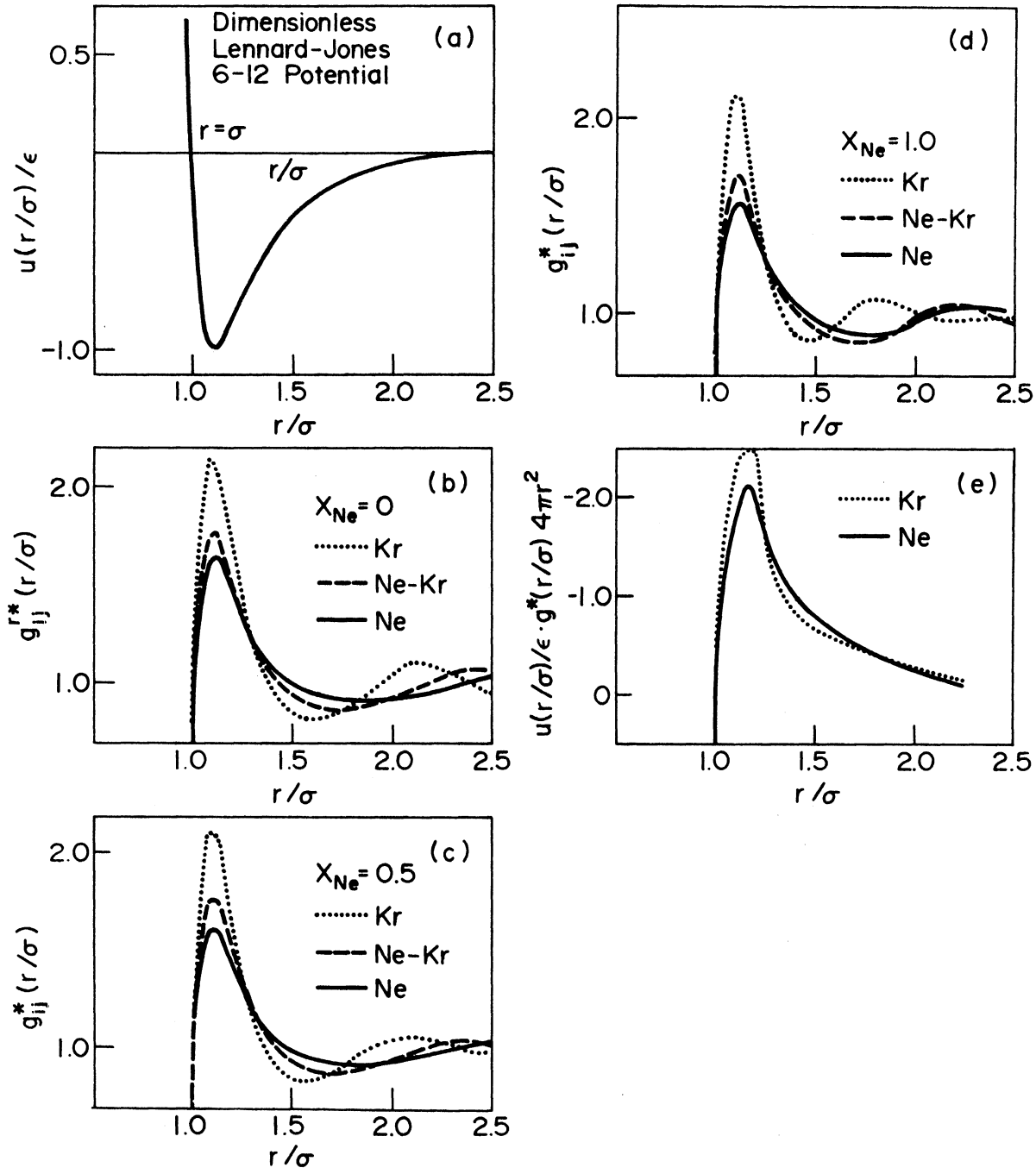

Figure IV-3. The Radial Distribution Function $g_{ij}(\frac{r}{\sigma})$ for All Pair Interactions in the Neon-Krypton System at 260K [266].

to differences in the value of ε for the various i-j pairs, then Equation (IV-41) suggests that a non-zero value for the exponential factor ν in the generalized one fluid model of Equation (IV-28) may allow us to compensate for the observed differences in $g_{ij}(r/\sigma)$. In fact, if we were to substitute Equation (IV-41) into Equation (IV-33) and repeat the derivation of the Van der Waal mixing rule for the generalized case with $\nu \neq 0$, we would find, for example, that

$$\frac{I_{ii}}{I_{jj}} = \frac{(\varepsilon_{ii}/kT)^{\nu}}{(\varepsilon_{jj}/kT)^{\nu}} \qquad \text{(IV-60a)}$$

where I is defined as before.

We may use the above equation to calculate the best value of ν from the data in Figure IV-4. In Figure IV-3e, we plot the quantity $y(r/\sigma)$ defined as

$$y(\tfrac{r}{\sigma}) = \frac{u(\frac{r}{\sigma})}{\varepsilon}\, g(\tfrac{r}{\sigma})\, 4\pi r^2 \qquad \text{(IV-60b)}$$

for each like pair interaction for the case of the 50% mixture. The quantity I_{ij} in Equation (IV-34) is defined in terms of $y_{ij}(r/\sigma)$ by the relation

$$I_{ij} = 4\pi \int_0^{\infty} y_{ij}(\tfrac{r}{\sigma})\, d(\tfrac{r}{\sigma}) \qquad \text{(IV-61)}$$

Integration of the curves in Figure IV-3e yield a value of 1.15 for I_{jj}/I_{ii}. Therefore, given the fact that $\varepsilon_{jj}/\varepsilon_{ii} = 0.7$, Equation (IV-60a) yields the optimum value of ν as 0.09. In any case, a cursory glance at Figures IV b, c, and d suggests that the assumption

$$\overset{*}{g}_{ij}(\tfrac{r}{\sigma}) = [g_{ii}(\tfrac{r}{\sigma}) + \overset{*}{g}_{jj}(\tfrac{r}{\sigma})]/2 \quad \text{(for all } \tfrac{r}{\sigma}) \qquad \text{(IV-61a)}$$

as embodied by the two fluid model with $\nu = 0$ would provide a more realistic representation of the microstructure of the mixture particularly at the first maximum in $g(r/\sigma)$ than the assumption of Equation (IV-36) corresponding to the one fluid case.

Irrespective of how the various dimensionless pair distribution functions in the mixture relate to each other, the success of the

various corresponding states models still depends upon our ability to relate $g_{ij}(r/\sigma)$ in the mixture to that in the pure fluid. By following the variation of $g(r/\sigma)$ for each like pair as a function of composition in Figures IV-3 b,c, and d we note that, apart from a slight decrease in height of the first peak and a shortening of the distance between contiguous peaks as the mole fraction of neon increases, the approximation

$$g^{*}_{ii}\left(\frac{r}{\sigma}, \xi, T, [x]\right) \simeq g^{*}_{ii}\left(\frac{r}{\sigma}, \xi, T, x_i = 1.0\right) \qquad \text{(IV-62)}$$

appears to be reasonable for the particular case examined.

The implication of Equation (IV-62) is twofold. Firstly, it appears that the behaviour of any like pair distribution function in the mixture can be obtained from the corresponding pure component at the same temperature and volume density, and secondly, the optimum value of ν for the generalized Van der Waal models is independent of mixture composition at any fixed temperature as long as the volume density is constant. Unfortunately many more such calculations are needed if we are to obtain more than a partial answer to the interesting question of how the exponent ν varies with temperature, density, and composition, or for that matter with the energy and size parameter ratios of the constituent pure components. We emphasize again that although such calculations are tedious and perhaps impractical for design purposes, they promise to yield information that is less ambiguous than obtained from the correlation of real data.

The selection of the volume density ξ as a working parameter instead of the reduced density must be considered as a judicious one. Although the two quantities are equivalent for pure components differing only by the constant factor $1/6\ \pi$, the volume density in a mixture is defined by

$$\xi = \sum_i \frac{1}{6}\pi\, \rho_i \sigma_i^3 \qquad \text{(IV-63)}$$

where as the reduced density ρr is expressed as

$$\rho r = \rho N \sigma^3 \qquad \text{(IV-64)}$$

The use of ξ is preferred because, unlike ρr, it does not commit us to a specific corresponding states model and does not require us to specify the hypothetical size parameter σ_m. This author believes that the significance of the parameter ξ should also be investigated in developing practically oriented thermodynamic property correlations.

Throop and Bearman [268] have since calculated the excess properties H^E, G^E and V^E for various binary inert gas systems, Ne-Kr and Ne-Xe at the conditions corresponding to their earlier distribution function calculations using the same model. These results have unfortunately not as yet been tested against any of the corresponding states theories examined in this chapter but promise to be discriminating in the event of such an examination in the future.

i) Conclusion. The entire discussion on mixtures of molecules governed by artificial potential models including the consideration of the radial distribution function is to be considered valuable because the evidence, unlike the results for real conformal molecules, permits us to conclude with some confidence that the generalized one and two fluid VDW corresponding states models are superior to others in characterizing mixtures of substances that are conformal in two parameters. Of these two models, no one is clearly superior to the other although it appears that the two fluid version is to be preferred at higher densities while the one fluid version is more suitable in the gas phase at subcritical pressures. However, since such evidence does not extend to mixtures of pure substances that subscribe to a three parameter theory, (such as the n-alkanes in which we are primarily interested), it is also necessary to examine the literature for more empirically based efforts involved in the correlation of the thermodynamic properties of mixtures in such extended schemes.

The Macroscopic One Fluid Three Parameter Corresponding States Principle For Mixtures

a) The Pseudocritical Method. It has already been noted in Chapter III that the force constants ε_{ii} and σ_{ii}^3 for pure substances conforming to a two parameter theory are proportional to the critical temperature Tc_{ii} and the critical volume Vc_{ii}, respectively. In

examining the applicability of the one fluid model expressed by Equation (IV-22), to mixtures, one is tempted to replace the ratios $\varepsilon_m/\varepsilon_{oo}$, and σ_m^3/σ_{oo}^3 by Tc_x/Tc_{oo}, and Vc_x/Vc_{oo}, respectively, where Tc_x and Vc_x are the measured true critical properties of the mixture, in order to determine if the measured configurational enthalpies of the mixture can be represented by the function $\tilde{H}_{oo}$ over the single phase region in the P-T plane.

The thermodynamic criteria defining the critical point in a mixture are discussed at length by Prigogine and Defay [208]. In brief, the conditions

$$\left(\frac{\partial^2 G}{\partial x_2^2}\right)_{T,P} = 0 \qquad \text{(IV-65)}$$

$$\left(\frac{\partial^3 G}{\partial x_2^3}\right)_{T,P} = 0 \qquad \text{(IV-66)}$$

must be satisfied by a binary mixture at the critical point in contrast to the conditions expressed by Equations (V-15) and (V-16) that apply to the pure component case. Other distinctions include the fact that the heat capacity for a pure component approaches infinity at the critical point, but remains finite for a mixture as demonstrated by the experimental measurements of Manker [162] on the 0.949 mole fraction methane-propane mixture.

The most common procedure is to determine the parameters Tc_m and Vc_m that produce the best fit of the thermodynamic properties of the given mixture in the specified framework. These are called "pseudo-critical" parameters because they take the place of the pure component critical properties when used in corresponding states correlations, but unlike the latter, they are not accessible to direct experimental measurement. In fact, the "pseudo-critical point" always lies within the two phase region. For the special care of the Van der Waal equation of state, Rowlinson [226] has indicated that the pseudo-critical parameters and the critical parameters for a binary mixture are related by the expressions:

$$\frac{Tc_x - Tc_m}{Tc_m} = x(1-x)\left[\frac{3}{4}\frac{dTc_m}{dx}/Tc_x - \frac{1}{4}\frac{d}{dx}(RTc_m/Pc_m)/RTc_m/Pc_m\right]^2 \qquad \text{(IV-67)}$$

$$\frac{Pc_x - Pc_m}{Pc_m} = \left(\frac{\partial \ln P}{\partial \ln T}\right)_{V=Vc_m} \left(\frac{Tc_x - Tc_m}{Tc_m}\right) \qquad \text{(IV-68)}$$

where $(\partial \ln P/\partial \ln T)_{V=Vc_m}$ has a value of 4.0.

Kreglewski [133,134] determined that the empirical equation

$$Tc_x - Tc_m = 2.2\, x_1 (1-x_1) \frac{(Tc_{11} - Tc_{22})^2}{Tc_{11}x_1 + Tc_{22}(1-x_1)} \qquad \text{(IV-69)}$$

was satisfactory for binary n-alkane mixtures with ethane and n-heptane as extreme components. Equation (IV-68) was found to be considerably better in representing real fluid data if the slope of the pseudo-critical isochore is instead expressed by the relation

$$\left(\frac{\partial \ln P}{\partial \ln T}\right)_{V=Vc_m} = 5.808 + 4.93\,(\omega_1 x_1 + \omega_2 x_2) \qquad \text{(IV-70)}$$

where ω is the acentric factor.

b) Empirical Justification for Hydrocarbon Mixtures. The suitability of the three parameter pure component reduced function as a vehicle for the representation of mixture properties of normal fluids, was examined by Pitzer and Hultgren [197] who determined the pseudo-critical parameters for a number of mixtures containing at least one light hydrocarbon by fitting the mixture compressibility data near the minima in z along isotherms to the Pitzer pure component corresponding states framework. Comparisons then made outside this region, even for mixtures of components with significantly different values of Tc and Vc, indicated an agreement of better than 1% in most cases. In an extreme comparison of this type, the second virial coefficient for a mixture containing 40% n-butane and 60% methane was fitted to a worse case deviation of 6cc/mole using Equation (IV-21) and pseudo-critical constants obtained from dense fluid z values. However, as the Tc and Vc ratios for the constituent components of a mixture departed from unity, a trend towards poorer representation was observed. For example, in the case of a methane-pentane mixture, experimental isotherms fitted near their minima in z were found to lie about 2% below values predicted from the pure fluid reference at pressures

corresponding to half or twice the minimum.

Yesavage [284] noted that optimized sets of pseudo-parameters could be determined for each of five methane-propane mixtures that would represent the enthalpy departure over the range -240°F to +300°F and upto 2000 psia and including the single phase liquid, gaseous and dense fluid region to within 1 Btu/lb. The direct use of calorimetric data on the pure components methane and propane to define the reference enthalpy departure functions in the three parameter framework must be appreciated as an optimum choice for the binary system in question. Powers [202] later obtained essentially the same results with the PGC correlation.

It is, therefore, tempting to conclude that the one fluid corresponding states model is very suitable for the representation of the thermodynamic property of light hydrocarbon mixtures in the single phase region. This assumption, however, carries with it the implication that all thermodynamic properties can be represented with a single unique set of pseudo-parameters whereas, in fact, each investigation in this connection has been confined to the evaluation of the principle for one specific thermodynamic property. This distinction is an important one and is further clarified in Chapter IX.

c) Mixing Rules for Calculating the Pseudo-parameters for a Given Mixture. It is now obvious that the accuracy of the predictions for the thermodynamic properties of a given mixture using the corresponding states principle will depend very heavily on our ability to correctly estimate its pseudo-critical parameters. Much attention has been devoted to the calculation of such parameters as a function of the mole fractions, the true critical properties of the individual pure components and from additional empirically obtained terms that are characteristic of all constituent unlike pair binary interactions appropriate to the mixture.

The simplest and perhaps the most widely used rules are due to Kay [125,126] which combine the pure component properties in a linear fashion with respect to composition

$$Tc_m = \sum_{i=1}^{n} Tc_{ii} x_i \qquad \text{(IV-71)}$$

$$Pc_m = \sum_{i=1} Pc_{ii} x_i \qquad \text{(IV-72)}$$

In a three parameter framework, Kay's rule may be extended to impose a similar composition dependence on the third parameter. Thus, the acentric factor ω_m is defined as

$$\omega_m = \sum_{i=1}^{n} \omega_{ii} x_i \qquad \text{(IV-73)}$$

Garcia-Rangel and Yen [86] have, in a recent comprehensive study, tested these rules for their ability to predict the enthalpy data of a wide variety of mixtures containing both polar and non-polar components.

Kay's rule, however, suffers from the disadvantage of not being able to utilize binary mixture data when available. Pitzer and Hultgren [197] extended Kay's rule by adding an extra empirical parameter for each binary interaction expressed in terms of the pseudo-critical properties of the equimolar binary mixture.

$$Tc_m = \sum_{i=1}^{n} Tc_{ii} x_i + \sum_{j\neq i}^{n} \sum_{i\neq j}^{n} x_i x_j \left[2\, Tc_{0.5i,\, 0.5j} - Tc_{ii} - Tc_{jj} \right] \qquad \text{(IV-74)}$$

$$Pc_m = \sum_{i=1}^{n} Pc_{ii} x_i + \sum_{j\neq i}^{n} \sum_{i\neq j}^{n} x_i x_j \left[2\, Pc_{0.5i,\, 0.5j} - Pc_{ii} - Pc_{jj} \right] \qquad \text{(IV-75)}$$

$$\omega_m = \sum_{i=1}^{n} \omega_{ii} x_i + \sum_{j\neq i}^{n} \sum_{i\neq j}^{n} x_i x_j \left[2\, \omega_{0.5i,\, 0.5j} - \omega_{ii} - \omega_{jj} \right] \qquad \text{(IV-76)}$$

where the subscript 0.5_i, 0.5_j refers to the equimolar binary mixture of i and j. These rules are sometimes expressed in an alternate form that is completely quadratic in the composition dependence. For ω_m, for example, we obtain

$$\omega_m = \sum_{i=1}^{n} \sum_{j=1}^{n} x_i x_j \omega_{ij} \qquad \text{(IV-76a)}$$

where ω_{ij} $(i\neq j)$ is to be regarded strictly as an empirical constant. The authors have tabulated the equimolar mixture pseudo-critical properties for twelve systems including the methane-ethane and the

methane-propane systems. These forms all reduce to Kay's rule if the pseudo-critical properties of the equimolar mixture are given by the arithmetic average of the constituent pure component critical properties.

If it is assumed that ε/kTc, and $Vc/N\sigma^3$ are constant for every term in Equation (IV-29) and (IV-30) as required by two parameter corresponding states theory, then we obtain the mixing rules

$$Vc_m = \sum_{i=1}^{n} \sum_{j=1}^{n} x_i x_j \, Vc_{ij} \qquad \text{(IV-77)}$$

$$Tc_m \, Vc_m = \sum_{i=1}^{n} \sum_{j=1}^{n} x_i x_j \, Tc_{ij} \, Vc_{ij} \qquad \text{(IV-78)}$$

If we assume a value of 0.5 for ν in Equation (IV-27) and (IV-28), and assume zc is constant, again, as required by two parameter theory, then we obtain the rules

$$\frac{RTc_m}{Pc_m} = \sum_{i=1}^{n} \sum_{j=1}^{n} x_i x_j \, \frac{RTc_{ij}}{Pc_{ij}} \qquad \text{(IV-79)}$$

$$\frac{RTc_m}{Pc_m}^{2.5} = \sum_{i=1}^{n} \sum_{j=1}^{n} x_i x_j \, \frac{RTc_{ij}}{Pc_{ij}}^{2.5} \qquad \text{(IV-80)}$$

Equations (IV-77) and (IV-78) encompass the Van der Waal pseudo-critical mixing rules, whereas Equations (IV-79) and (IV-80) describe the Redlich-Kwong mixing rules. These rules obtain their name from the specific reduced equations of state from which they may be derived. This aspect is treated in greater detail in Chapter V. It must be emphasized that the equivalence between these rules and their microscopic counterparts is not assured in a three parameter framework with which they are frequently used. In such cases, as Leland et al. [144] point out, ε/kTc is a function of the third parameter whatever it may be, and one would therefore expect to see an αc or ω dependence in these rules. Such improvements have not yet found their way into the literature. In practice, an independent rule for the third parameter usually expressed in the form of Equation (IV-76a) is used concurrently with both sets of rules.

The Van der Waal rules of Equations, (IV-77) and (IV-78) are used by both Leland [81] and Powers [204] in applying their respective

corresponding states correlations to mixtures perhaps because of the excellent theoretical credentials behind these rules as noted earlier in this chapter. The approximations of Equations (IV-17) and (IV-19A) are applied to Vc_{ij} and $Tc_{ij}Vc_{ij}$, respectively, if and when appropriate mixture data are not available to permit empirical adjustment of the interaction parameters.

A number of such mixing rules have been summarized by Reid and Sherwood [214], many of which can be derived from the Van der Waal form by making simplifying assumptions for the interaction terms Tc_{ij} and Pc_{ij} or Vc_{ij} in terms of the pure component critical properties, or by fixing an empirically derived exponent different from unity on all Tc terms in Equation (IV-78).

The Use of Equations of State in the Calculation of the Thermodynamic Properties of Mixtures

The advantages of complex empirical equations of state such as the BWR over simpler forms like the Van der Waal and Redlich-Kwong equations in representing pure component properties do not extend to the representation of multi-component systems as a function of composition because of the increased difficulty in specifying the composition dependence of the equation of state constants.

The mixing rules for the Starling BWR equation [Equation (III-19)] for example, are presented in Appendix H-1 and are of empirical origin. The original BWR terms use the original BWR mixing rules. The additional terms D_o, E_o, and d for the mixture involve constants that must be determined from binary data. By determining the interaction constants $D_{o_{12}}$ and $E_{o_{12}}$ from the enthalpy data on the 50.6 mole percent methane-propane mixture, the enthalpy behaviour for all five methane-propane mixtures investigated at this facility were predicted to about 1.1 Btu/lb in the single phase region.

In working with the original BWR equation, Tiwari [268] suggested that mixture constants were better defined from the quadratic mixing rule

$$k_m = \sum_{i=1}^{n} \sum_{j=1}^{n} x_i x_j k_{ij} \qquad \text{(IV-81)}$$

where k_m is the mixture constant, if some mixture data were available to permit the empirical specification of the parameter k_{ij}.

The lack of equation of state constants for all systems of interest have lead to the use of simpler analytic forms whose constants are more manageably related to the critical constants of the constituent pure components of the mixture whose properties are desired. The Wilson [279] modified Redlich-Kwong equation is one such popular example and is expressed as

$$P = \frac{RT}{V - \sum_i x_i b_{ii}} - \frac{RT\sum\sum x_i x_j (fb)_{ij}}{V(V + \sum_i x_i b_{ii})} \qquad \text{(IV-82)}$$

where $b_{ii} = 0.0865\ RTc_{ii}/Pc_{ii}$

and $(fb)_{ij} = f(b_{ii}, Tr_{ii}, Tr_{jj}, \omega_{ii}, \omega_{jj}, a_{ij})$

where a_{ij} is an empirical binary interaction coefficient. The phase equilibria and enthalpy predictions are better than one would expect from the simplicity of the equation.

Another interesting approach is due to Vera and Prausnitz [274] who, in effect, combined Equations (IV-5) and (IV-7). z_m^{HS} was represented by the closed form mixture hard sphere equation of state due to Carnahan and Starling [41], while z_m was represented by a complex empirical reduced equation of state expressed in pure component form. The Van der Waal coefficient a_{ij} was then obtained as

$$a_{ij} = RTV_m[z_{ij}^{HS} - z_{ij}^{SG}] \qquad \text{(IV-83)}$$

where the superscript SG stands for the empirical Strobridge-Gosman equation of state [90]. The terms within the brackets were evaluated from independent estimates of the interaction parameters Tc_{ij} and Vc_{ij}. This technique, therefore, ascribes a temperature and density dependence to the term a_m that is constant in the treatment of Snider and Herrington [248] and ingeniously avoids the need to specify mixing rules for the individual constants in the complex empirical SG equation of state. Equation (IV-5) is now no longer restricted in application to liquids at low pressure. The technique was used to fit the phase equilibria of the constituent binaries of the ternary system N_2-O_2-Ar. The agreement was good (within 2% of the observed

mole fractions in the vapor phase). The predictions for the ternary system using the empirically determined constituent binary parameters were equally good. The method, however, has the disadvantage of being, for the present, restricted to mixtures of substances that are strictly conformal in a two parameter framework.

Comparative Studies of Enthalpy Prediction Techniques for Non-Polar Mixtures

The American Petroleum Institute [7] conducted a comprehensive survey of analytical and tabular correlations for both pure and mixed hydrocarbons and recommended the corresponding states approach of Pitzer and co-workers [195,197]. It was cautioned, however, that the paucity of directly obtained mixture enthalpy data at the time could subject their conclusions to reassessment in the future. Since then, the wide ranging mixture enthalpy data on the He-N_2, CH_4-N_2 and the CH_4-C_3H_8 systems obtained at this facility have served as standards for more recent comparison studies.

The recent comparison study of Starling et al. [253] with respect to eight enthalpy correlations, already discussed in Chapter III with respect to the prediction of pure components, also provided results on the calculation of mixture enthalpies. Fifteen mixed systems were examined including the University of Michigan data referred to above, the n C_5H_{12}-n C_6H_{12}, and the n C_5H_{12}-n C_8H_{18} enthalpy data of Lenoir and co-workers [149,150]. The PGC, the 1970 Rice Properties III correlation of Leland and co-workers [81], and the Starling modified BWR equation were measurably superior to the rest in that order, with mean deviations in the enthalpy departure varying from 1.57 Btu/lb to 1.67 Btu/lb, respectively. The performance of the PGC for the light hydrocarbon systems with propane as the heaviest component was spectacular, yielding a mean deviation of 0.7 Btu/lb. The Rice Properties III correlation is slightly superior for the heavier hydrocarbon mixtures again, no doubt because the heavier n-pentane reference that should be more suited to the prediction of these systems than the propane weighted reference tables in the PGC. The authors also concluded that the increased deviations noted for the best methods applied to the heavier systems could be attributed to errors in the

data.

Conclusion

The empirical evidence suggests that the PGC 3 parameter one fluid corresponding states framework appears to be most suited to the representation of the enthalpies of mixtures of light hydrocarbons. Although the examination of a two fluid model is also recommended from more theoretical considerations, the implementation of such a model has been generally avoided in practice, perhaps because it requires us to specify twice as many parameters as for the one fluid case. Also, Powers [202] has already characterized the methane-propane binary in the one fluid PGC framework. Therefore, for our purposes, less additional effort will be involved in adopting his model to predict the enthalpy of the ternary methane-ethane -propane mixture than a two fluid version of the PGC.

Chapter V

THE DEVELOPMENT OF ADDITIONAL MIXING RULES FOR THE PSEUDOCRITICAL METHOD

In Chapter III, it was concluded that the PGC was perhaps the most suitable three parameter corresponding states framework for the representation of the enthalpies of pure non-polar species including the light n-alkanes. In Chapter IV, it was noted that the PGC framework was also a very effective vehicle for the one fluid model representation of enthalpy data of light hydrocarbon mixtures. It was also shown that the estimation of the pseudoparameters for mixtures of substances which are conformal in a two parameter framework could, at least in theory, be best accomplished by mixing rules of the Van der Waal type [Equations (IV-27) and (IV-28)]. This section is concerned with the development of additional procedures for evaluating the pseudocritical constants of multicomponent mixtures from constituent binary data in a three parameter corresponding states framework. First, the basic assumptions necessary for the prediction of mixture properties in the specified framework are stated. Next, in a different approach from that of the previous chapter, the Van der Waal mixing rules are derived by restricting the theory to apply to a two parameter reduced equation of state. A modified reduced Van der Waal equation of state is also used to develop another set of concise mixing rules that incorporate the effect of the third parameter α_c.

A more rigorous procedure for estimating the pseudo parameters for a multicomponent mixture that does not yield concise mixing rules is also presented. Additional considerations and practical difficulties involved in the implementation of the proposed procedure are discussed. In this connection, considerable attention has been paid to the development of two new correlations for the reduced second virial coefficient in the low to moderate temperature region and in the vicinity of the maximum in B, respectively. The application of the developments in this Chapter to the systems investigated in this work is illustrated later in Chapter IX.

The Fundamental Principle in the Calculation of Pseudo-critical Parameters for Mixtures

It has already been indicated in the previous chapter that at any specified temperature, the configurational properties in the dilute gas region for all mixtures belonging to a given binary system may be calculated from experimental information on the configurational properties of the constituent pure components and any one binary mixture. In particular, we recall the relation for the second virial coefficient B_m of the mixture as

$$(B_m)_T = \sum_{i=1}^{n} \sum_{j=1}^{n} x_i x_j (B_{ij})_T \qquad (V\text{-}1)$$

Furthermore, we also recall that if B_{ij} values are also experimentally obtained for all constituent binaries of a multicomponent system at a specified temperature, then the value of B_m for the multicomponent mixture is rigorously known at the same temperature irrespective of marked differences in the nature and complexity of the constituent molecules. Unfortunately, such straight forward predictions for multicomponent systems cannot be invoked elsewhere in the fluid phase. However, if the calculated B_m values from Equation (V-1) can be coupled with a corresponding states framework with the expressed purpose of generating pseudocritical constants for a given mixture, then such information can be valuably utilized in predicting the configurational properties of the same mixture in the single phase region over the entire P-T plane. We next examine the additional restrictions that must be imposed on the intermolecular forces between all molecules in such a mixture if the procedure is to be justified.

The Basic Assumptions

I) It is assumed that all the constituent components of the mixture are restricted to a class of substances whose potentials are conformal in three parameters ε_{ii}, σ_{ii} and αc_{ii}.

$$u_{ii}\left(\frac{r}{\sigma_{ii}}\right) = \varepsilon_{ii} F\left(\frac{r}{\sigma_{ii}}, \alpha c_{ii}\right) \qquad (V\text{-}2)$$

It follows that the macroscopic configurational properties and

in particular the second virial coefficient, the compressibility factor and the residual enthalpy can all be represented by suitable three parameter corresponding states functions.

$$\frac{B_{ii}}{RTc_{ii}/Pc_{ii}} = f_B\left(\frac{T}{Tc_{ii}}, \alpha c_{ii}\right) \tag{V-3}$$

$$z_{ii} = f_z\left(\frac{T}{Tc_{ii}}, \frac{P}{Pc_{ii}}, \alpha c_{ii}\right) \tag{V-4}$$

$$\mathcal{H}_{ii} = f_{\mathcal{H}}\left(\frac{T}{Tc_{ii}}, \frac{P}{Pc_{ii}}, \alpha c_{ii}\right) \tag{V-5}$$

where f_B, f_z and $f_{\mathcal{H}}$ are universal functions, and Tc_{ii}, Pc_{ii} and αc_{ii} are the pure component critical parameters that can be unequivocally defined by direct measurement.

II) It is further assumed that the intermolecular forces between all unlike pairs in the mixture are conformal in the same sense. Thus

$$u_{ij}\left(\frac{r}{\sigma_{ij}}\right) = \varepsilon_{ij} F\left(\frac{r}{\sigma_{ij}}, \alpha c_{ij}\right) \tag{V-6}$$

Consequently, we are able to write

$$\frac{B_{ij}}{RTc_{ij}/Pc_{ij}} = f_B\left(\frac{T}{Tc_{ij}}, \alpha c_{ij}\right) \tag{V-7}$$

where it must be emphasized again that the unlike pair parameters Tc_{ij}, Pc_{ij} and αc_{ij}, cannot be uniquely specified by direct experimental measurements in contrast to the pure component case.

III) From the standpoint of the macroscopic consequences of the intermolecular forces in a mixture, it is assumed that all the different species in the mixture may be effectively replaced by a hypothetical pure species, the molecules of which interact according to a potential function conformal with that of Equation (V-2) for some optimum choice of the potential parameters ε_m, σ_m and α_m. Therefore

$$u_m = \varepsilon_m F\left(\frac{r}{\sigma_m}, \alpha c_m\right) \tag{V-8}$$

Also, we obtain as before

$$\frac{B_m}{(RTc_m/Pc_m)} = f_B\left(\frac{T}{Tc_m}, \alpha c_m\right) \qquad (V\text{-}9)$$

$$z_m = f_z\left(\frac{T}{Tc_m}, \frac{P}{Pc_m}, \alpha c_m\right) \qquad (V\text{-}10)$$

$$\mathcal{M}_m = f_{\mathcal{M}}\left(\frac{T}{Tc_m}, \frac{P}{Pc_m}, \alpha c_m\right) \qquad (V\text{-}11)$$

IV) In consequence of the above assumptions, if B_m values for multicomponent mixtures are calculated from experimental B_{ij} values for all constituent binary pairs over a wide range of temperatures, then it is, at least in theory, possible to extract the parameters Tc_m, αc_m and Pc_m for the mixture from Equation (V-9), and apply these values in Equations (V-10) and (V-11) to calculate z_m and $\mathcal{M}_m$ at any T and P in the single phase region. The suggested procedure is theoretically rigorous within the restrictions imposed by the three previous basic assumptions.

Rigorous Procedure for Evaluating Unlike Pair Interaction Parameters

Our only recourse in evaluating the validity of assumption II is to work with reducing parameters that are directly and unequivocally determinable from interaction second virial coefficient data. For example, the following procedure may be suggested.

a) Determine Tb_{ii}/Tc_{ii}, and $Vb_{ii}/(RTc_{ii}/Pc_{ii})$ for each of the conformal pure components where Tb_{ii} and Vb_{ii} are the Boyle temperature and Boyle volume, respectively, obtained from direct measurements on second virial coefficients.

b) Determine the value of the reduced second virial coefficient $B_{ii}/(RTc_{ii}/Pc_{ii})$ for each of the pure components at some low temperature that is a specified fraction of the Boyle temperature, i.e. at k(Tb), (k<1).

c) Correlate all three reduced variables as a function of αc_{ii}

$$\frac{Tb_{ii}}{Tc_{ii}} = G(\alpha c_{ii}) \qquad (V\text{-}12)$$

$$\frac{Vb_{ii}}{RTc_{ii}/Pc_{ii}} = H(\alpha c_{ii}) \qquad (V\text{-}13)$$

$$\left[\frac{B_{ii}}{(RTc_{ii}/Pc_{ii})}\right]_{T = k(Tb)} = K(\alpha c_{ii}) \qquad (V\text{-}14)$$

d) Measure Tb_{ij}, Vb_{ij} and B_{ij} at $T = k(Tb)$ for each i-j pair using interaction second virial coefficient data, and solve for Tc_{ij}, RTc_{ij}/Pc_{ij}, and αc_{ij} using the above three equations.

e) Substitute these parameters into Equation (V-3), and determine if the calculated reduced second interaction virial coefficients agree with those obtained from measured B_{ij} values over the entire range of the data, and in particular outside the limits $k(Tb) < T \leq Tb$.

Difficulties in Implementing the Rigorous Procedure

Unfortunately, experimental second virial coefficient data for pure n-alkanes heavier than methane do not extend to high enough reduced temperatures (>2.3 Tr) to permit the evaluation of the Boyle parameters. Furthermore, it is highly unlikely that such evidence may ever be obtained for the heavier hydrocarbons before the onset of thermal decomposition. Also, the specification of the Boyle parameters for any unlike pair interaction would require some mixture data to be available in the high temperature range. Therefore, it is apparent that establishing the identity of the function

$$\frac{B}{Vb} = g(T/Tb) \qquad (V\text{-}14a)$$

for both like and unlike pair interactions, in mixtures where all pair interactions are suspected to be conformal, is virtually beyond experimental corroboration.

Douslin and Harrison [65] have established the validity of the function (V-14a) for the pure components CH_4, CF_4, Ar, and Kr over the range $0.55 \leq T/Tb \leq 1.2$. It was determined that the second interaction virial coefficients for the system CH_4-CF_4 also subscribed to the same

function over the same range of T/Tb. To the best of this authors knowledge, this is the only case where enough experimental measurements have been obtained to allow the conformality of all pair interactions in a mixed system to be tested. The result is significant because the αc value of CF_4 is considerably different from that of CH_4, and approximately equal to that of n-C_4H_{10} in the n-alkane series.

The main purpose of the above arguments is to suggest that, in the absence of conclusive experimental evidence for other non-polar mixtures of interest, it is not unreasonable to assume that the function f_B in Equations (V-3) and (V-7) are the same, particularly if the span of αc values for the various components in the given mixture are smaller than for the CH_4-CF_4 system.

The Calculation of Mixture Pseudoparameters from the Van der Waal Equation of State

For illustrative purposes, we now apply the suggested procedure governed by assumptions I through IV to the limiting case when the reference generalized equation of state given by Equations (V-4) and (V-13) is replaced by the reduced two parameter Van der Waal equation of state. If the criteria

$$\left(\frac{\partial P}{\partial V}\right)_{T=Tc} = 0 \qquad \text{(V-15)}$$

$$\left(\frac{\partial^2 P}{\partial V^2}\right)_{T=Tc} = 0 \qquad \text{(V-16)}$$

are applied to the Van der Waal equation of state we obtain the result [165]

$$P = \frac{RT}{(V-Vc/3)} - \frac{9}{8}\frac{R\,Tc\,Vc}{V^2} \qquad \text{(V-17)}$$

The second virial coefficient for both like and unlike interactions is then obtained from the above equation as

$$B_{ij} = \frac{Vc_{ij}}{3} - \frac{9}{8}\frac{Tc_{ij}\,Vc_{ij}}{T} \quad \text{all } i,j \qquad \text{(V-18)}$$

By combining Equations (V-1) and (V-18) we can obtain the Van der Waal

mixing rules expressed by Equations (IV-77) and (IV-78), respectively.

a) The Modified Van der Waal Mixing Rules. If, for example, we apply the criteria

$$\left(\frac{\partial P}{\partial V}\right)_{T=Tc} = 0 \qquad \text{(V-19a)}$$

$$\left(\frac{d \ln P}{d \ln T}\right)_{V=Vc} = \alpha c \qquad \text{(V-19b)}$$

to the Van der Waal equation of state instead of Equations (V-15) and (V-16) we obtain the mixing rules

$$\frac{Tc_m}{Pc_m}\left(\frac{\alpha c_m - 2}{\alpha c_m^2}\right) = \sum_{i=1}^{n}\sum_{j=1}^{n} x_i x_j \left[\frac{Tc_{ij}}{Pc_{ij}}\left(\frac{\alpha c_{ij} - 2}{\alpha c_{ij}^2}\right)\right] \qquad \text{(V-20)}$$

$$\frac{Tc_m^2}{Pc_m}\frac{(\alpha c_m - 1)^3}{\alpha c_m^4} = \sum_{i=1}^{n}\sum_{j=1}^{n} x_i x_j \left[\frac{Tc_{ij}^2}{Pc_{ij}}\frac{(\alpha c_{ij} - 1)^3}{\alpha c_{ij}^4}\right] \qquad \text{(V-21)}$$

These rules are derived in Appendix G, and illustrate, typically, the procedure for obtaining mixing rules from two parameter reduced equations of state. By fitting the slope of the real fluid critical isochore at the critical point to the Van der Waal equation of state, we have been able to develop a mixing rule in a two parameter framework that involves the third parameter αc, and which must, at least in theory, be considered more attractive than the original Van der Waal mixing rules for use in a three parameter framework. However, a third independent relationship between the pseudocritical parameters Tc_m, Pc_m and αc_m is still necessary to specify each of them uniquely. The empirical rule

$$\alpha c_m = \sum_{i=1}^{n}\sum_{j=1}^{n} x_i x_j \alpha c_{ij} \qquad \text{(V-22)}$$

is invoked to satisfy this requirement for both sets of rules. This form is equivalent to the Pitzer-Hultgren rule for the third parameter ω_m shown as Equation (IV-76), if the linear relationship between the parameters αc and ω is recognized from Equation (III-32). Other mixing rules similar to Equations (V-20) and (V-21) may be obtained either by starting with a different two parameter equation of state, or by

choosing different criteria for defining the reduction parameters.

b) The Practical Utilization of Mixing Rules of the Van der Waal Type. None of the rules discussed so far can be implemented unless the interaction parameters Tc_{ij}, Vc_{ij} (or equivalently RTc_{ij}/Pc_{ij}), and αc_{ij} are first defined. The most rigorous way to accomplish this, without destroying the consistency with the original model in each case, is to fit B_{ij} data ($i \neq j$) to the specific reduced second virial coefficient function f_B that is used to generate the rules. Figure (V-1) compares the reduced second virial coefficient B/Vc of a non-polar spherically symmetric classical fluid as a function of Tr [145] with the calculated results from Equation (V-18), and from a combination of Equations (G-8) and (G-14) in Appendix G. The latter curve originates from the modified Van der Waal equation of state discussed above and is seen to be slightly superior to Equation (V-18) in representing real systems.

However, given B_{ii} data for real pure components, it is unlikely that the parameters Tc_{ii} and Vc_{ii} calculated from the best fit to either of the dashed curves in Figure (V-1) will be in strict agreement with the values obtained by direct measurement of pure component critical properties. This point is raised because Tc_{ij} and Vc_{ij} ($i \neq j$) cannot be measured directly and we need to find an attractive indirect technique to specify them. It may be anticipated that the technique proposed in the previous paragraph would not be very effective because neither of the dashed curves in Figure (V-1) can accurately represent real pure component data.

Recognizing the inadequacies of the Van der Waal and other two parameter equations of state, but impressed by the conciseness of the mixing rules that can be derived from them, it is reasonable to ask why attempts have not been made to generate concise mixing rules starting with empirical representations of the function f_B in Equation (V-3) that more accurately represent real data. The reason for this is that most of these functions have more than two constants, and do not lend themselves to the manipulations, typified in Appendix G, that will permit the straight forward extraction of mixing rules which directly relate the pseudocritical parameters of the mixture to the

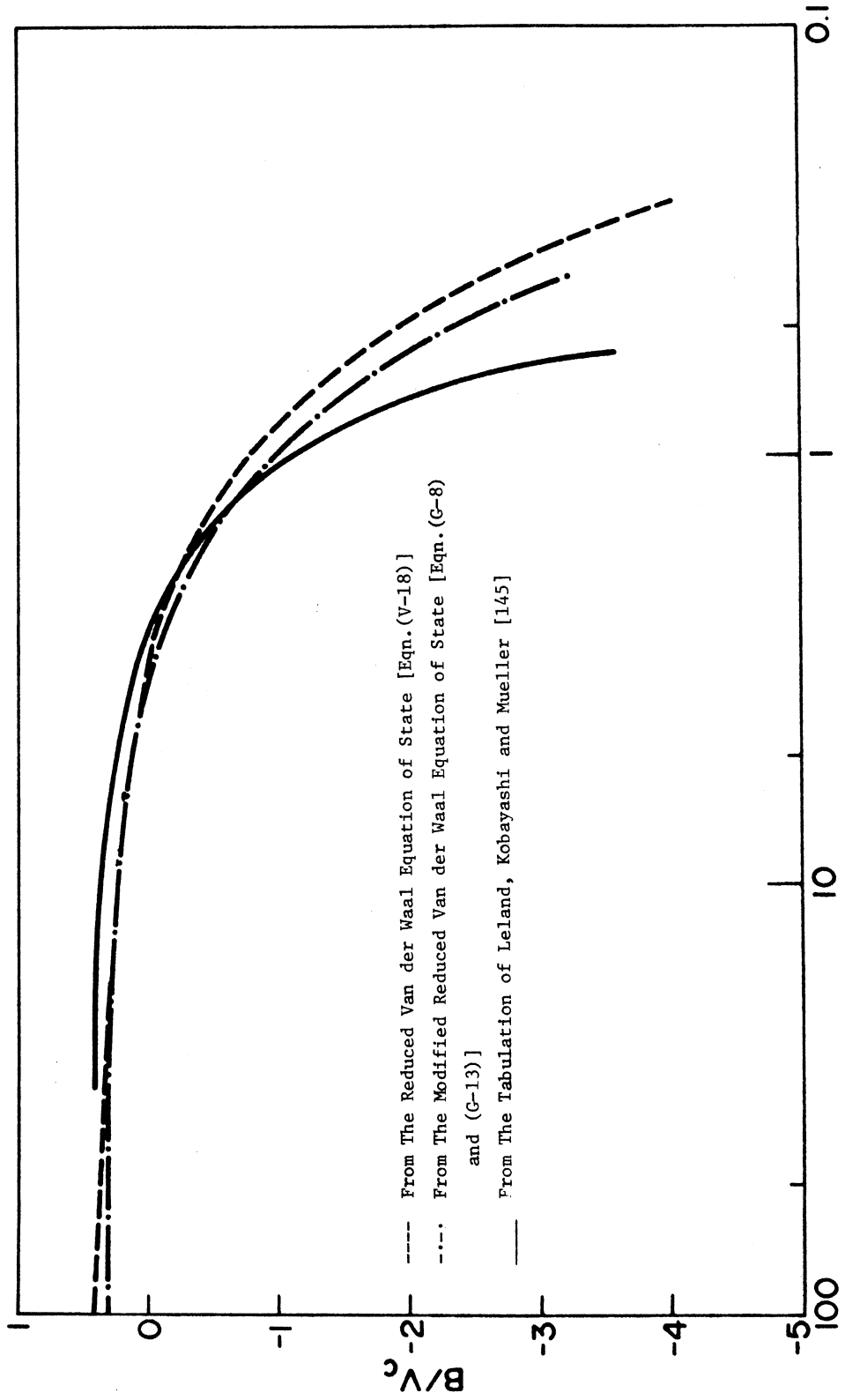

Figure V-1. The Reduced Second Virial Coefficient as a Function of Reduced Temperature for a Classical Spherically Symmetric Fluid.

composition and the constituent pair interaction parameters.

Another approach, somewhat less defensible in theory, but more successful in practice, is to fit experimental measurements on binary mixtures to the appropriate reduced thermodynamic functions defined by Equations (V-9), (V-10) and (V-11). The set of pseudoconstants Tc_m, Pc_m and αc_m generated for the best fit case may then be used together with the pure component critical properties to calculate the appropriate unlike pair parameters directly from some specified set of concise mixing rules, say for example, the rules expressed by Equations (V-20) through (V-22). Once all such unlike pair interactions have been determined from binary data, the mixing rules provide a concise technique for calculating the pseudoparameters, and hence the thermodynamic properties of multicomponent systems. Such procedures were indeed used by Pitzer and Hultgren [197], and Yesavage [284] to define binary interaction constants for other more empirical mixing rules from wide ranging volumetric and enthalpy data, respectively.

Difficulties Involved in Using Second Virial Coefficient Data to Obtain Pseudocritical Parameters

It is difficult to specify pseudocritical or interaction parameters solely from second virial coefficient measurements. The second virial coefficient is well known to be relatively insensitive to the form and details of the intermolecular function chosen to characterize the pair interaction [188]. Even if we were to specify an accurate empirical function f_B in Equation (V-3), the parameters for the optimum fit to pure component B data, for example, would not necessarily coincide with the true critical parameters unless the experimental measurements were to extend from at least 0.5Tc to 6Tc. B_m values for a multi-component mixture are, therefore, to be specified over approximately the same range of reduced temperatures if the "correct" pseudoparameters are to be extracted from the best fit to the specified function f_B. As the technique requires Equation (V-1) to determine the set of B_m values to be used, it is apparent that we will need B_{ij} data below 0.5 Tc_{ij} for interactions where $Tc_{ij} < Tc_m$, and above 6.0 Tc_{oj} for interactions where $Tc_{ij} > Tc_m$. Thus, the effective reduced

temperature range over which direct measurements are required to characterize the mixture pseudoparameters can be considerably broader than that required to determine the reduction parameters for the pure component case alone.

There are few pure compounds for which such wide ranging measurements are available in the literature. The situation is even worse with respect to measurements on unlike pairs. If, for example, we consider a multicomponent methane-ethane-propane mixture, the limited range of the constituent binary interaction virial coefficient data would probably not permit more than one pseudocritical parameter to be significantly optimized, forcing the other two parameters to be predetermined from mixing rules bases strictly on the constituent pure component parameters. Prausnitz and Gunn [206], for example, obtained Tc_{ij} ($i \neq j$) from a best fit to B_{ij} data using the reduced second virial coefficient correlation of Pitzer and Curl [Equations (III-40) through (III-42)], after having previously fixed ω_{ij} and Vc_{ij} from simplifying rules involving only pure component parameters.

Proposed Scheme for Calculating Mixture Pseudoparameters from Enthalpy Data

We now consider another approach for the calculation of B_m values for a multi-component mixture based on the indirect calculation of B_{ij} as a function of temperature for each of the constituent unlike pair interactions. From the considerations in Chapter IV, it appears that, given accurate wide ranging enthalpy data on a light hydrocarbon mixture, there exist suitable empirical representations of the function f_H in Equation (V-5) or (V-12), such as the PGC, that will define a pseudocritical parameter set for the mixture with reasonable selectivity. If it is further assumed that these pseudoparameters are also applicable to Equation (V-9), then the B_m values for the mixture may be calculated from a suitable function f_B over some fixed temperature range. The constituent pure component virial coefficients can also be calculated over the same range using the same function f_B as defined in Equation (V-5). If the mixture is restricted to two components, then B_{ij} values for the unlike pair interaction may now be computed over the same fixed temperature range using Equation (V-1).

The B_{ij} values as a function of temperature may be similarly computed for all the constituent unlike pair interactions in a multi-component mixture by obtaining and processing the enthalpy data on at least one binary mixture in each case. Reapplication of Equation (V-1) to the multi-component mixture yields the desired set of B_m values as a function of temperature. Equation (V-9) may now be used to evaluate the required parameters Tc_m, Pc_m and αc_m. The set of B_{ij} values determined for each i-j pair by this technique is now limited only by the range of of applicability of the function f_B and should extend considerably beyond the temperature range of direct measurements in almost all cases. A schematic of the proposed technique for the prediction of the enthalpies of a ternary mixture from the minimum amount of constituent binary enthalpy data is shown in Figure (V-2).

An important consequence of this technique is that it permits a direct comparison between experimentally determined B_{ij} values ($i \neq j$) when available, with results synthesized from wide ranging enthalpy data. Similar procedures could be invoked to obtain synthesized B_{ij} values as a function of temperature from other thermodynamic measurements; for example, using volumetric data in the liquid and dense fluid region. The consistency between such independently obtained values of B_{ij} as a function of temperature can then serve as a measure of the validity of the one fluid corresponding states model for mixtures of conformal substances. From the discussion in Chapter IV it may be anticipated that as the mixture becomes less random (as the size and energy parameter ratios for the various molecular species in the mixture depart from unity), the validity of the assumption should be more questionable and we may anticipate this to be reflected as an increased disparity between the independent B_{ij} sets obtained as above.

It is conceivable, however, that even though the assumption of Equation (V-11) may be valid, any <u>one</u> of the three functions f_B, f_Z and f_H in Equations (V-9) through (V-11) may not by itself be sufficiently selective enough to be able to generate from the appropriate configurational property precisely <u>those</u> pseudoparameters Tc_m, Pc_m and αc_m that can satisfy the conditions expressed by <u>all three</u> equations simultaneously. The desired parameter set will

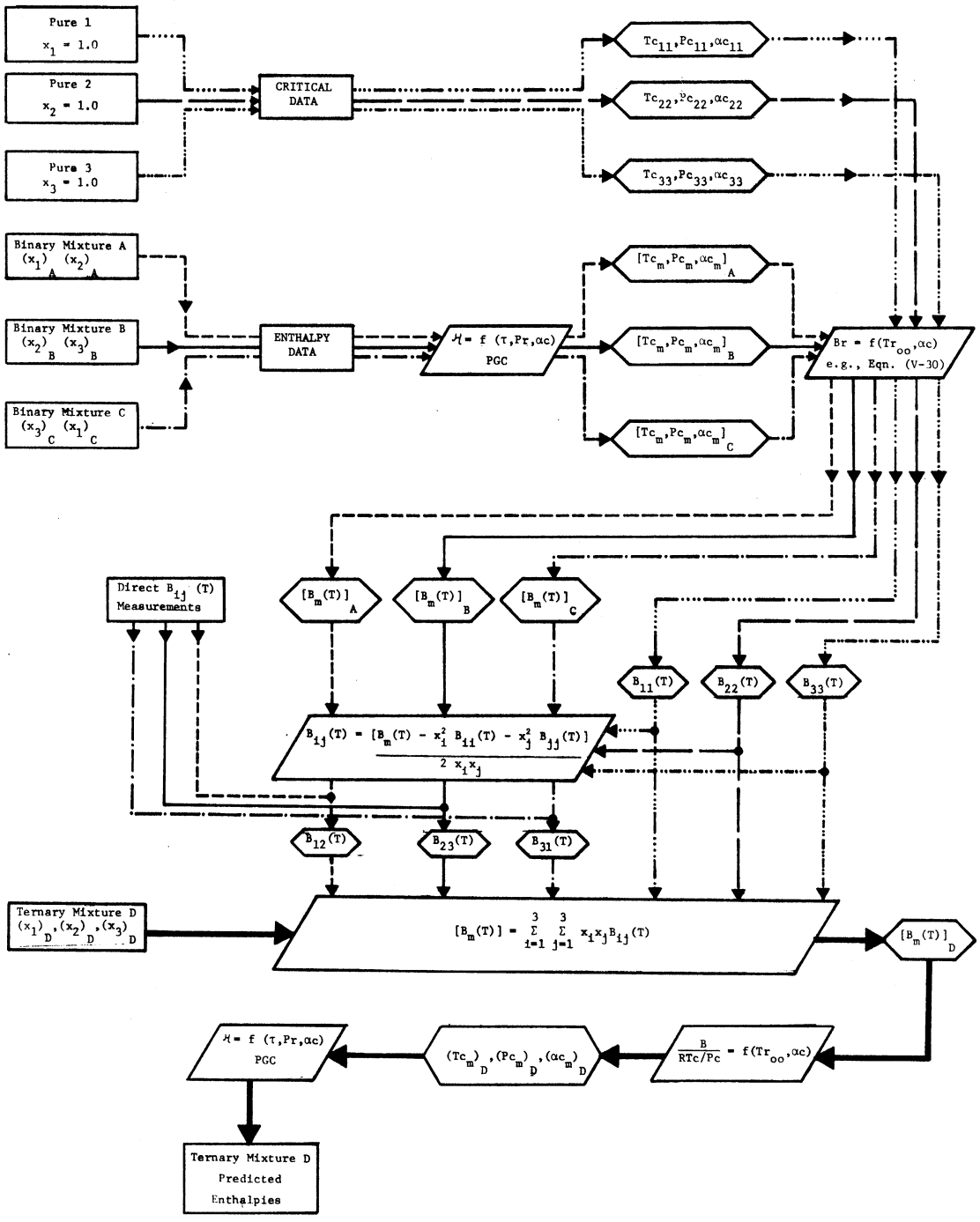

Figure V-2. Schematic of Proposed Scheme for Defining Pseudo-Critical Parameters for Multi-Component Mixtures.

hitherto be referred to as the "meaningful" set. In general, one can expect a particular configurational property to be most sensitive to the optimization of those pseudoparameters that are used to express it in reduced form. Given B_m data for example, we see from Equation (V-3) that the optimization should be uniformly sensitive to the reduction factor RTc_m/Pc_m regardless of the functional dependence of f_B on Tc_m and ωc_m. Similarly, an optimization using reduced enthalpies can be expected to be more selective of the pseudocritical temperature, Tc_m, as was verified by Yesavage [284] for several methane-propane mixtures. These considerations reveal that the success of the proposed procedure will depend very heavily upon our ability to extract meaningful pseudocritical parameters at every optimization step. Furthermore, if our primary objective is to be able to predict the enthalpy of mixtures, then we particularly need to obtain an accurate value of Tc_m. Unfortunately, it must be acquired from a property [Equation (V-9)] that is not particularly suited to this end. This suggests, therefore, that a critical factor in the performance of the proposed technique is the accuracy and temperature range of validity of the function f_B, and our ability to extract the correct value of Tc_m from a set of B_m values using the function.

Selection of a Method for the Representation of the Second Virial Coefficient in a Corresponding States Framework

Although we seek to select a function f_B that is universally suitable for the representation of the seconf virial coefficient of non-polar substances, it is more important that it satisfy the specific objective of representing the experimental measurements on methane, ethane and propane as our test multi-component mixture is composed of these components. The deficiencies of the existing three parameter correlations of Pitzer and Curl [196] and McGlashan and Potter [159] in this regard have already been noted in Chapter III from which it may be concluded that the development of a more accurate correlation is desirable.

The plan of attack is to develop a reduced correlation for some spherically symmetric non-polar substance, and to express the reduced second virial coefficients, Br, of other substances as a perturbation

about the reference fluid values using the third parameter αc as the perturbation variable.

a) Representation of the Reference Fluid: Methane. Methane was selected as the reference fluid in view of the availability of direct measurements over the extended reduced temperature range $0.58 < Tr < 3.26$. Furthermore, precise independent measurements [28,35,67,108,200] are in excellent agreement down to 190K. Below this temperature there appears to be significant differences between the precise measurements of Pope [200] and Byrne et al. [35] reaching a maximum of 6% at about 125K. The measurements from all sources were fitted by the empirical equation

$$\frac{B}{RTc/Pc} = 0.14416 - 0.49095(1-e^{0.6851/Tr}) \qquad \text{(V-23)}$$

The functional form of the above equation is dictated by the result obtained for the square well potential [167] of Equation (III-4), the theoretically equivalent parameters for which are given by

$$\sigma^3 = \frac{(0.14416)}{(2\pi/3)\,N_o}\left(\frac{RTc}{Pc}\right) \qquad \text{(V-23a)}$$

$$\frac{\varepsilon}{k} = 0.68511\,Tc \qquad \text{(V-23b)}$$

$$\left[1 - \left(1 + \frac{L}{\sigma}\right)^3\right] = \left[\frac{0.49095}{(2\pi/3)\,N_o\sigma^3}\right]\left(\frac{RTc}{Pc}\right) \qquad \text{(V-23c)}$$

where L is the well width. The constants in Equation (V-23) were obtained by a non-linear regression analysis. Although there are many experimental determinations of the second virial coefficient of methane, only those sources that were deemed to be precise were used in this work. With the exception of the data of Pope below 198.15K, the absolute average deviation for all measurements was under 0.6%. (See the bottom entry in Table V-1).

b) Representation of Substances with αc Values Different from Methane. Next, several hydrocarbons from ethane to n-octane, the inert gases Ar and Kr, and also CF_4 were examined to determine the

TABLE V-1

Summary of Results for the Reduced Second Virial Coefficient Correlation [Equation (V-30)] of This Work

System	Investigator	Reduced Temp. Range Low	Reduced Temp. Range High	No. of Points N	Mean Value of B cc/gm mole	Abs.* Avg. Dev. cc/gm mole	Abs. Avg. Dev. %	** % Bias	Reference
C2H6	POPE	.69	1.00	6.	216.6	7.5	3.4	+3.4	[200]
	MICHELS	.98	1.38	7.	141.8	1.1	0.8	+0.7	[174]
	DIAZ PENA	.65	1.63	13.	174.5	6.6	3.8	-3.2	[61]
	GUNN	1.23	1.67	3.	83.5	1.9	2.2	-0.7	[94]
C3H8	MCGLASHAN	.80	1.11	12.	278.2	7.4	2.7	+2.7	[159]
	KUNZ	.74	.86	3.	404.2	3.3	0.8	+0.4	[136]
	KAPALLO	.52	1.40	15.	464.4	4.4	1.0	-0.1	[122,123]
	DIAZ PENA	.68	1.48	13.	229.8	2.5	1.1	-0.4	[61]
	SILBERBERG	.66	.94	6.	448.3	6.0	1.3	-0.2	[240]
		1.00	1.48	9.	169.5	2.8	1.6	-1.6	[16]
	DESCHNER	.82	1.54	6.	223.6	10.3	4.6	-4.6	[60]
n-C4H10	BOTTOMLEY	.64	1.00	7.	644.4	19.5	3.0	-3.0	[27]
	KAPALLO	.57	1.00	6.	788.7	51.3	6.5	-6.5	[122]
	MCGLASHAN	.69	.97	11.	478.3	9.3	1.9	+1.8	[159]
n-C5H12	MCGLASHAN	.63	.88	11.	837.7	15.6	1.8	-1.1	[159]
	DIAZ PENA	.64	1.07	9.	649.7	11.4	1.7	-0.6	[61]
i-C5H12	SILBERBERG	.59	1.00	7.	888.1	29.3	3.3	-3.3	[241]
n-C8H18	MCGLASHAN	.65	.72	10.	1841.0	88.7	4.8	-4.8	[159]
CF4	DOUSLIN	1.20	2.73	9.	48.6	0.9	1.9	-1.4	[66]
	LANGE	.89	1.61	6.	128.6	4.0	3.1	+2.9	[137]
A	BYRNE	.57	1.80	18.	134.9	2.3	1.7	+1.7	[35]
KR	BYRNE	.56	1.20	12.	208.1	6.6	3.2	+3.0	[35]
	BREWER	.58	1.54	8.	127.3	4.4	3.4	+1.9	[28]
CH4	BYRNE, HOOVER, BREWER, DOUSLIN	.58	3.26	42.	104.5	0.6	0.6	0.0	[35] [108] [28] [67]
	POPE	.66	1.00	6.	175.4	5.2	2.9	+2.9	[200]

* $\frac{\sum_N |B - B_{cal}|}{N}$

** $\frac{\sum_N B - B_{cal}}{B\ N}$

effect of the third parameter αc. It was decided to use a modified reduced temperature parameter Tr_{oo} to correlate these measurements in view of the singular success obtained by Powers [204] using a similar approach in the correlation of pure component enthalpy data of non-polar compounds. The modified reduced temperature Tr_{oo} for a substance at reduced temperature Tr has already been defined on page 52. This approach is identical to that of Powers who suggests the parameter τ defined in Chapter III. The change in parameter was motivated by the belief that readers will have a better "feel" for the concept of a modified reduced temperature Tr_{oo} than for the parameter τ.

Heavy reliance was placed on the propane data in defining the function for several reasons. Firstly, its αc value is significantly different from that of methane. Secondly, the data extend to low reduced temperatures, ($Tr \leq 0.5$), and thirdly, since heavy reliance was placed on the propane measurements in defining the PGC enthalpy framework, it was felt that maximum consistency between the two correlations would be achieved. As measurements on propane were not available above 1.54 Tr, the precise measurements of Douslin et al. [66] on CF_4 extending to 2.73 Tr were emphasized in this range.

We now explain the first but somewhat abortive approach to the problem. The data for the substances examined were individually fit to the form

$$Br = a + b(1 - e^{c/Tr_{oo}}) \tag{V-24}$$

the rationale being that the constants a, b, and c could then be redefined as functions of $(\alpha c - \alpha c_{oo})$

$$\frac{B}{(RTc/Pc)} = 0.14416 + h(\alpha c-\alpha c_{oo}) + [0.49095 + k(\alpha c-\alpha c_{oo})][1-e^{\{0.68511 + g(\alpha c-\alpha c_{oo})\}/Tr_{oo}}] \tag{V-25}$$

where h, k and g are the functions to be specified, and αc_{oo} is the αc value for methane. The equation reduces to Equation (V-23) if $\alpha c \rightarrow \alpha c_{oo}$. The empirically observed and theoretically predicted restriction

$$\left(\frac{B}{RTc/Pc}\right)_{Tr_{oo},\alpha c} \rightarrow \left(\frac{B}{RTc/Pc}\right)_{Tr_{oo},\alpha c_{oo}} \text{ as } Tr_{oo} \rightarrow 1.0 \tag{V-26}$$

discussed in Chapter IV leads to the constraint

$$h(\alpha c-\alpha c_o) + k(\alpha c-\alpha c_{oo}) \left[1-e^{\{0.68511 + g(\alpha c-\alpha c_{oo})\}}\right] = 0 \qquad \text{(V-27)}$$

Most of the measurements were obtained over restricted temperature ranges. Furthermore, the reduced temperature range of the data varied considerably from one substance to the next. Consequently, values of a, b, and c for the individual compounds obtained in this manner were not specific enough to permit them to be reasonably correlated as functions of $(\alpha c - \alpha c_{oo})$.

The next approach was to select a functional relationship of the form

$$Br(Tr_{oo}) = Br_{oo}(Tr_{oo}) + \left[\frac{dBr}{d\alpha c}(Tr_{oo})\right]\left[\alpha c - \alpha c_{oo}\right] \qquad \text{(V-28)}$$

involving a linear dependence on $(\alpha c - \alpha c_o)$ where Br_{oo} is given by the right hand side of Equation (V-23). The slope function $(dBr/d\alpha c)$ was determined by investigating the quantity

$$[Br(Tr_{oo}) - Br_{oo}(Tr_{oo})]/(\alpha c-\alpha c_{oo}) \qquad \text{(V-29)}$$

as a function of Tr_{oo} for various compounds. This technique, unlike the previous one, has the advantage of allowing accurate data for various compounds in different regions of reduced temperature to be investigated on a common basis. The final result given by the expression

$$\frac{B}{(RTc/Pc)} = 0.14416+0.49095(1-e^{0.68511/Tr_{oo}}) + (\alpha c-5.82)\left(0.0175 - \frac{0.0220}{Tr_{oo}} - \frac{0.00614}{Tr_{oo}^2} + \frac{0.00281}{Tr_{oo}^3}\right) \qquad \text{(V-30)}$$

was obtained, where the last bracketed term in the above equation is a representation of the slope function in analytic form.

Figure V-3 shows a plot of Br for methane, ethane and propane as a function of Tr_{oo} designated as Tr_{CH_4} to indicate the use of methane as a reference fluid. The dotted line shows the smoothed location of the propane data using the actual reduced temperature Tr as the independant variable instead. The separation between the Br

Table V-2

Comparison of Second Virial Coefficient Correlations with Respect to Methane and Propane

Species	T	Tr	Tr_{oo}	B_{Expt}	B(I)	B(II)	B(III)	B(IV)	ϕ(I)	ϕ(II)	ϕ(III)	ϕ(IV)
					cc/gm. mole				Btu/lb/psia			
Methane	116.79	0.612	0.612	-295.5	-284.6	-284.0	-296.5	-311.9	-0.1483	-0.1468	-0.1609	-0.1757
	191.06	1.002	1.002	-116.3	-114.7	-113.5	-115.3	-116.0	-0.0624	-0.0625	-0.0633	-0.0647
	298.15	1.563	1.563	-42.1	-42.6	-41.7	-43.0	-44.3	-0.0291	-0.0285	-0.0290	-0.0282
	623.4	3.269	3.269	+9.7	+11.1	+9.3	+10.1	+5.1	-0.0060	-0.0056	-0.0061	-0.0064
Propane	244.0	0.660	0.627	-610.29	-618.6	-599.6	-610.2	-658.3	-0.1343	-0.1309	-0.1295	-0.1475
	369.97	1.000	1.000	-260.0	-250.6	-245.1	-248.8	-252.2	-0.0547	-0.0516	-0.0542	-0.0561
	523.16	1.414	1.476	-100.0	-104.8	-111.9	-105.0	-109.9	-0.0278	-0.0262	-0.0275	-0.0263

Key I - McGlashan and Potter [Eqn. (III-43)]

II - Pitzer and Curl [Eqn. (III-40, III-41, III-42)]

III - This Work [Eqn. V-30)]

IV - Starling BWR [Appendix H-1]

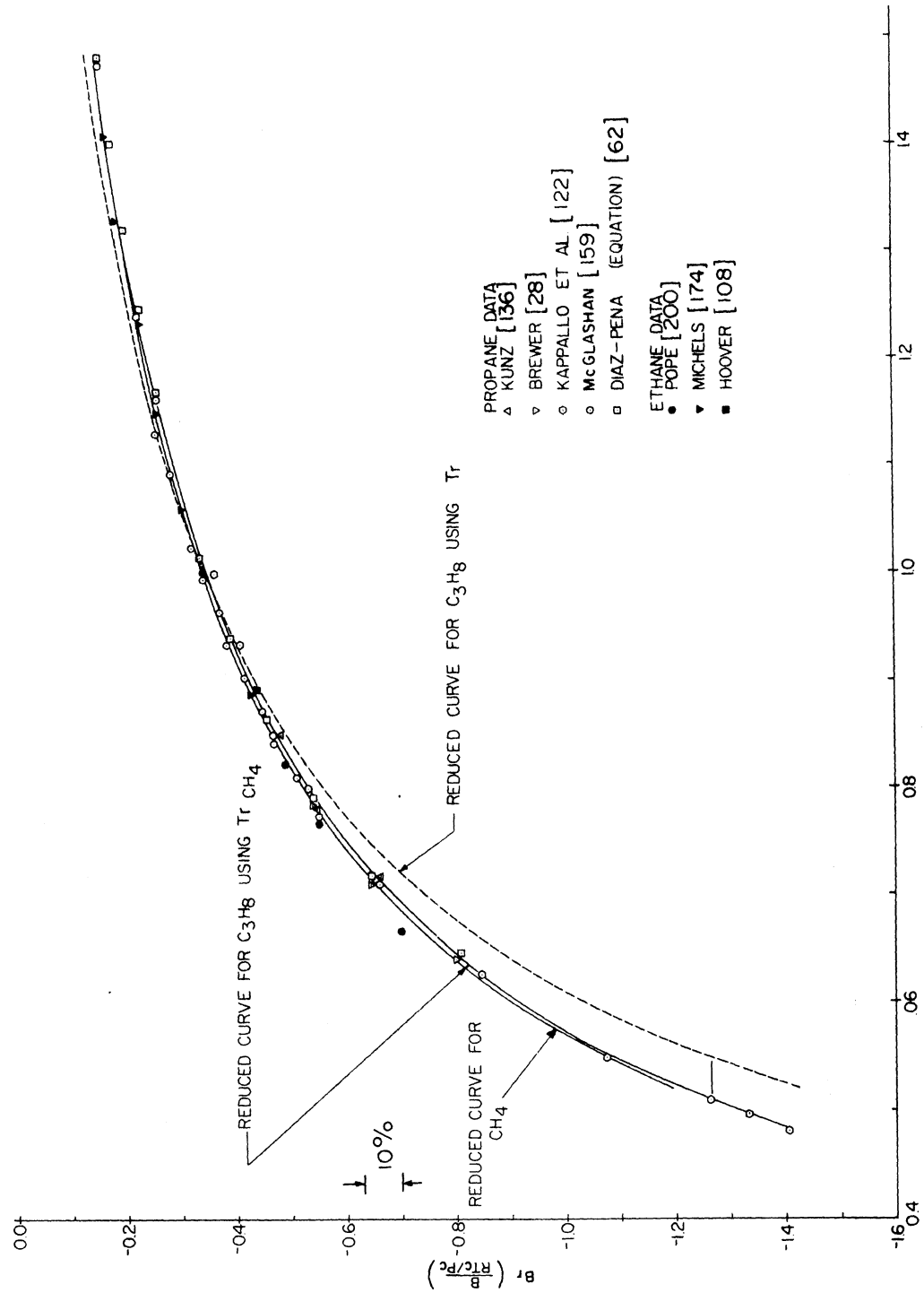

Figure V-3. The Reduced Second Virial Coefficient as a Function of the Modified Reduced Temperature Tr_{CH_4} for Methane, Ethane and Propane.

curves for the two substances is seen to be much smaller in the first case. A comparison between the equation and the measurements for the systems examined is summarized in Table V-1. The literature data on individual n-alkanes has also been examined and smoothed by Diaz-Pena [61,62] using a polynomial function in each case. The equation has also been compared with these smoothed values. Relevant critical properties for the substances examined are summarized in Table J-1, most of which were obtained from tabulations by Reid and Sherwood [214]. The results of Table V-1 are further amplified in Table J-3.

c) Performance of the Correlation. For the light hydrocarbons upto n-butane, the correlation is better than the scatter of the data around it. The precise measurements on methane and ethane obtained at Rice University [108,200] are consistently less negative at low reduced temperatures ($T_r < 1.0$) than predicted by the equation which appears to fit the other measurements more satisfactorily. We recall from Chapter III that similar trends with respect to the Rice University data were also observed for the correlation of Pitzer and Curl [196] and this observation was in part used to justify the need for improving upon the correlation. Thus, the two equations are less dissimilar than was originally anticipated. The predictions for propane at various reduced temperatures using Equations (III-40), (III-43) and (V-2) are compared in Table V-2. The values of ω and n in the first two of these equations were expressed in terms of α_c using Equations (III-32) and (III-43a), respectively, for the sake of uniformity. Values of the isothermal throttling coefficient $(\partial H/\partial P)_T$ at zero pressure were also calculated in each case using the identity

$$\left(\frac{\partial H}{\partial P}\right)_{T,P=0} \equiv \left(B - T\frac{dB}{dT}\right)_T \qquad \text{(V-31)}$$

The results indicate that the differences in B are small except at low reduced temperatures. Differences in $(\partial H/\partial P)_T$ are, percentage-wise somewhat larger and suggest that isothermal throttling coefficient data, if sufficiently precise, could serve to discriminate between the three correlations. Such direct calorimetric measurements at low

reduced temperatures are in general rare, extremely difficult, and usually of poor precision.

It is this author's belief that a comprehensive evaluation of the relative accuracy of the B measurements at low reduced temperatures for the various substances is needed before the superiority of any one functional form for the representation of Br can be unequivocally established. Nevertheless, two important statements may be made with respect to the correlation developed in this work. Firstly, by design, it fits the existing second virial coefficient data for methane and propane better than any existing reduced correlations available in the literature, and secondly, the use of the modified reduced temperature parameter represents a significant advance in our efforts to improve the correspondence between various substances subscribing to a three parameter framework.

d) Suggestions for Improving the Correlation. The results indicate some possibilities for the future improvement of the correlation and consequently a brief analysis merits consideration. The results for Ar, Kr and CF_4 at low reduced temperatures ($Tr < 0.9$) (See Table J-2) yielded a positive bias with respect to the measurements in all cases. The sign and magnitude of the bias may, in part, be explained by the neglect of quantum corrections for the reference substance methane. Leland et al. [145] have estimated the contribution to be 1 to 2% of the value of Br at a Tr value of approximately 0.7. This suggests that the correlation would probably have been better served using an argon reference with an additional term in Equation (V-18) to account for quantum effects in methane.

The deviations for krypton ($\alpha c = 5.94$) were significantly higher than those for argon ($\alpha c = 5.76$) particularly at low reduced temperatures where the contribution of αc becomes important. It is suspected that the αc value for krypton obtained from the tabulation of Reid and Sherwood [214] is too high. Koeppe [132] has suggested that Ar, Kr and Xe all have αc values of 5.79 ± 0.01. This seems more reasonable in view of the spectacular correspondence obtained between the reduced properties of these substances [226]. In any case, if the αc value of krypton were decreased to that for argon, the observed deviations

in the Br values for krypton would have been almost the same as for argon at any given reduced temperature.

A negative bias was consistently noted with respect to the experimental measurements for hydrocarbons heavier than n-butane. The extent of the bias was found to increase with increasing αc. Again, if argon, instead of methane, was used as the reference substance with propane retained as the pivot substance for determining the slope function $dBr/d\alpha c$, then this modification would have the effect of decreasing the negative bias for compounds with αc values higher than propane and decreasing the positive bias for substances with lower αc values. The necessity for using higher order terms in $(\alpha c - \alpha c_{oo})$ in Equation (V-30) should, however, not be discounted as a possible solution to decreasing the negative bias for markedly non-spherical molecules such as n-octane.

Development of a Mixing Rule for RTc_m/Pc_m

a) Need for the Development of a High Temperature Reduced Second Virial Coefficient Correlation. In preliminary application of Equation (V-30) to the extraction of mixture pseudoparameters from Equation (V-12) it was found that the range of the correlation was not sufficient to permit the unambiguous selection of the three parameters required. Even if αc_m were independently fixed, the specificity of the optimization in the remaining two parameters was found to be marginally acceptable for the parameter Tc_m if enthalpy values for the mixture are to be accurately predicted. This suggests that the range of the correlation should be further extended.

Measurements at reduced temperatures below 0.5 are generally unavailable. Measurements at high reduced temperatures extending beyond the maximum in Br are available only for helium [185]. The quantum effect contribution for helium is well known to be sizable at low temperatures, but only marginal in the vicinity of the maximum in Br [106]. Nevertheless the high temperature measurements on helium cannot be directly used in extending the correlation as its critical properties are themselves subject to quantum corrections. Leland, Kabayashi and Mueller [145] were able to develop a procedure to

calculate the deviations exhibited by quantum spherically symmetric fluids from classical behaviour in a corresponding states framework. An important consequence of this procedure, and the availability of measurements on quantum fluids, was their ability to calculate the reduced second virial coefficient as a function of reduced temperature for a classical fluid for Tr $\leq$ 30, well beyond actual measurements on such fluids. It was decided to use their tabulated values in extending the high temperature limit of the correlation from 3.26 Tc to 30 Tc.

b) Initial Efforts Towards the Development of the High Temperature Correlation. The functional form of Equation (V-30) suffers from the disadvantage of not being able to account for a maximum in Br at high reduced temperatures, contrary to fact. This shortcoming is attributed to the hardness of the repulsive forces for the square well potential. The Lennard-Jones potential function produces the required maximum in Br but the result cannot be expressed in closed form [92,167]. For a soft sphere conforming to the potential

$$u(r) = \varepsilon\left(\frac{\sigma}{r}\right)^{n} \qquad n \geq 3 \tag{V-32}$$

the result is [167]

$$\frac{B(T)}{N_o\sigma^3} = \frac{2\pi}{3}\left(\frac{\varepsilon}{kT}\right)^{\frac{3}{n}} f(n) \tag{V-33}$$

where f(n) is a gamma function in n diverging for n $\leq$ 3. The macroscopic two parameter equivalent is given by

$$Br = \beta(n)\, Tr^{3/n} \tag{V-34}$$

and expresses the effect obtained by softening the repulsive part of the potential. Consequently, we are tempted to empirically combine Equation (V-30) and (V-31) and write

$$Br_{oo}(Tr_{oo}) = Tr_{oo}^{3/n}\left[a + b\left(1-e^{c/Tr_{oo}}\right)\right] \tag{V-35}$$

to incorporate a maximum into the correlation.

The tabulation of Leland et al. [145] described above was used to generate B values for methane over the range $3.26 \leq Tr \leq 30$. These values were blended in with the experimental measurements extending upto 3.26 Tr and a least squares fit was obtained with respect to Equation (V-35) with n equal to 12. Although the fit to the high temperature data was improved, the fit to the data for $Tr < 1.0$ was not nearly as good as that obtained with Equation (V-30). This suggests that we need a harder repulsion as the temperature is lowered. In fact, Byrne et al. [35] have demonstrated that the low temperature second virial coefficient data for argon are represented better by the 18-6 Lennard-Jones potential than by the softer 12-6 form which was found to be more suitable at higher temperatures. This suggests that Equation (V-35) could be further improved by expressing n as a function of Tr_{oo} such that n decreases as Tr_{oo} increases. Further efforts in this direction were beyond the original scope of this work and consequently this pursuit, though attractive, was abandoned.

c) The Development of a High Temperature Mixing Rule for RTc_m/Pc_m. Next, a less ambitious, and perhaps more pragmatic approach was tried. An examination of the B/Vc vs T/Tc tabulation of Leland et al. [145] indicates that Br varies only 18% over the range $9.0 \leq Tr \leq 30.0$ and suggests that the required function f_B of Equation (V-12) is insensitive to the value of Tc in this range. Consequently, the difficulty in extracting at least two, if not three, meaningful pseudoparameters could be somewhat circumvented by splitting the function f_B into two parts. The high temperature function could be used to define the reduction parameter RTc/Pc using an approximate estimate of Tc, while the low temperature function given by Equation (V-30) could then be used to refine the estimate of Tc using the optimized value of RTc/Pc. The αc dependance of the high temperature part of the function f_B poses a problem in that it cannot be ascertained from the table of Leland et al. The assumptions involved in the development of an indirect technique to achieve this end are discussed below.

1) It is assumed that the two parameter corresponding states function

$$B/Vb = \theta(T/Tb) \qquad (V-36)$$

involving the Boyle point parameters is valid for all substances that satisfy the three parameter function f_B defined by Equation (V-12) regardless of the value of αc.

2) It is assumed that the two parameter corresponding states function

$$B/B_M = \phi(T/T_M) \qquad (V-37)$$

is also applicable to the non-polar substances that satisfy Equation (V-9) regardless of the value of αc, where B_M is the value of the second virial coefficient at the maximum, and T_M is the temperature at which the maximum occurs.

At first, these assumptions may seem implausible, but the reduction parameters are, in each case, directly derived from second virial coefficient data, and produce an exact fit at the Boyle and maximum points, respectively, regardless of how dissimilar the substances examined may be. One would further expect that the functions θ_A, ϕ_A and θ_B, ϕ_B specific to two substances A and B would be similar in varying degrees in the vicinity of the Boyle and the maximum point respectively.

It has already been noted earlier in this chapter that substances such as CH_4 and CF_4 with significant differences in αc could be fit within the limits of accuracy of precise experimental measurements to a single universal function of the form of Equation (V-36) over the range $1.20 \leq Tr \leq 2.73$, where the Boyle point occurs near the upper limit of the range. The more recent measurements of Lange and Stein [137] down to Tr values as low as 0.89 seem to suggest that the Boyle point conditions are less satisfactory as reducing parameters for these substances below a Tr value of 1.20. At the Boyle temperature, the positive and negative branches of the integrand in Equation (IV-10a) are of equal magnitude, and B is zero. (See Mason and Spurling [167] for a pictorial representation). It is not unreasonable to assume that if the universality of the function θ is valid for negative

excursions down to Br values of -0.22 (at Tr = 1.20), then it is also valid for positive excursions upto a Br value of 0.144, that is, upto and beyond the maximum. We may then confine the validity of assumptions 1 and 2 above to the range $Tb \leq Tr \leq 30$.

3) Assumptions 1 and 2 lead to the result that B_M/Vb and T_M/Tb are constants for all substances and independant of αc.

The tabulation of Leland et al. [145] was re-expressed in terms of the reduced parameters B/B_M vs T/T_M. These parameters were obtained from the same table with some slight modification to the value of B_M as discussed in Appendix F-5. A fit of better than 0.4% was obtained with respect to the modified tabular values using the equation.

$$\frac{B}{B_M} = 0.3517 + 1.5068 \left(\frac{T}{T_M}\right) - 1.11739 \left(\frac{T}{T_M}\right)^2 + 0.25874 \left(\frac{T}{T_M}\right)^3 \qquad \text{(V-38)}$$

The equation is plotted as Figure (V-4), and the regression details are presented in Table J-2. The equation was again transformed to involve the variables Tc, Pc, and αc by using the Boyle point data on CH_4 and CF_4 to establish T_M/Tc and $B_M/(RTc/Pc)$ as functions of αc. Further details are presented in Appendix F-5. The final result applicable over the range $Tb \leq Tr \leq 30$ is given by

$$Br = [h(\alpha c)]\,[g(\alpha c, Tr)] \qquad \text{(V-39)}$$

where

$$h(\alpha c) = Br_M = 0.7085\,[\,0.1590 + 0.0588(\alpha c - 5.82)\,] \qquad \text{(V-39a)}$$

and $g(\alpha c, Tr)$ is given by the right hand side of Equation (V-38) if we replace T_M in terms of Tc and αc as expressed by the relation

$$\frac{T_M}{Tc} = \frac{18}{[1.0 + 0.189(\alpha c - 5.82)]} \qquad \text{(V-40)}$$

By following the procedure similar to that suggested in Appendix G and applying Equation (V-39) to every component in the mixture one can obtain the mixing rule

$$\frac{RTc_m}{Pc_m} = \sum_{i=1}^{n}\sum_{j=1}^{n} x_i x_j \frac{RTc_{ij}}{Pc_{ij}} \frac{h(\alpha c_{ij})}{h(\alpha c_m)} \frac{g(\alpha c_{ij}, Tr_{ij})}{g(\alpha c_m, Tr_m)} \qquad \text{(V-41)}$$

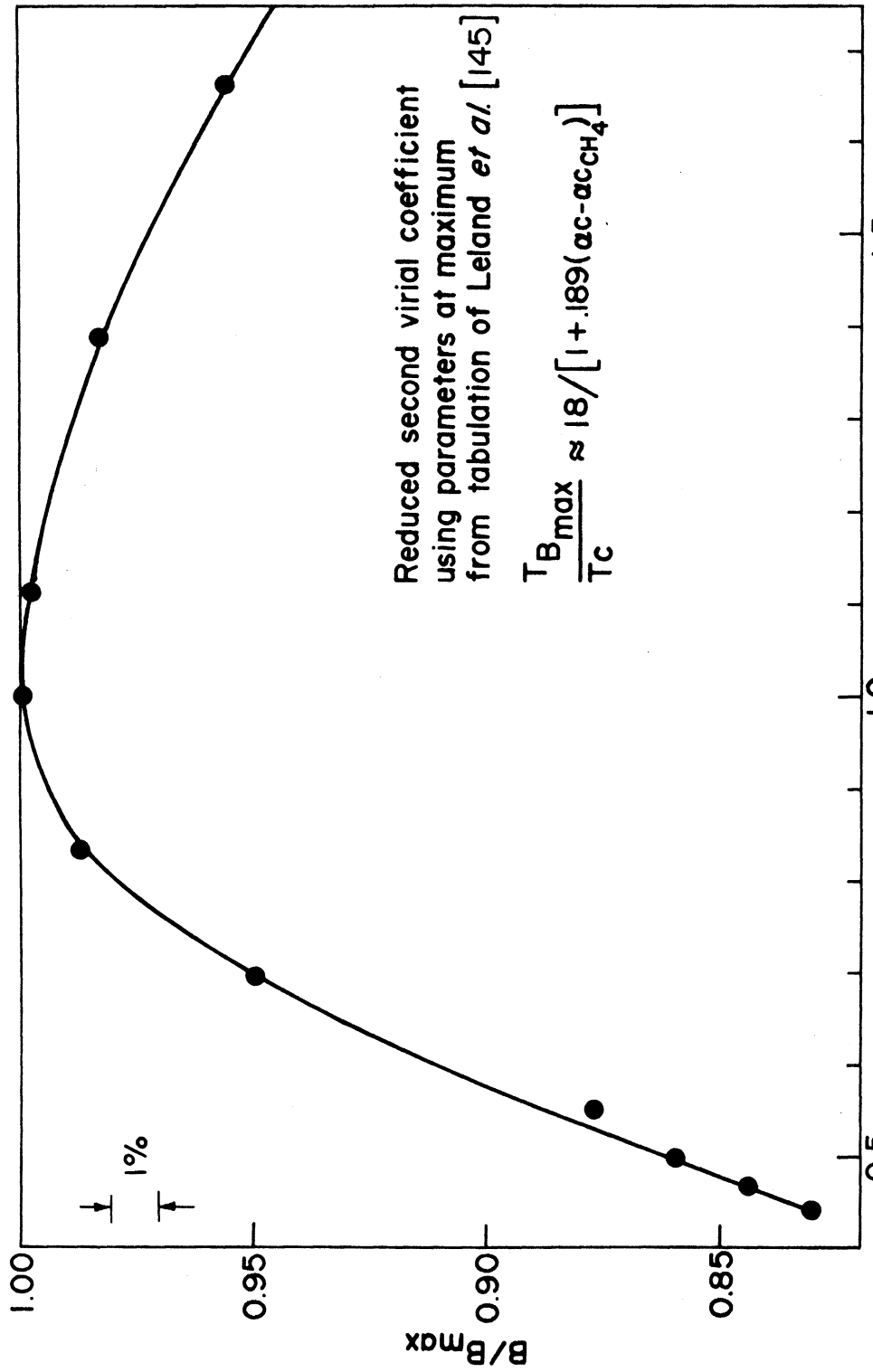

Figure V-4. Dimensionless Second Virial Coefficient for a Classical Fluid in the Vicinity of the Maximum.

if $Tb_{ij} \leq Tr \leq 30$ for all i,j. This reduces exactly to the Van der Waal rule for Vc_m if the $h(\alpha c)$ and $g(\alpha c,Tr)$ ratios in the above equation assume unity values, and if all substances are assumed to have the same value for zc.

We now have several options for calculating the pseudo-parameters for multi-component mixtures using the basic framework explained in this Chapter. Given B_M values, and α_{ij} values for all i,j, Equation (V-22) may be used to determine αc_m. The optimum values of Tc_m and RTc_m/Pc_m may then be calculated using Equation (V-30). Alternately, RTc_m/Pc_m may be independantly established from Equation (V-41) at some high temperature such that $Tb_{ij} \leq Tr \leq 30$, assuming predetermined values of αc_{ij} and αc_m, and from independently specified approximate estimates of Tc_{ij} and Tc_m. Equation (V-30) may then be used to optimize the parameter Tc_m alone from a given set of B_m values. These options will be further examined in Chapter IX.

Summary

In conclusion, the basic logic in the formulation of mixing rules for the evaluation of mixture pseudoparameters within the one fluid three parameter corresponding states framework has been defined and the rationale behind some additional recipes developed in this work and utilized in Chapter IX has been indicated. The general goal of this work is to predict multi-component mixture enthalpies from constituent binary enthalpy data over the single phase fluid region. More specifically, the goal is to test the technique against the enthalpy data for a ternary methane-ethane-propane mixture using enthalpy measurements on the methane-ethane, ethane-propane and methane-propane binaries, respectively. Before the technique can be applied, the enthalpy data relevant to the examination of the problem must be completely defined. Therefore, the next three chapters are concerned with the experimental aspects of this investigation, and in sequence deal with the experimental method, the data reduction techniques and the experimental results.

Chapter VI
THE EXPERIMENTAL METHOD

Before the experimental results of this investigation are discussed, it is first useful to describe the experimental setup and the operation of the calorimetric facility at the Thermal Properties of Fluids Laboratory (TPFL) at the University of Michigan. This section is devoted to the description of the recycle system, the two calorimeters, and the measuring instruments. Operating procedures and instrument calibration techniques are also briefly discussed. As the evolution of the facility can be comprehensively traced through a number of doctoral theses [119,161,162,168,284], beginning with the pioneering efforts of Faulkner [79], only modifications with respect to both equipment and operating procedure made during the course of this work are emphasized.

The Recycle System

The modified recirculating system, incorporating both isobaric and throttling calorimeters for the direct measurement of the effect of temperature and pressure on the enthalpy of multicomponent mixtures of light hydrocarbons, is shown in Figure VI-1. The function of the recycle system as a whole is to provide a steady continuous supply of fluid to the appropriate calorimeter under prescribed and carefully maintained conditions of temperature, pressure, and flowrate which extend from -240°F to +300°F, from 80 psig to 2000 psia, and upto 4 standard cubic feet per minute (SCFM), respectively.

The flow stream in Figure VI-1 may be traced starting at the compressor inlet buffer. The fluid is compressed from about 80 psig to some high pressure varying from 1000 psia to an upper limit of 2500 psia using a two stage diaphragm compressor (Item 2, Appendix D) operating at a constant volume rate of 4 SCFM. The fluid subsequently passes through a bomb containing copper fittings located in a heated air bath which serves as an effective oxygen scavenger, and then enters an insulated box containing the control valve mainfold.

The outlet pressure at the compressor is adjusted with the compressor throttle CT. The flow is then split between the calorimeter feed

and bypass lines by relative adjustment of the calorimeter throttle (9T), and bypass throttle (BT) valves, respectively. The two lines eventually merge at approximately 80 psig at the compressor inlet buffer enroute to the compressor. The pressure at the calorimeter is principally determined by the adjustment of the calorimeter throttle. Mather [168] and Yesavage [284] introduced heating tapes ahead of such throttling valves to prevent the condensation of the system fluid due to Joule-Thomson cooling at the valve outlets. The fluid in the calorimeter feed line then enters a buffer tank that is located in an insulated controlled temperature heated air bath, and serves to stabilize the flow conditions. Also located in the same bath, are a bank of five storage tanks that act either as a source or sink for the recycling fluid. The air bath is usually maintained at about 50°F higher than the cricondentherm temperature of the mixture to ensure that fractionation does not occur when the fluid is being initially supplied from the storage tanks to the recycle system.

The fluid then travels through a series of conditioning baths designed to bring it to the temperature desired at the calorimeter. In order to reduce holdups, particularly under two phase flow conditions, the baths and the fluid line are arranged to ensure a downward flow path at all times, and the inside diameter of the fluid line is reduced to 1/8" just as it enters the first conditioning bath. A micron filter between the high pressure buffer and the baths serves to trap any particulate thermal decomposition products. A "double pipe" water coil, 15 feet in length, is used to cool the fluid if the desired temperature is below ambient conditions. The coil is bypassed at higher operating temperatures. The first bath that the fluid enters contains 175 feet of 3/16" O.D. copper tubing which serves to bring the fluid temperature to about -100°F, if necessary, when a dry ice-acetone mixture is used as the bath fluid.

The system fluid next enters the "heat exchanger" bath containing 325 feet of 3/16" O.D. copper tubing, and maintained to within $\pm$ 0.5°F of the desired temperature at the calorimeter using an electronic controller (Item 7, Appendix D) driving a 50 watt immersion heater. The fluid leaves within $\pm$ 1°F of the desired temperature and then passes into the bath where the two calorimeters are located.

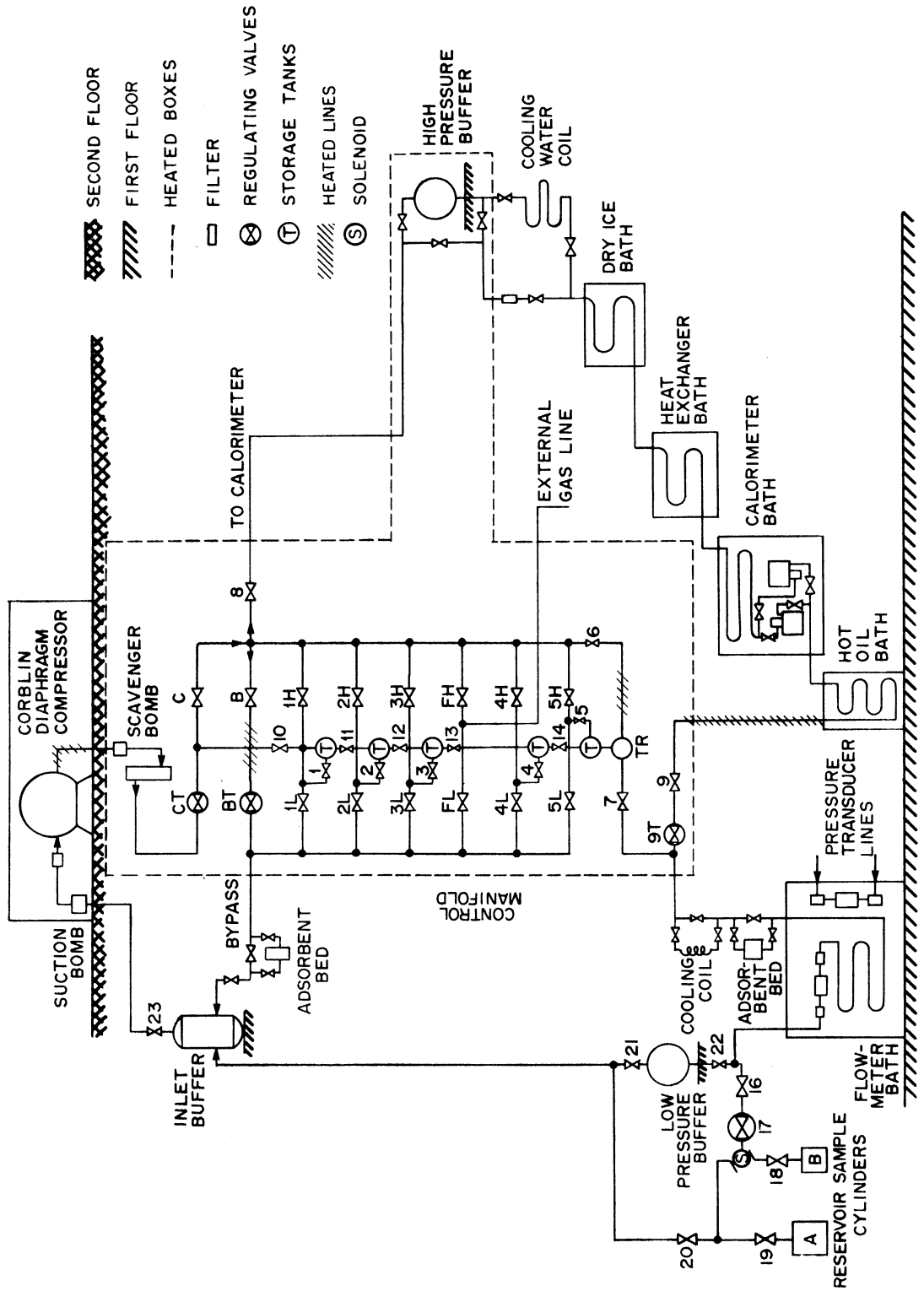

Figure VI-1. The Recycle System (Schematic).

There are four cryogenic valves (Item 1n, Appendix D) inside the calorimeter bath which can be manipulated to guide the fluid through the appropriate calorimeter after it has passed through 100 feet of 3/16" O.D. copper coil for a final temperature conditioning. The choice of bath fluid for the last two baths in the series depends on the operating temperature. Isopentane is used below -50°F. Kerosene is used in the range -25°F to 75°F. Above 75°F, 30 wt. lubricating oil was found to be more suitable. At below ambient temperatures, the bath fluid is cooled by liquid nitrogen supplied from externally located 50 litre dewars. The liquid nitrogen flowrate can be adjusted if the pressure at the dewar is varied by regulating the outlet driving pressure of a nitrogen cyclinder connected to it, or by adjusting a valve located in the effluent vaporized nitrogen line outside the bath.

The inlet temperature and pressure, the difference between the inlet and outlet temperature, the pressure drop, and the electrical energy input are the key measurements that are next obtained as the fluid passes through the calorimeter. After it leaves the calorimeter, the fluid enters a temperature controlled hot oil bath designed to vaporize it completely before returning to the valve mainfold where it is throttled (9T) to 80 psig, the selected pressure for the measurement of the flowrate. The fluid leaves the valve mainfold to enter a water bath, where the flowmeter is located. The bath temperature is controlled to 27 $\pm$ 0.1°C by balancing the cooling effect of a water coil against the heating effect of a 100 watt tubular heater operated by an electronic relay, and actuated by a mercury contact switch (Item 8d, Appendix D). The fluid enters a multiple channel flowmeter (Item 8a, Appendix D) after passing through 50 feet of 3/8" ID copper tubing for temperature conditioning. Micron filters are located on either side of the flowmeter to remove entrained solids from the flowing stream. The fluid passes through another 50 feet of copper tubing after the flowrate is measured and returns to the compressor inlet buffer where it joins the bypass stream prior to being recycled.

Modifications to the Recycle System

Mather [168], and later Yesavage [284] reported that the recycling fluid stream was in some circumstances contaminated with oil that leaked from the compressor heads around the edges of the oil to gas pressure transmitting metal diaphgrams. A bed of activated charcoal and dehydrite located in the heated air bath just after the compressor was found by Yesavage to be quite inefficient in adsorbing the oil in the fluid stream. This oil had a tendency to separate out at the low pressure of the flowmeter causing serious fouling problems and flowmeter calibration changes. A glass wool bomb placed just before the flowmeter by the same investigator to remedy the problem was also found to be ineffective in this work.

The phase equilibria for an oil-gas system are such that the desorption or the condensation of oil from the gas stream is facilitated if the process is conducted at the lowest possible pressure and temperature in that order. A twelve foot double pipe water cooling coil with provisions for bypass was placed in the fluid stream before the flowmeter bath to decrease its temperature from a maximum of 175°F to below the flowmeter bath temperature of 27°C as part of the strategy for condensing as much oil as possible prior to the desorption process. A bypassable adsorbent bed of about 800 cc capacity (Item 13, Appendix D) containing molecular sieves 3A and 4A, activated charcoal and drierite was placed in the flow stream after the water coil. A similar bed was also installed in the bypass stream to the compressor buffer. The molecular sieves effect the removal of nitrogen and unsaturated hydrocarbons, and together with the charcoal, serve to remove the oil. As these beds also adsorb significant quantities of the light saturated hydrocarbons that vary with the temperature of the bed, it is imperative that the temperature of the bed in the flowstream be strictly controlled to prevent spurious contributions to the measured flowrate.

During the investigation of the 76% ethane-propane mixture, a severe explosion caused serious damage to the valve manifold resulting in the deposition of carbon black in the manifold lines. The damage is typically illustrated in Figure VI-2. The entire valve manifold had to be completely rebuilt, and the valves replaced. The monitoring of leaks within the control manifold required the frequent removal of

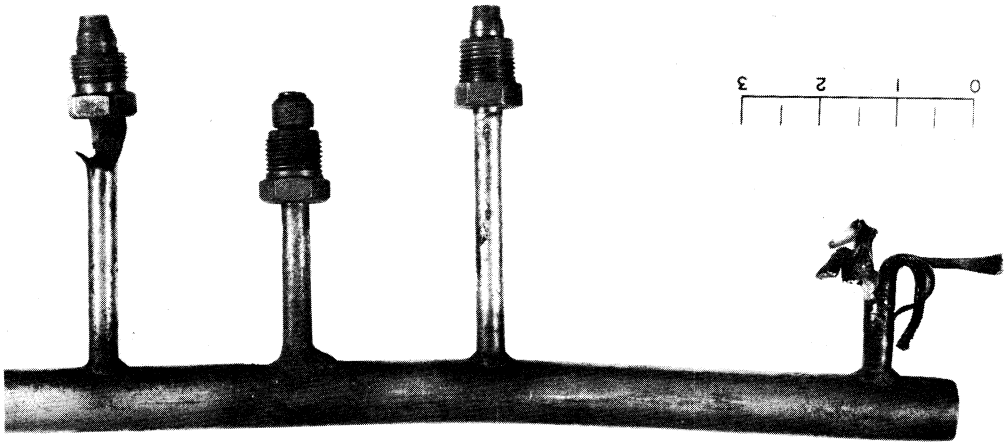

Figure VI-2. View of Control Valve Manifold Line Following Explosion.

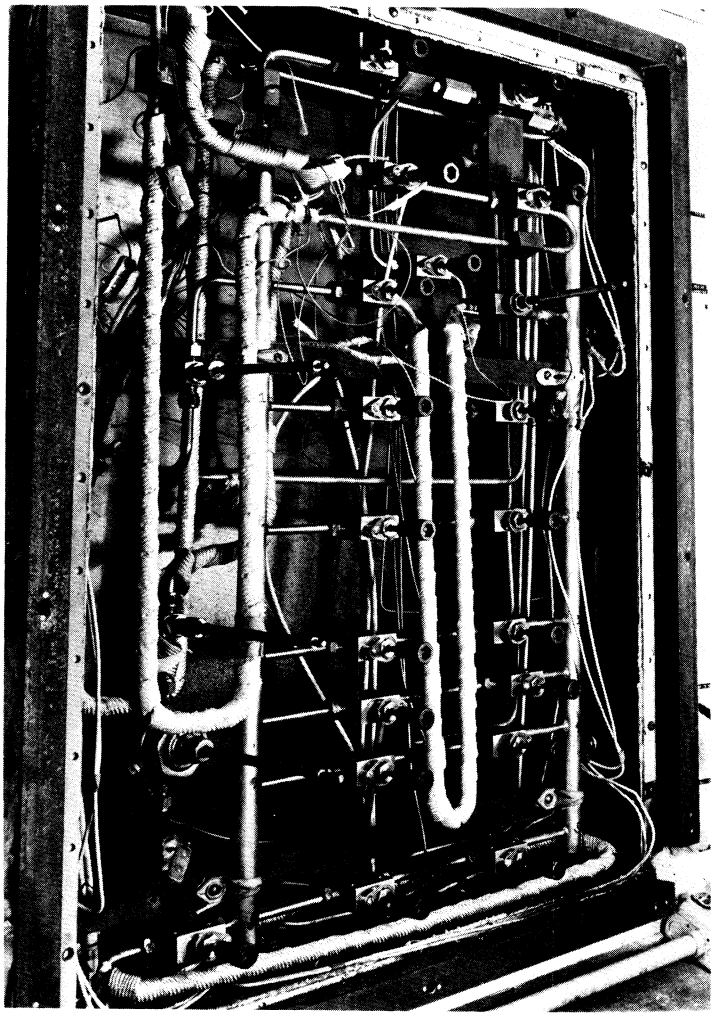

Figure VI-3. View of Rebuilt Valve Manifold.

the insulated front panel during regular operation. Originally a time consuming process, it was speeded up by the replacement of the single piece valve stems by split stem quick-snapout valve extensions. This modification provided instant control of any valve in the manifold for the duration of such tests. The rebuilt manifold is shown in Figure VI-3.

The initial introduction of fluid to the system was previously accomplished through valve 20 ahead of the low pressure buffer which required the fluid to be compressed before it could be stored in a tank. The inclusion of valve FH in this work provides for the direct transfer of fluid at high pressure between the recycle system and an external storage tank if necessary. Other modifications include the use of a water coil as a less expensive replacement for gaseous nitrogen to provide the necessary cooling for the control of the calorimeter bath at above ambient temperatures, the installation of a relief valve (Item 8c, Appendix D) just before the flowmeter, venting at 100 psig, to prevent possible deformation of the flowmeter, and the addition of a shut-off valve at the bypass stream before the compressor inlet buffer to prevent it from overpressurizing in the event of a leakage across any shut-off valve on the low pressure side of the valve manifold when the compressor is shut down.

The Isobaric Calorimeter of Faulkner [79]

The calorimeter is shown in Figure VI-4. The fluid enters the calorimeter through the tubing in the lower section, passes through the inlet thermowell (1) and into the calorimeter heater capsule (3) where the electrical power is delivered. Passage through a series of baffles (5) brings the fluid to a uniform temperature as it leaves the capsule through tubing H via outlet thermowell J. Previous tests indicate that the exposed surface of the capsule is essentially at constant temperature [119]. Heat leakage is compensated by the use of a Nichrome wire wrapped radiation shield or "guard heater" maintained at the exit gas temperature by appropriate adjustment of a variac. Jones [119] introduced a thermocouple gland (Item 1g, Appendix D) to improve the pressure seal on the power input leads. Further modifications relating to the inlet thermowell, the lead wires for the main

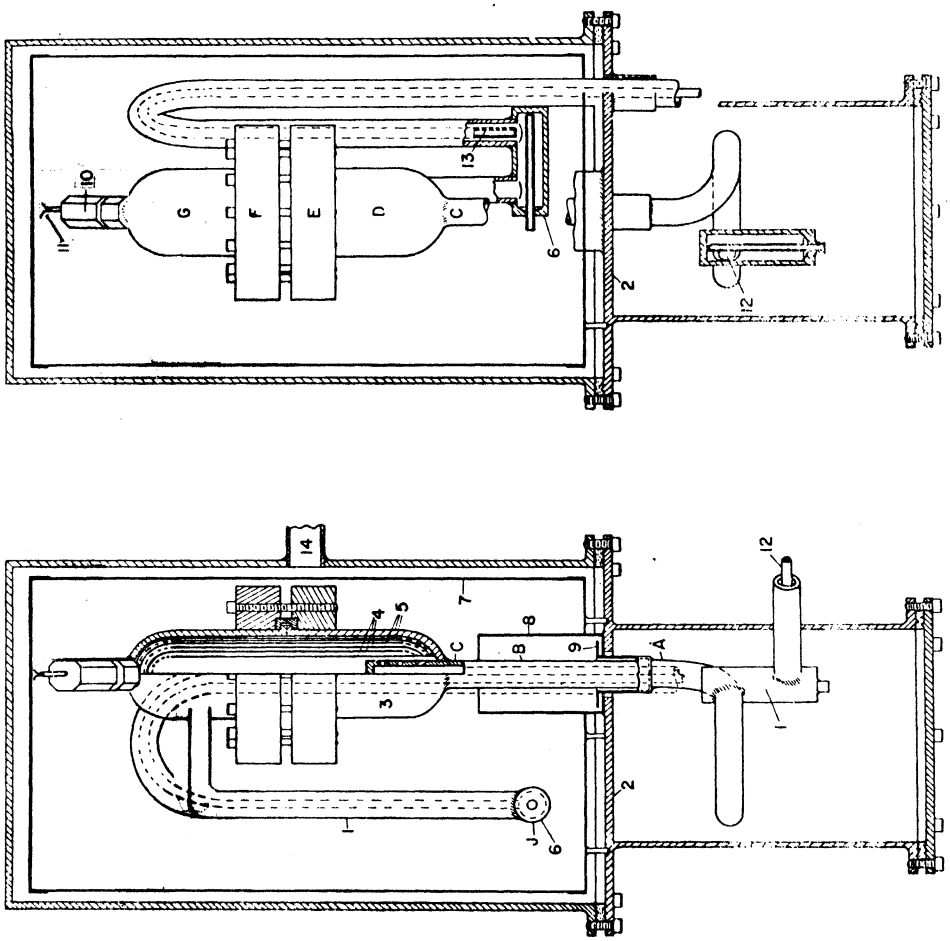

Figure VI-4. The Isobaric Calorimeter of Faulkner [79] After Modifications of this Work.

heater, and vacuum seals were reported by Yesavage [284].

A major contribution to this calorimeter was the design and construction of a new heater capsule whose parts are shown in Figure VI-5a. In the original design of Faulkner, the baffles consisted of concentric copper cylindrical shells with hemispherical shells soldered at either end. Frequent burnout of the calorimeter heater resulted in permanent breaches at these soldered joints permitting the fluid to bypass the heater wire and reach the outer shells directly. This resulted in fluctuations in the observed value of the outlet temperature which increased the uncertainty in evaluating the approach of steady state conditions and aggravated the likelihood of more burnouts (See Figure VI-5b).

The modified capsule consists of six shells varying from approximately 0.46" O.D. to 1.00" O.D. that are screwed onto a capsule mount. The detailed drawings are presented in Appendix E. The shells and mount are each made of tellurium copper alloy because of its superior machining characteristics. The alternate ends of contiguous baffles are perforated with small holes to permit the counter-current flow of the fluid across each baffle surface. Each shell was machined as a single piece unit to include the upper hemispherical portion where protruding tabs serve to keep the annular spaces uniform at all times. In every case, the shell is 0.01" thick except at the wider threaded portions near the bottom.

The three innermost shells are wound with Nichrome wire (Item 1i, Appendix D) while the rest serve to thermally equilibrate the fluid before it leaves the capsule. The heating wire is glued to the shells by a thermally conducting electrically insulating resin (Item 1m, Appendix D). The two outermost shells, silver soldered to each other near the base, appear as a single unit in Figure VI-5a. The tabs on the outside shell serve to prevent the heater capsule from being pushed flush against the outlet tube on the capsule housing causing the flow of gas to be arrested. The tabs are also threaded to accomodate a ring which clamps the heater wires in place. A pair of grooves running along the length of the shell permits the capsule to fit easily in the housing by providing a recessed resting place for the insulated heater wires.

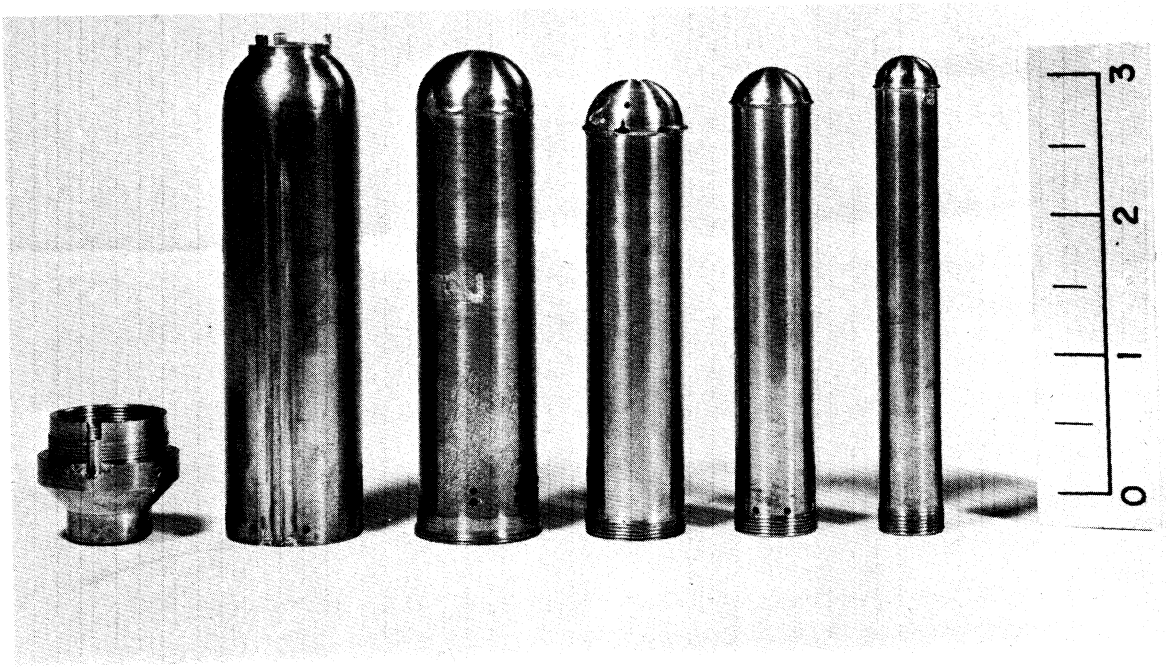

Figure VI-5a. View of the Parts of the Modified Heater Capsule.

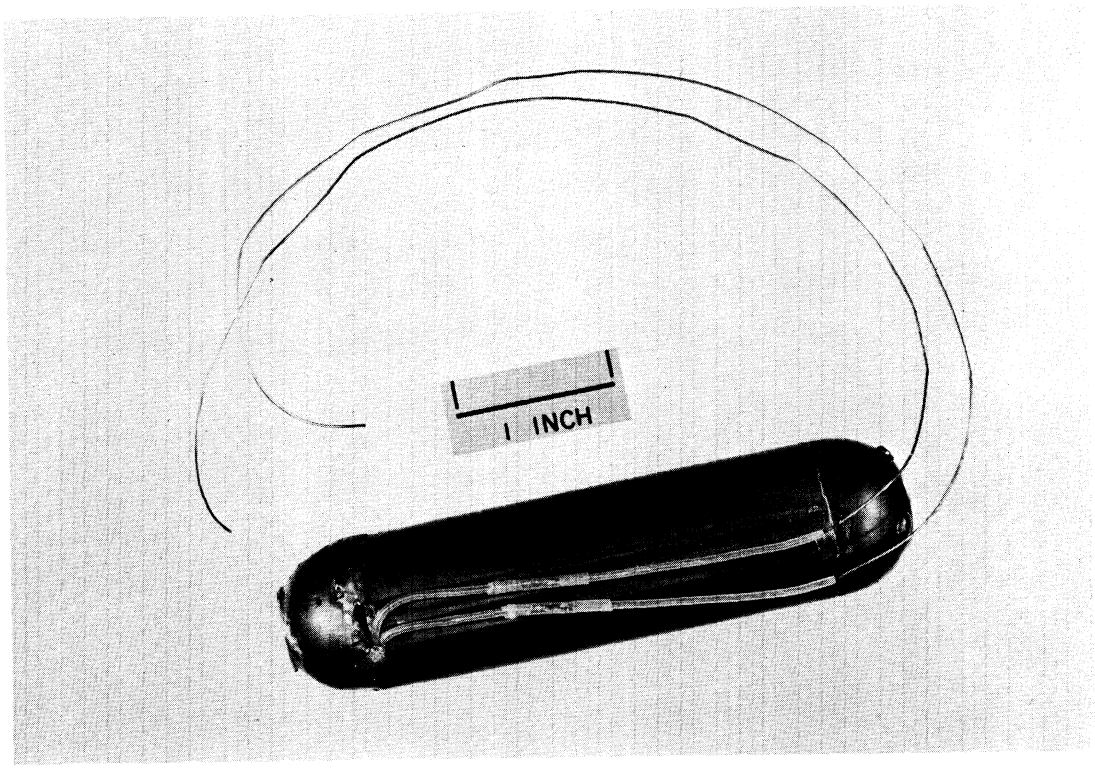

Figure VI-5b. View of the Original Heater Capsule.

A number of slots appear on the capsule mount and are designed to carry the bifilarly wound heating wire from shell to shell. The shells are screwed on the mount so as to exert firm pressure on the heating wire in the slots to prevent any leakage of fluid along such paths. The third shell from the inside requires both the heater wire and the fluid to be transferred out at the top, hence the larger opening in this case. The threads on the mount are arranged to stack the shells in a staircase configuration. The threaded bases of the three innermost shells are screwed to the mount in ascending order. The remaining shells are arranged in descending order as the shell diameter increases. This particular feature was incorporated in the design to increase the limited scavenging surface available to the fluid at the mount. The main difference between the original design of Faulkner [79], and the modified version lies in the replacement of the hemispherical shells bottoms by the heavier threaded mount. In effect, the better scavenging characteristics and lighter weight of the original mount design are somewhat compromised in favor of a design that emphasizes ruggedness and ease of accessibility to the heater element in case of repair.

Finally, before inserting the capsule into the calorimeter, the uniformity of flow through the perforated holes is carefully checked by passing gas under slight pressure through the bottom of the capsule mount and observing the heating wire slots for leakages with the shells in place. The modified capsule weighs 4.75 oz. This is about 1.5 oz. heavier than the original version and is chiefly due to the increased weight of the new mount. This increase in mass is less significant from the standpoint of the increased time required to attain steady state conditions if it is noted that the flanged capsule housing alone weighs 32 oz. The pressure drop across the capsule for average operating conditions varied from 0.1 psid at high pressures to about 1.0 psid at 250 psia. The efficiency of heat transfer was so improved as a result of the precautions taken, both in design and installation, that the power supply with a rating of 325 volts and 2 amps became the limiting factor in the rate of heat input. To obtain the maximum power consistent with the supply restrictions, the amount of heating wire used should correspond to a total resistance of about 162 ohms.

Another modification to the calorimeter was the interchange in the positions of the outlet flow tube H and the heater wire gland 11 in the upper half of the flanged capsule housing. In the original configuration, considerable difficulty was experienced in drawing the heater lead wires through the gland, a necessary step for the removal of the capsule. The abrasion of the insulation on the wires at the sharp bend would sometimes result in a short circuit. This problem was eliminated in the modified housing. The conax gland was swaged due to frequent tightening and was also replaced. Both versions are seen in Figure VI-6.

The Throttling Calorimeter of Mather [168]

This calorimeter is shown in Figure VI-7. The fluid enters the upper section near 9 and passes into a capillary coil in the lower section which causes the pressure drop. A grounded insulated wire running through the coil serves to supply a manually adjustable energy input to maintain isothermal conditions when operating within the Joule-Thomson inversion curve. After passing through a number of baffles to stabilize its temperature, the fluid leaves through exit thermowell 5. Outside the Joule-Thomson curve, the calorimeter is operated in the isenthalpic mode. The heat leak is balanced by adjusting the power to the radiation shield H such that a three junction differential thermopile between the outermost baffle and the shield indicates zero temperature difference.

In Figure VI-7, the inlet thermowell is seen to be in mechanical and thermal contact with the outer wall of the calorimeter, insuring that the bath temperature is, in effect, measured at the thermowell. If, for simplicity, it is assumed that the fluid enters the calorimeter bath at the desired bath temperature, the pressure drop caused by its passage through 100 ft. of 3/16" O.D. thick wall copper tubing before the calorimeter serves to cool or heat the fluid to an extent that, in some circumstances, is not quite matched by the heat transferred between the coil and the bath fluid. These conditions occur chiefly when the magnitudes of the flowrate, the viscosity, and the adiabatic Joule-Thomson coefficient for the fluid are all high and can result in temperature differences as high as 0.4°F between the inlet thermowell

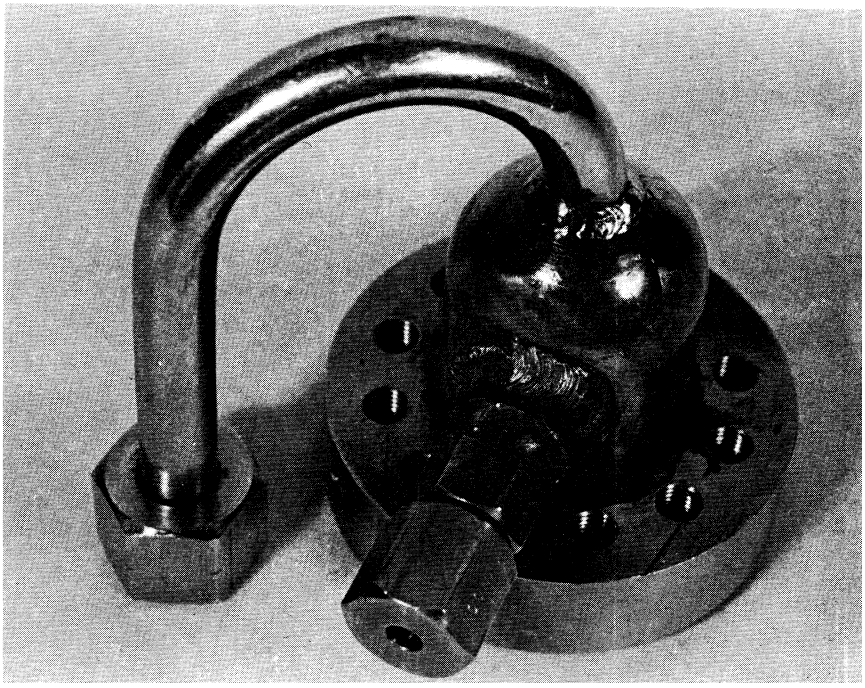

(a) Original Half.

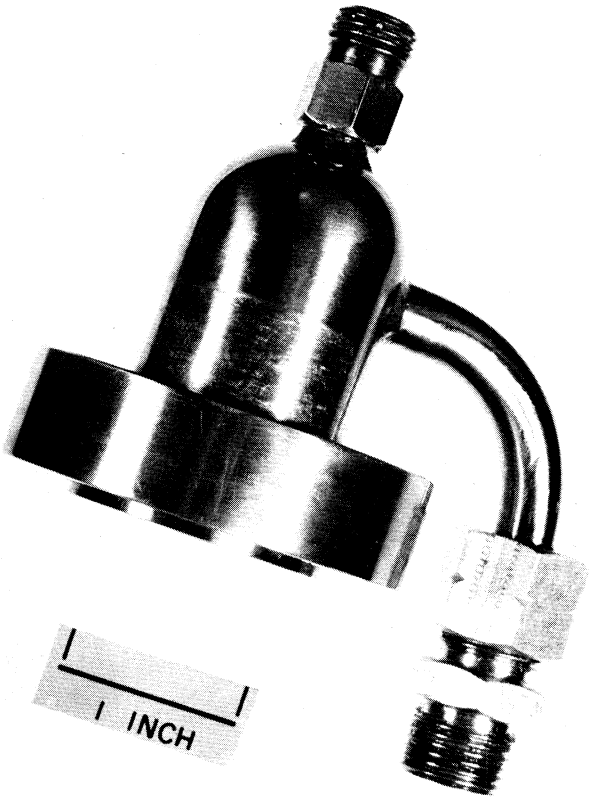

(b) Modified Half.

Figure VI-6. The Original and Modified Upper Half of the Heater Capsule Housing.

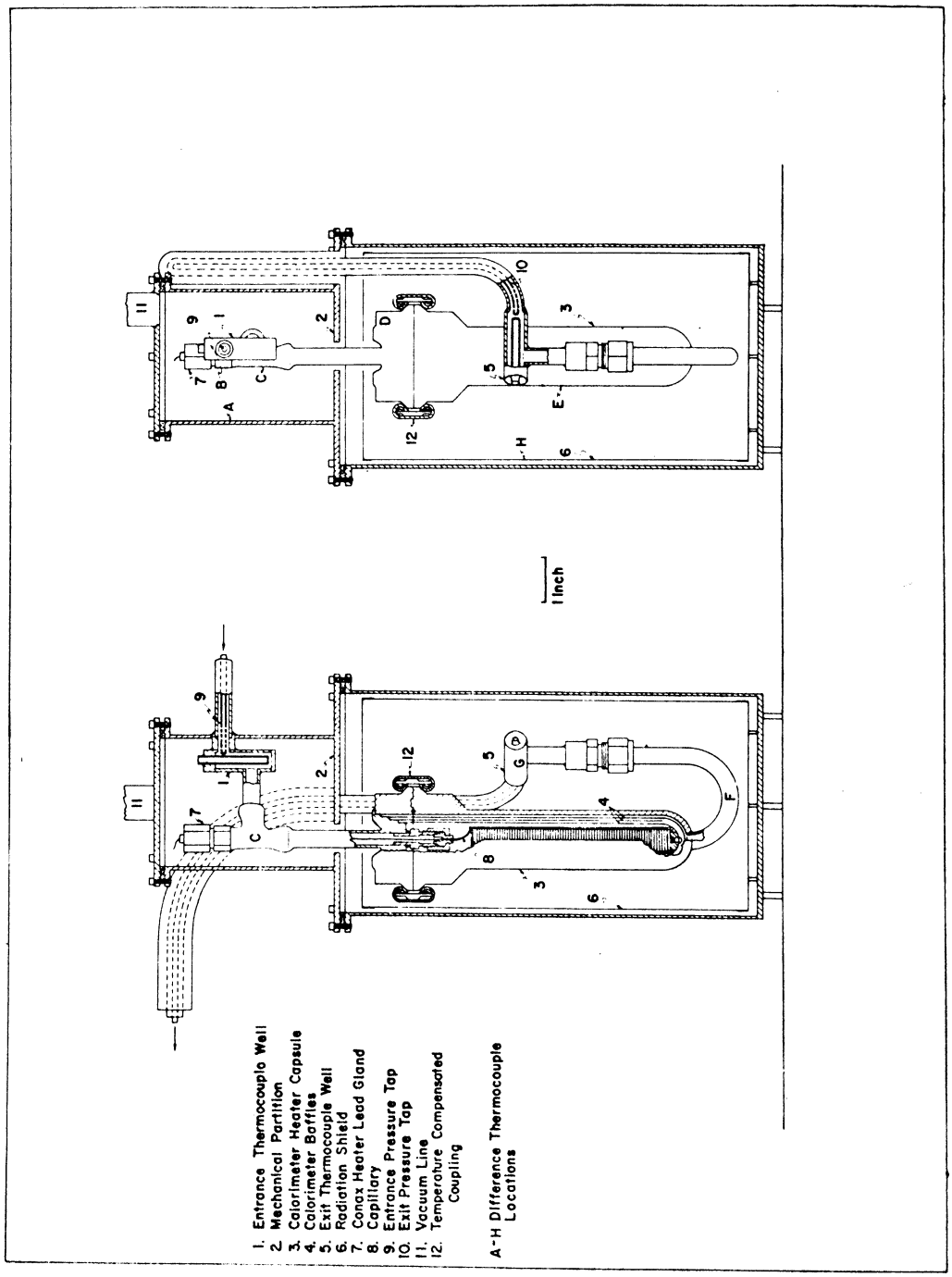

Figure VI-7. The Throttling Calorimeter of Mather [168] Before Modification.

and the bath. The inlet thermowell was moved by interposing a 4 inch piece of coiled stainless steel tubing between its original location and the wall. Although the discrepancy between the bath and the thermowell temperature is still retained, it no longer appears in the measured temperature difference where the contributing error to the measured mean heat capacity is usually far more serious.

Serious leakage problems were found to occur at the pressure seal (12) at cryogenic operating temperatures. It was determined that the temperature compensating clamp (Item 1c, Appendix D), and one of the grooves on the seal were deformed. The clamp was replaced, and the sealing problems were minimized by using nickel gaskets with a thicker teflon coating.

Measuring Instruments

a) Electrical Measurements. All electrical and electrically transduced measurements are made on a K3 potentiometer (Item 3a, Appendix D) using standard resistors to scale down the voltages to the range of the potentiometer. The circuitry for the potentiometer, and the calibration data for the standard resistors is given by Jones [119]. The worst case accuracy is 0.01% of reading $\pm$ 0.2 microvolts (μv) for the range 0 to 0.01611 volts. Manker [162] has discussed techniques for maintaining the precision of the measurements. In this work, the standard cell for the potentiometer was calibrated by adjusting the cell voltage setting on the potentiometer until the measured value of the EMF of another sparingly used standard cell was equal to its NBS calibrated value corrected for ageing according to a previous history pattern that predicted a steady decrease of 75 μv/year out of a total value of approximately 1.019 volts. The latest calibration for the reference cell is indicated in Table A-1.

b) Temperature Measurement. The temperature of the calorimeter bath as measured by a four lead platinum thermometer (Item 5, Appendix D) is assumed to be the inlet temperature of the calorimeter. As discussed earlier, a worst case discrepancy of 0.4°F may occur. The constants for a modified Callendar equation representing resistance as a function of temperature, the circuitry for the thermometer and

a sample calculation of the temperature from two voltage measurements at the K3 potentiometer are presented by Jones [119]. A second thermometer in a metal housing (Item 5a, Appendix D) was used beginning with the examination of the 0.27 mole fraction ethane-propane system. The Callendar equation constants determined by the NBS are shown in Table A-2. The accuracy of the bath temperature measurement is 0.04°F. The original thermometer was recently recalibrated by Miyazaki [178] against a Hewlett-Packard Model 2841-A quartz crystal thermometer. The resistance at 0°C was computed as 25.519 ohms, as opposed to the original calibrated value of 25.513 ohms. The discrepancy between the two sources did not exceed 0.01°C, the estimated accuracy of the quartz thermometer.

c) Temperature Difference. The temperature difference between the calorimeter inlet and outlet is normally measured using duplicate six junction copper/constantan (Cu/Con) thermopiles calibrated by the NBS at 20°C intervals from -100°C to 160°C, and including calibration points at -183°C and -196°C. The estimated accuracy of the calibration tables for the thermopiles is $\pm$ 0.1°C. The calibration data for thermocouples 3M, 4M, 5M, and 6M used in the isothermal and isobaric calorimeters, respectively, are reported by Yesavage [284].

A fourth degree least squares polynomial fit of EMF vs T was considered adequate for the measurement conditions at the isobaric calorimeter. A typical regression analysis is indicated in Table A-3. The first constant or intercept obtained from the regression was adjusted to indicate a value of 0μv at 0°C. It was initially felt that a divided difference polynomial would more accurately calculate the small temperature differences involved in the throttling calorimeter. Both techniques were simultaneously used in this work. An average discrepancy of 0.03% in the calculated values of the temperature difference was observed. However, in the case of Joule-Thomson data obtained for ethane at -246°F, the discrepancy between a fifth order Lagrange interpolating polynomial and the fourth degree least square approach increased to 3%, as seen in Figure VIII-13. The discrepancy could not be improved by changing the order of the interpolating polynomial.

difference curve was constructed between the calibration table EMF values of thermopile 6M and an archetypical 6 junction thermopile derived from the comprehensive single junction NBS reference tables [184] as a function of temperature. The results indicated that the estimate from the least square technique was more accurate below -240°F. The inferior performance of the interpolating polynomial is thought to have occurred because the interpolation interval was as high as 83°C in this region, as opposed to 20°C at higher temperatures.

In order to improve the sensitivity of the measurement over temperature differences of the order of a few degrees, the thermopiles in the isothermal calorimeter were permanently replaced by a single 15 junction unit. A similar replacement was also made for the isobaric calorimeter over the limited period involving the investigation of the heat capacity maxima for ethane and part of the measurements for the 0.76 mole fraction ethane-propane mixture. The four calibration points initially determined by the NBS are listed in Table A-4, and apply to both thermopiles #1 and #2. The isobaric calorimeter was recalibrated at the four points in Table A-5, including two conditions repeated from the previous calibration. In spite of considerable handling, and a time period lapse of eight months, the calibrations agreed to 0.01%.

The four original and the two additional calibration points are not sufficient to obtain an accurate fit over the temperature range from -240°F to +300°F. The following indirect procedure was used to generate additional synthetic data points:

i) A fifteen junction thermopile was first synthesized from the calibration data for the six junction thermopile 6M by multiplying the EMF values for the latter by 2.5.

ii) A fifteen junction thermopile was also constructed from the archetypical single junction thermopile data presented in the NBS tables at the 17 temperature conditions corresponding to the calibration data of 6M.

iii) Differences in the EMF values between the two tables in i and ii were plotted as a function of temperature and connected with a smooth curve.

iv) A difference curve was also constructed between the EMF values

for the archetypical fifteen junction thermopile and the actual results for the fifteen junction thermopile #1 at the six calibration points for the latter.

v) The shape of the difference curve in step iv between -280°F and +300°F, with only six data points, was guided by the shape of the well established curve in step iii. Both curves are seen in Figure A-1. The difference values for thermocouple #1 were then recorded at 20°C intervals, and combined with the archetypical values from step i to yield a set of values summarized in Table A-6. The regression analysis for the synthesized calibration table for #1 is presented in Table A-7.

A sample calculation of the outlet temperature at the calorimeter from a knowledge of the EMF generated by the differential thermopile and the inlet temperature as measured by the platinum resistance thermometer is presented by Jones [119]. The measured error in the temperature difference was estimated at 0.2% by Manker [162] for differences greater than 10°F. For smaller differences of the order of 1°F, obtained primarily in the critical region and near the Cp maxima, the accuracy degrades to about 0.5% and 1.0% for the fifteen and six junction thermopiles, respectively, and is limited by the accuracy of the measurement at the potentiometer.

d) Measurement of Electrical Energy Input. The electrical energy input to the calorimeters is supplied by a Kepco D.C. power supply (Item 4, Appendix D). A wiring diagram for the power measurement circuit for both calorimeters has been made by Yesavage [284]. Human errors in recording the current or the voltage measurement can be detected as an unusual value in the computed resistance of the heating wire which varies less than 0.5% during the course of a run, and less than 3% over the entire range from -250°F to +300°F. Short circuits within the heater capsule are also detected in this manner.

e) Measurement of Flowrate. The mass flowrate is calculated from a knowledge of the pressure drop across a multichannel flowmeter (Item 8a, Appendix D), the density, and the viscosity of the fluid at

the flowmeter. The pressure drop is measured by the height difference across a precision 10 inch water manometer (Item 8b, Appendix D) corrected for variations in the water temperature. The density at the flowmeter inlet is estimated from the inlet flowmeter pressure as measured by a 180 inch mercury manometer (Item 8c, Appendix D) and from the measured flowmeter bath temperature, using a suitable equation of state. The flowmeter is calibrated by directly weighing the condensed system fluid accumulated over a measured time period in a liquid nitrogen cooled cylinder. The modified procedural details for the optimal operation of the calibration equipment are indicated in Appendix I-1. The flowrate in normal operation for the systems of this work varied from 0.10 lbs/min to 0.35 lbs/min; the upper limit depending chiefly on the density of the system examined at the flowmeter temperature and pressure. The high energy input required for the measurement of the enthalpy of vaporization required the flowrate to be reduced to below 0.1 lbs/min in most cases in view of power supply limitations.

Previous investigators at the laboratory [161,162,168,284] used the series

$$\frac{\rho\Delta P}{\mu F} = a + b\left(\frac{F}{\mu}\right) + c\left(\frac{F}{\mu}\right)^2 + d\left(\frac{F}{\mu}\right)^3 \qquad \text{(VI-1)}$$

to represent the calibration data where ρ, μ, and F are the density, viscosity, and mass flowrate of the system fluid, and ΔP is the pressure drop across the flowmeter. This form is seen to be an expansion of the Ergun equation [71] for packed beds given by

$$\frac{\rho\Delta P}{\mu F} = A + B\left(\frac{F}{\mu}\right) \qquad \text{(VI-2)}$$

where A and B are constants that are characteristic of a given flowmeter. An alternate form for representing the calibration data can be constructed from the Prandtl universal law

$$\frac{1}{\sqrt{f}} = 4.0 \ln \mathrm{Re}\sqrt{f} - 0.4 \ , \quad 2.1\times10^3 \leq \mathrm{Re} \leq 5\times10^6 \qquad \text{(VI-3)}$$

recommended in the stated range by Bird, Stewart and Lightfoot [23],

where f is the friction factor, and Re is the Reynolds number. If the proportionality between f and $\rho\Delta P/\mu^2$, and also between Re and F/μ for a given flowmeter configuration is recognized, Equation (VI-3) may be transformed to yield

$$\frac{F}{\sqrt{\rho\Delta P}} = A + B \ln(\rho\Delta P/\mu^2) \qquad \text{(VI-4)}$$

In this work, the above equation was expanded in the series

$$\frac{10\ F}{\sqrt{\rho\Delta P}} = a' + b'[\ln(\frac{\rho\Delta P}{\mu^2}\ 10^3)] + c'[\ln(\frac{\rho\Delta P}{\mu^2}\ 10^3)]^2 + d'[\ln(\frac{\rho\Delta P}{\mu^2}\ 10^3]^3 \qquad \text{(VI-5)}$$

to extend its range of applicability.

The precision of the flowmeter calibration data over the entire range of measurements for all substances investigated was better than the fitting ability of either Equation (VI-1) or (VI-5) upto the third degree. At low flowrates Equation (VI-1) was preferable as it was observed that $\rho\Delta P/\mu F$ was a linear function of F/μ. [Figure VI-8]. Equation (VI-6) was found to be better in the intermediate and high flow region. The calibration data were consequently split into two or three regions, and separately fitted in each region using the most appropriate functional form. In Figure (VI-9) we see that $F/\sqrt{\rho\Delta P}$ approaches a constant value at high flowrates. Equation (VI-5) is still not the most desirable functional representation for this region because it does not extrapolate to the asymptotic high flow limit of $F/\sqrt{\rho\Delta P}$, and in retrospect an equation of the form

$$\frac{\rho\Delta P}{F^2} = a'' + b''(\frac{\mu}{F}) + c''(\frac{\mu}{F})^2 + d''(\frac{\mu}{F})^3 \qquad \text{(VI-6)}$$

which satisfies this criterion would have been preferred. We also see that if Equation (VI-6) is truncated upto the second term on the right hand side, it may in fact be obtained by a simple rearrangement of the Ergun equation (VI-2).

If the density and the viscosity of the fluid are accurately estimated, then all substances should lie on a single generalized curve, assuming no change in the flowmeter configuration with time. Such a curve would then permit the identification of major errors in the

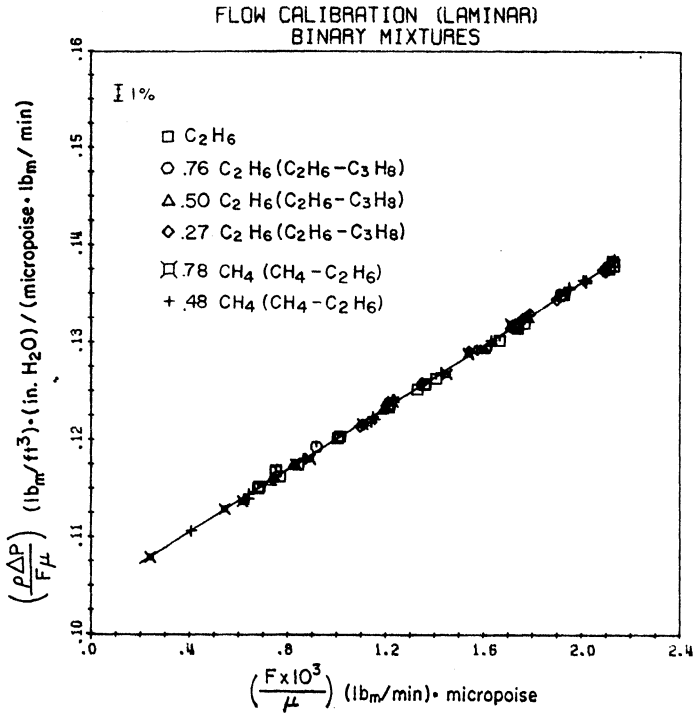

Figure VI-8. Flowmeter Calibration Results at Low Flowrates for all Systems of this Investigation Excluding the Ternary Mixture.

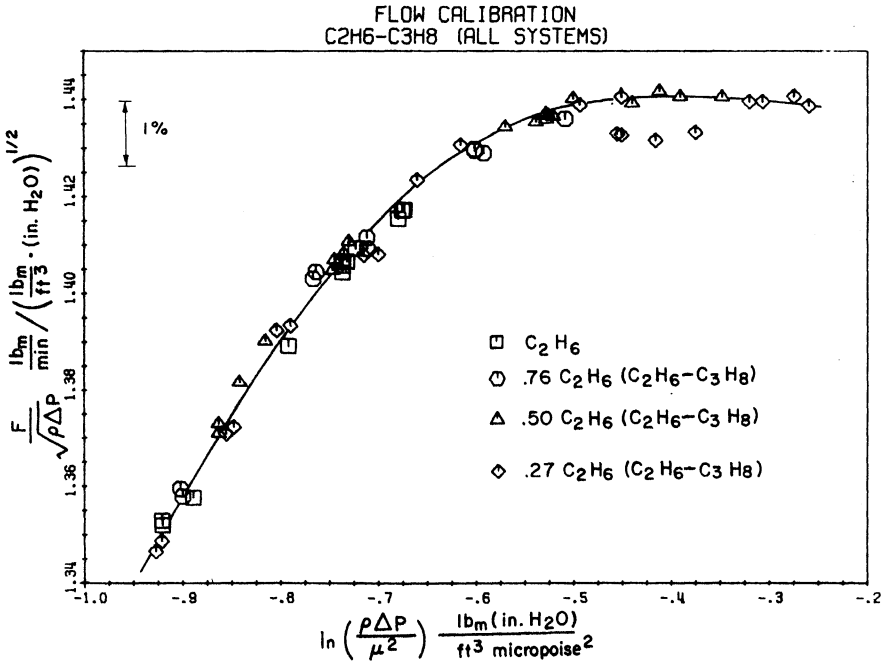

Figure VI-9. Flowmeter Calibration Results at High Flowrates.

calibration process. The densities of the mixtures were estimated using the virial equation truncated at the second virial coefficient. Both the value and the slope with respect to temperature at 27°C for the like and unlike pair second virial coefficients B_{ij} relevant to the ternary methane-ethane-propane mixture were obtained by interpolating the data in the literature. This procedure enables the variation of density with respect to the fluid composition, and with respect to the temperature and pressure of the flowmeter to be calculated to a high degree of accuracy. A calculation of the density at the flowmeter is presented as part of Appendix F-1.

The viscosity of the fluid at the flowmeter was estimated from the correlation of Lee et al. [143], given by the relation

$$\mu(T,\rho) = \mu^{\circ}(T,\rho) \exp[X(T)\rho^{Y(T)}] \qquad \text{(VI-7)}$$

where

$$X(T) = K1 + K2/T + K5\sqrt{W_i} \qquad \text{(VI-8)}$$

$$Y(T) = K3 + K4\,X(T) \qquad \text{(VI-9)}$$

K1, K2, K3, K4 and K5 are empirically determined constants that have been tabulated by the authors and are applicable to a number of light hydrocarbons including methane, ethane, and propane. W_i is the molecular weight of component i. The temperature dependence of the zero pressure viscosity μ^0 was determined using the Sutherland [260] equation

$$\mu^{\circ} = \frac{AT^{3/2}}{T + S} \qquad \text{(VI-10)}$$

for each of the pure components. The zero pressure viscosity of a mixture μ^0_m was also determined by Equation (VI-10) after applying the mixing rules

$$A_m = \frac{\sum_{i=1}^{n} x_i A_i \sqrt{W_i}}{\sum_{i=1}^{n} x_i \sqrt{W_i}} \qquad \text{(VI-11a)}$$

$$S_m = \sum_{i=1} x_i S_i \qquad \text{(VI-11b)}$$

prescribed by Lee et al. [143] to describe the mixture constants A_m and S_m.

Although the variation in the viscosity within the normal operating temperature and pressure limits of the flowmeter is calculated to be less than 0.1% for any given fluid, the actual value of the viscosity itself is not known to within the precision and repeatability of the flowmeter calibration. Consequently, the Sutherland constants A_i and S_i for the pure components methane, ethane and propane as determined by Lee and Eakin [142] were adjusted within the limits of accuracy of the data from which they were derived so as to force selected flowmeter calibration data for the three systems ethane, propane, and the 0.95 mole fraction methane-propane mixture to lie on a single curve. A calculation of the viscosity is illustrated in Appendix F-1.

Figures VI-8 and VI-9 illustrate the flowmeter calibration results for pure ethane and the binary mixtures investigated in this work using the variables in Equations (VI-1) and (VI-5) for the low and high flowrate regions, respectively. Except for the 27 mole percent ethane-propane mixture in the highly turbulent region, the results for which are interpreted in Chapter IX, a single function is seen to fit the data to all the systems examined to better than 0.25% on the average, attesting to the success of the viscosity mixing rules for the binary systems. In the case of the ternary mixture, (not plotted in these figures), the ordinate values for the curve corresponding to Equation (VI-1) were 0.5% higher than the rest. This may be attributed either to the inferior performance of the viscosity mixing rule for the ternary mixture, or due to a shift in the flowmeter characteristics caused possibly by oil that was entrained prior to the installation of the adsorbent beds.

A complete summary of all the flowmeter calibration regression results using the functional representations expressed by Equations (VI-1) and (VI-5) are presented in Table (VI-1). The calculated flowrates in either case are within 0.1% of each other. Although the accuracy of the measurement is estimated at 0.2% [119,162,284], the

TABLE VI-1

Summary of Flowmeter Calibration Equations for All Systems of This Work

System	Points	Using Equation (VI-1) Range (F/μ)+ Low	High	% Std.Dev. (Flowrate)	Least Sq. Regression Constants a	b	c	d	Using Equation VI-6 Range++ (ρΔP/μ²) Low	High	% Std.Dev. (Flowrate)	Least Sq. Regression Constants a'	b'	c'	d'
All except Ternary Mix	65	.0026	.0040	.26	.30250	-144.23	38393.	-.2288 E07	.39	.77	.15	1.4300	-.01693	.11666	.24915
All except Ternary Mix	90	.0002	.0022	.18	.10407	15.984			.025	.30	.16	1.6811	.34037	-.03125	-.91358 E-02
Ternary Mixture	44	.0008	.0030	.12	.10454	18.301	-2330.4	.6140 E06	.07	.46	.11	1.5736	.14668	-.14081	-.2885 E-01
C_2H_6 (Upto Calibration 5)	26	.0007	.0032	.18	.10368	18.558	-2681.9	.7166 E06	.09	.51	.16	1.5475	.08738	-.17510	-.35150 E-01
C_2H_6 (Beyond Calibration 5)	18	.0007	.0031	.11	.10198	21.528	-4264.7	.9534 E06	.08	.49	.14	1.5563	.09204	-.17716	-.36174 E-01
C_2H_6 (Combined)	44	.0007	.0032	.19	.10250	20.645	-3812.0	.8933 E06	.08	.51	.17	1.5498	.08570	-.17866	-.36177 E-01
0.50 C_2H_6 - C_3H_8	20	.0007	.0025	.13	.10179	21.426	-3851.8	.8107 E06	.08	.38	.11	1.6237	.21109	-.11152	-.24783 E-01
All C_2H_6- C_3H_8 Systems	45	.0007	.0027	.18	.10257	19.512	-2434.5	.5186 E06	.08	.40	.15	1.6379	.24548	-.08854	-.20155 E-01
All C_2H_6- C_3H_8 Systems	29	.0007	.0021	.16	.10417	15.954			.08	.29	.14	1.7504	.44189	.02207	
All C_2H_6- C_3H_8 Systems	19	.0021	.0027	.18	.10351	15.249	417.1		.30	.40	.14	1.6587	.31724	-.01793	
All C_2H_6- C_3H_8 Systems	37	.0027	.0040	.13	.22288	-70.510	15787.		.40	.77	.08	1.4289	-.02794	.10344	.24469
0.77 CH_4- C_2H_6	12	.0002	.0017	.14	.10436	15.017	567.1		.02	.23	.11	1.6639	.35180	-.03882	-.94379 E-02
0.48 CH_4- C_2H_6	24	.0004	.0023	.15	.10462	14.639	572.5		.04	.32	.13	1.6434	.27545	-.06110	-.13591 E-01

+ Units are lbs/min/micropoise

++ Units are $lbm/ft^3 \cdot (in.\ H_2O)/micropoise^2$

frequent occurence of an undetermined mass leakage between the calorimeter inlet and the flowmeter outlet does not always ensure that the flow at the calorimeter is accurately measured at the flowmeter. In fact, on infrequent occasions errors as high as 5% have been observed due to this effect.

f) Pressure and Differential Pressure Measurement. The arrangement of the pressure and differential pressure measurement devices used in this work is shown in Figure VI-10. The gauge pressure at the inlet to the calorimeter is measured by a dead weight gauge (Item 10a, Appendix D) using a Ruska gas to oil pressure transmitter and an electronic null detector (Item 10b, Appendix D) sensitive to imbalances as low as 0.05 psid. The resolution of the M & G dead weight gauge is 0.2 psig. The instrument was tested against a calibration standard Model 2400 Ruska dead weight gauge whose accuracy is estimated at 10 ppm. The results are reported in Table A-9. The two sources agreed to 0.1% over the entire pressure range from 250 to 2000 psia. In a previous calibration Mather [168] indicated that the error in the pressure measurement at the dead weight gauge was about 0.03%. The precision of the corrected measurement in this work is estimated at 0.05%. A mass leakage from the line connecting the calorimeter to the dead weight gage can, particularly at low pressures, cause significantly higher errors to occur.

i) Measurement Scheme for the Isobaric Calorimeter: The pressure drop across the isobaric calorimeter is measured using a 40 inch differential mercury manometer (item 10e, Appendix D) enclosed in an insulated air bath heated above the critical temperature of the system fluid to prevent liquid holdup in the lines in low temperature operation, and to prevent system fluid head corrections to the mercury level in the manometer. In the latter case, the correction can be substantial (upto 2 in. Hg.) for measurements across the two phase region. With the modified heater capsule, the pressure drop rarely exceeds one inch of mercury for the systems investigated. A precision of 0.05 inches mercury is normally obtained except if some surging action common to measurements in the two phase region, occurs.

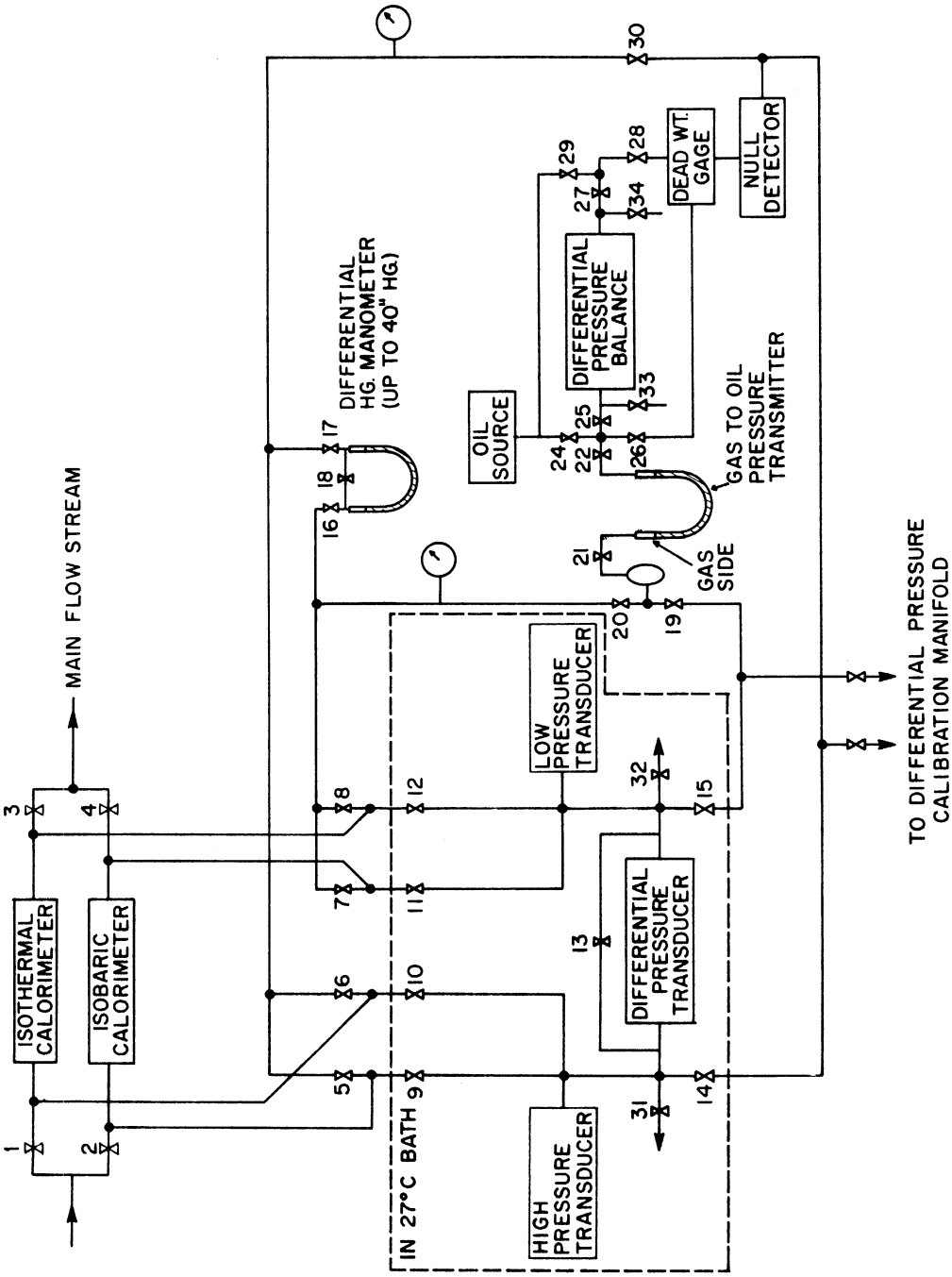

Figure VI-10. Pressure and Differential Pressure Measurement Scheme at the Recycle Flow Facility.

ii) Original Measurement Scheme for the Throttling Calorimeter: The pressure drop across the throttling calorimeter was originally measured using the differential pressure dead weight balance due to Roebuck [218] as modified by Mather [168], and Yesavage [284]. The high side pressure transmitted to the instrument is that measured at the M & G dead weight gauge. The outlet pressure at the calorimeter is transmitted to the Roebuck balance through a 36 inch mercury U leg between the system fluid and the oil on its low pressure side. The pressure differential across the balance causes the movement of a piston about a null position. The counterweight necessary to restore the piston to the balance point is equivalent to 19.998 psid/lb. mass according to the calibration of Manker [162]. Under optimum conditions, the accuracy of the measurement is estimated at $\pm$ 1% by Mather for pressure drops equal to and beyond 100 psid. In this work, the U leg was modified to include sight glasses (Item 10g, Appendix D) in each arm to permit a visual observation of the mercury imbalance previously monitored by a set of frequently malfunctioning electrical probes.

The Roebuck balance will unfortunately not sense the true inlet pressure at the calorimeter unless the M & G dead weight gauge is correctly balanced at the instant of measurement. If an imbalance exists, then it will, in effect, be incorporated as a more serious error in the differential pressure. The simultaneous adjustment of both instruments usually requires two operators, particularly, in view of pressure drop fluctuations of the order of 1% in normal operation.

iii) Modified Measurement Scheme for the Throttling Calorimeter: In this work, two strain gage transducers (Item 10c, Appendix D) each with an operating range from 0 to 2000 psia were added to determine the inlet and outlet pressure, respectively, at the calorimeter. A similar transducer (Item 10d, Appendix D) with an operating range from 0 to 1000 psid upto inlet pressure levels of 2000 psia served to measure the differential pressure across the throttling calorimeter. The three transducers together, are not only a more convenient substitute for the Roebuck balance, but also provide a redundant determination of the pressure drop.

The transducers were placed in the fixed temperature flowmeter

bath instead of the calorimeter bath to eliminate the effect of temperature on the transducer output. They were connected to the calorimeters through four 1/8" stainless steel lines welded to a stainless steel block in the wall of the flowmeter bath to which values 9,10,11 and 12 located in the bath were also attached as seen in Figure VI-10. The valves serve to connect the appropriate calorimeter to the pressure measurement section. The four lines are lead in a gently downward sloping plane through the styrofoam insulation surrounding the calorimeter bath and into the flowmeter bath through a stainless steel block in the bath wall. By confining the lines to an essentially horizontal plane, fluid head corrections at the pressure measurement system are avoided. Before the lines reach the flowmeter bath, they are tied to another set of four lines connected to the original system through valves 5,6,7 and 8 to allow one to revert to the original measurement scheme as a standby in case of transducer malfunctions. Valves 14 and 15 connect the transducer section to the M & G dead weight gauge and the Roebuck balance, respectively.

iv) Electrical Circuitry and Calibration Equations for the Pressure Transducers: The electrical circuitry for the transducers is presented in Figure VI-11. An adjustable Kepco power supply (Item 10f, Appendix D) constantly delivers an excitation voltage of approximately 10 volts to each transducer via switch S1. Switch S2 inserts a voltage divider into the circuit that permits the excitation voltage to be scaled within the measurement range of the K-3 potentiometer. The calibrations for the scaling resistors are summarized in Table A-10. A rotary switch connects any desired transducer to the K3 potentiometer. The sensitivity of the pressure transducers is 3 millivolts per excitation volt for a full scale pressure of 2400 psia. The output in each case is very linearly dependent upon pressure. For the differential pressure transducer, the sensitivity is 2 millivolts/volt for a full scale differential pressure of 1000 psid.

The pressure transducers were calibrated against the M & G dead weight gauge taking into account the calibration corrections for the latter as described earlier. The calibration equations

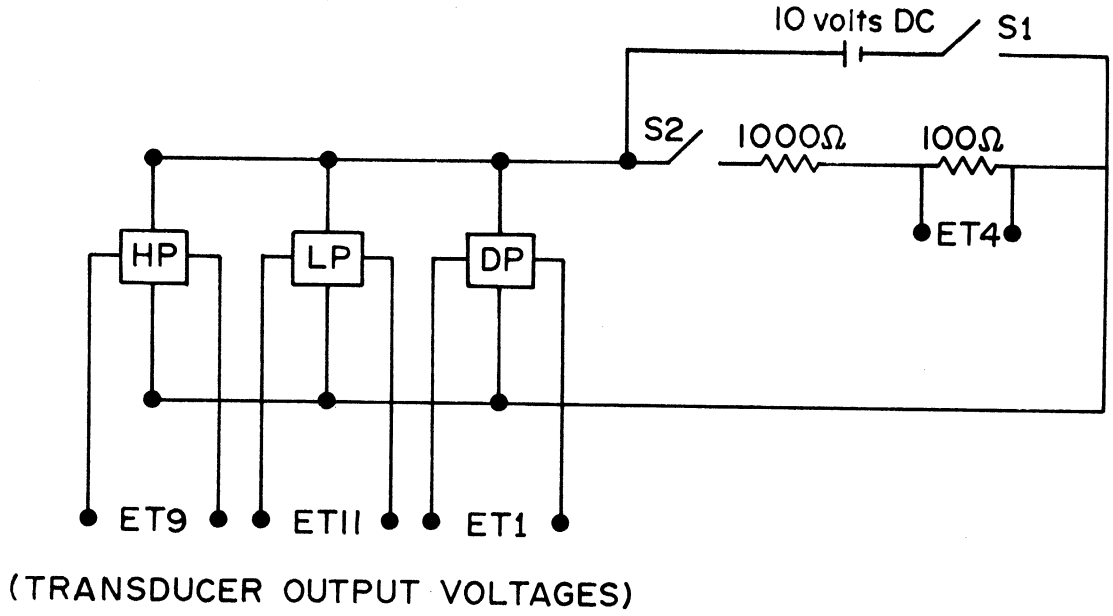

Figure VI-11. Electrical Circuit Diagram for Pressure and Differential Pressure Transducers.

$$E_h/10 = a_h + b_h P + c_h P^2 \quad \text{(VI-12)}$$

$$E_l/10 = a_l + b_l P + c_l P^2 \quad \text{(VI-13)}$$

for the high and low pressure transducers, respectively, were found to be sufficient to represent individual calibrations over the range 100 to 2000 psia with an average deviation of better than 0.06% of reading, where E is the output voltage in microvolts, and P is the pressure in psia. Sample calibration results for the pressure transducers are shown in Tables A-12 and A-13, respectively.

The representation of the calibration data for the differential pressure transducer by a suitable function is a more difficult problem because the output voltage varies not only with the differential pressure, but also with the pressure level. The output voltage is the result of an imbalance in a Wheatstone bridge circuit containing a strain gage in each arm whose resistance varies only with the absolute pressure impressed. The differential voltage is generated by the electrical subtraction of voltages produced by absolute pressure on the strain gages. Consequently the transducer, unlike the Roebuck balance is not a true differential pressure measuring device. If the high and low side are respectively represented by the individual equations

$$E_{HD}/10 = \alpha + \beta P_h + \delta P_h^2 + 3\gamma P_h^3 \quad \text{(VI-14)}$$

$$E_{LD}/10 = \alpha' + \beta' P_l + \delta' P_l^2 + 3\gamma' P_l^3 \quad \text{(VI-15)}$$

then the measured difference $(E_{HD} - E_{LD})/10$ is given by

$$\frac{E_{HD} - E_{LD}}{10} = (\alpha-\alpha') + \beta P_h - \beta' P_l + 2\delta P_h^2 - 2\delta' P_l^2 + 3\gamma P_h^2 - 3\gamma P_l^2 \quad \text{(VI-16)}$$

If the output voltage is also obtained for zero pressure difference at $P = P_h$, then the null point voltage $E_{null}/10$ is given as a function of pressure by

$$E_{null}/10 = (\alpha-\alpha') + (\beta-\beta')P_h + (\delta-\delta')P_h^2 + (\gamma-\gamma')P_h^3 \quad \text{(VI-17)}$$

By substituting P_l by P_h in Equation (VI-16), the above equation can be rewritten in the form

$$E_{null}/10 = a_n + b_n P_h + c_n P_h^2 + d_n P_h^3 \qquad \text{(VI-18)}$$

where a_n, b_n, c_n, d_n are empirical constants obtained by calibrating the null voltage as a function of pressure. Equation (VI-16) can now be rewritten in the form

$$\frac{E_{DP}}{10} = \frac{E_{HD} - E_{LD}}{10} = \beta'\Delta P + \delta'\Delta P(P_h - \frac{\Delta P}{2}) + \gamma'\Delta P(P_h^2 - P_h\Delta P + \frac{\Delta P^2}{3}) + E_{null}/10 \qquad \text{(VI-19)}$$

where $E_{null}/10$ can be determined either from direct measurement at any given time, or from a previous calibration as summarized by Equation (VI-18).

In theory therefore, the behaviour of the transducer can be completely characterized from a knowledge of the output voltage as a function of pressure drop at some fixed pressure level, and from the null point voltage as a function of pressure level. In practice, daily shifts equivalent to as much as $\pm$ 2 psid are noted in the null voltage corresponding to a given pressure level. These shifts could be attributed to hysteresis effects that are more pronounced during the dynamic conditions of actual measurement than from the relatively static calibration conditions. Therefore, it is believed that a better estimate of the true differential pressure may be obtained by measuring E_{null} at P_h for each measurement of E_{DP} instead of calculating it from Equation (VI-18).

The differential pressure transducer was calibrated using the pre-calibrated M & G dead weight gauge and the Ruska dead weight calibration standard to measure the pressure at the high and the low side, respectively. The results are shown in Table A-14. The calculated value of $[E_{DP} - E_{null}]/[10 \Delta P]$ as a function of pressure level for a fixed pressure drop of 200 psid is shown in Table A-15, and is seen to vary upto 0.35%. A sample calculation of the pressure drop, given

the calibration equations for the absolute and the differential pressure transducers, is indicated as part of Appendix F-2.

v) Chronological Survey of Pressure and Differential Pressure Measurements in This Work: The Roebuck balance and the M & G dead weight gauge were used to investigate the ternary mixture prior to the installation of the transducers. In the case of ethane, the measured pressures using the M & G gauge and the high pressure transducer are compared in Table VI-2. The pressure drop, as measured separately by the Roebuck balance and the differential pressure transducer is also tabulated. In the first case, the discrepancy between the two instruments is, in certain instances, beyond that expected from the goodness of fit to the transducer calibration data and may be attributed to hysteresis effects. Although the average agreement between the pressure drop measurements was within 1%, discrepancies upto 6%, particularly for pressure drops below 80 psid, were observed. The measured values from the Roebuck balance were almost always higher, and in retrospect these differences warranted further consideration.

Serious electrical problems in the internal circuitry caused chiefly by corrosion due to prolonged immersion in the flowmeter bath required each transducer to be returned at least once to the manufacturer. As a result, the low pressure transducer was not in service until the investigation of the 0.27 mole fraction ethane-propane system.

The constants a_h and a_l for the pressure transducers were adjusted in the time span between formal calibration and actual measurement to improve the agreement with the M & G dead weight gauge if deemed necessary. The practice of measuring all three transducer outputs at the inlet pressure corresponding to each data point as determined by the M & G dead weight gauge provides a simultaneous check on the calibrations for all three instruments during the operation of the isothermal calorimeter. As the transducers could not match the accuracy, or significantly improve the convenience of the original measurement system consisting of the M & G dead weight gauge and the 40 inch mercury differential manometer for the small pressure drops (< 2 in. Hg)

TABLE VI-2

Comparison Between Original and Modified Pressure and Differential Measurement Schemes with Ethane as the Test Fluid

RUN NO.	INLET * PRESSURE M & G PSIA	INLET + PRESSURE TRANSDUCER PSIA	ROEBUCK * PRESSURE DROP PSID	TRANSDUCER + PRESSURE DROP PSID
1.010	2001.3	2001.6	53.2	50.1
1.040	1648.5	1649.1	64.6	62.2
2.020	1165.3	1164.7	135.6	134.7
2.040	853.6	853.7	210.6	207.5
2.050	650.6	648.0	236.8	237.0
2.060	426.3	426.0	175.4	174.7
3.020	2001.0	2001.6	270.2	271.2
3.070	1142.7	1143.1	181.6	181.0
4.040	217.9	217.9	119.0	117.4
5.020	2001.4	2001.1	190.4	189.8
5.060	1192.4	1188.9	246.8	244.2
5.090	233.6	228.4	151.0	147.3
6.020	1999.5	1999.6	97.6	98.3
7.060	991.7	992.7	222.6	221.8
7.080	267.2	267.9	113.6	113.1
8.010	2002.4	2003.0	321.6	321.5
9.050	1032.5	1033.3	101.4	99.9
10.010	370.9	366.3	260.0	258.8
12.010	2013.6	2016.0	288.4	286.9
12.070	1150.5	1147.9	315.2	311.5
14.025	448.1	447.8	88.0	85.6
15.010	1996.6	1997.9	255.8	255.2
15.020	1997.2	1996.7	113.8	111.6
15.060	1198.7	1198.3	289.8	285.8
15.090	620.7	620.7	499.6	496.6
16.010	2014.0	2014.7	356.2	354.4
16.070	893.5	895.2	410.4	409.6
16.090	398.7	399.1	296.6	293.7

* Original Scheme
\+ Modified Scheme

encountered in the operation of the Faulkner calorimeter, they were not utilized for isobaric measurements.

vi) The Differential Pressure Calibration Manometer: It was originally intended to use a 200 in. multileg differential mercury manometer specially constructed in this work to serve as a calibration standard for any differential pressure device used at the facility. Although operating difficulties precluded the regular use of this instrument, it is nevertheless believed that a brief description of the manometer and the calculation of the differential pressure from the actual measurements would serve a useful purpose.

The manometer and the associated control panel is shown in Figures VI-12a through VI-12c. A schematic of the differential pressure calibration facility is shown in Figure VI-13. The manometer consists of five legs extending to a height of about 250 inches, and supported on a unistrut frame. The pressure to legs I and V constructed of 1/4" stainless steel tubing, and to legs II, III, and IV made from 1/8" stainless steel tubing is supplied by high pressure nitrogen cylinders equipped with relief venting regulators (Item 14b, Appendix D).

The mercury reservoirs at the bottom were constructed by welding together hemispherical forged steel caps for 6 inch pipe. A pressure differential between legs I and II can be created by raising a column of mercury in leg I through controlled venting of nitrogen at the top of the leg. If the mercury column is restricted to appear in sightglass A or B, corresponding approximately to 50 or 100 psid, respectively, then the actual difference in the mercury level between leg I and that in sightglass C, directly connected to leg II, can be measured by a freely suspended vertical ruled tape (Item 14e, Appendix D). The NBS calibration for the tape is presented in Table A-11. In practice, a system of front surface mirrors is used in conjunction with a telescope (Item 14d, Appendix D) to read the tape within the travel span of the telescope that is located, for convenience, at the control panel. The pressure in leg II is recorded at the dead weight gauge by suitable manipulation of the valves on the control panel shown in Figure VI-12c.

If legs IV and V are together cautiously brought to the pressure of leg I, then the subsequent venting of nitrogen gas from the top of

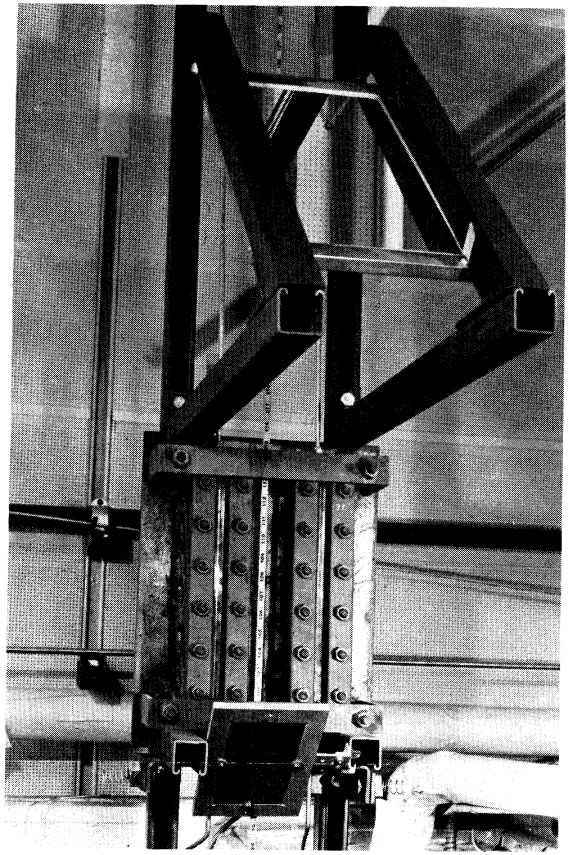

Figure VI-12a. View of Differential Pressure Calbration Manometer (D.P.C.M.) Sight Glasses.

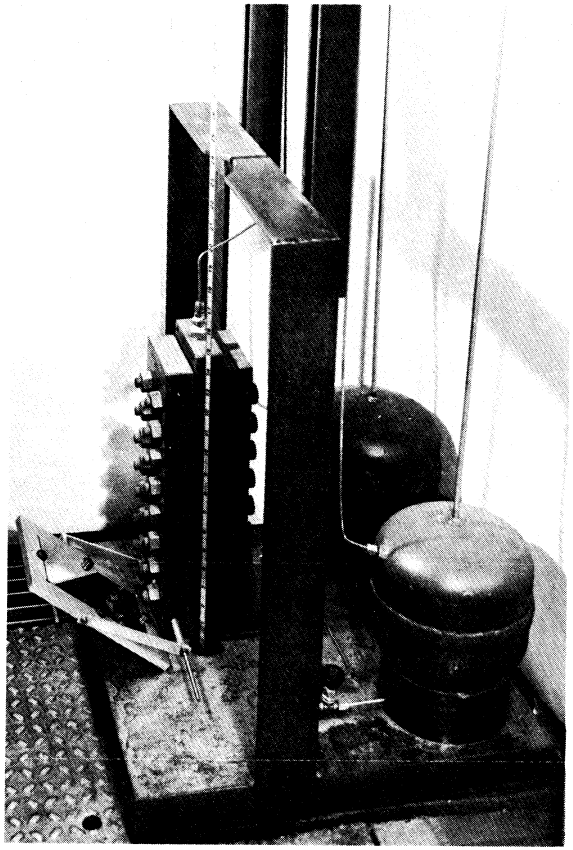

Figure VI-12b. View of (D.P.C.M.) Base.

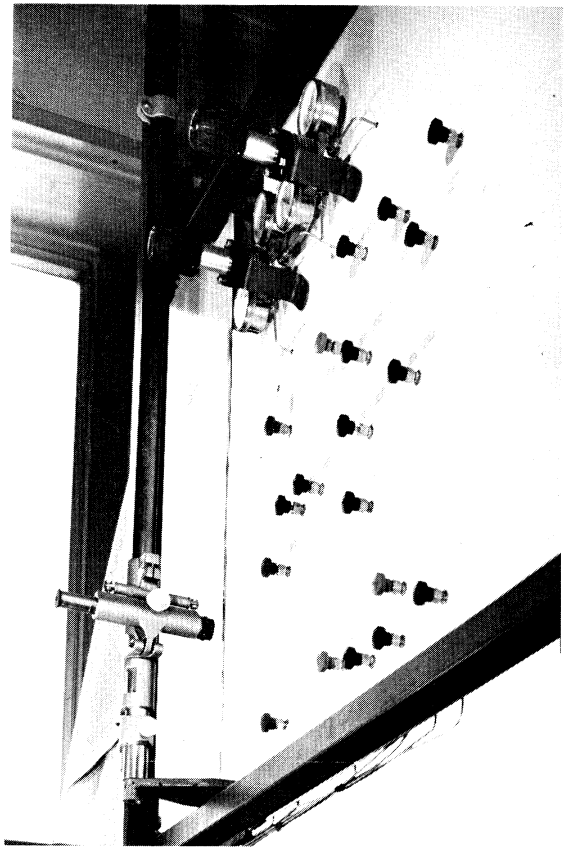

Figure VI-12c. View of (D.P.C.M.) Valve Manifold.

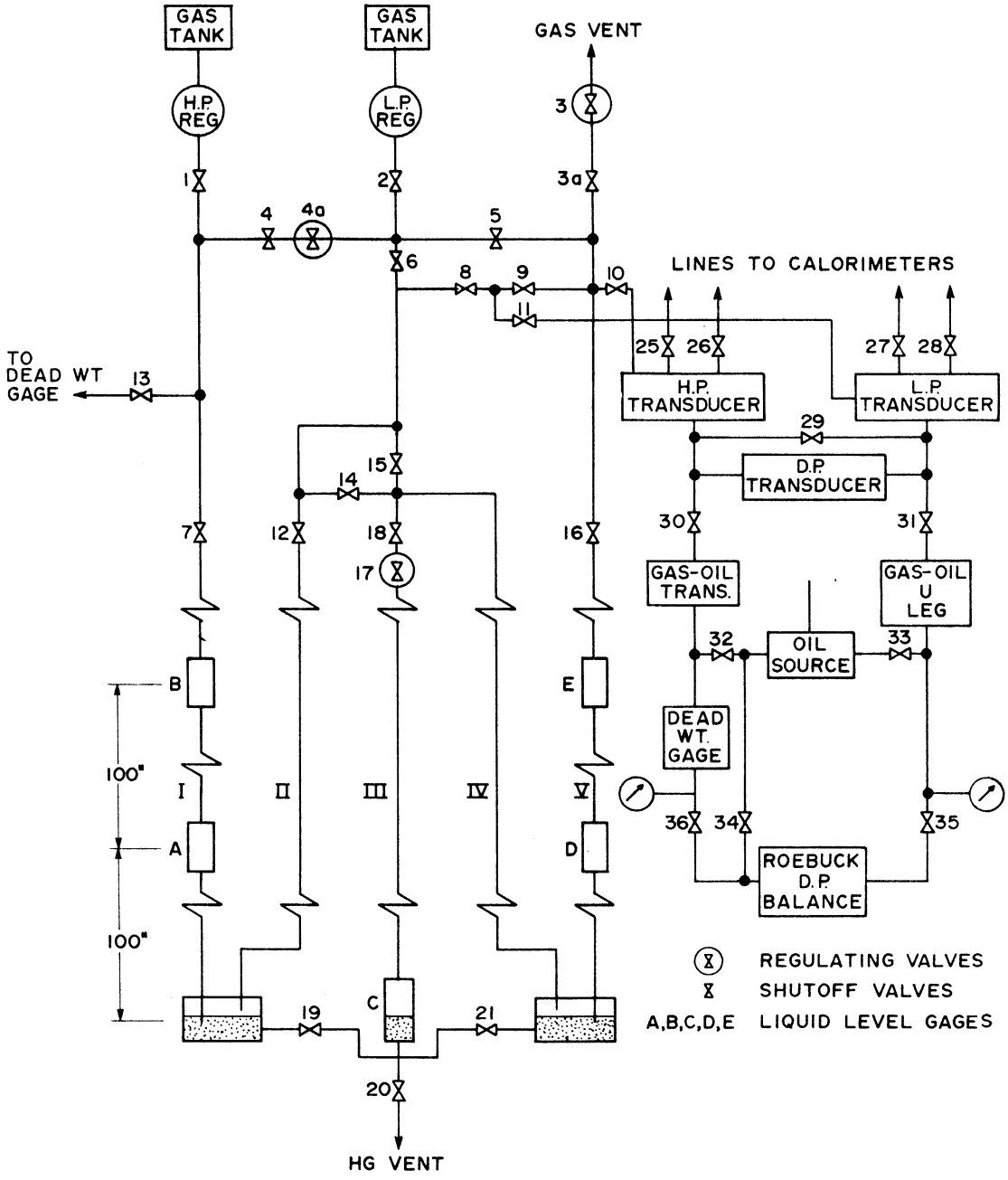

Figure VI-13. Schematic of Differential Pressure Calibration Facility.

leg V can raise a column of mercury into sightglass D or E permitting pressure differentials of about 200 psid with respect to leg II to be established. Mercury reservoirs constructed from 3" weld caps (not shown in the schematic) are also placed above sightglasses B and E to check surges in the mercury columns and to prevent contamination of the other legs or the control valve manifold.

The system is designed to permit the simultaneous calibration of all three transducers and the Roebuck balance, but is restricted to pressure differentials under 200 psid. Various corrections that are involved in the conversion of a measured mercury head into pressure units have been comprehensively reviewed by Brombacher [29]. A sample calculation involving such corrections including the contribution of a gas head to the difference in pressure between the gas in sightglass C and the M & G dead weight gage is illustrated in Appendix F-2. Difficulties in the use of the instrument can be ascribed to the simultaneous effect of poor definition of the mercury-gas interface in the reflected field sightglasses A,B,D and E, and the uncontrolled surging of the mercury column caused by sluggish regulator control in the gas venting operation.

g) Composition Analysis. The composition of the major components in each system is determined by gas-solid chromatographic analysis with a thermal conductivity detector (Item 9a, Appendix D) using helium as a carrier gas. The column and the detector are immersed in the flowmeter bath at 27°C to ensure isothermal operation. The output from the detector is traced on a strip chart recorder (Item 9b, Appendix D).

Various techniques for effecting the separation of light hydrocarbons and inorganic gases have been discussed by Chang [43]. A variety of column materials were investigated in this work including HMPA on chromasorb P (Item 93, Appendix D) Porapek Q, silica gel and alumina (Item 9d, Appendix D) in an attempt to obtain a sharp separation of methane, ethane, and propane in a reasonable time period at 27°C. Although alumina was very satisfactory at 100°C, its use would have required the installation of an additional controlled temperature bath. At room temperature, the propane elution curve is very diffuse.

A 30 foot column of HMPA on Chromasorb P produced satisfactory peaks for the individual components at room temperature, but required 12 minutes per analysis. When the column length was decreased to 15 feet, with a foot length of alumina added ahead in series, complete separation was effected in 3 minutes.

A sample chromatographic output for the ternary mixture is presented in Figure VI-14. The operating conditions for the column are indicated in Figure F-1. The propane peak height for a sample of fixed composition was found to vary from day to day. This behaviour was not observed by previous investigators at the facility who did not use alumina in the column packing. The chromatographic properties of alumina were investigated in depth by Scott [237], who concluded that trace amounts of water vapor had a significant effect on its performance, particularly with reference to the heavier hydrocarbons. Presaturation of the carrier gas was recommended for improving the reproducibility of the measurements, but was not undertaken in this work.

The system composition is analysed by comparing the individual component peak heights of a sample obtained from the flow or bypass stream just before being recycled to the compressor against the peak heights obtained for a standard sample of fixed and predetermined composition. The two samples are always analyzed together to ensure that the propane peaks are always consistent. The standard sample for each system is isolated by filling up a heated evacuated full size (size A) gas cylinder to 80 psig through valve FL on the low pressure side of the control manifold, as seen in Figure VI-1, as soon as the fluid in the system is adjudged to be completely mixed. The pressure in the cylinder is kept low, and the temperature kept high to prevent any fractionation during sampling. A sample calculation of the system composition is shown in Appendix F-4.

The composition of the standard samples was determined in the following manner. First, samples for each system investigated were obtained from the standard tank in each case and stored. A number of binary reference mixtures were prepared from ultra-pure constituent pure component samples in 180 cc containers by direct weighing using a precision Christian Becker balance sensitive to 0.1 milligram.

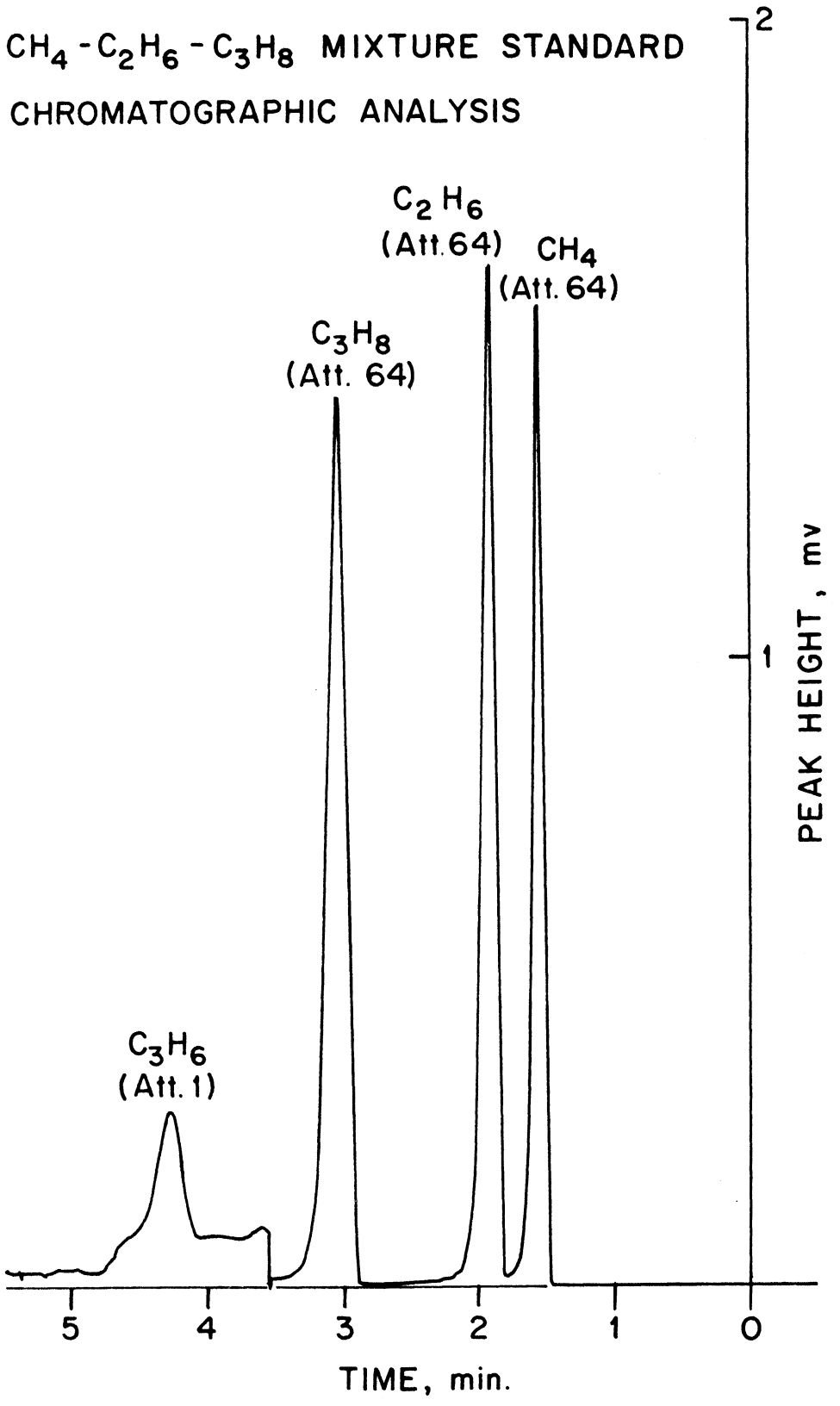

Figure VI-14. Sample Chromatographic Output for the Ternary Mixture.

Recent simplifications in the experimental technique including a sample calculation are described in Appendix F-3. The reference mixture compositions were designed to lie in the vicinity of the individual system samples and are believed to be known to an accuracy of better than 0.2%. The reference and the standard samples were then analyzed in sequence. A plot of peak height vs. mole fraction was made for each component using all the reference sample results as illustrated in Figure F-1. The propane calibration curve shows the greatest degree of non-linearity. The concentration of a given component in each standard sample was calculated from the appropriate calibration curve given the measured peak height. The departure from unity in the sum of the independently determined mole fractions, including trace components, for any given sample served as a consistency check, and was found to vary between 0.997 and 1.004.

Trace components in the standard samples were analyzed by mass spectrometry, and are assumed to be essentially invariant for all samples of a given system. Attempts to obtain corroborative evidence of the major component mole fractions by this technique were almost always unsuccessful, as the agreement was almost never better than 2%. A similar problem was reported by Manker [162]. Persistent work on the pure components, and some reference mixtures led to the discovery of an error in the experimental technique relating to the leakage of a variable quantity of air into the given sample as it was being transferred from the 180 cc can to the evacuated bulb of the mass spectrometer. The extent of the air contamination was evaluated by the discrepancy between the chromatographic and mass spectrometric determinations of the mole fraction of the major components, and an attempt was made to evaluate the trace amounts of nitrogen, oxygen, and carbon dioxide in the system by compensating for the air leakage. As the latter accounted for over 90% of the peak valve in each case, the estimated values of these trace impurities are only approximate. Fortunately, the analysis of the major impurity propylene, introduced into every system because of its occurence in the pure ethane feed, was not complicated by the air leakage.

The accuracy of the composition analysis of the major components as obtained during calorimetric measurements is a function of the

departure of the system composition at the flowmeter from that of the sample in the standard tank (see Appendix F-3) and averages to ± 0.25% for the systems investigated in this work. The average value of the composition for the individual systems is indicated in Table VI-3.

Procedure

An excellent procedure for starting, operating and shutting down the system is presented by Manker [162] and is applicable to this work with only minor modifications relating to the equipment changes discussed earlier. The operating procedures specific to the acquisition of a particular type of thermal data are outlined below.

As Manker explains, a very complex situation exists even before measurements can be attempted. The period between start-up and measurement is devoted to achieving the desired inlet conditions of temperature, pressure, and flowrate at the calorimeter. This period may vary anywhere from two to six hours. However, as Jones [119] indicates, true steady state conditions are never reached, and constant adjustment of the appropriate control valves are required to maintain quasi-steady state conditions if the accuracy of the measurements is to be ensured. The constant monitoring of leaks from diverse sources such as the valves in the control manifold and on the various storage cylinders, from fittings, particularly on the instrumentation lines leaving the calorimeter and the flowmeter, and at the compressor heads is a critical aspect of normal operation. If a leak is suspected, further measurements are postponed until the source is determined and the leak arrested. Consecutive measurements are usually spaced thirty to forty-five minutes apart. Jones has listed the more crucial observations that are recorded per isobaric measurement. Upto thirty observations noted over a period of five minutes or less, are made per data point.

a) Single Phase Isobaric Operation. A single run consists of a series of data points that are obtained by varying the outlet temperature through suitable adjustment of the heat input rate for a fixed set of inlet conditions. Four to five data points are obtained per run at a reasonably constant flowrate involving temperature rises

TABLE VI-3

Summary of the Composition Analysis for the Systems of this Investigation

NOMINAL COMPOSITIONS	.76 C2H6 .24 C3H8	.50 C2H6 .50 C3H8	.27 C2H6 .73 C3H8	.78 CH4 .22 C2H6	.48 CH4 .52 C2H6	.37 CH4 .31 C2H6 .32 C3H8	1.00 C2H6
COMPONENTS	MOLE FRACTION						
METHANE	.0023	.0037	.0006	.7771	.4790	.3690	.0004
ETHANE	.7598	.4940	.2746	.2210	.5170	.3045	.9960
PROPANE	.2350	.5002	.7235	.0003	.0003	.3232	.0003
PROPYLENE	.0019	.0015	.0003	.0005	.0029	.0025	.0026
NITROGEN	.0006	.0003	.0004	.0008	.0005	.0005	.0005
CARBON DIOXIDE	.0004	.0003	.0006	.0003	.0003	.0003	.0002
MOL. WT.	33.358	37.054	40.218	19.181	23.390	29.460	30.099

from 10°F to 125°F. Contiguous runs along a given isobar are usually arranged so that their temperature spans overlap. This permits their consistency with respect to each other to be evaluated.

Over the course of a given run, an average inlet temperature variation of about 0.2°F is observed, as opposed to 0.03°F reported by Manker [162]. Inlet pressure variations upto $\pm$ 2 psia per run were allowed. Manker [162] restricted such variations to $\pm$ 0.3 psia. Such stringent regulation of inlet conditions would have considerably increased the time period for this investigation, and were considered only for measurements in the vicinity of the heat capacity maxima, where the techniques used to compensate the data for variations in inlet conditions, as discussed in the next chapter, are less reliable. The precise location of the heat capacity maximum requires successive data points to be spaced as close as a degree apart in some cases. The solid horizontal bars in Figure VIII-10 for example are typical of single phase isobaric measurements.

b) Two Phase Isobaric Operation. For a given system, the dew and bubble points for a specified pressure are first approximately located from the data in the literature when available or by a prediction technique such as the NGPA K value charts [156]. The inlet temperature for the run is chosen to be at least 10°F below the estimated bubble point. Initially, the power at a fixed flowrate is adjusted to generate data points over small temperature increments. The bubble point is judged to have been exceeded, if the rate of increase of power is disproportionately high for a given temperature increment. At this point, a couple of additional measurements are made, sufficient to locate the bubble point as a discontinuity in a plot of heat input vs. temperature rise. The flowrate is then dropped to a low value commensurate with the limitations on the power supply, and the measurements are continued over larger temperature intervals until another change of slope is apparent on the same plot. The power is decreased if necessary, and closely spaced measurements that clearly serve to define the dew point are made. Although as many as fifteen data points may be involved in such a run [162], as few as nine may be sufficient to characterize an isobaric run across the two phase region. Again, as no provisions are made to compensate for variations in inlet pressure within the two phase region, such variations must be minimized.

Similar precautions must extend over the course of the entire run for measurements near the critical region in view of the extreme sensitivity of the enthalpy of vaporization to pressure in such cases. A typical enthalpy traverse is shown in Figure VIII-38.

c) Isothermal and Isenthalpic Operation. For the throttling measurements, the inlet pressure is initially set at 2000 psia, and a pressure drop usually in the range 50-400 psid is generated depending on the flowrate and the I.D. and length of the capillary element that is used to create the pressure drop. If the outlet temperature drops below the inlet temperature, an adjustable amount of power is supplied to the heating wire located within the capillary to raise the outlet temperature to within 0.02°F of the inlet temperature if possible. If the outlet temperature before the addition of power is above that of the inlet, the operation is restricted to the isenthalpic mode. The heating wire in the capillary is inactive, but the guard heater surrounding the outlet section is supplied with a small adjustable amount of power to balance the heat leak.

In either case, the inlet pressure is then decreased to a value near the outlet pressure of the previous data point, and the process repeated until an outlet pressure of approximately 100 psia is obtained. Measurements below 100 psia are restricted by the operating pressure (80 psig) of the flowmeter. Typical isothermal and isenthalpic runs are illustrated in Figures VIII-52 and VIII-41, respectively. In rare cases, two consecutive measurements are initiated at the same inlet pressure, and the pressure drop varied by suitable adjustment of the flowrate. Different size capillary coils should be used for the cryogenic liquid and the gaseous regions if comparable pressure drops for normal flow conditions are to be generated. In this work, a twelve foot 18-19 B & S gauge capillary was used in the liquid region, while a 16-17 B & S gauge capillary was found to be satisfactory for gas phase measurements. It is necessary to place greater emphasis in limiting the fluctuations in the calorimeter bath temperature in order to prevent relatively significant spurious contributions to the small temperature differences characteristic of such measurements.

Although previous investigators at the laboratory [168,284] have

reported isothermal enthalpy traverses across the two phase region, the measurement, and in particular the location of the dew point, is experimentally difficult, and has generally been avoided in this work. The chief difficulty is due to severe fluctuations in the flowrate and pressure drop that are observed within the two phase region and caused by the changing quality of the two phase mixture as one almost futilely attempts to adjust the outlet temperature to that of the inlet.

Operating Schedule

As a rule of thumb, a day of maintenance was found to be necessary per day of operation and illustrates to some extent the difficulty of the experiment. Furthermore, the recycle system was found to suffer from a high degree of inertia. Consequently, it was felt that round the clock operation, with twelve hour shifts, terminated only by the occurrence of a major malfunction would be most productive. This schedule was accordingly implemented.

Chronology of the Experimental Investigation

The chronological order of examination of the systems of this study was in part dictated by the need to minimize the total investment in the gas fed to the system. A 23.4% methane-propane mixture was left in the storage tanks from a previous investigation [284]. Ethane, and make up quantities of methane, and propane (Item 15a, 15c and 15d, respectively) were added until the system was filled to capacity with the ternary mixture of required composition. After its completion, the entire system including the fluid in the storage tanks was evacuated, flushed, and then filled with ethane. The three ethane-propane mixtures, investigated in order of increasing propane concentration, were prepared by adding propane and make up amounts of ethane to each system in sequence. Upon completion of the investigation, the system was re-evacuated, and appropriate quantities of methane, and ethane were mixed to yield a mixture containing 78% methane. Further addition of ethane was required to generate the 48% methane-ethane mixture. The procedure for mixing the pure fluids in the recycle systems to achieve the desired mixture in the shortest possible time was improved from that of previous investigations and is discussed in Appendix I-2.

Chapter VII

DATA REDUCTION

This section describes how smoothed tabulated values of the enthalpy function and its appropriate derivatives with respect to temperature and pressure are generated so as to accurately reflect the basic data of this work within the constraints of thermodynamic consistency. In sequence, the errors in the original observations must be weeded out and corrected where possible, the basic data must then be interpreted to yield smoothed values of Cp or ϕ which are in turn integrated along isobars and isotherms, respectively, to generate smoothed enthalpy values. After the enthalpies are examined and adjusted for self consistency, it is possible to proceed with the construction of smoothed enthalpy tables or diagrams using auxiliary enthalpy data at zero pressure.

Reduction of Raw Data to Basic Data

The basic observations are entered on punched cards, and fed to a master data reduction program in Fortran IV on file at the TPFL and processed on an IBM 360-67 digital computer. The program is designed to accomodate any system consisting primarily of the components methane, ethane and propane. The specific mode of calorimeter operation, the calibration data for those instruments whose characteristic tend to change with time, and information that indicates the desired weighting whenever redundant measurements are obtained must be fed as part of the input in addition to the observations specific to each given data point. The computer output is screened for errors in the noted observations using in part diagnostic techniques discussed in the previous chapter. This basic processed data are generated by the computer in punched card form in which the composition of the three major components, the inlet temperature, the temperature difference, the inlet pressure, the pressure drop, the experimentally observed enthalpy change, and the approximate average value of the enthalpy derivative appropriate to the calorimeter operating mode are recorded. The basic format for the ternary mixture for example is seen in Tables B-19 through B-21. The basic technique for the reduction of the raw data has been

excellently illustrated by Jones [119] and is utilized in this work with the exception of the modifications discussed in the previous chapter. Sample calculations that illustrate data reduction procedures that are modified in this work are presented in Appendix F-1 through F-4.

Determination of Enthalpy Derivatives Cp, ϕ and μ From the Basic Data

The determination of the differential thermal properties Cp and ϕ from the basic data requires the operating mode of the calorimeter to be such that the fluid stream is confined to a path where the effect of a single independent variable may be isolated. In general, simultaneous variations in other independent variables, however small, cannot be entirely avoided during the actual measurement and must be compensated for.

a) Thermodynamic Analysis for Isobaric Data. If the reference pressure and composition for an isobaric run are represented by P_o and $[x_o]$, respectively, then every data point in the run obtained at slightly different inlet conditions P_i and $[x]$ must be corrected to the reference point. Furthermore, the pressure drop $(P_i - P_f)$ must also be compensated for. The equation

$$\left(\underline{H}_{T_f,P_o,[x_o]} - \underline{H}_{T_i,P_o,[x_o]}\right) = \left(\underline{H}_{T_f,P_f,[x]} - \underline{H}_{T_i,P_i,[x]}\right) + \left(\underline{H}_{T_f,P_o,[x]} - \underline{H}_{T_f,P_f,[x]}\right) +$$

$$\left(\underline{H}_{T_f,P_o,[x_o]} - \underline{H}_{T_f,P_o,[x]}\right) + \left(\underline{H}_{T_i,P_i,[x]} - \underline{H}_{T_i,P_o,[x]}\right) + \left(\underline{H}_{T_i,P_o,[x]} - \underline{H}_{T_i,P_o,[x_o]}\right) \qquad \text{(VII-1)}$$

expresses the desired enthalpy difference on the left hand side in terms of the actually measured enthalpy difference (the first bracketed quantity on the right hand side) and additional correction terms. Combining Equation (I-21) with (VII-1), and expressing the correction terms on the right hand side in terms of the appropriate enthalpy derivatives, we obtain

$$\left(\underline{H}_{T_f,P_o,[x_o]} - \underline{H}_{T_i,P_o,[x_o]}\right) = \frac{EI}{\dot{m}} + \int_{P_f}^{P_o} (\phi)_{T_f,[x]}\, dP + \int_{[x]}^{[x_o]} \sum_{j=1}^{n} \left(\frac{\partial \underline{H}_j}{\partial x_j}\right)_{T_f,P_o,x_{i\neq j}} dx_j + \int_{P_o}^{P_i} (\phi)_{T_i,[x]}\, dP$$

$$+ \int_{[x_o]}^{[x]} \sum_{j=1}^{n} \left(\frac{\partial \underline{H}_j}{\partial x_j}\right)_{T_i,P_o,x_{i\neq j}} dx_j \qquad \text{(VII-2)}$$

The mean heat capacity over the interval between T_i and T_f may now be determined from the corrected enthalpy change as

$$\bar{C}_p = \int_{T_i}^{T_f} (Cp)_{P_o,[x_o]}\, dT/(T_f - T_i) = (\underline{H}_{T_f,P_o,[x_o]} - \underline{H}_{T_i,P_o,[x_o]})/(T_f - T_i) \qquad \text{(VII-3)}$$

The solid horizontal bars in Figure (VIII-10) for example, represent the mean heat capacities over the interval of the bar length, and are derived from the basic data after correction. A smoothed heat capacity curve can now be constructed along the entire isobar under the constraint of Equation (VII-3) which requires the area under the solid horizontal bars to equal the area under the smoothed curve.

As an isobaric run consists of a series of measurements where the inlet conditions are held fairly constant, the corrected basic data may be differenced after making additional corrections for small variations in the inlet conditions. Thus, if T_o is the reference inlet temperature for a given isobaric run containing two data points A and B with inlet temperatures T_{iA} and T_{iB}, and outlet temperatures T_{fA} and T_{fB}, respectively, then the mean heat capacity over the interval T_{fA} to T_{fB} is given by

$$\bar{C}_p = [(\underline{H}_{T_{fA},P_o,[x_o]} - \underline{H}_{T_{iA},P_o,[x_o]}) - (\underline{H}_{T_{fB},P_o,[x_o]} - \underline{H}_{T_{iA},P_o,[x_o]}) - \int_{T_{iA}}^{T_o} (Cp)_{T_o,P_o}\, dT + \int_{T_{iB}}^{T_o} (Cp)_{T_o,P_o}\, dT]/(T_{fA} - T_{fB}) \qquad \text{(VII-4)}$$

where the value of the heat capacity at the inlet condition T_o, P_o is necessary to provide the corrections for the variation in the inlet temperature.

If the interval $(T_{fA} - T_{fB})$ is small with respect to the temperature rises $(T_{fA} - T_{iA})$ and $(T_{fB} - T_{iB})$ for the data points A and B, then errors or inconsistencies in the basic data are magnified and consequently more easily spotted if such differenced mean heat capacity values are also plotted as indicated by the dashed lines in Figure VIII-10. This information is also seen to be more useful than the basic data in guiding the course of the equal area heat capacity curve by manual techniques.

The evaluation of the last four terms in Equation (VII-2) by direct measurement could be very time consuming. Therefore, the estimation of these terms from an enthalpy prediction technique of proven reliability is to be preferred. A satisfactory technique for the accurate estimation of thermal property derivatives is yet to

be found. Such difficulties forced previous investigators at the laboratory [162,168,284] to ignore the corrections for all but the pressure drop term in isobaric operation, and the temperature difference term for isothermal runs, both of which were calculated by the original BWR equation of state, unless more reasonable estimates could be obtained from other direct measurements

b) The Use of the PGC for the Correction of the Basic Data. Although the PGC was found to be excellent for the prediction of pure component and mixture enthalpies, the tabular nature of the correlation does not ensure that accurate values of enthalpy derivatives can also be calculated. To partially circumvent this problem, a modified data correction technique was used in this work which involved the computation of enthalpy difference ratios using the PGC predictions. For the isobaric case we obtain

$$(\underline{H}_{T_f,P_o,[x_o]} - \underline{H}_{T_o,P_o,[x_o]}) = [\underline{H}_{T_f,P_f,[x]} - \underline{H}_{T_i,P_i,[x]}]_{Expt} [(f_{[x_o]})(f_{T_o})(f_{P_o})(f_{\Delta P_f})] \quad \text{(VII-5)}$$

where

$$f_{[x_o]} = (\underline{H}_{T_f,P_f,[x_o]} - \underline{H}_{T_i,P_i,[x_o]})/(\underline{H}_{T_f,P_f,[x]} - \underline{H}_{T_i,P_i,[x]}) \quad \text{(VII-5a)}$$

$$f_{T_o} = (\underline{H}_{T_f,P_f,[x_o]} - \underline{H}_{T_o,P_i,[x_o]})/(\underline{H}_{T_f,P_f,[x_o]} - \underline{H}_{T_i,P_i,[x_o]}) \quad \text{(VII-5b)}$$

$$f_{P_o} = (\underline{H}_{T_f,P_f,[x_o]} - \underline{H}_{T_o,P_o,[x_o]})/(\underline{H}_{T_f,P_f,[x_o]} - \underline{H}_{T_o,P_i,[x_o]}) \quad \text{(VII-5c)}$$

$$f_{\Delta P_f} = (\underline{H}_{T_f,P_o,[x_o]} - \underline{H}_{T_o,P_o,[x_o]})/(\underline{H}_{T_f,P_f,[x_o]} - \underline{H}_{T_o,P_o,[x_o]}) \quad \text{(VII-5d)}$$

The last four terms on the right hand side represent fractional corrections to the basic data for variations in composition, inlet temperature, inlet pressure, and pressure difference, respectively. The corrections for variations in inlet temperature are only required if the basic isobaric data are to be differenced. For the isothermal case, one obtains

$$\underline{H}_{T_o,P_f,[x_o]} - \underline{H}_{T_o,P_i,[x_o]} = (\Delta H)_{Expt}[(f_{[x_o]})(f_{T_o})(f_{\Delta T})] \quad \text{(VII-6)}$$

where

$$f_{\Delta T} = (\underline{H}_{T_o,P_f,[x_o]} - \underline{H}_{T_o,P_i,[x_o]})/(\underline{H}_{T_f,P_f,[x_o]} - \underline{H}_{T_o,P_i,[x_o]}) \quad \text{(VII-6a)}$$

and corrects for the temperature difference between the calorimeter outlet and the reference temperature T_o for the isotherm.

Special care is required in applying such correction procedures in the vicinity of the heat capacity maxima, as discrepancies between the PGC and the actual data with respect to the location of the maximum can result in substantial errors in the correction terms. The average total correction was about 0.2% for the isobaric measurements, and about 1% for the isothermal data.

In all cases, unreasonably large correction terms were either ignored or substituted by experimentally derived values of Cp or ϕ where possible. Thus, corrections for the temperature difference in isothermal measurements, and for variations in inlet temperature in the isobaric data were, in some cases, obtained from Cp values that were determined by preliminary processing of the experimental results. As the PGC was not equipped for the prediction of the phase behaviour of mixtures at the time, two phase data remained uncorrected.

In all cases, unreasonably large correction terms were either ignored or substituted by experimentally derived values of Cp or ϕ where possible. Thus corrections for the temperature difference in isothermal measurements, and for variations in inlet temperature in the isobaric data were, in some cases, obtained from Cp values that were determined by preliminary processing of the experimental results. Special care is required in applying such correction procedures in the vicinity of the heat capacity maxima, as discrepancies between the PGC and the actual data with respect to the location of the maximum can result in substantial errors in the correction terms. The average total correction was about 0.2% for the isobaric measurements, and about 1% for the isothermal data.

c) Interpretation of Joule-Thomson Coefficient Data. It is evident that the fractional correction scheme cannot work for situations involving little or no enthalpy change, i.e., for isenthalpic operation. In this case the fractional correction may be computed with respect to the observed temperature difference. Thus

$$[T_f([x_o],P_f) - T_i([x_o],P_i)]_{\Delta H=0} = [T_f([x],P_f) - T_i([x],P_i)]_{\substack{\Delta H=0 \\ Expt}} \left[\frac{T_f([x_o],P_f) - T_i([x_o],P_i)}{T_f([x],P_f) - T_i([x],P_i)} \right]_{PGC} \quad \text{(VII-7)}$$

However, the PGC predictions were such that irregular variations were observed with respect to both the sign and magnitude of the enthalpy deviations for the individual data points in a given run. These variations were, in part, also attributed to truncation effects. It was felt that the PGC corrections for such data, as incorporated in Equation (VII-7), were best ignored in view of the demonstrated irregularities.

Isenthalpic measurements are typically illustrated in Figure (VIII-13) where the average value of the Joule-Thomson coefficient $\bar{\mu}$ is plotted over the pressure interval for each data point. It is important to note that successive data points do not, strictly speaking, lie on the same isenthalp if the inlet pressure is varied and the inlet temperature is kept constant throughout the run. Furthermore, the point value of μ at any point cannot, in rigid accordance with thermodynamics, be obtained by constructing an equal area curve through the data points in Figure VIII-13. From the standpoint of constructing an enthalpy diagram from such measurements, it is best to interpret the isenthalpic data to generate a pressure-enthalpy isotherm corresponding to the inlet temperature of the run.

Recalling Equations (I-27) through (I-30), an experimental determination of $\bar{\mu}$, and an independent estimate of $\bar{C}p$ over the interval $(T_f - T_i)$ permits the value of $(\bar{\phi})_{T_i}$ over the interval $(P_f - P_i)$ to be calculated. Point values of ϕ at T_i may now be obtained as a function of pressure by the equal area technique. On integration, the desired pressure-enthalpy isotherm is generated.

As the temperature rise ΔT across individual isenthalpic data points is usually less than 1°F, $\bar{C}p$ may be approximated by the point value Cp at the arithmetic mean temperature $T_o = (T_i + T_f)/2$. The required estimate of Cp at T_o and P_f was obtained by cross plotting Cp values obtained along isobars as a function of pressure at $T = T_o$. The generation of a pressure enthalpy isotherm from isenthalpic data has been illustrated for propane as Figure 18 in the thesis of Yesavage [284].

In this work, the experimental heat capacity data at the temperature of interest T_o were sometimes restricted to a single isobar at P_o, and required a different technique to be used for the estimation of Cp at the desired pressure P_f. It was necessary to assume that

dCp/dPr was uniquely determined at a given Tr and Pr. It was further assumed that the variation of Cp with reduced pressure could be determined from the Cp vs P plot of Yesavage [284] for the 23% methane-propane mixtures as a function of temperature in the liquid and dense fluid region. If the pseudocritical properties of the mixture are approximately estimated (the mixing rules expressed by Equations (IV-77), (IV-78) and (V-22) with the approximations of Equations (IV-17), (IV-19a) and the arithmetic mean for αc_{ij} were used), then the variation of Cp with pressure over the interval P_o to P_f at temperature T_o for a substance with pseudocritical parameters Tc_m and Pc_m is given by

$$Cp(T_o,P_f) - Cp(T_o,P_o) = \left[Cp\left(T_o \frac{Tc_{mr}}{Tc_m}, P_f \frac{Pc_{mr}}{Pc_m}\right) - Cp\left(T_o \frac{Tc_{mr}}{Tc_m}, P_o \frac{Pc_{mr}}{Pc_m}\right)\right] \frac{Pc_{mr}}{Pc_m} \qquad \text{(VII-7a)}$$

where the square bracketed term on the right hand side represents the quantity evaluated from the plot of Yesavage, and Tc_{mr}, Pc_{mr} are the pseudocritical parameters for the 23% methane-propane mixtures. Thus, Cp at P_f may be estimated if Cp at P_o is independently known. Although this appears to be an approximate technique it must be recognized that the variation of Cp with pressure from saturation conditions in the liquid phase upto pressures as high as 2000 psia rarely exceeds 1.5% in the region of isenthalpic measurements. Consequently errors in the estimation of $\overline{\phi}$ from such data are bounded by this value even if corrections for the variation of Cp with pressure are completely ignored.

Techniques for Constructing Equal Area Curves

Unless errors in constructing and integrating equal area curves for the properties Cp and ϕ from the basic enthalpy data are scrupulously avoided, all the effort that has been expended in preserving the accuracy of the basic measurements will have been essentially wasted. The construction and integration of these curves was one of the most time consuming problems of this work. The merits and deficiencies of techniques attempted in previous investigations are also discussed along with those tried in this work.

a) Graphical. Manker [162], Jones [119] and Mather [168] obtained

heat capacities from experimental isobaric data by graphical integration involving a visual judgement of the equal area criterion and claimed a precision of 0.5%. The reported enthalpy values of Manker were, however, directly derived from experimental data by plotting the measured enthalpy change vs temperature rise for each data point in a given run, and by connecting the points with a smooth curve using the inlet temperature as a temporary enthalpy reference. The value of the inlet temperature enthalpy for successive runs along a given isobar were related to each other either from overlapping data or through graphical integration of interpolated heat capacity values when no such overlap existed. Such a procedure does not ensure consistency between the enthalpy and heat capacity values.

Bhirud and Powers [22] have used Simpson's rule both to plot the Cp curve from the mean heat capacity values and to integrate the plotted curve to yield consistent enthalpy values. In brief, if Cp is assumed to be a cubic function of T in the interval T_i to T_f for which the mean heat capacity is known, and plotted as a bar over the given interval, then, at the midpoint of the bar, the vertical distance between the bar and the equal area heat capacity curve must be half of the distance between the bar and the straight line joining the point values of Cp at the extremities T_i and T_f of the bar. Mathematically

$$\bar{C}p - (Cp)_{(T_i+T_f)/2} = \frac{1}{2}\left[\{(Cp)_{T_i} + (Cp)_{T_f}\}/2 - \bar{C}p\right] \qquad \text{(VII-8)}$$

This technique is very arduous and is susceptible to an indeterminate degree of human error.

2) Linear Regression Techniques. Yesavage [284] assumed that the heat capacity could be expressed as a power series

$$Cp = b + 2cT + 3dT^2 + 4eT^3 \qquad \text{(VII-9)}$$

On integration, the result

$$\frac{H_f - H_i}{T_f - T_i} = \bar{C}p = b + c\frac{(T_f^2 - T_i^2)}{(T_f - T_i)} + d\frac{(T_f^3 - T_i^3)}{(T_f - T_i)} + e\frac{(T_f^4 - T_i^4)}{(T_f - T_i)} \qquad \text{(VII-10)}$$

was obtained. The constants b,c,d, and e are determined by a multivariable linear least squares regression analysis using T_i and T_f as the independent variables, and $\overline{Cp}$ as the dependent variable, and may now be used to calculate smoothed values of heat capacity and enthalpy relative to some base temperature. The number of data points for a given set of regression constants was fixed at eight. This technique consequently gave rise to discontinuities in the value of the heat capacity at the interface of successive regression sets along a given isobar. Furthermore, in the absence of weighting procedures, the use of marginal data points in the regression was observed to cause ripples in the heat capacity function in some cases. The method also produced a poor fit in the region of the Cp or ϕ maxima where supplementary graphical processing was found to be necessary.

c) Non-Linear Regression Techniques. In this work, an attempt was made to process a complete isobar or isotherm with observed maxima using a single analytic functional relationship between Cp and T, or between ϕ and P. This technique was tested with the 126.2°F isotherm for the ternary mixture seen in Figure (VIII-52), primarily because of the even distribution of data about the maximum point, and their excellent consistency with respect to each other. Provisions were made for performing a multiple, and if necessary, non-linear regression analysis on a flexible combination of a wide variety of functions using the Gauss method of least squares. A discussion of the technique, and an algorithm is provided by Wolberg [282] which also includes provisions for weighting the data used in the regression.

Initially, the form

$$\phi = a + bP + cP^2 + dP^3 + gfe^{-f(P-P_k)^2} \qquad \text{(VII-11)}$$

was attempted, where P_k is the pressure corresponding to the maximum value of ϕ along the isotherm. The polynomial terms have some theoretical justification in the gas phase and may be regarded as a truncated version of the virial equation for ϕ. The true virial coefficients cannot, however, be expressed solely in terms of the polynomial constants

because of the contribution of the gaussian function to each term. The gaussian function was selected for the specific purpose of fitting the data in the vicinity of the maximum because, unlike most other functional forms, its contribution away from the maximum can be made to decay rapidly, if necessary, by suitable adjustment of the parameter f in Equation (VII-11). The regression constants were determined from the basic data using the equation

$$\frac{H_f-H_i}{P_f-P_i} = \bar{\phi} = a + b\frac{(P_f^2-P_i^2)}{2(P_f-P_i)} + c\frac{(P_f^3-P_i^3)}{3(P_f-P_i)} + d\frac{(P_f^4-P_i^4)}{4(P_f-P_i)} + \frac{\sqrt{\pi}}{2} g \left[\text{erf}\{f(P_f-P_k)\} - \text{erf}\{f(P_i-P_k)\}\right] \qquad \text{(VII-12)}$$

obtained by integration of Equation (VII-11). Convergence was obtained for reasonable initial values of the constants. The value of P_k can be fairly well estimated from the basic data. Reasonable estimates of a, b, c, d, and g were obtained by initially fixing f and P_k, and then conducting a regression on the rest of the linear terms, because convergence is always assured for the linear case. The results of the regression are shown in Table C-2. The fit to the basic data is about 0.6%. The smoothed ϕ curve resulting from the regression and indicated by the dashed line in Figure VIII-52 does not fit the low pressure data very well and suggests that the representation of ϕ by Equation (VII-11) is not the final answer.

Other possibilities for improving upon Equation (VII-11) are discussed in Chapter X. Several factors precluded the further pursuit of this technique in this work. Firstly, the range and distribution of the basic data about the peak value influence the type and number of terms to be used in the regression analysis, requiring considerable experimentation to find the best combination. For example, an isolated isobaric run, or a complete isothermal run in the liquid region would be completely insensitive to the gaussian function, as both Cp and ϕ vary only slightly in the cryogenic liquid region. On the other hand, a run that consists, for example, of only four data points around the maximum in Cp, though accessible to graphical analysis, would demand considerable skill in locating just the right combination of functions that could fit the data within experimental accuracy, without involving three or more adjustable constants. Secondly, the weighting procedure is arbitrary and could involve a

number of trials before the most desirable weighting scheme from the combined standpoint of smoothness and goodness of fit is obtained.

d) Computer Aided Graphical Techniques. Although a graphical construction of the equal area curve circumvents the problem of specifying an appropriate analytic functional form for the least squares fitting of the basic data in different regions, and furthermore permits a visual weighting of the data without requiring the assignment of quantitative weighting factors to each data point, it is nevertheless desirable to monitor such a subjective procedure by computer techniques. A more objective assessment of the equal area curve can be made if the area under the curve so constructed is integrated on the computer and compared with the basic data.

The Simpson's rule technique was used to manually construct a smoothed plot of ϕ vs P, or Cp vs T from large sized graphs of the basic corrected data plotted as horizontal bars. These plots were generated using a Model 763 Digital Calcomp Plotter. To avoid clutter, only the differenced values between contiguous data points, arranged in order of increasing temperature rise, are plotted in addition to the basic data for the isobaric measurements. Point values of Cp or ϕ were obtained from such graphs at frequent intervals of temperature or pressure. The interval between the selected data points was such that rapid changes in the value of the slope dCp/dT or $d\phi/dP$ were avoided. In the isobaric case, the spacing was usually of the order of 10°F, decreasing to 1°F in the vicinity of the maxima. The interval for isothermal data was about 200 psid decreasing to 50 psid near the maxima. The functional relationship in the interval between any two such points was represented by successive five point Lagrange interpolating polynomials. The desired interval is arranged to lie between the third and the fourth of five points whenever possible.

The integral over each such interval was also calculated to yield enthalpy differences using Gauss-Legendre quadrature. An algorithm and an excellent discussion of the technique is provided by Carnahan et al. [40]. The integral under the curve was also computed over the intervals corresponding to the basic and differenced data and compared with the experimental values. The overall bias and percentage bias for each loop

were calculated in terms of the enthalpy difference ΔH_i for each arm as

$$\text{Bias} = \sum_{i=1}^{4} \left[\left(\Delta H_i \right)_{\text{Expt}} - \left(\Delta H_i \right)_{\text{Cal}} \right] \qquad \text{(VII-13)}$$

$$\% \text{ Bias} = \sum_{i=1}^{4} \left[\left(\Delta H_i \right)_{\text{Expt}} - \left(\Delta H_i \right)_{\text{Cal}} \right] / \sum_{i=1}^{4} \left[\Delta H_i \right]_{\text{Expt}} \times 100 \qquad \text{(VII-13a)}$$

These computations provide a check on the graphical technique and indicate regions where adjustments are necessary. The actual curve is then replotted, and appropriate adjustments are made in the point values of Cp or ϕ until the bias, after ignoring the contribution of data points with percentage deviations greater than four times the average, is less than 0.25%. At this stage, the Cp, ϕ and enthalpy values are uniformly adjusted to compensate for the remaining bias if necessary.

The effect of the order of the interpolating polynomial on the integration of tabulated values of ϕ vs T was investigated for the 126.2°F isotherm for the ternary mixture. Maximum local variations of 0.2%, and an average variation of 0.05% was noted on comparing the three and the five point case. The variation in the total enthalpy change from 0 to 2000 psia was less than 0.1%. To ensure that the Lagrange polynomial integration was accurate, values of ϕ at 100 psi intervals were obtained from the multiple, non-linear regression analysis results for the same isotherm, and integrated using the five point interpolating polynomial. The agreement with the analytically integrated regression equation [Equation (VII-12)] was better than 0.1%. An examination of the data for the systems of this work indicates that on an average, the goodness of fit is better than 0.3% for the isobaric data, and about 1% for the isothermal measurements. Sample results for the equal area determination of heat capacities and enthalpies from the basic isobaric data are indicated in Table C-3.

Consistency Checks

The acquisition of isobaric and isothermal data over common regions permits them to be compared for self-consistency. Figure VIII-14, for example, summarizes the consistency checks on the ethane data. The

enthalpy loop from -246.3°F to -123.3°F and from 250 psia to 1000 psia is regarded to indicate how such checks may be accomplished. The enthalpy change across each arm of the loop is calculated from the integrated equal area Cp or ϕ curve discussed in the previous section. As enthalpy is a point function of state, the net enthalpy change across any path forming a closed loop should be zero. In practice, the algebraic sum across such a loop is a finite quantity (+0.55 Btu/lb in this case) that serves as a measure of the thermodynamic consistency of the data. Before enthalpy tables can be constructed, it is necessary that the values ascribed to each arm of every loop be optimally adjusted, preferably within the estimated accuracy of the data, so that each loop is exactly balanced.

In the particular case examined, the initial smoothed value of the enthalpy change at 1000 psia between -246.6°F and -123.3°F is 0.65 Btu/lb higher than the final adjusted value of 68.91 Btu/lb; an inconsistency of about 1%. The percentage inconsistency for the entire loop defined by $(\sum_{i=1}^{4} \Delta H_i / \sum_{i=1}^{4} |\Delta H_i|)(100)$ is only 0.4%. Thus, the percentage adjustment to the enthalpy difference ΔH_i across an individual arm of a loop may be considerably higher than that required for the loop as a whole. This behaviour is caused by the fact that the value of $\sum_i \Delta H_i$ for any given loop is relatively insensitive to large consistent errors in parallel arms, particularly, when the enthalpy changes along such arms are not significantly different from each other.

In order to avoid a concentration of errors in a small end loop, the largest loop (-24.5°F to 200.6°F, and from 500 to 2000 psia) is balanced first, and bounds are established on the total acceptable variation for the individual arms. The smaller constituent loops are than adjusted within these constraints. Errors common to both isobaric and isothermal measurements, such as a mass leak before the flowmeter, are not easily spotted unless one arm of a loop occurs at zero pressure where the enthalpy difference is defined by the API tables [220] which serve as a completely independent data source. The loop from 125°F to 200°F, and from 0 to 250 psia is just such an example. The smoothed Cp and ϕ values for the individual arms generated by the techniques of the previous section are now readjusted, usually

by uniform scaling, to conform to the final value of the enthalpy change assigned to the given arm. Particular difficulties exist when the corrections to contiguous arms along isobars or isotherms are in opposite directions, and some smoothness is sacrificed in the values of the appropriate enthalpy derivatives near the junction point.

Preparation of Pressure-Temperature-Enthalpy Diagrams and Tables

Although the interpretation of the data so far has generated useful results, enthalpy changes across any two conditions not restricted to experimental isotherms or isobars cannot be easily determined from such information. The construction of pressure-temperature-enthalpy diagrams or tables which serve to define the enthalpy at any specified point in relation to the enthalpy at some reference pressure and temperature would be very useful in making such calculations.

For reference, an enthalpy value of zero was attributed to each pure component in a mixture in the saturated liquid state at -280°F. This choice of reference conditions is consistent with the reported enthalpy values for previous systems investigated at the facility [119, 162,168,284], and conveniently ascribes positive values to the enthalpies over the range of application of the tables.

The computation of the enthalpy of a mixture at the reference condition, i.e., at the saturated liquid state at -280°F is troublesome because it requires the heat of mixing of the constituent pure components to be first established. The ideal gas state is a more desirable reference point for mixtures because the value of the zero pressure enthalpy at any temperature can be rigorously determined from the constituent pure component enthalpy values at the same temperature using the relation

$$\underline{H}_m = \sum_i w_i \underline{H}_i \qquad \text{(VII-14)}$$

where $\underline{H}_m$ is the specific enthalpy of the mixture, and w_i and $\underline{H}_i$ represent the mass fraction and the specific enthalpy for the ith component. Therefore, to circumvent the problem of computing the heat of mixing for the mixture at -280°F, the enthalpy change for each of the constituent pure components in going from the saturated liquid state at -280°F to the ideal gas state at some arbitrary temperature

is first calculated, and the mixture enthalpy at this temperature is then rigorously fixed by Equation (VII-14) above.

For convenience, the temperature selected for the definition of the mixture enthalpy at zero pressure is usually chosen to coincide with a measured isotherm in the gaseous phase beyond the cricondentherm temperature. A knowledge of the enthalpy behaviour along the given isotherm, previously calculated as a function of pressure, now specifies a reference enthalpy for every experimental isobar at that temperature. This information in conjunction with isobaric measurements across the given isotherm permits an enthalpy value to be assigned to the mixture at other temperatures along the isobars relative to the saturated liquid pure component references at -280°F. In this fashion, a pressure-temperature network of enthalpy values can be generated.

The following calculations illustrate the determination of the reference point for the ternary mixture at 192°F. First, the enthalpy of each of the pure components at 192°F and 0 psia is established below.

a) Methane	ΔH (Btu/lb)
Enthalpy of saturated liquid at -280°F and 5 psia	0.00
Enthalpy of vaporization at -280°F and 5 psia, (Frank and Clusius [84])	227.72
Enthalpy change from saturated vapor at 5 psia to the ideal gas at 0 psia and -280°F (Virial equation, this work)	1.15
Enthalpy change as an ideal gas from -280°F to 192°F, (Rossini [220])	243.32
Enthalpy of methane at 0 psia and 192°F	472.19

b) Ethane	
Enthalpy of saturated liquid at -280°F	0.00
Enthalpy change from saturated liquid at -280°F to saturated liquid at -128.1°F and 14.7 psia (Witt and Kemp [280])	84.50
Enthalpy of vaporization at -128.1°F and 14.7 psia (Witt and Kemp [280])	210.90
Enthalpy change from saturated vapor at 14.7 psia to 0 psia and -128.3°F (Virial equation, this work)	2.40

	ΔH (Btu/lb)
Enthalpy change as an ideal gas from -128.1°F to 192°F (Rossini [220])	127.70
Enthalpy of ethane at 0 psia and 192°F	425.50

c) Propane

Enthalpy of saturated liquid at -280°F	0.00
Enthalpy change from saturated liquid at -280°F to saturated liquid at 43.7°F and 14.7 psia (Kemp and Egan [127])	183.17
Enthalpy change from saturated vapor at 14.7 psia to 0 psia and -43.7°F (Virial Equation, this work)	2.43
Enthalpy change as an ideal gas from -280°F to 192°F	93.73
Enthalpy of propane at 0 psia and 192°F	394.63

As the contribution of other components are minor, only the final results are given in the following cases

d) Enthalpy of nitrogen at 0 psia and 192°F	193.60
e) Enthalpy of carbon dioxide at 0 psia and 192°F	182.00
f) Enthalpy of propylene at 0 psia and 192°F	370.00

g) Enthalpy of ternary methane-ethane-propane mixture at 0 psia and 192°F using the compositions in Table VI-3 converted to mass fraction for use in Equation (VII-14) 418.70

The calculation of the enthalpy departure for the saturated vapor was in each case accomplished by using the reduced second virial coefficient correlation of this work [Equation (V-30)], and the reduced third virial coefficient correlation of Chueh and Prausnitz [Equation (III-44)]. The appropriate thermodynamic relationships for calculations based on Equation (V-30) are summarized in Appendix H-3. The enthalpy differences at zero pressure were calculated by interpolating the heat content function values $[H(T°K) - H(0°K)]/T$ tabulated at regular intervals by Rossini [220].

Chapter VIII

EXPERIMENTAL AND SMOOTHED CALORIMETRIC DATA

This section summarizes the results obtained from the isobaric, isothermal and isenthalpic calorimetric investigation of ethane, three ethane-propane mixtures, two methane-ethane mixtures, and a ternary mixture of methane, ethane and propane over the liquid, gaseous, critical and two phase regions. Only basic data are reported for the methane-ethane mixtures. For the rest of the systems, the basic data, consistency checks on the smoothed data, and tabulated values of the enthalpy and its appropriate derivative Cp or ϕ are presented at the conditions of measurement. Enthalpy diagrams are also prepared both for ethane and the ternary mixture. The techniques employed to achieve these final results have already been discussed in the previous section. Typical results involving various operating modes for the calorimeters are graphically illustrated for each system. Difficulties in the acquisition and interpretation of the data that are specific to a given system are outlined here. Some comparisons are made with limited sources of data available in the literature. The results of special tests on the calorimeters are also discussed prior to the presentation of the data to examine the validity of several assumptions with respect to operating practice.

Special Tests on Calorimeters

a) Unsteady State Behaviour of the Isobaric Calorimeter. The estimation of the amount of time required to achieve quasi-steady state conditions for a given data point in normal operation after the initial input of power was made difficult because of observed fluctuations in the temperature rise. These fluctuations appear to be related to problems in maintaining the state and the flowrate of the system fluid at the calorimeter inlet at some fixed pre-determined conditions, and complicated the determination of the time period required for the quantity $dU/d\theta$ in Equation (I-17) to vanish, where U is the energy of the calorimeter.

The effect of varying flowrate on the final approach to quasi-steady

state conditions is minimized if the decay in the temperature difference between the inlet and outlet, caused by suddenly removing the power input to a calorimeter at quasi-steady state, is followed with time instead of the temperature rise. In practice, the power to the calorimeter and the guard heater was switched off after maintaining quasi-steady state conditions for about four hours. The experiment was conducted on the 0.49 mole fraction ethane-propane system at a flowrate of 0.244 lbs/min., and for an initial quasi-steady state temperature rise of 100°F. As soon as the power was switched off, the evacuated section between the guard heater and the outlet section of the calorimeter was quickly brought to atmospheric pressure to allow rapid equilibration between their respective temperatures, arresting the radiative and conductive heat transfer to the calorimeter from the guard heater.

The results for both the original and modified heater capsules are shown in Figure VIII-1, and indicate that the latter has better heat transfer characteristics. The graph establishes that a 99.9% approach to steady state occurs in a period of about 50 minutes for the modified capsule. For very small temperature differences, (≤ 0.05°F), the analysis is complicated by the relatively significant contribution of variations in the calorimeter bath temperature to fluctuations in the observed temperature difference. Although such effects have been qualitatively observed in the time period before the initial input of power to the first data point for a given run, no attempt has been made to quantitatively define such observations as the time interval for the unsteady state experiment would have to be greatly extended.

b) Heat Leak Test. If Equations (I-17), (I-18) and (I-19) are combined, and if the temperature difference between the calorimeter bath and the calorimeter inlet T_i is ignored in Equation (I-18), we obtain the result

$$\underline{H}_{T_f,P_f} - \underline{H}_{T_i,P_i} = \frac{E\,I}{\dot{m}} + h_f A_f (Ts_f - T_f) - \frac{1}{\dot{m}} \frac{d\mathcal{U}}{d\theta} \qquad \text{(VIII-1)}$$

If the left hand side of the above equation is expressed in terms of

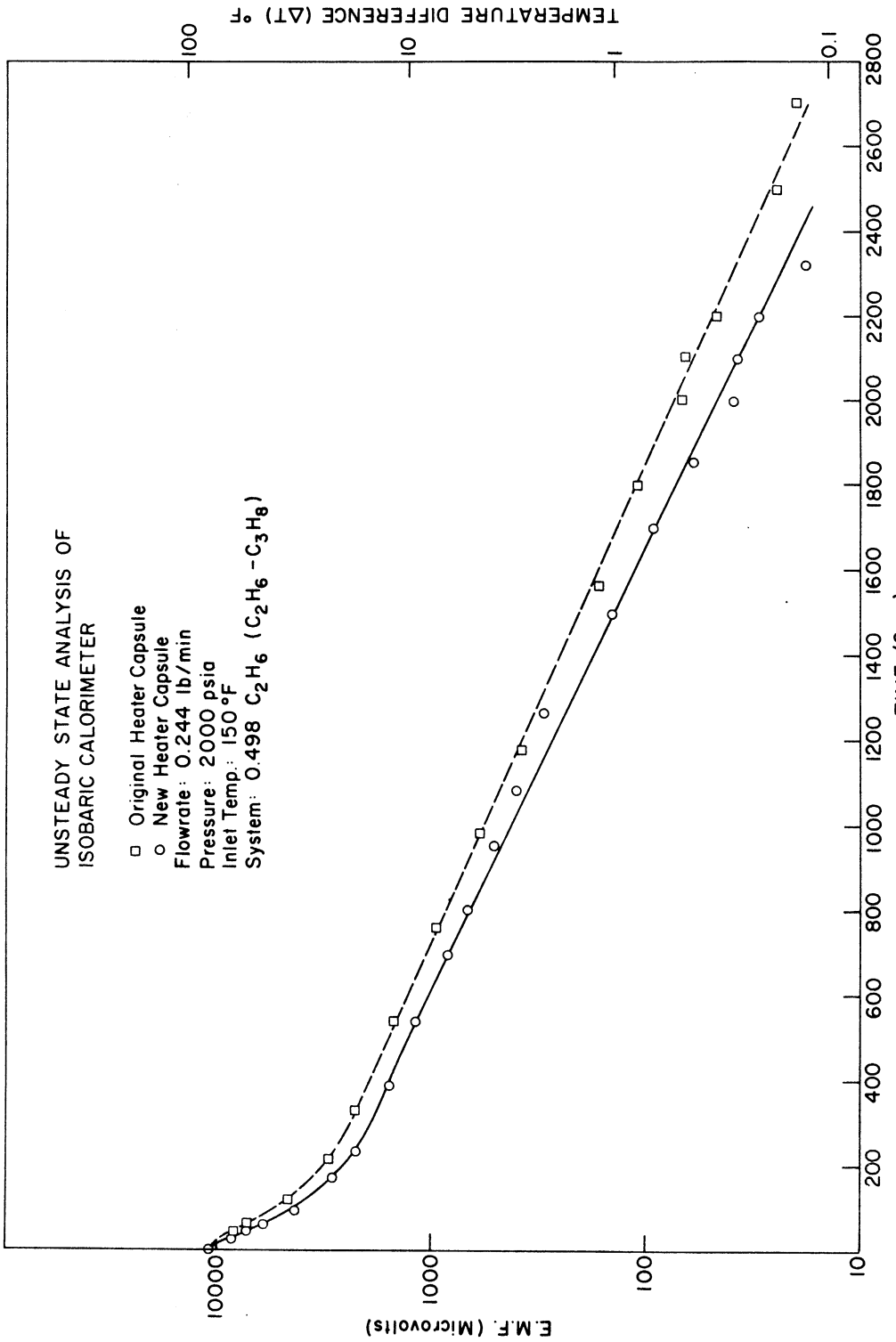

Figure VIII-1. Approach to Steady State as a Function of the Heater Capsule Within the Isobaric Calorimeter.

the enthalpy derivatives Cp and ϕ, as in Equation (I-25), then we obtain the result

$$\bar{C}p = \frac{\bar{H}_{T_f,Ps} - \bar{H}_{T_i,Ps}}{(T_f - T_i)} = \left[\frac{E\,I}{\dot{m}} + \frac{h_f A_f (Ts_f - T_f)}{\dot{m}} - \frac{1}{\dot{m}} \frac{d\mathcal{U}}{d\theta} + \int_{Ps}^{P_f} (\phi)_{T_f} dP - \int_{P_i}^{Ps} (\phi)_{T_i} dP \right] / (T_f - T_i) \qquad \text{(VIII-2)}$$

on dividing by $(T_f - T_i)$ and rearranging, where Ps is the reference pressure to which the actual measurements are corrected. If heat leak and unsteady state effects are ignored, then the apparent heat capacity $\bar{C}p_A$ is defined by the relation

$$\bar{C}p_A = \left[\frac{E\,I}{\dot{m}} + \int_{Ps}^{P_f} (\phi)_{T_f} dP - \int_{P_f}^{Ps} (\phi)_{T_i} dP \right] / (T_f - T_i) \qquad \text{(VIII-3)}$$

Therefore, the true mean heat capacity Cp is defined in terms of the apparent mean heat capacity $\bar{C}p_A$ by the relation

$$\bar{C}p_A = \bar{C}p + \left[\frac{1}{\dot{m}} \frac{d\mathcal{U}}{d\theta} - \frac{h_f A_f (Ts_f - T_f)}{\dot{m}} \right] / (T_f - T_i) \qquad \text{(VIII-4)}$$

A plot of apparent mean heat capacity vs reciprocal flowrate $1/\dot{m}$ has been prepared for ethane over a fixed temperature rise of 15°F for inlet conditions at 146.67°F and 1000 psia as illustrated in Figure VIII-2. Successive measurements were taken in order of increasing flowrate. A new point is initiated by first increasing the flowrate, and then adding power till the original specified temperature rise is obtained. In such situations $d\mathcal{U}/d\theta$ is always initially positive. In the absence of heat leak and unsteady state effects, the plot should yield a horizontal line. Except for the point at the lowest flowrate, the data lie within a span of 0.3%, and the trend is in the opposite direction from that anticipated due to heat leak and unsteady state effects. It is conceivable that the location of the heat shield differential thermopile is such that the guard heat at the observed balance point over-compensates for the true heat leak causing $\bar{C}p_A$ to rise with increasing reciprocal flowrate. The estimated precision of the measured flowrate is also indicated in the figure, and suggests that it may be the limiting factor in this analysis.

Point 1 at the lowest flowrate merits further discussion as the computed value of $\bar{C}p$ is higher than the rest by about 0.5%. Although

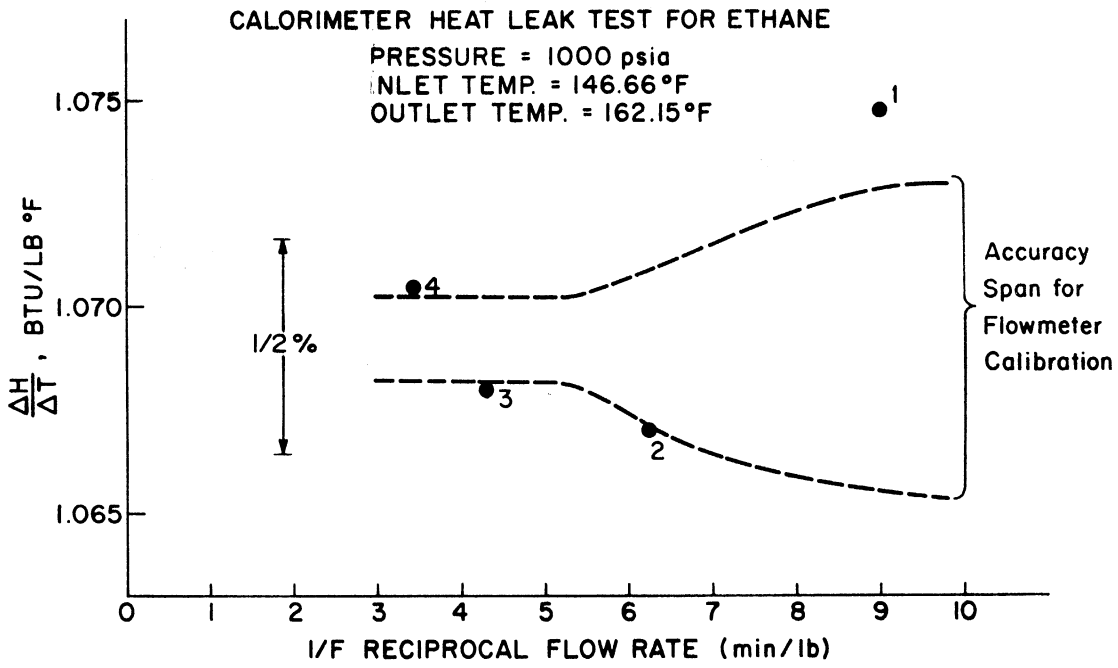

Figure VIII-2. Heat Leak Test for the Isobaric Calorimeter, Heat Capacity of Ethane as a Function of Reciprocal Flowrate.

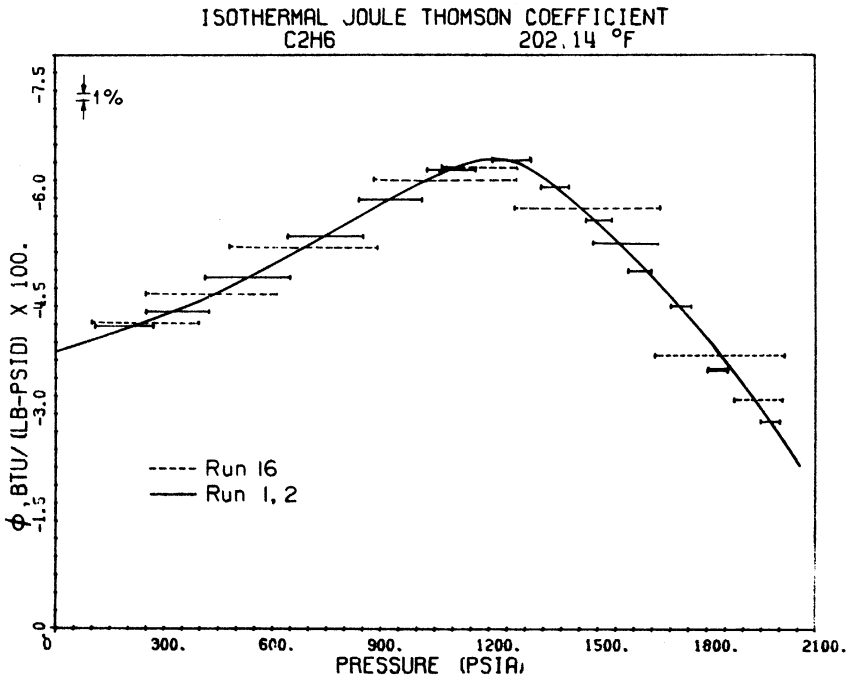

Figure VIII-3. Effect of the Size of the Capillary Coil on the Measured Value of $(dH/dP)_T$ for Ethane Along the 202.14°F Isotherm.

the accuracy of the flowmeter calibration is lower at these flowrates, the observed discrepancy is beyond this consideration. The first data point for a given run is not usually initiated until it is judged that the calorimeter inlet temperature has been equilibriated with the bath temperature. In order that the desired state may be more quickly attained, it is normal to pass the fluid through the calorimeter for about 50 minutes after the bath temperature is on control before a measurement is initiated. It is conceivable that since the operating flowrate for the first data point in this experiment was much lower than normal, the desired equilibration did not, in fact, take place before the completion of the measurement. In summary, it is believed that the higher discrepancy for this point is predominantly attributable to unsteady state effects.

It is believed that the masking effect of the unsteady state term on the evaluation of the heat leak effect as a function of flowrate could be minimized in future experiments if the measurements were initiated at the highest flowrate instead of the lowest, and if the time period between the data points was increased from 40 minute to at least an hour. The operating flowrates for the systems of the study were, however, generally restricted to the range between points 2 and 3 in Figure VIII-2, where it is felt that corrections for heat leak and unsteady state are, in practice, unnecessary, within the limits of precision of the flow measurements. Nevertheless, Equation (VIII-4) implies that we have a better chance of measuring the true mean heat capacity if the flowrate and temperature rise $(T_f - T_i)$ are both large.

c) Capillary Coil Test. The effect of pressure on the enthalpy of a fluid, at a given temperature, as measured by the isothermal calorimeter, should be independent of the characteristics of the throttling device used. Measurements were initially obtained on pure ethane at 200.6°F using a 15 BWG capillary coil [Runs 1, 2 in Figure VIII-3]. The occurence of a leak in the calorimeter bath necessitated a subsequent repetition of the run. The repeated run was conducted at 202.14°F using a 17 BWG capillary coil. The data at 200.6°F were corrected to 202.14°F using the PGC as explained in Chapter VII, and

plotted as the dashed lines in Figure VIII-3. The measured pressure drops in Run 16 are about double those in Run 2 for comparable flowrates. The integration of the smoothed ϕ curve in the figure, over the interval of the basic data points, indicates that the two sets of measurements agree within $\pm$ 1%, the results for Runs 1 and 2 being generally higher than those for Run 16. This may in part be attributed to the observed leak during the investigation of Runs 1 and 2.

d) Test for Consistency Between the Faulkner and the Mather Calorimeters. Although the throttling calorimeter is usually operated either in isothermal or in isenthalpic mode, it is possible to cause a large temperature rise if sufficient power is supplied. Furthermore, the guard heater for the calorimeter can also function to balance the heat leak in non-isothermal operation. Nevertheless, the extraction of the mean heat capacity from such measurements is to be considered less reliable in view of the substantial correction for the pressure drop across the calorimeter.

The performance of both calorimeters may be adequately compared with each other if the operating conditions are confined to the liquid region across the Joule-Thomson inversion curve, where the contribution to the measured enthalpy change in the throttling calorimeter due to a pressure drop is considerably minimized. The basic test data in Table (VIII-1) were, in fact, obtained under such conditions.

TABLE VIII-1

Direct Comparison of the Enthalpy Data from the Isobaric and Throttling Calorimeters

RUN	COMPOSITION MOLE PERCENT CH4 C2H6 C3H8	INLET TEMP. (°F)	OUTLET TEMP. (°F)	INLET PRESSURE (PSIA)	PRESSURE DROP (PSID)	ΔH BTU/LB	ΔH CORRECTED BTU/LB
3.010	.001 .279 .720	0.82	10.59	1001.1	0.12	5.689	5.689 +
4.110	.001 .276 .723	1.58	11.45	1043.4	75.25	5.777	5.722 *

+ISOBARIC CALORIMETER
*THROTTLING CALORIMETER (CORRECTED TO CONDITIONS OF ISOBARIC CALORIMETER)

In both cases, sufficient power was supplied to cause a temperature rise of about 9.9°F. Run 4.110 was obtained with the throttling calorimeter. The last column in the table indicates the enthalpy change as corrected to the operating conditions of the isobaric calorimeter using the PGC correlation and the Joule-Thomson data obtained in this

work. The major contribution to the correction term stemmed from the slight difference in the temperature rise for the two cases, and amounted to 0.057 Btu/lb. A comparison between the two measurements after the appropriate adjustments indicates that the throttling calorimeter yields an enthalpy change that is 0.7% higher than for the isobaric case. This discrepancy is higher than anticipated and may possibly be attributed to unsteady state effects in the former case.

Error Analysis

A comprehensive error analysis of the basic isobaric measurements and the reduced data was initially undertaken by Jones [119] and subsequently extended by Manker [162]. The accuracy of the throttling data was discussed by Mather [168]. Table VIII-2 indicates the major sources of errors and their effect on the accuracy of the basic enthalpy data. In the latter case, only approximate estimates are possible in view of the highly variable dependence of the enthalpy on temperature, pressure, and composition. Furthermore, the precise contribution of unsteady state and mass leakage is almost always uncertain, and underscores the difficulty of evaluating the quality of such measurements. It is felt that the most reliable index of the accuracy of the results is obtained from the observed discrepancy between the original and adjusted values of the enthalpy difference for each arm of every enthalpy loop for any given system.

Experimental Measurements on Ethane

The range of experimental determinations is indicated on a P-T diagram shown as Figure (VIII-4). The horizontal lines represent distinct isobaric runs, the vertical lines represent isothermal data. The adiabatic Joule-Thomson data in the liquid region are indicated by lines that are slightly inclined to the vertical. The vapor pressure curve is also indicated to permit the identification of the phase corresponding to each run. As the diagram indicates, the critical region was given special consideration in view of the recognized deficiencies of most empirically fitted PVT equations of state in predicting the enthalpy behaviour in this area. The run numbers are assigned to indicate the chronological order of the investigation.

TABLE VIII-2

Summary of Estimates of Measurement and Data Interpretation Errors for the Calorimetric Data of this Work

MEASUREMENT	%ERROR			%CONTRIBUTION TO	
	OPTIMUM	AVERAGE	WORST	$\Delta H/\Delta T$ (AV. CASE)	$\Delta H/\Delta P$
POWER INPUT	0.02	0.05	0.1	0.05	0.05
INLET PRESSURE	0.02	0.03	0.2	<0.02	<0.02
PRESSURE DROP (ISOBARIC)	3.0	5.0	30.0	<0.02	
PRESSURE DROP (ISOTHERMAL)	0.5	2.0	4.0		2.0
INLET TEMP.	<0.01	0.02	0.05	<0.01	0.05
TEMP. RISE (ISOBARIC)	0.02	0.10	0.5	0.10	
TEMP. DIFF.(ISOTHERMAL)	1.0	2.0	5.0		0.05
MASS FLOWRATE	0.1	0.2	4.0	0.2	0.2
COMPOSITION	0.1	0.2	1.0	0.02	0.1
ANCILLIARY ERROR SOURCES					
UNSTEADY STATE	0.1	0.2	2.0	0.25	0.4
HEAT LEAKAGE (ISOBARIC)	0.0	0.05		0.05	
MASS LEAKAGE*	0.00	0.25	4.0	0.25	0.25
INTEGRATION OF BASIC DATA	0.1	0.25	0.5	0.25	0.2

* Systematic error which tends to increase the measured value of $\Delta H/\Delta T$ or $\Delta H/\Delta P$

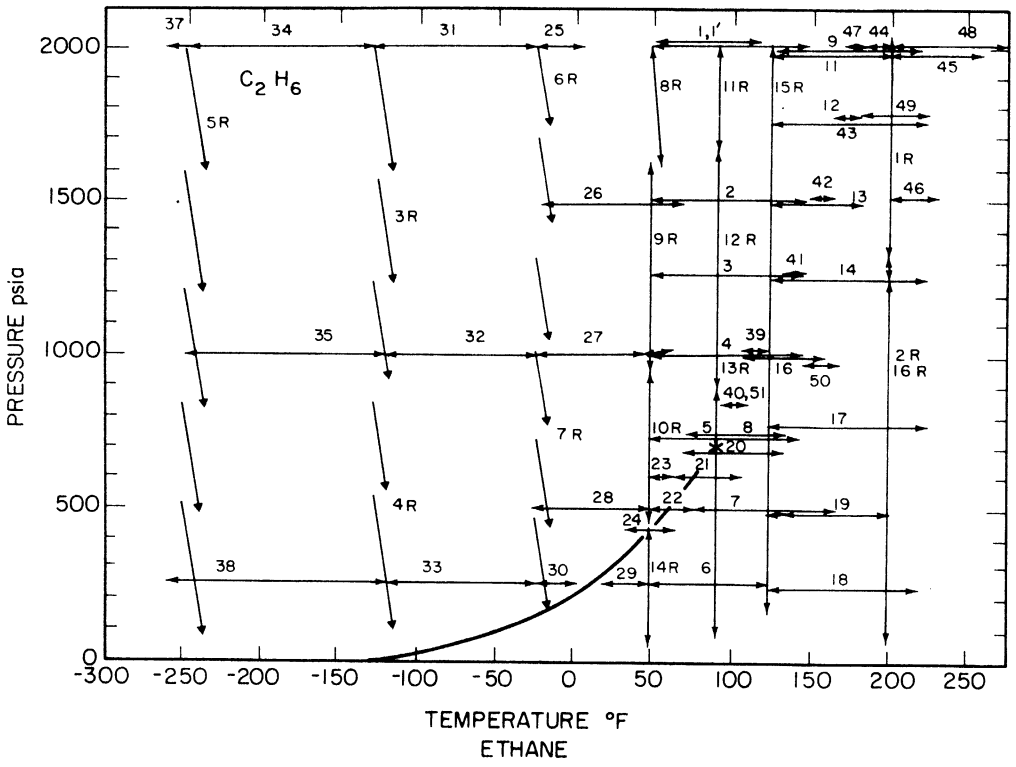

Figure VIII-4. Temperature and Pressure Range of Calorimetric Measurements of Ethane in this Work, as a Function of Run Number.

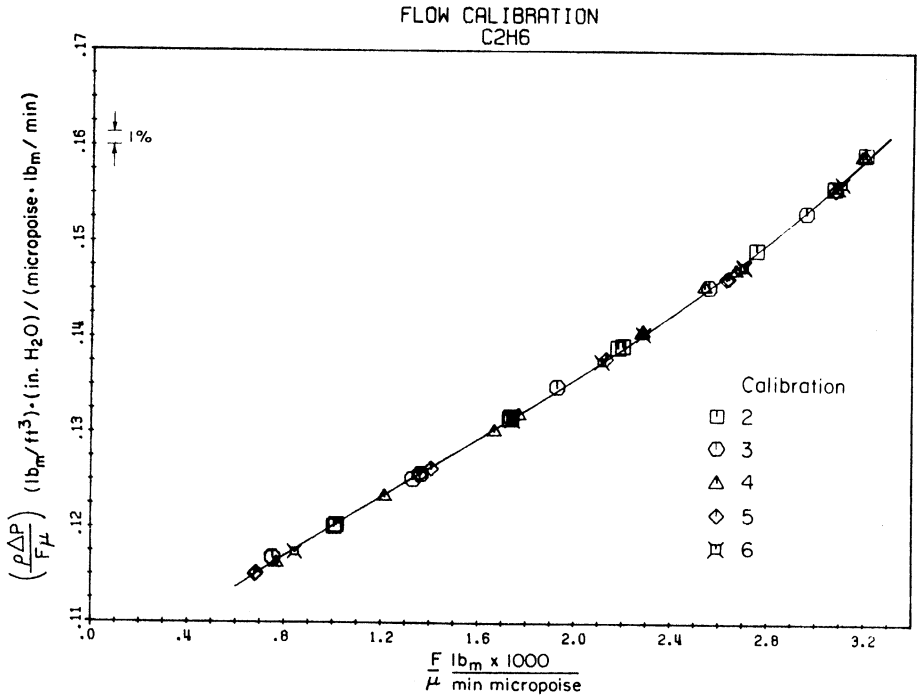

Figure VIII-5. Flowmeter Calibration Results for Ethane.

The composition of the system presented in Table VI-3 was essentially constant throughout the investigation; the major impurity being 0.3% propylene. Consequently, the results reported apply to the mixture and not to pure ethane. The flowmeter calibration results are summarized in Table VI-1. The data for these five calibrations are also plotted in Figure VIII-5. The basic isobaric, isothermal, and isenthalpic data are presented in Tables B-1, B-2, and B-3 respectively.

The P-T diagram of Figure VIII-4 indicates that extensive measurements were also made in the single phase liquid and gaseous regions at 250 psia, and in the supercritical region at 1000 psia and 2000 psia. Isobaric determinations across the two phase region were made at 410, 500, 600 and 677 psia, respectively. A limited number of additional measurements, concentrated chiefly in the vicinity of the heat capacity maxima, were also obtained at 713, 750, 819, 2150, 1500 and 1750 psia.

A typical isobar in the supercritical region is illustrated in Figure VIII-6, where the data extends from -260°F to beyond 170°F. At low temperatures, the heat capacity increases only slightly with temperature. As the temperature is further increased, the heat capacity rises sharply, reaching a maximum at a temperature somewhat beyond the critical temperature, and then begins to fall just as rapidly. Previous similar investigations on light hydrocarbons [119, 162] suggest that, beyond 170°F, the heat capacity would go through a broad mimimum, and then rise with a gentle slope.

Figure VIII-7 represents an isobar at 713 psia which is less than 5 psia beyond the critical pressure for ethane. Mean heat capacities as high as 9 Btu/lb/°F were obtained on differencing the data for this particular run. Successive data points were, however, not closely spaced enough to define the precise shape of the equal area heat capacity curve between 88 and 92°F. The equal area curve in the vicinity of the heat capacity maximum was more clearly defined for the measurements at 819 psia shown in Figure VIII-8. In this particular case, the difference in outlet temperature between successive measurements is of the order of 1°F. Special efforts were made to maintain the inlet pressure within $\pm$ 0.5 psia for the entire duration of the run which was conducted at a high flowrate of 0.28 lbs/min. The excellent agreement between the basic (solid bars) and differenced (dotted bars) data

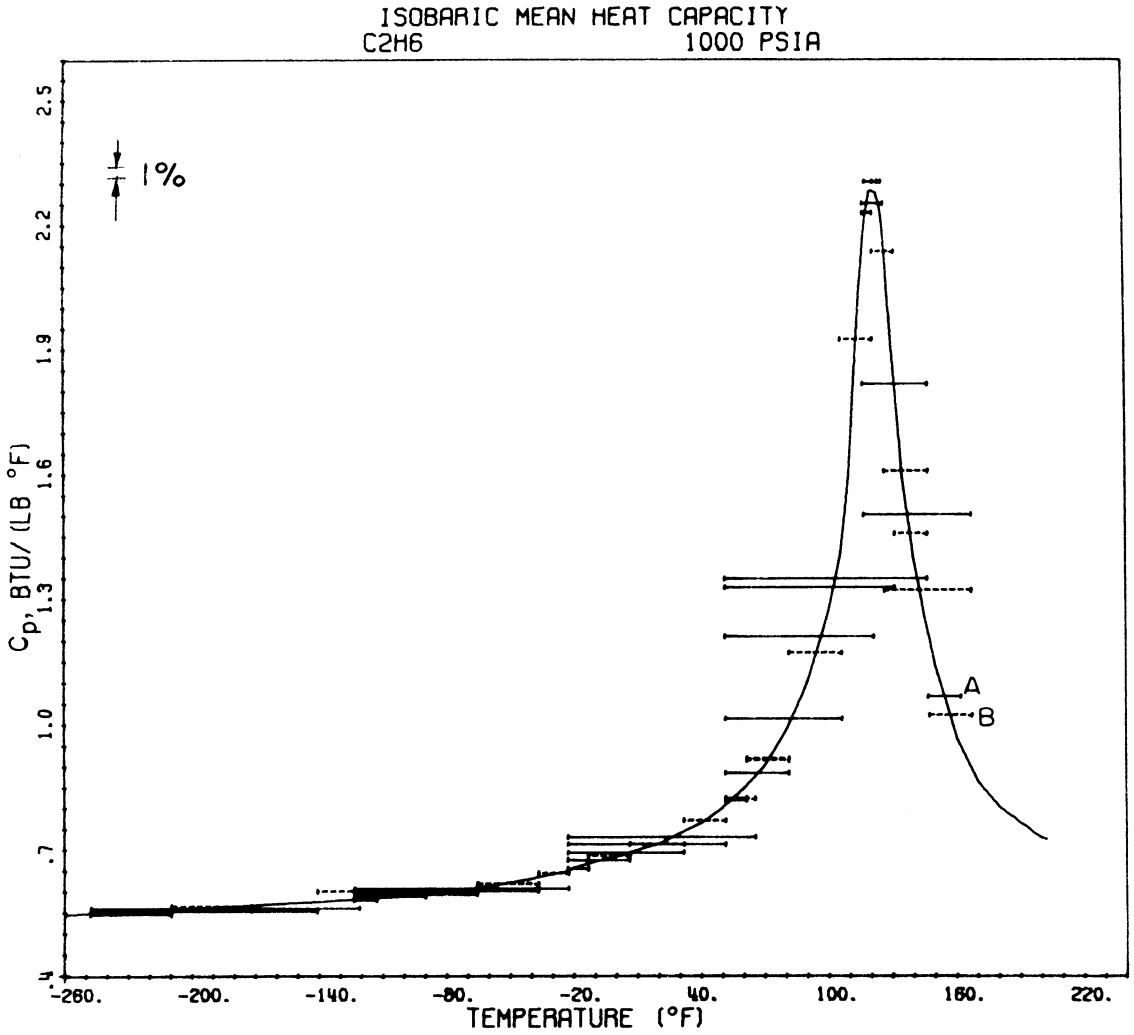

Figure VIII-6. Isobaric Heat Capacity for Ethane at 1000 psia.

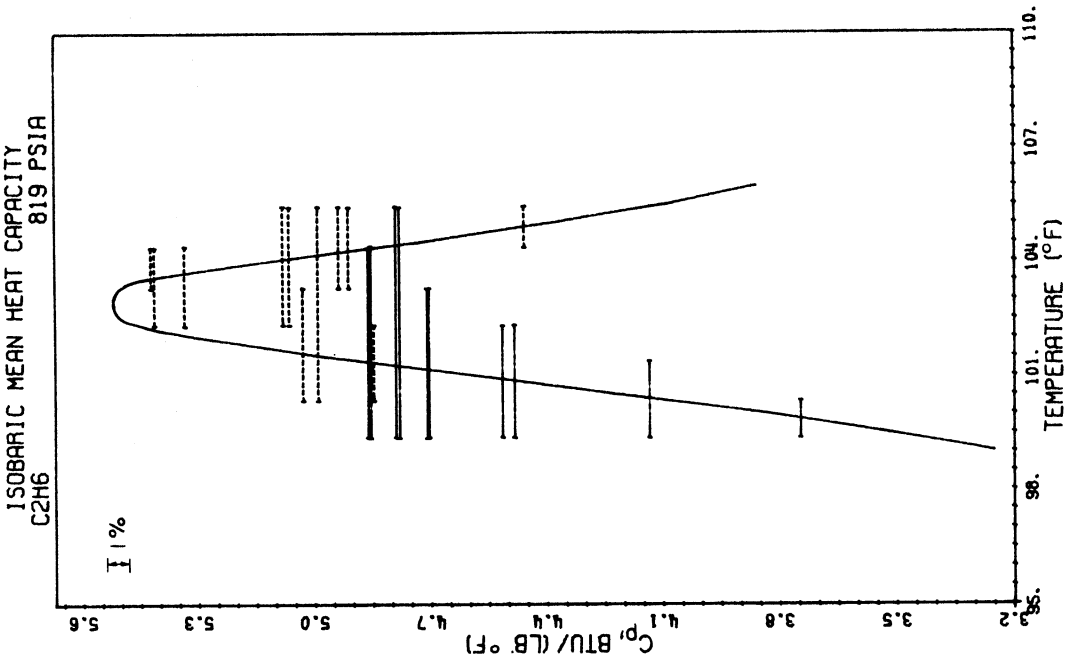

Figure VIII-8. Isobaric Heat Capacity for Ethane at 819 psia.

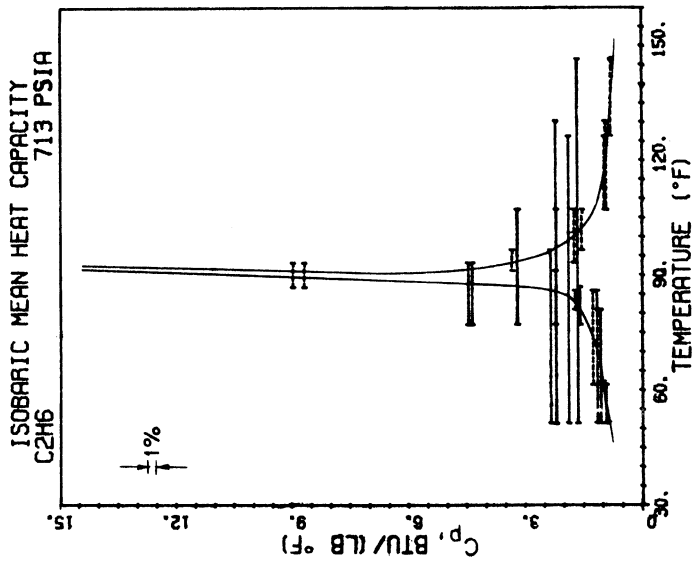

Figure VIII-7. Isobaric Heat Capacity for Ethane at 713 psia.

attest to the precision of the measurements. Although the temperature span for the entire run was only 6°F, the time span for its completion was extended to 12 hours from the point of initial input of power in order to ensure attainment of quasi-steady state conditions. Such careful measurements, though desirable, were unfortunately undertaken in very limited cases only due to the breadth of the experimental commitment of this work.

With reference to Figure VIII-4, additional runs were obtained at high flowrates, principally in the 40 series, with the specific purpose of defining the heat capacity more clearly in the vicinity of the maxima. An undetected leak at the calorimeter pressure to vacuum seal during the course of these runs resulted in Cp values that were 1 to 3% too high when compared with the earlier measurements. These results were basically disregarded in all further interpretation of the data. The correspondence between Run 50 at 1000 psia from 146.7°F to 162.2°F, (Point A in Figure VIII-6) obtained after the leak was arrested, and the differenced data for Run 16 from 147.4°F to 167.5°F (Point B in Figure VIII-6) was good.

Figure VIII-9 illustrates an enthalpy traverse across the two phase region at 500 psia. The heat capacities for the liquid and vapor upto the saturation point as determined from the same run (Run 22) are also shown in Figures VIII-11 and VIII-10, respectively. The bubble point, as determined by the technique described in Chapter VII is 0.6°F below the dew point. This difference can only be ascribed to the presence of impurities in the ethane, and has the effect of increasing the measured enthalpy of vaporization. The equivalent pure component enthalpy of vaporization is extracted from the measurements, as plotted in Figure VIII-9b, if the two phase region is expressed as a flat line at some mean temperature, (61.1°F in this case) between the observed dew and bubble points, and if the curve through the enthalpies in the single phase liquid and gaseous regions are extrapolated to intersect the two phase line

Isothermal runs were made at 49.2°F, 89.8°F, 125°F, 200.6°F and 202.14°F, and include measurement in the liquid, critical, and gaseous regions. The measurements at 89.8°F, near the critical isotherm, are illustrated in Figure VIII-12. Again, a very sharp maximum is observed

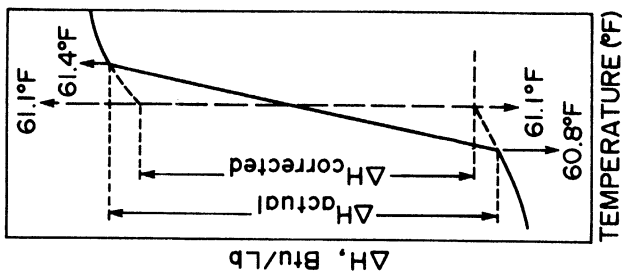

Figure VIII-9b. Graphical Procedure for Estimating the Enthalpy of Vaporization at Constant Pressure of the Pseudo-pure Fluid from Actual Measurements on an Impure System.

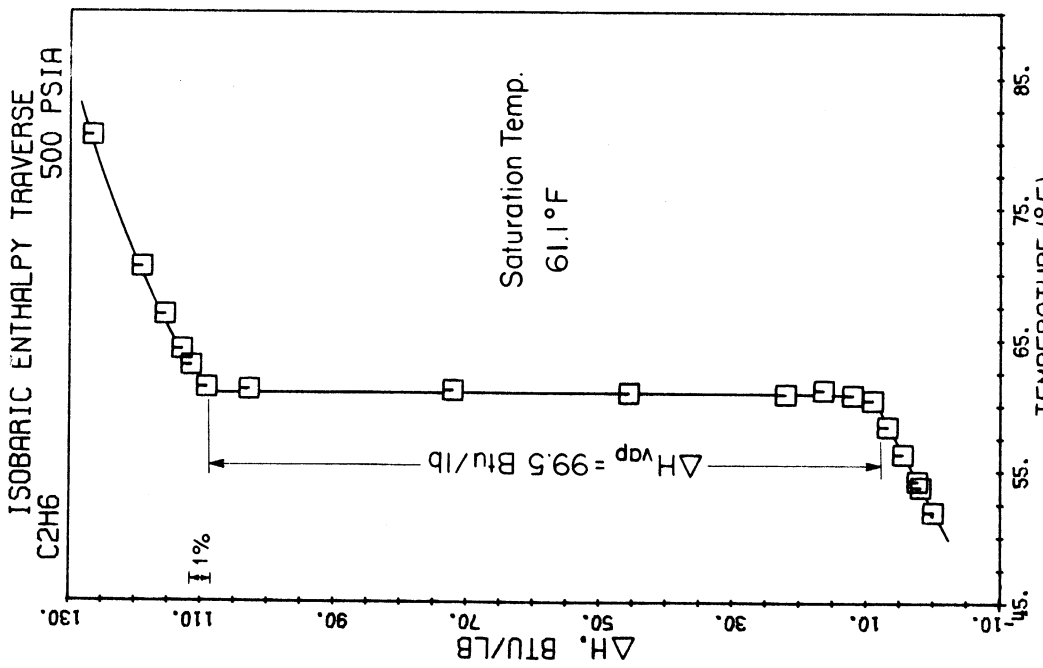

Figure VIII-9a. Isobaric Enthalpy Traverse for Ethane Across the Two Phase Region at 500 Psia.

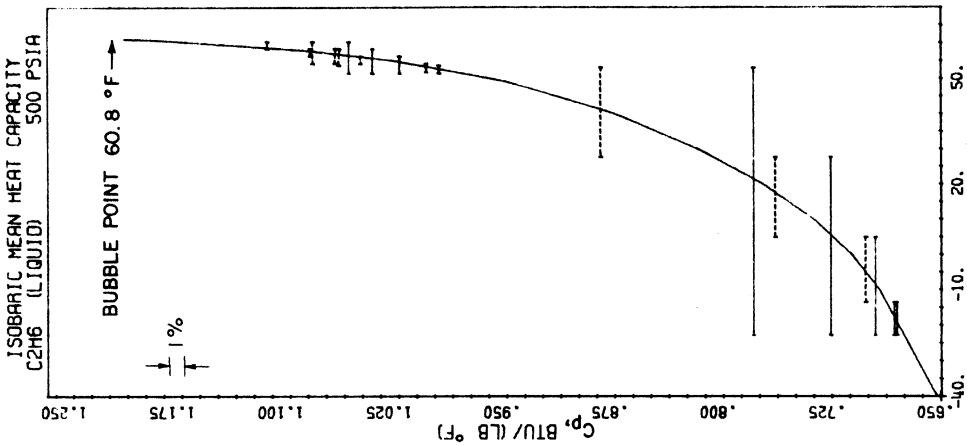

Figure VIII-11. Isobaric Heat Capacity for Ethane in the Liquid Phase upto the Saturation Boundary at 500 psia.

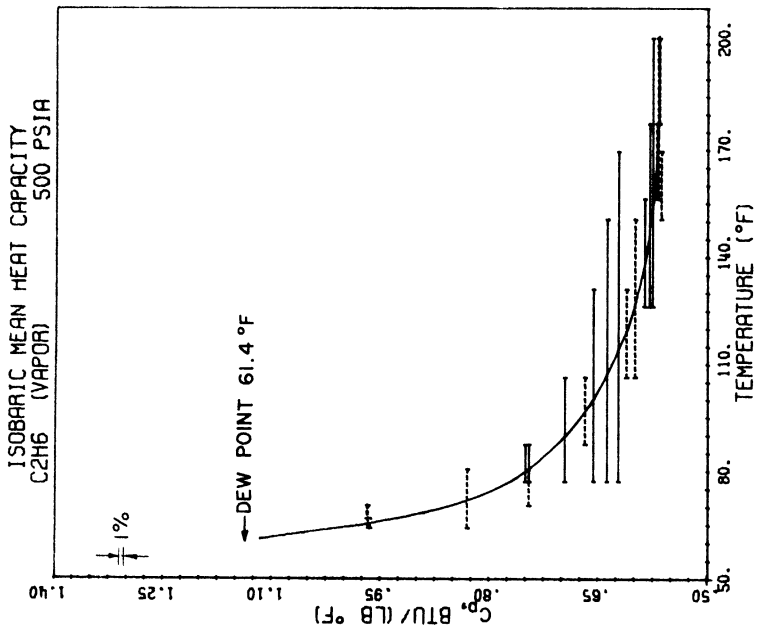

Figure VIII-10. Isobaric Heat Capacity for Ethane in the Vapor Phase upto the Saturation Boundary at 500 psia.

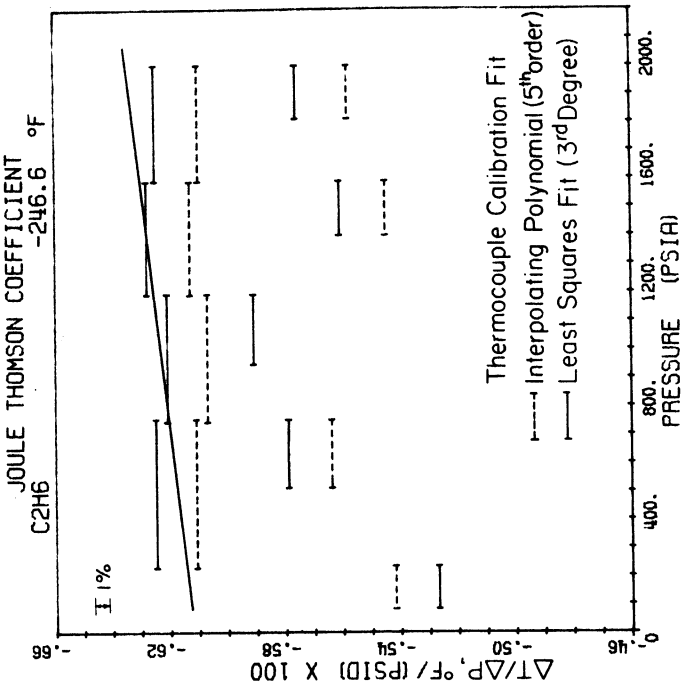

Figure VIII-13. Joule-Thomson Coefficient Measurements on Ethane at -246.6°F.

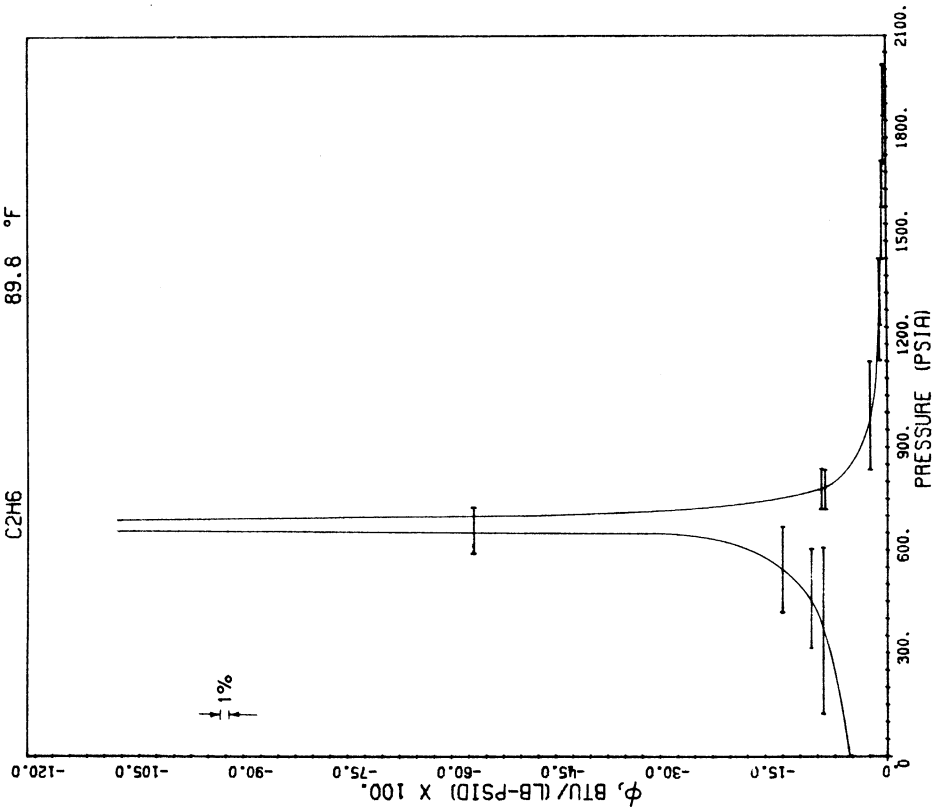

Figure VIII-12. Isothermal Joule-Thomson Coefficient for Ethane at 89.8°F.

to occur near the critical point, and in fact, mean ϕ values as high as 0.5 Btu/lb/psid were actually measured. Nevertheless, it must be emphasized that the precise shape of the equal area ϕ curve cannot be uniquely established in the vicinity of the maximum for this particular case unless an additional set of closely spaced measurements with pressure drops as low as or below 5 psid are obtained in the maximum region.

Adiabatic Joule-Thomson measurements were made at -246.6°F, -123,3°F, -24.5°F, and in the high pressure region at 49.2°F. The precision of the data as illustrated in Figure VIII-13 was particularly poor. In this case, the data obtained at the lower flowrates were effectively ignored. In any case, the discrepancy between the two sets results in a difference of only 0.5 Btu/lb in the enthalpy change from 2000 psia down to the saturated liquid state.

Consistency Checks

The consistency checks between the isobaric and throttling measurements for ethane are presented in Figure VIII-14. The reader is referred to Chapter VII for an interpretation of the diagram. The average and maximum inconsistency for the enthalpy loops is 0.64 Btu/lb or 0.4%, and 1.29 Btu/lb or 1.2%, respectively. The accuracy of the isobaric and isothermal data is estimated at 0.7% and 1.5%, respectively.

Thermal Property Tables

The enthalpy diagram in Figure VIII-15 illustrates the variation in the enthalpy as a function of temperature for ethane containing 0.4% impurities. The diagram was generated primarily from the calorimetric measurements of this work and the zero pressure enthalpies tabulated by Rossini [220]. Table VIII-3 contains numerical values for the enthalpies at regular intervals, including those for the measured isobars and isotherms.

The saturated liquid boundary upto the normal boiling point on the enthalpy diagram was obtained by integrating the saturated liquid heat capacities of Witt and Kemp [280] along the vapor pressure curve calculated by the Riedel correlation [Equation (III-36) through

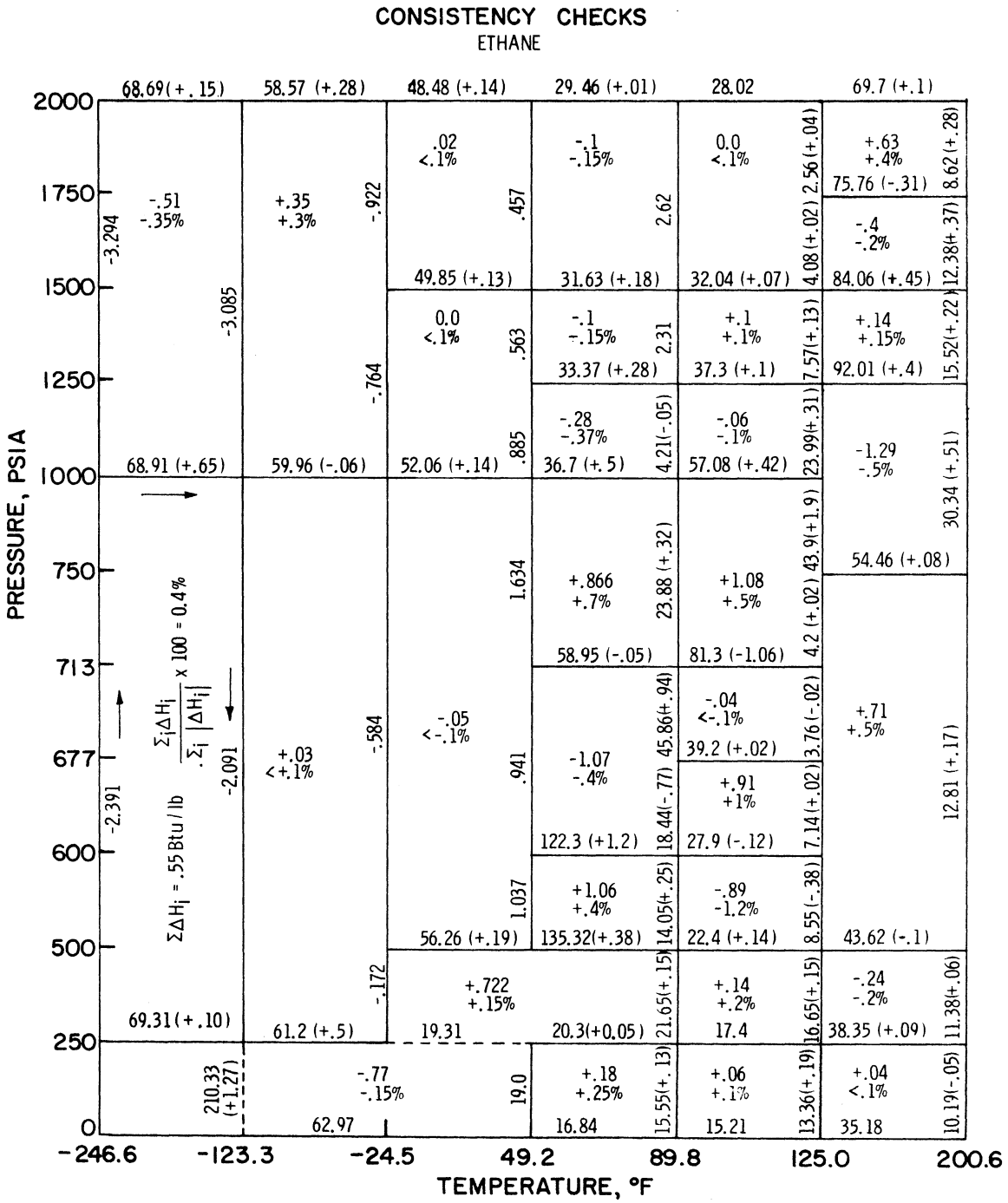

Figure VIII-14. Thermodynamic Consistency Checks for the Ethane Calorimetric Data of this Work.

TABLE VIII-3

Smoothed Enthalpy++ Values for 0.996 Ethane at Regular Intervals

TEMP.(°F)	0.*	100.	200.	250.	300.	400.	500.	600.	677.	700.	713.	800.	900.
-280.	250.6	0.3	0.7	0.8	1.0	1.3	1.6	1.9	2.1	2.2	2.2	2.5	2.8
-260.	256.4	11.1	11.4	11.6	11.8	12.1	12.4	12.7	12.9	13.0	13.1	13.3	13.7
-246.6	260.3	18.4	18.7	19.0	19.1	19.4	19.7	20.1	20.2	20.4	20.4	20.7	21.1
-240.	262.2	22.1	22.4	22.5	22.7	23.0	23.3	23.6	24.0	24.1	24.1	24.3	24.7
-220.	268.2	33.2	33.5	33.6	33.8	34.1	34.4	34.7	34.9	35.0	35.0	35.4	35.7
-200.	274.3	44.3	44.6	44.7	44.9	45.2	45.5	45.8	46.0	46.0	46.1	46.4	46.7
-180.	280.5	55.4	55.7	55.8	56.0	56.3	56.6	56.9	57.1	57.2	57.3	57.5	57.8
-160.	286.8	66.7	67.0	67.1	67.2	67.5	68.0	68.2	68.3	68.5	68.7	68.9	69.1
-140.	293.2	78.3	78.6	78.7	78.8	79.0	79.3	79.6	79.8	79.9	79.9	80.2	80.4
-123.3	298.6	88.0	88.1	88.2	88.4	88.6	88.9	89.2	89.4	89.4	89.6	89.8	90.0
-120.	299.7	90.0	90.1	90.2	90.4	90.6	90.8	91.1	91.3	91.4	91.4	91.7	92.0
-100.	306.4	101.9	101.9	102.0	102.0	102.1	102.2	102.4	102.6	102.8	102.9	103.1	103.4
-80.	313.2	114.0	114.0	114.0	114.1	114.3	114.5	114.8	115.0	115.2	115.1	115.4	115.6
-60.	320.2	126.3	126.3	126.4	126.5	126.7	126.8	127.0	127.1	127.3	127.4	127.6	127.8
-40.	327.4	316.4	139.2	139.2	139.3	139.4	139.5	139.6	139.7	139.8	139.8	139.9	140.1
-24.5	333.4	323.1	149.5	149.5	149.6	149.6	149.7	149.8	149.8	149.9	149.9	150.0	150.1
-20.	334.7	325.0	152.6	152.7	152.8	152.8	152.8	152.9	152.9	153.0	153.0	153.0	153.1
0.	342.3	333.7	322.8	167.2	167.0	166.8	166.6	166.4	166.3	166.2	166.3	166.4	166.4
20.	350.0	342.0	332.8	327.0	182.0	182.5	181.2	181.0	181.0	181.0	181.0	180.8	180.6
40.	357.9	350.5	342.4	337.8	332.3	198.5	197.6	196.9	196.6	196.3	196.2	195.9	195.0
49.2	361.6	354.3	346.8	342.6	337.8	325.5	205.9	204.9	204.2	204.1	204.0	203.4	202.8
60.	366.0	359.2	352.0	348.0	343.7	332.8	217.2	215.1	214.0	213.7	213.6	212.5	211.7
80.	374.3	368.1	361.6	358.0	354.3	345.7	334.3	316.3	238.3	237.4	237.0	233.9	231.1
89.8	378.5	372.5	366.4	363.0	359.5	351.4	341.2	327.2	309.2	298.0	260.0	245.3	241.6
100.	382.8	377.1	371.1	368.0	364.6	357.1	348.1	336.8	325.1	320.5	317.3	275.1	256.1
120.	391.5	386.2	380.7	377.7	374.6	368.0	360.5	352.0	344.3	341.8	340.1	326.9	305.1
125.	393.7	388.4	383.0	380.2	377.3	370.8	363.5	355.4	348.2	345.9	344.2	333.6	316.8
140.	400.4	395.5	390.4	387.8	385.0	379.0	372.6	365.4	359.3	357.2	356.1	347.7	336.3
160.	409.5	404.9	400.2	398.8	395.1	389.9	384.2	378.0	373.0	371.3	370.3	363.9	355.4
180.	418.9	414.6	410.2	408.0	405.7	400.9	395.6	390.1	384.5	384.3	383.4	378.0	371.2
200.	428.5	424.5	420.5	418.4	416.2	411.6	406.9	402.0	397.8	396.6	396.0	391.1	385.4
200.6	428.8	424.9	420.8	418.7	416.5	412.1	407.3	402.4	398.4	397.2	396.4	391.6	386.0
220.	438.5	434.8	430.9	428.9	426.8	422.6	418.3	413.9	410.2	409.2	408.5	404.4	399.6
240.	448.6	445.0	441.3	439.5	437.6	433.8	429.9	425.7	422.6	421.3	420.9	417.0	412.4
260.	459.0	455.6	452.2	450.4	448.7	445.0	441.2	437.4	435.8	433.5	433.0	429.6	425.5
280.	469.5	466.2	462.9	461.3	459.7	456.3	452.8	449.3	446.8	445.6	445.1	441.9	438.2
300.	480.1	477.1	474.1	472.5	471.	467.8	464.5	461.2	458.8	457.8	457.2	454.4	450.9

* ZERO PRESSURE VALUES OBTAINED BY INTERPOLATION OF (H(T)-H(0))/T VALUES AS TABULATED BY THE API [220]

++ REFERENCE ENTHALPY H=0 FOR EACH PURE COMPONENT AS A SATURATED LIQUID AT -280F

TABLE VIII-3

(CONTINUED)

TEMP.(°F)	1000.	1100.	1200.	1250.	1300.	1400.	1500.	1600.	1700.	1750.	1800.	1900.	2000.
-280.	3.2	3.5	3.8	4.0	4.2	4.5	4.8	5.1	5.4	5.6	5.8	6.1	6.5
-260.	14.1	14.4	14.8	15.0	15.1	15.4	15.7	16.0	16.3	16.5	16.8	17.1	17.4
-246.6	21.4	21.7	22.0	22.2	22.4	22.7	23.0	23.4	23.7	23.8	24.0	24.3	24.6
-240.	25.0	25.3	25.7	25.9	26.0	26.3	26.7	27.0	27.3	27.3	27.7	28.0	28.3
-220.	36.0	36.4	36.7	36.9	37.0	37.4	37.7	38.0	38.3	38.5	38.6	39.0	39.3
-200.	47.0	47.3	47.7	47.9	48.1	48.4	48.8	49.1	49.4	49.5	49.7	50.0	50.4
-180.	58.2	58.5	58.8	59.0	59.2	59.5	59.8	60.2	60.5	60.6	60.8	61.1	61.4
-160.	69.4	69.7	70.0	70.1	70.3	70.5	70.9	71.3	71.6	71.7	71.9	72.2	72.5
-140.	80.7	81.0	81.2	81.5	81.8	82.0	82.3	82.6	82.9	83.0	83.2	83.5	83.9
-123.3	90.3	90.6	90.9	91.1	91.2	91.5	91.8	92.1	92.4	92.6	92.8	93.1	93.4
-120.	92.3	92.5	92.8	93.0	93.1	93.4	93.7	94.0	94.3	94.5	94.7	95.0	95.3
-100.	103.7	104.0	104.2	104.3	104.5	104.8	105.1	105.4	105.7	105.9	106.0	106.3	106.6
-80.	115.8	116.0	116.2	116.3	116.4	116.7	116.9	117.2	117.5	117.6	117.7	118.0	118.2
-60.	128.0	128.2	128.4	128.5	128.6	128.8	129.2	129.4	129.6	129.7	129.8	130.0	130.2
-40.	140.3	140.5	140.7	140.8	140.9	141.0	141.2	141.5	141.7	141.8	141.9	142.1	142.3
-24.5	150.2	150.3	150.5	150.6	150.7	150.9	151.0	151.1	151.2	151.3	151.5	151.7	151.9
-20.	153.1	153.2	153.3	153.4	153.6	153.7	153.8	154.0	154.1	154.2	154.3	154.6	154.8
0.	166.5	166.6	166.6	166.7	166.7	166.8	166.8	166.9	167.0	167.1	167.2	167.4	167.6
20.	180.4	180.2	180.1	180.1	180.1	180.1	180.1	180.1	180.2	180.2	180.3	180.4	180.5
40.	195.2	194.9	194.7	194.6	194.5	194.3	194.1	193.9	193.9	193.9	194.0	194.0	194.0
49.2	202.3	201.9	201.5	201.4	201.3	201.1	200.9	200.9	200.6	200.6	200.5	200.5	200.4
60.	211.0	210.4	209.9	209.8	209.5	209.1	208.8	208.5	208.3	208.2	208.1	208.1	208.1
80.	229.0	227.3	226.3	226.0	225.6	224.9	224.5	223.8	223.4	223.2	223.0	222.7	222.4
89.8	239.9	236.9	235.4	234.8	234.2	233.2	232.4	231.8	231.2	231.0	230.7	230.3	229.9
100.	251.1	248.0	245.4	244.5	243.6	242.2	241.2	240.4	239.7	239.2	238.9	238.2	237.7
120.	285.0	274.3	268.2	266.0	264.2	261.5	259.4	257.9	256.6	256.0	255.5	254.4	253.6
125.	296.0	281.9	274.7	272.2	270.0	266.8	264.5	262.5	260.9	260.2	259.8	258.7	257.8
140.	322.7	308.5	297.0	292.6	289.1	283.9	280.2	277.5	275.3	274.3	273.4	272.0	270.8
160.	346.0	335.2	325.0	320.5	316.3	308.9	303.2	298.8	295.3	294.0	292.7	290.7	289.9
180.	363.9	356.0	348.0	344.1	340.3	333.3	327.0	321.6	317.1	315.3	313.5	310.4	307.9
200.	379.4	373.0	366.6	363.5	360.2	354.0	348.0	342.7	338.0	336.9	333.9	330.3	327.1
200.6	380.0	373.7	367.4	364.1	360.8	354.5	348.7	343.2	338.4	337.4	334.2	330.6	327.6
220.	394.2	388.6	383.0	380.2	377.5	372.2	367.0	362.0	357.3	355.1	353.0	349.2	346.3
240.	407.8	403.2	398.5	396.1	393.9	389.2	384.6	380.0	375.6	373.4	371.6	368.1	364.9
260.	421.2	417.0	412.8	410.0	408.6	404.4	400.2	396.3	392.5	390.8	389.0	385.9	382.9
280.	434.4	430.6	426.8	425.0	423.1	419.4	415.8	412.3	408.9	407.2	405.5	402.3	399.6
300.	447.4	443.9	440.4	438.1	437.2	434.0	430.7	427.6	424.5	422.9	421.4	418.4	415.8

(III-36c)] using the critical parameters Tc = 305.4K, Pc = 48.2 atm., and αc = 6.275. Beyond the normal boiling point, the saturated liquid enthalpies were obtained by linearly extrapolating the isotherms in the subcooled liquid region upto the estimated saturation pressure.

Having specified the location of the saturated liquid boundary on the diagram, the saturated vapor boundary above 410 psia was estimated from the calorimetric measurements of this work made across the two phase region. The gas phase enthalpies below 300 psia and upto the saturation curve were obtained from the reduced virial equation truncated at the third virial coefficient as discussed previously on page 196. The saturated vapor boundary on the enthalpy diagram between 300 and 410 psia was obtained by extending and blending the two curves on either side. Thus, the enthalpy of vaporization below 410 psia can now be specified from the relative locations of the saturated liquid and vapor boundaries on the enthalpy diagram even though direct calorimetric measurements of ΔH^{v} were not obtained in this region. Table VIII-4 lists the smoothed enthalpy values for ethane at saturation.

The variation in the heat capacity as a function of temperature and pressure is presented in Table VIII-5. Above 250 psia, the tabulated values are restricted to the results obtained from the isobaric measurements of this work. The accuracy of these values is estimated at 0.7% on the average. Supplementary heat capacity and enthalpy values in the vicinity of the saturation curve and the heat capacity maxima are presented in Table VIII-6. The heat capacity values at saturation, particularly for the vapor phase, are only approximately determined ($\pm$ 3%) from the experimental measurements. The smoothed ϕ values for the throttling measurements are shown in Table VIII-7. The procedure for calculating ϕ values from the basic isenthalpic measurements has already been described in Chapter VII.

Comparisons with Literature Data and Compilations

In order to permit a comparison between the isobaric heat capacity data of this work at 250 psia and the heat capacities in the liquid phase along the saturation curve due to Witt and Kemp [280] and Wiebe et al. [277], we first need to express the enthalpy change across any two temperatures at 250 psia, in terms of the integral of the heat

TABLE VIII-4

Smoothed Enthalpy Values for Ethane at Saturation

TEMP. (°F)	PRESSURE (PSIA)	LIQUID ENTHALPY BTU/LB	VAPOR ENTHALPY BTU/LB
-128.01	14.7	84.6	294.6
-47.3	100	134.4	313.4
-6.6	200	162.3	319.3
8.3	250	173.2	320.5
21.2	300	183.0	321.0
44.8	410 *	202.9	320.7
61.1	500 *	218.4	317.7
76.5	600 *	235.4	310.3
86.5	677 *	253.0	298.9
90.1	709.2	277.7	277.7

* ENTHALPY OF VAPORIZATION MEASUREMENTS OF THIS WORK

TABLE VIII-5

Smoothed Values of the Heat Capacity of Ethane as a Function of Temperature and Pressure

HEAT CAPACITY, CP, (BTU/LB/°F)

TEMP (°F)	PRESSURE (PSIA)											
	0.*	250.	500.	600.	677.	713.	750.	1000.	1250.	1500.	1750.	2000.
-280.	.285	.544										
-260.	.290	.546						.545				.542
-246.6	.294	.547						.546				.544
-240.	.296	.548						.547				.545
-220.	.302	.550						.549				.548
-200.	.308	.555						.554				.552
-180.	.312	.562						.560				.557
-160.	.318	.568						.566				.561
-140.	.324	.576						.571				.565
-123.3	.329	.583						.576				.569
-120.	.331	.584						.582				.570
-100.	.338	.596						.588				.578
-80.	.346	.610						.599				.588
-60.	.354	.627						.612				.599
-40.	.362	.652	.650					.630				.613
-24.5	.369	.678	.671					.645		.633		.625
-20.	.371	.683	.678					.655		.637		.628
0.	.381	.748	.709					.681		.658		.645
20.	.391	.552	.770					.711		.683		.663
40.	.401	.518	.872					.761		.714		.686
49.2	.405	.509	.948	.887		.843		.786	.754	.730		.697
60.	.411	.503	1.135	1.030		.947		.834	.786	.753		.713
80.	.420	.496	.782	1.509	1.58	1.414		.889	.860	.808		.739
89.8	.423	.494	.692	.973	2.38	9.0		1.090	.911	.840		.754
100.	.428	.493	.654	.832	1.183	1.590		1.260	.981	.877		.778
120.	.439	.495	.606	.709	.946	.865	1.000	2.265	1.192	.971		.825
125.	.442	.496	.601	.691	.778	.810	.929	2.243	1.273	1.005	.904	.838
140.	.450	.499	.586			.758	.789	1.403	1.435	1.096	.953	.878
160.	.462	.506	.574				.706	.980	1.286	1.199	1.031	.927
180.	.478	.513	.568				.660	.830	1.065	1.120	1.052	.956
200.	.490	.519	.568				.630	.751	.908	1.008	.986	.959
200.6	.491	.520	.568				.629	.749	.906	1.005	.984	.941
220.	.502	.526					.610		.808	.928	.932	.895
240.	.513											
260.	.523											
280.	.529											
300.	.539											

*ZERO PRESSURE VALUES OBTAINED BY NUMERICAL DIFFERENTIATION OF (H(T)-H(0))/T AS TABULATED BY THE API [220]

TABLE VIII-6

Supplementary Smoothed Enthalpy and Isobaric Heat Capacity Values for 0.996 Mole Fraction Ethane in the Vicinity of the Heat Capacity Maxima and in the Two Phase Region

250 PSIA

TEMP. °F	H BTU/LB	CP BTU/LB/°F
-10.	159.6	.710
-5.	163.1	.726
0.	167.7	.748
5.	171.5	.785
8.25	173.2	.822 *
8.25	320.5	.606 **
10.	321.5	.591
13.	323.3	.578
18.	326.1	.558

410 PSIA

TEMP. °F	H BTU/LB	CP BTU/LB/°F
40.	198.4	.917
42.	200.2	.923
44.	202.1	.943
44.8	202.9	.973 *
44.8	320.7	
47.	322.3	
49.2	324.2	
50.	324.8	
55.	328.9	

500 PSIA

TEMP. °F	H BTU/LB	CP BTU/LB/°F
55.	211.7	1.024
58.	214.8	1.088
60.	217.2	1.135
61.1	218.4	1.210 *
61.1	317.7	1.110 **
63.	319.8	1.046
65.	321.8	.972
67.	323.7	.919
70.	326.4	.852
75.	330.4	.783

600 PSIA

TEMP. °F	H BTU/LB	CP BTU/LB/°F
70.	225.9	1.285
73.	230.0	1.425
75.	233.0	1.550
76.5	235.4	1.690 *
76.5	310.0	1.905 **
78.	312.7	1.755
80.	316.0	1.510
81.5	318.1	1.340
82.5	319.4	1.254
85.	322.3	1.096

677 PSIA

TEMP. °F	H BTU/LB	CP BTU/LB/°F
77.5	234.5	1.39
80.	238.3	1.58
81.5	241.1	1.76
82.5	243.0	1.91
84.	246.1	2.22
85.	248.4	2.55
85.5	249.8	2.80
86.	251.2	3.19
86.5	253.0	3.77 *
86.5	298.9	3.86 **
87.5	302.6	3.38
88.	304.2	2.80
90.	309.2	2.33
91.	311.4	2.08
92.5	314.3	1.78
95.	318.3	1.47
97.5	321.7	1.29
100.	325.1	1.18
105.	330.3	1.04
110.	335.3	.956

713 PSIA

TEMP. °F	H BTU/LB	CP BTU/LB/°F
50.	204.6	.848
60.	213.6	.947
70.	223.6	1.077
75.	229.3	1.185
77.2	232.0	1.245
80.	237.0	1.414
82.	238.6	1.535
84.	241.9	1.728
85.	243.6	1.838
86.	245.5	1.959
87.	247.4	2.181
88.	251.0	4.5
89.	257.0	5.5
89.8	263.0	8.0
90.	264.5	
91.	287.3	
92.	297.0	4.4
93.	301.3	3.88
94.	304.5	2.985
95.	307.5	2.642
97.	312.2	2.081
100.	317.3	1.590
105.	324.5	1.257
110.	330.4	1.077
130.	334.4	.815

* SATURATED LIQUID
** SATURATED VAPOR

TABLE VIII-6

(CONTINUED)

819 PSIA

TEMP. °F	H BTU/LB	CP BTU/LB/°F
99.	263.5	3.25
99.5	265.2	3.53
100.0	267.0	3.84
100.5	269.0	4.22
101.	271.2	4.59
101.5	273.6	4.98
102.	276.2	5.30
102.2	277.2	5.41
102.4	278.3	5.48
102.7	280.0	5.51
103.0	281.6	5.52
103.2	282.7	5.51
103.4	283.8	5.50
103.6	284.9	5.40
104.	287.0	5.12
104.5	289.5	4.73
105.	291.8	4.39
105.5	293.9	4.09
106.	295.9	3.86

1000 PSIA

TEMP. °F	H BTU/LB	CP BTU/LB/°F
106.	259.0	1.402
110.	264.9	1.591
112.	268.3	1.770
115.	274.0	2.021
117.	278.2	2.151
118.	280.3	2.208
120.	285.9	2.265
121.2	287.5	2.270
123.	291.6	2.267
125.	296.1	2.240
126.	298.3	2.203
128.	302.6	2.053
130.	306.6	1.915
135.	315.3	1.594
145.	329.4	1.263
150.	335.4	1.142

1250 PSIA

TEMP. °F	H BTU/LB	CP BTU/LB/°F
110.	254.7	1.070
120.	266.0	1.192
130.	278.6	1.337
135.	285.4	1.400
140.	292.6	1.435
143.	296.9	1.440
147.	302.6	1.433
150.	306.9	1.412
155.	313.8	1.353
160.	320.5	1.286
170.	332.7	1.180

1500 PSIA

TEMP. °F	H BTU/LB	CP BTU/LB/°F
110.	250.2	.919
120.	259.6	.971
130.	269.6	1.033
140.	280.2	1.096
150.	291.5	1.151
160.	303.2	1.199
161.2	304.6	1.206
163.	307.5	1.204
167.	311.7	1.201
170.	315.3	1.186
175.	321.2	1.151
180.	327.0	1.120
190.	337.2	1.052

1750 PSIA

TEMP. °F	H BTU/LB	CP BTU/LB/°F
150.	284.1	.991
160.	294.0	1.031
165.	299.4	1.046
170.	304.7	1.055
173.5	308.4	1.058
174.5	309.4	1.059
180.	315.3	1.052
185.	320.5	1.036
190.	325.6	1.020

TABLE VIII-7

Smoothed Values of the Isothermal Throttling Coefficient
for 0.996 Mole Fraction Ethane

$(DH/DP)_T \times 100$ (BTU/LB/PSID)

PRESSURE (PSIA)	TEMPERATURE (°F)						
	-246.6	-123.3	-24.5	49.2	89.8	125.0	200.6
0.*	-48.20	-15.05	-8.70	-6.36	-5.50	-4.90	-3.88
100.	.312	.194	-11.30	-6.78	-5.70	-5.25	-3.98
200.	.313	.215	.046	-8.25	-6.67	-5.72	-4.18
250.	.314	.223	.053	-9.50	-7.10	-5.92	-4.28
300.	.315	.232	.060	.	-7.45	-6.17	-4.38
400.	.316	.246	.074	.	-8.43	-6.78	-4.60
500.	.317	.258	.085	-1.14	-11.30	-7.59	-4.82
600.	.318	.268	.096	-0.94	-18.60	-8.67	-5.09
677.	.319	.273	.102	-0.80	-34.70	-10.0	-5.30
700.	.320	.274	.105	-0.76	.	-10.5	-5.36
713.	.320	.275	.106	-0.74	.	-10.8	-5.39
750.	.320	.280	.109	-0.69	-9.83	-12.1	-5.49
800.	.321	.284	.114	-0.63	-4.86	-13.7	-5.62
900.	.322	.290	.124	-0.52	-3.13	-20.3	-5.87
1000.	.323	.294	.133	-0.43	-2.28	-20.2	-6.10
1100.	.325	.298	.142	-0.37	-1.74	-10.0	-6.31
1200.	.326	.302	.150	-0.31	-1.36	-5.35	-6.40
1250.	.326	.303	.154	-0.28	-1.21	-4.36	-6.52
1300.	.327	.304	.157	-0.26	-1.08	-3.68	-6.49
1400.	.328	.307	.164	-0.22	-0.84	-2.75	-6.10
1500.	.330	.308	.170	-0.17	-0.75	-2.13	-5.65
1600.	.331	.310	.177	-0.13	-0.64	-1.68	-5.10
1700.	.332	.310	.182	-0.10	-0.56	-1.39	-4.51
1750.	.332	.312	.185	-0.090	-0.52	-1.24	-4.20
1800.	.333	.312	.188	-0.072	-0.47	-1.15	-3.88
1900.	.334	.313	.192	-0.053	-0.40	-0.99	-3.29
2000.	.336	.313	.197	-0.036	-0.35	-0.87	-2.76

* THE VALUE OF $(DH/DP)_T$ AT ZERO PRESSURE IS OBTAINED FROM EQUATIONS (V-30) AND (V-31) IN CONJUNCTION WITH THE CRITICAL PARAMETERS IN TABLE IX-1

capacity at constant pressure along the saturation curve. Thus

$$\int_{T_i}^{T_f} (Cp)_{250\ psia}\, dT = \int_{T_i}^{T_f} (Cp)_{P=Ps}\, dT + \int_{T_i}^{T_f} \left[\int_{Ps}^{250} \left(\frac{dCp}{dP} \right)_T dP \right] dT \qquad \text{(VIII-5)}$$

where Ps is the saturation pressure. If Cp at the saturation pressure is next expressed in terms of the saturated heat capacity Cs as defined by Equation (I-8), we obtain the result

$$\int_{T_i}^{T_f} (Cp)_{250\ psia}\, dT = \int_{T_i}^{T_f} (Cp)_T\, dT + \int_{T_i}^{T_f} \left[-T\left(\frac{dV}{dT} \right)_P \left(\frac{dP}{dT} \right)_{Sat} \right] dT + \int_{T_i}^{T_f} \left[\overline{\Psi}\,(250-Ps) \right] dT \qquad \text{(VIII-6)}$$

where $\overline{\Psi}$ is the mean value of dCp/dP over the interval (250-Ps) at any given temperature. In order to obtain an estimate of the last term in Equation (VIII-6) from the experimental data of this work, it was necessary to further assume that $\overline{\Psi}$ was a constant over the interval T_i to T_f, and that it could be estimated from the ϕ values reported for the two isenthalps at -246.6°F and -123.3°F using the approximation

$$\overline{\Psi} = \Delta\phi/\Delta T = (\overline{\phi}_{-246.6°F} - \overline{\phi}_{-123.3°F})/(-246.6 + 123.3) \qquad \text{(VIII-7)}$$

where $\overline{\phi}$ is the mean value of ϕ over the interval 250 psia to Ps. The above approximation can be derived from the thermodynamic identity in Equation (I-1), which expresses Ψ in terms of $(dH/dP)_T$. The value of $\overline{\Psi}$ was estimated to be 0.00011 Btu/lb/°F/psi from Equation (VIII-7).

The argument for ignoring the contribution of the middle term in Equation (VIII-6) upto the NBP will now be presented. Eubank [70] has indicated that the term, V(dP/dT), along the saturation curve is about 0.4% of the saturated heat capacity Cs at the NBP. If the ratio $[-T(dV/dT)_P/V]$ can be determined at the NBP, then the relative contribution of the middle term in Equation (VIII-6) can be established. The saturated volume V at the NBP is 55.02 cc/gm mole according to the compilation of Eubank [70]. The value of ϕ at the NBP was approximately estimated at 42cc/gm mole from the equal area ϕ curve for the -123.3°F isotherm of this work extrapolated to its saturation pressure. If the thermodynamic identity expressed as Equation (I-2) is now used, then the estimated values of ϕ and V yield a value of 0.235 for the ratio

$[- T (dV/dT)_p/V]$. Therefore, the maximum contribution of the middle term upto the NBP is about 0.1%, confirming the general rule of Ginnings and Stinson [87] in this regard.

As the maximum value of Ps upto the NBP is 14.7 psia, the contribution of Ps to the last term in Equation (VIII-6) was also ignored along with the middle term. On rearranging and dividing by ΔT, we obtain the result

$$\bar{C}_s = \int_{T_i}^{T_f} \frac{C_s dT}{\Delta T} = \left(\frac{\Delta H}{\Delta T}\right)_{250 \text{ psia}} + 0.00011 (250) \text{ Btu/lb/°F} \qquad \text{(VIII-8)}$$

espressed in Btu/lb/°F. The quantity on the right hand side of Equation (VIII-8) was computed from the basic data of Run 38 and plotted as the horizontal bars in Figure VIII-16. The differenced data plotted as the dashed bars are of lower precision than the basic data of this work, but were plotted in preference to the latter in order to visually highlight the discrepancy between the curve through the point data in the literature and the bar data of this work. For perfect consistency, a curve through the points must realize an equal area curve with respect to the solid and dashed bars. The results of this work at -260°F appear to be too high, and may be attributed to the melting of previously solidified unsaturated hydrocarbon impurities trapped in the heater capsule and also possibly to unsteady state effects that appear to be more prevalent for the first data point in a given run. An accuracy of 0.5% is claimed for both literature sources of Cs data. Apart from the first data point, the agreement between all sources is approximately 0.7%.

Comparisons were also made against the smoothed heat capacity values of Michels et al. [174] in the gaseous and supercritical regions as derived from accurate volumetric data along isotherms, and the Cp° values of Smith [247] derived from spectroscopic data. The results are illustrated in Figure VIII-17. In some cases, the agreement, even at low pressure, was no better than 2%. It was later discovered that the enthalpy change at zero pressure from 77°F to 212°F was calculated as 50.1 Btu/lb from the tables of Michels et al., whereas the API results [220] used in this work yielded a higher value of 51.4 Btu/lb. The discrepancies between the two sources deserves further consideration,

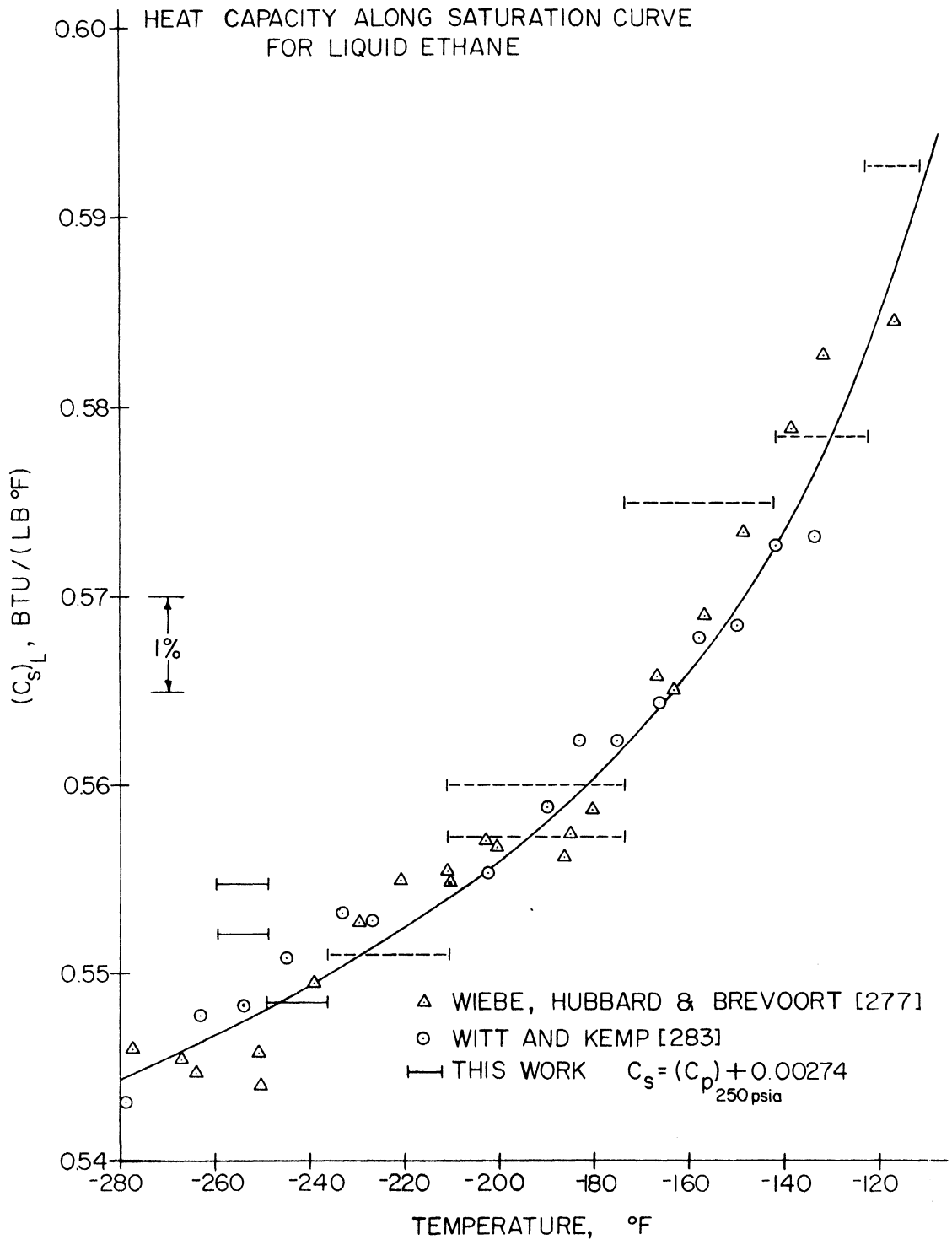

Figure VIII-16. Comparison Between the Measured Mean Heat Capacities of Ethane From this Investigation with the Saturated Liquid Heat Capacity Data in the Literature.

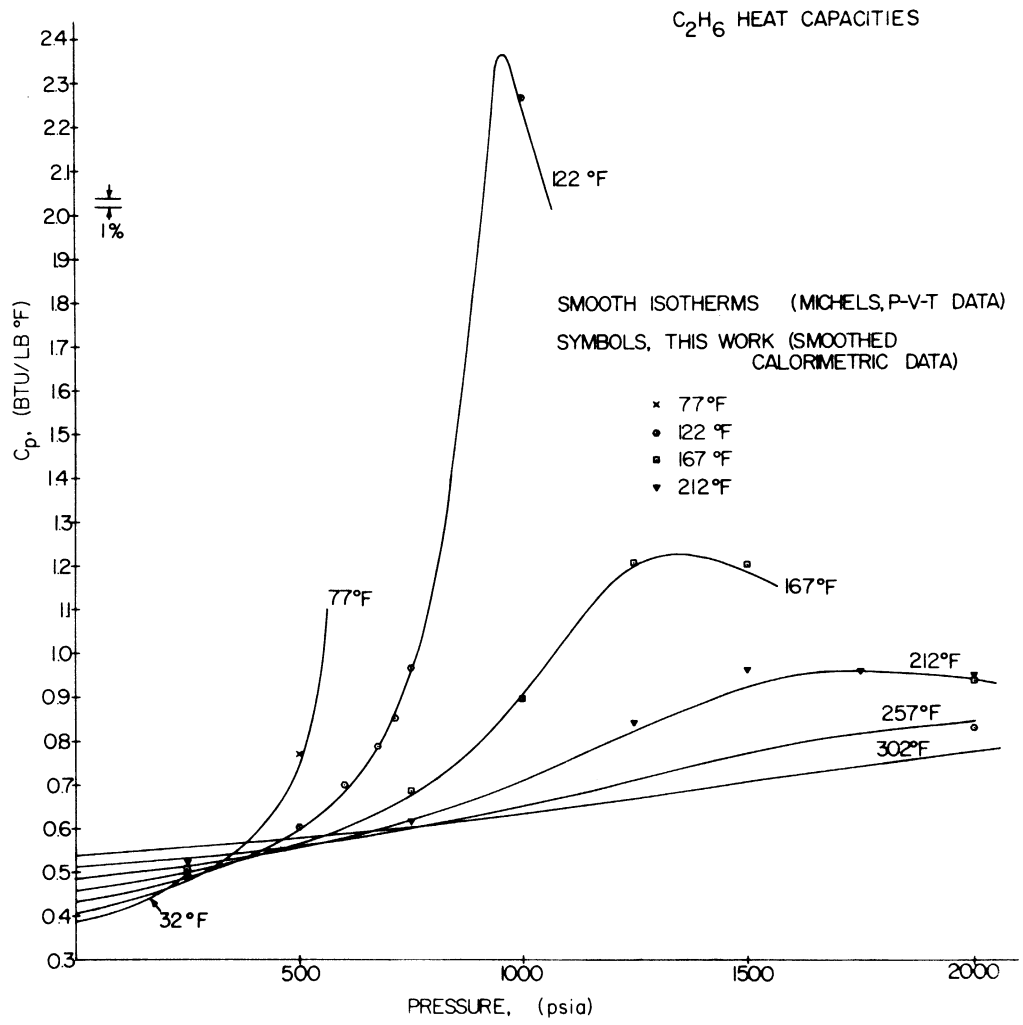

Figure VIII-17. Comparison Between the Smoothed Heat Capacities of this Work and the Smoothed Values of Michels et al.[174] Obtained from PVT Data.

TABLE VIII-8

Comparison of the Smoothed Heat Capacities of this Work with the Tabulated Results of Michels et al. in the Gaseous and Supercritical Regions

TEMP. (°F)	PRESSURE (PSIA)	CP (THIS WORK) (BTU/LB/°F)	CP (MICHELS)+ (BTU/LB/°F)	CP (MICHELS) CORRECTED * BTU/LB/°F	% DEV.
77	0	.418	.409	.418	
77	500	.770	.760	.769	-0.1
122	0	.440	.432	.440	0.0
122	250	.524	.514	.523	-0.2
122	500	.604	.596	.605	+0.2
122	600	.702	.681	.689	-1.6
122	677	.790	.790	.799	+1.1
122	713	.851	.862	.871	+2.3
122	750	.966	.952	.961	-0.4
167	0	.468	.458	.468	0.0
122	1000	2.268	2.247	2.256	-0.5
167	250	.508	.497	.507	-0.2
167	750	.966	.952	.962	-0.4
167	1000	.920	.905	.915	-0.5
167	1250	1.215	1.200	1.210	-0.4
167	1500	1.201	1.185	1.195	-0.5
212	0	.497	.485	.497	0.0
212	250	.524	.514	.526	+0.4
212	750	.619	.619	.631	+5.0
212	1250	.843	.822	.834	-1.1
212	1500	.961	.924	.934	-2.8
212	2000	.949	.938	.950	+0.1

* ZERO PRESSURE HEAT CAPACITIES ADJUSTED TO AGREE WITH VALUES USED IN THIS WORK

+ Ref [174]

particularly since Hill [105] points out that a torsional vibration component of Cp° that is approximately 5% of the total vibration effect escapes detection in spectroscopic analysis. Next, the Cp° values of Michels et al. were corrected to correspond to those used in this work, and the comparisons repeated. The results are presented in Table VIII-8. The agreement is, on the average, better than 1%, and is of the order of the precision of the interpretation of the volumetric measurements. An unusually high discrepancy of 5%, considerably beyond the estimated limits of accuracy for the data of this work, was however obtained at 750 psia and 212°F.

The enthalpies of vaporization calculated from the smoothed data and the enthalpy diagram of this work are compared with the values from the compilations of Tester [264] and Eubank [75], the experimental data of Witt and Kemp [280] at the NBP, the measurements of Dana et al. [57] at higher pressures, and the calculated results of Powers [20] using the Riedel three parameter reduced vapor pressure, saturated liquid, and saturated vapor volume correlations in conjunction with Equation (I-6). The comparisons are indicated in Figure VIII-18 and Table VIII-9. The solid line in the figure represent the smoothed values obtained from the enthalpy diagram of this work. The results of Dana et al. are about 1 to 2% above the line, as are the values of Eubank near the critical region. The calculation procedure of Powers is seen to be less satisfactory below the normal boiling point. The value of the enthalpy of vaporization at the NBP was calculated as 210.1 Btu/lb from the enthalpy diagram of this work, and compares favorably with the value of 210.91 Btu/lb obtained by Witt and Kemp from direct calorimetric measurements.

Discussion on the Maxima in Cp and ϕ

The saturation data, the Cp maxima along isobars, and the ϕ maxima along isotherms are all plotted on ln P vs ln T coordinates as seen in Figure VIII-19. The particular choice of coordinates is dictated by the general observation that the vapor pressure curve is approximately linear as one approaches the critical point on such a plot. The Cp maxima appear to lie on, or close to, the linear extrapolation of the vapor pressure curve beyond the critical temperature.

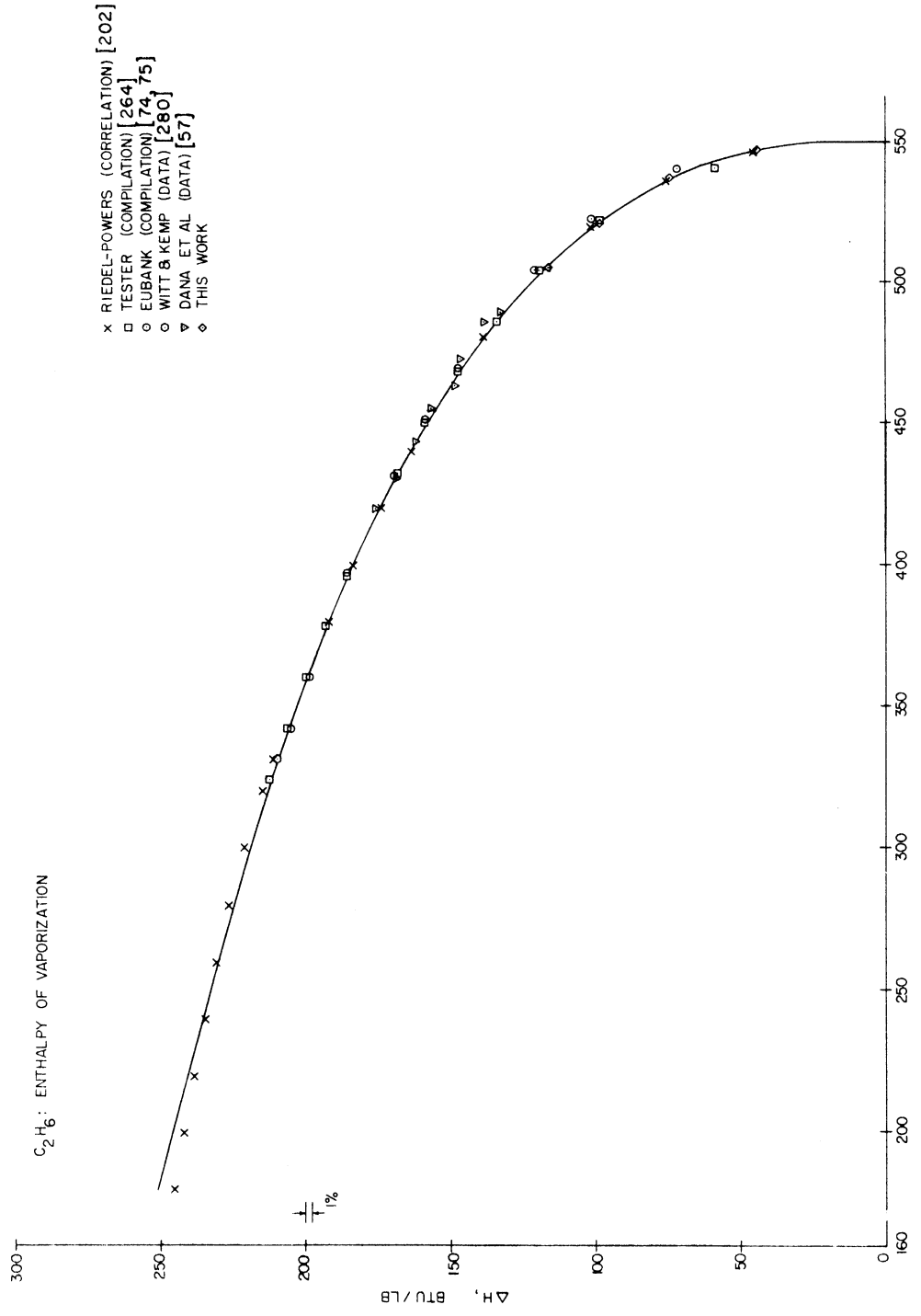

Figure VIII-18. Comparison Between the Enthalpies of Vaporization for Ethane as Derived from this Investigation with Some Results from the Literature.

TABLE VIII-9

Comparison Between the Enthalpy of Vaporization as a Function of Temperature as Obtained from The Enthalpy Diagram of This Work with The Results from The Literature

TEMP. (°R)	ENTHALPY OF VAPORIZATION (BTU/LB)*					
	TESTER [264]	EUBANK [74]	WIEBE ET AL [277]	RIEDEL [216]	WITT ET AL [280]	THIS WORK
180				245.4		251.0
200				242.2		244.9
240			236.3	235.4		236.0
280			225.6	226.8		225.5
300			220.1	221.5		219.6
324	212.9	212.8	214.3	214.0		212.2
331.4	210.9	210.9	210.0	211.8	210.9	210.0
342	207.0	206.1	197.1	207.8		206.3
360	200.5	199.5	193.1	201.0		199.6
378	193.6	192.8	188.5	193.6		193.0
396	186.3	185.8	183.2	186.0		186.0
414	178.4	178.1	176.8	177.2		177.9
432	169.5	169.4	169.4	168.0		169.0
450	159.4	159.3	160.7	158.0		158.3
468	148.1	147.8	150.1	147.2		147.2
486	134.8	134.9	137.1	134.7		134.7
504	119.6	120.6	120.6	119.5		118.0
522	98.8	101.5	98.1	98.2		98.2
540	58.8	71.9	61.4	65.2		66.0

* The values of Wiebe et al, Witt and Kemp, and the results of this work are derived from calorimetric measurements.

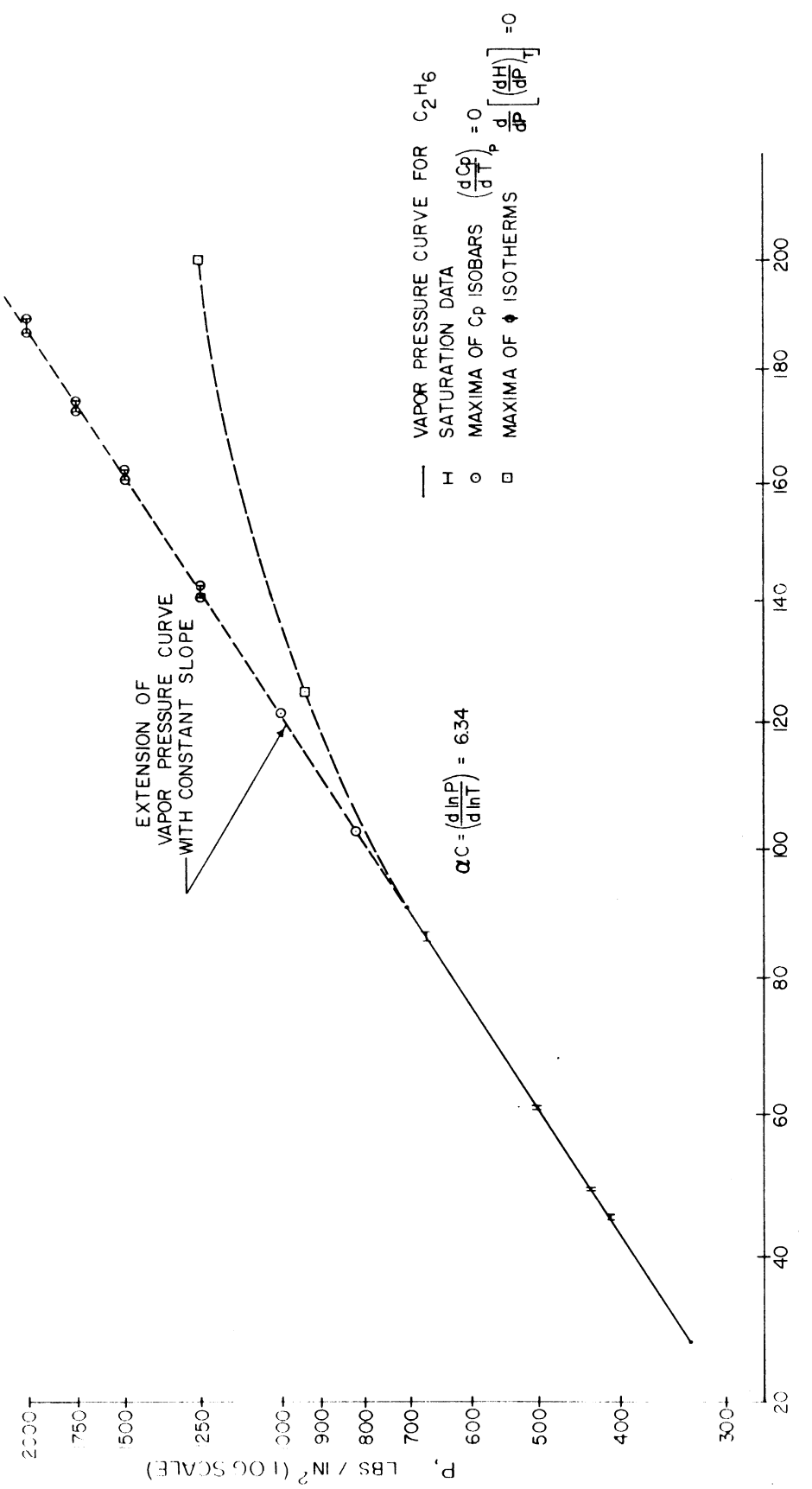

Figure VIII-19. The Location of the Cp Maxima Along Isobars, and the ϕ Maxima Along Isotherms Relative to the Linear Extrapolation of the Vapor Pressure Curve for Ethane on Logarithmic Coordinates.

Qualitatively speaking, the slight trend towards the right of the extrapolated line as the pressure is increased could be reversed by plotting the locus of the maxima in $(Cp - Cp^{\circ})$ along isobars instead, to compensate for the increase of Cp° with temperature. Such a plot would, in fact, be more proper because the quantity $(Cp - Cp^{\circ})$, unlike Cp, is a true configurational property and is recommended for future analyses along such lines.

An αc value of 6.34 was computed for the best straight line fit to the saturation data and the Cp maxima along isobars as opposed to the suggested value of 6.275 [214]. Table VIII-10 lists the location, the value of Cp, and the value of $\underline{H}$ for the heat capacity maxima at several isobars as determined from the measurements of this work. Also listed, are the predicted temperatures for the heat capacity maxima for a fixed αc value of 6.34. These are seen to agree fairly well with the measured temperatures. The ϕ maxima are found to lie on the gas side of the extrapolated vapor pressure line, moving further away from the Cp maxima as the pressure is increased.

Other thermodynamic and transport properties are known to follow a similar behaviour in the critical region. Bailey and Kellner [8] observed that the thermal conductivity maxima for Argon were near the location of the critical isochore. Noury et al. [186,187] have obtained minima in the ultrasonic velocities for propane in the supercritical region. Sirota and co-workers [245] have established from precise data on water, that the locus for the maxima in Cp along isotherms, $(dCp/dP)_T = 0$, would appear to the right of the locus of $(dCp/dT)_P = 0$, if plotted with the coordinates of Figure VIII-19, with the critical isochore lying, for the most part, in between the two curves but closer to the former. These considerations indicate that though there is a change from a more liquid-like phase to a more gas-like phase across the supercritical region, there is no unique prescription for locating a phase transition boundary.

The explanation for such phenomena is not yet clear. The absence of discontinuities in the second and higher order derivatives of the heat capacity with respect to temperature along isobars, or with respect to pressure along isotherms, precludes the occurence of a higher order transition in the supercritical region as a possible extension of the

TABLE VIII-10

Thermal Properties for Ethane at the Heat Capacity Maxima along Isobars

PRESSURE (PSIA)	TEMP. THIS WORK (°F)	PREDICTED TEMP.* ALPHAC=6.340 (°F)	$(C_P)_{max}$ THIS WORK BTU/LB/°F	H THIS WORK BTU/LB
819.	103.0	103.0	5.52	281.6
1000.	121.2	121.6	2.27	287.5
1250.	143.0	141.7	1.44	296.9
1500.	161.2	161.1	1.206	304.6
1750.	174.5	174.6	1.059	309.4
2000.	190.0	188.1	0.963	317.3

* Predicted results assuming that the heat capacity maxima lie on a linear extrapolation of the vapor pressure curve on a log P vs log T plot.

first order transition across the vapor pressure curve. It may be conjectured that the supercritical phase is composed of a variable number of clusters of molecules, with fewer larger clusters occuring at lower temperatures. The addition of energy to such a phase may be assumed to be partly utilized in raising the kinetic energy of such clusters, and thus the temperature of the phase, and partly in breaking down such clusters into smaller ones. The fraction of energy utilized in the latter case has little or no effect on raising the temperature. At the maximum in Cp, the cluster distribution is such that the fraction of added energy utilized in the breakup of clusters is highest relative to that used in increasing their kinetic energy. Beyond this point, the phase is more gas like, consisting of smaller, more stable clusters, and the added energy is principally used in raising the temperature.

Measurements on Ethane-Propane Mixtures

An attempt was made in this work to characterize the enthalpy behaviour of the ethane-propane system as a function of composition with the minimum experimental effort necessary to effectively represent the system in some established enthalpy correlation framework. An analysis of the enthalpy data for five methane-propane systems using an equation of state led Starling [249,250] to conclude that the examination of three well spaced mixtures could permit a level of description that was adequate for engineering purposes. A similar conclusion was independently reached by Powers [202]. Consequently, the investigation of the ethane-propane system was restricted to three such ethane-propane mixtures.

A further examination of the methane-propane data in the PGC framework suggested that a sufficiently significant set of optimized pseudo-parameters for any given mixture could be obtained from limited experimental data carefully selected to include.

1) A wide ranging isobar at high pressure.

2) Limited range isobaric data at various pressures in the region of the heat capacity maxima, and specifically just above the cricondenbar.

3) An isotherm near, and preferably just beyond, the

cricondentherm.

4) An adiabatic Joule-Thomson run in the liquid region outside the inversion dome, and preferably, at the lowest possible temperature.

Although the above criteria were used in selecting the location of the runs for the various ethane-propane mixtures, additional data were also obtained to provide the necessary thermodynamic consistency checks. The three mixtures examined contained 0.76, 0.50 and 0.27 mole fraction ethane, respectively. The compositions and the flowmeter calibration results for these mixtures are summarized in Tables VI-3 and VI-1, respectively. These mixtures are individually discussed below.

a) Nominal 0.76 Mole Fraction Ethane-Propane Mixture. The measurement conditions are illustrated in Figure VIII-20. All runs are numbered in chronological sequence. Extensive isobaric data were obtained at 1000 psia and 1500 psia. Isothermal measurements were taken at 50°F, 151.65°F, and 250.74°F from about 100 psia to 2000 psia, and over a limited range at 102.4°F. Adiabatic Joule-Thomson data were obtained at -50.12°F and in the high pressure region at 50°F. Isobaric enthalpy data in the two phase region were taken at 250, 500, and 716 psia. The basic isobaric, isothermal, and isenthalpic measurements are reported in Tables B-4, B-5, and B-6, respectively.

The variation of the system composition as a function of run number is shown in Figure VIII-21, where the ethane and propane mole fractions are each normalized to include the impurities at their respective ends of the spectrum. The dotted line indicates the selected normalized ethane composition for the system. Most of the values lie within $\pm$ 0.6% of this line. Isobaric results at 1000 psia illustrating the variation of the mixture heat capacity in the supercritical region are indicated in Figure VIII-22. The behaviour of the heat capacity variation with temperature is similar to that for pure ethane. A typical isothermal run in the gas phase is shown in Figure VIII-23. Adiabatic Joule-Thomson data at -50.18°F are plotted in Figure VIII-24. For this particular case the precision of the measurements is about 2%. An isobaric enthalpy traverse at 716 psia through the two phase region (Run 18.1) is illustrated in Figure VIII-25. This particular run was a repeat of an earlier

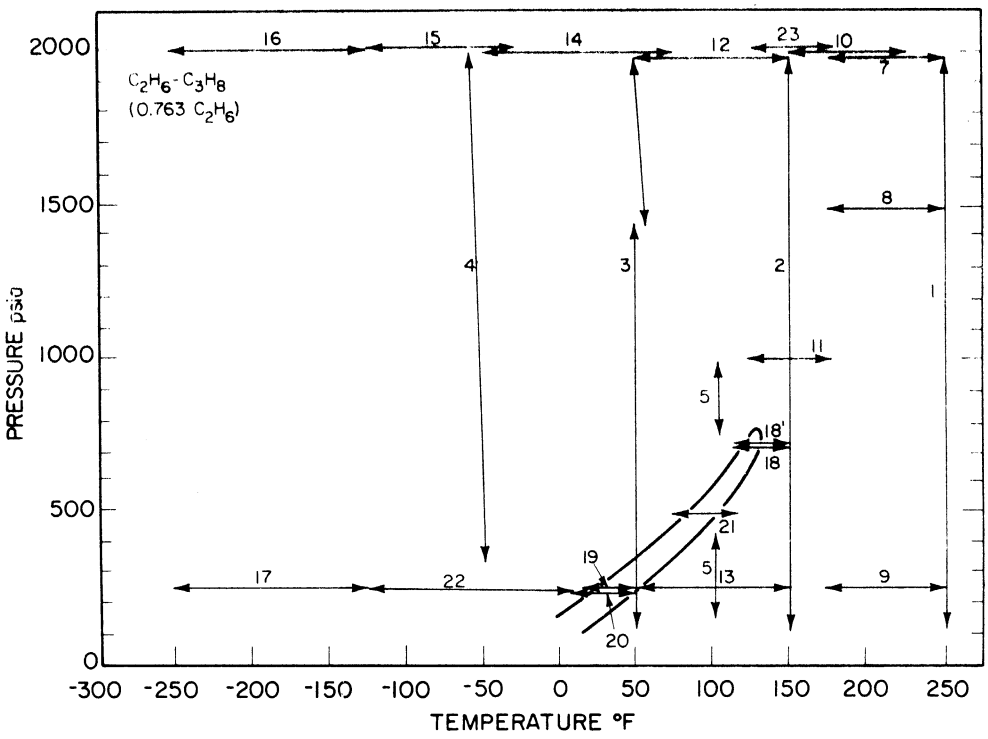

Figure VIII-20. Temperature and Pressure Range of the Calorimetric Measurements for the Nominal 0.76 Mole Fraction Ethane-Propane Mixture as a Function of Run Number.

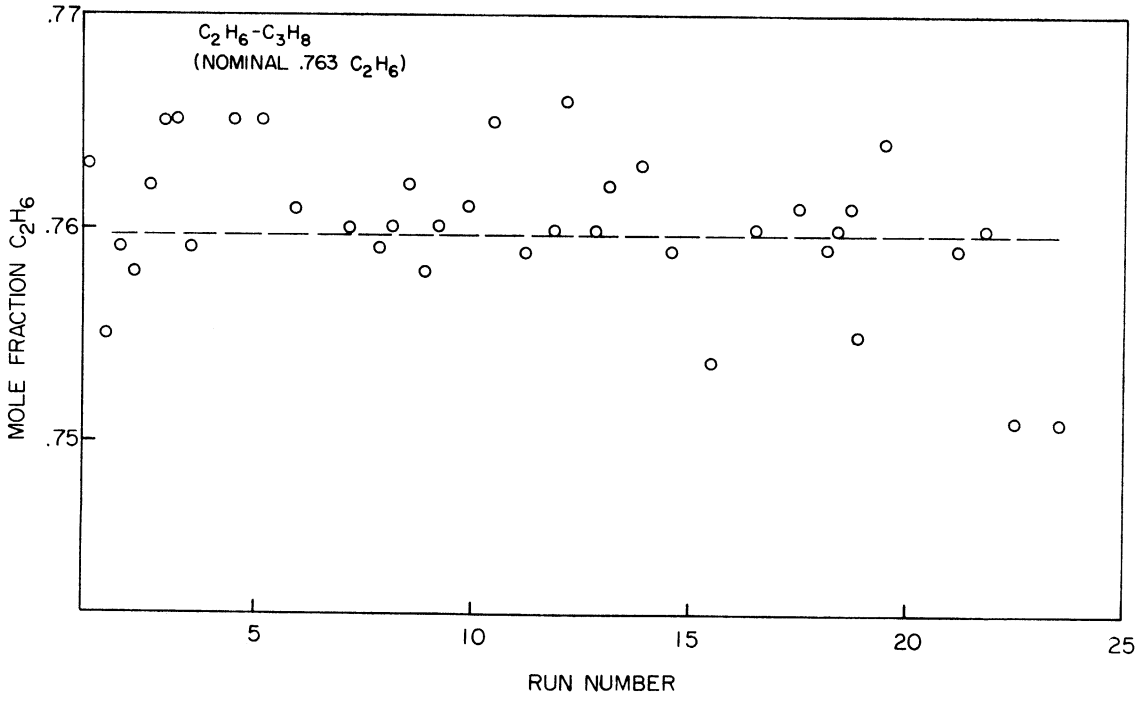

Figure VIII-21. Variation of Composition for the Nominal 0.76 Mole Fraction Ethane-Propane Mixture as a Function of Run Number.

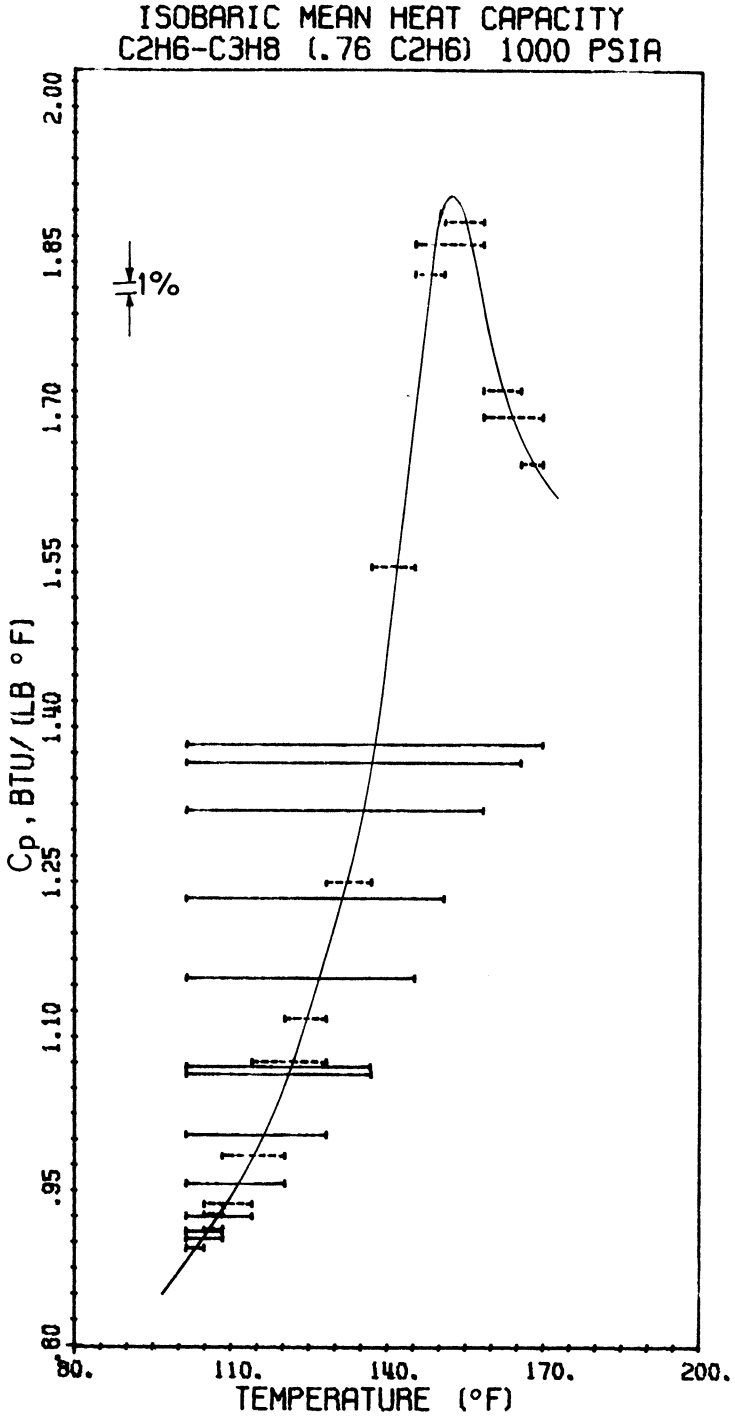

Figure VIII-22.
Isobaric Heat Capacity for the Nominal 0.76 Mole Fraction Ethane-Propane Mixture at 1000 psia.

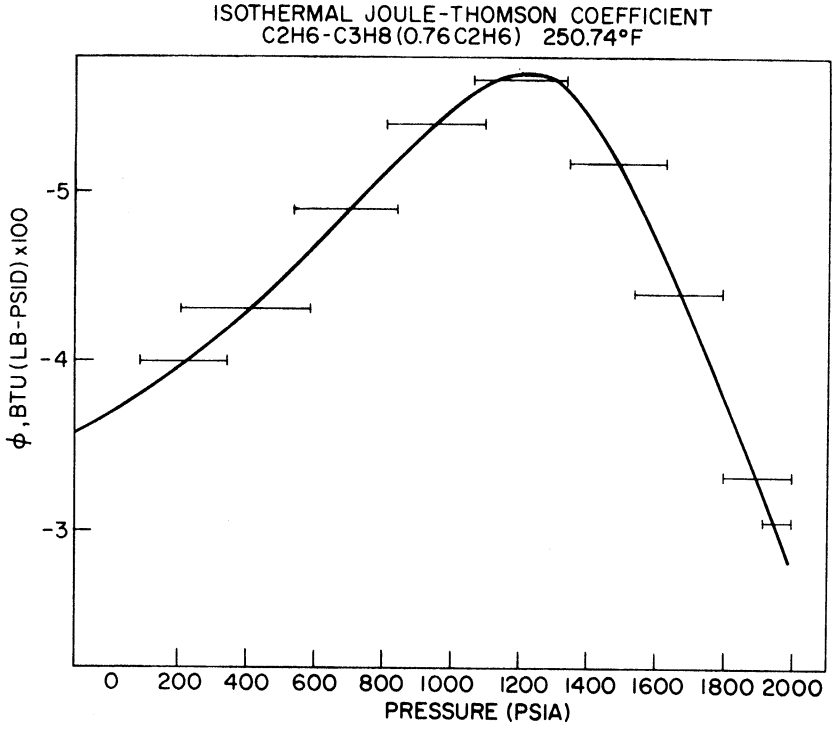

Figure VIII-23. Isothermal Joule-Thomson Coefficient for the Nominal 0.76 Mole Fraction Ethane-Propane Mixture at 250.74°F.

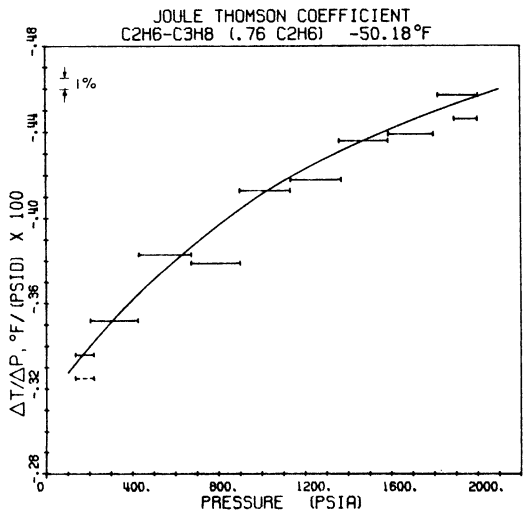

Figure VIII-24. Adiabatic Joule-Thomson Coefficient Data for the Nominal 0.76 Mole Fraction Ethane-Propane Mixture at -50.18°F.

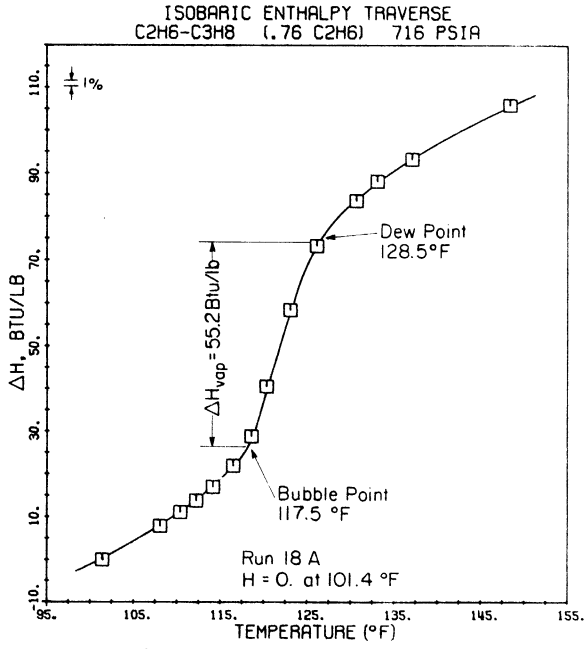

Figure VIII-25. Isobaric Enthalpy Traverse for the Nominal 0.76 Mole Fraction Ethane-Propane Mixture at 716 psia.

attempt (Run 18.0), where a leak occured in the flowmeter section. The use of low flowrates in these runs magnified the errors, and resulted in discrepancies that were as large as 5%, emphasizing again, the importance of eliminating such problems.

The consistency checks on the smoothed data are summarized in Figure VIII-26. The discrepancy between the "experimental" and adjusted enthalpy differences for the arms of several loops involving Runs 7 through 10 (see Figure VIII-20) is worse than indicated in Figure VIII-26. The adjustment of the basic data before the consistency checks is justified as follows: A pressure dependent mass leak across the pressure to vacuum seal of the isobaric calorimeter was found to have occured for the runs in question. Run 23 was then attempted to estimate the magnitude of the error, and the results were about 2% below those for Run 10 over the common range extending between 156.5°F and 180°F. The enthalpy values for Runs 7 through 10 were uniformly decreased by about 2% in the initial processing of the basic data for obtaining smoothed Cp and enthalpy values.

The loop checks for Runs 7 through 10 were still uncertain, as a pressure dependent leak was also observed for the 250.74°F isotherm. In consequence, the rest of the basic data were used to determine the optimum pseudo-parameters for the mixture in the PGC framework by techniques to be explained in Chapter IX. These parameters were than used to predict the enthalpy values for the leak-plagued measurements using the PGC at high pressures, and the reduced virial equation in the gas phase upto 500 psia. These predictions were also used as a guide in extrapolating the results of Run 8 and 9 to 151.65°F to permit additional consistency checks to be made. The 50°F isotherm could not serve as an arm of a loop from 2000 to 250 psia as severe instability in the flow conditions did not permit the evaluation of the enthalpy change across the entire two phase region. The maximum and average error in the consistency checks were 1.8 Btu/lb or 0.8%, and 0.83 Btu/lb or 0.45%, respectively. Smoothed Cp and H values for the isobaric measurements are presented in Table VIII-11. The smoothed ϕ and H values for the isothermal and isenthalpic measurements are summarized in Table VIII-12.

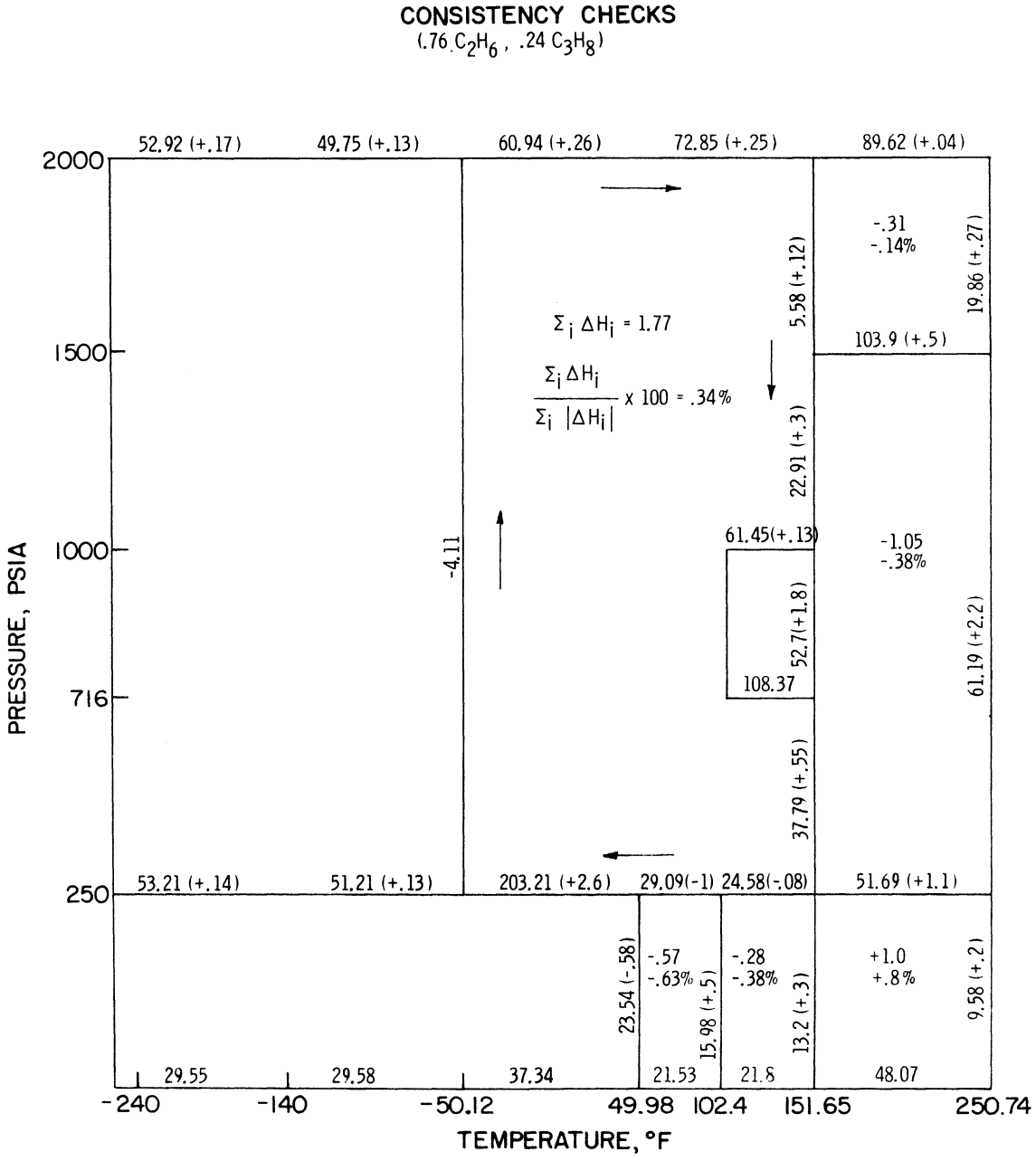

Figure VIII-26. Thermodynamic Consistency Checks for the Calorimetric Data on the 0.76 Mole Fraction Ethane-Propane Mixture.

TABLE VIII-11

Tabulated Values of the Enthalpy[++] and the Heat Capacity
for the Nominal 0.76 Mole Fraction Ethane-Propane Mixture

0 PSIA ***			250 PSIA			500 PSIA			716 PSIA		
TEMP. °F	H BTU/LB	CP BTU/LB/°F	TEMP. °F	H BTU/LB	CP BTU/LB/°F	TEMP. °F	H BTU/LB	CP BTU/LB/°F	TEMP. °F	H BTU/LB	CP BTU/LB/°F
-280.	245.2	.265	-280.	0.7	.517	-50.12	126.4		-50.12	127.5	
-260.	250.6	.272	-260.	11.0	.520	49.98	192.1		49.98	191.0	
-240.	256.1	.279	-240.	21.4	.523	68.	207.9	.857	100.	234.0	1.03
-220.	261.8	.286	-220.	31.9	.526	70.	209.6	.871	102.4	236.6	1.04
-200.	267.6	.293	-200.	42.4	.529	72.	211.3	.888	108.	243.4	1.30
-180.	273.5	.298	-180.	53.2	.534	75.	214.1	.914	110.	246.1	1.40
-160.	279.5	.305	-160.	63.8	.539	78.	216.9	.946	112.	249.0	1.55
-140.	285.7	.312	-140.	74.6	.547	80.	218.8	.968	114.	252.3	1.76
-120.	292.0	.319	-120.	85.7	.557	82.2	221.0	.980 *	115.	254.1	1.94
-100.	298.4	.327	-100.	96.9	.566	83.	225.1		116.	256.3	2.40
-80.	305.1	.335	-80.	108.3	.578	85.	241.3		117.	258.9	2.90
-60.	311.9	.343	-60.	120.0	.591	90.	276.8		117.5	260.4	3.10 *
-50.12	315.3	.348	-50.12	125.9	.598	95.	305.3		120.	274.7	
-40.	318.8	.353	-40.	132.0	.606	100.	329.5		122.5	291.2	
-20.	325.9	.362	-20.	144.3	.623	100.4	330.7	.868 **	125.	303.7	
0.	333.3	.373	0.	157.0	.655	102.4	332.3	.840	128.5	315.5	2.30 **
20.	340.9	.383	10.	163.7	.693	105.	334.4	.808	130.	318.6	1.75
40.	348.7	.393	15.	167.2	.732	110.	338.3	.756	132.5	322.6	1.50
49.98	352.6	.398	20.	171.1	.796	115.	342.0	.726	135.	326.4	1.30
60.	356.6	.404	22.5	173.1	.832	151.65	365.7		140.	332.5	1.15
80.	364.8	.414	24.2	174.5	.863 *	250.74	424.1		151.65	344.9	
100.	373.1	.424	25.	179.1					250.74	414.3	
102.4	374.1	.425	30.	218.6							
120.	381.7	.435	35.	253.6							
140.	390.5	.446	40.	283.9							
151.65	395.9	.453	45.	310.3							
160.	399.6	.458	49.98	329.1							
180.	408.9	.473	52.2	332.0	.622 **						
200.	418.5	.485	55.	333.7	.602						
220.	428.3	.497	60.	336.7	.568						
240.	438.4	.508	65.	339.4	.538						
250.74	444.0	.514	70.	342.1	.523						
260.	448.6	.519	80.	347.1	.502						
280.	459.1	.527	100.	357.1	.493						
300.	469.7	.537	102.4	358.2	.493						
			120.	367.0	.494						
			140.	376.9	.497						
			151.65	382.7	.499						
			160.	386.9	.501						
			180.	397.1	.511						
			200.	407.4	.521						
			220.	418.0	.533						
			240.	428.6	.544						
			250.74	434.4	.551						
			260.	439.9	.557						
			280.	451.1	.570						

++ REFERENCE ENTHALPY H=0 FOR EACH PURE COMPONENT AS A SATURATED LIQUID AT -280F

* SATURATED LIQUID

** SATURATED VAPOR

*** ZERO PRESSURE ENTHALPIES AND HEAT CAPACITIES CALCULATED FROM HEAT CONTENT FUNCTION AS TABULATED BY THE API [220]

TABLE VIII-11

(CONTINUED)

1000 PSIA				1500 PSIA				2000 PSIA		
TEMP. °F	H BTU/LB	CP BTU/LB/°F		TEMP. °F	H BTU/LB	CP BTU/LB/°F		TEMP. °F	H BTU/LB	CP BTU/LB/°F
-50.12	126.8			-50.12	128.7			-280.	6.6	.516
49.98	191.5			49.98	190.7			-260.	16.9	.519
100.	228.7	.869		151.65	269.3	.963		-240.	27.2	.522
102.4	230.8	.887		160.	277.5	1.000		-220.	37.7	.525
120.	247.7	1.046		170.	293.0	1.042		-200.	48.3	.527
125.	253.1	1.130		180.	298.4	1.091		-180.	58.9	.530
135.	265.1	1.302		190.	309.5	1.118		-160.	69.5	.534
140.	272.0	1.499		194.	314.0	1.122	+	-140.	80.2	.539
142.	275.1	1.587		200.	320.7	1.107		-120.	91.0	.544
144.	278.4	1.670		210.	331.8	1.097		-100.	101.9	.551
147.	283.6	1.797		220.	342.6	1.061		-80.	113.1	.558
150.	289.1	1.876		230.	353.0	1.020		-60.	124.4	.568
151.65	292.2	1.893		240.	363.0	.976		-50.12	130.0	.573
153.	294.8	1.896	+	250.74	373.2	.928		-40.	135.8	.580
155.	298.6	1.888						-20.	147.5	.593
160.	307.8	1.796						0.	159.4	.607
162.5	312.3	1.746						20.	171.8	.624
165.	316.6	1.696						40.	184.5	.643
170.	324.8	1.612						49.98	190.9	.653
250.74	400.1							60.	197.6	.663
								80.	211.0	.683
								100.	224.0	.709
								102.4	226.8	.713
								120.	239.4	.740
								140.	254.6	.776
								151.65	263.8	.803
								160.	270.6	.830
								180.	287.7	.881
								200.	305.7	.917
								220.	323.7	.937
								240.	343.2	.948
								250.74	353.4	.949

+ THE HEAT CAPACITY MAXIMUM POINT ALONG THE GIVEN ISOBAR

TABLE VIII-12

++

Tabulated Values of the Enthalpy and the Isothermal Throttling Coefficient for the Nominal 0.76 Mole Fraction Ethane-Propane Mixture

TEMPERATURE (°F)

	-50.12°F		50.0°F		151.65°F		250.74 F	
P	H	$(DH/DP)_T$ X100	H	$(DH/DP)_T$ X100	H	$(DH/DP)_T$ X100	H	$(DH/DP)_T$ X100
PSIA	BTU/LB	BTU/LB/ PSID	BTU/LB	BTU/LB/ PSID	BTU/LB	BTU/LB/ PSID	BTU/LB	BTU/LB/ PSID
**								
0.	315.3	-10.6	352.6	-6.8	395.9	-4.72	444.0	-3.69
100.	125.53	.195	345.2	-8.0	391.0	-5.15	440.3	-3.81
200.	125.73	.200	345.0	-10.0	385.6	-5.64	436.4	-3.93
250.	125.85	.203	329.1	.	382.7	-5.93	434.4	-3.99
300.	125.94	.206	264.2	.	379.7	-6.24	432.4	-4.04
400.	126.15	.210	192.42	-.392	373.1	-6.96	428.3	-4.18
500.	126.36	.215	192.06	-.328	365.7	-7.91	424.1	-4.35
600.	126.58	.219	191.76	-.274	357.2	-9.21	419.7	-4.52
700.	126.80	.223	191.51	-.226	346.9	-11.78	415.1	-4.71
716.	126.83	.224	191.48	-.220	344.9	-12.18	414.3	-4.75
750.	126.91	.225	191.40	-.204	339.9	-14.24	412.7	-4.82
800.	127.03	.227	191.30	-.185	332.4	-18.63	410.3	-4.92
900.	127.26	.230	191.14	-.148	309.9	-21.75	405.3	-5.11
1000.	127.50	.234	191.01	-.116	292.2	-13.07	400.1	-5.28
1100.	127.73	.237	190.90	-.088	282.6	-6.90	394.8	-5.42
1200.	127.97	.240	190.83	-.062	277.2	-4.15	389.3	-5.51
1250.	128.09	.241	190.80	-.051	278.9	-3.54	386.5	-5.51
1300.	128.21	.243	190.78	-.040	273.8	-2.93	383.7	-5.50
1400.	128.45	.245	190.75	-.020	271.3	-2.21	378.4	-5.33
1500.	128.70	.248	190.74	-.002	269.3	-1.73	373.2	-5.04
1600.	128.95	.250	190.75	+.014	267.8	-1.37	368.8	-4.61
1700.	129.20	.252	190.77	+.028	266.5	-1.16	363.9	-4.16
1750.	129.32	.253	190.79	+.034	266.0	-1.07	361.9	-3.94
1800.	129.45	.254	190.80	+.040	265.4	-0.97	359.9	-3.71
1900.	129.70	.256	190.85	+.050	264.5	-0.86	356.4	-3.27
2000.	129.96	.258	190.90	+.060	263.8	-0.74	435.3	-2.79

	102.38°F*		151.65°F*		
P	H	$(DH/DP)_T$ X100	P	H	$(DH/DP)_T$ X100
PSIA	BTU/LB	BTU/LB/ PSID	PSIA	BTU/LB	BTU/LB/ PSID
0.	374.1	-5.6	810.	330.4	-20.4
250.	358.2	-7.6	825.	327.2	-22.2
500.	332.3		830.	326.1	-22.6
716.	236.6		850.	321.5	-23.2
800.	233.4		860.	319.1	-23.3
1000.	230.8		880.	314.5	-23.2
			890.	312.2	-22.9
			925.	304.8	-20.0
			950.	300.0	-17.7

* SUPPLEMENTARY VALUES

** THE VALUE OF $(DH/DP)_T$ AT ZERO PRESSURE IS OBTAINED FROM EQUATIONS (V-30) AND (V-31) IN CONJUNCTION WITH THE PSEUDO-PARAMETERS (I) FOR THE GIVEN MIXTURE IN TABLE IX-13

++ REFERENCE ENTHALPY H=0 FOR EACH PURE COMPONENT AS A SATURATED LIQUID AT -280F

b) Nominal 0.50 Mole Fraction Ethane-Propane Mixture. The measurement conditions are illustrated in Figure VIII-27. Isobaric data were obtained in an unbroken stretch from -246°F to 293°F at 2000 psia. Additional limited measurements are reported at 760 and 1000 psia. Isobaric runs across the two phase region were made at 250 and 500 psia. Isothermal runs were obtained at 151.1°F and 251.1°F. Isenthalpic data are reported at 37.5°F and -125.5°F. The basic isobaric, isothermal, and isenthalpic measurements are reported in Tables B-7, B-8 and B-9.

The variation in composition during the course of the investigation is illustrated in Figure VIII-28, and is seen to be more severe than usual. The dotted line indicates the selected normalized ethane mole fraction used in the thermal property tabulations. The 2000 psia isobar is shown in Figure VIII-29. The heat capacity maximum is located very near the 300°F high temperature operating limit of the system. Consequently, it was not possible to obtain measurements that would characterize the behaviour of Cp with temperature beyond the maximum. An isobaric enthalpy traverse is plotted as Figure VIII-30. The sharpness in the definition of the dew and bubble points in this case is typical of the traverses obtained at lower pressures. The vapor phase heat capacity at 250 psia, including the best differenced data beyond the dew point for Run 9, and the results of Runs 4 and 5 are plotted. in Figure VIII-31, and illustrates the broad minimum observed in this region. The isothermal measurements in the gas phase at 251.1°F and the isenthalpic measurements in the liquid phase at 37.5°F are illustrated in Figures VIII-32 and VIII-33, respectively. The measurements in the latter case are more precise than usual.

The consistency checks are summarized in Figure VIII-34. Seven enthalpy loops were examined. The maximum and average inconsistencies in the loops were - 0.5 Btu/lb or - 0.2%, and 0.3 Btu/lb or 0.14%, respectively. It is felt that these data are among the most precise ever obtained at the facility. Table VIII-13 contains the smoothed H and Cp values for the isobaric data. Table VIII-14 summarizes the smoothed H and ϕ values for the isothermal and isenthalpic throttling data.

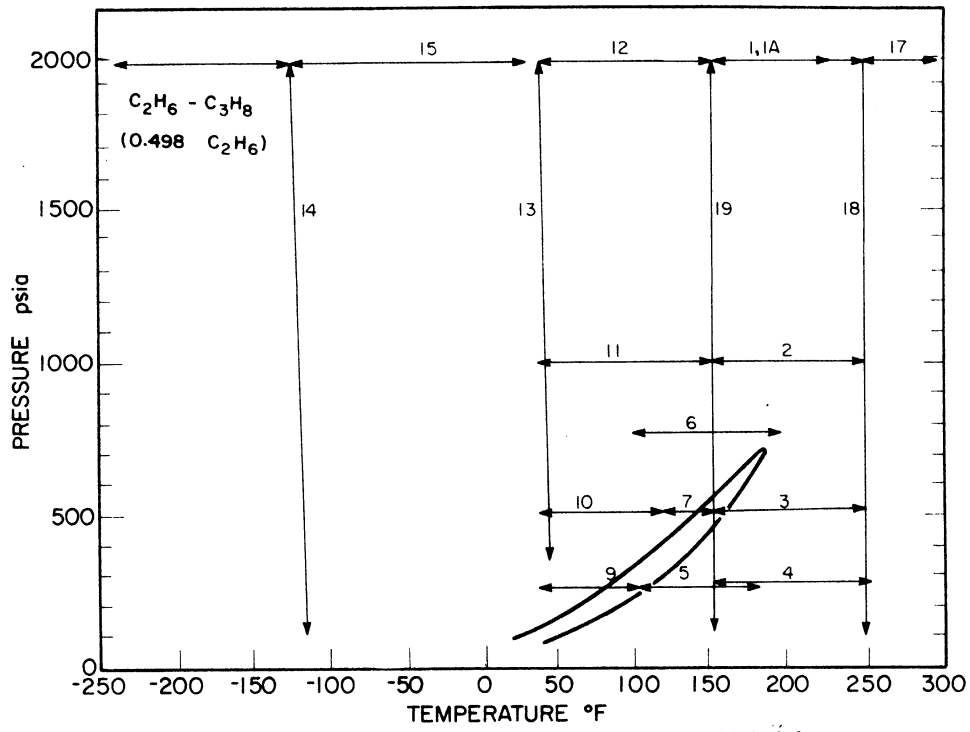

Figure VIII-27. Range of Calorimetric Measurements Obtained in This Work for the Nominal 0.50 Mole Fraction Ethane-Propane Mixture.

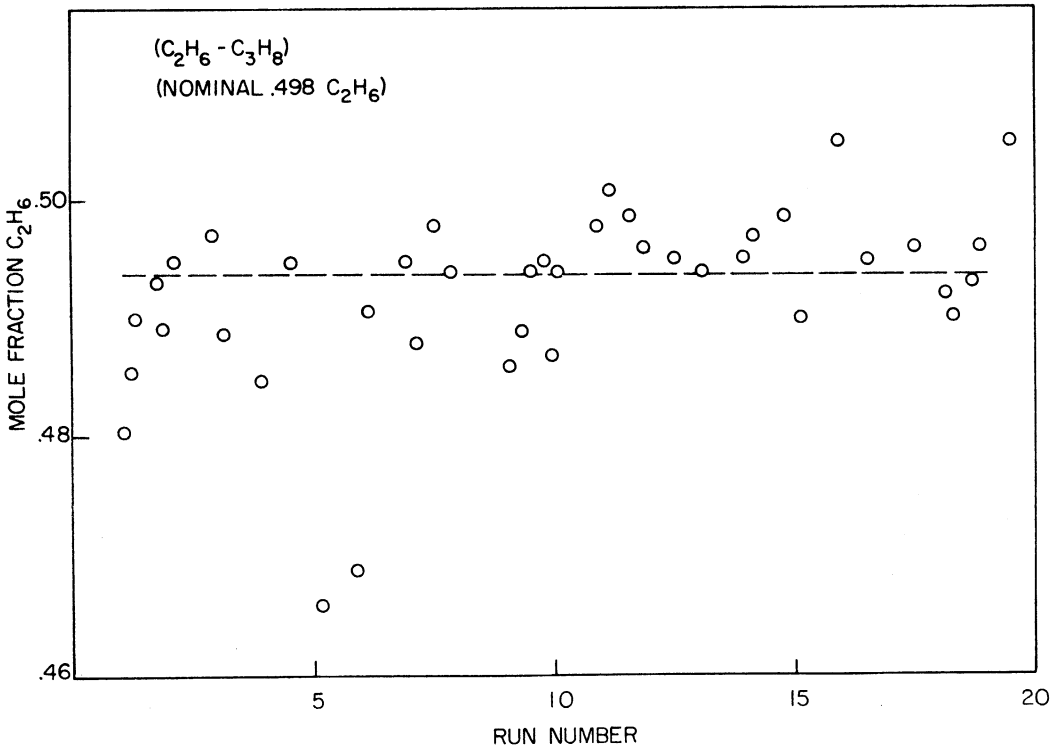

Figure VIII-28. Variation of Composition for the Nominal 0.50 Mole Fraction Ethane-Propane Mixture as a Function of Run Number.

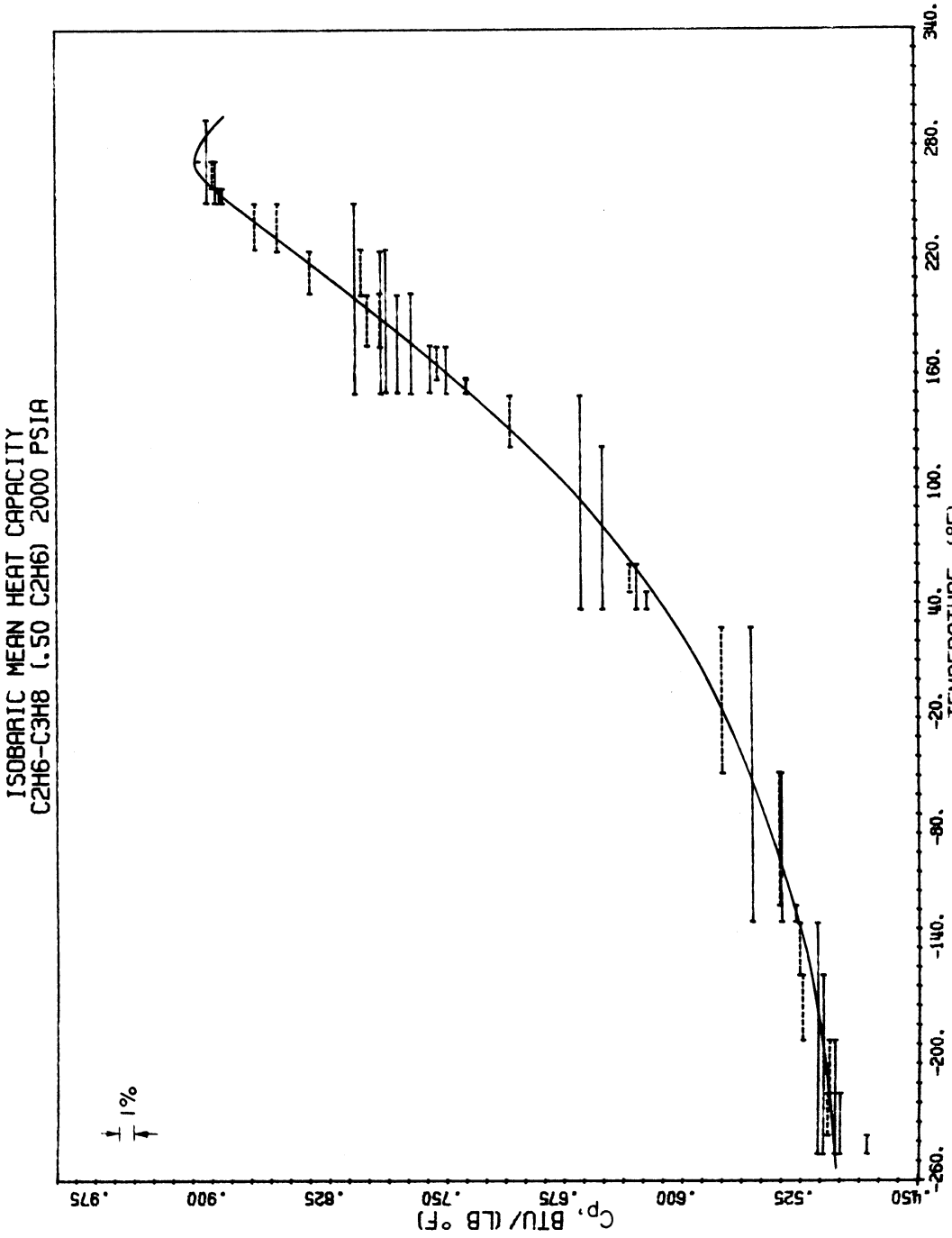

Figure VIII-29. Isobaric Heat Capacity for the Nominal 0.50 Mole Fraction Ethane-Propane Mixture at 2000 Psia.

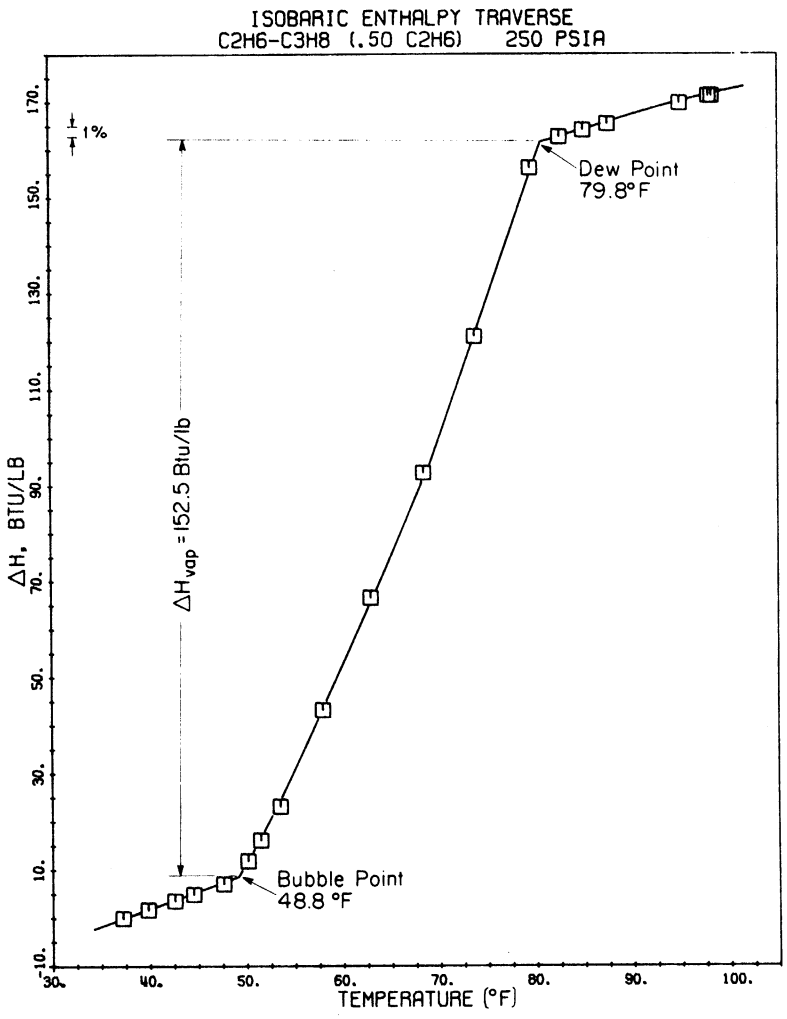

Figure VIII-30. Isobaric Enthalpy Traverse Across the Two Phase Region for the Nominal 0.50 Ethane-Propane Mixture at 250 Psia.

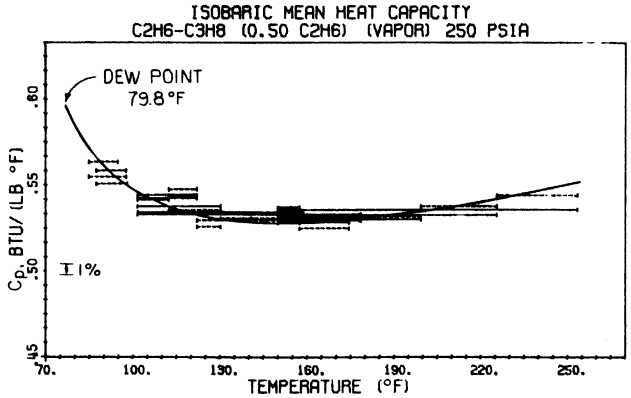

Figure VIII-31. Isobaric Heat Capacity for the Nominal 0.50 Mole Fraction Ethane-Propane Mixture in the Vapor Phase upto the Saturation Boundary at 250 Psia.

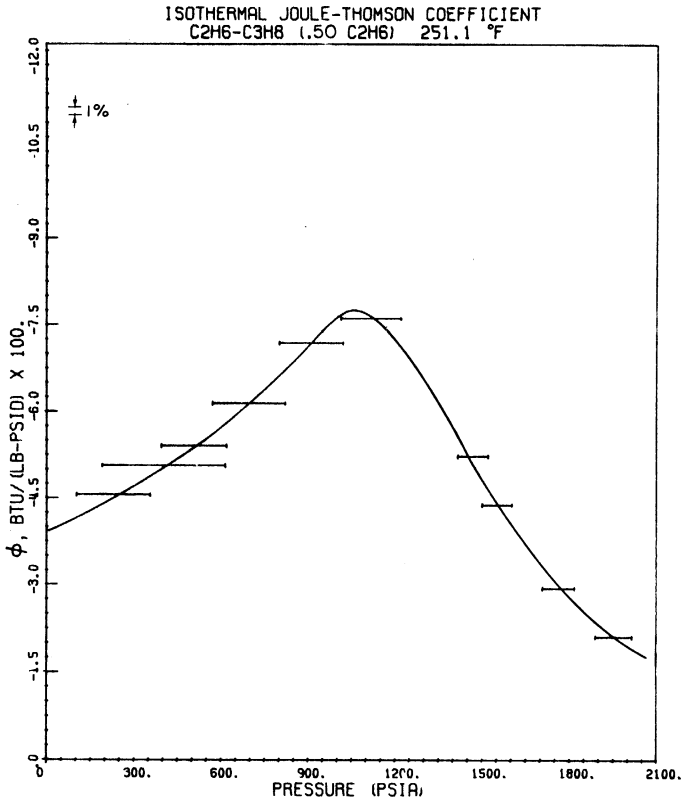

Figure VIII-32. Isothermal Joule-Thomson Coefficient for the Nominal 0.50 Mole Fraction Ethane-Propane Mixture at 251.1°F.

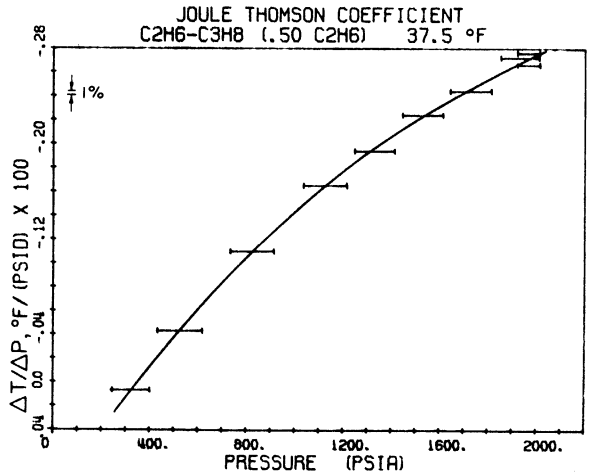

Figure VIII-33. Adiabatic Joule-Thomson Coefficient for the Nominal 0.50 Mole Fraction Ethane-Propane Mixture at 37.5°F.

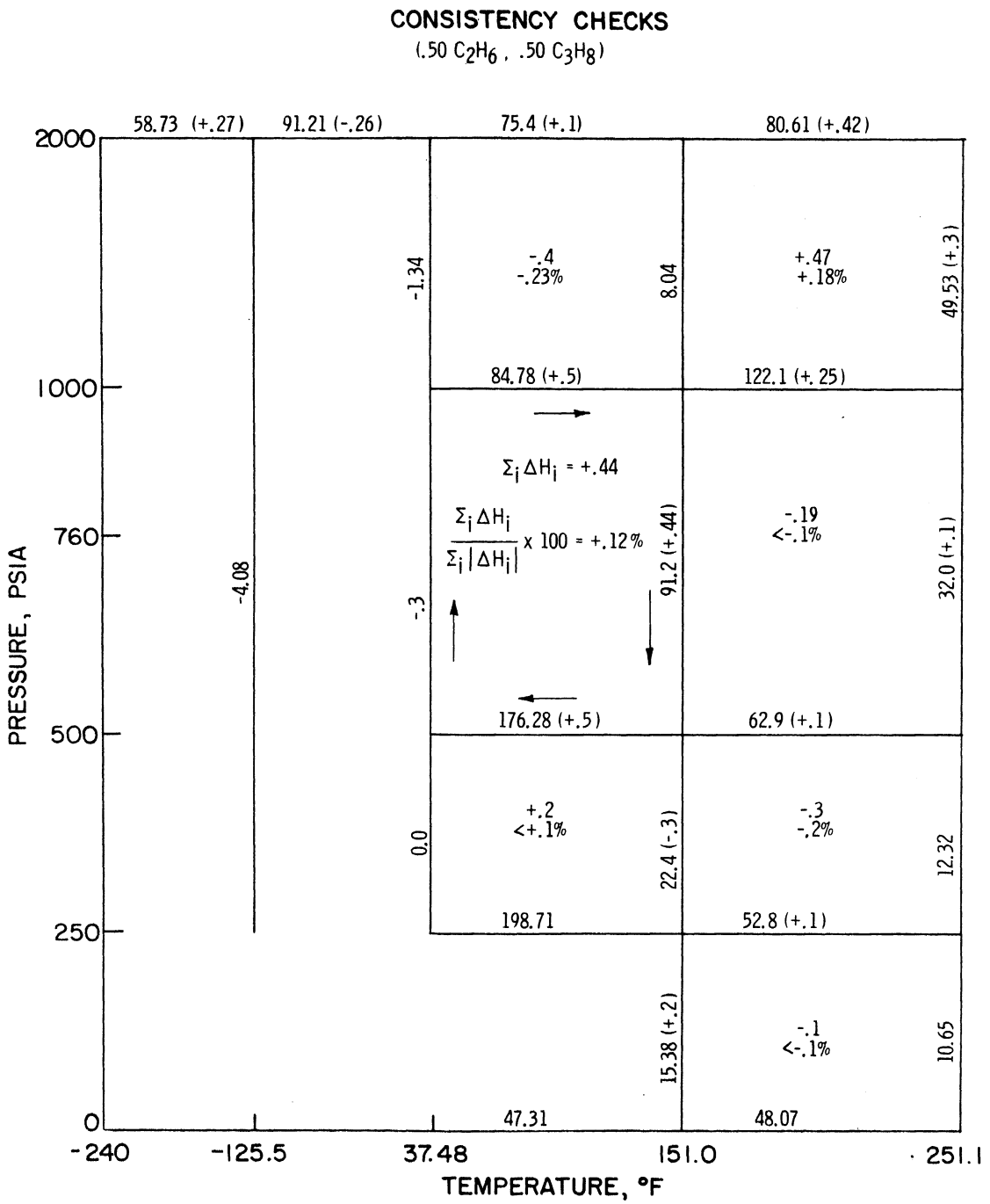

Figure VIII-34. Thermodynamic Consistency Checks for the Calorimetric Data on the Nominal 0.50 Mole Fraction Ethane-Propane Mixture.

TABLE VIII-13

++

Tabulated Values of Enthalpy and Heat Capacity for the Nominal 0.50 Mole Fraction Ethane-Propane Mixture

0 PSIA ***			250 PSIA			500 PSIA		
TEMP. °F	H BTU/LB	CP BTU/LB/°F	TEMP. °F	H BTU/LB	CP BTU/LB/°F	TEMP. °F	H BTU/LB	CP BTU/LB/°F
-280.	240.9	.248	37.48	173.4	.670	-125.5	80.14	
-260.	246.0	.256	40.	175.4	.675	30.	168.4	.657
-240.	251.5	.264	44.	177.8	.685	37.48	173.4	.666
-220.	256.8	.272	48.8	181.1	.699 *	40.	175.0	.669
-200.	262.4	.280	50.	184.4		50.	181.8	.683
-180.	268.0	.285	55.	202.9		60.	188.7	.700
-160.	273.8	.293	60.	226.4		70.	195.8	.722
-140.	279.7	.301	65.	250.2		80.	203.2	.750
-125.5	284.1	.306	70.	274.2		90.	210.8	.790
-120.	285.8	.309	75.	302.6		95.	214.9	.818
-100.	291.7	.317	79.8	333.6	.598 **	100.	219.0	.851
-80.	298.5	.326	80.	333.7	.596	105.	223.4	.895
-60.	305.1	.335	90.	339.5	.568	108.	226.1	.929
-40.	311.9	.344	100.	345.1	.550	110.	228.0	.957
-20.	318.9	.354	110.	350.6	.537	111.8	229.8	.980 *
0.	326.1	.365	120.	355.9	.530	115.	241.3	
20.	333.5	.375	140.	366.4	.520	120.	263.5	
37.48	340.1	.385	151.1	372.1	.518	125.	289.2	
40.	341.1	.386	160.	376.7	.517	130.	316.3	
60.	348.9	.397	180.	387.1	.520	134.	336.5	.844 **
80.	357.0	.408	200.	397.5	.524	135.	337.3	.836
100.	365.3	.419	220.	408.1	.532	140.	341.4	.786
120.	373.8	.431	240.	418.8	.542	145.	345.2	.747
140.	382.5	.443	251.1	424.9	.548	150.	348.9	.717
151.1	387.5	.449	260.	429.8	.555	151.1	349.7	.711
160.	391.5	.455				155.	352.5	.693
180.	400.7	.468				160.	355.9	.673
200.	410.2	.481				170.	362.4	.645
220.	419.9	.493				180.	368.8	.630
240.	429.9	.504				190.	375.2	.620
251.1	435.5	.511				200.	381.2	.616
260.	440.1	.515						
280.	450.5	.525						
300.	461.1	.536						

* SATURATED LIQUID

** SATURATED VAPOR

*** ZERO PRESSURE ENTHALPIES AND HEAT CAPACITIES CALCULATED FROM HEAT CONTENT FUNCTION AS TABULATED BY THE API [220]

++ REFERENCE ENTHALPY H=0 FOR EACH PURE COMPONENT AS A SATURATED LIQUID AT -280F

TABLE VIII-13

(CONTINUED)

760 PSIA

TEMP. °F	H BTU/LB	CP BTU/LB/°F
100.	212.5	.782
110.	220.5	.814
120.	228.9	.873
130.	238.2	.995
140.	249.1	1.218
150.	262.9	1.556
151.1	264.5	1.596
155.	271.4	1.867
160.	281.7	2.289
165.	294.3	2.741
170.	308.4	2.849
175.	322.3	2.620
180.	334.6	2.300
190.	354.9	1.810
200.	371.2	1.480
210.	384.8	1.360

1000 PSIA

TEMP. °F	H BTU/LB	CP BTU/LB/°F
37.48	173.7	.639
40.	175.3	.642
60.	188.3	.649
80.	201.8	.662
100.	216.2	.695
120.	231.4	.737
140.	248.2	.793
151.1	258.5	.893
160.	267.7	.980
165.	273.3	1.164
170.	279.4	1.267
175.	286.1	1.402
177.5	289.7	1.480
180.	293.5	1.537
183.	298.2	1.590
186.	303.0	1.610
190.	309.4	1.620
195.	317.5	1.600
198.	322.3	1.566
200.	325.4	1.530
205.	332.8	1.422
210.	339.6	1.325
220.	352.0	1.147
230.	362.7	.993
251.1	380.6	.731

2000 PSIA

TEMP. °F	H BTU/LB	CP BTU/LB/°F
-280.	5.3	.492
-260.	15.2	.495
-240.	25.1	.499
-220.	35.1	.503
-200.	45.3	.507
-180.	55.5	.511
-160.	65.9	.515
-140.	76.3	.520
-125.5	83.9	.523
-120.	86.7	.525
-100.	97.3	.531
-80.	108.0	.538
-60.	118.9	.548
-40.	129.9	.558
-20.	141.2	.569
0.	152.6	.581
20.	164.4	.596
37.48	175.0	.609
40.	176.6	.611
60.	188.9	.628
80.	201.7	.647
100.	214.8	.668
120.	228.4	.690
140.	242.5	.716
151.1	250.4	.731
160.	257.0	.744
180.	272.2	.774
200.	287.9	.804
220.	304.2	.835
240.	321.2	.866
251.1	331.0	.884
260.	338.9	.897
280.	357.0	.909
300.	375.0	.883

TABLE VIII-14

Tabulated Values of the Enthalpy[++] and the Isothermal Throttling Coefficient for the Nominal 0.50 Mole Fraction Ethane-Propane Mixture

	TEMPERATURE (°F)							
	-125.5°F		37.48°F		151.1°F		251.1°F	
P PSIA	H BTU/LB	$(DH/DP)_T$ X100 BTU/LB/PSID	H BTU/LB	$(DH/DP)_T$ X100 BTU/LB/PSID	H BTU/LB	$-(DH/DP)_T$ X100 BTU/LB/PSID	H BTU/LB	$-(DH/DP)_T$ X100 BTU/LB/PSID
0.**	284.13	-18.94	340.14	-7.88	387.5	5.18	435.5	4.02
100.	79.20	.228	.	-.050	381.9	5.86	431.3	4.24
200.	79.44	.230	173.37	-.027	375.6	6.68	426.9	4.42
250.	79.52	.231	173.36	-.017	372.1	7.20	424.9	4.60
300.	79.67	.232	173.35	-.008	368.4	7.81	422.5	4.70
400.	79.91	.234	173.35	.009	359.8	9.40	417.7	5.00
500.	80.14	.236	173.37	.025	349.7	11.42	412.6	5.34
600.	80.37	.237	173.40	.040	336.8	13.90	407.0	5.70
700.	80.62	.239	173.44	.055	270.8	*	401.1	6.13
750.	80.74	.240	173.47	.061	264.7	7.20	398.0	6.38
800.	80.86	.241	173.51	.068	262.8	3.00	394.8	6.62
900.	81.10	.242	173.58	.080	260.0	2.24	387.9	7.13
1000.	81.35	.244	173.67	.092	258.5	1.72	380.6	7.53
1100.	81.60	.246	173.76	.103	256.7	1.49	372.9	7.66
1200.	81.84	.247	173.88	.112	255.4	1.17	365.3	7.42
1250.	81.96	.247	173.93	.117	254.8	1.05	361.7	7.11
1300.	82.09	.248	173.99	.121	254.3	.951	358.2	6.73
1400.	82.34	.250	174.11	.128	253.4	.787	351.9	5.86
1500.	82.60	.251	174.25	.135	252.7	.660	346.6	4.83
1600.	82.85	.253	174.39	.142	252.1	.560	342.2	3.93
1700.	83.10	.254	174.54	.148	251.6	.480	338.6	3.26
1750.	83.22	.254	174.62	.151	251.3	.450	337.0	2.98
1800.	83.35	.255	174.69	.154	251.1	.417	335.6	2.73
1900.	83.60	.256	174.84	.160	250.7	.363	333.1	2.28
2000.	83.80	.258	175.01	.165	250.4	.304	331.0	1.94

* DATA LIES WITHIN THE TWO PHASE REGION

** THE VALUE OF $(DH/DP)_T$ AT ZERO PRESSURE IS OBTAINED FROM EQUATIONS (V-30) AND (V-31) IN CONJUNCTION WITH THE PSEUDO-PARAMETERS (I) FOR THE GIVEN MIXTURE IN TABLE IX-14

++ REFERENCE ENTHALPY H=0 FOR EACH PURE COMPONENT AS A SATURATED LIQUID AT -28°F

c) Nominal 0.27 Mole Fraction Ethane-Propane Mixture. The range of measurement conditions for this mixture is indicated in Figure VIII-35. The high pressure isobar examined for this system was reduced to 1000 psia so that the region around and beyond the maximum in Cp could be experimentally characterized within the 300°F operating limit. The lower pressure also served to decrease the cooling effect and attendant composition upsets involved in throttling the fluid from the calorimeter outlet to the compressor inlet conditions. An isobaric enthalpy traverse was made across the two phase region at 500 psia. Isothermal data were obtained at 127.4°F, and 269°F, and 269°F. Adiabatic throttling measurements were made at -150.2°F, 1.6°F, and in the high pressure region at 127.4°F. Additional isobaric measurements were obtained over a limited range at 2000 psia to provide the necessary consistency checks for the high temperature data. The basic isobaric, isothermal and isenthalpic measurements are summarized in Tables B-10, B-11, and B-12, respectively.

The variation in composition with run number is illustrated in Figure VIII-36. The mole fraction of ethane decreased by over 1% during the course of the first five runs, and is attributed to the cumulative fractionation effects occuring at mass leaks from high pressure sources into the atmosphere. The isobaric run at 1000 psia is illustrated in Figure VIII-37. The enthalpy traverse at 500 psia is illustrated in Figure VIII-38, and the liquid phase heat capacities as obtained from this run are shown in Figure VIII-39. The isothermal data at 269°F are shown in Figure VIII-40 while the isenthalpic throttling measurements at 1.6°F are demonstrated in Figure VIII-41.

Difficulties in sustaining the high temperature required to maintain the mixture in the gas phase outside of the calorimeter section, contributed substantially to the premature termination of the investigation. The consistency checks for the three enthalpy loops are summarized in Figure VIII-42. The absolute average deviation is 1.96 Btu/lb or 0.72%. The maximum deviation is 3.25 Btu/lb and occurs in the loop from 500 to 1000 psia and from 127.4°F to 203.1°F. These rather large inconsistencies were traced to the occurence of a leak at the differential pressure transducer that was used to measure the pressure drop for the throttling measurements. The adjustment of the

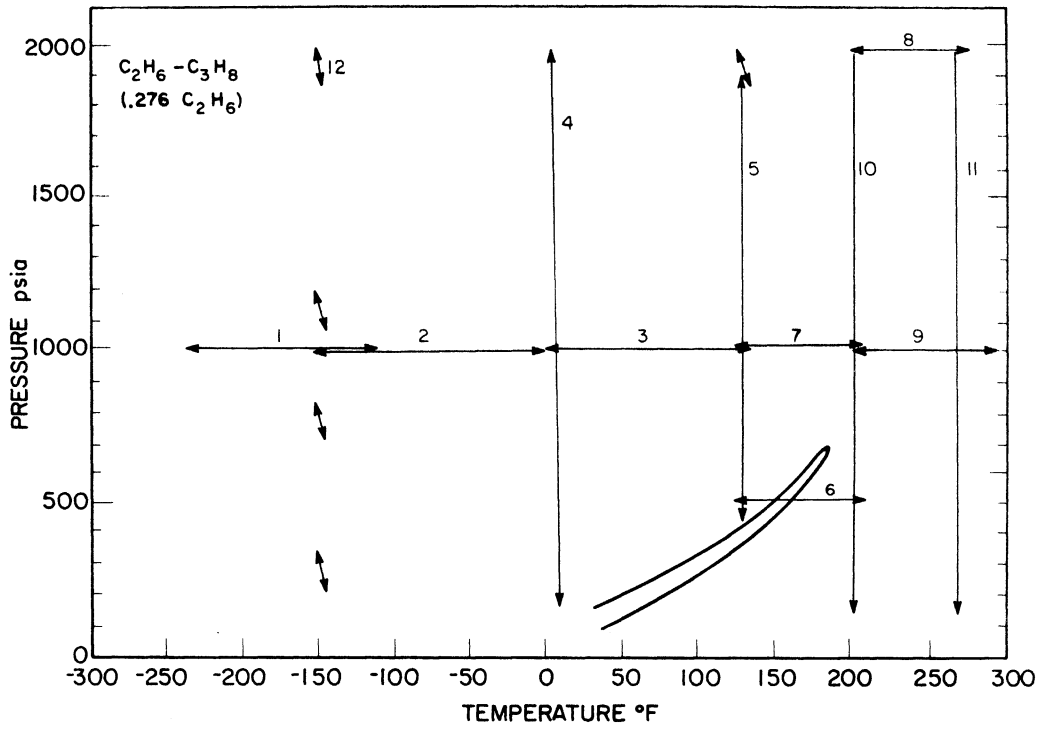

Figure VIII-35. Range of Calorimetric Measurements Obtained in this Work for the Nominal 0.27 Mole Fraction Ethane-Propane Mixture.

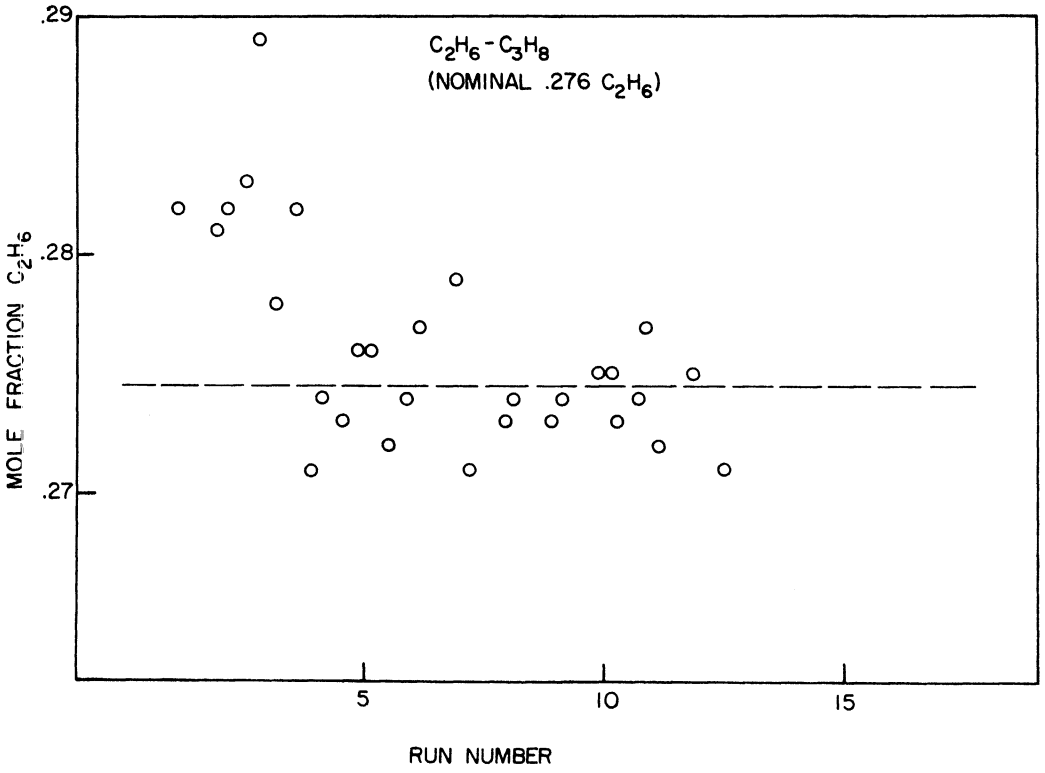

Figure VIII-36. Variation of Composition for the Nominal 0.27 Mole Fraction Ethane-Propane Mixture.

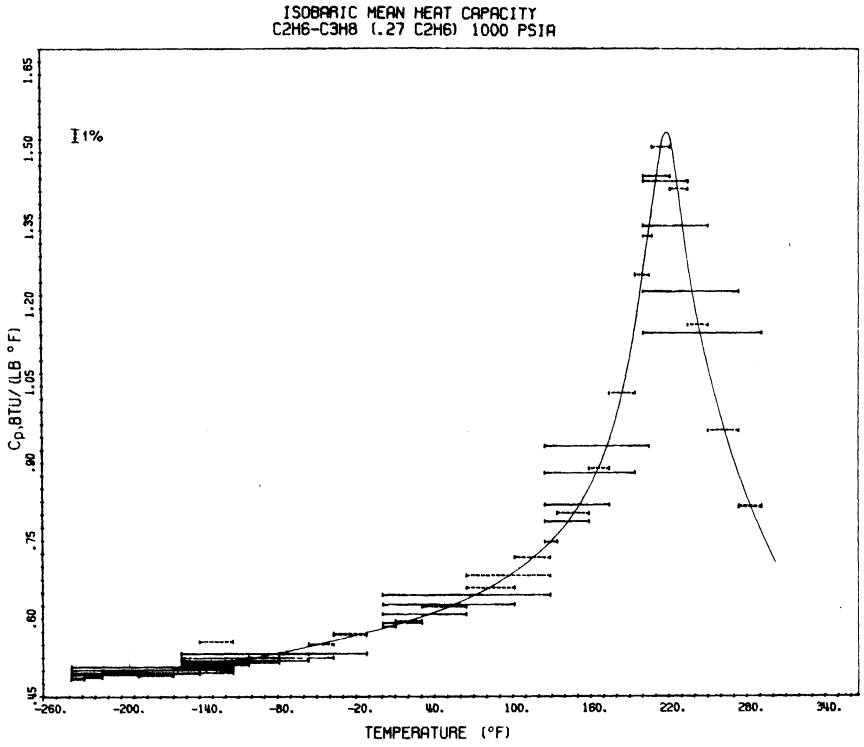

Figure VIII-37. Isobaric Heat Capacity for the Nominal 0.27 Mole Fraction Ethane-Propane Mixture.

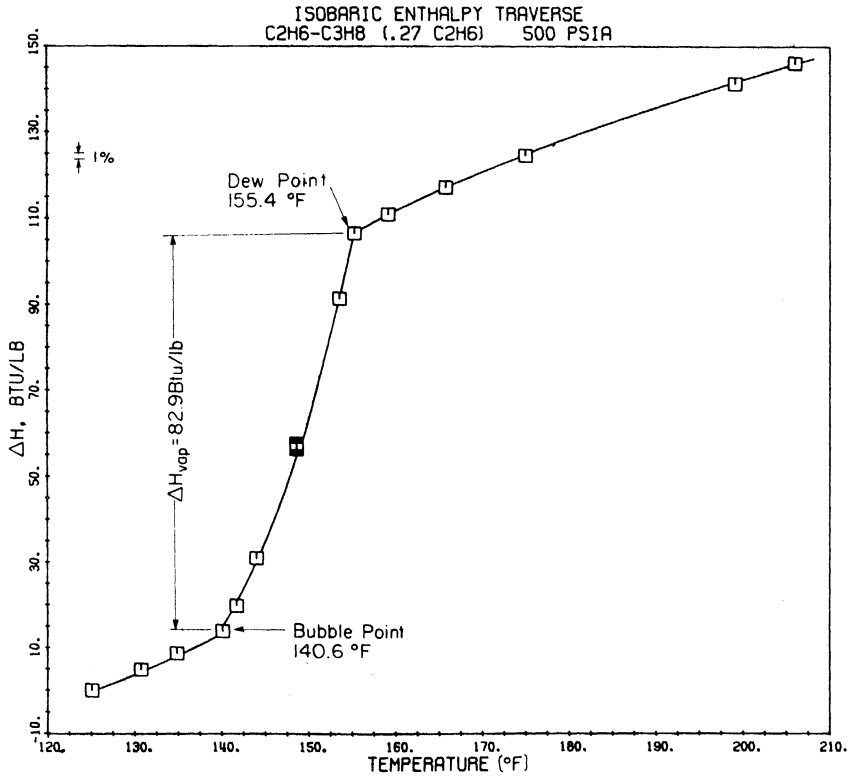

Figure VIII-38. Isobaric Enthalpy Traverse for the Nominal 0.27 Mole Fraction Ethane-Propane Mixture at 500 psia.

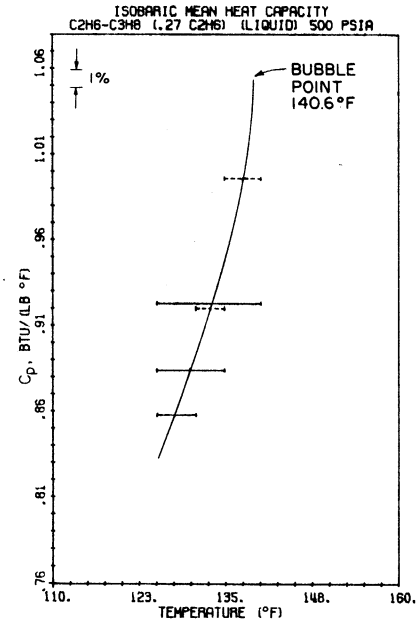

Figure VIII-39. Isobaric Liquid Phase Heat Capacity for the Nominal 0.27 Mole Fraction Ethane-Propane Mixture upto the Saturation Boundary at 500 Psia.

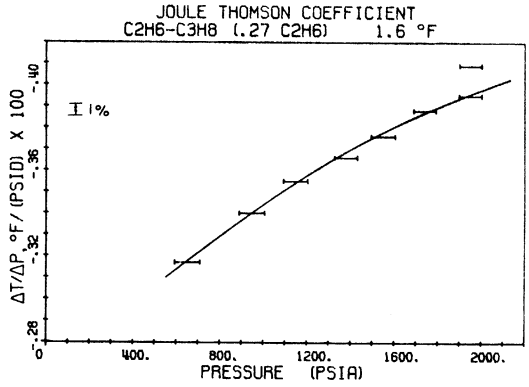

Figure VIII-41. Adiabatic Joule-Thomson Coefficient for the Nominal 0.27 Mole Fraction Ethane-Propane Mixture at 1.6°F.

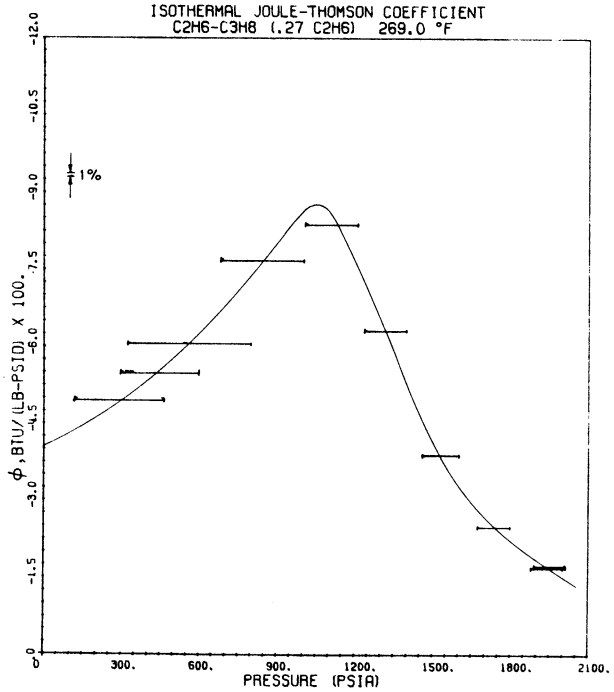

Figure VIII-40. Isothermal Joule-Thomson Coefficient for the Nominal 0.27 Mole Fraction Ethane-Propane Mixture at 269°F.

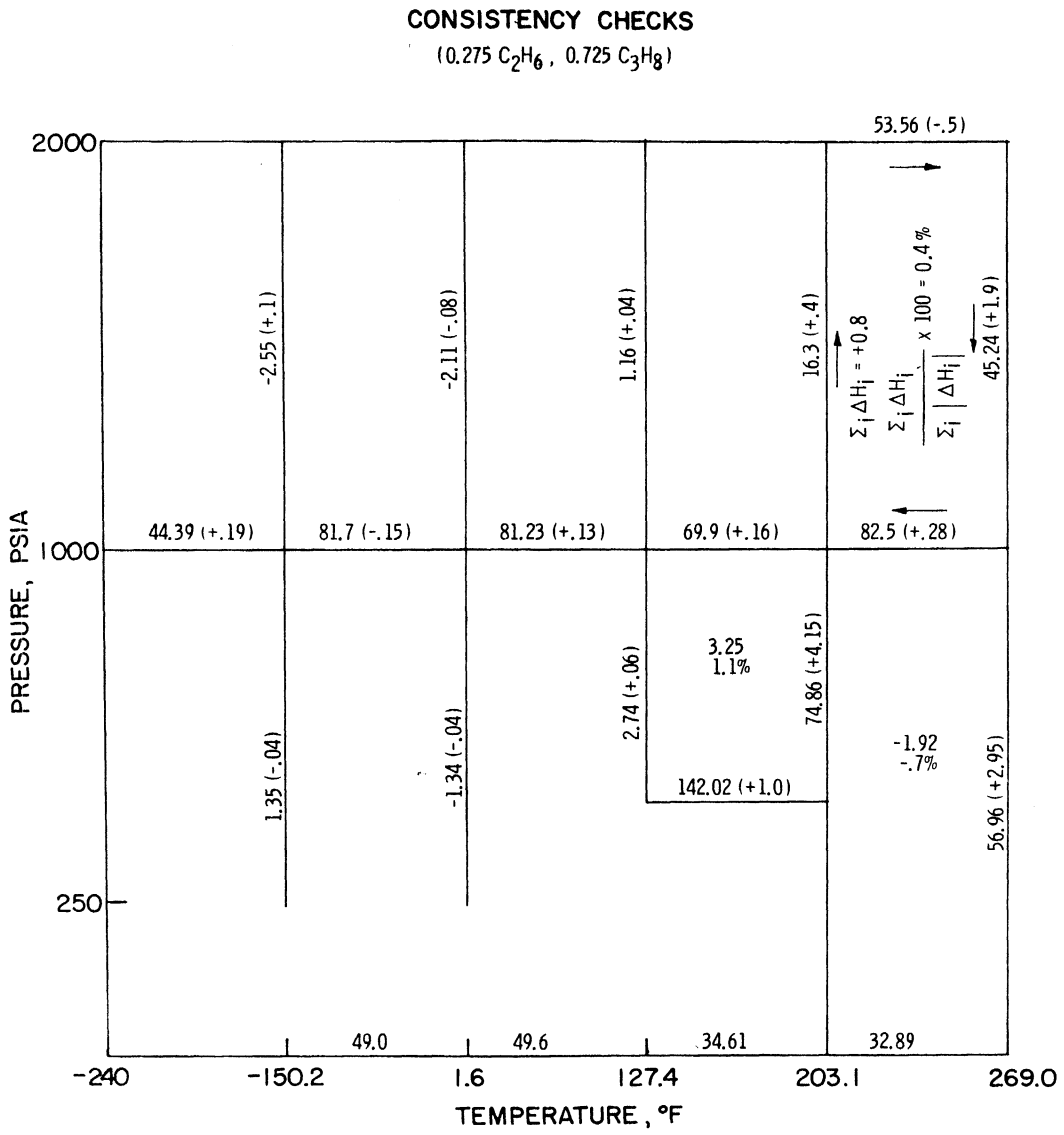

Figure VIII-42. Thermodynamic Consistency Checks for the Calorimetric Data on the Nominal 0.27 Mole Fraction Ethane-Propane Mixture.

isothermal measurements posed a problem that was attacked in the following fashion.

1) Cutler and Morrison [55] have calculated the heat of mixing for saturated liquid mixtures of methane and propane at -280°F from experimental data on the enthalpy of vaporization for both pure components and for several binary mixtures. The maximum value of the excess enthalpy was calculated as 52 Btu/lb mole of mixture.

2) As the size and energy parameter ratios for the pure components of the ethane-propane system are closer to unity than the corresponding ratios for the methane-propane system, it is reasonable to expect that the heat of mixing at -280°F is lower in the former case.

3) For this particular mixture, the lowest temperature of investigation was -240°F. The assumption of ideal mixing for ethane and propane at -280°F and 1000 psia establishes the enthalpy of the mixture as 21.82 Btu/lb at -240°F and 1000 psia, if the ethane enthalpy table of this work and the propane enthalpy table of Yesavage [284] are used in the calculation. A reasonable, but arbitrarily chosen heat of mixing of 11 Btu/lb mole of mixture, assumed constant over the interval from -280°F to -240°F, assigned an enthalpy value of 22.1 Btu/lb to the mixture at -240°F and 1000 psia.

4) The results for the 1000 psia isobar were integrated without adjustments from -240°F upto 203.1°F and 269.0°F, respectively, to fix the enthalpy value at 1000 psia for each experimentally obtained isotherm in the gas phase.

5) The enthalpy values for a given mixture at zero pressure are independently established from the constituent pure component enthalpies at any given temperature using Equation (VII-14). If this is done, then the enthalpy departure at 1000 psia can be independently calculated for each of the two experimental isotherms in the gas phase. These values were about 5% lower in magnitude than that obtained from the analysis of the basic data.

6) Based on the assumption that the isobaric data were relatively free from error, the isothermal enthalpy departures obtained from the basic data at 203.1°F and 269°F were adjusted downwards to conform to the values calculated in Step 5. The PGC enthalpy calculations, using a set of pseudocritical parameters obtained from the

optimization of the basic isobaric data alone, as explained in the next chapter, were also instrumental in providing reasonable adjustments to the isothermal data particularly in the range from 1000 psia to 2000 psia.

7) The isenthalpic results were not affected by the mass leakage proper, as the flowrate itself is not involved in the measurements. They are, however, susceptible to errors in the measurement of differential pressure itself, as a consequence of the leak. Such errors, though lower in magnitude than the effect of mass leakage, cannot be precisely evaluated and were arbitrarily set at 2%. Such a correction has a very minor effect on the enthalpies in the liquid phase and, in fact, decreases the enthalpy change from 2000 psia down to the saturated liquid by only 0.1 Btu/lb.

Smoothed values of $\underline{H}$ and Cp for the isobaric conditions are listed in Table VIII-15, while the smoothed $\underline{H}$ and ϕ values obtained from the isothermal and isenthalpic throttling data are presented in Table VIII-16.

d) Generation of Enthalpy Tables in the Single Phase Region upto Saturation.

The construction of comprehensive enthalpy tables extending from -280°F to 300°F and upto 2000 psia for each of the ethane-propane mixtures from the interpretation of the limited data obtained from these systems was one of the major goals of this work. The skeleton enthalpy values obtained from the smoothing of the basic data for each system were used to determine a set of pseudo-critical parameters that would, in each case, produce the best fit in the PGC enthalpy departure framework. The detailed enthalpy networks in Tables K-4 through K-6 were then generated using the optimum pseudo-parameters for each mixture. These tabulations are only applicable in the single phase region, and are consistent with the skeleton tables for the individual mixtures to within 2 Btu/lb. The procedure for determining the optimum parameters from the smoothed enthalpy data is discussed in some depth in Chapter IX.

Although the enthalpy correlation technique specifically utilized in this work is restricted to the single phase region, the enthalpy

TABLE VIII-15

++

Tabulated Values of the Enthalpy and the Heat Capacity for the
Nominal 0.27 Mole Fraction Ethane-Propane Mixture

0 PSIA ***			500 PSIA			1000 PSIA			2000 PSIA		
TEMP. °F	H BTU/LB	CP BTU/LB/°F	TEMP. °F	H BTU/LB	CP BTU/LB/°F	TEMP. °F	H BTU/LB	CP BTU/LB/°F	TEMP. °F	H BTU/LB	CP BTU/LB/°F
-280.	238.6	.235	-150.2	65.5		-280.	2.9	.477	200.	280.6	.770
-260.	243.4	.244	1.6	147.3		-260.	12.5	.480	203.1	283.0	.774
-240.	248.3	.253	120.	226.2	.783	-240.	22.1	.484	220.	298.7	.791
-220.	253.5	.262	125.	230.2	.828	-220.	31.8	.488	240.	314.8	.815
-200.	258.8	.271	127.5	232.2	.852	-200.	41.7	.493	260.	331.4	.839
-180.	264.3	.276	130.	234.5	.880	-180.	51.6	.498	269.	336.6	.853
-160.	269.9	.284	132.5	236.7	.913	-160.	61.6	.503	280.	348.4	.866
-150.2	272.7	.288	135.	239.1	.950	-150.2	66.5	.505	300.	366.0	.888
-140.	275.7	.293	137.5	241.5	1.002	-140.	71.7	.507			
-120.	281.6	.301	140.6	244.7	1.050 *	-120.	81.9	.514			
-100.	287.7	.310	145.	266.4		-100.	92.3	.521			
-80.	294.0	.319	150.	295.6		-80.	102.8	.531			
-60.	300.5	.329	155.	335.1		-60.	113.6	.543			
-40.	307.1	.338	155.4	337.6	1.030 **	-40.	124.6	.555			
-20.	314.0	.348	157.5	339.9	.985	-20.	135.8	.566			
0.	321.1	.359	160.	342.2	.933	0.	147.3	.582			
1.6	321.7	.360	162.5	344.5	.873	1.6	148.2	.583			
20.	328.4	.370	165.	346.6	.853	20.	159.0	.595			
40.	335.9	.381	170.	350.8	.799	40.	171.2	.613			
60.	343.6	.392	180.	358.4	.731	60.	183.6	.633			
80.	351.6	.404	190.	365.4	.689	80.	196.5	.655			
100.	359.8	.416	200.	372.2	.662	100.	209.9	.685			
120.	368.2	.427	203.1	374.2	.655	120.	224.0	.724			
127.4	371.3	.432	210.	378.7	.642	127.4	229.4	.738			
140.	376.9	.440				140.	239.0	.775			
160.	385.8	.452				160.	255.2	.850			
180.	395.0	.465				170.	263.2	.905			
200.	404.4	.477				180.	273.7	.980			
203.1	405.9	.479				190.	285.3	1.085			
220.	414.1	.489				200.	295.1	1.255			
240.	424.0	.501				203.1	299.3	1.330			
260.	434.1	.513				210.	308.9	1.450			
269.	438.8	.517				212.	311.8	1.485			
280.	444.5	.524				214.	314.8	1.519			
300.	455.1	.535				216.	317.9	1.529			
						220.	324.0	1.536			
						223.	328.6	1.537 +			
						225.	331.7	1.533			
						230.	338.9	1.465			
						240.	351.7	1.206			
						250.	363.1	1.074			
						260.	373.3	.977			
						269.	381.8	.905			
						280.	391.3	.835			
						300.	407.0	.728			

* SATURATED LIQUID

** SATURATED VAPOR

*** ZERO PRESSURE ENTHALPIES AND HEAT CAPACITIES CALCULATED FROM HEAT CONTENT FUNCTION AS TABULATED BY THE API [220]

\+ THE HEAT CAPACITY MAXIMUM ALONG THE GIVEN ISOBAR

++ REFERENCE ENTHALPY H=0 FOR EACH PURE COMPONENT AS A SATURATED LIQUID AT -280F

TABLE VIII-16

Tabulated Values of the Enthalpy[++] and the Isothermal Throttling Coefficient for the Nominal 0.27 Mole Fraction Ethane-Propane Mixture

TEMPERATURE (°F)

	-150.2°F		1.6°F		127.4°F		203.1°F		269.0°F		203.1°F		
P PSIA	H BTU/LB	$(DH/DP)_T$ X100 BTU/LB/PSID	H BTU/LB	$(DH/DP)_T$ X100 BTU/LB/PSID	H BTU/LB	$(DH/DP)_T$ X100 BTU/LB/PSID	H BTU/LB	$-(DH/DP)_T$ X100 BTU/LB/PSID	H BTU/LB	$-(DH/DP)_T$ X100 BTU/LB/PSID	P PSIA	H BTU/LB	$-(DH/DP)_T$ X100 BTU/LB/PSID
0.*	272.7	-26.0	321.7	-10.26	371.4	-6.2	405.91	4.96	438.84	4.00	760.	339.15	22.98
100.	65.04	.126	146.64	.150	364.8	-7.1	400.74	5.35	434.70	4.08	775.	335.50	24.89
200.	65.10	.145	146.79	.157	357.0	-8.5	395.21	5.78	430.33	4.22	795.	330.26	28.06
250.	65.16	.152	146.87	.160	352.5	-9.7	392.20	6.07	428.06	4.46	810.	321.11	28.73
300.	65.23	.160	146.96	.164	347.2	-11.4	389.10	6.40	425.70	4.59	832.	317.52	28.23
400.	65.38	.174	147.12	.170	233.10	1.195	382.30	7.33	420.75	4.74	840.	315.13	25.77
500.	65.54	.186	147.29	.176	232.18	.915	374.20	8.32	415.50	5.05	850.	313.15	21.97
600.	65.72	.197	147.46	.181	231.37	.713	364.30	8.81	409.94	5.42	860.	306.89	17.62
700.	65.91	.207	147.65	.183	230.72	.570	350.80	13.40	403.80	5.85			
750.	66.00	.211	147.73	.186	230.45	.513	341.35	19.34	400.48	6.42			
800.	66.10	.216	147.82	.190	230.21	.466	328.84	28.06	397.11	6.81			
900.	66.30	.224	148.10	.195	229.79	.386	307.40	11.46	389.74	7.06			
1000.	66.51	.232	148.21	.198	229.44	.319	299.34	8.15	381.84	7.70			
1100.	66.73	.239	148.40	.202	229.14	.260	294.65	6.22	373.57	8.19			
1200.	66.96	.245	148.60	.206	228.90	.212	291.83	3.51	365.73	8.10			
1250.	67.09	.247	148.70	.208	228.8	.187	290.75	2.34	362.10	7.50			
1300.	67.19	.251	148.80	.210	228.71	.169	289.80	2.03	358.82	6.93			
1400.	67.43	.257	149.00	.212	228.56	.129	288.22	1.78	353.26	6.21			
1500.	67.67	.262	149.21	.215	228.44	.096	286.95	1.42	348.82	4.97			
1600.	67.90	.269	149.42	.219	228.36	.070	285.88	1.15	345.28	3.95			
1700.	68.16	.272	149.64	.221	228.30	.046	285.00	.956	342.42	3.15			
1750.	68.29	.274	149.74	.222	228.28	.035	284.60	.805	341.27	2.54			
1800.	68.43	.276	149.85	.223	228.26	.025	284.22	.747	340.13	2.30			
1900.	68.69	.281	150.06	.225	228.27	.005	283.63	.683	338.25	2.10			
2000.	68.96	.284	150.32	.228	228.28	-.015	283.04	.585	336.60	1.76			

* THE VALUE OF $(DH/DP)_T$ AT ZERO PRESSURE IS OBTAINED FROM EQUATIONS (V-30) AND (V-31) IN CONJUNCTION WITH THE PSEUDO-PARAMETERS (I) FOR THE GIVEN MIXTURE IN TABLE IX-15

++ REFERENCE ENTHALPY H=0 FOR EACH PURE COMPONENT AS A SATURATED LIQUID AT -28°F

values at the two phase boundary may be determined if the dew and bubble points are also known. The saturated liquid and vapor enthalpies for each of the mixtures were calculated in the following manner. First, the dew and bubble point conditions at a series of selected isobars and isotherms were calculated from the phase equilibria data of Djordjevich [63] below 0°F, of Price and Kobayashi [207] from 0°F to 50°F, and of Matschke and Thodos [169] from 100°F to 200°F. The PGC enthalpies at these conditions, using the optimum pseudo-parameters in each case, served to define the enthalpy values for the saturated phase. Below 300 psia the enthalpy values for the vapor phase were obtained from the reduced virial equation defined by the combination of (III-44) and (V-30).

The calculated enthalpies at saturation are presented in Tables VIII-17 through VIII-19. The experimental dew and bubble point determinations of this investigation and their corresponding enthalpy values are also included for comparison purposes. The results indicate that the two phase region as determined in this work is generally wider than predicted from the results of Matschke and Thodos [169].

Measurements on the Methane-Ethane System

Enthalpy data on two methane-ethane mixtures containing 0.78 and 0.48 mole fraction methane, respectively, were obtained at the existing facility subsequent to the completion of the ethane-propane system as part of a continuing effort to characterize the enthalpy behaviour of light hydrocarbon mixtures. It was originally intended to use the enthalpy compilations in the literature to generate the appropriate interaction parameters for the system in the PGC framework with the specific objective of using such information to improve the enthalpy predictions for the ternary mixture. However, as explained in Chapter II, it was felt that neither the quality nor the range of the experimental or correlated enthalpy values in the literature could compete with the results normally obtained at this facility. The modified objective, then, was to carry the interpretation of the raw data for the mixtures investigated in this facility only as far as was necessary to specify the methane-ethane binary interaction parameters. Accordingly, the processing of the measurements was preliminarily

TABLE VIII-17

Saturated Liquid and Vapor Enthalpies for the Nominal 0.76 Mole Fraction Ethane-Propane Mixture+

TEMP. (°F)	PRESSURE (PSIA)	LIQUID ENTHALPY (BTU/LB)	TEMP. (°F)	PRESSURE (PSIA)	VAPOR ENTHALPY (BTU/LB)	
-100.	24.	96.8	-100.	9.	297.1	ISOTHERMAL
- 50.	70.	125.8	-50.	33.	311.6	
0.	162.	159.9	0.	106.	323.1	
50.	340.	194.4	50.	242.	331.7	
102.4	600	240.2	102.4	510.	331.6	
120.	715.	267.3	120.	633.	325.3	
26.5	250.	277.7	52.0	250.	331.8	ISOBARIC
24.2 *	250.	175.8	52.2 *	250.	331.9	
24.2 **	250.	174.5	52. **	250.	332.0	
85.0	500.	223.4	101.	500.	331.5	
82.2 *	500.	220.6	100.4 *	500.	331.0	
82.2 **	500.	221.0	100.4 **	500.	330.7	
119.	716.	262.5	127.	716.	314.9	
117.5 *	716.	258.4	128.5 *	716.	316.9	
117.5 **	716.	260.4	128.5 **	716.	315.5	
127.3	755.	285.5	127.3	755.	285.5	

TABLE VIII-18

Saturated Liquid and Vapor Enthalpies for the Nominal 0.50 Mole Fraction Ethane-Propane Mixture+

TEMP. (°F)	PRESSURE (PSIA)	LIQUID ENTHALPY (BTU/LB)	TEMP. (°F)	PRESSURE (PSIA)	VAPOR ENTHALPY (BTU/LB)	
-100.	17.	92.7	-100.	5.8	291.1	ISOTHERMAL
-50.	47.	119.6	-50.	17.	305.7	
0.	114.	150.6	0.	66.	319.0	
50.	246.	182.9	50.	160.	330.0	
100.	427.	219.8	100.	320.	337.2	
120.	525.	236.4	120.	415.	338.7	
151.1	700.	270.2	151.1	595.	333.4	
161.	737.	290.7	161.	737.	290.7	
51.	250.	183.5	78.	250.	333.4	ISOBARIC
48.8 *	250.	182.1	79.8 *	250.	334.4	
48.8 **	250.	181.1	79.8 **	250.	333.6	
115.	500.	232.1	133.	500.	335.2	
111.8 *	500.	229.0	134. *	500.	336.1	
111.8 **	500.	229.8	134. **	500.	336.5	

TABLE VIII-19

Saturated Liquid and Vapor Enthalpies for the Nominal 0.27 Mole Fraction Ethane-Propane Mixture+

TEMP. (°F)	PRESSURE (PSIA)	LIQUID ENTHALPY (BTU/LB)	TEMP. (°F)	PRESSURE (PSIA)	VAPOR ENTHALPY (BTU/LB)	
-100.	11.	91.1	-100.	4.	287.0	ISOTHERMAL
-50.	30.	116.8	-50.	14.	301.8	
0.	82.	145.4	0.	48.	315.7	
50.	176.	178.9	50.	125.	327.4	
100.	318.	213.2	100.	240.	338.4	
120.	390.	229.1	120.	319.	339.9	
140.	485.	245.6	140.	407.	342.2	
160.	585.	265.5	160.	515.	340.0	
180.	680.	312.7	180.	639.	333.4	
184.3	697.	321.7	184.3	697.	321.7	
143.	500.	248.2	158.5	500.	341.5	ISOBARIC
140.6 *	500.	245.7	155.4 *	500.	338.5	
140.6 **	500.	244.7	155.4 **	500.	337.6	

+ Unless otherwise indicated, phase equilibria are calculated from the date in the literature (see Text). The enthalpy values are generated by the PGC using the optimum pseudo-critical parameters in each case, except for the gas phase below 300 psia, where the combination of Equations (V-30) and (III-44) is used to generate enthalpies instead.

* Saturation temperatures obtained from this work, enthalpy values obtained as above.

** Saturation conditions and enthalpies obtained from the measurements of this work.

terminated at the basic data stage.

The regions of measurement for the 0.78 mole fraction methane-ethane mixture are indicated in Figure VIII-43. Extended data were obtained from -240°F to +300°F along an isobar at 1000 psia. Additional isobaric data were concentrated in the peak region. Enthalpy traverses across the two phase region were made at 250 and 500 psia. Isothermal data were obtained at 79.1°F, and at 255°F. Adiabatic Joule-Thomson measurements were taken at -58.4°F, -150.5°F and at -253.2°F, respectively. A detailed composition analysis is indicated in Table VI-3. The flowmeter calibration data, summarized earlier in Table VI-1, are plotted in Figure VIII-44. The basic isobaric, isothermal, and isenthalpic measurements are summarized in Tables B-13, B-14, and B-15, respectively.

The range of data obtained for the 0.48 mole fraction methane-ethane mixture is summarized in Figure VIII-45. Isobaric data extending from -230°F to just over 300°F were obtained at 1500 psia. Additional isobaric measurements were taken in the vicinity of the heat capacity maxima at 975, 1250, 1500 and 2000 psia. Isobaric determinations were also made across the two phase region at 250, 500 and 750 psia. Isothermal measurements were obtained at 1.8°F, 101.4°F and 252.4°F, respectively. Adiabatic Joule-Thomson data were taken at -228.5°F and -99.1°F, respectively. The composition, including impurities, is indicated in Table VI-3. The flowmeter calibration data are shown in Figure VIII-46. The basic isobaric, isothermal, and isenthalpic measurements are summarized in Tables B-16, B-17 and B-18, respectively.

Although the data were not evaluated for self-consistency in this work, preliminary predictions with the PGC, using pseudo-parameters obtained from isobaric data alone, suggest that the isothermal data are about 5% too high. It is probable that the mass leakage at the differential pressure transducer, first observed during the examination of the 0.27 mole fraction ethane-propane mixture, also extended through the investigation of these systems. The smoothed thermal properties, including the consistency checks as obtained from the measurements of this work, have recently been reported by Kant, Furtado and Powers [121].

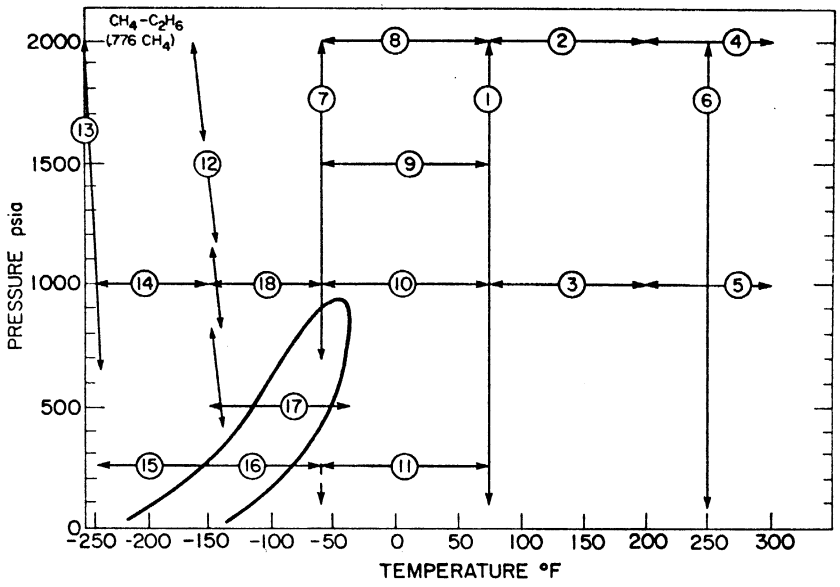

Figure VIII-43. Range of Calorimetric Measurements Obained in This Work for the Nominal 0.78 Mole Fraction Methane-Ethane Mixture.

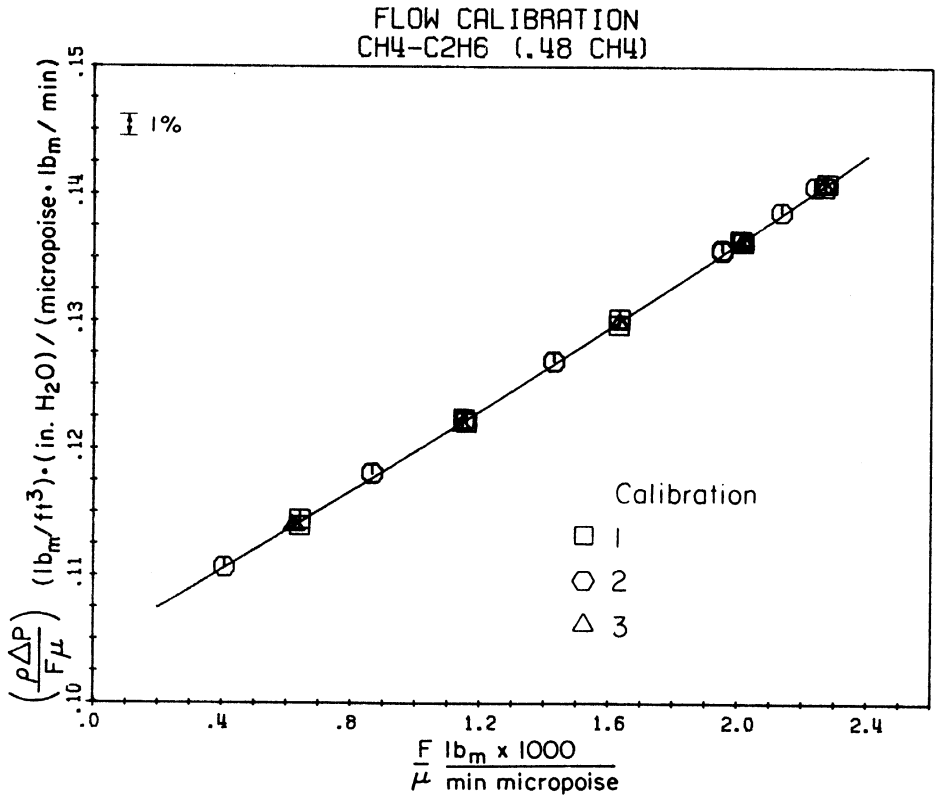

Figure VIII-44. Flowmeter Calibration Results for the Nominal 0.78 Mole Fraction Methane-Ethane Mixture.

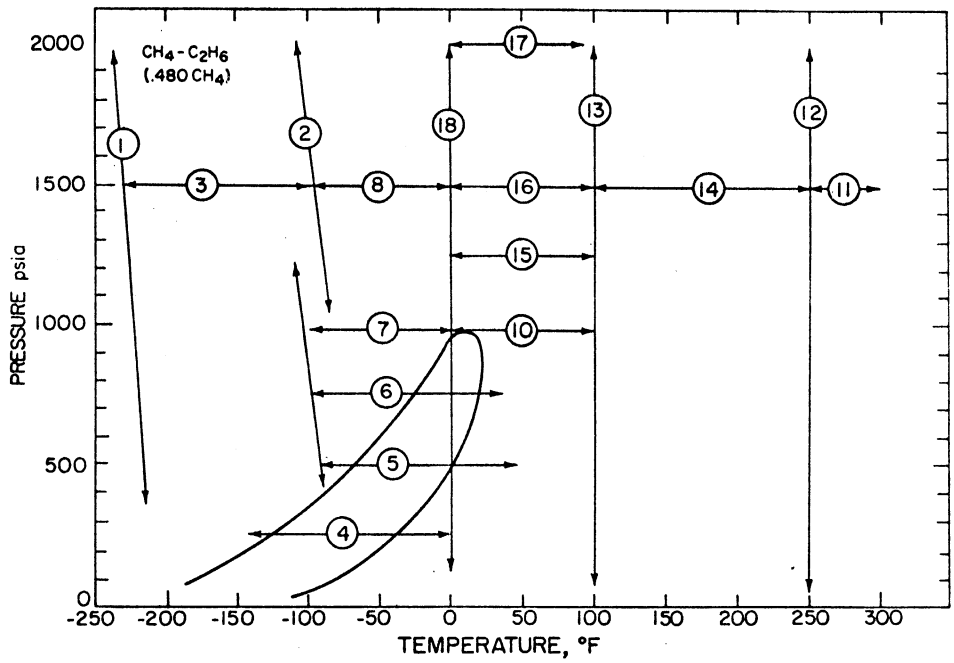

Figure VIII-45. Range of Calorimetric Measurements Obtained in This Work for the Nominal 0.48 Mole Fraction Methane-Ethane Mixture.

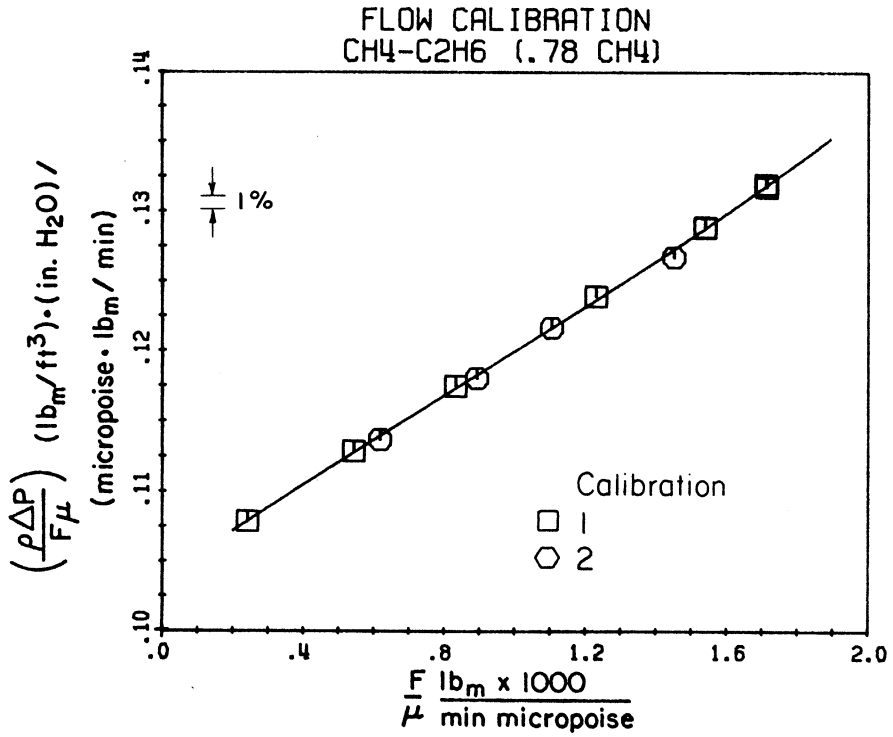

Figure VIII-46. Flowmeter Calibration Results for the Nominal 0.48 Mole Fraction Methane-Ethane Mixture.

Measurements on the Methane-Ethane-Propane System

The range of the experimental determinations is indicated on Figure VIII-47. The data extend from -236°F to 267°F, and cover the liquid, gaseous and two phase regions. Extensive isobaric measurements have been obtained in the single phase region. Enthalpy traverses were made across the two phase region at 250, 500, 750 and 1000 psia. Isothermal throttling measurements were taken in the liquid region at -16.04°F near the two phase envelope, at 52.04°F, 126.2°F and 192.0°F. Adiabatic throttling data were obtained in the high pressure region at -16.04°F and at -234°F.

The variation in composition as a function of hours of compressor operation is shown in Figure VIII-48. While the ethane analysis was fairly constant to within 0.5%, the methane and propane mole fractions varied over a span of 1.5%. The steady increase in the propane fraction can be attributed to the fractionation that often takes place when a mass leak to the atmosphere occurs from a high pressure point. These leaks were fortunately located in non-critical areas, and, apart from increasing the effort necessary to achieve quasi-steady state conditions, had little effect on the accuracy of the measurements themselves. The detailed analysis, including trace components, for the average mixture composition, whose nominal value is indicated by the solid lines in Figure VIII-48, is shown in Table VI-3. The flowmeter calibration results for the system are plotted in Figure VIII-49. All five calibrations were fit to a single curve to better than 0.08%. The basic isobaric, isothermal, and isenthalpic data are summarized in Tables B-16, B-17 and B-18, respectively.

The isobar at 2000 psia (Figure VIII-50) illustrates, typically, the variation in the heat capacity of a dense fluid mixture in going from -236°F to 267°F. The sharpest heat capacity maximum occurs closest to the two phase boundary at 1100 psia as shown in Figure VIII-51. Although the ternary isotherm of Rutherford [230] at 110°F suggests that the mixture is in the single phase region at 1100 psia, it is not certain whether the measurements at the peak and those below 110°F are also in the supercritical region. Figure VIII-52 illustrates the occurence of a maximum in ϕ for Run 1R at 126.2°F; slightly beyond the cricondentherm temperature. Adiabatic Joule-Thomson data in the

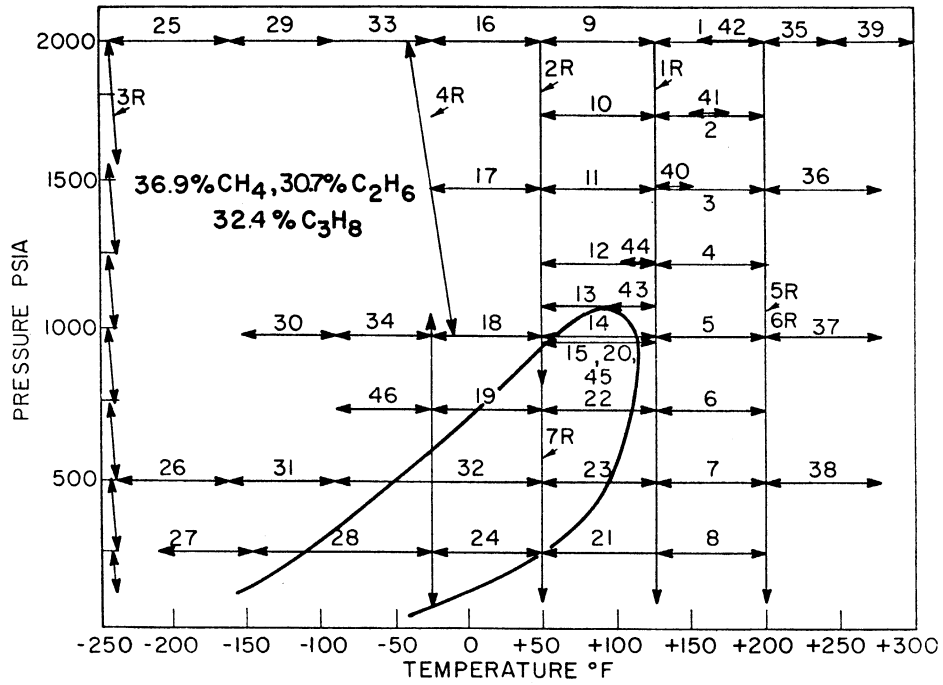

Figure VIII-47. Range of Calorimetric Measurements Obtained in this Work for the Ternary (0.369 CH_4, 0.305 C_2H_6, 0.325 C_3H_8) Mixture.

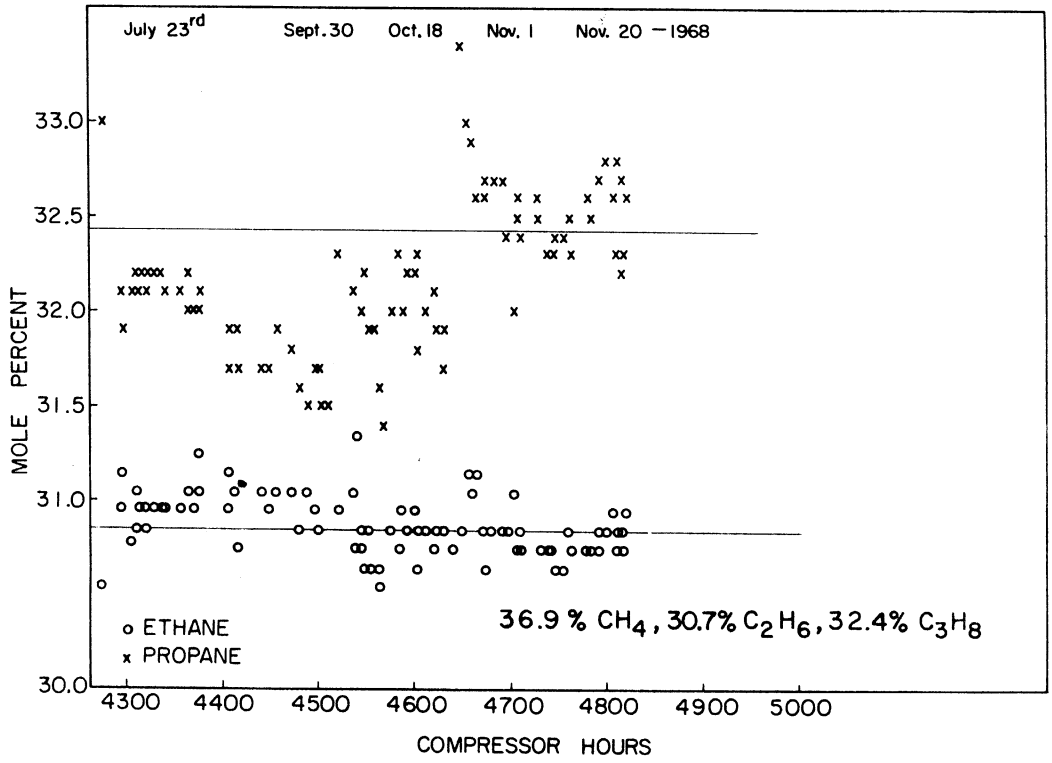

Figure VIII-48. The Variation of Composition for the Ternary Mixture for the Duration of the Investigation.

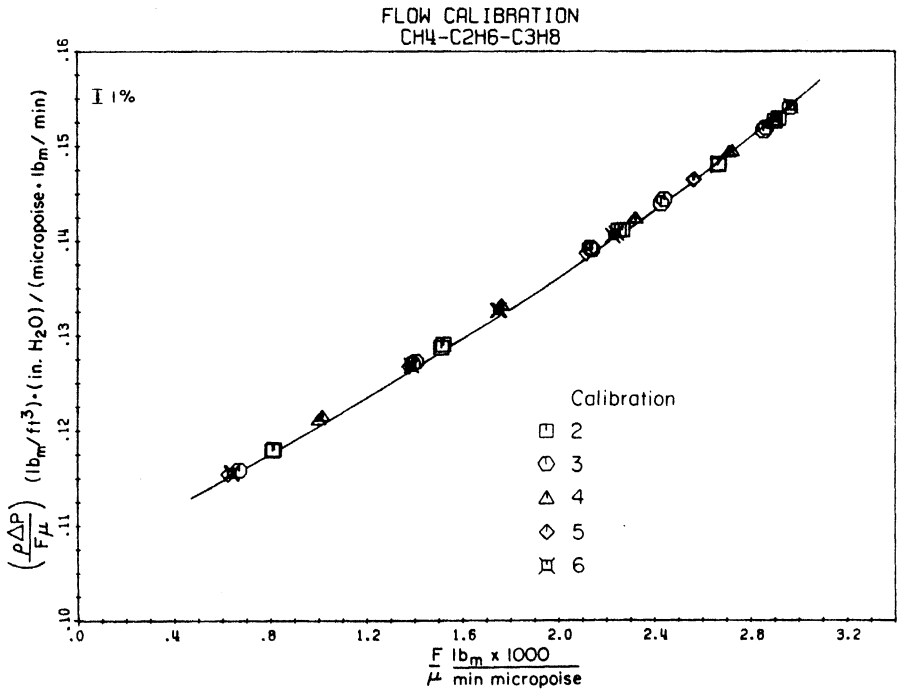

Figure VIII-49. Flowmeter Calibration Results for the Ternary Mixture.

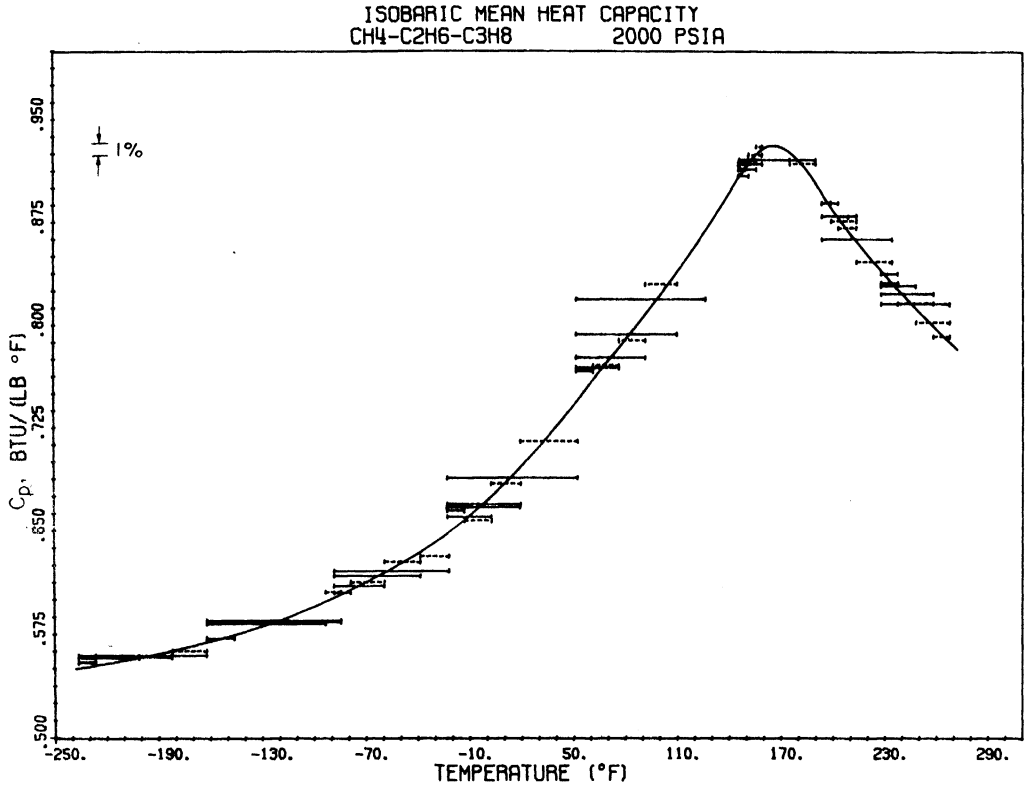

Figure VIII-50. Isobaric Heat Capacity for the Ternary Mixture at 2000 Psia.

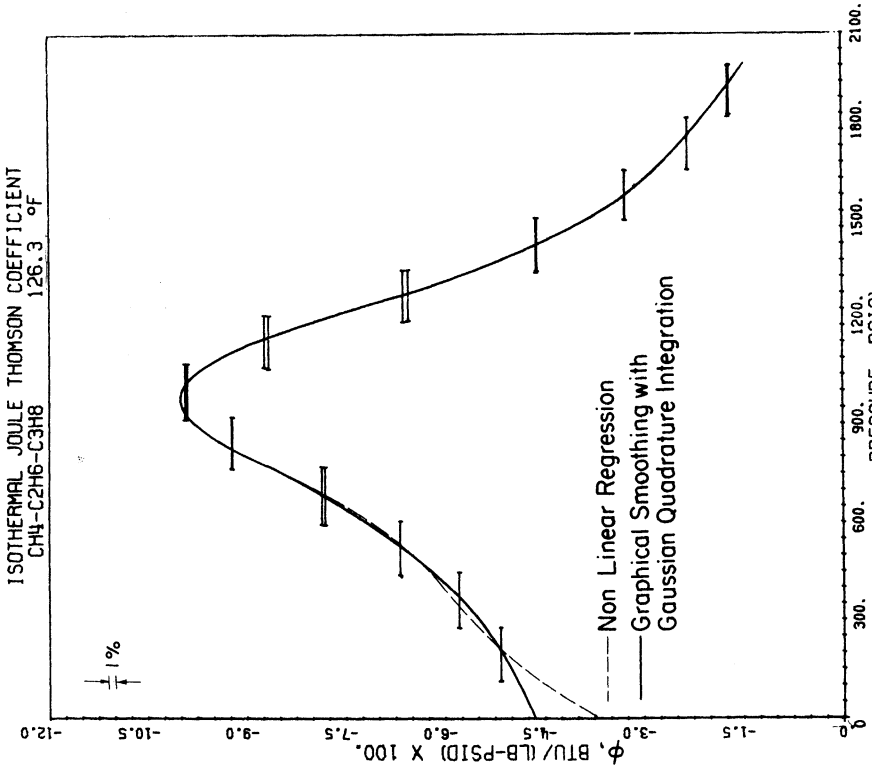

Figure VIII-52. Isothermal Joule-Thomson Coefficient for the Ternary Mixture at 126.3°F.

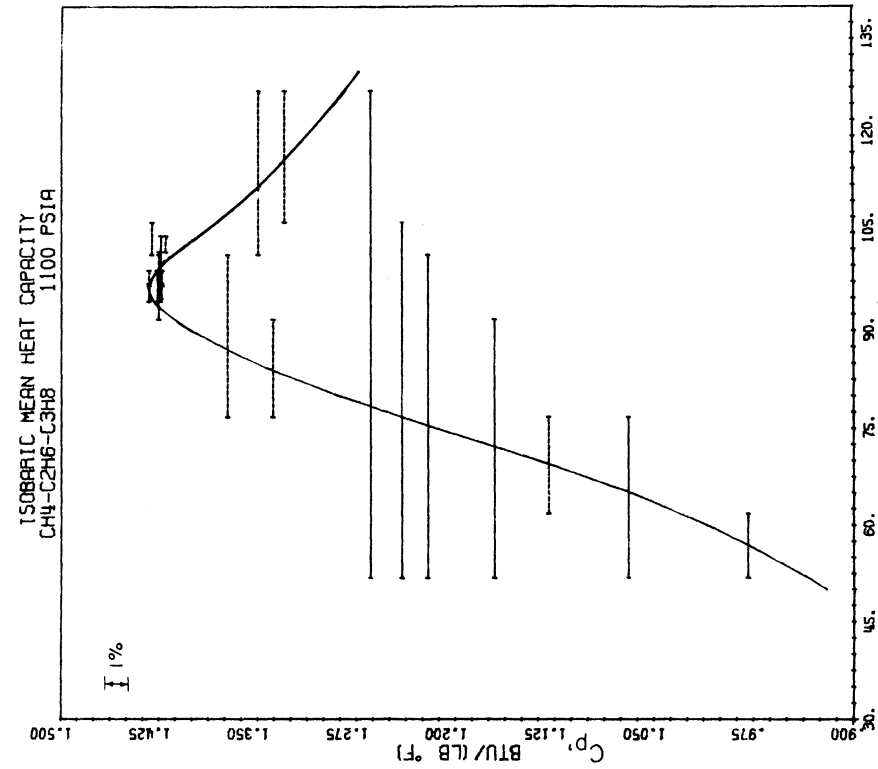

Figure VIII-51. Isobaric Heat Capacity for the Ternary Mixture at 1100 Psia.

liquid phase at -236.48°F are shown in Figure VIII-53. Difficulties in maintaining the calorimeter bath temperature at a fixed value contributed to the lower precision of the measurements in the latter case.

An enthalpy traverse across the two phase region at 500 psia, composed of Run 32 from -88.2°F to 59.9°F and Run 23 from 52.2°F upto 127.5°F, is shown in Figure VIII-54. The two separate runs were necessary to establish the enthalpy of vaporization because power supply limitations at the time did not permit a single traverse across the entire two phase region. These runs were meshed together at a temperature of 59.9°F. The results for these runs are compared in Table VIII-20 with the basic enthalpy data obtained at CB & I [138], and with enthalpy values from the same source normalized to 100°F inlet temperature. All the data sources were corrected for small differences in pressure and composition using the PGC as explained in Chapter VII. The normalized values are also compared with the results of this work in Figure VIII-54 bases on the assumption that the enthalpies match at 100°F. An absolute average discrepancy of 0.7% between the two sources suggests that the agreement is satisfactory within the precision of the CB & I results. The heat capacity in the liquid phase upto the saturation temperature at 500 psia and also derived from Run 22 is shown in Figure VIII-55.

Consistency Checks for the Ternary Mixture

A total of 26 enthalpy loops as summarized in Figure VIII-56 were examined for consistency. An absolute average deviation of 0.35% or 0.6 Btu/lb was noted. The maximum deviation amounted to 1.1% or 2.25 Btu/lb. A maximum adjustment of 1.9 Btu/lb was made in the arm at 500 psia between 52.04 and 126.2°F, and served to significantly improve the consistency for both enthalpy loops involving the given arm. The smoothed $\underline{H}$ and Cp values for the isobaric data are presented in Table VIII-21. The smoothed $\underline{H}$ and ϕ values for the isothermal and isenthalpic throttling data are indicated in Table VIII-22.

Enthalpy Tables and Diagrams

The detailed enthalpy diagram shown as Figure VIII-57 a and b

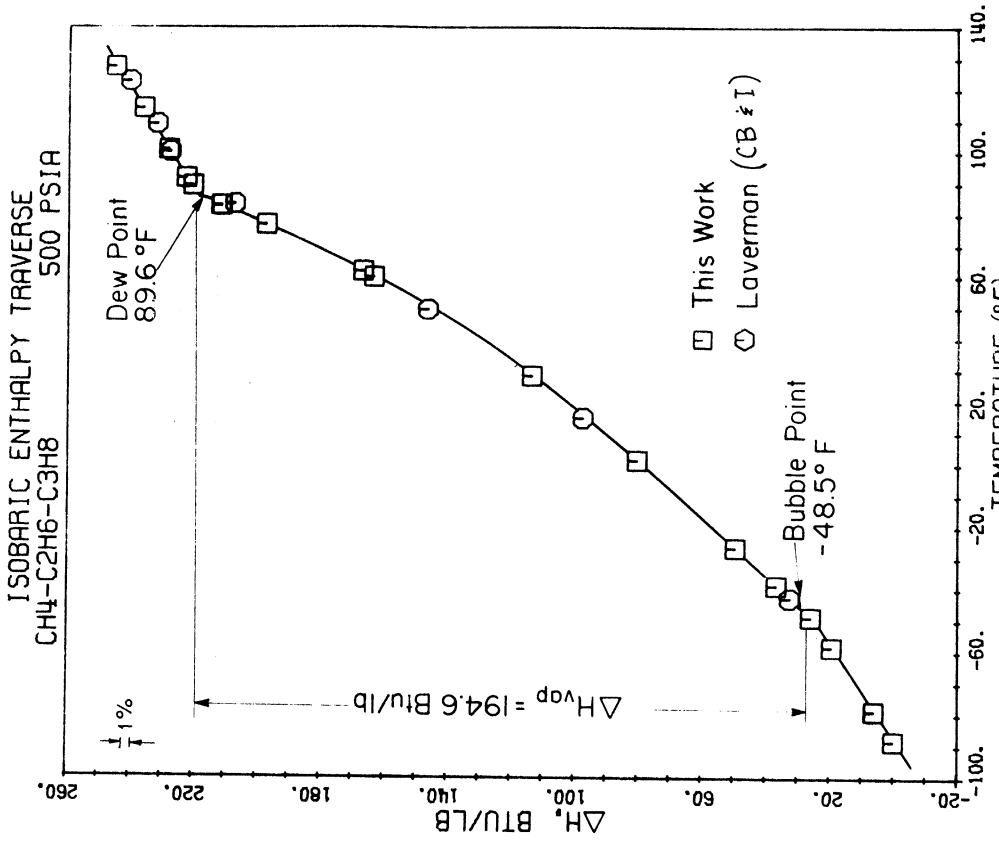

Figure VIII-54. Isobaric Enthalpy Traverse for the Ternary Mixture Across the Two Phase Region at 500 psia.

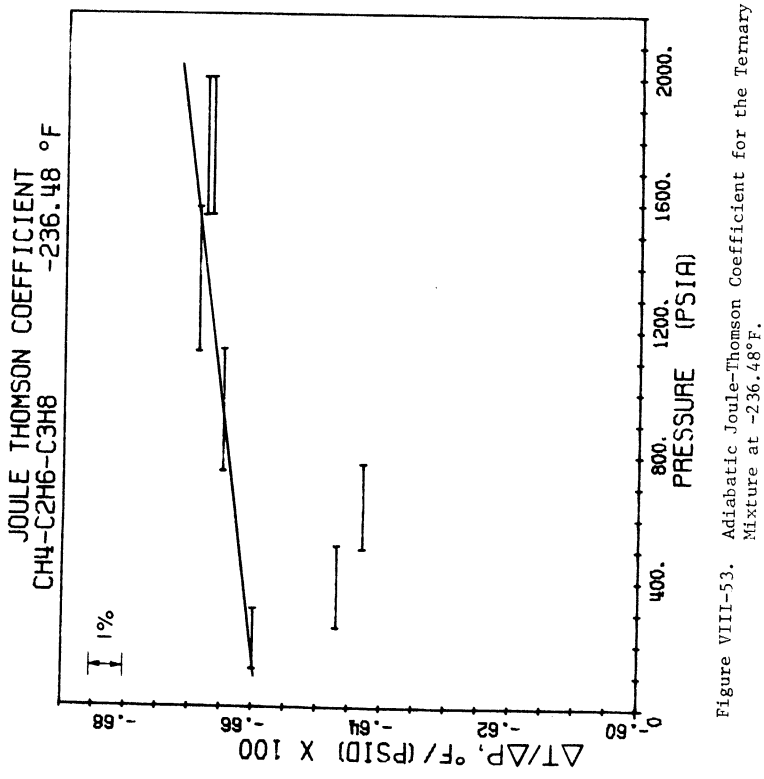

Figure VIII-53. Adiabatic Joule-Thomson Coefficient for the Ternary Mixture at -236.48°F.

TABLE VIII-20

Comparison Between the Calorimetric Data of This Work and the Results from CB&I for the Ternary Mixture at 500 psia

INLET TEMP. (°F)	OUTLET TEMP. (°F)	PRESSURE (PSIA)	ΔH (CB&I)* BTU/LB	ΔH (CB&I)** CORRECTED BTU/LB	ΔH THIS WORK BTU/LB
120.8	49.3	498.5	92.7	92.2	94.0
109.0	14.6	502.0	134.3	134.0	135.4
98.4	-42.7	499.5	193.8	193.9	193.8
122.8	-111.1	500.4	257.2	257.5	258.8
119.8	-142.0	504.3	276.4	277.2	275.7
83.2	-208.8	496.5	282.3	283.0	283.1
100.	49.3	498.5	81.4	81.2	83.1
100.	14.6	502.0	130.5	130.2	130.0
100.	-42.7	499.5	195.1	195.2	195.0
100.	-111.1	500.4	244.3	244.7	245.2
100.	-142.0	504.3	265.4	266.3	263.7
100.	-208.8	496.5	303.3	303.5	302.1

* For a mixture containing 0.359 CH_4, 0.314 C_2H_6 and 0.327 C_3H_8 [138].

** Corrected to the composition of the ternary mixture in this work as indicated in Table VI-3.

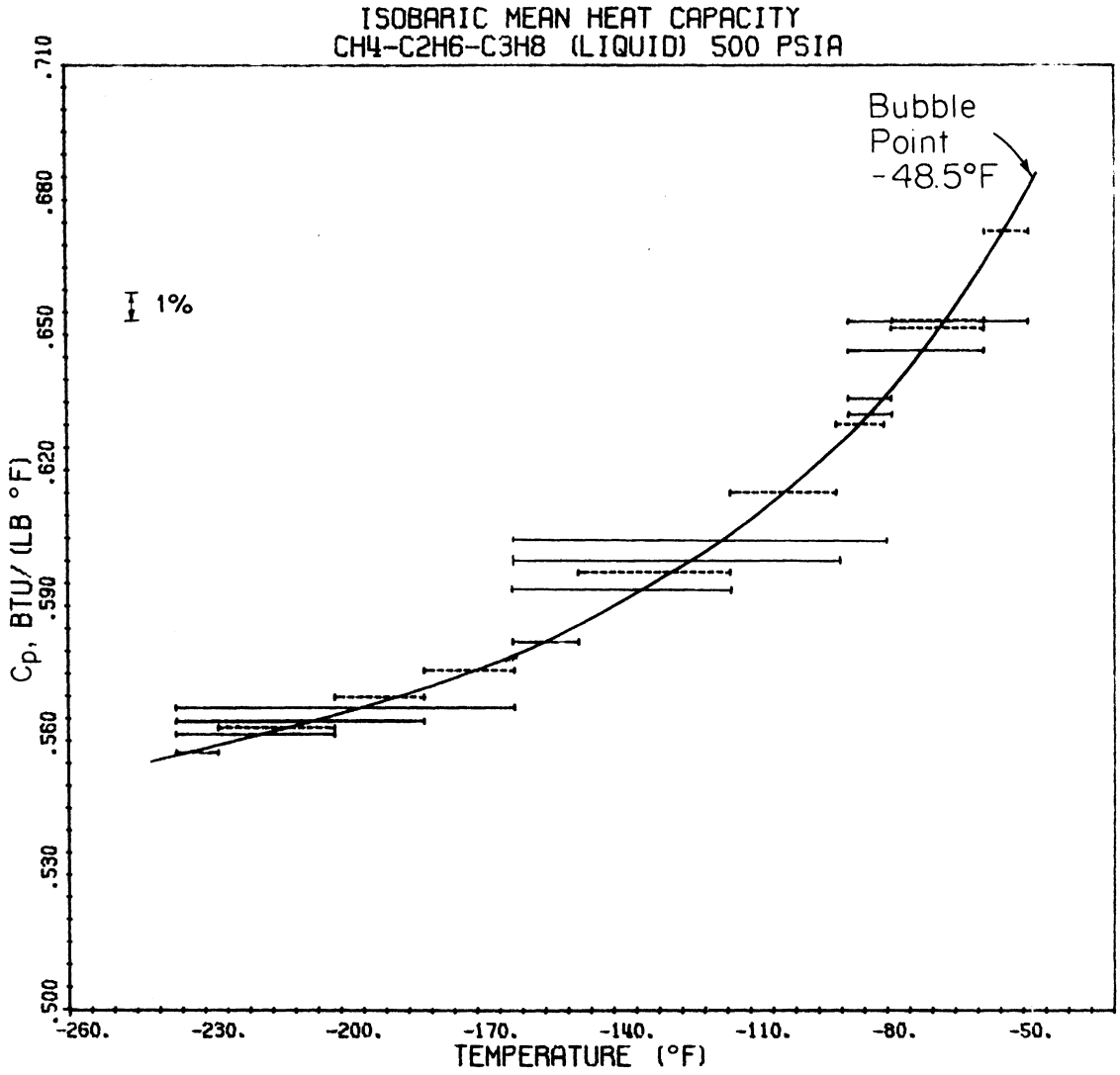

Figure VIII-55. Isobaric Liquid Phase Heat Capacity Data for the Ternary Mixture at 500 Psia upto the Saturation Boundary.

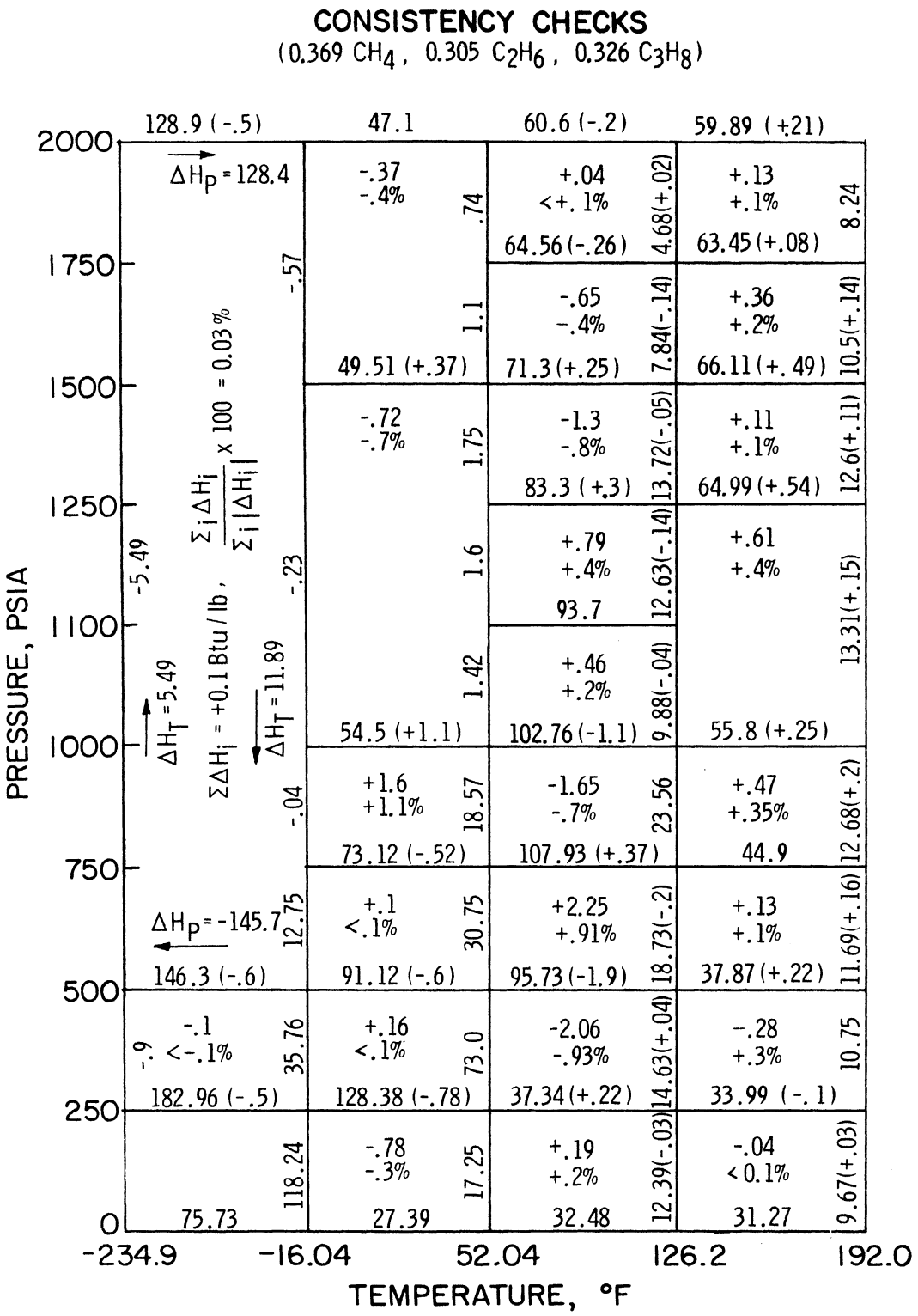

Figure VIII-56. Thermodynamic Consistency Checks for the Calorimetric Data on the Ternary Mixture.

TABLE VIII-21

++

Tabulated Values of the Enthalpy and the Heat Capacity for the Ternary Mixture

0 PSIA ***			250 PSIA			500 PSIA			750 PSIA			1000 PSIA		
TEMP. °F	H BTU/LB	CP BTU/LB/°F	TEMP. °F	H BTU/LB	CP BTU/LB/°F	TEMP. °F	H BTU/LB	CP BTU/LB/°F	TEMP. °F	H BTU/LB	CP BTU/LB/°F	TEMP. °F	H BTU/LB	CP BTU/LB/°F
-280.	238.2	.297	-280.	1.3	.548	-280.	2.2	.551	-100.	106.4	.616	-180.	60.0	.576
-260.	244.2	.303	-260.	12.6	.552	-260.	13.5	.554	-80.	118.7	.625	-160.	71.6	.581
-240.	250.3	.310	-240.	23.5	.556	-240.	24.3	.557	-60.	131.3	.641	-140.	83.2	.587
-234.9	251.9	.312	-234.9	26.4	.557	-234.9	27.3	.558	-40.	144.3	.665	-120.	95.0	.594
-220.	256.6	.316	-220.	34.8	.561	-220.	35.7	.561	-20.	158.1	.711	-100.	107.0	.605
-200.	263.0	.323	-200.	46.2	.567	-200.	46.9	.567	-16.04	160.9	.722	-80.	119.2	.620
-180.	269.5	.327	-180.	57.5	.572	-180.	58.3	.572	-10.	165.3	.756	-60.	131.8	.637
-160.	271.6	.333	-160.	69.0	.580	-160.	69.9	.580	-5.	169.2	.795	-40.	144.7	.660
-140.	282.8	.339	-140.	80.7	.594	-140.	81.6	.590	0.	173.3	.848	-20.	158.1	.691
-120.	289.6	.346	-120.	92.7	.615	-120.	93.5	.603	0.5	173.7	.857 *	-16.04	160.9	.699
-100.	296.6	.353	-117.	94.6	.618	-100.	105.7	.619	10.	185.0		0.	172.2	.730
-80.	303.7	.360	-115.3	95.7	.620 *	-80.	118.2	.638	20.	196.1		20.	187.2	.795
-60.	311.0	.368	-100.	113.6		-60.	131.3	.664	40.	220.0		40.	203.9	.900
-40.	318.5	.376	-80.	136.4		-50.	138.0	.678	52.04	234.0		52.04	215.4	.996
-20.	326.1	.385	-60.	156.9		-48.5	139.0	.681 *	60.	246.6		53.0	216.4	1.004 *
-16.04	327.6	.387	-40.	179.4		-40.	147.6		80.	276.7		60.	224.8	
0.	333.9	.394	-16.04	209.4		-20.	169.0		100.	312.5		80.	251.2	
20.	341.8	.403	-20.	203.8		-16.04	173.6		107.9	325.5	1.037 **	100.	280.1	
40.	349.9	.413	0.	233.5		0.	193.5		110.	327.6	.992	112.3	300.1	1.444 **
52.4	355.0	.418	20.	273.3		20.	217.1		115.	332.3	.900	117.	306.7	1.315
60.	358.3	.422	40.	320.3		40.	245.4		120.	336.7	.835	120.	310.8	1.251
80.	366.9	.432	47.	335.1	.520 **	60.	279.4		126.2	341.7	.784	126.2	318.2	1.112
100.	375.6	.443	50.	336.7	.518	80.	320.2		140.	352.0	.714	130.	322.0	1.067
120.	384.6	.454	60.	341.8	.510	89.6	338.3	.643 **	160.	365.7	.665	140.	332.3	.946
126.2	387.5	.457	70.	346.9	.505	90.	338.5	.640	180.	378.8	.651	160.	349.7	.812
140.	393.8	.465	80.	351.9	.502	95.	341.7	.628	192.	386.6	.650	180.	365.2	.741
160.	402.8	.476	100.	361.9	.498	100.	344.1	.617	200.	391.8	.655	192.	374.0	.712
180.	412.8	.489	120.	372.0	.503	120.	356.0	.590	220.	404.9	.663	200.	379.6	.700
192.	418.7	.496	140.	382.1	.508	126.2	360.5	.584				220.	393.3	.677
200.	422.7	.500	160.	392.3	.514	140.	368.5	.578				240.	406.9	.663
220.	432.8	.512	180.	402.7	.524	160.	380.0	.575				260.	419.9	.655
240.	443.2	.523	192.	409.1	.529	180.	391.4	.573						
260.	453.8	.533	200.	413.3	.534	192.	389.3	.573						
280.	464.5	.542	220.	423.9	.540	200.	402.9	.573						
300.	475.4	.553	240.	434.8	.549	220.	414.4	.575						
			260.	445.8	.557	240.	425.9	.578						
			280.	457.0	.564	260.	437.5	.582						
			300.	468.4	.574	280.	449.2	.587						
						300.	461.0	.594						

* SATURATED LIQUID

** SATURATED VAPOR

*** ZERO PRESSURE ENTHALPIES AND HEAT CAPACITIES CALCULATED FROM HEAT CONTENT FUNCTION AS TABULATED BY THE API [220]

++ REFERENCE ENTHALPY H=0 FOR EACH PURE COMPONENT AS A SATURATED LIQUID AT -280F

TABLE VIII-21

(CONTINUED)

1100 PSIA ++			1250 PSIA			1500 PSIA			1750 PSIA			2000 PSIA		
TEMP. °F	H BTU/LB	CP BTU/LB/°F	TEMP. °F	H BTU/LB	CP BTU/LB/°F	TEMP. °F	H BTU/LB	CP BTU/LB/°F	TEMP. °F	H BTU/LB	CP BTU/LB/°F	TEMP. °F	H BTU/LB	CP BTU/LB/°F
52.04	214.0	.941	52.04	212.4	.862	-20.	158.5	.667	40.	200.2	.768	-280.	8.0	.547
60.	221.8	1.016	60.	219.5	.916	-16.04	161.1	.672	52.04	209.5	.784	-260.	19.2	.550
70.	232.5	1.144	80.	239.4	1.082	0.	172.0	.695	60.	215.8	.798	-240.	30.0	.553
75.	238.5	1.223	95.	256.7	1.219	20.	186.2	.731	80.	232.2	.844	-234.9	32.8	.554
80.	244.8	1.296	100.	262.8	1.248	40.	201.1	.776	100.	249.6	.897	-220.	41.1	.556
85.	251.4	1.361	105.	269.1	1.266	52.04	210.6	.814	120.	268.1	.955	-200.	52.3	.560
90.	258.3	1.410	107.	271.7	1.270 +	60.	217.2	.839	126.2	274.1	.970	-180.	63.5	.565
95.	265.5	1.441	108.	273.0	1.269	80.	234.8	.921	135.	282.7	.993	-160.	74.8	.570
100.	272.7	1.437	110.	275.5	1.268	90.	244.2	.968	140.	287.7	1.000	-140.	86.3	.576
105.	279.8	1.406	115.	281.8	1.260	100.	254.1	1.014	145.	292.7	1.003	-120.	97.9	.584
100.	286.8	1.370	120.	288.1	1.241	110.	264.5	1.054	146.	293.7	1.004 +	-100.	109.7	.592
120.	300.2	1.324	126.2	295.7	1.208	120.	275.2	1.089	150.	297.7	1.001	-80.	121.6	.604
126.2	308.2	1.295	140.	311.6	1.110	123.2	281.9	1.099 +	155.	302.7	.994	-60.	133.8	.616
			160.	332.4	.970	130.	286.1	1.091	160.	307.7	.975	-40.	146.3	.631
			180.	350.7	.858	140.	296.9	1.073	170.	317.3	.952	-20.	159.1	.649
			192.	360.6	.803	150.	306.4	1.044	180.	326.7	.920	-16.4	161.7	.653
			200.	366.9	.771	160.	317.8	1.009	192.	337.5	.883	0.	172.3	.672
						180.	337.2	.930	200.	344.5	.864	20.	185.9	.698
						192.	348.0	.881				40.	200.1	.725
						200.	354.9	.852				52.4	208.8	.742
						220.	371.4	.801				60.	214.8	.754
						240.	386.9	.762				80.	230.3	.790
						260.	401.8	.733				100.	246.6	.825
						280.	416.6	.719				120.	263.8	.865
						300.	431.0	.708				126.2	269.4	.877
												140.	281.7	.903
												160.	299.9	.935
												162.	303.6	.937 +
												180.	318.3	.917
												192.	329.3	.900
												200.	336.4	.887
												220.	353.8	.855
												240.	370.6	.825
												260.	386.8	.800
												280.	402.6	.779

\+ THE HEAT CAPACITY MAXIMUM ALONG THE GIVEN ISOBAR

++ THE TABULATED HEAT CAPACITIES BETWEEN 95 F AND 105 F MAY APPLY TO THE TWO PHASE MIXTURE

TABLE VIII-22

Tabulated Values of the Enthalpy[++] and the Isothermal Throttling Coefficient for the Ternary Mixture

	TEMPERATURE (°F)									
	-234.9°F		-16.04°F		52.04°F		126.2°F		192.0°F	
P PSIA	H BTU/LB	$(DH/DP)_T$ X100 BTU/LB/PSID	H BTU/LB	$(DH/DP)_T$ X100 BTU/LB/PSID	H BTU/LB	$(DH/DP)_T$ X100 BTU/LB/PSID	H BTU/LB	$(DH/DP)_T$ X100 BTU/LB/PSID	H BTU/LB	$(DH/DP)_T$ X100 BTU/LB/PSID
0.*	251.87	-36.3	327.6	-7.8	355.0	-5.9	387.5	-4.59	418.7	-3.68
100.	25.86	.359	295.0	.	348.6	-6.7	382.7	-4.87	415.0	-3.82
200.	26.22	.359	225.3	.	341.4	-7.4	377.7	-5.18	411.1	-3.98
250.	26.40	.360	209.4	.	337.7	-8.0	375.1	-5.37	409.1	-4.08
300.	26.58	.360	199.0	.	320.0	.	372.3	-5.55	407.0	-4.17
400.	26.94	.361	184.0	.	286.4	.	366.6	-5.99	402.7	-4.35
500.	27.30	.361	173.5	.	264.7	.	360.5	-6.56	398.3	-4.52
600.	27.66	.362	165.2	.	250.2	.	353.4	-7.23	393.8	-4.63
700.	28.13	.363	160.78	.	238.8	.	345.8	-8.00	389.0	-4.81
750.	28.20	.363	160.85	.	234.0	.	341.7	-8.43	386.6	-4.90
800.	28.38	.363	160.90	-.020	229.7	.	337.4	-8.88	384.2	-4.98
900.	28.75	.364	160.89	-.004	222.0	.	328.1	-9.69	379.1	-5.13
1000.	29.12	.364	160.89	.010	215.40	1.57	318.2	-10.07	374.0	-5.25
1100.	29.48	.365	160.91	.025	213.98	1.27	308.3	-9.49	368.6	-5.34
1200.	29.85	.366	160.94	.040	212.85	1.00	299.5	-8.03	363.3	-5.34
1250.	30.03	.366	160.96	.046	212.38	.89	295.7	-7.19	360.6	-5.28
1300.	30.21	.366	160.99	.052	211.95	.81	292.3	-6.42	358.0	-5.22
1400.	30.57	.367	161.04	.068	211.23	.66	286.5	-5.09	352.9	-4.99
1500.	30.95	.368	161.12	.082	210.63	.54	281.9	-4.06	348.0	-4.70
1600.	31.31	.368	161.21	.095	210.13	.45	278.3	-3.25	343.6	-4.30
1700.	31.68	.369	161.32	.104	209.71	.38	275.3	-2.60	339.5	-3.92
1750.	31.86	.369	161.37	.114	209.53	.35	274.1	-2.34	337.5	-3.74
1800.	32.15	.370	161.43	.120	209.36	.33	273.0	-2.12	335.7	-3.60
1900.	32.41	.370	161.55	.133	209.06	.29	271.0	-1.75	332.3	-3.20
2000.	32.79	.371	161.69	.144	208.79	.25	269.4	-1.51	329.3	-2.80

++ REFERENCE ENTHALPY H=0 FOR EACH PURE COMPONENT AS A SATURATED LIQUID AT -280F

* THE VALUE OF $(DH/DP)_T$ AT ZERO PRESSURE IS OBTAINED FROM EQUATIONS (V-30) AND (V-31) IN CONJUNCTION WITH THE PSEUDO-PARAMETERS (I) FOR THE TERNARY MIXTURE IN TABLE IX-21

was constructed from the smoothed enthalpy values adjusted for thermodynamic consistency. Table VIII-23 contains essentially the same information in tabular form. The reported enthalpy values are believed to be precise to within 1 Btu/lb. The two phase envelope on the enthalpy diagram from 250 to 1000 psia was guided by the smoothed data of this work. The phase equilibria data of Price and Kobayashi [207] upto 50°F were used to determine the dew and bubble points for the mixture below 250 psia. The enthalpies in the liquid phase at saturation were obtained by extrapolating the subcooled liquid enthalpy lines at any given temperature to the calculated saturation pressure. The saturated vapor phase enthalpies below 250 psia were evaluated from the reduced virial equation truncated at the third virial coefficient as suggested on page 196. The shape of the two phase envelope is somewhat uncertain above 1000 psia. About the only information available in this region is the phase equilibria data of Rutherford [230] at 110°F which predicts a dew point pressure of about 1075 psia. The enthalpies for the liquid and vapor phase at saturation, including the experimental results of this work, are presented in Table VIII-24.

TABLE VIII-23

Smoothed Values of the Enthalpy[++] for the Ternary Mixture as Obtained from the Enthalpy Diagram

H (BTU/LB)

TEMP. (°F)	PRESSURE (PSIA) 0.*	250.	500.	750.	1000.	1250.	1500.	1750.	2000.
-280.	238.2	1.3	2.2	3.2	4.1	5.1	6.0	7.0	8.0
-260.	244.2	12.6	13.5	14.5	15.4	16.3	17.3	18.2	19.2
-240.	250.3	23.5	24.3	25.3	26.2	27.1	28.1	29.0	30.0
-234.9	251.9	26.4	27.3	28.2	29.1	30.0	31.0	31.9	32.8
-220.	256.6	34.8	35.7	36.6	37.5	38.4	39.3	40.7	41.1
-200.	263.0	46.2	47.0	47.8	48.7	49.5	50.5	51.4	52.3
-180.	269.5	57.5	58.3	59.1	60.0	60.9	61.8	62.6	63.5
-160.	276.1	69.0	69.9	70.7	71.6	72.4	73.2	74.0	74.8
-140.	282.8	80.7	81.6	82.4	83.2	84.0	84.7	85.5	86.3
-120.	289.6	92.7	93.5	94.3	95.0	95.7	96.4	97.1	97.9
-100.	296.6	113.6	105.7	106.4	107.0	107.6	108.3	108.9	109.7
-80.	303.7	136.4	118.2	118.7	119.2	119.8	120.3	120.9	121.6
-60.	311.0	156.9	131.3	131.3	131.8	132.2	132.7	133.3	133.8
-40.	318.5	179.4	147.6	144.3	144.7	145.1	145.4	145.8	146.3
-20.	326.1	203.8	169.0	158.0	158.1	158.3	158.5	158.8	159.1
-16.04	327.6	209.4	173.6	160.9	160.9	161.0	161.1	161.4	161.7
0.	333.9	233.5	193.5	173.3	172.2	172.4	172.0	172.3	172.3
20.	341.8	273.3	217.1	196.1	187.2	186.7	186.2	186.0	185.9
40.0	350.0	320.3	245.4	220.0	203.9	202.2	201.1	200.2	200.1
52.04	355.0	337.7	264.7	234.0	215.4	212.4	210.6	209.5	208.8
80.	366.9	351.9	320.2	276.7	251.2	239.4	234.8	232.2	230.3
60.	358.3	341.8	279.4	246.6	224.8	219.5	217.2	215.8	214.8
100.	375.6	361.9	344.1	312.5	280.1	262.8	254.1	249.6	246.6
120.	384.6	372.0	356.0	336.7	310.8	288.1	275.2	268.1	263.8
126.2	387.5	375.1	360.5	341.7	318.2	295.7	281.9	274.1	269.4
140.	393.8	382.1	368.5	352.0	332.3	311.6	296.9	287.7	281.7
160.	402.8	392.3	380.0	365.7	349.7	332.4	317.8	307.7	299.9
180.	412.8	402.7	391.4	378.8	365.2	350.7	337.2	326.7	318.3
192.	418.7	409.1	398.3	386.6	374.0	360.6	348.1	337.5	329.3
200.	422.7	413.3	402.9	391.8	379.6	366.9	354.9	344.5	336.4
220.	432.8	423.9	414.4	404.8	393.3	382.0	371.4	361.8	353.8
240.	443.2	434.8	425.9	416.5	406.7	397.0	386.9	378.5	370.6
260.	453.8	445.8	437.5	428.9	419.9	410.9	401.8	393.5	386.8
280.	464.5	457.0	449.2	441.1	432.9	424.9	416.6	409.1	402.6
300.	475.4	468.4	461.0	453.4	445.8	438.5	431.0	424.4	418.3

++ REFERENCE ENTHALPY H=0 FOR EACH PURE COMPONENT AS A SATURATED LIQUID AT -280F

* ZERO PRESSURE VALUES OBTAINED BY INTERPOLATION OF (H(T)-H(0))/T VALUES AS TABULATED BY THE API [220]

TABLE VIII-24

Saturated Liquid and Vapor Phase Enthalpies for the Ternary Mixture

TEMP. (°F)	PRESSURE (PSIA)	LIQUID ENTHALPY++ BTU/LB	TEMP. (°F)	PRESSURE (PSIA)	VAPOR ENTHALPY++ BTU/LB	
-198.5	50.	47.0	-39.	50.	313.8	ISOBARIC
-168.3	100.	63.8	-6.5	100.	323.0	
-130.2	200.	86.2	33.	200.	332.7	
-115.3	250. *	95.7	47.	250. *	335.1	
-100.2	300.	105.2	58.2	300.	337.6	
-72.8	400.	122.8	76.5	400.	339.0	
-48.5	500. *	139.0	89.6	500. *	338.3	
-27.3	600.	153.1	99.	600.	334.9	
-8.5	700.	167.0	104.4	700.	329.1	
0.5	750. *	173.7	105.9	750. *	325.5	
53.	1000. *	216.4	112.3	1000.	300.1	
-40.	537.	144.5	-40.	47.5	313.1	ISOTHERMAL
-20.	636.	158.2	-20.	77.	319.6	
-16.04	655. *	160.8	-16.04	83.	320.8	
0.	746.	172.4	0.	113.	324.8	
20.	847.	187.7	20.	162.	329.8	
40.	943.	204.3	40.	223.	334.2	
52.04	996. *	215.8	52.04	273.	336.7	
60.	1025.	223.1	60.	309.	337.8	

* SMOOTHED EXPERIMENTAL MEASUREMENTS OF THIS WORK

++ REFERENCE ENTHALPY H=0 FOR EACH PURE COMPONENT AS A SATURATED LIQUID AT -260F

Chapter IX

THE EVALUATION OF ENTHALPY CORRELATION AND PREDICTION METHODS

Chapters VI, VII and VIII have focussed on the experimental aspects of this investigation concluding with the interpretation of the basic measurements to yield smoothed enthalpy values for ethane, three ethane-propane mixtures, and for a ternary methane-ethane-propane mixture over a broad range of temperatures and pressures. Additionally, the calorimetric measurements on two methane-ethane mixtures, investigated after the completion of the ethane-propane system, were processed upto the basic data stage. The enthalpies of five methane-propane mixtures have already been adequately characterized in previous investigations at the facility [162, 168, 284]. Therefore, the necessary data has now been accumulated to pursue the objective outlined at the conclusion of Chapter IV, i.e., the prediction of multi-component mixture enthalpies from constituent pure component and binary enthalpy data.

Before any technique can be applied to predict multi-component mixture enthalpies, it is first necessary to establish its ability to accurately represent all the constituent pure component and binary enthalpy data. Furthermore, if the technique is to be utilized for characterizing a variety of systems, it is imperative for such data to be concisely encoded, and rapidly decoded when necessary. The evidence presented in Chapter IV suggested that the thermodynamic properties of a mixture may, for engineering purposes, be adequately encoded in a corresponding states framework given an optimum set of three pseudo-critical parameters. It was further established that the PGC one fluid model was perhaps the most suitable of such frameworks for representing light hydrocarbons and "normal" fluids.

In this chapter, the procedure for calculating the pseudo-parameters RTc_m/Pc_m, Tc_m and αc_m that produce the best fit to the enthalpy data for each individual mixture taken separately is first outlined. This also provides us with a quantitative measure of the ability of the PGC to encode the enthalpy data of individual mixtures. In the particular case of the ethane-propane system, this analysis allows us to generate comprehensive enthalpy tables in the

single phase region from skeleton calorimetric data. An important test is then performed for each binary system that evaluates the consistency between the prescribed pseudo-parameters for all mixtures belonging to a given binary system if the one fluid corresponding states model is assumed to be rigorously true for every mixture examined.

Next, ten mixing rules, including four developed in this work, are examined for their ability to characterize the enthalpy data for the methane-ethane and the methane-propane binaries as a function of composition. For eight of these rules, the binary unlike pair interaction parameters are empirically adjusted so that the calculated pseudo-parameters are in close agreement with the optimum pseudo-parameters for each mixture. Having specified all the constituent binary like and unlike pair interaction parameters, the rules are subsequently evaluated for their ability to predict the enthalpy of the ternary mixture. Topographical plots are prepared which illustrate the performance of the PGC and other prediction techniques in calculating the enthalpies for the systems of this work.

Prediction of Pure Component Enthalpies

Before proceeding with the optimization of the pseudo-parameters for each of the mixtures examined in this work, it is necessary to ensure that the PGC framework can adequately represent the enthalpies of the pure components methane, ethane, and propane that constitute the ternary mixture. The PGC enthalpy predictions for the three components using the appropriate critical parameters from Table J-1 are presented in Tables K-1, K-2 and K-3, respectively. The enthalpy values in these tables are obtained by combining the PGC enthalpy departure calculations with the zero pressure enthalpy values of Rossini [220]. As the smoothed methane calorimetric data of Jones [19] and the smoothed propane calorimetric data of Yesavage [284] were mainly used to develop the reference reduced enthalpy tables for the PGC, the accurate prediction of these measurements is virtually assured [203].

Table IX-1 compares the PGC enthalpy predictions with the smoothed enthalpy data of this work for the system containing 0.996 mole fraction ethane. The critical parameters used in the analysis (also indicated

TABLE IX-1

The PGC Enthalpy Predictions Compared With Smoothed Data
Using the Critical Parameters for Ethane

TEMP. (DEG F) INLET	TEMP. (DEG F) OUTLET	PRESS. (PSIA) INLET	PRESS. (PSIA) OUTLET	ENTHALPY CHANGE EXP'TAL BTU/LB	ENTHALPY CHANGE CALC'D BTU/LB	DIFFERENCE BTU/LB	DIFFERENCE %
-246.60	-246.60	2000.00	0.0	235.58	236.12	-0.54	-0.23
-246.60	-246.60	2000.00	100.00	-6.15	-5.75	-0.40	6.50
-123.30	-123.30	2000.00	0.0	205.26	205.60	-0.34	-0.16
-123.30	-123.30	2000.00	250.00	-5.07	-5.51	0.44	-8.59
-24.50	-24.50	2000.00	0.0	181.11	181.26	-0.15	-0.08
-24.50	-24.50	2000.00	250.00	-2.44	-1.72	-0.72	29.69
49.20	49.20	2000.00	700.00	3.64	2.73	0.91	24.92
80.00	80.00	2000.00	1000.00	6.38	6.55	-0.17	-2.63
80.00	80.00	1000.00	713.00	6.72	7.19	-0.47	-6.94
89.80	89.80	250.00	0.0	15.55	15.06	0.49	3.13
89.80	89.80	500.00	0.0	37.20	36.00	1.20	3.24
89.80	89.80	677.00	0.0	69.69	69.61	0.08	0.12
89.80	89.80	819.00	0.0	133.03	132.40	0.63	0.47
89.80	89.80	1000.00	0.0	139.43	138.69	0.74	0.53
89.80	89.80	1500.00	0.0	145.16	145.43	-0.27	-0.18
89.80	89.80	2000.00	0.0	148.57	148.29	0.28	0.19
125.00	125.00	250.00	0.0	13.36	12.99	0.37	2.78
125.00	125.00	750.00	0.0	53.66	53.69	-0.03	-0.05
125.00	125.00	1000.00	0.0	97.56	98.88	-1.32	-1.35
125.00	125.00	1250.00	0.0	121.55	121.18	0.37	0.30
125.00	125.00	1500.00	0.0	129.12	128.53	0.59	0.46
125.00	125.00	2000.00	0.0	135.76	135.22	0.54	0.40
200.60	200.60	250.00	0.0	10.19	9.98	0.21	2.04
200.60	200.60	750.00	0.0	34.30	34.12	0.18	0.52
200.60	200.60	1000.00	0.0	48.90	48.78	0.12	0.24
200.60	200.60	1500.00	0.0	80.24	80.90	-0.66	-0.82
200.60	200.60	2000.00	0.0	101.24	101.67	-0.43	-0.43
300.00	300.00	500.00	0.0	15.73	15.41	0.32	2.03
300.00	300.00	1000.00	0.0	32.73	31.82	0.91	2.77
300.00	300.00	2000.00	0.0	64.33	65.88	-1.55	-2.41
60.00	63.00	500.00	500.00	102.82	103.48	-0.66	-0.64
50.00	80.00	713.00	713.00	31.03	32.62	-1.59	-5.14
82.00	93.00	713.00	713.00	62.73	56.16	6.57	10.48
99.00	106.00	819.00	819.00	32.41	28.22	4.19	12.91
170.00	200.60	2000.00	2000.00	29.39	29.37	0.02	0.06

AVERAGE ENTHALPY DIFFERENCE	72.0 BTU/LB
STD. DEV. (BTU/LB)	1.49 BTU/LB
TC	305.44 K
PC	708.33 PSIA
ALPHAC	6.270

in the same table) differ slightly from the true critical parameters for ethane because the PGC mixing rules were used to adjust the parameters to account for the propylene impurity. The data used for comparison purposes consists of a representative set of smoothed isothermal and isobaric enthalpy differences extending from -246.6°F to 300°F and upto 2000 psia. Although the standard deviation of 1.49 Btu/lb in the enthalpy difference is not as good as might be expected, its magnitude would be considerably lower but for the relatively large enthalpy deviations of 6.57 and 4.19 Btu/lb observed for two isobaric enthalpy differences across the heat capacity maxima at 713 and 819 psia, respectively. Some rather large percentage deviations are also noted at 24.5°F and 49.2°F. The observations correspond to isothermal enthalpy differences in the liquid phase in the vicinity of the Joule-Thomson inversion curve and involve rather small enthalpy changes. A slight error in predicting the exact location of the Joule-Thomson curve can, therefore, result in large percentage deviations in such cases.

Although Yesavage [284] and Powers [203] have previously used the methane and propane enthalpy data to predict the enthalpy departures for nitrogen to within 1 Btu/lb using three parameter corresponding states frameworks, such predictions did not adequately test the techniques with respect to variations in the third parameter αc, because the αc value for methane and nitrogen are not much different (See Table J-1). The successful prediction of the enthalpy of ethane in the PGC framework is considerably more significant in this respect because its αc value lies in between those for methane and propane.

Optimization of Pseudo-parameters

a) General Procedure. This section is concerned with the determination of the three pseudo-critical parameters Tc_m, Pc_m, and αc_m that will produce the best fit to the enthalpy data for each of the mixtures investigated in this work using the PGC framework. Although it is possible to use all the data for each mixture in the optimization scheme, expressed as enthalpy departures at regular intervals over the entire measurement range, the number of calculations in such a trial and error operation may be significantly reduced if a

restricted set of test data that cover the entire measurement range are carefully chosen so as to be selective of each of the three pseudo-critical parameters desired. By experience obtained from preliminary attempts at optimization, it was determined that isobaric enthalpy differences across the heat capacity maxima were very selective of αc. The same was true of enthalpy of vaporization data for mixtures with narrow two phase regions. The data just above the critical point were relatively sensitive to Pc. As indicated in Chapter V, enthalpy data are always selective of Tc regardless of location.

A representative set of 25 to 35 isobaric and isothermal enthalpy differences were selected from the smoothed enthalpy table for a given mixture. The set was further divided into three subgroups each containing about 5 to 10 points. The data were re-arranged such that each subgroup was independently selective of the pseudo-parameters. The optimization was intially restricted to the first subgroup. The starting estimates for the pseudo-parameters were provided by the PGC mixing rules.

The pseudo-parameters were always incremented one at a time in the sequence Tc_m, Pc_m and αc_m. The smoothed enthalpy differences were compared with the PGC predictions for each such pseudo-parameter set. A particular parameter was negatively incremented about a central value only if the positive increment yielded a higher standard deviation in the enthalpy difference. The optimization is terminated after the cycle is repeated for a specified number of times (usually twice). The results were examined at this point to determine if further optimization was necessary. If not, another subgroup was added and the process repeated. When little or no movement of the optimum condition was observed, the step size for each pseudo-parameter was reduced to half its original value and the process repeated.

The search was conducted with initial increments of $\pm$ 0.5°F in Tc, $\pm$ 2 psia in Pc, and $\pm$ 0.02 in αc, respectively. A histogram showing the distribution of the PGC predictions as a function of the magnitude and sign of the deviation in Btu/lb from -2 to +3 Btu/lb, in increments of 0.25 Btu/lb, was also generated for each trial. The histogram is useful in monitoring the optimization and can serve to

ferret out persistent and unusually high deviations that decrease the selectivity of the optimization. It can also indicate if further optimization from a different starting point is necessary, as for example, when the enthalpy deviations in the histogram show a marked bias at the termination of an optimization step.

b) Pseudo-parameter Optimization for Ethane. In order to ensure that the optimum pseudo-parameters obtained within the PGC framework by the technique described above are truly meaningful, it is desirable to apply the procedure to a substance whose pseudo-critical parameters are otherwise unequivocally defined. If the ethane enthalpies of this work are subjected to a pseudo-parameter optimization, then the optimized pseudo-critical parameters may be compared with the critical parameters in Table IX-1 to establish the reliability of the technique. The results obtained in the final stages of the optimization, including the histogram, are summarized in Table IX-2 illustrating the general procedure discussed in the previous section. The data involving isobaric enthalpy differences across the two phase region were spread over an interval of a few degrees to prevent the predicted location of the vapor pressure curve from completely dominating the optimization of the pseudo-parameters. Nevertheless, some pseudo-parameter combinations did not predict the observed phase change within the selected latitude, thereby resulting in standard deviations of over 20 Btu/lb.

The smoothed experimental data are compared with the enthalpy predictions for the optimum pseudo-parameters in Table IX-3. In this case the input data are arranged in the subgroups used to optimize the pseudo-parameters. The standard deviation in the enthalpy difference for the optimum fit was 1.03 Btu/lb. A relatively high deviation of 3.11 Btu/lb was obtained for an isobaric enthalpy difference of 32.41 Btu/lb at 819 psia in the vicinity of the heat capacity maximum. This suggests that either the smoothed reference enthalpy tables involving the methane and propane data, or the αc dependence of the reduced enthalpy function in Equation (III-35) require some improvement in this region. Nevertheless, it is significant that the optimum pseudo-parameters were within 0.22°F in Tc, 1.8 psia in Pc, and 0.01 in αc with respect to the critical properties in Table

TABLE IX-2

Summary of Results in the Final Stages of Pseudo-parameter Optimization
for Ethane in the PGC Framework

TC (°K)	PC (PSIA)	ALPHAC	ZC	STD.DEV. BTU/LB	NO.OF POINTS	TRIAL NO.	DEVIATION HISTOGRAM (BTU/LB) −2	−1	0	1	2	3	>4
305.4	710.	6.280	.2848	1.43	10	1		2 1 1 1 3					1
305.5	710.	6.280	.2848	1.88		2		1 1 1 3 1					1
305.3	710.	6.280	.2848	1.05		3		2 1 0 2 0 4			1		
305.3	712.	6.280	.2848	33.4		4		1 1 0 2 0 4 1					1
305.3	708.	6.280	.2845	1.70		5		1 2 1 1 2 2					1
305.3	710.	6.300	.2845	1.34		6		2 1 0 1 1 1 2 2		1			
305.3	710.	6.260	.2858	1.04		7		2 0 1 2 3 1			1		
305.4	710.	6.260	.2858	1.44		8		2 0 1 2 3 1					1
305.2	710.	6.260	.2858	33.4		9		1 0 0 3 2 1	1				1
305.3	712.	6.260	.2858	33.4		10		1 0 1 2 2 3	1				1
305.3	708.	6.260	.2858	1.73		11		1 1 1 4 1 1	1				1
305.3	710.	6.280	.2848	1.05		12		2 1 0 2 0 4			1		
305.3	710.	6.240	.2858	33.4		13		1 0 0 2 2 1 1 1				1	1
305.3	710.	6.260	.2845	0.98	15	14		1 2 1 3 4 2 0 1				1	
305.4	710.	6.260	.2845	1.21		15		2 1 1 3 5 1 1					1
305.2	710.	6.260	.2845	26.8		16		1 1 0 3 4 1 2 0 1 1					1
305.3	712.	6.260	.2845	26.8		17		1 1 1 3 3 4 0 1					1
305.3	708.	6.260	.2845	1.46		18		1 2 1 5 2 2 1					1
305.3	710.	6.280	.2845	0.91		19		2 1 2 2 1 5 1				1	
305.4	710.	6.280	.2845	1.18		20		2 1 3 1 2 5					1
305.2	710.	6.280	.2845	26.8		21		1 1 1 3 0 6 0 0 1 1					1
305.3	712.	6.280	.2845	26.8		22		1 1 2 2 1 5 1 1					1
305.3	708.	6.280	.2845	1.40		23		1 2 3 1 3 3 1					1
305.3	710.	6.300	.2845	1.16		24		2 2 0 2 2 2 4		1			
305.3	710.	6.260	.2858	0.97		25		1 2 1 3 4 2	1	0	1		
305.3	710.	6.280	.2848	0.91	15	26 *		2 1 2 2 5 1			1		
305.3	710.	6.280	.2845	1.03		27		2 1 3 1 2 4 1				1	
305.2	710.	6.280	.2845	0.84		28		2 1 1 3 0 6 0 1		1			
305.2	711.	6.280	.2845	26.8		29		1 1 1 3 0 6 0 1 1					1
305.2	709.	6.280	.2845	1.01		30		1 2 1 3 1 5 0 1				1	
305.2	710.	6.290	.2848	0.93		31		1 2 0 2 2 1 5 0 1		1			
305.2	710.	6.270	.2848	0.84		32		2 1 4 0 4 2 0 1		0			
305.3	710.	6.280	.2848	0.91		33		2 1 2 2 1 5 0 1		1			
305.2	710.	6.280	.2848	26.8		34		1 1 1 3 0 6 0 0 1 1					1
305.25	711.	6.280	.2848	26.8		35		1 1 2 2 0 6 0 1 1					1
305.25	709.	6.280	.2848	1.01		36		1 2 1 3 1 5 0 1				1	
305.25	710.	6.290	.2848	0.93		37		1 2 0 2 2 1 5 0 1		1			
305.25	710.	6.270	.2848	0.84		38		2 1 4 0 4 2	1	1			
305.25	710.	6.280	.2848	0.94	23	39	1	2 1 3 4 0 6 1 2 1 1 0 1					
305.28	710.	6.280	.2848	0.94		40	1	2 1 4 3 1 5 2 1 1 1		1			
305.22	710.	6.280	.2848	0.92		41	1	2 1 2 4 1 6 1 2 1 1					
305.22	711.	6.280	.2848	21.3		42	1	1 1 2 4 0 6 3 1 2 1					1
305.22	709.	6.280	.2848	1.00		43	1	1 2 3 4 0 6 1 2 1 1				1	
305.22	710.	6.285	.2849	0.95		44	1	2 2 2 3 1 6 1 2 1 2					
305.22	710.	6.275	.2852	21.4		45	1	1 0 2 5 1 5 2 1 2 1 1					1
305.25	710.	6.280	.2849	0.94		46		2 1 4 3 0 6 1 2 1 1	1				
305.19	710.	6.280	.2849	21.4		47	1	1 1 2 4 1 6 1 1 3 1					1
305.22	711.	6.280	.2849	21.4		48	1	1 1 2 4 0 6 3 1 2 1					1
305.22	709.	6.280	.2849	1.00		49	1	1 2 3 4 0 6 1 2 1 1				1	
305.22	710.	6.285	.2849	0.95		50	1	2 2 2 3 1 6 1 2 1 2					
305.22	710.	6.280	.2849	1.03	35	51	1	1 2 2 3 4 2 9 3 2 2 1 1 1				1	

* OPTIMIZATION REPEATED WITH SMALLER INCREMENTS FOR THE PSEUDO-PARAMETERS

TABLE IX-3

The PGC Enthalpy Predictions Compared with Smoothed Data
Using the Optimum Pseudo-critical Parameters for Ethane

TEMP. (DEG F) INLET	OUTLET	PRESS. (PSIA) INLET	OUTLET	ENTHALPY CHANGE EXP'TAL (BTU/LB)	CALC'D	DIFFERENCE BTU/LB	%
-246.00	-246.60	2000.00	0.0	235.58	236.79	-1.21	-0.51
-123.30	-123.30	2000.00	250.00	-5.07	-5.48	0.41	-8.00
-24.50	-24.50	2000.00	250.00	-2.44	-1.66	-0.78	31.93
125.00	125.00	750.00	0.0	53.66	53.27	0.39	0.73
125.00	125.00	2000.00	0.0	135.76	135.14	0.62	0.46
200.60	200.60	750.00	0.0	34.30	33.96	0.34	0.98
200.60	200.60	2000.00	0.0	101.24	101.33	-0.09	-0.09
60.00	63.00	500.00	500.00	102.82	103.64	-0.82	-0.79
82.00	98.00	713.00	713.00	62.73	61.19	1.54	2.46
170.00	200.60	2000.00	2000.00	29.39	29.45	-0.06	-0.20
-246.60	-246.60	2000.00	100.00	-6.15	-5.71	-0.44	7.19
-24.50	-24.50	2000.00	0.0	181.11	181.54	-0.43	-0.24
89.80	89.80	819.00	0.0	133.03	131.65	1.38	1.03
89.80	89.80	2000.00	0.0	148.57	148.00	0.57	0.38
125.00	125.00	250.00	0.0	13.36	12.94	0.42	3.17
125.00	125.00	1000.00	0.0	97.56	97.46	0.10	0.10
200.60	200.60	1500.00	0.0	80.24	80.45	-0.21	-0.26
300.00	300.00	1000.00	0.0	32.73	31.67	1.06	3.25
50.00	80.00	713.00	713.00	31.03	33.03	-2.00	-6.45
-123.30	-123.30	2000.00	0.0	205.26	206.04	-0.78	-0.38
89.80	89.80	500.00	0.0	37.20	35.78	1.42	3.81
89.80	89.80	1000.00	0.0	139.43	138.16	1.27	0.91
125.00	125.00	1250.00	0.0	121.55	120.76	0.79	0.65
300.00	300.00	500.00	0.0	15.73	15.34	0.39	2.50
125.00	125.00	1500.00	0.0	129.12	128.30	0.82	0.63
99.00	106.00	819.00	819.00	32.41	29.30	3.11	9.59
49.20	49.20	2000.00	700.00	3.64	2.83	0.81	22.33
60.00	60.00	2000.00	1000.00	6.38	6.72	-0.34	-5.35
80.00	80.00	1000.00	713.00	6.72	7.46	-0.74	-11.08
89.80	89.80	250.00	0.0	15.55	15.01	0.54	3.47
89.80	89.80	677.00	0.0	69.69	67.86	1.83	2.62
89.80	89.80	1500.00	0.0	145.16	145.05	0.11	0.08
300.00	300.00	2000.00	0.0	64.33	65.56	-1.23	-1.90
200.60	200.60	250.00	0.0	10.19	9.94	0.25	2.48
200.60	200.60	1000.00	0.0	48.90	48.51	0.39	0.80

AVERAGE ENTHALPY DIFFERENCE	72.0
STD. DEV. (BTU/LB)	1.03
TC (K)	305.22
PC (PSIA)	710.1
ALPHAC	6.28
ZC	0.2849

IX-1. Therefore, it is possible to conclude that, given sufficient, accurate and discriminating input data, the PGC optimization should provide selective and meaningful pseudo-critical parameters.

c) Pseudo-parameter Optimization for Mixtures. The pseudo-parameter optimization results for the mixtures belonging to the methane-ethane, ethane-propane and methane-propane systems are summarized in Column I of each table from Table IX-11 to Table IX-20, respectively. The results for the ternary mixture are indicated in Column I of Table IX-21. The PGC enthalpy predictions for each condition in the data set, the average value of the enthalpy difference, the standard deviation for the predicted enthalpy differences, and the optimum pseudo-parameters are all indicated for each mixture. As the interpretation of the calorimeteric measurements for the methane-ethane mixtures did not extend to the preparation of consistency checks or smoothed enthalpy tables, it was necessary to use the basic processed data for the determination of the optimum parameters in these cases.

With the exception of some mixtures belonging to the methane-propane system, the standard deviation in the enthalpy difference is below 1 Btu/lb, and suggests that the PGC is eminently suitable for correlating the enthalpy data on individual light hydrocarbon mixtures. The fact that the standard deviation for ethane is higher than for most mixtures examined may initially lead us to conclude either that the ethane data are of poorer quality, or that the PGC framework is perhaps better suited to represent mixture enthalpies. Such implications are false. The accurate prediction of the enthalpy change experienced by a pure component in the vicinity of the saturation line or the critical point is very taxing of any correlation. In the case of mixtures these areas are progressively removed from consideration as the two phase region excluded from the corresponding states analysis increases in size, resulting in a lower overall standard deviation.

The optimum pseudo-parameter for the methane-propane mixtures were not directly determined in this work from the data sets in Tables IX-16 through IX-20. The predictions in Column I for these tables correspond to a set of pseudo-critical parameters that were optimized by Powers [202] with respect to a different set of data selected by

Yesavage [284] that were confined only to enthalpy departures along isotherms. The standard deviation of these enthalpy departures as reported by Yesavage, and later confirmed by Powers using the PGC framework, was better than 1 Btu/lb for all mixtures belonging to the methane-propane system. This is generally better than the performance obtained for the same systems in this work.

Two reasons may be forwarded to explain such discrepancies. Firstly, although Yesavage and Powers used three times as much enthalpy data in optimizing the pseudo-parameters, the enthalpies of vaporization and the difficulty predictable single phase region in the immediate vicinity of the two phase envelope were not emphasized. Secondly, it is now believed that some of the isobaric enthalpy differences incorporated in the data sets of this work, and ignored by Powers and Yesavage, are in error. In the case of the 0.883 mole fraction methane-propane mixture, for example, (Table IX-17), such data resulted in deviations as high as 8.85 Btu/lb and were indirectly responsible for raising the standard deviation for the entire data set to 2.65 Btu/lb. Preliminary work with the original enthalpy tabulations of Mather [168] for the 0.946 mole fraction methane-propane mixture indicated similar trends which disappeared after the re-interpreted enthalpy values of Bhirud and Powers [22] for the same mixture were used. The predictions with respect to the latter set of enthalpy values are indicated in Table IX-16 and yield a very respectable standard deviation of 0.64 Btu/lb.

It must be emphasized, however, that the relatively high errors in the values of the enthalpy of vaporization for the methane-propane mixtures as tabulated by Mather [168] are primarily incurred in the estimation of the phase boundaries from the basic data and should not reflect on the established accuracy of the basic calorimetric measurements themselves.

It is strongly recommended that the critically chosen enthalpy differences in Tables IX-3, and IX-12 through IX-21 (except those values otherwise identified to be in error) be used in preference to isothermal enthalpy departures in evaluating enthalpy correlations.

Consistency Test for Examining the Validity of the One Fluid Corresponding States Principle

As indicated in Chapter V, if we are to assume that the one fluid model is applicable to mixtures, then Equations (V-12), (V-13) and (V-14) are all simultaneously valid. In this particular work, we have chosen to define the parameters Tc_m, Pc_m and ωc_m from enthalpy data using Equation (V-14) where f_H represents the PGC. Therefore, we may now, in particular, calculate B_m for each mixture over a range of temperatures for a specified function f_B. If the pure component second virial coefficients B_{ii} and B_{jj} are also known at each such temperature for a binary mixture, then Equation (V-1) may be utilized to specify the value of the unlike pair interaction virial coefficient B_{ij} at the same temperature. If the functions f_B and f_H, chosen to represent the reduced second virial coefficient and the reduced enthalpy departure, respectively, are accurate and if the pseudo-parameters that best satisfy Equations (V-12) and (V-14) simultaneously can be obtained from Equation (V-14) alone, and if the principle of corresponding states is valid for every mixture belonging to a given binary system, then the B_{ij} values so computed should be independent of composition at any specified temperature and should be identical to those obtained by direct measurement.

In this work the function f_B defined by Equation (V-30) is used to characterize the reduced second virial coefficients for both pure components and mixtures. As the equation is valid over the range $0.52 \leq Tr_{oo} \leq 3.26$, the B_m values for the 0.484 mole fraction methane-propane mixture can, for example, be computed over the approximate temperature range $151K \leq T \leq 945K$ given the optimum pseudo-critical parameters in column I of Table IX-19. The B values for methane and propane can also be calculated over the ranges 99K to 623K, and 192K to 1205K, respectively, using the same equation. Therefore, if we plan to calculate the methane-propane interaction virial coefficient $B_{ij}(i \neq j)$ from such information in conjunction with Equation (V-1), it is immediately clear that reliable estimates of B_{ij} can only be obtained over the restricted range $0.52\ Tc_{jj} \leq T \leq 3.26\ Tc_{ii}$, $(Tc_{ii} \leq Tc_{jj})$. This translates to an approximate temperature range from 192K to 623K for the methane-propane system. In effect, the range of validity of

the calculations is limited by the critical temperature ratio of the pure components in the mixture. In particular, the method is completely inapplicable if the ratio Tc_{jj}/Tc_{ii} exceeds 3.26/0.52 unless the range of validity of Equation (V-30) is further expanded.

In extending the technique to the calculation of B_m values for a multi-component mixture from Equation (V-1), the effective range over which reliable estimates of B_m may be obtained is still governed by the extreme pure components. In particular, reliable calculated values of B_m for the ternary mixture of this work are still confined to the range 192K to 623K. In practice, however, all calculations involving Equation (V-1) and (V-30) were restricted to the temperature range from 198.15K to 510K, at regular intervals of 25K. Calculations were also made at a few additional temperatures in this range for which independent direct measurements were available.

The B_{ij} values calculated in the above fashion for the mixtures belonging to the methane-ethane, ethane-propane, and methane-propane systems are summarized in Tables IX-4, IX-5 and IX-6, respectively, and include comparisons with direct measurements. These results are also illustrated in Figures IX-1, IX-2 and IX-3, respectively. The consistency between the B_{ij} values derived from enthalpy data for the two methane-ethane mixtures are believed to be within the limits of accuracy of the enthalpy data and the optimization procedure in each case. It is less likely that the differences between the enthalpy based and directly measured $B_{CH_4-C_2H_6}$ values can be similarly reconciled. The two data points of Hoover [108] at 215K and 240K which seem to differ from the enthalpy based B values are suspect because the ethane second virial coefficients used by Hoover in calculating the B_{ij} values for these two cases are believed to be in error as previously noted in Chapter V. The B_{ij} values obtained from direct measurement are distinctly lower in magnitude than those derived from enthalpy data.

The agreement between the B_{ij} values calculated from the enthalpy data for the 0.498 mole fraction ethane-propane mixture and the direct measurements of Dantzler et al. [59] is excellent (See Figure IX-2). The calculated B_{ij} values for the other mixtures are slightly more positive. Nevertheless, the agreement between the enthalpy based B_{ij}

TABLE IX-4

The Variation of the Calculated Interaction Virial Coefficient as a Function of Composition as a Measure of the Consistency Between the Pseudo-parameters for the Various Methane-Ethane Mixtures

T(°K)	B_{ij} Values in cc/gm mole Obtained by Interpretation of Enthalpy Data		Experimental B_{ij} Values				Selected Values* cc/gm mole
	.778 CH_4	.479 CH_4	GUNN [94]	DANTZLER ET AL[59]	GUGGENHEIM ET AL[173]	HOOVER [108]	
198.15	-198.69	-192.42					-198.69
223.15	-157.87	-153.69					-157.87
248.15	-127.69	-124.77					-127.69
273.16	-104.53	-102.42	-111.9		-109.0	-111.9	-104.53
298.15	-86.27	-84.71	-92.0	-93.	-90.		-86.27
310.90	-78.36	-77.02					-78.36
323.15	-71.50	-70.34	-75.6	-79.±5	-77.		-71.50
348.15	-59.32	-58.45		-68.±4			-59.32
373.15	-49.12	-48.47		-56.±4			-49.12
398.15	-40.45	-39.97					-40.45
423.15	-33.00	-32.65					-33.00
444.30	-27.48	-27.22					-27.48
473.15	-20.87	-20.71					-20.87
510.90	-13.53	-13.47					-13.53

TABLE IX-5

The Variation of the Calculated Interaction Virial Coefficient as a Function of Composition as a Measure of the Consistency Between the Pseudo-parameters for the Various Ethane-Propane Mixtures

T(°K)	B_{ij} Values in cc/gm mole Obtained by Interpretation of Enthalpy Data			Experimental B_{ij} Values	Selected Values* cc/gm mole
	.763 C_2H_6	.498 C_2H_6	.276 C_3H_8	DANTZLER ET AL[59]	
198.15	-600.06	-626.74	-602.14		-614.00
223.15	-468.73	-489.74	-470.04		-478.00
248.15	-377.04	-394.01	-377.53		-387.00
273.16	-309.80	-323.79	-309.56		-317.00
298.15	-258.63	-270.34	-257.74	-274.±11	-263.50
310.90	-236.98	-247.73	-235.79		-242.50
323.15	-218.42	-228.35	-216.97	-230.±11	-223.00
348.15	-186.11	-194.58	-184.15	-193.±11	-189.50
373.15	-159.63	-166.91	-157.26	-165.±11	-163.00
398.15	-137.57	-143.86	-134.85		-140.00
423.15	-118.91	-124.37	-115.91		-120.00
444.30	-105.25	-110.10	-102.03		-106.00
473.15	-89.14	-93.28	-85.67		-90.00
510.90	-71.52	-74.87	-67.77		-70.00

* Selected for application in mixing rules VII, IX and X of Table IX-5.

TABLE IX-6

The Variation of the Calculated Interaction Virial Coefficient as a Function of Composition as a Measure of the Consistency Between the Pseudo-parameters for the Various Methane-Propane Mixtures

T(°K)	$B_{CH_4-C_3H_8}$ Values in cm^3/gm mole Obtained by Interpretation of Enthalpy Data					Experimental $B_{CH_4-C_3H_8}$ Values			*Selected Values cc/gm mole
	.948 CH_4	.883 CH_4	.720 CH_4	.484 CH_4	.234 CH_4	MICHELS ET AL.[173]	DANTZLER ET AL.[59]	GUNN [94]	
198.15	-289.24	-290.60	-277.41	-264.86	-236.10				-277.41
223.15	-229.42	-231.36	-223.11	-216.02	-196.81				-223.11
248.15	-185.39	-187.57	-182.20	-178.13	-164.33				-182.20
273.16	-151.74	-154.01	-150.44	-148.10	-137.65				-150.44
298.15	-125.26	-127.57	-125.18	-123.85	-115.54	-136.	-139.±12		-125.18
310.90	-113.82	-116.14	-114.21	-113.24	-105.70			-122.5	-114.21
323.15	-103.90	-106.22	-104.66	-103.96	-97.02	-114.	-116.±12		-104.66
348.15	-86.34	-88.65	-87.69	-87.42	-81.44	-93.	-93.±12		-87.69
373.15	-71.66	-73.95	-73.44	-73.48	-68.23	-81.	-75.±10		-73.44
398.15	-59.21	-61.49	-61.32	-61.56	-56.88			-55.1	-61.32
423.15	-48.53	-50.80	-50.90	-51.27	-47.01			-34.8	-50.90
444.30	-40.61	-42.87	-43.15	-43.61	-39.64				-43.15
473.15	-31.16	-33.41	-33.88	-34.43	-30.76				-33.88
510.90	-20.69	-22.92	-23.59	-24.20	-20.84				-23.59

* Selected for application of mixing rules VII, IX and X of Table IX-10

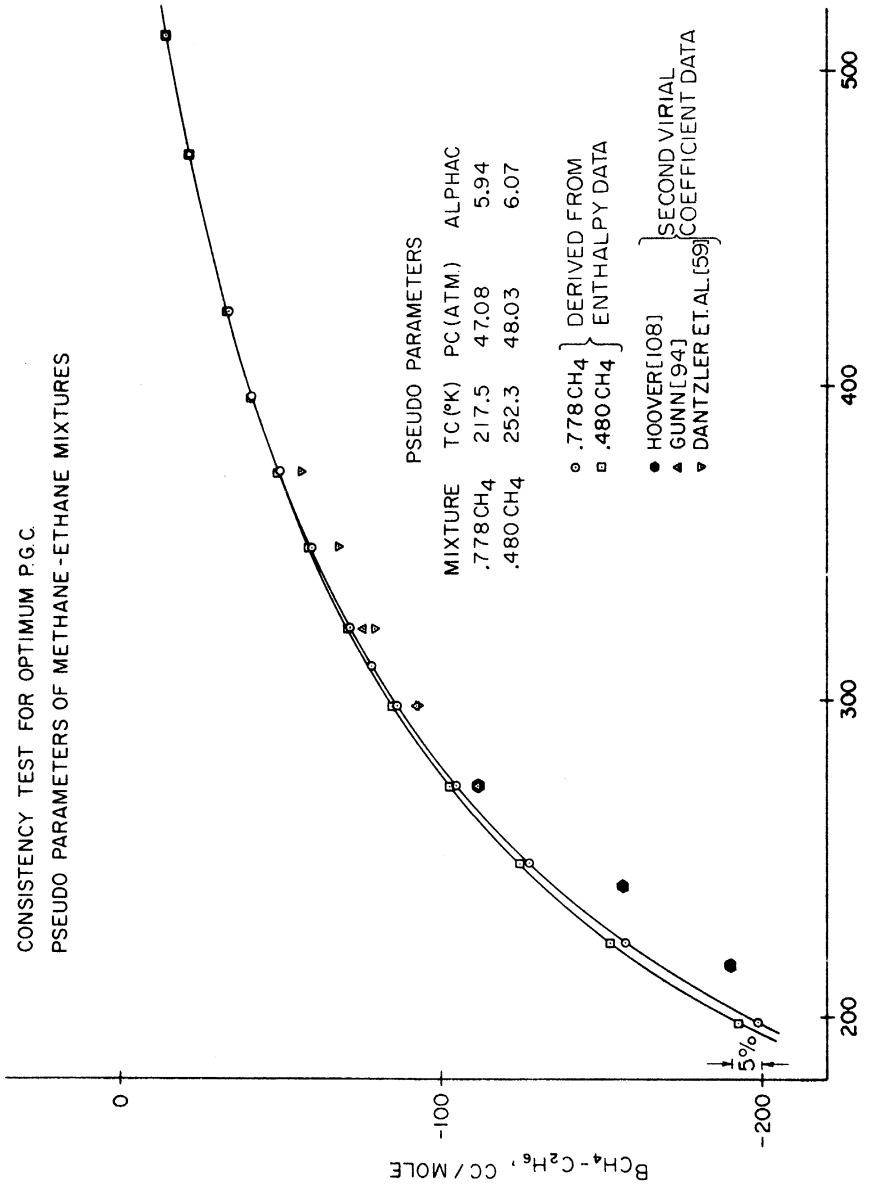

Figure IX-1. The Use of the Interaction Second Virial Coefficient as a Measure of the Ability of the Corresponding States Principle to Correlate the Thermodynamic Properties of the Methane-Ethane System.

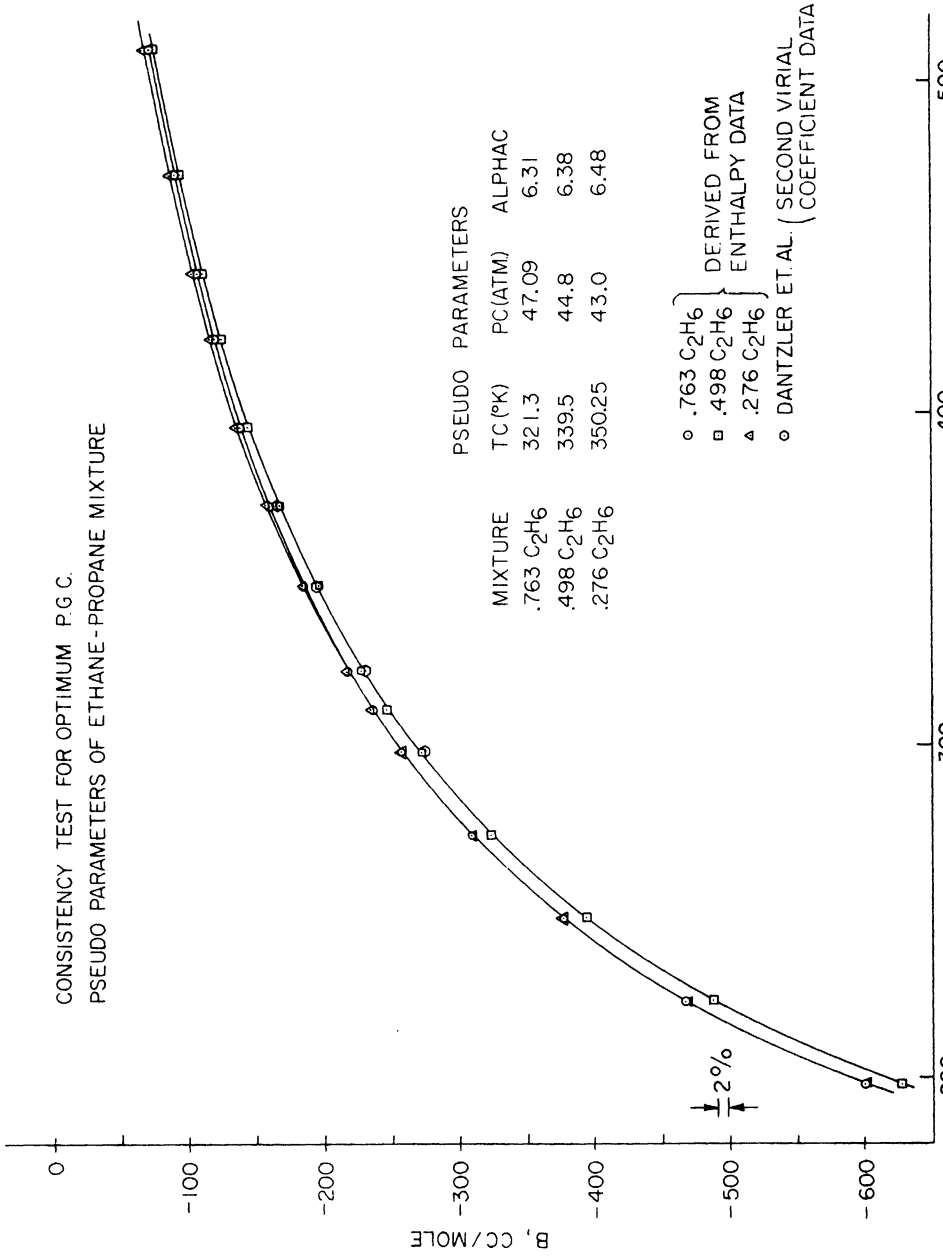

Figure IX-2. The Use of the Interaction Second Virial Coefficient as a Measure of the Ability of the Corresponding States Principle to Correlate the Thermodynamic Properties of the Ethane-Propane System.

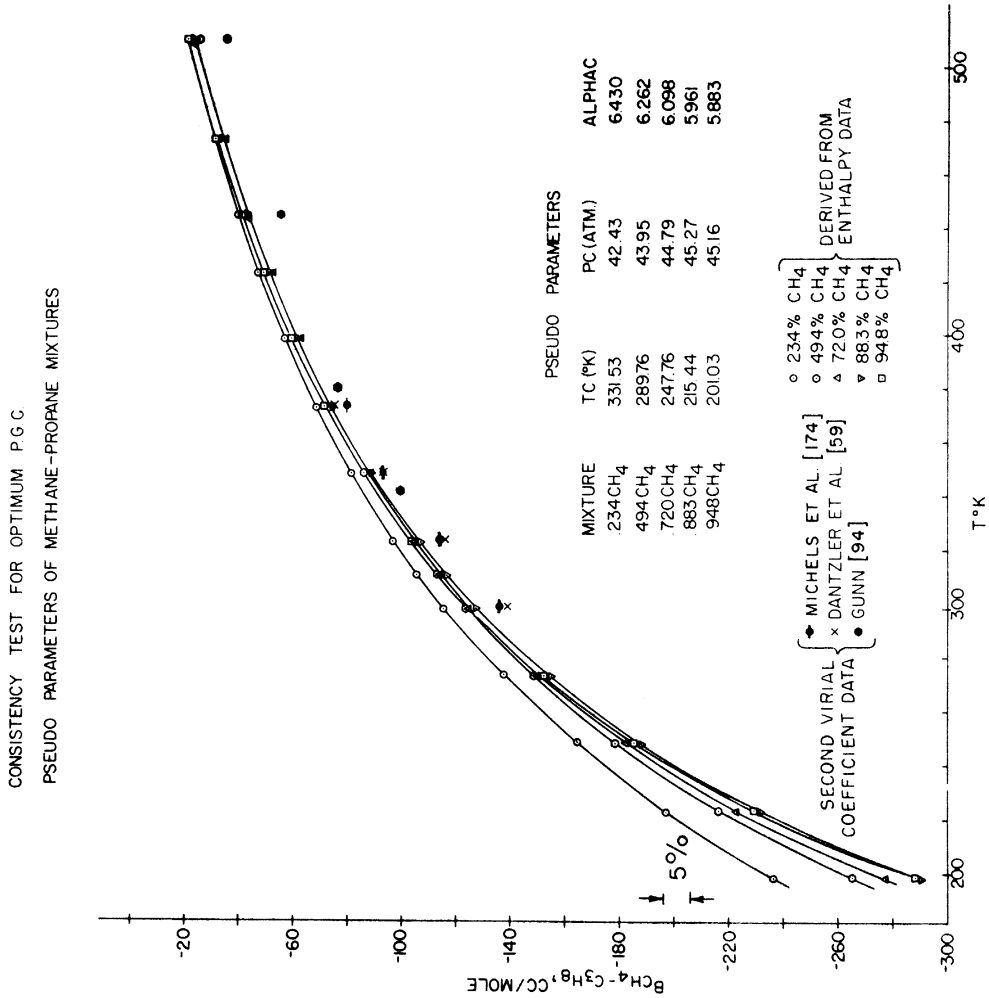

Figure IX-3. The Use of the Interaction Second Virial Coefficient as a Measure of the Ability of the Corresponding States Principle to Correlate the Thermodynamic Properties of the Methane-Propane System.

values is, on a percentage basis, considerably better than that obtained for the methane-ethane mixtures at the lower temperatures. The reverse is true at higher temperatures.

A similar analysis for the five mixtures belonging to the methane-propane system as seen in Figure IX-3 reveals a significant lack of consistency between the B_{ij} values for the individual mixtures. In general, the calculated B_{ij} values become less negative as the mole fraction of propane increases. Again, the experimental B_{ij} values are more negative than the enthalpy based values. The high temperature results of Gunn [94] appear to be somewhat inconsistent with the values of Michels et al. [174] and Dantzler et al. [59] at lower temperatures and are believed to be less accurate than the latter.

The B_{ij} values for the 0.234 mole fraction methane-propane mixture appear to be much more positive than the rest. It is conceivable that the pseudo-parameters for this particular mixture are not truly optimum as they were not obtained from the carefully chosen data sets in Tables IX-16 through IX-20. For example, the low B_{ij} values could have resulted if the "optimum" value of RTc_m/Pc_m for the mixture was underestimated.

To ensure that the calculated B_{ij} values were not influenced by any errors introduced by using Equation (V-30) to calculate B_m, B_{ii} and B_{jj}, a further analysis was undertaken. As seen in Table J-3, the methane second virial coefficient data from different reliable sources are in excellent agreement with the predictions from Equation (V-30) down to about 190K. The propane data of Kapallo [122,123] and Kunz [136] were subjectively emphasized in relation to the measurements of Brewer [28] and McGlashan et al. [159] in defining the αc dependence of the correlation at low temperatures. Considering the possibility that the latter measurements might be more accurate than the former, the αc dependence of the correlation was redefined by focusing instead on the data of Brewer and McGlashan et al. The sample calculation in Appendix F-6 in this regard, and the results of Table F-3 show that even though the discrepancy between the enthalpy based and directly measured B_{ij} values is slightly decreased, the consistency between the enthalpy based B_{ij} values for the individual mixtures shows no improvement. This analysis therefore suggests that the inaccuracies

in the reduced second virial coefficient correlation are not instrumental in causing the observed inconsistencies.

The consistency tests for the three binary systems suggest that the application of the corresponding states principle to mixtures is apt to be less successful as the size and energy parameter ratios for the constituent pure components depart from unity. In particular, the results hint that a set of pseudo-parameters that are optimal for the representation of a given configurational property such as the enthalpy departure, may be less suitable when applied to the estimation of other thermodynamic properties for the same system.

The Selection of Mixing Rules for This Investigation

Although the enthalpies for the individual mixtures of this study appear to be adequately correlated within the PGC framework, we would now like to determine whether the enthalpies for each of the binary systems that constitute the ternary mixtures can be satisfactorily characterized as a function of composition given enthalpy data on a few selected mixtures.

The most concise approach to the problem is to examine various mixing rules that compute the pseudo-parameters as a function of composition for each binary system investigated. A knowledge of the enthalpy behaviour and the optimum pseudo-parameters for each of the selected mixtures of this investigation can serve to evaluate the performance of the mixing rule examined.

The mixing rules examined in this chapter are summarized in Table IX-10. These include the more popular recipes discussed in Chapter IV and other rules developed in Chapter V. All rules except VI and VIII are set up to allow empirical adjustment of the unlike pair interaction parameters. Originally, the Pitzer-Hultgren rules (II) prescribed a quadratic mixing rule for the acentric factor ω_m but the linear relationship between ω and αc as given by Equation (III-32) suggests that the quadratic mixing rule for αc_m used in this work is essentially equivalent. This mixing rule for αc_m is also used to supplement rules III, IV, and V which, strictly speaking, apply only to the two parameter case.

Rules V, VII, IX and X are all developed in this work. The

basis for each of these rules is explained in Chapter V. Rules VII, IX and X each require B_m values for the given mixture to be provided over a range of temperatures. Rule VII uses these B_m values in conjunction with Equation (V-30) to optimize the value of Tc_m alone. The values of RTc_m/Pc_m and αc_m are predetermined by application of the high temperature mixing rule of Equation (V-38) and the quadratic mixing rule for αc_m, respectively. Rule X optimized both Tc_m and RTc_m/Pc_m from the set of B_m values but defines αc_m from the quadratic rule. Rule IX also optimizes Tc_m and RTc_m/Pc_m but instead presupposes that the optimum value of αc_m for the mixture is somehow known. Therefore, in the strictest sense, it is not a true prediction method. Nevertheless, the various approaches permit us to study the influence of the precise choice of αc_m on the optimized values of Tc_m and Pc_m from a given set of B_m values. By examining Rules VII, IX and X we are, in effect, evaluating different compromises to circumvent the practical difficulty of unequivocally defining three pseudo-critical parameters from B_m data over a limited range of temperatures.

Calculation of Optimum Binary Interaction Parameters for Several Mixing Rules

The enthalpy data on each of the constituent binaries of the ternary mixture can now be used to specify an optimum set of the appropriate unlike pair interaction parameters for each mixing rule in Table IX-10 except rules VI and VIII for which the parameters are independently defined from approximations involving pure component critical properties. There are two procedures for accomplishing this objective.

In the first approach, the enthalpy data for all mixtures belonging to a given binary system are simultaneously utilized in optimizing the interaction parameters for each mixing rule. In the second case, the interaction parameters are adjusted to yield the best fit to the pseudo-parameters obtained by optimizing the enthalpy data for each mixture taken separately. The two procedures are equivalent only if the unlike pair interaction parameters for a binary system are characterized from enthalpy data on a single mixture.

When data are available on more than one mixture, then the first

procedure is the more reliable. It is, however, unquestionably more demanding of computer time because not only must all the mixture data for a given binary system be collectively used in the optimization of the interaction parameters, but the optimization process must also be separately repeated for all but two of the mixing rules examined in this work. The second procedure allows us to accomplish our objective given only the optimum pseudo-parameters in Column I of Tables IX-11 through IX-21, and was therefore used in this work.

For example, using the second technique, the optimum value of RTc_{ij}/Pc_{ij}, $i \neq j$, for the Redlich-Kwong mixing rule (III) can be determined from the optimum pseudo-parameters for each of the three ethane-propane mixtures by minimizing the quantity

$$\sum_{k=1}^{k=3} \left[w_k \left(\frac{RTc_m}{Pc_m} \right)_k - (x_2)_k^2 \left(\frac{RTc_{22}}{Pc_{22}} \right) - (x_3)_k^2 \left(\frac{RTc_{33}}{Pc_{33}} \right) - 2(x_2)_k (x_3)_k \left(\frac{RTc_{23}}{Pc_{23}} \right) \right] \qquad \text{(IX-1)}$$

where w_k is a subjectively defined weighting factor for the optimum pseudo-parameters (RTc_m/Pc_m) for the kth mixture which accounts for relative differences in the quality of the enthalpy data and the estimated reliability of the optimum pseudo-parameters, and x_{2_k}, x_{3_k} are the ethane and propane mole fractions, respectively, for the kth mixture. The value of (RTc_m/Pc_m) for each of the three mixtures is obtained from column I of Tables IX-13 through IX-15, respectively. The values of (RTc_{22}/Pc_{22}) and (RTc_{33}/Pc_{33}) for the pure components ethane and propane, respectively, are defined in Table J-1.

The interaction parameter RTc_{23}/Pc_{23} for the Redlich-Kwong rule can also be determined for each mixture separately using the relation

$$\left(\frac{RTc_{23}}{Pc_{23}} \right)_k = \frac{\left(\frac{RTc_m}{Pc_m} \right)_k - (x_2)_k^2 \left(\frac{RTc_{22}}{Pc_{22}} \right) - (x_3)_k^2 \left(\frac{RTc_{33}}{Pc_{33}} \right)}{2 x_{2_k} x_{3_k}} \qquad \text{(IX-2)}$$

Therefore, by making use of Equation (IX-2) we may instead minimize the quantity

$$\sum_{k=1}^{k=3} w_k (x_2)_k (x_3)_k \left[\left(\frac{RTc_{23}}{Pc_{23}} \right)_k - \left(\frac{RTc_{23}}{Pc_{23}} \right)_{Opt.} \right]^2 \qquad \text{(IX-3)}$$

to specify the optimum value of RTc_{23}/Pc_{23} from the values calculated

for each of the k mixtures taken separately. Thus, in the general case, the optimum interaction parameters $(RTc_{ij}/Pc_{ij})_{Opt}$, $(RTc^2_{ij}/Pc_{ij})_{Opt}$ and $(\alpha c_{ij})_{Opt}$ for the Redlich-Kwong rule are defined by minimizing the quantities

$$\sum_{k=1}^{p} w_k (x_i)_k (x_j)_k \left[\left(\frac{RTc_{ij}}{Pc_{ij}} \right)_k - \left(\frac{RTc_{ij}}{Pc_{ij}} \right)_{Opt.} \right]^2 \quad i \neq j \qquad \text{(IX-4)}$$

$$\sum_{k=1}^{p} w_k (x_i)_k (x_j)_k \left[\left(\frac{RTc^2_{ij}}{Pc_{ij}} \right)_k - \left(\frac{RTc^2_{ij}}{Pc_{ij}} \right)_{Opt.} \right]^2 \quad i \neq j \qquad \text{(IX-5)}$$

$$\sum_{k=1}^{p} w_k (x_i)_k (x_j)_k [(\alpha c_{ij})_k - \alpha c_{Opt.}]^2 \qquad \text{(IX-6)}$$

for the p mixtures for a given binary system taken together. Similar criteria may be used to specify the interaction pseudo-parameters for rules II, IV and V in Table IX-10, respectively.

Although the final results are entirely equivalent, the forms represented by (IX-4), (IX-5) and (IX-6) were preferred to the form (IX-1) for specifying the optimum interaction parameters for the Redlich-Kwong rule (III) because the variation in the interaction parameters as a function of composition is obtained in the first case and serves as a measure of the ability of the rule to represent the entire binary system. The forms specified by (IX-4) through (IX-6) also illustrate that the interaction parameters calculated for each mixture must be weighted with respect to the composition product $x_i x_j$ to best define its optimum value.

Although each mixture of components i and j provides us with a B_{ij} values at each of the fourteen specified temperatures from 198.15K to 510K, rules VII, IX and X require us to specify a single B_{ij} value for the whole system at each temperature. The averaging of the B_{ij} values could have been achieved in a fashion similar to that illustrated for the Redlich-Kwong rule by minimizing the quantity

$$\sum_{k=1}^{p} w_k (x_i)_k (w_j)_k \left[(B_{ij})_k - (B_{ij})_{Opt.} \right]^2 \qquad \text{(IX-7)}$$

instead at each selected temperature. However, such an averaging procedure would have totally ignored the B_{ij} data obtained from volumetric measurements. In actual practice the final set of B_{ij} values were

selected by visual examination of the data in each figure from Figure IX-1 through IX-3. In general, more weight was given to the mixtures whose B_{ij} values were closer to those obtained from direct measurement. Consequently, it is to be anticipated that the use of such values may sacrifice the goodness of fit to the enthalpy data for the binary systems in question to yield some improvement in the fit to low pressure volumetric measurements.

The final selected set of B_{ij} values for the methane-ethane, the ethane-propane and the methane-propane systems are also presented in Tables IX-4, IX-5 and IX-6, respectively. The final B_{ij} values for the methane-ethane system were selected to correspond to those for the 0.778 mole fraction methane-ethane mixture. The B_{ij} values for the ethane-propane system were obtained by averaging the results for all three mixtures. In retrospect this was a poor choice, and the results for the 0.498 mole percent mixture should have been weighted more heavily as they agree very well with the second virial coefficient data of Dantzler et al. [59]. The final B_{ij} values for the methane-propane system were selected to correspond to those for the 0.72 mole fraction methane-propane mixture. The results for the 0.234 mole fraction methane-propane mixture were effectively ignored in view of the observed discrepancy with the results for the other mixtures.

The calculated values of the interaction pseudo-parameters for mixing rules II, III, IV and V as a function of composition for the methane-ethane, the ethane-propane and the methane-propane systems are presented in Tables IX-7 through IX-9. The value of the parameter (RTc_{ij}/Pc_{ij}) determined for Rule VII using Equation (V-41) is also indicated. The value of αc_{ij} used in the equation is independently obtained from the quadratic mixing rule for αc_m. Unlike other mixing rules, the function g in Equation (V-4) also varies with reduced temperature T/Tc_{ij}. The temperature of application of the rule must be such that $8.0 \leq Tr_{ij} \leq 30$ for all i,j as explained earlier (See page 131), and should not be confused with the actual temperature at which enthalpy predictions are desired.

A sample calculation of RTc_{ij}/Pc_{ij} and αc_{ij} for Rule VII using the optimum pseudo-parameter for the 0.498 mole fraction ethane-propane

TABLE IX-7

The Calculated Interaction Parameters for Rules II, III, IV, V and VII
of Table IX-10 as a Function of Composition for the Methane-Ethane System

Rule	Code (Table IX-10)	.778 CH4(CH4-C2H6)				.479 CH4(CH4-C2H6)				WEIGHTED AVERAGE			
		TC_{ij} (°K)	$(R*TC/PC)_{ij}$ CC/MOL	PC_{ij} ATM	$ALPHAC_{ij}$	TC_{ij} (°K)	$(R*TC/PC)_{ij}$ CC/MOL	PC_{ij} ATM	$ALPHAC_{ij}$	TC_{ij} (°K)	$(R*TC/PC)_{ij}$ CC/MOL	PC_{ij} ATM	$ALPHAC_{ij}$
PITZER-HULTGREN	II	251.9	420.5	49.16	6.102	251.9	422.1	48.96	6.074	251.9	421.3	49.07	6.080
VAN DER WAAL	III	240.9	423.9	46.64	6.102	240.6	423.6	46.62	6.074	240.75	423.7	46.63	6.080
REDLICH-KWONG	IV	236.9	424.6	45.78	6.102	236.3	424.0	45.74	6.074	236.6	424.3	45.76	6.080
MOD. VAN DER WAAL	V	240.7	425.6	46.40	6.102	240.5	425.9	46.35	6.074	240.6	425.8	46.38	6.080
THIS WORK	VII	234.6	422.2	45.60	6.102	231.9	422.8	45.00	6.074	233.3	423.5	45.20	6.080
ARITHMETIC MEAN											424.6		6.047
GEOMETRIC MEAN										241.3			
HARMONIC MEAN										234.8			

TABLE IX-8

The Calculated Interaction Parameters for Rules II, III, IV, V and VII
of Table IX-10 as a Function of Composition for the Ethane-Propane System

Rule	Code (Table IX-10)	.763 C2H6(C2H6-C3H8)				.498 C2H6(C2H6-C3H8)				.276 C2H6(C2H6-C3H8)				WEIGHTED AVERAGE			
		TC_{ij} (°K)	$(R*TC/PC)_{ij}$ CC/MOL	PC_{ij} ATM	$ALPHAC_{ij}$	TC_{ij} (°K)	$(R*TC/PC)_{ij}$ CC/MOL	PC_{ij} ATM	$ALPHAC_{ij}$	TC_{ij} (°K)	$(R*TC/PC)_{ij}$ CC/MOL	PC_{ij} ATM	$ALPHAC_{ij}$	TC_{ij} (°K)	$(R*TC/PC)_{ij}$ CC/MOL	PC_{ij} ATM	$ALPHAC_{ij}$
PITZER-HULTGREN	II	339.3	604.2	46.09	6.331	341.2	628.9	44.52	6.350	330.0	630.9	43.31	6.440	338.0	625.0	44.38	6.380
VAN DER WAAL	III	334.9	595.2	46.17	6.331	336.4	622.3	44.36	6.350	328.0	625.5	43.03	6.440	332.0	618.0	44.09	6.380
REDLICH-KWONG	IV	333.7	599.0	45.71	6.331	335.2	621.9	44.23	6.350	326.5	625.5	42.83	6.440	331.0	618.0	43.95	6.380
MOD. VAN DER WAAL	V	334.3	602.3	46.17	6.331	336.0	624.5	44.15	6.350	328.0	623.3	43.19	6.440	331.6	620.0	43.19	6.380
THIS WORK	VII	332.2	597.0	45.67	6.331	333.3	618.2	44.24	6.350	321.8	634.9	41.59	6.440	331.0	612.0	44.38	6.380
ARITHMETIC MEAN															615.7		6.407
GEOMETRIC MEAN														336.1			
HARMONIC MEAN														334.6			

TABLE IX-9

The Calculated Interaction Parameters for Rules II, III, IV, V and VII of Table IX-10 as a Function of Composition for the Methane-Propane System

Rule	Code (Table IX-10)	.948 CH4(CH4-C3H8) T_{Cij} (°K)	.948 CH4(CH4-C3H8) $(R*TC/PC)_{ij}$ CC/MOL	.948 CH4(CH4-C3H8) P_{Cij} ATM	.948 CH4(CH4-C3H8) $ALPHAC_{ij}$	.883 CH4(CH4-C3H8) T_{Cij} (°K)	.883 CH4(CH4-C3H8) $(R*TC/PC)_{ij}$ CC/MOL	.883 CH4(CH4-C3H8) P_{Cij} ATM	.883 CH4(CH4-C3H8) $ALPHAC_{ij}$	.72 CH4(CH4-C3H8) T_{Cij} (°K)	.72 CH4(CH4-C3H8) $(R*TC/PC)_{ij}$ CC/MOL	.72 CH4(CH4-C3H8) P_{Cij} ATM	.72 CH4(CH4-C3H8) $ALPHAC_{ij}$
PITZER-HULTGREN	II	290.6	605.0	39.41	6.439	298.6	563.4	43.49	6.455	297.4	554.2	44.03	6.369
VAN DER WAAL	III	254.0	574.8	36.27	6.439	262.3	559.1	38.50	6.455	264.6	551.8	39.34	6.369
REDLICH-KWONG	IV	247.2	570.6	35.54	6.439	254.2	552.9	37.73	6.455	255.8	546.0	38.45	6.369
MOD. VAN DER WAAL	V	252.6	577.9	35.87	6.439	261.3	558.1	38.42	6.455	263.6	552.6	39.15	6.369
THIS WORK	VII	248.6	538.5	37.89	6.439	252.4	527.1	39.29	6.455	248.6	530.2	38.48	6.369

Rule	Code (Table IX-10)	.50 CH4(CH4-C3H8) T_{Cij} (°K)	.50 CH4(CH4-C3H8) $(R*TC/PC)_{ij}$ CC/MOL	.50 CH4(CH4-C3H8) P_{Cij} ATM	.50 CH4(CH4-C3H8) $ALPHAC_{ij}$	.234 CH4(CH4-C3H8) T_{Cij} (°K)	.234 CH4(CH4-C3H8) $(R*TC/PC)_{ij}$ CC/MOL	.234 CH4(CH4-C3H8) P_{Cij} ATM	.234 CH4(CH4-C3H8) $ALPHAC_{ij}$	WEIGHTED AVERAGE T_{Cij} (°K)	WEIGHTED AVERAGE $(R*TC/PC)_{ij}$ CC/MOL	WEIGHTED AVERAGE P_{Cij} ATM	WEIGHTED AVERAGE $ALPHAC_{ij}$
PITZER-HULTGREN	II	297.1	553.5	44.04	6.335	290.2	559.1	42.6	6.310	295.0	560.0	43.22	6.350
VAN DER WAAL	III	268.1	550.9	39.94	6.335	265.6	560.3	38.90	6.310	264.0	555.0	39.03	6.350
REDLICH-KWONG	IV	258.5	545.4	38.89	6.335	254.3	553.8	37.69	6.310	255.0	549.0	38.11	6.350
MOD. VAN DER WAAL	V	267.2	551.9	39.73	6.335	264.5	558.3	38.80	6.310	263.1	558.0	38.69	6.350
THIS WORK	VII	244.9	535.2	37.55	6.335	232.9	550.9	34.70	6.310	244.0	540.0	37.08	6.350
ARITHMETIC MEAN											508.6		6.180
GEOMETRIC MEAN										265.6			
HARMONIC MEAN										251.7			

mixture is illustrated in Appendix F-7, part 3. It is established there that the rule may be applied at any temperature between 2960K and 5720K for any system with methane and propane as the extreme components. In this work a temperature of 5000K was arbitrarily selected for the calculation. However, the temperature dependence of the function g(αc, Tr) is very weak, and additional calculations at 4000K and 6000K showed negligible changes ($\leq$ 0.2K) in the computed value of RTc_{ij}/Pc_{ij}. The results of Table IX-7 through IX-9 indicate that the variation in the interaction parameters Tc_{ij} and RTc_{ij}/Pc_{ij} with composition is minimal for the Redlich-Kwong rule (III), although the performance of the other rules is only slightly inferior. More significantly, we note that the calculated values of the interaction parameters for a given mixture vary from rule to rule. The Redlich-Kwong Tc_{ij} for example is almost always lower than for the Van der Waal (IV) case. The Tc_{ij} value for the modified Van der Waal rule (V) lies in between the two but is closer to the Van der Waal result. The value of RTc_{ij}/Pc_{ij} for the modified Van der Waal rule (V) is usually higher than for the Redlich-Kwong rule. The Pitzer-Hultgren (II) interaction constant Tc_{ij} is considerably different from values calculated for the rest of the rules in the case of the methane-propane system. This is not surprising as the interaction parameters for the rule have no theoretical value and are merely empirical constants.

In summary, the analysis of the results for Rules III, IV and V indicate that considerable caution is to be exercised in applying empirically obtained interaction parameters from the literature to a particular mixing rule if a different rule is used to specify these parameters from experimental measurements.

The geometric and harmonic mean assumptions for Tc_{ij} suggested by Equation (IV-19) with k_{ij} equal to 1.0, and by Equation (IV-20), respectively, and the arithmetic mean assumption for αc_{ij} and RTc_{ij}/Pc_{ij} (the latter being expressed by Equation (IV-18)) are also included in Tables IX-7 through IX-9 for comparison purposes as they are frequently used with various mixing rules in the absence of binary data. The effectiveness of these assumptions depends on the mixing rule with which they are used. The geometric mean rule for

TABLE IX-10

Summary of Mixing Rules Examined in This Investigation for the Calculation of Pseudoparameters

Code	Rules	Designation
I	PGC optimized pseudo-parameters using enthalpy data for individual mixtures	Optimum
II	$Pc_m = \sum_j \sum_i x_i x_j \, Pc_{ij}$	
	$Tc_m = \sum_j \sum_i x_i x_j \, Tc_{ij}$	Pitzer-Hultgren
	$\alpha c_m = \sum_j \sum_i x_i x_j \, \alpha c_{ij}$	
III	$\frac{RTc_m}{Pc_m} = \sum_j \sum_i x_i x_j \frac{RTc_{ij}}{Pc_{ij}}$	
	$\frac{RTc_m}{Pc_m^{2.5}} = \sum_j \sum_i x_i x_j \frac{RTc_{ij}}{Pc_{ij}^{2.5}}$	Redlich-Kwong
	$\alpha c_m = \sum_j \sum_i x_i x_j \, \alpha c_{ij}$	
IV	$Vc_m = \sum_i \sum_j x_i x_j \, Vc_{ij}$	
	$Tc_m \, Vc_m = \sum_i \sum_j x_i x_j \, Tc_{ij} \, Vc_{ij}$	Van der Waal
	$\alpha c_m = \sum_i \sum_j x_i x_j \, \alpha c_{ij}$	

TABLE IX-10 (contd.)

V

$$\left(\frac{RTc_m}{Pc_m}\right)\left(\frac{\alpha c_m - 2}{\alpha c_m^2}\right) = \sum_i \sum_j x_i x_j \frac{RTc_{ij}}{Pc_{ij}} \left(\frac{\alpha c_{ij} - 2}{\alpha c_{ij}^2}\right)$$

$$\left(\frac{RTc_m^2}{Pc_m}\right)\left(\frac{[\alpha c_m - 1]^3}{\alpha c_m^4}\right) = \sum_i \sum_j x_i x_j \left(\frac{RTc_{ij}^2}{Pc_{ij}}\right)\left(\frac{[\alpha c_{ij} - 1]^3}{\alpha c_{ij}^4}\right)$$

Modified Van der Waal (This Work)

$$\alpha c_m = \sum_i \sum_j x_i x_j \alpha c_{ij}$$

VI

$$Pc_m = \sum_i x_i Pc_{ii}$$

$$Tc_m = \sum_i x_i Tc_{ii}$$

Kay

$$\alpha c_m = \sum_i x_i \alpha c_{ii}$$

VII

$$\alpha c_m = \sum_i \sum_j x_i x_j \alpha c_{ij}$$

$$\frac{RTc_m}{Pc_m} = \sum_i \sum_j x_i x_j \left[\frac{RTc_{ij}}{Pc_{ij}}\right][h_r(\alpha c_{ij})][g_r(\alpha c_{ij}, Tr_{ij})]$$

where

$$hr(\alpha c_{ij}) = \frac{0.15903 + 0.0588\ (\alpha c_{ij} - 5.82)}{0.15903 + 0.0588\ (\alpha c_m - 5.82)}$$

$$gr(\alpha c_{ij}, Tr_{ij}) = \frac{g(\alpha c_{ij}, Tr_{ij})}{g(\alpha c_m, Tr_m)}$$

$$g(\alpha c_{ij}, Tr_{ij}) = 0.3517 + 1.5068\left[\frac{Tr_{ij}}{18} \cdot f(\alpha c_{ij})\right] - 1.11739\left[\frac{Tr_{ij}}{18} \cdot f(\alpha c_{ij})\right]^2 + 0.25874\left[\frac{Tr_{ij}}{18} \cdot f(\alpha c_{ij})\right]^3,\ 8.0 \leq Tr_{ij} \leq 30 \text{ all } i,j$$

TABLE IX-10 (contd.)

$$f(\alpha c_{ij}) = 1.0 + 0.189\ (\alpha c_{ij} - 5.82)$$

Tc_m is obtained by minimizing the function

$$\sum_{k=1}^{1} [Br_m - F[(Tr_{oo})_m]^2$$

over a selected set of temperatures, $T_1 \ldots T_k \ldots T_1$.

where

$$F[Tr_{oo}] = 0.14416 + 0.49095\ [1 - \exp\ (\frac{0.68511}{Tr_{oo}})] + (\alpha c_m - 5.82)[0.0175 - \frac{0.0220}{Tr_{oo}} - \frac{0.00614}{Tr_{oo}^2} + \frac{0.00281}{Tr_{oo}^3}]$$

$(Tr_{oo})_m$ is defined by the relation

$$-\phi\ (Tr_m) - [\alpha c_m - 7.0][\Psi(Tr_m)] = -\phi\ (Tr_{o_m}) - [5.82 - 7.0][\Psi(Tr_{o_m})]$$

where the functions ϕ and Ψ are defined in Equations III-36 Through III-36c

$$Br_m(T_k) = \frac{\sum \sum x_i x_j B_{ij}\ (T_k)}{RTc_m/Pc_m}$$

For i=j, $B_{ij}(T_k) = (\frac{RTc_{ij}}{Pc_{ij}})\ [F(Tr_{oo})_{ij}]_{T=T_k}$

For i≠j, $B_{ij}(T_k)$ values are independantly obtained from binary mixture data.

TABLE IX-10 (contd.)

VIII Same as IV with

$$Tc_{ij} = (Tc_{ii}\ Tc_{jj})^{1/2}$$

$$Vc_{ij} = \left[\frac{Vc_{ii}^{1/3} + Vc_{jj}^{1/3}}{2}\right]^3$$

$$\alpha c_{ij} = (\alpha c_{ii} + \alpha c_{jj})/2$$

Van der Waal with Lorentz-Berthelot approximations

IX αc_m assumed to be independantly known, i.e., from rule I

$\frac{RTc_m}{Pc_m}$ and Tc_m are then simultaneously obtained

by minimization of the function

$$\sum_{k=1}^{1} \left\{ Br_m - F[(Tr_{oo})_m] \right\}^2$$

using the same procedure as in rule VII

X $$\alpha c_m = \sum_i \sum_j x_i x_j\ \alpha c_{ij}$$

$\frac{RTc_m}{Pc_m}$ and Tc_m obtained as in rule IX

Tc_{ij} is best suited to the Van der Waal rule (IV), while the harmonic mean rule for Tc_{ij} is preferable when used in conjunction with the Redlich-Kwong mixing rule. For the methane-propane system, the arithmetic mean rules for (RTc_{ij}/Pc_{ij}) and αc_{ij} yield values that are considerably lower than those calculated by the rules examined in Table IX-9. The agreement is better for the methane-ethane and the ethane-propane systems. It is therefore safe to conclude that the effectiveness of these two rules decreases as the differences in the size and energy parameters for the constituent pure components of a binary mixture increase.

The Evaluation of the Mixing Rules of Table IX-10

Having specified the optimum values of the interaction parameters, the pseudo-critical parameters for each of the mixtures investigated in this work can now be recalculated for every mixing rule in Table IX-10 and compared with the optimum values obtained earlier. The results for the individual systems are summarized in Tables IX-11 through IX-21. However, a better measure of the relative performance of these rules can be obtained by comparing the predicted enthalpy values for the specified pseudo-parameters in the PGC framework with the smoothed experimental enthalpy data in each case. These calculations are also reported in the same tables. No such enthalpy calculations are reported for the methane-ethane mixtures because the basic enthalpy data used in obtaining the optimum pseudo-parameters for these systems have not yet been evaluated for accuracy and self-consistency. The enthalpy deviations for the mixing rules averaged over all the mixtures for each of the binary systems methane-propane, and ethane-propane are summarized in Table IX-22 along with the results for the ternary mixture. All these results are analyzed below.

a) Methane-Ethane. A comparison between the calculated Tc_m values for the various rules in Tables 11b and 12b indicate that the predictions in every case are within 1.3K and 2.5K of the optimum Tc_m values for the 0.778 and 0.478 methane-ethane mixtures, respectively. The agreement between the optimum parameters (I) and the calculated values of Tc_m and RTc_m/Pc_m for rules II through V is particularly

TABLE IX-11

a) The PGC Enthalpy Predictions for the 0.78 Mole Fraction Methane-Ethane System Using the Optimum Pseudo-parameters (I) of Table IX-11 b.

RUN NUMBER	TEMP. (DEG F) INLET	TEMP. (DEG F) OUTLET	PRESS. (PSIA) INLET	PRESS. (PSIA) OUTLET	ENTHALPY CHANGE EXP'TAL BTU/LB	ENTHALPY CHANGE CALC'D BTU/LB	DIFFERENCE BTU/LB	DIFFERENCE %
8.010	-59.23	-38.57	2000.10	2000.03	19.69	19.09	0.60	3.03
8.050	-59.27	37.80	1999.80	1999.73	101.56	100.38	1.18	1.16
4.040	202.31	277.43	2002.60	2002.46	52.85	52.20	0.65	1.23
9.010	-59.44	-40.36	1502.20	1502.15	21.46	21.04	0.42	1.96
9.030	-59.46	-29.25	1503.40	1503.35	35.03	35.77	-0.75	-2.13
9.060	-59.37	25.36	1499.30	1499.25	106.82	106.77	0.04	0.04
14.020	-240.76	-189.32	1000.40	1000.35	38.00	37.29	0.71	1.87
18.040	-152.10	-60.85	1002.10	1002.04	90.20	91.94	-1.74	-1.93
10.020	-59.45	-49.65	1001.40	1001.34	19.05	16.85	2.20	11.54
10.030	-59.47	-40.21	1000.10	1000.04	41.63	40.01	1.63	3.90
10.040	-59.47	-29.23	1001.80	1001.74	64.72	65.81	-1.10	-1.69
10.090	-59.49	75.58	1000.90	1000.84	164.54	163.68	0.86	0.52
3.050	77.92	202.95	1000.00	999.81	80.21	79.41	0.80	1.00
5.050	202.17	300.70	1001.40	1001.22	63.21	61.60	1.61	2.54
17.020	-152.29	-126.03	500.10	500.03	22.95	22.40	0.55	2.40
17.100	-152.20	-42.23	499.00	498.83	206.37	207.39	-1.02	-0.50
15.030	-240.70	-158.85	251.30	251.20	62.59	62.91	-0.32	-0.51
16.130	-165.75	-59.92	249.10	248.76	227.10	227.05	0.05	0.02
11.060	-59.56	75.29	252.10	251.71	71.29	70.46	0.84	1.18
7.050	-58.49	-58.45	1390.50	995.70	10.13	9.92	0.21	2.07
1.026	79.14	79.13	2000.00	1584.02	15.66	15.44	0.21	1.36

b) The Calculated Pseudo-critical parameters for the 0.78 Mole Fraction Methane-Ethane System Using the Mixing Rules of Table IX-10

		THE CALCULATED PSEUDO-PARAMETERS FOR THE VARIOUS MIXING RULES									
		I	II	III	IV	V	VI	VII	VIII	IX	X
TC	(K)	217.5	217.5	217.4	217.4	217.5	216.2	217.0	217.7	217.5	216.8
PC	(PSIA)	692.0	691.6	691.9	692.4	692.5	680.2	689.6	692.5	692.0	685.8
R*TC/PC	(CC/MOLE)	379.2	379.4	379.0	378.8	378.9	383.4	379.6	379.1	379.2	381.5
ALPHAC		5.940	5.932	5.932	5.932	5.932	5.921	5.932	5.921	5.940	5.932
ZC		.289	.290	.290	.290	.290	.290	.290	.290	.288	.290

TABLE IX-12

a) The PGC Enthalpy Predictions for the 0.50 Mole Fraction Methane-Ethane System Using the Optimum Pseudo-parameters (I) of Table IX-12b.

RUN NUMBER	TEMP. (DEG F) INLET	OUTLET	PRESS. (PSIA) INLET	OUTLET	ENTHALPY CHANGE EXP'TAL	CALC'D	DIFFERENCE BTU/LB	%
					BTU/LB		BTU/LB	
3.050	-229.94	-99.68	1490.40	1490.35	85.41	86.17	-0.75	-0.88
4.110	-136.75	-18.40	251.60	251.53	228.97	230.17	-1.19	-0.52
5.090	-99.33	9.43	500.70	500.56	195.93	197.55	-1.62	-0.83
5.010	-99.42	-78.40	499.70	499.56	16.35	15.84	0.51	3.13
6.010	-101.11	-70.33	749.90	749.55	23.26	22.49	0.77	3.30
6.080	-101.41	39.13	749.70	749.48	194.94	197.00	-2.06	-1.06
7.040	-100.04	4.68	974.50	974.42	98.22	97.12	1.10	1.12
8.010	-100.17	-69.83	1499.50	1499.44	21.83	22.27	-0.44	-2.01
8.030	-100.13	0.53	1501.30	1501.24	80.00	79.99	0.01	0.01
11.030	249.96	302.80	1500.90	1500.80	36.34	35.73	0.60	1.66
14.050	100.20	251.34	1499.90	1499.75	117.74	115.62	2.12	1.80
15.030	0.31	25.69	1253.90	1253.80	31.43	29.38	2.06	6.54
15.070	0.25	58.62	1251.90	1251.80	80.49	80.16	0.33	0.41
15.080	-0.44	108.37	1249.60	1249.50	133.89	133.38	0.51	0.38
16.020	0.36	45.82	1502.00	1501.90	49.85	49.87	-0.03	-0.06
16.060	0.21	80.47	1499.10	1499.00	93.32	91.98	1.34	1.44
17.045	0.32	81.41	2002.80	2002.67	75.99	75.08	0.91	1.20

b) The Calculated Pseudo-critical Parameters for the 0.50 Mole Fraction Methane-Ethane System Using the Mixing Rules of Table IX-10

		THE CALCULATED PSEUDO-PARAMETERS FOR THE VARIOUS MIXING RULES											
		I	II	III	IV	V	VI	VII	VIII	IX	X	XI	XII
TC	(K)	252.0	252.3	252.4	252.4	252.3	250.4	253.0	252.6	250.5	250.8	251.0	256.4
PC	(PSIA)	708.0	706.8	706.2	706.0	706.0	691.3	707.7	706.0	683.8	681.6	706.1	713.0
R*TC/PC	(CC/MOLE)	429.3	430.6	431.2	431.1	431.1	436.9	431.3	431.6	442.0	443.9	428.8	433.8
ALPHAC		6.073	6.073	6.073	6.073	6.073	6.057	6.073	6.057	6.073	6.073	6.057	6.010
ZC		.288	.288	.288	.288	.288	.289	.288	.289	.288	.289	.282	.279

* Using the mixing rules and the binary interaction constant for the pseudo-critical temperature as tabulated by Barner and Quinlan [15].

** Using mixing rule (II) with interaction pseudo-parameters determined by Pitzer and Hultgren [197] from high pressure volumetric data.

striking and suggests that these rules are equally capable of codifying the composition dependence of the pseudo-parameters for mixtures belonging to this particular system, in spite of differences in functional form, by suitable adjustment of the interaction parameters. The predicted values of Tc_m and RTc_m/Pc_m using the Van der Waal rule with the Lorentz-Berthelot assumptions (VIII) are comparable with the results obtained using the Van der Waal rule (IV) with empirically specified interaction parameters.

Additional sets of pseudo-parameters XI and XII have been specified for the 0.479 methane-ethane mixture in Table 12b. Set XI corresponds to the results obtained with the Barner and Quinlan [15] mixing rules discussed in Chapter IV. Only the rule for Tc_m contains an empirically defined interaction constant derived from second virial coefficient data. The entries in Column (XII) correspond to those obtained with the Pitzer-Hultgren rules [Equations (IV-74) through (IV-76)] with the interaction constants obtained from mixture volumetric data in the single phase region above the cricondenbar pressure [197]. The rules for Tc_m and Pc_m in this case are the same as those for rule (II) in Table IX-10. The differences in the calculated values of Tc_m and αc_m for II and XII are significant. Interestingly, the results for rule XI based on limited dilute gas volumetric data are closer to the optimum values (I) determined from enthalpy data.

b) Ethane-Propane. Table IX-22 indicates that Rules II, III and IV are about equivalent in overall performance. The deviations for the modified Van der Waal rule (V) which takes into account the effect of αc in specifying the mixing rules for each of the three pseudo-parameters are unexpectedly 0.5 Btu/lb higher than for the simpler and theoretically less appealing Van der Waal rule (IV) More disturbing is the fact that Kay's rule (VI) with the most primitive assumptions in regard to the interaction parameters works better than rule (VIII) with a supposedly more refined estimate for Tc_{ij}. Furthermore, its performance is superior to almost all the other rules where the interaction parameters are calculated with the additional benefit of enthalpy data.

TABLE IX-13

The Calculated Pseudo-critical Parameters and the PGC Enthalpy Predictions for the 0.763 Mole Fraction Ethane-Propane System Using the Mixing Rules of Table IX-10

TEMP. (DEG F) INLET	OUTLET	PRESS. (PSIA) INLET	OUTLET	ΔH(EXPT) BTU/LB	DEVIATION IN BTU/LB FROM THE EXP'TAL ENTHALPY DIFFERENCE FOR EACH MIXING RULE I	II	III	IV	V	VI	VII	VIII	IX	X
-280.00	-280.00	250.00	0.0	244.53	0.55	0.39	0.74	0.74	2.24	-1.22	0.30	-2.30	3.27	2.15
-280.00	-280.00	2000.00	250.00	-5.90	0.01	0.09	0.11	0.13	0.21	-0.05	0.07	-0.02	0.34	0.25
-160.00	-160.00	2000.00	0.0	210.00	-0.44	-0.37	-0.01	0.00	1.55	-1.63	-0.47	-2.65	2.55	1.50
-50.12	-50.12	250.00	0.0	189.41	-0.59	-0.47	-0.11	-0.11	1.45	-1.37	-0.56	-2.46	2.30	1.36
-50.12	-50.12	2000.00	0.0	185.30	0.07	0.23	0.58	0.60	2.13	-0.71	0.13	-1.75	3.01	2.08
-50.12	-50.12	2000.00	100.00	-4.43	0.36	0.40	0.40	0.41	0.42	0.33	0.39	0.37	0.46	0.44
52.20	52.20	250.00	0.0	21.90	1.64	1.35	1.38	1.32	1.39	1.44	1.38	1.04	1.22	1.24
49.98	49.98	500.00	0.0	160.54	-0.09	0.17	0.61	0.60	2.46	-0.35	0.07	-1.79	3.25	2.31
49.98	49.98	2000.00	0.0	161.70	0.48	0.68	1.04	1.04	2.55	0.05	0.59	-1.01	3.30	2.47
102.40	102.40	250.00	0.0	15.98	0.12	-0.05	-0.01	-0.05	0.07	0.02	-0.03	-0.26	-0.03	-0.04
102.40	102.40	716.00	0.0	137.56	-0.20	0.29	0.96	0.91	3.73	0.10	0.15	-2.17	4.67	3.40
102.40	102.40	1000.00	0.0	143.34	1.20	1.50	1.98	1.95	4.02	1.19	1.40	-0.41	4.79	3.84
102.40	102.40	2000.00	0.0	147.33	0.17	0.40	0.76	0.76	2.30	-0.09	0.31	-1.22	2.97	2.19
151.65	151.65	250.00	0.0	13.20	0.30	0.17	0.20	0.17	0.25	0.24	0.19	0.04	0.16	0.16
151.65	151.65	500.00	0.0	30.24	0.42	0.08	0.18	0.08	0.41	0.27	0.11	-0.38	0.21	0.17
151.65	151.65	1000.00	0.0	103.69	0.14	-0.20	0.66	0.38	3.63	0.61	-0.23	-3.12	3.73	2.76
151.65	151.65	1200.00	0.0	118.71	0.86	1.07	1.69	1.59	4.17	1.24	0.98	-0.97	4.73	3.74
151.65	151.65	1500.00	0.0	125.60	-0.04	0.15	0.62	0.57	2.55	0.04	0.07	-1.56	3.12	2.27
151.65	151.65	2000.00	0.0	132.18	0.91	1.08	1.48	1.44	3.08	0.87	1.00	-0.50	3.62	2.88
250.74	250.74	250.00	0.0	9.60	0.31	0.24	0.26	0.24	0.30	0.30	0.25	0.16	0.24	0.25
250.74	250.74	500.00	0.0	19.90	0.18	-0.02	0.03	-0.02	0.11	0.10	0.00	-0.22	-0.03	-0.02
250.74	250.74	1000.00	0.0	43.90	-0.61	-1.02	-0.87	-0.99	-0.50	-0.69	-0.98	-1.60	-0.78	-0.83
250.74	250.74	1250.00	0.0	57.50	-0.85	-1.36	-1.14	-1.30	-0.55	-0.95	-1.31	-2.22	-0.85	-0.98
250.74	250.74	1500.00	0.0	70.80	-1.22	-1.70	-1.41	-1.58	-0.53	-1.28	-1.67	-2.82	-0.76	-1.00
250.74	250.74	2000.00	0.0	90.60	-1.31	-1.51	-1.16	-1.29	0.06	-1.19	-1.52	-2.74	0.08	-0.33
24.20	52.20	250.00	250.00	157.46	-0.59	-0.11	0.35	0.38	2.25	-0.74	-0.24	-1.94	3.22	2.28
82.20	100.40	500.00	500.00	109.75	-1.69	-0.60	-0.18	-0.03	1.96	-1.26	-0.80	-1.89	3.33	2.20
115.00	130.00	716.00	716.00	64.04	0.11	2.00	2.28	2.58	4.21	1.01	1.72	0.08	6.17	5.05
115.00	130.00	716.00	716.00	64.04	0.11	2.00	2.28	2.58	4.21	1.01	1.72	0.08	6.17	5.05
120.00	140.00	1000.00	1000.00	24.30	0.27	0.50	0.34	0.44	-0.14	0.00	0.47	0.82	0.12	0.15
140.00	170.00	1000.00	1000.00	52.80	0.81	1.70	1.83	1.99	2.83	1.06	1.57	1.44	3.75	3.14
160.00	180.00	1500.00	1500.00	20.90	-0.50	-0.28	-0.26	-0.20	0.06	-0.52	-0.32	-0.28	0.40	0.18
180.00	200.00	1500.00	1500.00	22.27	1.06	1.34	1.40	1.44	1.69	1.19	1.31	1.13	1.95	1.77
200.00	220.00	1500.00	1500.00	21.98	1.30	1.34	1.37	1.37	1.43	1.30	1.33	1.20	1.42	1.42
220.00	250.74	2000.00	2000.00	29.66	1.62	1.83	1.88	1.91	2.15	1.68	1.79	1.66	2.36	2.22
AVERAGE ENTHALPY DIFFERENCE				86.0										
STD. DEV. (BTU/LB)					0.79	1.01	1.12	1.17	2.26	.92	.95	1.59	2.93	2.27
TC	(K)				321.3	320.8	320.4	320.4	318.7	320.7	320.9	321.9	318.1	318.8
PC	(PSIA)				692.1	683.1	681.8	680.3	673.3	686.7	684.4	684.7	665.2	670.0
R*TC/PC	(CC/MOLE)				560.0	566.5	566.8	568.1	570.9	563.3	565.6	567.2	577.0	574.0
ALPHAC					6.31	6.317	6.317	6.317	6.317	6.337	6.317	6.337	6.31	6.317
ZC					.284	.284	.284	.284	.284	.284	.284	.283	.284	.284

TABLE IX-14

The Calculated Pseudo-critical Parameters and the PGC Enthalpy Predictions for the 0.498 Mole Fraction Ethane-Propane System Using the Mixing Rules of Table IX-10

TEMP. (DEG F) INLET	OUTLET	PRESS. (PSIA) INLET	OUTLET	ΔH(EXPT) BTU/LB	DEVIATION IN BTU/LB FROM THE EXPTAL ENTHALPY DIFFERENCE FOR EACH MIXING RULE I	II	III	IV	V	VI	VII	VIII	IX	X
-240.00	-240.00	2000.00	0.0	226.30	1.16	2.50	2.91	2.99	3.00	0.30	1.99	-0.99	6.03	6.03
-125.50	-125.50	100.00	0.0	204.90	0.04	1.36	1.76	1.84	1.86	-0.17	0.89	-1.46	4.59	4.59
-125.50	-125.50	2000.00	100.00	-4.40	0.19	0.22	0.22	0.22	0.23	0.10	0.19	0.08	0.50	0.50
37.48	37.48	2000.00	250.00	-1.48	-0.71	-0.89	-0.95	-0.96	-0.97	-1.06	-0.85	-0.84	-1.19	-1.19
37.48	37.48	1000.00	0.0	166.47	-0.70	0.67	1.10	1.19	1.24	-0.23	0.19	-1.62	4.22	4.22
37.48	37.48	2000.00	0.0	165.13	-0.25	1.05	1.46	1.55	1.59	0.06	0.60	-1.24	4.46	4.46
80.00	80.00	500.00	0.0	153.84	-1.04	0.62	1.14	1.25	1.31	-0.03	0.09	-1.75	4.60	4.60
80.00	80.00	1000.00	0.0	155.15	-0.56	0.87	1.33	1.42	1.48	0.14	0.38	-1.31	4.62	4.62
80.00	80.00	2000.00	0.0	155.30	-0.03	1.26	1.66	1.75	1.80	0.43	0.82	-0.87	4.64	4.64
120.00	120.00	250.00	0.0	17.88	0.41	0.76	0.85	0.87	0.86	0.89	0.71	0.49	0.84	0.84
120.00	120.00	1000.00	0.0	142.36	-0.73	0.95	1.51	1.63	1.72	0.46	0.39	-1.27	5.19	5.19
120.00	120.00	2000.00	0.0	145.34	-0.29	1.11	1.55	1.65	1.71	0.41	0.64	-1.01	4.58	4.58
151.10	151.10	250.00	0.0	15.38	0.38	0.61	0.66	0.68	0.67	0.71	0.58	0.44	0.58	0.58
151.10	151.10	500.00	0.0	37.80	0.30	1.10	1.29	1.35	1.31	1.60	1.04	0.61	1.27	1.27
151.10	151.10	750.00	0.0	122.80	1.42	4.85	6.00	6.26	6.41	5.26	3.86	1.43	13.50	13.50
151.10	151.10	1000.00	0.0	129.00	-0.43	1.77	2.41	2.54	2.62	1.56	1.16	-0.72	6.29	6.29
151.10	151.10	1500.00	0.0	134.75	-0.66	1.14	1.64	1.74	1.80	0.71	0.65	-1.11	4.90	4.90
151.10	151.10	2000.00	0.0	137.04	-0.53	1.05	1.49	1.57	1.63	0.55	0.61	-1.03	4.35	4.35
251.10	251.10	250.00	0.0	10.65	0.24	0.37	0.40	0.41	0.41	0.48	0.36	0.31	0.31	0.31
251.10	251.10	500.00	0.0	22.97	0.02	0.36	0.44	0.47	0.45	0.56	0.32	0.14	0.30	0.30
251.10	251.10	1000.00	0.0	54.97	-0.25	0.88	1.18	1.26	1.24	1.60	0.74	0.23	1.25	1.25
251.10	251.10	1500.00	0.0	88.95	-1.23	0.68	1.22	1.35	1.38	1.30	0.26	-0.85	3.12	3.12
251.10	251.10	2000.00	0.0	104.50	0.00	1.63	2.12	2.23	2.27	1.93	1.22	0.13	4.25	4.25
48.80	79.80	250.00	250.00	152.53	-1.31	-0.42	-0.08	-0.01	0.06	-1.38	-0.83	-2.21	3.70	3.70
111.90	134.00	500.00	500.00	106.64	-0.65	0.24	0.64	0.70	0.84	-0.69	-0.30	-1.51	5.56	5.56
160.00	180.00	760.00	760.00	52.88	-1.25	3.01	4.44	4.75	4.95	4.01	1.67	-1.07	11.49	11.49
186.00	198.00	1000.00	1000.00	19.30	-0.22	-1.02	-1.07	-1.08	-1.03	-1.61	-1.01	-0.93	0.56	0.56
251.10	300.00	2000.00	2000.00	43.99	1.17	1.32	1.37	1.38	1.40	1.08	1.23	0.96	2.00	2.00
AVERAGE ENTHALPY DIFFERENCE				102.0										
STD. DEV. (BTU/LB)					.74	1.53	1.99	2.09	2.15	1.58	1.14	1.10	5.04	5.04
TC	(K)				339.6	338.0	337.5	337.4	337.3	337.8	338.5	339.4	333.9	333.9
PC	(PSIA)				658.5	657.5	656.6	656.6	655.7	662.6	659.7	661.9	631.4	631.4
R*TC/PC	(CC/MOLE)				622.1	620.0	620.1	619.8	620.5	614.9	618.9	618.6	638.0	638.0
ALPHAC					6.379	6.379	6.379	6.379	6.379	6.408	6.379	6.408	6.379	6.379
ZC					.282	.282	.282	.282	.282	.281	.282	.281	.282	.282

TABLE IX-15

The Calculated Pseudo-critical Parameters and the PGC Enthalpy Predictions for the 0.276 Mole Fraction Ethane-Propane System Using the Mixing Rules of Table IX-10

TEMP. (DEG F) INLET	TEMP. (DEG F) OUTLET	PRESS. (PSIA) INLET	PRESS. (PSIA) OUTLET	ΔH(EXPT) BTU/LB	DEVIATION IN BTU/LB FROM THE EXP'TAL ENTHALPY DIFFERENCE FOR EACH MIXING RULE I	II	III	IV	V	VI	VII	VIII	IX	X
-200.00	-200.00	1000.00	0.0	217.12	-0.44	0.38	0.61	0.76	-1.60	-1.06	-0.09	-2.07	-2.58	3.28
-150.20	-150.20	2000.00	1000.00	-2.45	1.14	1.21	1.21	1.20	1.13	1.13	1.21	1.15	1.11	1.30
-150.20	-150.20	2000.00	0.0	203.44	0.34	0.93	1.16	1.31	-0.85	-0.40	0.45	-1.41	-1.84	3.93
1.60	1.60	100.00	0.0	175.06	-0.28	-0.45	-0.20	-0.04	-1.50	-1.28	-0.95	-2.36	-2.51	2.56
1.60	1.60	1000.00	100.00	-1.57	-0.01	0.01	-0.00	-0.01	0.04	0.02	0.03	0.08	0.08	-0.10
1.60	1.60	2000.00	100.00	-3.68	0.34	0.49	0.48	0.46	0.41	0.42	0.52	0.51	0.46	0.38
127.40	127.40	500.00	0.0	139.13	0.32	-1.05	-0.70	-0.44	-1.33	-1.33	-1.72	-2.89	-2.63	2.88
127.40	127.40	750.00	0.0	140.85	-0.07	-1.08	-0.78	-0.58	-1.41	-1.51	-1.69	-2.83	-2.67	2.11
127.40	127.40	1000.00	0.0	141.86	-0.07	-0.99	-0.71	-0.52	-1.39	-1.40	-1.54	-2.61	-2.49	2.24
127.40	127.40	1500.00	0.0	142.86	-0.37	-0.96	-0.72	-0.55	-1.53	-1.45	-1.45	-2.52	-2.49	1.82
127.40	127.40	2000.00	0.0	143.02	-0.80	-1.39	-1.15	-1.00	-2.00	-1.94	-1.87	-2.98	-2.98	1.59
203.10	203.10	250.00	0.0	13.71	0.48	0.40	0.43	0.48	0.42	0.50	0.37	0.33	0.40	0.33
203.10	203.10	500.00	0.0	31.71	-0.06	-0.23	-0.15	-0.02	-0.23	-0.02	-0.31	-0.41	-0.26	-0.45
203.10	203.10	750.00	0.0	64.56	0.54	-1.62	-1.07	-0.44	-0.84	-0.27	-2.45	-3.06	-1.85	-0.23
203.10	203.10	1000.00	0.0	106.57	0.65	-2.10	-1.60	-1.15	-1.51	-1.60	-2.99	-3.90	-3.13	2.23
203.10	203.10	1500.00	0.0	118.96	-0.30	-1.50	-1.20	-0.97	-1.57	-1.60	-2.10	-3.01	-2.70	1.39
203.10	203.10	2000.00	0.0	122.87	-1.42	-2.40	-2.14	-1.95	-2.63	-2.62	-2.89	-3.77	-3.59	0.30
269.90	269.90	250.00	0.0	10.74	0.29	0.21	0.23	0.26	0.24	0.30	0.18	0.17	0.23	0.14
269.90	269.90	500.00	0.0	23.30	-0.08	-0.24	-0.18	-0.09	-0.21	-0.05	-0.31	-0.37	-0.25	-0.34
269.90	269.90	1000.00	0.0	56.96	0.12	-0.90	-0.66	-0.36	-0.50	-0.19	-1.23	-1.40	-0.87	-0.50
269.90	269.90	1500.00	0.0	89.98	-0.57	-2.20	-1.86	-1.53	-1.82	-1.70	-2.75	-3.30	-2.73	0.01
269.90	269.90	2000.00	0.0	102.20	-0.61	-1.98	-1.70	-1.45	-1.77	-1.77	-2.48	-3.09	-2.68	0.33
140.60	155.35	500.00	500.00	92.90	-0.00	-0.69	-0.62	-0.74	-1.02	-1.70	-1.04	-1.83	-2.06	3.24
210.00	230.00	1000.00	1000.00	30.00	0.25	0.19	0.14	0.01	-0.11	-0.47	0.19	-0.08	-0.44	1.80
240.00	269.90	2000.00	2000.00	23.94	-1.45	-1.33	-1.34	-1.36	-1.51	-1.53	-1.34	-1.48	-1.57	-1.00
-240.00	-100.00	1000.00	1000.00	70.16	-0.48	0.28	0.29	0.29	-0.50	-0.22	0.28	-0.21	-0.49	0.32
170.00	210.00	1000.00	1000.00	44.90	0.55	1.90	1.72	1.50	1.12	1.10	2.16	2.04	1.48	1.44
AVERAGE ENTHALPY DIFFERENCE				86.0										
STD. DEV. (BTU/LB)					0.60	1.24	1.05	0.92	1.29	1.26	1.61	2.26	2.07	1.79
TC	(K)				350.3	352.3	352.0	351.8	351.7	352.1	352.9	353.4	352.9	348.7
PC	(PSIA)				632.0	638.4	638.1	639.0	637.4	642.7	640.3	642.8	643.3	615.9
R*TC/PC	(CC/MOLE)				668.4	665.7	665.4	664.2	665.5	660.8	664.9	663.2	662.0	683.0
ALPHAC					6.480	6.444	6.444	6.444	6.444	6.467	6.444	6.467	6.480	6.444
ZC					.279	.280	.280	.280	.280	.279	.280	.279	.279	.280

The results for rules IX and X are poor when compared with the results for the other mixing rules, particularly for the 0.498 ethane-propane mixture (Table IX-14) where the standard deviation for the enthalpy differences is as high as 5.04 Btu/lb. This tends to confirm our earlier suspicion that the final B_{ij} values for the ethane-propane system as tabulated in Table IX-5 and later used in specifying Tc_m and RTc_m/Pc_m for these rules should have instead been selected to emphasize the values calculated from the 0.498 ethane-propane mixture. On the contrary, however, the standard deviation is lowest for rule VII which uses the very same set of B_{ij} data to specify the parameter Tc_m.

c) Methane-Propane. The summary results in Table IX-22 indicate that, in contrast to our conclusions for the ethane-propane systems, the deviations for rules VII and IX are higher than for all the other rules that permit empirical adjustment of the interaction parameters. The lowest standard deviation on the other hand is observed for rule X which operates on the same set of B_m data as rule IX. It is only the differences in the choice of αc_m that cause the calculated pseudo-parameters Tc_m and RTc_m/Pc_m, and hence the enthalpy deviations, to differ in the two cases. Differences in the standard deviations for the two rules are particularly significant for the 0.484 and the 0.234 mole fraction methane-propane mixtures as seen in Tables IX-19 and IX-20, respectively.

In examining the standard deviations for the mixing rules, we observe that, for all but the 0.95 mole fraction methane-propane mixture, there is at least one rule that yields better results than the "optimum" case in column I.

When the differences are small, ($\leq$ 0.1 Btu/lb) they may be rationalized by the fact that the pseudo-parameters in column I were obtained by optimizing on a different set of data. The superiority of the results for rule X in comparison to rule I for the 0.484 and the 0.234 modification methane-propane mixtures is beyond this consideration and leads us to conclude that the pseudo-critical parameters reported for these mixtures in column I are not optimally defined.

The predictions for rules II, III and IV are about equally satisfactory, but are again superior to the results for the modified Van der Waal rule (V). Of the methods based on pure component critical properties alone, the predictions for Kay's rule (VI) are considerably poorer than the rest. In the worst case, the standard deviation in the enthalpy differences for the 0.484 methane-propane mixture (Table IX-19) is as high as 7.4 Btu/lb. The performance of the Van der Waal rule with the Lorentz-Berthelot assumptions (VIII) is more encouraging. The standard deviation for this case is only 0.3 Btu/lb higher than for the equivalent case IV where the parameters are calculated using binary data.

The results in columns XI and XII in Table IX-19 correspond to the pseudo-critical parameters calculated for the 0.484 mole fraction methane-propane mixture by the Barner and Quinlan [15], and the Pitzer-Hultgren [197] mixing rules using B_{ij} data and high pressure volumetric measurements, respectively. The calculated value of Tc_m in XII is in reasonably good agreement with the optimum case (X). Furthermore, as volumetric data are particularly selective of RTc/Pc, one would normally have to conclude that the estimated value of RTc_m/Pc_m using rule XII should be superior to that for rule XI which uses the arithmetic mean rule to calculate Vc_m and, hence, RTc_m/Pc_m. For the same reason, the RTc_m/Pc_m value for rule XII should also be more reliable than the values obtained for rules that use binary enthalpy data.

A comparison between the calculated RTc_m/Pc_m values for rule X (which provides the best fit to the enthalpy data), rule XI, and rule XII reveals disconcertingly large discrepancies that extend over a span of 20%, with the enthalpy based value of rule X lying in between the volumetrically based values. Such observations do not augur well for the accurate prediction of volumetric data in the supercritical region if the interaction parameters for any given mixing rule are based on second virial coefficient or enthalpy data, and also seem to offer strong evidence that the optimization of pseudo-critical parameters using a single thermodynamic property, no matter how extensive, can be dangerous if we then wish to calculate other thermodynamic properties.

The entire picture is somewhat clouded because Joffe and

Zudkevitch [117] have disputed the accuracy of the Pitzer-Hultgren parameters [159] for the methane-propane system. Barner and Quinlan [15] have since compared the pseudo-critical parameters Tc_m and Pc_m obtained from their mixing rules with those of Pitzer and Hultgren for twelve equimolar binary mixtures including mixtures with components as dissimilar as methane- n-butane. In almost all cases, the values of the Barner and Quinlan parameters were close to (within 2%), but generally below, the corresponding Pitzer-Hultgren parameters.

However, an unusually high worst case discrepancy of 20% was obtained on comparing the Pc_m values for the equimolar methane-propane mixture lending further credibility to the arguments of Joffe and Zudkevitch. Furthermore, the standard deviation in the enthalpy difference for the Pitzer-Hultgren parameters (XII) in Table IX-19, is, at 5.15 Btu/lb, considerably worse than the standard deviation of 2.42 Btu/lb obtained for the Barner and Quinlan parameters (XI). This is all the more remarkable because the value of the parameter Tc_m (to which the enthalpy predictions appears to be most sensitive) for rule XI is as much as 5.5K above that for the best fit case (X), whereas the Tc_m value for rule (XII) is only 1.5K above that for rule X.

d) Ternary Methane-Ethane-Propane Mixture. It must be emphasized that the enthalpy data for this system have been completely ignored in specifying any interaction parameters for the rules investigated. Therefore, except for rules VI and VII, the performance of a mixing rule is, for the first time, more an index of its ability to predict enthalpy data than to fit it. From Table IX-21 or IX-22 it is seen that the best predictions are obtained for rule VII and rule II in that order. The standard deviation in each case is less than 1.1 Btu/lb. With the exception of Kay's rule (VI), whose performance is to be considered poor, the standard deviation over the single phase liquid and gaseous regions does not exceed 2 Btu/lb for any rule. Sample calculation illustrating the application of rules VII, IX and X in calculating the pseudo-parameters for the ternary mixture are presented in Appendix F-7.

TABLE IX-16

The Calculated Pseudo-critical Parameters and the PGC Enthalpy Predictions for the 0.95 Mole Fraction Methane-Propane System Using the Mixing Rules of Table IX-10

TEMP. (DEG F) INLET	OUTLET	PRESS. (PSIA) INLET	OUTLET	ΔH(EXPT) BTU/LB	DEVIATION IN BTU/LB FROM THE EXP'TAL ENTHALPY DIFFERENCE FOR EACH MIXING RULE I	II	III	IV	V	VI	VII	VIII	IX	X
-280.00	-280.00	2000.00	0.0	218.70	-0.08	-0.32	-1.04	-1.31	-1.46	2.32	1.60	-0.12	-1.91	-0.79
-280.00	-280.00	2000.00	250.00	-8.50	-0.90	-0.97	-1.00	-1.00	-1.01	-0.98	-0.83	-1.08	-1.14	-1.04
-180.00	-180.00	2000.00	0.0	188.10	0.29	-0.10	-0.81	-1.08	-1.23	2.34	1.77	-0.08	-1.46	-0.55
-180.00	-180.00	2000.00	500.00	-4.10	0.78	0.80	0.85	0.88	0.89	0.62	0.73	0.77	0.78	0.80
-147.00	-147.00	2000.00	500.00	-1.40	0.80	0.89	1.02	1.08	1.10	0.30	0.54	0.85	0.97	0.93
-147.00	-147.00	500.00	0.0	177.40	-0.64	-1.15	-1.99	-2.32	-2.49	1.83	1.06	-1.12	-2.51	-1.62
-100.00	-100.00	2000.00	800.00	13.00	0.48	1.12	1.89	2.20	2.34	-1.38	-0.72	1.29	2.00	1.51
-100.00	-100.00	800.00	0.0	144.90	-0.40	-1.43	-2.87	-3.46	-3.72	4.01	2.40	-1.47	-3.28	-2.14
-27.00	-27.00	2000.00	0.0	116.60	-0.12	-0.54	-1.39	-1.78	-1.93	2.52	1.31	-0.29	-1.29	-0.82
-27.00	-27.00	1000.00	0.0	60.30	-0.18	-0.16	-0.67	-0.97	-1.03	2.06	0.67	0.57	0.05	-0.05
-27.00	-27.00	500.00	0.0	25.90	0.43	0.49	0.35	0.27	0.25	1.17	0.67	0.76	0.59	0.55
-50.00	-50.00	2000.00	0.0	131.40	0.14	-0.43	-1.33	-1.72	-1.89	2.59	1.69	-0.45	-1.59	-0.88
-50.00	-50.00	1500.00	0.0	118.60	0.87	0.45	-0.55	-1.04	-1.20	4.31	2.61	0.96	-0.24	0.21
-50.00	-50.00	1000.00	0.0	77.10	-0.76	-0.93	-1.91	-2.44	-2.57	3.05	0.87	0.11	-0.87	-0.87
-50.00	-50.00	250.00	0.0	12.90	-0.56	-0.52	-0.59	-0.63	-0.63	-0.21	-0.45	-0.39	-0.46	-0.49
91.60	91.60	2000.00	0.0	60.90	1.32	1.19	0.76	0.53	0.47	2.88	2.01	1.52	1.12	1.17
91.60	91.60	1500.00	0.0	46.60	0.26	0.23	-0.05	-0.21	-0.24	1.44	0.72	0.56	0.29	0.27
91.60	91.60	1000.00	0.0	30.90	-0.16	-0.11	-0.25	-0.35	-0.36	0.66	0.12	0.23	0.09	-0.01
91.60	91.60	500.00	0.0	15.30	0.07	0.10	0.03	-0.01	-0.02	0.45	0.19	0.24	0.18	0.14
260.00	260.00	2000.00	0.0	32.30	-0.31	-0.37	-0.56	-0.67	-0.69	0.42	-0.01	-0.20	-0.34	-0.36
260.00	260.00	250.00	0.0	4.20	-0.31	-0.31	-0.34	-0.35	-0.35	-0.21	-0.28	-0.28	-0.30	-0.31
-95.20	-37.50	800.00	800.00	115.10	-0.94	-2.21	-3.48	-3.94	-4.17	2.52	1.80	-2.69	-4.25	-3.05
-166.50	-60.50	250.00	250.00	221.00	-1.12	-1.63	-2.36	-2.63	-2.79	0.68	0.33	-1.77	-3.06	-2.13
AVERAGE ENTHALPY DIFFERENCE				79.5										
					0.64	0.92	1.47	1.73	1.84	2.11	1.28	1.02	1.71	1.19
STD. DEV. (BTU/LB)					201.0	201.5	202.0	202.2	202.3	200.0	200.2	201.7	202.2	201.8
TC (K)					663.7	669.4	671.2	671.2	671.9	670.2	660.8	677.5	679.3	673.8
PC (PSIA)					365.3	363.1	363.2	363.5	363.2	360.0	365.3	359.1	359.0	361.0
R*TC/PC (CC/MOLE)					5.883	5.877	5.877	5.877	5.877	5.870	5.877	5.870	5.883	5.877
ALPHAC					.289	.289	.289	.289	.289	.289	.289	.289	.289	.289
ZC														

TABLE IX-17

The Calculated Pseudo-critical Parameters and the PGC Enthalpy Predictions for the 0.883 Mole Fraction Methane-Propane System Using the Mixing Rules of Table IX-10

TEMP. (DEG F) INLET	OUTLET	PRESS. (PSIA) INLET	OUTLET	ΔH(EXPT) BTU/LB	DEVIATION IN BTU/LB FROM THE EXP'TAL ENTHALPY DIFFERENCE FOR EACH MIXING RULE I	II	III	IV	V	VI	VII	VIII	IX	X
-280.00	-280.00	2000.00	0.0	221.20	-1.58	0.66	-0.56	-0.96	-1.10	7.97	3.46	3.28	-3.32	-0.89
-280.00	-280.00	2000.00	250.00	-8.60	-1.95	-1.91	-1.94	-1.95	-1.96	-1.86	-1.73	-2.07	-2.16	-2.02
-160.00	-160.00	2000.00	0.0	185.50	-0.49	1.22	0.04	-0.36	-0.49	7.05	3.86	2.52	-2.11	-0.26
-160.00	-160.00	2000.00	500.00	-5.80	-1.28	-1.32	-1.24	-1.21	-1.20	-1.63	-1.47	-1.31	-1.28	-1.27
-70.00	-70.00	2000.00	1000.00	11.70	2.44	2.02	2.57	2.76	2.82	-0.15	0.93	2.32	3.11	2.66
-70.00	-70.00	1000.00	0.0	141.30	-1.98	-0.07	-1.82	-2.41	-2.60	7.68	3.65	0.67	-4.60	-2.04
10.00	10.00	2000.00	0.0	109.20	-1.10	0.28	-1.08	-1.57	-1.72	6.07	2.72	1.15	-1.98	-1.01
10.00	10.00	1500.00	0.0	89.80	0.06	1.56	0.08	-0.46	-0.62	7.91	3.96	3.02	-0.35	0.38
10.00	10.00	1000.00	0.0	57.60	1.69	2.49	1.75	1.47	1.39	5.98	3.48	3.82	2.01	2.11
10.00	10.00	500.00	0.0	27.30	3.26	3.53	3.31	3.22	3.20	4.77	3.79	4.10	3.43	3.45
80.00	80.00	2000.00	0.0	74.70	-0.06	0.87	-0.09	-0.44	-0.54	4.97	2.49	1.78	-0.21	0.14
80.00	80.00	1000.00	0.0	37.10	0.35	0.75	0.39	0.24	0.21	2.57	1.18	1.48	0.58	0.59
80.00	80.00	250.00	0.0	8.60	-0.02	0.05	-0.02	-0.04	-0.05	0.38	0.09	0.21	0.05	0.03
120.00	120.00	2000.00	1500.00	14.40	0.65	0.87	0.60	0.51	0.48	1.76	1.39	0.81	0.40	0.58
120.00	120.00	1500.00	0.0	47.40	0.50	0.99	0.49	0.30	0.25	3.29	1.70	1.67	0.60	0.69
180.00	180.00	2000.00	0.0	48.40	0.86	1.31	0.85	0.67	0.62	3.46	1.95	1.82	0.88	1.00
180.00	180.00	1500.00	0.0	37.20	0.30	0.65	0.30	0.16	0.12	2.33	1.05	1.23	0.47	0.48
180.00	180.00	500.00	0.0	12.40	-0.32	-0.21	-0.30	-0.34	-0.35	0.32	-0.11	0.04	-0.20	-0.23
-172.00	-34.00	200.00	200.00	248.30+	3.29	5.10	3.82	3.40	3.25	10.89	7.92	6.36	1.51	3.49
-124.00	4.00	500.00	500.00	200.10+	-8.85	-7.31	-8.54	-8.93	-9.06	-1.87	-4.30	-6.85	-10.76	-8.95
-49.40	4.00	1100.00	1100.00	82.00+	-4.18	-2.87	-4.30	-4.79	-4.96	2.41	0.46	-3.62	-6.51	-4.79
AVERAGE ENTHALPY DIFFERENCE				79.5										
STD. DEV. (BTU/LB)					2.65	2.51	2.63	2.74	2.78	5.13	3.12	3.04	3.43	2.76
TC	(K)				215.4	214.7	215.6	215.9	216.0	211.7	212.7	215.2	216.6	215.8
PC	(PSIA)				665.3	664.6	667.4	668.0	668.4	666.6	652.4	681.9	680.6	672.8
R*TC/PC	(CC/MOLE)				390.5	389.7	389.8	389.9	389.8	383.1	393.2	380.6	384.0	387.0
ALPHAC					5.961	5.946	5.946	5.946	5.946	5.904	5.946	5.904	5.961	5.946
ZC					.287	.288	.288	.288	.287	.288	.288	.288	.287	.288

+ These values suspected to be in error

TABLE IX-18

The Calculated Pseudo-critical Parameters and the PGC Enthalpy Predictions for the 0.72 Mole Fraction Methane-Propane System Using the Mixing Rules of Table IX-10

TEMP. (DEG F) INLET	OUTLET	PRESS. (PSIA) INLET	OUTLET	ΔH(EXPT) BTU/LB	DEVIATION IN BTU/LB FROM THE EXP'TAL ENTHALPY DIFFERENCE FOR EACH MIXING RULE I	II	III	IV	V	VI	VII	VIII	IX	X
-280.00	-280.00	2000.00	0.0	223.80	**-0.70**	0.09	-0.60	-0.71	**-0.48**	12.73	1.73	5.32	-0.40	-0.96
-280.00	-280.00	2000.00	250.00	-6.50	**-0.08**	-0.05	-0.05	-0.05	**-0.04**	-0.32	0.00	-0.43	-0.07	-0.08
-160.00	-160.00	2000.00	0.0	192.60	**0.92**	1.82	1.13	1.01	**1.13**	12.50	3.43	5.07	1.22	0.77
-160.00	-160.00	2000.00	250.00	-5.40	**0.37**	0.38	0.39	0.39	**0.40**	0.14	0.38	0.19	0.38	0.37
-60.00	-60.00	2000.00	1000.00	-2.10	**-1.33**	-1.47	-1.39	-1.38	**-1.35**	-2.06	-1.66	-1.13	-1.36	-1.35
-60.00	-60.00	1000.00	0.0	161.70	**-1.77**	-0.65	-1.43	-1.56	**-1.55**	9.66	1.20	0.98	-1.43	-1.83
40.00	40.00	2000.00	1500.00	12.10	**0.44**	0.36	0.44	0.46	**0.55**	-1.59	0.31	-0.98	0.40	0.40
40.00	40.00	2000.00	250.00	110.00	**-1.84**	-0.74	-1.48	-1.61	**-1.70**	8.38	0.94	-0.11	-1.52	-1.82
-167.00	11.00	200.00	200.00	259.60	**-0.63**	0.21	-0.44	-0.55	**-0.42**	10.38	1.77	3.31	-0.35	-0.80
-110.00	55.00	500.00	500.00	221.90	**-3.34+**	-2.48	-3.08	-3.18	**-3.07**	5.58	-0.98	-1.20	-3.07	-3.45
-47.00	79.00	1000.00	1000.00	155.00	**-4.70+**	-3.98	-4.42	-4.49	**-4.33**	0.96	-2.67	-5.01	-4.50	-4.80
-4.00	64.00	1300.00	1300.00	78.00	**-6.29**	-6.07	-6.16	-6.16	**-5.96**	-5.11	-5.49	-8.06	-6.25	-6.39
80.00	80.00	2000.00	0.0	103.80	**-0.62**	0.39	-0.33	-0.45	**-0.63**	9.88	1.83	2.17	-0.32	-0.55
80.00	80.00	1500.00	0.0	85.90	**0.59**	1.62	0.86	0.72	**0.48**	11.66	3.04	4.34	0.90	0.68
80.00	80.00	1000.00	0.0	55.80	**2.72**	3.15	2.79	2.72	**2.56**	8.89	3.73	5.50	2.86	2.77
80.00	80.00	500.00	0.0	24.30	**1.39**	1.50	1.39	1.37	**1.32**	3.55	1.65	2.51	1.43	1.40
140.00	140.00	1000.00	0.0	39.80	**1.86**	2.11	1.90	1.86	**1.75**	5.58	2.44	3.56	1.95	1.90
180.00	180.00	2000.00	0.0	64.90	**0.91**	1.54	1.08	1.00	**0.83**	7.48	2.40	2.91	1.10	0.98
180.00	180.00	250.00	0.0	7.90	**0.19**	0.21	0.19	0.18	**0.17**	0.68	0.23	0.49	0.20	0.20
300.00	300.00	2000.00	0.0	40.60	**-0.29**	-0.02	-0.23	-0.27	**-0.38**	3.13	0.33	0.84	-0.21	-0.24
300.00	300.00	1000.00	0.0	22.00	**0.59**	0.69	0.60	0.58	**0.53**	2.34	0.81	1.38	0.62	0.60
300.00	300.00	250.00	0.0	5.50	**-0.12**	-0.09	-0.12	-0.12	**-0.14**	0.30	-0.06	0.05	-0.11	-0.12
AVERAGE ENTHALPY DIFFERENCE				86.5										
STD. DEV. (BTU/LB)					2.16	2.05	2.08	2.10	2.02	7.18	2.22	3.41	2.11	2.21
TC (K)					247.8	246.8	247.4	247.5	247.6	240.9	245.4	247.6	247.5	247.7
PC (PSIA)					658.3	653.5	655.6	655.9	655.2	657.4	646.1	683.6	657.2	658.3
R*TC/PC (CC/MOLE)					454.1	455.5	455.2	455.2	455.8	442.0	458.1	436.8	454.8	454.0
ALPHAC					6.098	6.102	6.102	6.102	6.102	6.022	6.102	6.022	6.098	6.102
ZC					.285	.285	.285	.285	.286	.286	.285	.286		

+ These values might be in error

TABLE IX-19

The Calculated Pseudo-critical Parameters and the PGC Enthalpy Predictions for the 0.494 Mole Fraction Methane-Propane System Using the Mixing Rules of Table IX-10

TEMP. (DEG F) INLET	TEMP. (DEG F) OUTLET	PRESS. (PSIA) INLET	PRESS. (PSIA) OUTLET	ΔH(EXPT) BTU/LB	DEVIATION IN BTU/LB FROM THE EXP'TAL ENTHALPY DIFFERENCE FOR EACH MIXING RULE I	II	III	IV	V	VI	VII	VIII	IX	X	XI*	XII**
-280.00	-280.00	2000.00	0.0	226.20	-0.98	-1.76	-1.11	-0.72	**-0.60**	13.08	-2.57	5.50	4.78	0.48	3.12	-9.68
-280.00	-280.00	2000.00	250.00	-6.00	0.77	0.75	0.73	0.73	**0.75**	0.63	0.73	0.61	1.10	0.93	0.62	1.38
-200.00	-200.00	1000.00	0.0	211.10	-1.35	-1.70	-1.03	-0.64	**-0.53**	11.43	-2.50	3.79	4.29	0.46	1.47	-7.86
-149.00	-149.00	1000.00	0.0	198.80	-0.53	-0.72	-0.34	0.35	**0.46**	11.61	-1.52	3.97	5.10	1.45	1.60	-6.00
-149.00	-149.00	2000.00	250.00	-5.50	0.29	0.29	0.27	0.27	**0.28**	0.05	0.28	0.14	0.52	0.43	0.17	1.17
-50.00	-50.00	2000.00	750.00	-1.90	0.89	0.77	0.72	0.69	**0.69**	0.28	0.80	1.08	0.64	0.67	1.19	0.73
-50.00	-50.00	750.00	0.0	173.30	-0.92	-0.70	0.01	0.42	**0.53**	10.63	-1.52	2.34	4.75	1.48	-0.17	-4.43
50.00	50.00	2000.00	1250.00	2.80	0.16	-0.13	-0.31	-0.41	**-0.42**	-2.12	0.03	0.14	-1.18	-0.55	0.75	0.29
100.00	100.00	1500.00	0.0	119.80	-1.57	-0.65	0.40	0.95	**1.00**	11.87	-1.62	1.29	4.18	1.46	-2.14	-5.45
130.00	150.00	1250.00	1250.00	21.80	-0.97	-0.36	-0.07	0.10	**0.16**	2.06	-0.82	-1.10	0.88	0.49	-2.66	0.32
140.00	160.00	1750.00	1750.00	18.90	-0.71	-0.60	-0.55	-0.50	**-0.45**	0.13	-0.73	-0.92	0.54	-0.05	-1.14	0.82
130.00	130.00	1250.00	750.00	43.10	-3.46	-2.55	-1.85	-1.50	**-1.47**	4.92	-3.27	-2.04	0.07	-1.28	-5.10	-4.19
110.00	110.00	500.00	0.0	31.40	2.59	2.59	2.87	2.96	**2.89**	5.79	2.53	4.34	2.15	2.20	3.72	-3.70
-149.00	50.00	200.00	200.00	260.70	-2.05	-2.28	-1.71	-1.36	**-1.24**	8.82	-3.02	1.94	3.38	-0.13	-0.21	-5.95
152.20	152.20	2000.00	0.0	105.90	-0.68	0.05	0.91	1.34	**1.32**	10.05	-0.65	1.95	3.08	1.24	-0.96	-5.85
152.20	152.20	1250.00	0.0	76.80	0.19	0.69	1.66	2.10	**1.97**	11.55	0.21	4.52	2.12	0.91	1.94	-10.69
152.20	152.20	500.00	0.0	25.00	1.25	1.27	1.48	1.55	**1.50**	3.69	1.22	2.52	1.02	1.02	2.09	-2.96
251.30	251.30	2000.00	0.0	70.80	0.79	1.35	2.01	2.32	**2.26**	8.49	0.92	3.12	2.74	1.77	1.30	-4.80
251.30	251.30	1750.00	0.0	63.30	0.72	1.11	1.71	1.96	**1.88**	7.62	0.80	3.22	1.82	1.18	1.69	-5.85
251.30	251.30	1000.00	0.0	36.20	1.68	1.80	2.11	2.23	**2.16**	5.07	1.71	3.25	1.55	1.53	2.53	-3.41
251.30	251.30	250.00	0.0	8.60	0.71	0.73	0.78	0.80	**0.78**	1.30	0.72	1.03	0.57	0.63	0.92	-0.43
300.00	300.00	2000.00	0.0	59.10	1.96	2.42	2.96	3.21	**3.15**	8.00	2.10	3.78	3.19	2.63	2.27	-3.26
-63.00	104.00	500.00	500.00	226.10	-3.04	-3.01	-2.60	-2.30	**-2.11**	5.22	-3.73	-1.12	2.99	-0.46	-2.90	-0.77
11.00	137.00	1000.00	1000.00	142.20	-3.65	-3.75	-3.90	-3.82	**-3.56**	-1.55	-4.18	-4.98	1.47	-1.31	-5.25	6.27
79.00	114.00	1300.00	1300.00	41.10	2.70	2.34	2.02	1.92	**2.01**	1.10	2.44	1.67	3.54	2.33	2.99	6.74
AVERAGE ENTHALPY DIFFERENCE				87.3												
STD. DEV. (BTU/LB)					1.73	1.72	1.72	1.75	1.69	7.37	2.02	2.91	2.81	1.34	2.42	5.15
TC (K)					289.8	288.7	288.0	287.6	287.5	281.4	289.5	289.5	284.2	286.6	292.1	288.1
PC (PSIA)					645.9	640.0	639.9	638.9	636.9	644.9	644.4	671.5	602.6	619.8	678.5	556.5
R*TC/PC (CC/MOLE)					541.1	544.2	542.9	543.1	544.5	526.3	541.8	519.9	569.0	558.0	519.3	624.4
ALPHAC					6.262	6.284	6.284	6.284	6.284	6.184	6.284	6.184	6.262	6.284	6.184	6.383
ZC					.282	.281	.281	.281	.282	.284	.284	.282	.282	.281	.284	.282

* Using the mixing rules and the binary interaction constant for the pseudo-critical temperature as tabulated by Barner and Quinlan [15].

** Using mixing rule (III) and the interaction pseudo-parameters determined by Pitzer and Hultgren [197] from high pressure volumetric data

TABLE IX-20

The Calculated Pseudo-critical Parameters and the PGC Enthalpy Predictions for the 0.234 Mole Fraction Methane-Propane System Using the Mixing Rules of Table IX-10

TEMP. (DEG F) INLET	OUTLET	PRESS. (PSIA) INLET	OUTLET	ΔH(EXPT) BTU/LB	DEVIATION IN BTU/LB FROM THE EXP'TAL ENTHALPY DIFFERENCE FOR EACH MIXING RULE I	II	III	IV	V	VI	VII	VIII	IX	X
-280.00	-280.00	2000.00	0.0	226.90	**-1.57**	-4.06	-2.98	-2.47	**-2.52**	5.97	-5.59	1.27	2.02	-0.96
-280.00	-280.00	2000.00	250.00	-6.80	**-1.23**	-1.93	-1.32	-1.31	**-1.53**	-1.09	-1.43	-1.29	-0.81	-1.03
-200.00	-200.00	1000.00	0.0	213.10	**-1.08**	-3.34	-2.26	-1.76	**-1.70**	5.54	-4.64	0.92	2.30	-0.37
-150.00	-150.00	1000.00	0.0	201.90	**-0.94**	-3.11	-2.02	-1.52	**-1.45**	5.19	-4.40	0.81	2.41	-0.14
-96.80	-96.80	2000.00	250.00	-4.80	**0.50**	0.50	0.47	0.47	**0.30**	0.39	0.45	0.40	0.75	0.65
-96.80	-96.80	2000.00	0.0	187.70	**0.25**	-1.82	-0.76	-0.27	**-0.28**	6.01	-3.10	1.50	3.66	1.16
-0.00	-0.00	2000.00	500.00	-2.70	**0.02**	0.08	-0.01	-0.04	**-0.16**	-0.06	0.13	0.18	-0.00	-0.00
-0.00	-0.00	2000.00	0.0	166.70	**0.14**	-1.76	-0.72	-0.23	**-0.18**	5.26	-3.02	0.76	3.44	1.13
100.00	100.00	2000.00	1000.00	1.80	**-0.16**	-0.03	-0.18	-0.25	**-0.35**	-0.44	0.08	0.22	-0.45	-0.32
100.00	100.00	2000.00	250.00	123.20	**-1.68**	-3.42	-2.40	-1.92	**-2.28**	2.19	-4.83	-2.22	2.14	-0.14
102.00	178.00	800.00	800.00	104.90	**-2.61**	-2.04	-3.11	-3.37	**-6.92**	-4.44	-2.30	-4.43	1.43	-0.19
12.00	147.00	500.00	500.00	183.50	**-1.78**	-2.86	-2.58	-2.28	**-3.92**	0.59	-3.85	-2.42	2.85	0.53
-100.00	83.00	200.00	200.00	242.10	**-2.65**	-4.78	-3.67	-3.15	**-3.28**	2.64	-6.18	-1.73	0.96	-1.58
160.00	160.00	2000.00	1000.00	14.60	**0.87**	1.67	0.87	0.51	**-0.79**	-2.10	2.12	1.34	-0.31	0.48
201.00	201.00	2000.00	0.0	114.30	**-0.46**	-2.23	-0.93	-0.35	**0.50**	4.21	-3.49	-0.90	2.19	0.40
201.00	201.00	1500.00	0.0	106.10	**-0.28**	-2.15	-0.69	-0.05	**1.58**	5.23	-3.37	-0.43	1.74	0.16
201.00	201.00	1250.00	0.0	97.10	**0.96**	-1.54	0.53	1.37	**3.21**	7.00	-3.21	0.40	3.02	1.43
201.00	201.00	1000.00	0.0	76.40	**0.12**	-2.40	-0.08	0.82	**4.54**	7.41	-3.72	0.75	0.79	-0.45
201.00	201.00	750.00	0.0	49.60	**2.01**	0.91	1.95	2.32	**4.30**	5.44	0.56	3.06	1.21	1.12
201.00	201.00	500.00	0.0	27.70	**0.48**	0.10	0.47	0.60	**1.63**	2.10	0.08	1.27	-0.28	-0.18
251.00	251.00	2000.00	0.0	96.40	**-1.02**	-2.58	-1.31	-0.77	**0.66**	3.39	-3.58	-1.18	0.48	-0.73
251.00	251.00	1000.00	0.0	52.40	**0.32**	-0.04	0.30	0.65	**2.69**	3.74	-0.92	1.30	-0.46	-0.58
251.00	251.00	1500.00	0.0	81.70	**-1.20**	-2.95	-1.45	-0.83	**1.29**	3.99	-3.97	-1.03	-0.18	-1.27
251.00	251.00	250.00	0.0	10.10	**-0.02**	-0.12	-0.01	0.03	**0.34**	0.42	-0.11	0.18	-0.27	-0.22
300.00	300.00	2000.00	0.0	80.30	**-0.91**	-2.26	-1.08	-0.60	**1.03**	3.08	-3.06	-0.88	0.03	-0.89
300.00	300.00	1000.00	0.0	41.90	**0.79**	0.14	0.76	1.02	**2.49**	3.21	-0.81	1.52	0.13	0.11
300.00	300.00	500.00	0.0	17.70	**-1.01**	-1.23	-1.01	-0.93	**-0.33**	-0.08	-1.26	-0.63	-1.32	-1.30
300.00	300.00	250.00	0.0	8.60	**-0.10**	-0.19	-0.09	-0.05	**0.23**	0.29	-0.19	0.05	-0.29	-0.25
AVERAGE ENTHALPY DIFFERENCE				91.1										
STD. DEV. (BTU/LB)					**1.17**	**2.25**	**1.61**	**1.45**	**2.48**	**4.03**	**3.13**	**1.52**	**1.71**	**0.80**
TC	(K)				331.5	333.2	331.9	331.3	331.1	328.0	334.7	333.6	327.7	329.8
PC	(PSIA)				623.6	627.0	626.1	625.0	642.7	630.4	635.2	646.4	589.9	603.7
R*TC/PC	(CC/MOLE)				641.2	641.2	639.5	639.4	621.4	627.6	635.8	622.6	669.0	659.0
ALPHAC					6.430	6.443	6.443	6.443	6.443	6.372	6.443	6.372	6.430	6.443
ZC					.279	.279	.279	.279	.279	.280	.280	.280	.279	.279

TABLE IX-21

The Calculated Pseudo-critical Parameters and the PGC Enthalpy Predictions for the (0.369 CH_4, 0.305 C_2H_6, 0.326 C_3H_8) Ternary Mixture Using the Mixing Rules of Table IX-10

TEMP. (DEG F) INLET	TEMP. (DEG F) OUTLET	PRESS. (PSIA) INLET	PRESS. (PSIA) OUTLET	ΔH(EXPT) BTU/LB	DEVIATION IN BTU/LB FROM THE EXPTAL ENTHALPY DIFFERENCE FOR EACH MIXING RULE I	II	III	IV	V	VI	VII	VIII	IX	X
-234.90	-234.90	100.00	0.0	226.01	-0.82	-0.18	0.41	0.60	0.70	7.32	-0.76	1.89	4.33	2.00
-234.90	-234.90	2000.00	100.00	-6.93	-0.66	-0.81	-0.79	-0.79	-0.77	-0.85	-0.83	-0.90	-0.59	-0.54
-200.00	-200.00	250.00	0.0	216.80	-0.73	-0.12	0.46	0.65	0.74	6.95	-0.70	1.66	3.98	1.97
-200.00	-200.00	2000.00	250.00	-6.10	-0.35	-0.52	-0.49	-0.49	-0.46	-0.37	-0.54	-0.61	-0.18	-0.16
-140.00	-140.00	100.00	0.0	202.39	-0.67	-0.18	0.40	0.59	0.69	6.55	-0.75	1.14	3.52	1.95
-140.00	-140.00	2000.00	250.00	-5.57	0.14	0.04	0.04	0.04	0.05	-0.05	0.05	0.02	0.16	0.18
-60.00	-60.00	500.00	0.0	179.74	-0.65	-0.26	0.36	0.56	0.66	6.14	-0.88	0.38	2.90	1.99
-60.00	-60.00	2000.00	0.0	177.21	0.22	0.54	1.13	1.33	1.43	6.72	-0.05	1.28	3.84	2.80
-16.04	-16.04	750.00	0.0	166.75	-0.26	0.07	0.71	0.93	1.03	6.36	-0.57	0.21	2.95	2.40
-16.04	-16.04	2000.00	750.00	-0.84	0.52	0.48	0.33	0.28	0.98	6.65	0.64	0.98	1.11	0.87
52.04	52.04	250.00	0.0	17.25	0.82	1.24	1.28	1.31	1.28	2.07	1.17	1.54	1.13	0.93
52.04	52.04	1000.00	0.0	139.59	-0.25	0.22	1.05	1.34	1.45	8.73	-0.61	-0.12	2.83	2.94
52.04	52.04	1250.00	0.0	142.61	0.05	0.54	1.26	1.52	1.61	8.20	-0.20	0.39	2.98	2.98
52.04	52.04	2000.00	0.0	146.20	0.20	0.59	1.17	1.37	1.45	6.96	0.01	0.79	2.90	2.52
80.00	80.00	250.00	0.0	14.96	0.51	0.87	0.90	0.93	0.90	1.55	0.81	1.11	0.74	0.59
80.00	80.00	1250.00	0.0	127.49	-1.13	-0.37	0.52	0.86	0.95	7.93	-1.32	-0.97	1.90	2.17
80.00	80.00	2000.00	0.0	136.61	0.11	0.59	1.21	1.43	1.51	6.72	-0.05	0.61	2.75	2.53
100.00	100.00	250.00	0.0	13.71	0.43	0.74	0.77	0.80	0.77	1.36	0.69	0.95	0.61	0.49
100.00	100.00	500.00	0.0	30.90	0.65	1.54	1.65	1.73	1.67	3.36	1.36	2.06	1.28	0.95
100.00	100.00	1250.00	0.0	112.80	-1.91	-0.75	0.22	0.60	0.66	8.81	-1.80	-1.38	1.04	1.52
100.00	100.00	1500.00	0.0	121.53	-0.64	0.25	1.06	1.37	1.44	7.89	-0.61	-0.09	2.10	2.28
100.00	100.00	2000.00	0.0	129.00	-0.14	0.48	1.11	1.34	1.39	6.44	-0.17	0.39	2.29	2.16
126.20	126.20	250.00	0.0	12.39	0.44	0.71	0.74	0.76	0.74	1.23	0.67	0.87	0.58	0.49
126.20	126.20	500.00	0.0	27.02	0.54	1.26	1.32	1.37	1.32	2.62	1.15	1.76	0.99	0.69
126.20	126.20	750.00	0.0	45.75	0.56	1.93	2.13	2.26	2.18	5.08	1.66	2.70	1.52	1.18
126.20	126.20	900.00	0.0	59.36	0.77	2.69	3.00	3.19	3.08	6.94	2.23	3.53	2.06	1.73
126.20	126.20	1000.00	0.0	69.31	-0.17	2.14	2.66	2.94	2.82	9.24	1.43	2.82	1.57	1.48
126.20	126.20	1100.00	0.0	79.19	-0.68	1.72	2.40	2.74	2.63	9.10	0.85	2.15	1.46	1.51
126.20	126.20	1500.00	0.0	105.54	-1.07	0.51	1.19	1.49	1.46	7.60	-0.23	0.67	1.24	1.15
126.20	126.20	2000.00	0.0	118.06	-0.59	0.16	0.84	1.09	1.14	6.44	-0.57	-0.27	1.68	1.78
160.00	160.00	250.00	0.0	10.51	-0.13	0.11	0.13	0.15	0.13	0.53	0.08	0.25	-0.03	-0.09
160.00	160.00	500.00	0.0	22.86	-0.03	0.54	0.60	0.65	0.61	1.68	0.44	0.90	0.32	0.11
160.00	160.00	1000.00	0.0	53.10	-0.44	1.09	1.30	1.45	1.35	4.37	0.75	1.81	0.49	0.18
160.00	160.00	1250.00	0.0	70.43	-1.09	0.83	1.25	1.49	1.38	6.14	0.25	1.57	0.50	0.26
160.00	160.00	1500.00	0.0	85.07	-1.63	0.10	0.67	0.94	0.88	6.42	-0.61	0.45	0.27	0.23
160.00	160.00	2000.00	0.0	102.98	-0.95	0.18	0.75	0.99	0.98	5.91	-0.48	0.03	0.89	0.95
192.00	192.00	250.00	0.0	9.67	0.14	0.35	0.38	0.40	0.38	0.78	0.31	0.44	0.23	0.20
192.00	192.00	500.00	0.0	20.42	0.20	0.69	0.74	0.78	0.74	1.62	0.61	0.99	0.48	0.31
192.00	192.00	1000.00	0.0	44.79	-0.17	0.98	1.16	1.27	1.20	3.50	0.72	1.50	0.54	0.29
192.00	192.00	1500.00	0.0	70.70	-0.74	0.86	1.22	1.42	1.33	5.41	0.38	1.49	0.63	0.41
192.00	192.00	2000.00	0.0	89.44	-1.19	0.12	0.60	0.83	0.79	5.36	-0.47	0.26	0.35	0.44
260.00	260.00	250.00	0.0	7.95	0.22	0.39	0.40	0.41	0.39	0.64	0.36	0.48	0.27	0.22
260.00	260.00	1000.00	0.0	33.86	0.52	1.30	1.39	1.45	1.40	2.81	1.16	1.67	0.90	0.73
260.00	260.00	1500.00	0.0	51.96	0.39	1.59	1.77	1.90	1.82	4.32	1.32	2.14	1.08	0.93
260.00	260.00	2000.00	0.0	66.92	-0.57	0.56	0.90	1.07	1.03	4.38	0.13	0.74	0.42	0.54
-115.30	47.00	250.00	250.00	239.40	-1.61	-1.57	-1.02	-0.86	-0.73	4.21	-2.09	-0.72	2.15	0.94
0.50	107.90	750.00	750.00	153.27	-1.86	-3.30	-2.87	-2.81	-2.60	-0.59	-3.60	-4.24	0.04	0.09
95.00	110.00	1250.00	1250.00	18.81	-0.14	-0.81	-0.86	-0.89	-0.84	-0.15	-0.63	-0.88	-0.17	-0.18
AVERAGE ENTHALPY DIFFERENCE				83.3										
STD. DEV. (BTU/LB)					0.76	1.06	1.24	1.38	1.37	5.41	1.03	1.47	1.83	1.44
TC	(K)				288.4	288.4	287.8	287.6	287.5	283.9	289.0	289.6	287.1	286.2
PC	(PSIA)				654.3	668.6	665.8	665.6	663.8	665.0	670.3	684.6	651.7	642.0
R*TC/PC	(CC/MOLE)				531.8	520.3	521.5	521.3	522.4	515.0	520.2	510.1	531.5	535.0
ALPHAC					6.245	6.236	6.236	6.236	6.236	6.192	6.236	6.192	6.245	6.236
ZC					.284	.284	.284	.284	.284	.285	.284	.285	.285	.284

TABLE IX-22

Summary of the PGC Enthalpy Predictions for the Mixing Rules of this Investigation

ENTHALPY DEVIATIONS IN (BTU/LB)

SYSTEM	MIXING RULES									
	OPT.	II	III	IV	V	VI	VII	VIII	IX	X
CH4-C3H8	1.67	1.89	1.92	1.95	2.18	5.15	2.35	2.20	2.35	1.66
C2H6-C3H8	0.71	1.26	1.39	1.39	1.90	1.29	1.23	1.82	3.35	3.03
TERNARY	0.76	1.06	1.24	1.38	1.37	5.41	1.03	1.47	1.83	1.44

Critique of Mixing Rules

While no mixing rule is consistently superior in performance for every system considered in this investigation, the Pitzer-Hultgren rule (II) appears to work best on an overall basis. However, as the rule has little, if any, theoretical basis, it is difficult to forecast a similar degree of success in applying the rule to other multi-component systems. The fact that rule VII provides the least deviation for the ethane-propane system and the ternary mixture, and rule X provides the best results for the methane-propane system suggests that the basic approach for calculating mixture pseudo-parameters as a function of composition from a set of extensive second virial coefficient values for the same mixture (synthetically generated if necessary) is fundamentally sound. The three separate techniques encompassed by Rules VII, IX and X for the practical implementation of the same basic scheme were developed and tested to determine if any one approach was consistently superior. The inconclusive nature of the results suggest that further work is needed to refine the technique.

It is, however, still unclear whether the relative performance of the mixing rules based on binary enthalpy data can be indisputably evaluated from the results of this investigation. The fact that Kay's rule (VI) works better for the ethane-propane system than other rules with empirically determined interaction parameters (see Table IX-22) clearly indicates that our procedure for specifying these interaction parameters is not yet optimally defined. The fact that the enthalpy predictions for rule V in Table IX-15 are, for example, poorer than for rules III and IV, even though the Tc_m and RTc_m/Pc_m values in the former case are closer to the "optimum" values in I appears to confirm this conclusion. Furthermore, the fact that rules IX and X yield relatively poor results for the ethane-propane system, a system for which the fundamental assumptions used in deriving the rules are least questionable, suggests the possibility that the optimal averaging of the B_{ij} values for these rules is yet to be achieved.

In retrospect, such inconsistencies could have been avoided if the more time consuming but less uncertain approach of specifying the interaction parameters for each mixing rule by optimizing the fit to the enthalpy data for all mixtures of a binary system taken together

were utilized instead. In effect, such a scheme optimizes the three separate mixing rules involving various combinations of the pseudo-parameters simultaneously. In particular, the scheme has the added flexibility of permitting the optimum value of the parameter αc_{ij} to vary from rule to rule even when the quadratic mixing rule for αc_m is common to many different sets of rules in Table IX-10.

The analysis of mixing rules based strictly on pure component critical properties is more straight-forward. In general, their performance degrades as the size and energy parameter ratios for the constituent pure components of a mixture depart from unity. For example, Kay's rule would appear to be inadequate for enthalpy predictions on mixtures whose components are as dissimilar as methane and propane. The Van der Waal mixing rule with the Lorentz-Berthelot assumptions (VIII) appears to be preferable to Kay's rule, particularly for the prediction of the ternary mixture enthalpies. The results in Tables IX-4 through IX-6 suggest, however, that the Redlich-Kwong rule with the harmonic mean assumption for Tc_{ij} and the arithmetic mean assumption for $(RTc_{ij}/Pc_{ij})^{1/3}$, has the potential to do as well, even though it was not included in Table IX-10.

In comparing the pseudo-parameters and the standard deviation in the enthalpy differences for rules VIII and X in Table IX-21 and rules I and X in Table IX-19, it appears that equivalent low deviations can be produced for substantially different pseudo-parameter sets. In particular, large variations (upto 5%) in the value of RTc_m/Pc_m are permissible. This appears to conflict with the highly specific and accurate definition of the optimum pseudo-parameters obtained from the enthalpy data for ethane. The decrease in the specificity of the optimization in going from pure components to mixtures may be explained by the fact the data in the vicinity of the critical point, and information on the precise location of the vapor pressure curve that are so useful in selecting the parameters for pure components are inaccessible in the case of mixtures because the pseudo-critical point and the pseudo-reduced vapor pressure curve lie deep within the excluded two phase region. The only alternative to improve the optimization in such cases would be to simultaneously use as many thermodynamic properties as are required to unequivocally define the three desired

pseudo-parameters.

Notwithstanding our reservations about the theoretical validity of the one fluid corresponding states model for mixtures, and the imperfections in the technique used in this work for specifying the binary interaction parameters from enthalpy data, one can conclude that the enthalpy behaviour of complete binary systems in the single phase region can, for engineering purposes, be adequately characterized as a function of composition in the PGC framework using almost any mixing rule where the interaction parameters are empirically adjusted from limited enthalpy data on the same system. Furthermore, the application of these rules to multi-component systems also appears to be adequate and does not require the use of additional empirical parameters. It is important to emphasize that these conclusions are, for the present, restricted to non-polar systems whose extreme components are not more dissimilar than methane and propane in terms of the ratios of their respective size and energy parameters.

Illustrative Contour Plots for Some Enthalpy Prediction and Correlation Schemes

The performance of selected correlations over the entire P-T range of measurements is succinctly illustrated in the contour plots of Figures IX-4 through IX-8 for ethane, the three ethane-propane mixtures, and for the ternary mixture respectively. The deviation at any P and T is, in each case, expressed by the experimental minus the calculated enthalpy departure. The reduced virial equation, the PGC with optimum pseudo-parameters, and the PGC with pseudoparameters defined by rule VII of Table IX-10 were tested in every case.

The reduced virial equation uses Equations (V-30) and (III-44) to define the reduced second and third virial coefficients respectively. The enthalpy departure is calculated using relevant thermodynamic identities in Appendix H-3. The optimum pseudoparameters were used in each case to illustrate the limitations of the range of applicability of the method without introducing the additional uncertainties imposed by mixing rules. The application of the technique was restricted to the gas phase and to the dense fluid above the critical temperature. The

truncated virial equation appears to be satisfactory at least upto 500 psia. Its reliability at higher pressures increases as one moves towards the right of the heat capacity maxima.

A comparison between the performance of the PGC using optimum pseudoparameters and that obtained with rule VII is a measure of the extent to which the representation of individual mixture enthalpies in a corresponding states framework is degraded by further codifying the results as a function of composition through a mixing rule.

The Starling BWR was tested for its ability to represent the ethane enthalpy data using a set of constants provided by the author [249] that were determined primarily by interpreting the volumetric data of Sage and coworkers [209]. The calculations were, however, not extended below -70°F because of calculation errors introduced by this author in applying the technique in the cryogenic liquid region.

The ternary mixture enthalpies were compared against six methods including the Rice Properties III [81], the Starling BWR [254] and the Johnson-Colver [118] correlations, all of which are discussed in Chapter III. These three additional methods were already evaluated by Starling et al. in a previous comparison study [253]. However, the "experimental" enthalpies used in the study were actually obtained from a preliminary PGC fit to the basic data and the comparisons have therefore been repeated using the correct results.

This author is at present not familiar with how much or what type of constituent binary data was utilized by Starling in applying the above three methods to the ternary mixture. Certainly, the enthalpies for the methane-propane binary were available for some time before the study was initiated. In any case, the PGC predictions using mixing rule VII is seen from Figure IX-8 to be superior to all these methods. We may therefore conclude that the prediction of multi-component mixture can be more fruitfully accomplished if constituent pure component and binary enthalpy data are used in the prediction scheme.

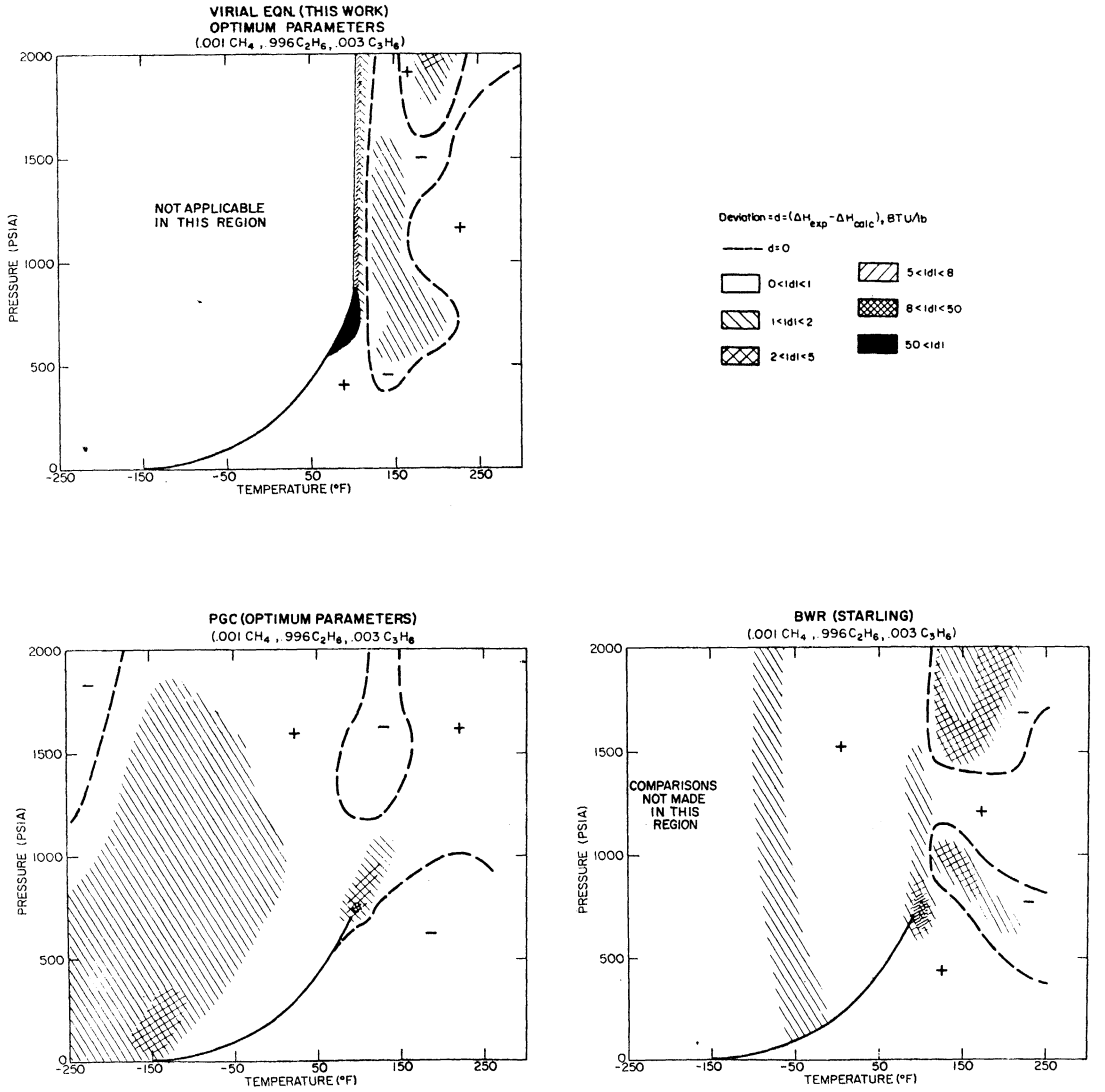

Figure IX-4. The Performance of Some Corresponding States Techniques in Calculating the Enthalpy Departure for 0.996 Ethane.

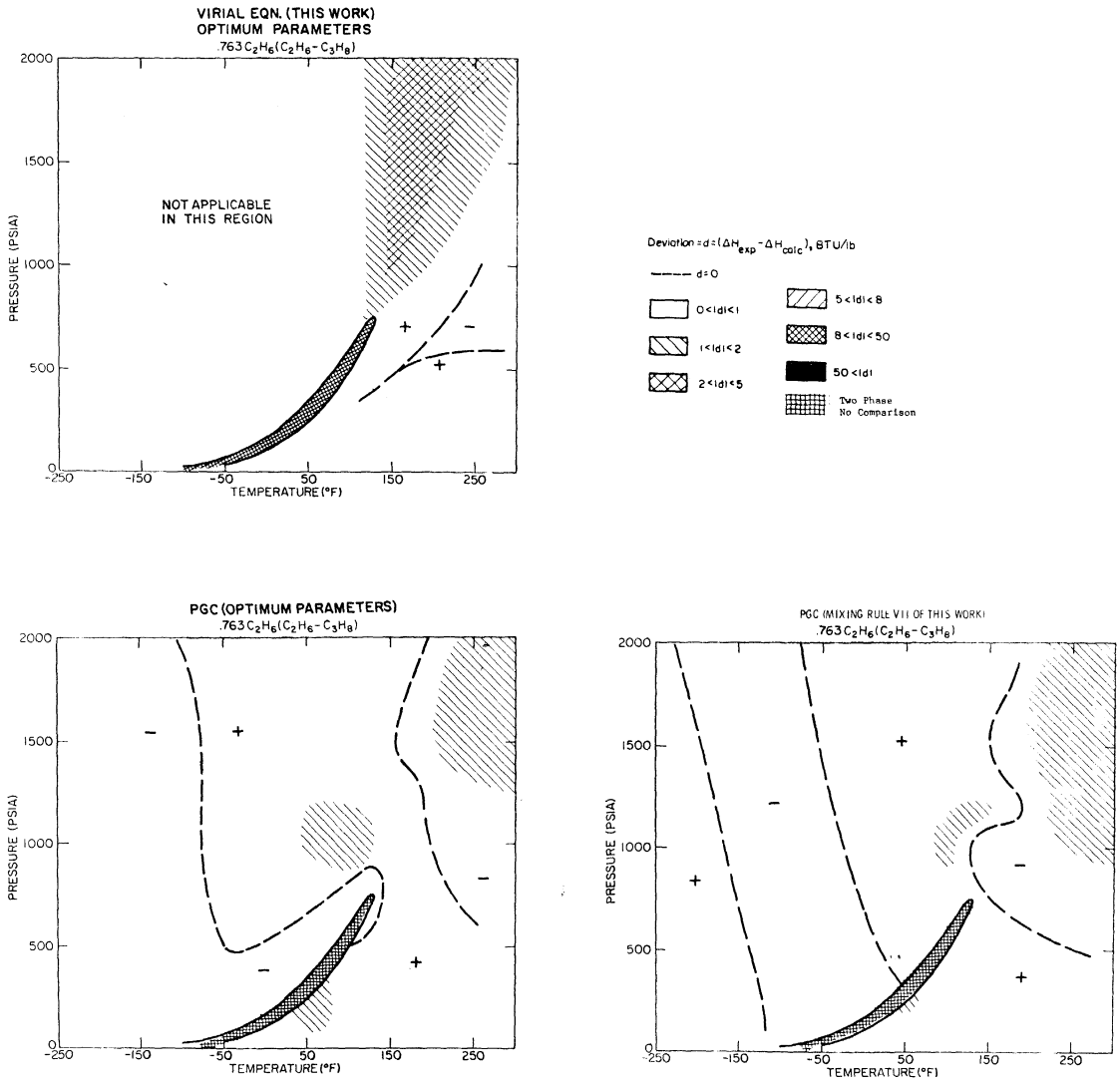

Figure IX-5. The Performance of Some Corresponding States Techniques in Calculating the Enthalpy Departure for the 0.76 Mole Fraction Ethane-Propane Mixture.

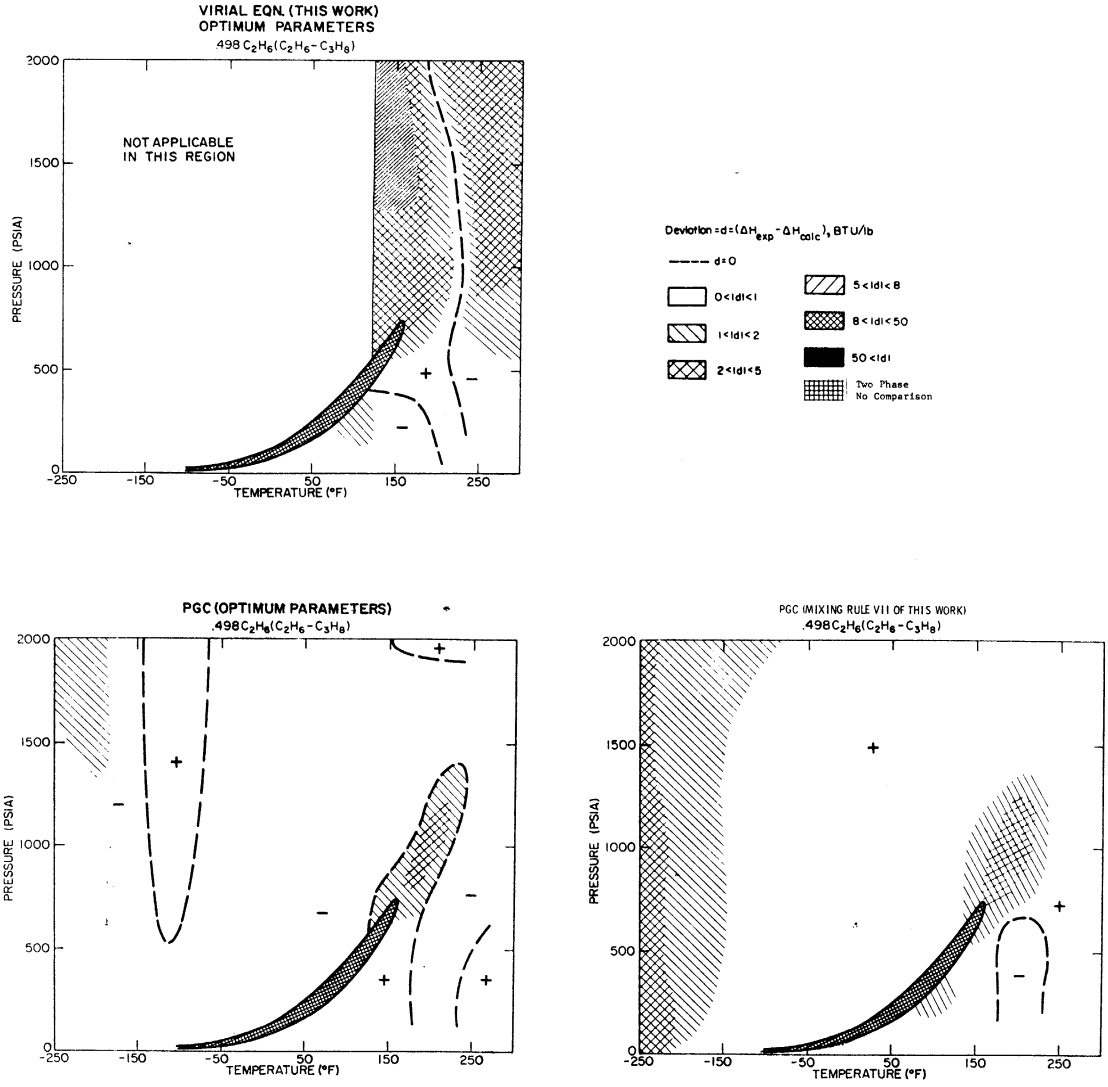

Figure IX-6. The Performance of Some Corresponding States Techniques in Calculating the Enthalpy Departure for the 0.50 Mole Fraction Ethane-Propane Mixture.

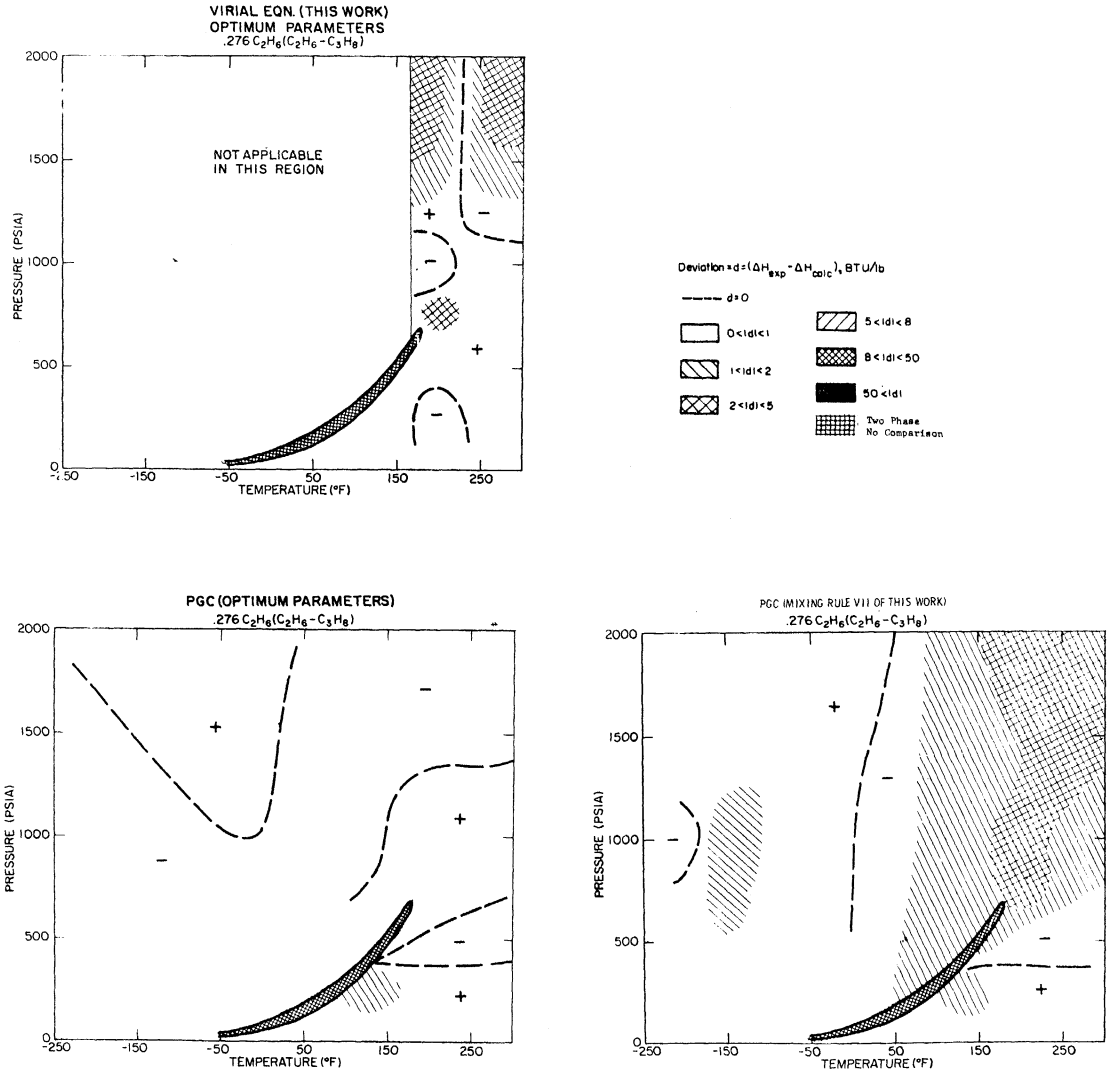

Figure IX-7. The Performance of Some Corresponding States Techniques in Calculating the Enthalpy Departure for the 0.27 Mole Fraction Ethane Propane Mixture.

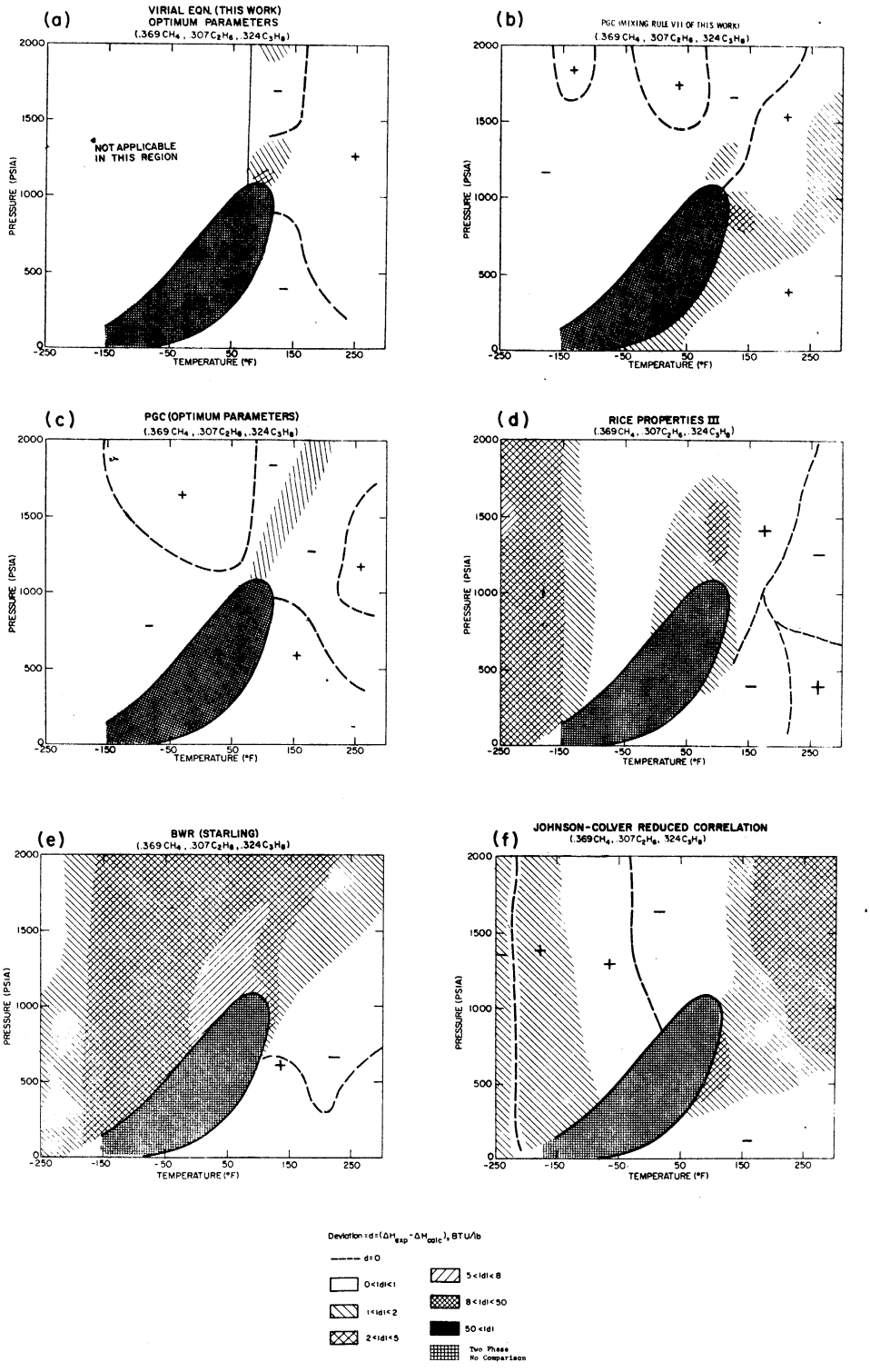

Figure IX-8. The Performance of Some Enthalpy Prediction Techniques with Respect to the Ternary (0.369 CH_4, 0.305 C_2H_6, 0.323 C_3H_8) Mixture.

Chapter X
SUGGESTIONS FOR FURTHER RESEARCH

Specific suggestions for further improvements with respect to various aspects of this investigation have been distributed throughout the text where appropriate. The discussion in this chapter is primarily meant to provide the reader with an overall perspective of various courses for further research as suggested by this study.

a) Suggested Improvements for the Operating of the Existing Facility. As the experimental investigation of this work was essentially conducted on a production basis, it was difficult to continuously monitor the precision of the measurements. Under optimum operating conditions, it is believed that the accuracy of the measured enthalpy change can be increased to better than 0.2%. The care and effort necessary to achieve these conditions will undoubtedly require a much longer investment in time and energy per investigation as evidenced by the painstaking work of Manker [162]. The high degree of inertia present in the existing facility, coupled with its enormous maintenance requirements, makes its continued operation prohibitively expensive. Accordingly, the establishment of a less complex facility characterized by minimum valving and quick response is recommended. Notwithstanding the severity of the operating problems in the present faciltiy, the fortunate use of high flowrate has, in the ultimate analysis, prevented the quality of the measurements from being severely compromised.

If, however, the continued operation of the existing facility is necessary, then the following improvements are recommended.

1) Assuming that all system variables such as temperature, pressure, flowrate and compositions at the calorimeter inlet are steadily maintained, a minimum wait of at least sixty minutes, after the intial addition of power to the calorimeter, is recommended to achieve quasi-steady state conditions.

2) During the course of a run, at least one data point, and preferably the first, should be repeated at a significantly different flowrate to evaluate the contributions due to unsteady state and heat

or mass leaks at the calorimeter. Furthermore, a set of chronologically dispersed replicate measurements should be obtained for some arbitrarily chosen data point to monitor undesirable and otherwise undetectable changes in instrument calibrations or calorimeter operation.

3) As indicated in Appendix F-4, the calculation of the system composition will be more accurately accomplished in the face of composition variations of about 1% or more, if the system fluid is chromatographically analyzed along with two pre-calibrated mixtures differing slightly in the mole fractions of the individual components, instead of the one pre-calibrated standard currently used.

4) The control of the calorimeter and the pre-conditioning baths for operating temperatures below -150°F was seriously disrupted by the periodic replacement of 50 litre liquid nitrogen dewars. It is felt that larger dewars with a capacity of 150 litre or more, providing a steady liquid nitrogen flowrate, would provide a smoother operation.

5) A high precision differential pressure transducer with a measurement range from 0 to 500 psid at pressure levels upto 2000 psia, with a repeatability of better than 0.1% full scale and negligible hysteresis would, in conjunction with the transduer calibration facility, serve to increase the accuracy of the isothermal and isenthalpic measurements. A similar transducer with 1% precision in the range 0 to 5 psid could be used to record the small pressure drops obtained for the isobaric measurements. If all the variables involved in the measurement of composition and flowrate can be similarly transduced to provide an electrical output, then all the critical measurements could be obtained on a high precision (0.01% or better) automatic-switching, self-balancing potentiometer with provisions for direct recording of the data. Such measures would reduce both manpower requirements and human error.

6) The contamination of the valve manifold for the differential pressure transducer calibration manometer due to mercury blowback may be controlled by the installation of a differential pressure gauge (for example, Item 14f, Appendix D) between the gas and the mercury legs for each section of the manometer, permitting the mercury level in the latter case to be more accurately estimated. The use of pressure snubbers to check surges in the mercury filled legs is also

recommended.

b) Suggestions for Improving the Interpretation of the Basic Data. Although the non-linear least squares regression technique was rejected in favor of the Lagrange polynomial representation of the thermal properties Cp and ϕ, its attractiveness could be enhanced if it were possible to separately fit the measurements on either side of the peak for a given isobar or isotherm while ensuring the continuity of the function Cp or ϕ and the appropriate first derivative at the peak itself. Two separate polynomial expansions on either side of the peak each incorporating a gaussian term appear to be eminently suitable to meet these requirements.

For example, the isothermal throttling coefficient ϕ may be represented along an isotherm by the functional forms

$$\phi = a + b(P - P_k) + c(P - P_k)^2 + d(P - P_k)^3 + fg\, e^{-f(P - P_k)^2}, \quad P \leq P_k \tag{X-1a}$$

$$\phi = a' + b'(P - P_k) + c'(P - P_k)^2 + d'(P - P_k)^3 + f'g'e^{-f(P - P_k)^2}, \quad P \geq P_k \tag{X-1b}$$

The requirement of continuity in the value of ϕ at the peak, $P = P_k$, leads to the restriction

$$a + fg = a' + f'g' \tag{X-2}$$

The requirement

$$\left(\frac{d\phi}{dP}\right)_{P=P_k} = 0 \tag{X-3}$$

must be satisfied by Equations (X-1a) and (X-1b) separately, and leads to the restriction

$$b = b' = 0 \tag{X-4}$$

Additional polynomial terms may be added as necessary. Asymmetry in the peak region may be obtained by adjustment of the ratio f/f' away from unity. This is advantageous, because the presence of peak

asymmetry was noted for both the isobaric and isothermal data of this work. Sirota et al. [244] have also confirmed that the Cp maxima along isobars are steeper on the liquid side near the critical temperature, pass through a point of symmetry, and appear at higher temperatures to be sharper on the gas side.

c) Suggestions for Further Experimental and Correlative Research.

1) The enthalpy departures for the propane reference table in the PGC were found to be in error at 150K (near 0.4Tr for propane). The error was traced to a misprint in the zero pressure tables for the function [H(T) - H(0)]/T as compiled by the American Petroleum Institute [220], and used in conjunction with the data of Yesavage [284] to establish the reference table. If the value of the function is changed from 8.14 cal/gm mole K to 8.44 cal/gm mole K, so as to be consistent with the [H(T) - H(0)] tables from the same reference, then the performance of the correlation may be improved in the vicinity of 0.4 Tr for all other substances also.

2) It is suggested that the PGC correlation for the enthalpy departure featuring the αc dependent reduced temperature parameter be extended to include the prediction of other thermodynamic properties including the volume and the heat capacity departure, $Cp - Cp^\circ$. Although separate reference tables may be used to represent each property, the development and use of a precise equation of state to represent the reference fluid properties over the range of the calorimetric investigation of this work affords a more concise alternative and provides a consistent set of smoothed thermodynamic properties, not assured in the tabular approach. It is, however, doubtful whether any PVT equation of state currently used in engineering design calculations can provide a precise fit to the heat capacity departures for light hydrocarbons over the entire fluid phase. The problem may, perhaps, be more fruitfully tackled by concentrating future efforts on the development of a thermal property equation of state expressing $Cp - Cp^\circ$, or ϕ, or even the property Ψ in Equation (I-1) as a function of temperature and pressure. Most thermodynamic properties may then be obtained with little loss in precision, by integration rather than differentation of an equation of state.

3) Calorimetric measurements involving enthalpy traverses into, and across, the two phase region for a mixture of fixed overall composition rarely, if ever, specify the quantity and composition of the individual phases. As such information is necessary for the prediction of total mixture enthalpies by most techniques, two phase enthalpy data are consequently ignored in most comparative studies. It is urged that each enthalpy prediction method be accompanied by a technique for the estimation of phase equilibria to permit the extension of such comparisons into the two phase region. In particular, as the phase predictions for techniques based on the corresponding states principle depend on the derivatives of the various pseudo-parameters with respect to composition, (See reference [206] for further information), the analysis of two phase data has the potential of being far more selective of mixing rules than single phase data alone

4) The success of the modified reduced temperature parameter Tr_{oo} in decreasing the contribution of the perturbation term $(Br - Br_{oo})$ in Equation (V-30), when compared with the equivalent term in other reduced second virial coefficient correlations [159,195] that use the unmodified reduced temperature Tr as the correlating parameter suggests that it may also be useful in correlating higher order virial coefficients. The availability of the precise third and fourth virial coefficient data of Douslin [67] on CH_4 and CF_4 makes this a feasible venture, but additional measurements below 1.5Tr are also desirable.

5) The accurate estimation of the second virial coefficient from the critical properties of a pure substance and vice-versa, is a crucial factor in the performance of the pseudo-critical parameter calculation technique as encompassed by rules VII, IX and X (See Table IX-10) developed in the work. In particular, if the range of the second virial coefficient correlation used in such calculations can be increased, then it may be possible to increase the range of the B_m data used to optimize the pseudo-parameters for such rules. In turn, one would expect to obtain a more selective set of optimum parameters, particularly for rules IX and X.

The form of Equation (V-35) with n expressed as a function of Tr_{oo} is suggested as a starting point for extending the correlation expressed by Equation (V-30) so as to cover the range $0.5 \leq Tr \leq 20$. Additional

second virial coefficient measurements are necessary if such a correlation is to be used with confidence. Accurate low temperature data on n alkanes ($Tr \leq 0.7$) would be especially useful in resolving inconsistences in the current data in the literature. Measurements at high reduced temperature ($Tr \geq 3.0$), particularly in the vicinity of the maximum in B for substances whose αc values are significantly different from the simple fluid case, as for example, CF_4, would be very useful in defining the slope term $dBr/d\alpha c$ in this region.

6) The discrepancy between the optimum pseudo-parameters of Yesavage [284] and those of Pitzer and Hultgren [197] obtained for individual methane-propane mixtures from wide-ranging thermal and volumetric data, respectively, suggests that the methane-propane system should be completely reanalyzed from the standpoint of the pseudo-critical method. The pseudo-parameters for the individual methane-propane mixtures should be recalculated using the enthalpy data sets in Tables IX-16 through IX-20, as they are believed to be more selective than the original set of enthalpy data used in the optimization. The consistency test in Figure IX-6 should then be repeated with the new set of parameters to determine if any change in behaviour results from the reinterpretation.

It is possible that the discrepancies may have occurred because the reference enthalpy tables of Yesavage [284] or Powers [304] were not consistent with the volume tables of Curl and Pitzer [54]. Ideally, therefore, both volumetric and enthalpy data should be separately interpreted in thermodynamically consistent schemes, if we wish to determine whether the correlation of any one of the two properties in a corresponding states framework is sufficient to accurately predict the other.

It is also possible that the Pitzer optimization was not selective enough because the volumetric data were optimized over the restricted range from 40°F to 460°F. For better selectivity it is recommended that additional PVT measurements be obtained in the liquid phase from -250°F to +40°F and used in the optimization. In fact, Huang, Swift and Kurata [110] have already obtained some data in this region.

Several possibilities could be investigated if the PGC were extended to include the correlation and prediction of volumetric properties. Firstly, the existing volumetric data alone could be used

generate interaction parameters. These parameters could then be tested for their ability to predict the enthalpies of the methane-propane system. The revised pseudo-parameters based on the optimization of enthalpy data alone could also be used to predict the volumetric behaviour of the methane-propane system. It would also be interesting to determine whether the addition of second virial coefficient measurements to enthalpy data is of any significance in influencing the optimization to yield a set of pseudo-parameters that would improve the fit to the rest of the volumetric data over the entire fluid phase. Lastly, a multi-property optimization using enthalpy, volumetric and second virial coefficient measurements should be attempted to determine if a single set of pseudo-critical parameters can be defined without compromising the goodness of fit relative to the situation where each property is optimized separately. In essence, it is hoped that such a study would provide us with a better idea of the type and extent of experimental measurements that are necessary to accurately characterize a system of two or more non-polar substances in the one fluid corresponding states framework when their size and energy parameters are appreciably different.

7) The new set of interaction constants for the methane-propane system could then be used to reexamine the performance of the various rules in predicting the enthalpies for the ternary mixture.

8) Instead of using the body of enthalpy data on hydrocarbon mixtures now accumulated under the sponsorship of the NGPA and the API merely for the purpose of testing prediction methods, one can incorporate such information directly into the prediction techniques themselves. The enthalpy departure of an unknown mixture m, can be expressed in terms of the enthalpy departure of a reference mixture s at the same temperature and pressure by the relation

$$H - H^{\circ}(T,P)_m = H - H^{\circ}(T,P)_s + \left\{ [H - H^{\circ}(T,P)_m] - [H - H^{\circ}(T,P)_s] \right\} \qquad (X\text{-}5)$$

A judicious choice of the reference mixture s, i.e., one whose pseudo-critical parameters are close to that for a given mixture, can serve to significantly decrease the contribution of the second term on the right hand side. As any error involved in the first term

is only limited by the accuracy of the data on the reference mixture, any uncertainties involving the adequacy of either the specific corresponding states framework selected, or the particular mixing rule utilized, apply only to the prediction of the second term.

The success of the method depends, of course, on the extent and reliability of the data on the reference mixtures, and the availability of a reference whose components and pseudo-critical properties are similar to that for the unknown fluid. Even then, any incentive to develop such a method for practical use would depend upon our ability to accurately codify the properties of the reference mixture in concise form. The advantage of this technique, however, is that we are not subjected to the restrictions imposed by the corresponding states approach in representing the reference mixture properties in concise form.

One potential application of the technique involves the use of the methane-propane mixtures containing 0.946 and 0.883 mole fraction methane, respectively, as standards for predicting the properties of natural gas mixtures. For example, if we were confronted with determining the enthalpies of a mixture containing 0.92 mole fraction CH_4, 0.01 mole fraction C_2H_6 and 0.07 mole fraction C_3H_8, we would use the 0.946 methane-propane mixture as our reference. The second term on the right hand side of Equation (X-5) may be evaluated in one of two ways. In the first case, one may evaluate the term using the PGC framework with the pure component reference tables and some specified mixing rule (not necessarily involving empirically determined interaction parameters). In a different approach, both the 0.946 and the 0.883 mole fraction mixtures may be used to define a new set of reference data in the PGC framework replacing the original tables. The calculation may then be repeated as before.

9) In the continuing search for the utopian mixing rule, one is at first tempted to develop and test as many mixing rules as possible. For example, another modification of the Van der Waal mixing rules, similar to rule VIII of Table IX-10, may be developed using the general procedure outlined in Appendix G if the criterion in Equation (V-19a) is replaced by the condition $(\partial^2 P/\partial V^2)_T = 0$ at the critical point. The result is given by

$$\frac{Tc_m}{Pc_m}\left[\left\{\frac{3(\alpha c_m - 1)}{\alpha c_m^3}\right\}^{1/2} - \frac{1}{\alpha c_m}\right] = \sum_{i=1}^{n}\sum_{j=1}^{n} x_i x_j \frac{Tc_{ij}}{Pc_{ij}}\left[\left\{\frac{3(\alpha c_{ij} - 1)}{\alpha c_{ij}^3}\right\}^{1/2} - \frac{1}{\alpha c_{ij}}\right] \qquad (X\text{-}6)$$

$$\frac{Tc_m^2}{Pc_m}\frac{(\alpha c_m - 1)^2}{\alpha c_m^3} = \sum_{i=1}^{n}\sum_{j=1}^{n} \frac{Tc_{ij}^2}{Pc_{ij}}\frac{(\alpha c_{ij} - 1)^2}{\alpha c_{ij}^3} \qquad (X\text{-}7)$$

Similar rules involving the effect of αc could be developed starting with the reduced Redlich-Kwong equation of state.

As long as the interaction parameters are empirically adjusted to suit individual rules, one cannot anticipate significant differences in their performance, unless perhaps such rules are applied to systems where the critical properties of the constituent pure components are markedly different, as for example, in the methane-octane system. To complicate the analysis further, an additional degree of freedom is contributed by the specific corresponding states model used. For example, the entire investigation in Chapter IX could be reworked using the two fluid model. It is clearly questionable whether the repetition of the entire process for other systems, as more data becomes available, is of any real fundamental value to our understanding of the problem.

Although statistical thermodynamics is not yet competitive with empirical methods in predicting the configurational properties of real substances, it has advanced enough to permit us to evaluate mixing rules and corresponding states models with little ambiguity for simpler systems, such as Lennard-Jones molecules, because the interaction parameters in such cases can be unequivocally specified. The differences between the various mixing rules and the corresponding states models can, as we have seen in Chapter IV, be accentuated by careful choice of the molecular parameters for the pure components; a luxury that one rarely obtains in working with real systems. Although one must be careful in extrapolating such results to real systems of interest, the fact that such models approximately simulate real fluid behaviour permits us, at least, to reject those rules that perform poorly. It is this author's opinion that further research in this area has considerably more potential for improving our fundamental understanding of the application of the corresponding states principle to real systems than our success or failure in representing real data with empirically adjusted mixing rules.

10) The use of the pseudo-critical technique for the correlation of the thermodynamic properties of fluid mixtures suffers from one serious drawback in that the mixture parameters, unlike pure component critical properties, are not subject to direct experimental verification. Consequently, values ascribed to such parameters by indirect techniques often depend upon the type and range of the data analyzed, or on the specific corresponding states framework used.

The trajectories of characteristic curves in the P-T plane common to both pure components and mixtures have been traced on reduced coordinates by Brown [30]. These include the Joule-Thomson inversion curve, $[(dH/dP)_T = 0]$, the Boyle curve, $[(dz/dV)_T = 0]$, and the locii of the heat capacity maxima $[(dCp/dP)_T = 0$, or $(d(Cp - Cp°)/dT)_p = 0]$. Characteristic points of special interest include the Boyle temperature Tb in the dilute gas, and the maximum in the Joule-Thomson inversion curve in the dense fluid.

An experimental program to map such locii for selected pure components and mixtures would provide incontrovertible evidence in regard to the validity of the corresponding states principle particularly for the mixed systems so mapped. Such measurements would also permit the correlation of the thermodynamic properties of mixtures to be anchored to unequivocally defined parameters. By restricting the degrees of freedom in this manner, it may be possible to make more meaningful improvements in existing correlations.

APPENDIX A

Sample Calibration Results for Various Instruments Used in Obtaining the Basic Measurements

TABLE A-1

National Bureau of Standards Calibration for the Reference Cell

FORM NBS-70
(3-67)

U.S. DEPARTMENT OF COMMERCE
NATIONAL BUREAU OF STANDARDS
INSTITUTE FOR BASIC STANDARDS
WASHINGTON, D.C. 20234

REPORT OF CALIBRATION
UNSATURATED STANDARD CELL

Manufacturer: Eppley Laboratory Inc. Cell No. 650924

Submitted by

The University of Michigan
Research Administration Building
Ann Arbor, Michigan 48105

The electromotive force of this cell at 24 °C was, at the time of test, 1.01880 volts. This value, correct to 0.005 percent, is the mean of a series of measurements concluded April 23, 1969. The stated uncertainty (0.005%) includes an allowance of ± 50 microvolts for variability in the emf of the cell during test.

This is an unsaturated cell of the cadmium sulfate type, suitable for work requiring no greater accuracy than 0.005 percent. Such cells have a temperature coefficient that is negligible within the ordinary range of room temperature. Rapid changes in temperature may, however, produce temporary alterations of several hundredths of one percent in the electromotive force.

Precautions in using standard cells: (1) the cell should not be exposed to temperatures below 4 °C, (2) abrupt changes in temperature should be avoided, (3) all parts of the cell should be at the same temperature, (4) current in excess of 0.0001 ampere should never pass through the cell, (5) unsaturated standard cells should be recalibrated at intervals of a year or two because the electromotive force of an unsaturated cell usually decreases with time.

For the Director, Institute for Basic Standards

Walter J. Hamer
Chief, Electrochemistry Section
Electricity Division

Date: April 24, 1969
Test No.: 211.02/198463
Ref. No.: R 101443

USCOMM-DC 37289-P67

Table A-2

Callendar Equation Constants for the New Platinum Thermometer.

U.S. DEPARTMENT OF COMMERCE
NATIONAL BUREAU OF STANDARDS
INSTITUTE FOR BASIC STANDARDS
WASHINGTON D.C. 20234

REPORT OF CALIBRATION

PLATINUM RESISTANCE THERMOMETER
SERIAL NO. 586

SUBMITTED BY
UNIVERSITY OF MICHIGAN
CHEMICAL AND METALLURGICAL ENGINEERING

THIS THERMOMETER WAS CALIBRATED FOR USE WITH CONTINUOUS CURRENT OF 1.0 MA. THROUGH THE THERMOMETER.
THE FOLLOWING VALUES WERE FOUND FOR THE CONSTANTS IN THE INTERNATIONAL PRACTICAL TEMPERATURE SCALE (1946) FORMULAS:

ALPHA = 3.9261045-03	A = 3.9846691-03
DELTA = 1.4916703	B = -5.8564536-07
BETA = .1101008	C = -4.3229875-12

FOR T > 0 DEGREES 0, BETA = C = 0, BY DEFINITION.

THE PERTINENT INTERNATIONAL PRACTICAL TEMPERATURE FORMULAS ARE GIVEN IN THE DISCUSSION ON THE FOLLOWING PAGE.

THE RESISTANCE AT 0 DEGREES 0 WAS FOUND TO BE 25.5548 ABSOLUTE OHMS. DURING CALIBRATION, THIS RESISTANCE CHANGED BY THE EQUIVALENT OF .0008 DEG C.

THIS THERMOMETER IS SATISFACTORY AS A DEFINING STANDARD IN ACCORDANCE WITH THE TEXT OF THE INTERNATIONAL PRACTICAL TEMPERATURE SCALE.

FOR THE DIRECTOR,
INSTITUTE FOR BASIC STANDARDS

HARMON H. PLUMB
CHIEF, TEMPERATURE SECTION
HEAT DIVISION

TEST NO.639288
COMPUTED JUNE 1968
JLR/UNIVAC

Temperatures on the International Practical Temperature Scale of 1948 (IPTS-48) between -182.97 °C and 631.5 °C are defined by the indications (resistance values) of standard platinum resistance thermometers together with either of the following formulas.

$$R_t = R_o (1 + At + Bt^2 + Ct^3 (t-100))$$

or,
$$t = \frac{1}{\alpha}\left(\frac{R_t}{R_o} - 1\right) + \delta \left(\frac{t}{100} - 1\right) \frac{t}{100} + \beta \left(\frac{t}{100} - 1\right) \left(\frac{t}{100}\right)^3$$

where t is the temperature, at the outside surface of the tube protecting the platinum resistor, in °C on International Practical Temperature Scale of 1948 and R_t and R_o are the resistances of the platinum resistor at t° and 0 °C, respectively, measured with a continuous current through the platinum resistor. The value of this current, together with the constants A, B, and C for the first form of the equation, and α, δ, and β for the second form of the equation, is given on the previous page. The formulas are completely equivalent, the choice between them concerns only which form is less difficult to calculate.

TABLE A-3

Sample Regression Results for the Six Junction Copper-Constantan Thermopile 6M

Temp. (°K) T	Measured* Emf (Microvolts)	Calculated** Emf (Microvolts) E	Difference (Microvolts)	% Error
-196.00	-33339.0	-33324.4	-2.6	0.017
-183.00	-31986.0	-31989.8	3.8	-0.012
-160.00	-29286.0	-29289.7	3.7	-0.012
-140.00	-25140.0	-25145.0	5.0	-0.020
-100.00	-20338.0	-20334.1	-3.9	0.019
-80.00	-16781.0	-16776.9	-4.1	0.024
-60.00	-12956.0	-12953.7	-2.3	0.018
-40.00	-8877.0	-8875.9	-1.1	0.012
-20.00	-4557.0	-4555.0	-2.0	0.044
0.01	2.3	0.4	2.0	84.956
20.00	4775.0	4772.3	2.7	0.057
40.00	9761.0	9757.1	3.9	0.040
60.00	14944.0	14942.2	1.7	0.012
80.00	20322.0	20317.5	4.5	0.022
100.00	25868.0	25872.9	-4.9	-0.019
120.00	31593.0	31599.0	-6.0	-0.019
140.00	37484.0	37486.1	-2.1	-0.006
160.00	43530.0	43525.3	4.7	0.011

PERCENT STD. DEVIATION = 0.02174

* NBS Calibration

** Calculated using the Equation:

$$E = 1.9179 + 233.271T + 0.27651T^2 - 0.22361x10^{-3}T^3 + 0.62684x10^{-7}T^4$$

TABLE A-4

Original National Bureau of Standards Calibration
for the Fifteen Junction Thermopile

FORM NBS-417F
(7-65)

U.S. DEPARTMENT OF COMMERCE
NATIONAL BUREAU OF STANDARDS
INSTITUTE FOR BASIC STANDARDS
WASHINGTON, D.C. 20234

REPORT OF CALIBRATION

THERMOCOUPLE

COPPER CONSTANTAN
(15 junctions)
(Tagged #2)

Submitted by

The University of Michigan
Ann Arbor, Michigan

Electromotive Force as a Function of Temperature of
Measuring Junction (reference junctions at 32°F)

Degrees F*	Absolute Microvolts	Degrees F*	Absolute Microvolts
-166	-54995		
+ 32	0		
122	30800		
212	64665		

*In this table Degrees F is defined as 9/5×°C (Int. 1948) + 32.

The uncertainty in the above values is: ±0.2 °F

A discussion of uncertainties inherent in thermocouple calibrations is given in National Bureau of Standards Circular 590, Methods of Testing Thermocouples and Thermocouple Materials.

A True Copy
August 11, 1969
NMcB

For the Director, Institute for Basic Standards

/s/ Harmon H. Plumb

Harmon H. Plumb
Chief, Temperature Section
Heat Division

Test No. 197667
Completed: January 23, 1969
JAW:dh

TABLE A-5

NBS-497F

Repeated National Bureau of Standards Calibration
for the Fifteen Junction Thermopile

U.S. DEPARTMENT OF COMMERCE
NATIONAL BUREAU OF STANDARDS
INSTITUTE FOR BASIC STANDARDS
WASHINGTON, D.C. 20234

REPORT OF CALIBRATION
THERMOCOUPLE

Copper Constantan (15 Junctions)
(Tagged #2)

Submitted by
University of Michigan
Ann Arbor, Michigan

Electromotive Force as a Function of Temperature of Measuring Junction (reference junctions at 32°F)

Degrees F*	Absolute Microvolts	Degrees F*	Absolute Microvolts
-297.13	-79856		
-166.00	-54988		
32.00	0		
300.00	100316		

*In this table Degrees F is defined as 9/5 x °C (IPTS-68) + 32.

The uncertainty in the above values is: ±0.2 °F

A discussion of uncertainties inherent in thermocouple calibrations is given in National Bureau of Standards Circular 590, Methods of Testing Thermocouples and Thermocouple Materials.

All temperatures in this report are based on the International Practical Temperature Scale of 1968, IPTS-68. This temperature scale was adopted by the International Committee of Weights and Measures at its meeting in October, 1968, and is described in "The International Practical Temperature Scale of 1968," Metrologia, Vol. 5, No. 2, 35 (April 1969).

For the Director, Institute for Basic Standards

Harmon Blum

Test No. 199778
Completed: September 26, 1969
JAW:MJP

Chief, Temperature Section
Heat Division

USCOMM-DC 22429-P69

TABLE A-6

Calculation of the Fifteen Junction Thermopile EMF at Uncalibrated Temperatures by Comparison with a Calibrated 6 Junction Thermopile 6M

Temp	$15(\frac{E_{6M}}{6})$	$15(\frac{E_{6M}}{6} - E_{Std})$	$15(\frac{E_{15}}{15} - E_{Std})$ A	$15(\frac{E_{15}}{15} - E_{Std})$ B	E_{15}
°C	(μv)	(μv)	(μv)	(μv)	(μv)
-183.	-78927	-1095	-1024		-79856
-160.	-73215	-960		-900	-73155
-130.	-62850	-781		-737	-62807
-110.			-628		-54988
-100.	-50845	-610		-578	-50813
-80.	-41952	-492		-455	-41915
-60.	-32390	-365		-342	-32367
-40.	-22192	-247		-225	-22170
-20.	-11392	-127		-110	-11375
0.	0	0		0	0
20.	11937	132		111	11916
40.	24402	252		223	24373
50.			304.5		30800
60.	37360	356		328	37333
80.	50805	450		425	50780
100.	64670	515	510		64670
120.	78982	578		578	78982
140.	93710	650		645	93705
148.88			671		100316
160.	100882	705		710	100887

E_{6M} is the Emf of the 6 junction thermopile 6M, the calibration results for which are indicated in Table A-3.

E_{Std} is the Emf for a single Cu/Constanan thermopile as tabulated in [184].

E_{15} is the Emf of each of the 15 junction thermopiles used in this work.

Column A is obtained by considering the calibration data for the 15 junction thermopiles of this work as indicated in Tables A-4 and A-5.

Column B is obtained by interpolating the results of Column A plotted in Figure A-1.

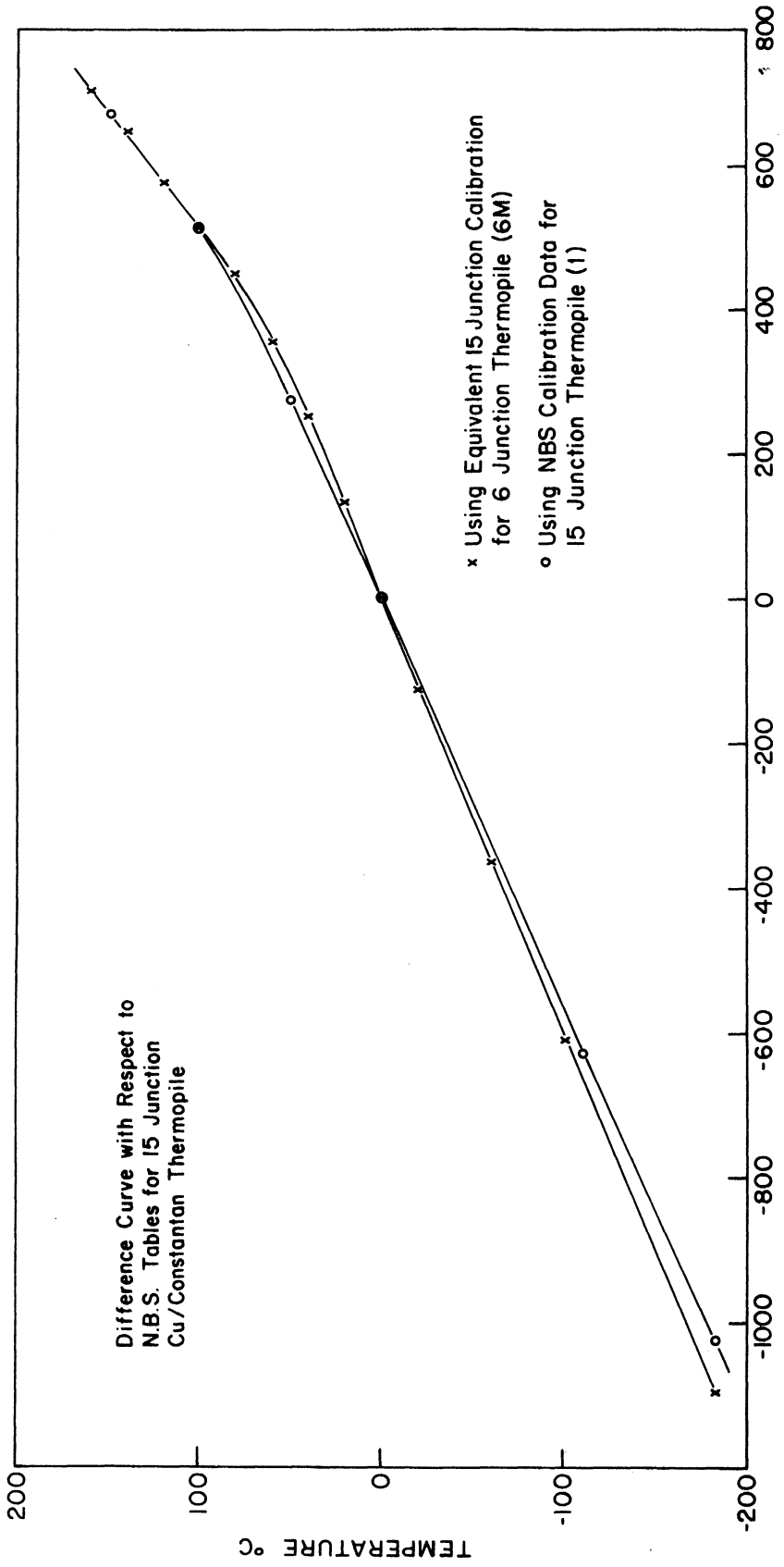

Figure A-1. The Interpolation of the Emf Values for the Fifteen Junction Thermopile Using Detailed Calibration Data on a Six Junction Thermopile

TABLE A-7

Least Squares Fit of EMF vs Temperature for the Fifteen Junction Thermopile

Temp. (°K) T	Emf* (Microvolts)	Calculated** Emf (Microvolts) E	Difference (Microvolts)	% Error
-182.85	-79856.0	-79849.3	-6.7	0.008
-160.00	-73155.0	-73162.8	7.8	-0.011
-130.00	-62807.0	-62819.6	12.6	-0.020
-110.00	-54995.0	-54987.7	-7.3	0.013
-100.00	-50813.0	-50803.0	-10.0	0.020
-80.00	-41915.0	-41915.5	0.5	-0.001
-60.00	-32367.0	-32362.8	-4.2	0.013
-40.00	-22170.0	-22174.3	4.3	-0.019
-20.00	-11375.0	-11378.8	3.8	-0.033
0.01	5.8	1.9	3.9	66.544
20.00	11916.0	11923.8	-7.8	-0.065
40.00	24373.0	24378.4	-5.4	-0.022
50.00	30800.0	30795.6	4.4	0.014
60.00	37333.0	37335.4	-2.4	-0.006
80.00	50780.0	50770.9	9.1	0.018
100.00	64670.0	64662.2	7.8	0.012
100.00	64665.0	64662.2	2.8	0.004
120.00	78982.0	78987.3	-5.3	-0.007
140.00	93705.0	93725.6	-20.6	-0.022
160.00	108870.0	108857.2	12.7	0.012

PERCENT STD. DEVIATION = 0.01923

* Obtained from Table A-6

** Calculated using the Equation:

$$E = -3.887 + 582.78T + 0.691T^2 - 0.54565\times10^{-3}T^3 + 0.253876\times10^{-6}T^4$$

TABLE A-8

Sample Flowmeter Calibration Results for the Ternary Mixture

TABLE OF RESIDUALS

RUN NO	X VALUE* (F/μ)	Y VALUE** (ρΔP/μF)	Y ESTIMATE+	RESIDUAL ($Y-Y_{est}$)	PCERR ($(Y-Y_{est})/(Y/100)$)
20.0	0.0032340	0.16103	0.16012	0.00091	0.568
21.0	0.0008148	0.11808	0.11824	-0.00016	-0.134
22.0	0.0008092	0.11796	0.11815	-0.00019	-0.161
23.0	0.0015165	0.12908	0.12911	-0.00003	-0.023
24.0	0.0015112	0.12874	0.12899	-0.00025	-0.197
25.0	0.0022499	0.14115	0.14091	0.00024	0.168
26.0	0.0022640	0.14121	0.14115	0.00006	0.040
27.0	0.0026625	0.14806	0.14833	-0.00027	-0.183
28.0	0.0026657	0.14819	0.14839	-0.00020	-0.135
29.0	0.0029143	0.15293	0.15328	-0.00035	-0.228
30.0	0.0028987	0.15262	0.15296	-0.00034	-0.223
31.0	0.0006703	0.11586	0.11594	-0.00008	-0.070
32.0	0.0028620	0.15197	0.15222	-0.00025	-0.167
33.0	0.0028510	0.15166	0.15200	-0.00034	-0.224
34.0	0.0029615	0.15412	0.15425	-0.00013	-0.083
35.0	0.0024256	0.14399	0.14398	0.00001	0.006
36.0	0.0024388	0.14445	0.14422	0.00023	0.162
37.0	0.0021296	0.13930	0.13887	0.00042	0.304
38.0	0.0021392	0.13912	0.13904	0.00008	0.059
39.0	0.0013908	0.12704	0.12714	-0.00010	-0.078
40.0	0.0014052	0.12727	0.12736	-0.00009	-0.068
41.0	0.0010167	0.12143	0.12138	0.00004	0.035
42.0	0.0010009	0.12104	0.12114	-0.00009	-0.078
43.0	0.0017624	0.13314	0.13291	0.00022	0.168
44.0	0.0017648	0.13308	0.13295	0.00012	0.093
45.0	0.0023174	0.14234	0.14208	0.00026	0.183
46.0	0.0023217	0.14229	0.14215	0.00014	0.097
47.0	0.0027092	0.14930	0.14922	0.00007	0.047
48.0	0.0027216	0.14943	0.14946	-0.00003	-0.021
49.0	0.0029013	0.15298	0.15301	-0.00004	-0.024
50.0	0.0028925	0.15259	0.15284	-0.00025	-0.163
52.0	0.0006240	0.11543	0.11520	0.00023	0.196
53.0	0.0025641	0.14654	0.14649	0.00005	0.034
54.0	0.0025587	0.14648	0.14639	0.00009	0.061
58.0	0.0013748	0.12672	0.12689	-0.00016	-0.130
60.0	0.0021150	0.13867	0.13863	0.00004	0.029
61.0	0.0006410	0.11570	0.11547	0.00023	0.198
62.0	0.0006392	0.11553	0.11545	0.00008	0.071
64.0	0.0029647	0.15423	0.15431	-0.00008	-0.051
65.0	0.0013875	0.12687	0.12708	-0.00022	-0.173
67.0	0.0017533	0.13273	0.13277	-0.00004	-0.031
68.0	0.0017445	0.13264	0.13263	0.00001	0.006
69.0	0.0022398	0.14082	0.14074	0.00008	0.056
70.0	0.0022254	0.14057	0.14049	0.00008	0.057

PERCENT AV. DEVIATION = 0.12014

* Units are $\frac{\text{lbs}}{\text{min. micropoise}}$

** Units are $(\frac{\text{lb}_m}{\text{ft}^3})$(in. H_2O)/(micropoise·lb_m/min)

\+ From Calibration Equation $Y = 0.10454 + 18.30116X - 2330.416X^2 + 0.61398 \times 10^6 X^3$

TABLE A-9

Calibration Results for Mansfield and Green Dead Weight Gage

P_{Ruska} +	$P_{M\&G}$	P
RUSKA DEAD WT. GAGE PRESSURE (PSIG)	M & G DEAD WT. GAGE PRESSURE (PSIG)	CALCULATED* CALIB. EQN. PRESSURE (PSIG)
264.8	264.6	264.8
537.8	537.4	537.8
961.1	960.6	961.2
960.0	959.4	960.0
1472.1	1471.4	1472.1
1461.5	1460.7	1461.4
2106.2	2105.0	2106.1

Calibration Date Dec. 16, 1969.

*Calibration Equation $P = P_{M\&G} + .49 \times 10^{-3}(P_{M\&G}) + 0.1$ psi

+ Calibration Standard Dead Wt. Gage

TABLE A-9

Calibration Results for Mansfield and Green Dead Weight Gage

P_{Ruska} +	$P_{M\&G}$	P
RUSKA DEAD WT. GAGE PRESSURE (PSIG)	M & G DEAD WT. GAGE PRESSURE (PSIG)	CALCULATED* CALIB. EQN. PRESSURE (PSIG)
264.8	264.6	264.8
537.8	537.4	537.8
961.1	960.6	961.2
960.0	959.4	960.0
1472.1	1471.4	1472.1
1461.5	1460.7	1461.4
2106.2	2105.0	2106.1

Calibration Date Dec. 16, 1969.

*Calibration Equation $P = P_{M\&G} + .49 \times 10^{-3}(P_{M\&G}) + 0.1$ psi

+ Calibration Standard Dead Wt. Gage

TABLE A-11

FORM NBS-580 (10-14-64)

National Bureau of Standards Calibration of 200 Inch Steel Tape

U.S. DEPARTMENT OF COMMERCE
NATIONAL BUREAU OF STANDARDS
WASHINGTON, D.C. 20234

NATIONAL BUREAU OF STANDARDS
REPORT OF CALIBRATION

300-Inch
STEEL TAPE

Maker: The Lufkin Rule Co. NBS No. 13872
No.

Submitted by

The University of Michigan
Department of Chemical and
Metallurgical Engineering
Ann Arbor, Michigan 48104

This tape has been compared with the standards of the United States, and the horizontal straight-line distance between the terminal points of the indicated intervals have the following lengths at 68° Fahrenheit (20 °Celsius) when subjected to horizontally applied tensions and conditions of support as indicated below:

Supported on a horizontal flat surface: tension, 10 pounds

Interval (inches)	Length (inches)	Interval (inches)	Length (inches)
0 to 1	0.999	0 to 150	150.002
7	6.997	160	160.001
10	9.995	170	170.007
20	20.006	180	180.007
30	30.003	190	190.001
40	40.004	200	200.013
50	50.001	210	210.006
60	60.007	212	212.004
70	70.006	220	220.006
80	80.005	230	230.006
90	90.008	240	240.010
99	99.005	250	250.007
100	100.005	260	260.007
110	110.007	270	270.008
120	120.010	280	280.008
130	130.006	290	290.005
140	140.004	300	300.004

The length values given above are not in error by more than 0.006 inch.

The average weight per inch of this tape ribbon is 0.0008372 pound.

Test No. 212.21/G-38740
Date : March 11, 1968

USCOMM-DC 26106-P64

TABLE A-11

(CONTINUED)

Report of Calibration continued
300-Inch Steel Tape

The average AE value of this tape is 88,200 pounds, where A is the cross-sectional area of the tape ribbon, and E is Young's Modulus of Elasticity.

The terminal points of the indicated intervals are defined as the centers of the graduations nearest the observer when the zero graduation is at his left.
The length of the indicated intervals when the tape is suspended vertically from a point above the desired interval with a weight attached to the free end can be computed from the length of the interval on a horizontal flat surface and the change in length (ΔL) due to the effective change in tension. The total effective change in tension is equal to the weight attached to the free end, the weight of the blank ribbon below the zero graduation (0.0042 pound), the weight of the finger ring (0.0078 pound), plus one half the ribbon weight of the interval, minus the tension applied when the tape was supported on a horizontal flat surface (10 pounds). However, if the attached weight is 10 pounds when the tape is suspended vertically, the length of the 300-inch interval will increase by only 0.0005 inch. Therefore, the lengths of the subintervals when suspended vertically are not stated in this report. If the attached weight is not 10 pounds, the effective change in tension should be recomputed and the change in length determined by the following expression:

$$\Delta L = (\text{effective change in tension}) \times (\text{length of interval})/AE.$$

For the Director,

J. S. Beers
Acting Chief, Length Section
Metrology Division, IBS

Test No. 212.21/G-38740
Date: March 11, 1968

TABLE A-12

Sample High Pressure Transducer Calibration Results

a) Least Squares Regression Results

HIGH PRESSURE TRANSDUCER CALIBRATION SET APRIL 1970

Observation	Pressure, P_h at Dead Wt. Cage (psig)	Measured Output $E_h/10$ (μv)	Calculated Output * (μv)	Percent Error
70.0	0.11427E 04	0.13649E 04	0.13654E 04	-0.36633E-01
72.0	0.10008E 04	0.11962E 04	0.11954E 04	0.65841E-01
74.0	0.80080E 03	0.95654E 03	0.95579E 03	0.78586E-01
76.0	0.31686E 03	0.37540E 03	0.37583E 03	-0.11407E 00
78.0	0.21281E 03	0.25103E 03	0.25111E 03	-0.32806E-01
80.0	0.21654E 04	0.25903E 04	0.25902E 04	0.16023E-02
82.0	0.20003E 04	0.23930E 04	0.23926E 04	0.18711E-01
84.0	0.15989E 04	0.19121E 04	0.19119E 04	0.13585E-01
86.0	0.13778E 04	0.16468E 04	0.16470E 04	-0.14855E-01
88.0	0.11679E 04	0.13953E 04	0.13956E 04	-0.23745E-01
90.0	0.13053E 04	0.12006E 04	0.12008E 04	-0.17000E-01
92.0	0.60820E 03	0.72592E 03	0.72499E 03	0.12763E 00
71.0	0.11247E 04	0.13437E 04	0.13438E 04	-0.47420E-02
73.0	0.10046E 04	0.12004E 04	0.12000E 04	0.39556E-01
75.0	0.80180E 03	0.95728E 03	0.95699E 03	0.30655E-01
77.0	0.29665E 03	0.35125E 03	0.35160E 03	-0.10092E 00
79.0	0.21351E 03	0.25187E 03	0.25195E 03	-0.32320E-01
81.0	0.21638E 04	0.25882E 04	0.25883E 04	-0.55183E-02
83.0	0.19977E 04	0.23897E 04	0.23895E 04	0.10942E-01
86.0	0.16009E 04	0.19243E 04	0.19251E 04	-0.37668E-01
88.0	0.13922E 04	0.16642E 04	0.16643E 04	-0.63082E-02
90.0	0.11713E 04	0.13989E 04	0.13997E 04	-0.53351E-01
92.0	0.13980E 04	0.12038E 04	0.12040E 04	-0.18171E-01

TABLE A-12

b) Interpolated Results from The Calibration Equation

P_h (Psig)	$E_h/10$ * (μv)
100.00	115.89
200.00	235.76
300.00	355.62
400.00	475.48
500.00	595.33
600.00	715.17
700.00	835.00
800.00	954.83
900.00	1074.65
1000.00	1194.46
1100.00	1314.27
1200.00	1434.07
1300.00	1553.86
1400.00	1673.65
1500.00	1793.43
1600.00	1913.20
1700.00	2032.96
1800.00	2152.72
1900.00	2272.47
2000.00	2392.21

* Calibration Equation $\frac{E_h}{10} = -3.9897 + 1.1988\ P_h - 0.35262 \times 10^{-6}\ P_h^2$

TABLE A-13

Sample Low Pressure Transducer Calibration Results

a) Sample Low Pressure Transducer Calibration Data

LOW PRESSURE TRANSDUCER CALIBRATION SET APRIL 1970

Observation	Pressure, P_1 at Dead Wt. Gage (Psia)	Measured Output, $E_1/10$ (μv)	Calculated* Output (μv)	Percent Error
70.0	0.11427E 04	0.13814E 04	0.13824E 04	-0.74299E-01
72.0	0.10008E 04	0.12131E 04	0.12129E 04	0.21614E-01
74.0	0.80080E 03	0.97455E 03	0.97369E 03	0.88407E-01
76.0	0.31686E 03	0.39364E 03	0.39417E 03	-0.13465E 00
78.0	0.21281E 03	0.26914E 03	0.26943E 03	-0.10831E 00
80.0	0.21654E 04	0.26020E 04	0.26020E 04	-0.28712E-02
82.0	0.20003E 04	0.24058E 04	0.24055E 04	0.13121E-01
84.0	0.15989E 04	0.19273E 04	0.19271E 04	0.12465E-01
86.0	0.13778E 04	0.16629E 04	0.16632E 04	-0.20672E-01
88.0	0.11679E 04	0.14122E 04	0.14126E 04	-0.28128E-01
90.0	0.10053E 04	0.12181E 04	0.12183E 04	-0.12928E-01
92.0	0.60820E 03	0.74432E 03	0.74318E 03	0.15354E 00

b) Interpolated Results from The Calibration Equation

P_1 (Psig)	$E_1/10$* (μv)
100.00	134.14
200.00	254.07
300.00	373.96
400.00	493.81
500.00	613.61
600.00	733.36
700.00	853.07
800.00	972.73
900.00	1092.35
1000.00	1211.92
1100.00	1331.45
1200.00	1450.93
1300.00	1570.37
1400.00	1689.76
1500.00	1809.10
1600.00	1928.40
1700.00	2047.66
1800.00	2166.87
1900.00	2286.03
2000.00	2405.15

* Calibration Equation $\frac{E_1}{10} = 14.155 + 1.2P_1 - 0.22708\times10^{-5}P_1^2$

TABLE A-14

Sample Differential Pressure Transducer Calibration Results

Obs. No.	Inlet Trans. Output, $E_h/10$ Microvolts	Outlet Trans. Output, $E_h/10$ Microvolts	Pressure, P_h (Psia) [+]	Pressure, P_l (Psia) [++]	Diff.Trans. Null, $E_{null}/10$ (microvolts) [*]	Diff.Trans. Output, $E_{DP}/10$ (Microvolts)	$P_h - P_l$ (Psid)	Measured $\frac{(E_{DP}-E_{null})}{10}$ (Microvolts)	Calculated [**] $\frac{(E_{DP}-E_{null})}{10}$ (Micorvolts)	% Error
71.	1343.75	1193.21	1138.79	998.56	74.18	354.38	140.23	280.20	279.60	0.213
73.	1200.45	975.85	1019.18	816.81	74.05	477.91	202.37	403.86	403.45	0.101
75.	957.28	740.30	816.23	620.00	74.44	465.96	196.23	391.52	391.23	0.073
77.	351.25	148.72	310.81	126.61	75.36	442.73	184.20	367.37	367.72	-0.096
79.	251.87	15.06	227.89	15.20	74.55	499.38	212.69	424.83	424.79	0.010
81.	2588.17	2387.72	2178.11	1999.87	62.02	419.12	178.24	357.10	357.09	0.003
83.	2389.72	2175.77	2012.37	1821.97	62.84	443.39	190.40	380.85	380.96	-0.030
86.	1924.33	1673.19	1623.74	1400.61	65.29	512.61	223.13	447.32	445.45	0.418
88.	1664.20	1408.56	1406.56	1179.01	66.44	516.93	227.55	450.49	453.92	-0.762
90.	1398.93	1168.66	1185.11	978.29	67.46	480.59	206.82	413.13	412.39	0.180
92.	1203.83	977.41	1022.26	818.38	68.15	474.93	203.88	406.78	406.46	0.078

\+ Determined from the M&G Dead Wt. Gage and the Barometric pressure
++ Determined from the calibration equation of Table A-13
* Differential tranaducer null determined at P_h
** Calculated using the equation

$$\frac{E_{DP}-E_{null}}{10} = 1.9985\,\Delta P - 0.56295\times10^{-5}\Delta P(2P_h - \Delta P) + 0.21745\times10^{-8}\Delta P(3P_h^2 - 3P_h\Delta P + \Delta P^2)$$

where $\Delta P = P_h - P_l$

TABLE A-15

The Variation of the Differential Pressure Transducer Output as a Function of Pressure Level for a Fixed Pressure Drop of 200 psid.

Transducer Output $[(\frac{E_{DP}-E_{null}}{10\,\Delta P})]_{200\ psid}$ (Microvolts/psid)	Pressure (psia)
1.9973	700.
1.9945	600.
1.9935	1000.
1.9963	1600.
2.0001	2000.

APPENDIX B

The Basic Calorimetric Data

TABLE B-1

Basic Isobaric Data for 0.996 Mole Fraction Ethane

RUN NO.	COMPOSITION (MOLE FRACTION) CH4	C2H6	C3H8	INLET TEMP. (°F)	OUTLET TEMP. (°F)	INLET PRES. (PSIA)	PRES. DROP (PSID)	HEAT INPUT (BTU/LB)	MEAN HEAT CAPACITY (BTU/LB°F)
37.010	0.001	0.996	0.003	-257.68	-246.43	1999.4	0.14	6.162	0.54747
34.010	0.001	0.996	0.003	-246.54	-231.81	2003.2	0.11	8.072	0.54802
34.020	0.001	0.996	0.003	-246.55	-206.83	2003.4	0.15	21.800	0.54886
34.030	0.001	0.996	0.003	-246.43	-171.55	2002.1	0.11	41.229	0.55062
34.040	0.001	0.996	0.003	-247.61	-140.05	2001.5	0.12	59.572	0.55385
34.041	0.001	0.996	0.003	-247.61	-139.30	2001.5	0.12	60.112	0.55498
34.050	0.001	0.996	0.003	-247.59	-119.16	1999.3	0.13	71.734	0.55854
34.051	0.001	0.996	0.003	-247.59	-118.66	1999.9	0.13	71.867	0.55739
31.010	0.001	0.996	0.003	-123.10	-113.16	2001.9	0.11	5.819	0.58509
31.015	0.001	0.996	0.003	-123.10	-113.16	2001.9	0.11	5.686	0.57175
31.020	0.001	0.996	0.003	-122.80	-88.81	2001.7	0.17	19.679	0.57895
31.021	0.001	0.996	0.003	-122.84	-87.33	2003.1	0.13	20.523	0.57799
31.030	0.001	0.996	0.003	-122.75	-63.13	1999.9	0.12	34.921	0.58572
31.040	0.001	0.996	0.003	-122.75	-37.74	1999.4	0.11	50.296	0.59166
31.050	0.001	0.996	0.003	-122.76	-21.62	2000.6	0.12	59.998	0.59326
25.010	0.001	0.996	0.003	-22.75	-12.72	2000.6	0.05	6.314	0.62913
25.011	0.001	0.996	0.003	-22.65	-12.64	2000.2	0.05	6.302	0.62994
25.020	0.001	0.996	0.003	-22.78	7.77	1999.7	0.09	19.601	0.64160
1.010	0.001	0.996	0.003	50.74	60.73	2001.4	0.06	7.074	0.70762
1.015	0.001	0.996	0.003	51.34	60.73	2001.4	0.06	6.654	0.70862
1.020	0.001	0.996	0.003	51.37	81.30	2002.2	0.06	21.575	0.72087
1.030	0.001	0.996	0.003	51.42	105.93	1999.3	0.07	40.423	0.74156
1.110	0.001	0.996	0.003	51.65	62.13	2000.3	0.07	7.342	0.70091
1.111	0.001	0.996	0.003	51.39	61.77	2002.4	0.07	7.332	0.70636
1.120	0.001	0.996	0.003	51.42	81.47	2001.9	0.07	21.700	0.72229
1.130	0.001	0.996	0.003	51.36	104.86	2000.6	0.07	40.262	0.75258
1.140	0.001	0.996	0.003	51.47	126.88	2000.1	0.09	58.146	0.77108
1.150	0.001	0.996	0.003	51.48	144.66	2000.1	0.09	73.607	0.78993
9.010	0.001	0.996	0.003	127.01	136.15	2000.9	0.09	7.864	0.86068
9.011	0.001	0.996	0.003	127.04	136.18	2003.0	0.07	7.845	0.85804
9.020	0.001	0.996	0.003	127.11	154.04	2001.8	0.07	23.643	0.87419
9.030	0.001	0.996	0.003	127.13	180.06	1999.8	0.09	48.232	0.91117
9.040	0.001	0.996	0.003	127.13	202.79	1999.2	0.12	70.014	0.92538
9.050	0.001	0.996	0.003	127.15	219.91	2001.2	0.12	86.253	0.92977
11.010	0.001	0.996	0.003	126.58	135.69	2001.5	0.10	7.807	0.85668
11.011	0.001	0.996	0.003	126.71	135.92	2000.9	0.07	7.893	0.85743
11.012	0.001	0.996	0.003	126.71	136.01	1999.7	0.07	7.979	0.85841
11.020	0.001	0.996	0.003	126.74	155.24	2001.1	0.12	25.147	0.88250
11.030	0.001	0.996	0.003	126.70	179.48	2002.1	0.10	48.038	0.91018
11.031	0.001	0.996	0.003	126.74	180.05	2002.0	0.10	48.507	0.90983
11.040	0.001	0.996	0.003	126.70	200.78	2001.2	0.09	68.514	0.92480
47.010	0.001	0.996	0.003	176.30	177.39	2000.0	0.15	1.082	0.98676
47.020	0.001	0.996	0.003	176.25	179.15	2000.0	0.15	2.840	0.98065
47.030	0.001	0.996	0.003	176.25	180.07	2000.2	0.15	3.768	0.98633
47.040	0.001	0.996	0.003	176.33	182.60	2000.4	0.15	6.179	0.98601
47.050	0.001	0.996	0.003	176.32	183.97	1999.7	0.15	7.552	0.98625
47.060	0.001	0.996	0.003	176.32	186.59	1999.6	0.12	10.139	0.98725
44.010	0.001	0.996	0.003	183.99	185.32	1999.4	0.14	1.327	0.99983
44.020	0.001	0.996	0.003	183.96	186.80	1999.4	0.14	2.820	0.99102
44.021	0.001	0.996	0.003	183.96	186.82	1999.6	0.14	2.824	0.98703
44.030	0.001	0.996	0.003	184.05	188.65	2002.2	0.14	4.547	0.98861
44.031	0.001	0.996	0.003	184.05	188.65	2000.6	0.14	4.538	0.98621
44.032	0.001	0.996	0.003	184.05	188.70	1999.4	0.14	4.559	0.98068
44.040	0.001	0.996	0.003	184.04	190.35	2000.2	0.15	6.252	0.99107
44.041	0.001	0.996	0.003	184.04	190.35	2000.0	0.15	6.251	0.99075
44.050	0.001	0.996	0.003	184.03	192.29	1999.4	0.15	8.132	0.98445
44.060	0.001	0.996	0.003	184.11	194.54	2002.4	0.15	10.276	0.98524
48.010	0.001	0.996	0.003	201.51	210.22	2003.3	0.10	8.560	0.98330
48.020	0.001	0.996	0.003	201.54	216.86	2002.9	0.09	14.956	0.97430
48.030	0.001	0.996	0.003	201.60	226.18	1999.9	0.09	23.843	0.96995
48.040	0.001	0.996	0.003	201.60	246.77	2003.4	0.09	42.986	0.95161
45.010	0.001	0.996	0.003	201.88	210.39	2002.9	0.10	8.312	0.97704
45.011	0.001	0.996	0.003	201.88	210.41	2002.6	0.10	8.358	0.98017
45.020	0.001	0.996	0.003	201.87	226.40	2001.8	0.10	23.619	0.96294
45.021	0.001	0.996	0.003	201.87	226.47	2000.5	0.10	23.703	0.96360
45.030	0.001	0.996	0.003	201.88	247.06	2003.1	0.10	42.546	0.94174
45.040	0.001	0.996	0.003	201.87	269.95	2000.1	0.10	63.062	0.92640
12.010	0.001	0.996	0.003	126.72	135.46	1750.7	0.11	8.051	0.92057
12.011	0.001	0.996	0.003	126.71	135.48	1751.9	0.12	8.073	0.92059
12.020	0.001	0.996	0.003	126.78	153.98	1753.4	0.13	25.908	0.95259
12.030	0.001	0.996	0.003	126.76	179.52	1750.5	0.12	52.638	0.99774
12.040	0.001	0.996	0.003	126.71	203.03	1752.6	0.13	76.761	1.00585
12.050	0.001	0.996	0.003	126.69	216.38	1752.2	0.13	90.095	1.00452
12.056	0.001	0.996	0.003	126.70	216.38	1750.1	0.09	89.430	0.99721

TABLE B-1.
(CONTINUED)

RUN NO.	COMPOSITION (MOLE FRACTION) CH4	C2H6	C3H8	INLET TEMP. (°F)	OUTLET TEMP. (°F)	INLET PRES. (PSIA)	PRES. DROP (PSID)	HEAT INPUT (BTU/LB)	MEAN HEAT CAPACITY (BTU/LB°F)
43.010	0.001	0.996	0.003	168.86	169.82	1749.2	0.15	1.033	1.06634
43.020	0.001	0.996	0.003	168.87	170.81	1750.3	0.15	2.033	1.04592
43.021	0.001	0.996	0.003	168.87	170.80	1749.7	0.15	2.067	1.06684
43.030	0.001	0.996	0.003	168.85	172.77	1750.8	0.15	4.172	1.06632
43.040	0.001	0.996	0.003	168.86	174.74	1749.6	0.15	6.301	1.07167
43.041	0.001	0.996	0.003	168.86	174.77	1754.8	0.15	6.261	1.05878
43.050	0.001	0.996	0.003	168.91	176.54	1749.7	0.15	8.169	1.07041
43.051	0.001	0.996	0.003	168.91	176.52	1751.5	0.15	8.146	1.07014
43.060	0.001	0.996	0.003	168.92	177.85	1750.0	0.15	9.567	1.07136
43.061	0.001	0.996	0.003	168.92	177.84	1750.5	0.15	9.568	1.07204
				TABLE					
49.010	0.001	0.996	0.003	179.15	186.56	1750.0	0.10	7.752	1.04674
49.030	0.001	0.996	0.003	179.18	223.99	1748.6	0.13	44.937	1.00289
49.031	0.001	0.996	0.003	179.18	224.11	1748.0	0.13	44.993	1.00138
26.010	0.001	0.996	0.003	-22.72	-12.84	1500.9	0.10	6.351	0.64289
26.011	0.001	0.996	0.003	-22.68	-12.73	1502.3	0.10	6.377	0.64061
26.020	0.001	0.996	0.003	-22.79	7.32	1499.5	0.10	19.628	0.65174
26.030	0.001	0.996	0.003	-22.77	31.91	1500.9	0.12	36.752	0.67218
26.040	0.001	0.996	0.003	-22.73	51.76	1499.6	0.16	51.036	0.68518
26.050	0.001	0.996	0.003	-22.74	71.80	1500.5	0.10	66.328	0.70159
2.010	0.001	0.996	0.003	51.54	61.28	1500.7	0.08	7.301	0.74990
2.011	0.001	0.996	0.003	51.55	61.23	1500.1	0.08	7.260	0.74941
2.020	0.001	0.996	0.003	51.60	81.42	1501.9	0.08	23.097	0.77465
2.030	0.001	0.996	0.003	51.59	107.32	1501.6	0.10	45.072	0.80880
2.040	0.001	0.996	0.003	51.59	126.77	1502.8	0.12	63.760	0.84808
2.050	0.001	0.996	0.003	51.63	139.84	1504.3	0.12	77.703	0.88086
13.010	0.001	0.996	0.003	126.70	136.50	1502.5	0.12	10.284	1.04921
13.011	0.001	0.996	0.003	126.70	136.57	1500.6	0.17	10.366	1.05020
13.020	0.001	0.996	0.003	126.64	157.13	1501.1	0.15	33.747	1.10682
13.030	0.001	0.996	0.003	126.77	172.14	1501.1	0.16	58.198	1.28274
13.035	0.001	0.996	0.003	126.77	172.14	1501.1	0.16	57.447	1.26619
13.036	0.001	0.996	0.003	126.77	172.14	1501.1	0.16	51.667	1.13879
13.040	0.001	0.996	0.003	126.65	201.33	1500.0	0.16	83.551	1.11870
13.050	0.001	0.996	0.003	126.71	221.47	1503.1	0.13	102.769	1.08457
42.010	0.001	0.996	0.003	157.29	158.28	1500.6	0.14	1.267	1.27693
42.011	0.001	0.996	0.003	157.26	158.28	1500.8	0.14	1.269	1.24175
42.020	0.001	0.996	0.003	157.31	159.27	1500.5	0.15	2.374	1.20686
42.021	0.001	0.996	0.003	157.32	159.30	1501.4	0.15	2.485	1.20844
42.030	0.001	0.996	0.003	157.30	161.09	1501.0	0.15	4.600	1.21348
42.031	0.001	0.996	0.003	157.30	161.06	1499.4	0.15	4.590	1.21993
42.040	0.001	0.996	0.003	157.21	163.08	1499.5	0.15	7.168	1.21942
42.041	0.001	0.996	0.003	157.21	163.09	1499.5	0.15	7.152	1.21603
42.050	0.001	0.996	0.003	157.26	165.00	1501.4	0.17	9.398	1.21358
42.060	0.001	0.996	0.003	157.18	166.20	1499.4	0.15	10.995	1.21848
42.061	0.001	0.996	0.003	157.23	166.21	1500.0	0.15	10.893	1.21315
46.010	0.001	0.996	0.003	201.88	210.17	1500.1	0.10	8.221	0.99141
46.011	0.001	0.996	0.003	201.87	210.18	1500.4	0.10	8.252	0.99237
46.015	0.001	0.996	0.003	201.88	210.17	1500.1	0.10	8.249	0.99482
46.016	0.001	0.996	0.003	201.87	210.18	1500.4	0.10	8.275	0.99511
46.020	0.001	0.996	0.003	201.91	218.19	1501.5	0.10	15.937	0.97887
3.010	0.001	0.996	0.003	51.72	61.26	1251.3	0.05	7.504	0.78655
3.011	0.001	0.996	0.003	51.77	61.47	1251.2	0.07	7.578	0.78120
3.020	0.001	0.996	0.003	51.49	80.76	1251.2	0.10	23.970	0.81905
3.030	0.001	0.996	0.003	51.54	106.65	1251.8	0.10	47.949	0.87008
3.040	0.001	0.996	0.003	51.56	126.85	1250.1	0.11	71.802	0.95370
3.050	0.001	0.996	0.003	51.58	135.49	1249.0	0.12	83.188	0.99144
3.051	0.001	0.996	0.003	51.57	135.77	1250.4	0.12	83.429	0.99085
14.010	0.001	0.996	0.003	126.46	136.24	1249.2	0.16	13.437	1.37428
14.011	0.001	0.996	0.003	126.51	136.34	1249.2	0.16	13.494	1.37312
14.020	0.001	0.996	0.003	126.66	149.32	1249.6	0.16	32.087	1.41606
14.030	0.001	0.996	0.003	126.65	177.00	1250.5	0.16	67.303	1.33662
14.040	0.001	0.996	0.003	126.69	201.81	1250.8	0.12	92.066	1.22548
14.050	0.001	0.996	0.003	126.71	222.45	1251.4	0.12	108.979	1.13822
41.010	0.001	0.996	0.003	140.07	141.06	1252.1	0.17	1.517	1.52728
41.020	0.001	0.996	0.003	140.04	142.02	1253.0	0.15	2.996	1.51143
41.030	0.001	0.996	0.003	140.36	143.38	1252.0	0.15	4.560	1.50661
41.040	0.001	0.996	0.003	139.49	143.65	1252.9	0.15	6.201	1.49009
41.050	0.001	0.996	0.003	140.03	145.10	1252.9	0.15	7.613	1.50101
41.060	0.001	0.996	0.003	140.04	146.85	1252.0	0.15	10.241	1.50228
35.010	0.001	0.996	0.003	-247.72	-232.88	1001.7	0.12	8.188	0.55199
35.020	0.001	0.996	0.003	-247.61	-209.51	1001.4	0.12	20.835	0.54693
35.030	0.001	0.996	0.003	-247.59	-171.71	1000.6	0.12	42.212	0.55631
35.040	0.001	0.996	0.003	-247.62	-140.64	1003.6	0.12	59.289	0.55423
35.050	0.001	0.996	0.003	-247.55	-120.77	1001.3	0.12	71.211	0.56170
32.010	0.001	0.996	0.003	-123.30	-112.74	1002.1	0.07	6.140	0.58122
32.015	0.001	0.996	0.003	-123.30	-112.74	1002.1	0.07	6.156	0.58279
32.020	0.001	0.996	0.003	-123.32	-89.58	999.0	0.07	19.883	0.58934
32.030	0.001	0.996	0.003	-123.31	-65.35	999.1	0.10	34.459	0.59456
32.040	0.001	0.996	0.003	-123.26	-36.54	1001.9	0.10	52.266	0.60267
32.050	0.001	0.996	0.003	-123.15	-22.15	1001.5	0.12	61.472	0.60860

TABLE B-1.
(CONTINUED)

RUN NO.	COMPOSITION (MOLE FRACTION) CH4	C2H6	C3H8	INLET TEMP. (°F)	OUTLET TEMP. (°F)	INLET PRES. (PSIA)	PRES. DROP (PSID)	HEAT INPUT (BTU/LB)	MEAN HEAT CAPACITY (BTU/LB°F)
27.010	0.001	0.996	0.003	-22.74	-12.91	1000.8	0.10	6.441	0.65564
27.011	0.001	0.996	0.003	-22.72	-13.08	1000.3	0.10	6.328	0.65671
27.020	0.001	0.996	0.003	-22.70	6.59	999.2	0.10	19.801	0.67587
27.030	0.001	0.996	0.003	-22.73	32.00	1000.9	0.08	37.974	0.69385
27.040	0.001	0.996	0.003	-22.71	51.61	1002.7	0.10	53.057	0.71388
27.050	0.001	0.996	0.003	-22.66	65.74	997.2	0.10	64.685	0.73177
4.010	0.001	0.996	0.003	51.64	61.54	1001.0	0.08	8.179	0.82599
4.011	0.001	0.996	0.003	51.64	61.60	1000.5	0.05	8.180	0.82167
4.020	0.001	0.996	0.003	51.66	81.48	1001.8	0.05	26.415	0.88567
4.030	0.001	0.996	0.003	51.66	106.48	1002.4	0.10	55.570	1.01368
4.040	0.001	0.996	0.003	51.66	121.46	1002.4	0.10	84.196	1.20616
4.050	0.001	0.996	0.003	51.71	131.56	1001.0	0.10	105.888	1.32598
4.060	0.001	0.996	0.003	51.72	146.80	1002.8	0.10	127.899	1.34515
16.010	0.001	0.996	0.003	116.82	121.64	1001.3	0.16	10.661	2.21219
16.011	0.001	0.996	0.003	116.84	121.64	1000.0	0.16	10.700	2.22912
16.012	0.001	0.996	0.003	116.77	121.54	999.8	0.16	10.647	2.22882
16.020	0.001	0.996	0.003	116.78	126.69	998.8	0.16	22.312	2.25317
16.030	0.001	0.996	0.003	116.75	147.36	999.1	0.19	55.577	1.81564
16.040	0.001	0.996	0.003	116.72	167.46	1002.5	0.16	76.309	1.50400
39.010	0.001	0.996	0.003	117.80	118.89	1002.1	0.15	2.479	2.28365
39.020	0.001	0.996	0.003	117.86	119.96	1001.2	0.15	4.774	2.27418
39.030	0.001	0.996	0.003	117.77	120.93	1001.2	0.15	7.274	2.29977
39.040	0.001	0.996	0.003	117.76	121.96	1001.7	0.15	9.621	2.29120
39.050	0.001	0.996	0.003	117.88	123.13	1001.8	0.16	12.087	2.30063
39.060	0.001	0.996	0.003	117.76	124.06	999.8	0.15	14.509	2.30447
50.010	0.001	0.996	0.003	146.67	162.17	999.8	0.10	16.657	1.07473
50.020	0.001	0.996	0.003	146.68	162.22	998.0	0.10	16.576	1.06655
50.030	0.001	0.996	0.003	146.68	162.19	1000.1	0.20	16.554	1.06746
50.031	0.001	0.996	0.003	146.68	162.17	1000.1	0.20	16.540	1.06775
50.040	0.001	0.996	0.003	146.68	162.22	1002.6	0.22	16.622	1.0704
40.010	0.001	0.996	0.003	99.35	100.35	818.4	0.15	3.825	3.82454
40.020	0.001	0.996	0.003	99.37	101.38	819.8	0.15	8.355	4.14593
40.030	0.001	0.996	0.003	99.37	102.33	818.6	0.15	13.412	4.54513
40.031	0.001	0.996	0.003	99.37	102.31	818.6	0.15	13.415	4.56564
40.040	0.001	0.996	0.003	99.39	103.30	819.8	0.15	18.467	4.72778
40.041	0.001	0.996	0.003	99.39	103.30	819.5	0.15	18.471	4.72859
40.050	0.001	0.996	0.003	99.39	104.37	819.8	0.15	24.250	4.87076
40.051	0.001	0.996	0.003	99.39	104.40	820.0	0.15	24.225	4.83643
40.060	0.001	0.996	0.003	99.39	105.43	818.4	0.15	29.537	4.89497
40.061	0.001	0.996	0.003	99.39	105.45	818.8	0.15	29.517	4.87334
51.010	0.001	0.996	0.003	100.27	101.11	819.8	0.20	3.785	4.48389
51.020	0.001	0.996	0.003	100.77	101.56	819.8	0.20	3.777	4.78433
51.030	0.001	0.996	0.003	101.29	102.04	819.7	0.20	3.856	5.15570
51.040	0.001	0.996	0.003	101.95	102.74	819.9	0.20	4.273	5.41780
51.050	0.001	0.996	0.003	102.47	103.27	819.6	0.20	4.433	5.48134
51.060	0.001	0.996	0.003	103.06	103.90	819.8	0.20	4.450	5.29244
17.010	0.001	0.996	0.003	126.36	136.26	750.8	0.37	8.584	0.86728
17.011	0.001	0.996	0.003	126.43	136.39	750.4	0.37	8.591	0.86261
17.012	0.001	0.996	0.003	126.36	136.37	749.5	0.36	8.601	0.85951
17.020	0.001	0.996	0.003	126.48	157.15	749.3	0.39	24.205	0.78922
17.030	0.001	0.996	0.003	126.63	177.06	751.1	0.42	37.885	0.75120
17.040	0.001	0.996	0.003	126.37	201.99	749.9	0.47	54.157	0.71622
17.050	0.001	0.996	0.003	126.42	221.42	750.3	0.34	66.134	0.69615
5.010	0.001	0.996	0.003	51.49	61.54	714.1	0.05	9.210	0.91648
5.011	0.001	0.996	0.003	51.49	61.60	713.8	0.05	9.218	0.91761
5.020	0.001	0.996	0.003	51.46	81.09	712.0	0.06	31.388	1.05926
5.030	0.001	0.996	0.003	51.44	86.12	712.1	0.07	40.000	1.15336
5.040	0.001	0.996	0.003	51.32	91.26	712.3	0.11	88.130	2.20663
5.050	0.001	0.996	0.003	51.51	96.64	713.8	0.12	105.750	2.34317
5.060	0.001	0.996	0.003	51.52	107.28	713.4	0.09	122.128	2.19019
5.070	0.001	0.996	0.003	51.69	126.39	712.0	0.10	140.232	1.87729
5.080	0.001	0.996	0.003	51.73	146.66	713.9	0.10	155.812	1.64133
8.010	0.001	0.996	0.003	77.18	87.04	712.2	0.07	15.680	1.59143
8.021	0.001	0.996	0.003	77.20	93.34	711.6	0.17	72.134	4.46839
8.030	0.001	0.996	0.003	77.28	107.21	713.1	0.15	96.217	3.21445
8.035	0.001	0.996	0.003	77.28	107.21	713.1	0.15	95.351	3.18550
8.040	0.001	0.996	0.003	77.18	130.45	711.6	0.15	117.450	2.20485

TABLE B-1.
(CONTINUED)

RUN NO.	COMPOSITION (MOLE FRACTION) CH4	C2H6	C3H8	INLET TEMP. (°F)	OUTLET TEMP. (°F)	INLET PRES. (PSIA)	PRES. DROP (PSID)	HEAT INPUT (BTU/LB)	MEAN HEAT CAPACITY (BTU/LB°F)
20.010	0.001	0.996	0.003	78.48	80.74	676.2	0.05	3.527	1.55918
20.011	0.001	0.996	0.003	78.53	80.75	676.1	0.05	3.453	1.55447
20.012	0.001	0.996	0.003	78.56	80.75	675.8	0.04	3.410	1.55805
20.020	0.001	0.996	0.003	78.58	83.49	677.7	0.05	8.475	1.72580
20.030	0.001	0.996	0.003	78.56	84.57	676.4	0.04	10.998	1.83205
20.040	0.001	0.996	0.003	78.40	86.04	676.2	0.04	17.156	2.24356
20.051	0.001	0.996	0.003	78.58	86.39	676.8	0.11	26.777	3.43185
20.060	0.001	0.996	0.003	78.56	85.36	676.1	0.05	13.284	1.95596
20.070	0.001	0.996	0.003	78.63	86.55	677.6	0.06	35.764	4.51615
20.080	0.001	0.996	0.003	78.56	86.38	675.8	0.07	55.096	7.04687
20.090	0.001	0.996	0.003	78.58	89.42	676.7	0.11	74.091	6.83510
20.100	0.001	0.996	0.003	78.54	87.62	677.6	0.11	68.270	7.51963
20.110	0.001	0.996	0.003	78.52	92.83	677.2	0.12	81.002	5.66332
20.120	0.001	0.996	0.003	78.55	97.39	677.0	0.12	87.652	4.65363
20.130	0.001	0.996	0.003	78.58	101.37	676.4	0.14	92.534	4.06136
20.140	0.001	0.996	0.003	78.56	132.18	676.5	0.15	119.371	2.22648
23.010	0.001	0.996	0.003	52.04	60.45	602.4	0.11	8.217	0.97740
23.011	0.001	0.996	0.003	52.02	60.64	600.1	0.11	8.391	0.97350
23.020	0.001	0.996	0.003	52.07	68.57	601.4	0.08	17.241	1.04463
21.010	0.001	0.996	0.003	67.01	69.33	602.0	0.02	2.823	1.21419
21.011	0.001	0.996	0.003	66.97	69.32	599.8	0.02	2.848	1.21169
21.020	0.001	0.996	0.003	66.95	71.91	601.3	0.05	6.321	1.27451
21.030	0.001	0.996	0.003	66.94	73.10	600.2	0.04	8.031	1.30242
21.040	0.001	0.996	0.003	66.98	74.62	602.4	0.04	10.191	1.33326
21.050	0.001	0.996	0.003	67.21	76.13	600.6	0.06	12.508	1.40108
21.060	0.001	0.996	0.003	66.98	75.94	600.0	0.06	15.479	1.72649
21.070	0.001	0.996	0.003	66.95	75.96	600.2	0.06	17.840	1.97829
21.080	0.001	0.996	0.003	67.07	76.28	601.2	0.06	32.222	3.50049
21.090	0.001	0.996	0.003	67.13	76.33	601.1	0.08	53.390	5.80587
21.100	0.001	0.996	0.003	67.10	76.47	601.6	0.06	68.234	7.28658
21.110	0.001	0.996	0.003	67.13	76.94	601.2	0.06	88.064	8.97069
21.120	0.001	0.996	0.003	67.11	76.40	601.0	0.13	79.679	8.58008
21.130	0.001	0.996	0.003	67.10	79.30	601.4	0.14	92.592	7.58470
21.140	0.001	0.996	0.003	67.07	83.12	600.4	0.13	98.213	6.11792
21.150	0.001	0.996	0.003	67.09	86.01	600.4	0.13	101.391	5.35994
21.160	0.001	0.996	0.003	67.09	110.52	600.2	0.15	122.662	2.82393
28.010	0.001	0.996	0.003	-22.82	-13.49	501.5	0.07	6.370	0.68327
28.011	0.001	0.996	0.003	-22.80	-13.47	501.3	0.07	6.352	0.68037
28.020	0.001	0.996	0.003	-22.80	5.04	500.7	0.07	19.357	0.69528
28.030	0.001	0.996	0.003	-23.01	27.69	501.7	0.09	36.785	0.72558
28.040	0.001	0.996	0.003	-22.91	53.07	501.3	0.12	54.182	0.77840
22.010	0.001	0.996	0.003	51.91	54.26	500.1	0.02	2.361	1.00624
22.011	0.001	0.996	0.003	51.43	53.79	499.8	0.02	2.353	0.99995
22.020	0.001	0.996	0.003	51.56	56.30	500.0	0.03	4.859	1.02355
22.030	0.001	0.996	0.003	51.58	58.40	500.2	0.03	7.119	1.04338
22.040	0.001	0.996	0.003	51.56	60.40	499.8	0.04	9.381	1.06167
22.050	0.001	0.996	0.003	51.58	60.79	500.8	0.12	12.335	1.33955
22.060	0.001	0.996	0.003	51.97	61.17	500.6	0.08	16.300	1.77103
22.070	0.001	0.996	0.003	51.56	60.84	500.5	0.09	22.365	2.40971
22.080	0.001	0.996	0.003	51.54	60.92	500.4	0.10	45.911	4.89801
22.090	0.001	0.996	0.003	51.60	61.12	500.5	0.12	72.363	7.60735
22.100	0.001	0.996	0.003	51.57	61.19	500.3	0.15	103.116	10.71216
22.110	0.001	0.996	0.003	51.58	61.34	500.3	0.15	109.471	11.21786
22.120	0.001	0.996	0.003	51.59	64.25	500.5	0.15	113.183	8.93622
22.130	0.001	0.996	0.003	51.51	63.03	500.3	0.15	111.884	9.71160
22.140	0.001	0.996	0.003	51.58	66.90	500.1	0.15	115.820	7.56025
22.150	0.001	0.996	0.003	51.58	70.53	500.1	0.15	119.333	6.29717
22.160	0.001	0.996	0.003	51.56	80.58	500.1	0.15	126.843	4.37128
7.010	0.001	0.996	0.003	77.30	87.47	500.4	0.30	7.674	0.75412
7.011	0.001	0.996	0.003	77.32	87.57	501.0	0.30	7.700	0.75184
7.020	0.001	0.996	0.003	77.23	106.38	502.2	0.27	20.438	0.70099
7.030	0.001	0.996	0.003	77.23	131.15	499.7	0.37	35.406	0.65665
7.040	0.001	0.996	0.003	77.28	150.66	500.7	0.37	46.852	0.63844
7.050	0.001	0.996	0.003	77.22	169.66	501.5	0.39	57.684	0.62400
19.010	0.001	0.996	0.003	126.24	156.32	502.3	0.66	17.723	0.58915
19.027	0.001	0.996	0.003	126.29	177.47	502.3	0.68	29.753	0.58127
19.030	0.001	0.996	0.003	126.51	201.66	501.8	0.70	43.304	0.57617
24.010	0.001	0.996	0.003	40.57	42.64	410.4	0.05	1.914	0.92160
24.020	0.001	0.996	0.003	40.62	44.92	411.1	0.13	4.029	0.93179
24.030	0.001	0.996	0.003	40.61	43.60	410.3	0.05	2.772	0.92708
24.040	0.001	0.996	0.003	40.62	44.97	411.0	0.15	5.573	1.28278
24.050	0.001	0.996	0.003	40.61	45.07	411.1	0.18	22.422	5.02936
24.060	0.001	0.996	0.003	40.55	45.24	411.0	0.18	54.511	11.63423
24.070	0.001	0.996	0.003	40.55	45.66	410.9	0.20	121.843	23.87392
24.086	0.001	0.996	0.003	40.51	50.46	410.7	0.20	125.962	12.65245
24.090	0.001	0.996	0.003	40.53	57.19	410.7	0.20	131.384	7.88713
24.100	0.001	0.996	0.003	40.54	64.57	411.2	0.17	136.319	5.67340
38.010	0.001	0.996	0.003	-249.78	-236.22	249.1	0.22	7.486	0.55164
38.011	0.001	0.996	0.003	-249.75	-236.03	248.6	0.22	7.485	0.54977
38.020	0.001	0.996	0.003	-249.73	-211.11	250.9	0.17	21.231	0.54985
38.030	0.001	0.996	0.003	-249.63	-173.76	252.4	0.15	41.983	0.55335
38.040	0.001	0.996	0.003	-249.63	-142.14	249.7	0.15	60.091	0.55900
38.050	0.001	0.996	0.003	-249.63	-122.02	249.1	0.17	71.673	0.56166
38.110	0.001	0.996	0.003	-259.83	-248.39	248.5	0.17	6.316	0.55199
38.111	0.001	0.996	0.003	-259.87	-248.38	249.2	0.17	6.313	0.54930

TABLE B-1

(CONTINUED)

RUN NO.	COMPOSITION CH4	C2H6	C3H8 (MOLE FRACTION)	INLET TEMP. (°F)	OUTLET TEMP. (°F)	INLET PRES. (PSIA)	PRES. DROP (PSID)	HEAT INPUT (BTU/LB)	MEAN HEAT CAPACITY (BTU/LB°F)
33.010	0.001	0.996	0.003	-122.94	-112.63	251.7	0.05	6.088	0.59032
33.020	0.001	0.996	0.003	-122.93	-90.73	249.2	0.15	19.201	0.59618
33.030	0.001	0.996	0.003	-122.93	-64.34	248.9	0.20	35.602	0.60763
33.040	0.001	0.996	0.003	-123.01	-39.46	248.4	0.20	51.638	0.61807
33.050	0.001	0.996	0.003	-123.02	-24.32	248.9	0.15	61.760	0.62578
30.010	0.001	0.996	0.003	-23.37	-13.67	248.9	0.15	6.723	0.69309
30.011	0.001	0.996	0.003	-23.39	-13.69	248.9	0.15	6.728	0.69362
30.020	0.001	0.996	0.003	-23.32	6.94	248.8	0.17	21.897	0.72364
30.030	0.001	0.996	0.003	-23.37	8.26	249.1	0.29	30.156	0.95358
30.040	0.001	0.996	0.003	-23.35	1.87	249.2	0.10	17.916	0.71048
29.010	0.001	0.996	0.003	17.00	21.15	251.7	1.06	2.381	0.57520
29.011	0.001	0.996	0.003	17.00	21.15	248.5	1.06	2.405	0.57921
29.012	0.001	0.996	0.003	17.00	21.28	245.1	1.06	2.443	0.57073
29.020	0.001	0.996	0.003	17.00	27.71	250.4	1.08	5.927	0.55366
29.030	0.001	0.996	0.003	17.00	51.81	248.9	1.13	18.362	0.52752
6.010	0.001	0.996	0.003	51.52	61.54	252.4	0.64	5.105	0.50932
6.011	0.001	0.996	0.003	51.52	61.60	252.4	0.64	5.130	0.50921
6.020	0.001	0.996	0.003	51.62	82.02	251.3	0.69	15.223	0.50078
6.030	0.001	0.996	0.003	51.52	106.58	250.8	0.91	27.346	0.49667
6.040	0.001	0.996	0.003	51.59	126.85	251.2	0.69	37.360	0.49639
18.010	0.001	0.996	0.003	126.38	136.28	251.9	1.42	5.025	0.50732
18.011	0.001	0.996	0.003	126.32	136.26	252.3	1.42	5.029	0.50608
18.012	0.001	0.996	0.003	126.33	136.28	252.5	1.42	5.035	0.50597
18.020	0.001	0.996	0.003	126.33	156.71	252.0	1.43	15.294	0.50346
18.030	0.001	0.996	0.003	126.35	177.03	251.8	1.50	25.632	0.50579
18.031	0.001	0.996	0.003	126.44	177.35	251.0	1.50	25.737	0.50556
18.040	0.001	0.996	0.003	126.35	201.21	252.4	1.57	38.135	0.50937
18.050	0.001	0.996	0.003	126.42	221.71	250.6	1.65	48.819	0.51232

TABLE B-2

Basic Isothermal Data for 0.996 Mole Fraction Ethane

RUN NO.	COMPOSITION CH4	C2H6	C3H8 (MOLE FRACTION)	INLET TEMP. (°F)	OUTLET TEMP. (°F)	INLET PRES. (PSIA)	PRES. DROP (PSID)	HEAT INPUT (BTU/LB)	ISOTHERMAL J.T.COEFF. (BTU/LB PSIA)
9.010	0.001	0.996	0.003	49.18	49.18	1676.5	96.79	0.118	-0.00122
9.020	0.001	0.996	0.003	49.24	49.24	1585.5	95.39	0.158	-0.00165
9.030	0.001	0.996	0.003	49.26	49.26	1422.4	96.99	0.221	-0.00228
9.040	0.001	0.996	0.003	49.22	49.23	1216.9	100.99	0.337	-0.00334
9.050	0.001	0.996	0.003	49.22	49.22	1032.5	101.39	0.456	-0.00449
10.010	0.001	0.996	0.003	49.21	49.23	370.9	259.98	24.947	-0.09596
10.020	0.001	0.996	0.003	49.22	49.19	370.0	144.19	15.503	-0.10752
10.030	0.001	0.996	0.003	49.22	49.20	865.4	101.99	0.606	-0.00594
10.040	0.001	0.996	0.003	49.19	49.19	768.3	106.59	0.789	-0.00740
10.050	0.001	0.996	0.003	49.23	49.22	666.9	108.39	0.982	-0.00906
14.010	0.001	0.996	0.003	49.24	49.48	448.6	76.19	131.217	-1.72217
14.017	0.001	0.996	0.003	49.24	49.48	448.4	86.19	131.380	-1.52427
14.020	0.001	0.996	0.003	49.22	49.43	448.1	79.99	130.912	-1.63656
14.025	0.001	0.996	0.003	49.22	49.43	448.1	87.99	130.912	-1.48778
11.010	0.001	0.996	0.003	89.87	89.86	839.2	119.39	11.230	-0.09406
11.020	0.001	0.996	0.003	89.84	89.88	727.2	134.59	79.921	-0.59382
12.010	0.001	0.996	0.003	89.70	89.73	2013.6	288.37	1.241	-0.00430
12.015	0.001	0.996	0.003	89.70	89.73	2015.7	288.37	1.240	-0.00430
12.020	0.001	0.996	0.003	89.78	89.76	2011.7	147.79	0.541	-0.00366
12.030	0.001	0.996	0.003	89.79	89.78	1734.3	285.37	1.861	-0.00652
12.040	0.001	0.996	0.003	89.80	89.78	1732.3	133.59	0.752	-0.00563
12.050	0.001	0.996	0.003	89.80	89.79	1450.6	296.97	3.242	-0.01092
12.060	0.001	0.996	0.003	89.79	89.80	1449.9	192.78	1.894	-0.00983
12.070	0.001	0.996	0.003	89.84	89.85	1150.5	315.17	7.815	-0.02479
13.010	0.001	0.996	0.003	89.80	89.80	836.2	115.99	10.396	-0.08963
13.020	0.001	0.996	0.003	89.77	89.86	608.4	484.55	44.764	-0.09238
13.030	0.001	0.996	0.003	89.80	89.95	605.3	290.37	31.831	-0.10962
13.040	0.001	0.996	0.003	89.78	89.76	668.8	249.38	37.583	-0.15071
15.010	0.001	0.996	0.003	124.99	124.97	1996.6	255.78	2.686	-0.01050
15.020	0.001	0.996	0.003	124.96	124.96	1997.2	113.79	1.063	-0.00934
15.030	0.001	0.996	0.003	124.94	124.89	1742.1	262.58	4.429	-0.01687
15.040	0.001	0.996	0.003	124.96	125.02	1478.3	282.37	10.022	-0.03549
15.050	0.001	0.996	0.003	124.95	125.01	1309.2	114.79	5.219	-0.04546
15.060	0.001	0.996	0.003	124.97	125.04	1198.7	289.77	41.441	-0.14301
15.070	0.001	0.996	0.003	125.00	124.97	1197.8	153.19	13.886	-0.09065
15.080	0.001	0.996	0.003	125.00	125.03	914.2	512.35	57.873	-0.11296
15.090	0.001	0.996	0.003	124.96	124.87	620.7	499.55	34.148	-0.06836
15.100	0.001	0.996	0.003	124.98	125.03	760.5	620.74	48.491	-0.07812
15.110	0.001	0.996	0.003	124.95	124.97	758.2	503.75	41.645	-0.08267

TABLE B-2
(CONTINUED)

RUN NO.	COMPOSITION (MOLE FRACTION) CH4	C2H6	C3H8	INLET TEMP. (°F)	OUTLET TEMP. (°F)	INLET PRES. (PSIA)	PRES. DROP (PSID)	HEAT INPUT (BTU/LB)	ISOTHERMAL J.T.COEFF. (BTU/LB PSIA)
16.010	0.001	0.996	0.003	200.64	200.66	2014.0	356.17	13.481	-0.03785
16.020	0.001	0.996	0.003	200.68	200.65	2008.2	132.99	4.173	-0.03138
16.030	0.001	0.996	0.003	200.67	200.71	1672.2	399.96	23.645	-0.05912
16.040	0.001	0.996	0.003	200.59	200.61	1667.8	179.78	9.695	-0.05393
16.050	0.001	0.996	0.003	200.60	200.63	1278.7	394.96	25.155	-0.06369
16.060	0.001	0.996	0.003	200.60	200.56	1279.7	208.18	13.605	-0.06535
16.061	0.001	0.996	0.003	200.57	200.56	1281.5	208.18	13.604	-0.06535
16.070	0.001	0.996	0.003	200.62	200.61	893.5	410.36	22.026	-0.05367
16.080	0.001	0.996	0.003	200.62	200.66	614.1	362.57	17.111	-0.04719
16.090	0.001	0.996	0.003	200.61	200.56	398.6	296.57	12.762	-0.04303
1.010	0.001	0.996	0.003	202.14	202.16	2001.3	53.20	1.558	-0.02929
1.020	0.001	0.996	0.003	202.14	202.16	1857.8	56.79	2.066	-0.03638
1.021	0.001	0.996	0.003	202.14	202.18	1858.5	55.99	2.072	-0.03701
1.030	0.001	0.996	0.003	202.13	202.13	1758.6	58.39	2.626	-0.04497
1.040	0.001	0.996	0.003	202.12	202.14	1648.5	64.59	3.239	-0.05014
1.050	0.001	0.996	0.003	202.12	202.14	1540.0	71.79	4.106	-0.05720
1.060	0.001	0.996	0.003	202.15	202.17	1422.7	77.99	4.819	-0.06179
2.010	0.001	0.996	0.003	202.10	202.13	1318.0	107.39	7.047	-0.06562
2.020	0.001	0.996	0.003	202.08	202.09	1165.3	135.59	8.687	-0.06407
2.030	0.001	0.996	0.003	202.14	202.17	1016.8	175.98	10.543	-0.05991
2.040	0.001	0.996	0.003	202.13	202.14	853.6	210.58	11.519	-0.05470
2.050	0.001	0.996	0.003	202.15	202.16	650.6	236.78	11.602	-0.04900
2.060	0.001	0.996	0.003	202.14	202.18	426.3	175.38	7.780	-0.04436
2.070	0.001	0.996	0.003	202.13	202.15	272.2	162.38	6.870	-0.04231

TABLE B-3
Basic Isenthalpic Data for 0.996 Mole Fraction Ethane

RUN NO.	COMPOSITION (MOLE FRACTION) CH4	C2H6	C3H8	INLET TEMP. (°F)	OUTLET TEMP. (°F)	INLET PRES. (PSIA)	PRES. DROP (PSID)	HEAT INPUT (BTU/LB)	J.THOMSON COEFF. (°F/PSIA)
5.010	0.001	0.996	0.003	-246.57	-243.98	2002.8	414.96	0.000	-0.00625
5.020	0.001	0.996	0.003	-246.61	-245.52	2001.4	190.38	0.000	-0.00576
5.030	0.001	0.996	0.003	-246.54	-244.04	1588.4	398.76	0.000	-0.00628
5.040	0.001	0.996	0.003	-246.61	-245.54	1589.2	191.38	0.000	-0.00561
5.050	0.001	0.996	0.003	-246.61	-243.81	1193.2	449.96	0.000	-0.00621
5.060	0.001	0.996	0.003	-246.57	-245.12	1192.4	246.78	0.000	-0.00591
5.070	0.001	0.996	0.003	-246.59	-243.30	752.6	524.75	0.000	-0.00625
5.080	0.001	0.996	0.003	-246.61	-245.23	751.1	238.78	0.000	-0.00579
5.090	0.001	0.996	0.003	-246.60	-245.80	233.6	150.99	0.000	-0.00527
3.010	0.001	0.996	0.003	-123.30	-120.68	2003.2	484.15	0.000	-0.00541
3.020	0.001	0.996	0.003	-123.29	-121.92	2001.0	270.17	0.000	-0.00508
3.025	0.001	0.996	0.003	-123.29	-121.92	2001.0	270.17	0.000	-0.00508
3.030	0.001	0.996	0.003	-123.33	-123.11	1996.4	52.80	0.000	-0.00401
3.040	0.001	0.996	0.003	-123.35	-121.29	1520.8	388.56	0.000	-0.00529
3.050	0.001	0.996	0.003	-123.29	-122.02	1520.8	246.58	0.000	-0.00517
3.060	0.001	0.996	0.003	-123.31	-121.26	1141.9	394.56	0.000	-0.00519
3.065	0.001	0.996	0.003	-123.31	-121.26	1141.9	394.56	0.000	-0.00519
3.070	0.001	0.996	0.003	-123.14	-122.23	1142.7	181.58	0.000	-0.00502
4.010	0.001	0.996	0.003	-123.49	-121.81	760.1	392.96	0.000	-0.00429
4.015	0.001	0.996	0.003	-123.49	-121.81	760.1	392.96	0.000	-0.00429
4.020	0.001	0.996	0.003	-123.51	-122.52	761.8	239.38	0.000	-0.00413
4.030	0.001	0.996	0.003	-123.48	-122.50	393.1	248.78	0.000	-0.00394
4.040	0.001	0.996	0.003	-123.07	-122.76	217.9	118.99	0.000	-0.00262
6.010	0.001	0.996	0.003	-23.88	-22.96	2001.7	303.37	0.000	-0.00302
6.020	0.001	0.996	0.003	-23.80	-23.55	1999.5	97.59	0.000	-0.00263
7.010	0.001	0.996	0.003	-24.57	-23.61	1700.5	354.57	0.000	-0.00273
7.020	0.001	0.996	0.003	-24.58	-24.24	1702.3	137.59	0.000	-0.00253
7.030	0.001	0.996	0.003	-24.54	-23.71	1349.7	362.77	0.000	-0.00231
7.040	0.001	0.996	0.003	-24.56	-24.20	1349.6	166.78	0.000	-0.00215
7.050	0.001	0.996	0.003	-24.55	-23.90	991.6	363.37	0.000	-0.00179
7.060	0.001	0.996	0.003	-24.57	-24.17	991.6	222.58	0.000	-0.00183
7.070	0.001	0.996	0.003	-24.54	-24.10	635.7	377.36	0.000	-0.00118
7.080	0.001	0.996	0.003	-24.48	-24.44	267.2	113.59	0.000	-0.00035
8.010	0.001	0.996	0.003	49.75	49.45	2002.5	321.57	0.000	0.00095
8.020	0.001	0.996	0.003	49.75	49.68	2000.9	108.59	0.000	0.00066
8.030	0.001	0.996	0.003	44.46	44.44	1997.8	99.59	0.000	0.00024

TABLE B-4

Basic Isobaric Data for Nominal 0.76 C_2H_6, 0.24 C_3H_8 Mixture

RUN NO.	COMPOSITION (MOLE FRACTION) CH4	C2H6	C3H8	INLET TEMP. (°F)	OUTLET TEMP. (°F)	INLET PRES. (PSIA)	PRES. DROP (PSID)	HEAT INPUT (BTU/LB)	MEAN HEAT CAPACITY (BTU/LB°F)
16.010	0.003	0.760	0.237	-252.01	-241.58	2000.2	0.07	5.440	0.52185
16.020	0.003	0.760	0.237	-251.91	-232.09	2002.3	0.07	10.373	0.52324
16.021	0.003	0.760	0.237	-252.19	-232.27	2003.8	0.07	10.384	0.52120
16.030	0.003	0.760	0.237	-252.12	-191.76	2003.9	0.07	31.697	0.52514
16.031	0.003	0.760	0.237	-251.94	-191.16	2004.7	0.07	31.969	0.52394
16.040	0.003	0.760	0.237	-251.89	-150.93	2000.9	0.07	53.425	0.52913
16.041	0.003	0.760	0.237	-251.89	-150.60	2001.5	0.07	53.539	0.52954
16.050	0.003	0.760	0.237	-251.88	-131.84	1995.3	0.07	63.529	0.52923
15.010	0.003	0.754	0.243	-151.04	-140.80	2001.9	0.07	5.495	0.53646
15.020	0.003	0.754	0.243	-151.01	-131.05	2000.2	0.05	10.762	0.53915
15.030	0.003	0.754	0.243	-151.00	-90.57	2000.2	0.01	33.037	0.54677
15.040	0.003	0.754	0.243	-151.00	-49.73	2000.5	0.06	55.986	0.55282
15.050	0.003	0.754	0.243	-151.00	-24.35	2003.4	0.07	70.653	0.55783
14.010	0.003	0.760	0.237	-51.96	-41.72	1999.7	0.05	5.912	0.57754
14.020	0.003	0.760	0.237	-51.91	-32.24	2002.5	0.05	11.674	0.59360
14.030	0.003	0.760	0.237	-51.92	8.49	2001.7	0.06	35.912	0.59448
14.031	0.003	0.760	0.237	-51.92	8.64	2001.3	0.06	35.908	0.59291
14.040	0.003	0.760	0.237	-51.84	48.09	1997.5	0.07	60.871	0.60912
14.041	0.003	0.760	0.237	-51.84	48.37	1996.3	0.07	61.066	0.60937
12.010	0.003	0.766	0.231	47.99	58.87	1999.9	0.10	7.275	0.66860
12.020	0.003	0.766	0.231	47.95	68.58	2000.7	0.05	13.681	0.66314
12.030	0.003	0.761	0.236	47.99	98.34	2000.8	0.05	34.376	0.68280
12.040	0.003	0.761	0.236	47.93	128.74	2003.6	0.05	56.512	0.69933
12.050	0.003	0.761	0.236	47.94	148.59	2003.0	0.07	71.941	0.71481
23.010	0.003	0.751	0.246	125.64	137.99	2001.7	0.05	9.584	.77622
23.011	0.003	0.751	0.246	125.64	138.16	2004.2	0.05	9.556	.76320
23.020	0.003	0.751	0.246	125.75	153.99	2001.2	0.05	22.342	.79089
23.030	0.003	0.751	0.246	125.71	179.98	2002.8	0.05	44.061	.81184
10.010	0.003	0.765	0.232	149.81	156.46	2001.2	0.12	5.536	0.83195
10.011	0.003	0.765	0.232	149.82	156.37	2001.5	0.12	5.392	0.82239
10.020	0.003	0.765	0.232	149.83	164.62	2001.7	0.12	12.517	0.84597
10.030	0.003	0.765	0.232	149.92	175.68	2001.7	0.12	21.785	0.84563
10.040	0.003	0.765	0.232	149.84	201.95	2001.3	0.12	46.397	0.89032
7.010	0.003	0.760	0.237	175.31	185.58	2001.1	0.12	9.080	0.88348
7.020	0.003	0.760	0.237	175.34	195.61	2000.2	0.12	18.112	0.89378
7.030	0.003	0.760	0.237	175.26	230.04	1999.4	0.12	50.324	0.91862
7.040	0.003	0.760	0.237	175.39	251.09	2001.1	0.12	70.127	0.92634
8.010	0.003	0.761	0.236	175.23	181.80	1501.8	0.12	7.146	1.08874
8.020	0.003	0.761	0.236	175.35	190.61	1501.6	0.16	16.901	1.10722
8.030	0.003	0.762	0.235	175.33	198.91	1502.0	0.16	26.253	1.11306
8.040	0.003	0.759	0.238	175.32	230.30	1502.6	0.16	60.247	1.09577
8.050	0.003	0.759	0.238	175.31	248.29	1499.5	0.17	77.998	1.06866
8.051	0.003	0.759	0.238	175.31	248.69	1501.3	0.17	78.152	1.06505
11.010	0.003	0.760	0.237	101.35	104.93	999.1	0.15	3.203	0.89340
11.020	0.003	0.760	0.237	101.34	108.42	999.4	0.15	6.455	0.91160
11.021	0.003	0.760	0.237	101.38	108.50	999.9	0.15	6.440	0.90397
11.030	0.003	0.760	0.237	101.36	114.15	1000.1	0.15	11.852	0.92676
11.040	0.003	0.760	0.237	101.35	120.40	999.7	0.15	18.266	0.95875
11.050	0.003	0.760	0.237	101.32	128.41	1000.3	0.15	27.255	1.00605
11.060	0.003	0.760	0.237	101.43	136.87	999.4	0.15	38.087	1.07465
11.061	0.003	0.760	0.237	101.43	137.01	999.2	0.15	37.979	1.06745
11.070	0.003	0.760	0.237	101.38	145.36	999.6	0.15	51.046	1.16079
11.080	0.003	0.760	0.237	101.50	150.95	999.6	0.15	61.262	1.23881
11.090	0.003	0.760	0.237	101.38	158.39	999.6	0.15	75.540	1.32491
11.100	0.003	0.760	0.237	101.38	165.70	999.8	0.15	88.075	1.36937
11.110	0.003	0.760	0.237	101.42	169.84	999.2	0.15	94.961	1.38779
18.010	0.003	0.759	0.238	101.40	108.62	716.1	0.10	8.967	1.24355
18.020	0.003	0.759	0.238	101.40	110.15	715.9	0.10	11.155	1.27574
18.030	0.003	0.759	0.238	101.39	1112.07	715.9	0.10	14.146	1.3246
18.040	0.003	0.759	0.238	101.48	114.19	715.3	0.10	17.815	1.40077
18.050	0.003	0.759	0.238	101.45	116.65	716.1	0.10	22.875	1.50519
18.060	0.003	0.759	0.238	101.45	118.49	715.8	0.10	29.594	1.73662
18.070	0.003	0.759	0.238	101.44	120.12	715.4	0.10	41.481	2.21996
18.080	0.003	0.761	0.236	101.40	123.09	715.5	0.10	61.983	2.85702
18.090	0.003	0.761	0.236	101.40	125.83	715.8	0.15	75.991	3.11044
18.100	0.003	0.761	0.236	101.40	130.55	715.6	0.15	87.198	2.99137
18.110	0.003	0.761	0.236	101.41	132.92	715.6	0.15	91.419	2.90090
18.120	0.003	0.761	0.236	101.43	137.73	715.6	0.15	98.644	2.72744
18.130	0.003	0.761	0.236	101.43	151.47	715.5	0.15	115.040	2.29400
18.210	0.003	0.761	0.236	101.41	108.06	715.9	0.07	7.910	1.19424
18.220	0.003	0.761	0.236	101.39	110.38	715.5	0.07	11.105	1.23560
18.230	0.003	0.761	0.236	101.40	112.20	715.9	0.07	13.841	1.28195
18.240	0.003	0.761	0.236	101.40	114.13	715.7	0.07	17.087	1.34241
18.250	0.003	0.760	0.237	101.36	116.46	715.9	0.10	21.891	1.44918
18.260	0.003	0.760	0.237	101.41	118.54	715.7	0.10	28.722	1.67557
18.270	0.003	0.760	0.237	101.41	120.28	715.8	0.10	40.474	2.14503
18.280	0.003	0.760	0.237	101.44	123.03	715.9	0.10	58.362	2.70291
18.290	0.003	0.760	0.237	101.44	126.11	716.1	0.15	73.171	2.96552
18.300	0.003	0.760	0.237	101.44	130.67	716.0	0.15	83.799	2.86883
18.310	0.003	0.756	0.241	101.44	133.10	716.0	0.15	87.893	2.77590
18.320	0.003	0.756	0.241	101.42	137.11	716.0	0.15	93.207	2.61161
18.330	0.003	0.756	0.241	101.36	148.39	715.5	0.15	106.082	2.2556

TABLE B-4
(CONTINUED)

RUN NO.	COMPOSITION (MOLE FRACTION) CH4	C2H6	C3H8	INLET TEMP. (°F)	OUTLET TEMP. (°F)	INLET PRES. (PSIA)	PRES. DROP (PSID)	HEAT INPUT (BTU/LB)	MEAN HEAT CAPACITY (BTU/LB°)
21.010	0.003	0.760	0.237	68.95	72.87	499.7	0.07	3.474	0.886[illegible]
21.011	0.003	0.760	0.237	68.93	72.94	499.6	0.07	3.528	0.8785[illegible]
21.020	0.003	0.760	0.237	68.97	76.00	499.4	0.07	6.284	0.89392
21.021	0.003	0.760	0.237	68.93	75.75	499.6	0.07	6.084	0.89134
21.022	0.003	0.760	0.237	68.93	75.78	499.2	0.07	6.085	0.88732
21.030	0.003	0.760	0.237	68.97	78.19	499.6	0.07	8.320	0.90176
21.040	0.003	0.760	0.237	68.97	82.45	499.7	0.07	13.020	2.1730
21.050	0.003	0.760	0.237	68.93	83.52	500.0	0.07	20.968	1.43677
21.060	0.003	0.760	0.237	68.92	86.80	499.6	0.07	45.646	2.55287
21.070	0.003	0.760	0.237	68.92	92.91	499.7	0.07	85.553	4.56626
21.080	0.003	0.760	0.237	68.92	100.41	499.8	0.07	122.540	3.89131
21.090	0.003	0.760	0.237	68.99	109.91	499.9	0.07	129.681	3.16920
21.100	0.003	0.760	0.237	68.96	115.56	499.5	0.07	134.405	2.88434
17.010	0.003	0.761	0.236	-252.86	-242.55	250.4	0.05	5.384	0.52235
17.020	0.003	0.761	0.236	-252.85	-233.57	252.0	0.07	10.049	0.52102
17.030	0.003	0.761	0.236	-252.84	-194.06	252.3	0.07	30.989	0.52713
17.040	0.003	0.761	0.236	-252.80	-154.27	250.4	0.10	52.379	0.53160
17.050	0.003	0.761	0.236	-252.87	-130.83	251.2	0.10	65.197	0.53422
22.010	0.003	0.751	0.246	-119.25	-108.613	251.8	0.07	5.975	0.56172
22.020	0.003	0.751	0.246	-119.2	-94.729	252.1	0.01	13.805	.56367
22.030	0.003	0.751	0.246	-119.18	-56.962	252.2	0.07	35.786	.57517
22.040	0.003	0.751	0.246	-119.24	-22.46	251.6	0.07	56.849	.58738
22.050	0.003	0.751	0.246	-119.34	-4.23	250.8	0.07	68.861	.59820
22.060	0.003	0.751	0.246	-119.35	8.52	252.4	0.07	77.161	.60344
22.070	0.003	0.751	0.246	-119.35	17.74	250.9	0.07	83.307	.60769
20.010	0.003	0.761	0.236	8.27	11.28	249.7	0.05	2.086	0.69461
20.011	0.003	0.761	0.236	8.27	11.29	249.8	0.05	2.084	0.69026
20.020	0.003	0.761	0.236	8.27	15.16	249.8	0.05	4.780	0.69436
20.030	0.003	0.761	0.236	8.26	21.13	250.1	0.05	8.991	0.69861
20.040	0.003	0.761	0.236	8.25	24.24	249.8	0.17	12.160	0.76019
20.050	0.003	0.761	0.236	8.25	25.94	249.5	0.22	22.223	1.25623
20.060	0.003	0.761	0.236	8.26	29.51	249.4	0.20	52.700	2.47913
20.070	0.003	0.761	0.236	8.31	34.70	249.4	0.20	88.309	3.34611
20.071	0.003	0.761	0.236	8.31	34.43	248.8	0.20	88.238	3.37782
20.080	0.003	0.761	0.236	8.35	38.17	249.4	0.25	111.891	3.75200
20.090	0.003	0.761	0.236	8.25	45.18	249.2	0.25	148.214	4.01374
19.010	0.003	0.764	0.233	37.11	40.72	248.8	0.12	20.716	5.73564
19.020	0.003	0.764	0.233	37.11	43.93	250.4	0.17	37.685	5.52726
19.030	0.003	0.764	0.233	37.09	48.46	249.2	0.20	59.664	5.24836
19.040	0.003	0.764	0.233	37.10	52.20	250.1	0.22	65.208	4.31861
19.050	0.003	0.764	0.233	37.08	56.08	250.5	0.20	67.690	3.56292
19.060	0.003	0.764	0.233	37.10	59.58	250.8	0.20	70.048	3.11575
19.070	0.003	0.764	0.233	37.13	65.09	250.5	0.20	72.627	2.59682
13.010	0.003	0.763	0.234	48.90	58.98	248.9	0.32	7.578	0.75149
13.011	0.003	0.763	0.234	49.16	59.77	248.8	0.32	7.512	0.70823
13.020	0.003	0.763	0.234	49.01	68.53	249.7	0.32	13.228	0.67786
13.030	0.003	0.763	0.234	49.00	98.37	249.0	0.32	27.687	0.56086
13.031	0.003	0.763	0.234	49.00	98.76	248.8	0.32	27.667	0.55602
13.040	0.003	0.763	0.234	53.33	106.17	249.1	0.49	27.216	0.51506
13.050	0.003	0.763	0.234	53.34	128.32	249.1	0.49	38.369	0.51173
13.060	0.003	0.763	0.234	53.34	150.40	249.1	0.49	49.550	0.51052
9.010	0.003	0.761	0.236	175.25	185.19	250.8	1.38	5.231	0.52661
9.020	0.003	0.761	0.236	175.27	195.50	252.2	1.40	10.672	0.52760
9.030	0.003	0.761	0.236	175.35	227.82	251.0	1.47	28.108	0.53570
9.040	0.003	0.761	0.236	175.37	252.34	252.0	1.72	41.554	0.53988

TABLE B-5

Basic Isothermal Data for Nominal 0.76 C_2H_6, 0.24 C_3H_8 Mixture

RUN NO.	COMPOSITION CH4	C2H6	C3H8 (MOLE FRACTION)	INLET TEMP. (°F)	OUTLET TEMP. (°F)	INLET PRES. (PSIA)	PRES. DROP (PSID)	HEAT INPUT (BTU/LB)	ISOTHERMAL J.T.COEFF. (BTU/LB PSIA)
3.050	0.003	0.760	0.237	49.71	49.65	1418.3	202.32	0.041	-0.00020
3.060	0.003	0.760	0.237	49.88	49.80	1214.2	203.26	0.133	-0.00065
3.070	0.003	0.760	0.237	49.82	49.77	1015.1	202.53	0.259	-0.00128
3.080	0.003	0.760	0.237	49.96	49.90	816.2	202.24	0.415	-0.00205
3.090	0.003	0.760	0.237	49.84	49.83	646.9	222.58	0.710	-0.00319
3.100	0.003	0.760	0.237	50.03	50.02	441.4	96.38	0.392	-0.00407
5.010	0.003	0.765	0.232	102.38	102.37	398.1	290.79	23.823	-0.08193
5.020	0.003	0.761	0.236	102.36	102.24	1003.5	191.41	2.449	-0.01279
2.010	0.003	0.759	0.238	151.65	151.55	2003.3	199.96	1.645	-0.00823
2.015	0.003	0.759	0.238	151.65	151.55	2003.3	199.96	1.631	-0.00816
2.016	0.003	0.759	0.238	151.65	151.55	2003.3	199.96	1.660	-0.00830
2.020	0.003	0.759	0.238	151.85	151.80	1803.4	211.55	2.540	-0.01201
2.030	0.003	0.759	0.238	152.03	151.97	1602.0	214.01	3.839	-0.01794
2.040	0.003	0.759	0.238	152.16	152.08	1401.1	216.37	6.793	-0.03139
2.050	0.003	0.759	0.238	152.16	152.03	1204.8	250.97	23.154	-0.09226
2.060	0.003	0.762	0.235	152.03	152.00	1001.4	269.38	51.069	-0.18958
2.070	0.003	0.762	0.235	152.43	152.43	800.4	215.13	26.656	-0.12391
2.080	0.003	0.762	0.235	152.43	152.50	600.0	221.09	17.804	-0.08053
2.090	0.003	0.766	0.231	152.37	152.31	401.5	302.12	18.360	-0.06077
1.010	0.003	0.764	0.233	250.74	250.75	1998.3	203.24	6.847	-0.03369
1.020	0.003	0.764	0.233	250.83	250.85	1996.7	82.81	2.576	-0.03111
1.030	0.003	0.764	0.233	250.89	250.85	1798.6	258.77	11.428	-0.04416
1.040	0.003	0.764	0.233	250.84	250.76	1630.9	278.75	14.394	-0.05164
1.050	0.003	0.756	0.241	250.76	250.71	1349.3	279.03	15.833	-0.05674
1.060	0.003	0.756	0.241	250.75	250.75	1105.0	286.04	15.537	-0.05432
1.070	0.003	0.756	0.241	250.77	250.79	845.3	306.98	15.079	-0.04912
1.080	0.003	0.756	0.241	250.74	250.65	596.3	381.90	16.509	-0.04323
1.090	0.003	0.760	0.237	250.79	250.87	352.4	255.70	10.382	-0.04060

TABLE B-6

Basic Isenthalpic Data for Nominal 0.76 C_2H_6, 0.24 C_3H_8 Mixture

RUN NO.	COMPOSITION CH4	C2H6	C3H8 (MOLE FRACTION)	INLET TEMP. (°F)	OUTLET TEMP. (°F)	INLET PRES. (PSIA)	PRES. DROP (PSID)	HEAT INPUT (BTU/LB)	J.THOMSON COEFF. (°F/PSIA)
4.010	0.003	0.765	0.232	-50.12	-49.64	2002.1	107.38	0.000	-0.00453
4.020	0.003	0.765	0.232	-50.12	-49.27	2004.9	185.74	0.000	-0.00459
4.030	0.003	0.765	0.232	-50.18	-49.26	1798.4	209.18	0.000	-0.00442
4.040	0.003	0.765	0.232	-50.22	-49.23	1587.9	226.20	0.000	-0.00436
4.050	0.003	0.765	0.232	-50.21	-49.23	1371.2	235.12	0.000	-0.00418
4.060	0.003	0.765	0.232	-50.23	-49.27	1135.5	234.58	0.000	-0.00409
4.070	0.003	0.765	0.232	-50.21	-49.35	901.7	227.40	0.000	-0.00379
4.080	0.003	0.765	0.232	-50.19	-49.27	676.0	244.19	0.000	-0.00376
4.090	0.003	0.765	0.232	-50.20	-49.42	425.7	220.76	0.000	-0.00355
4.100	0.003	0.765	0.232	-50.23	-49.94	221.1	85.79	0.000	-0.00336
3.010	0.003	0.766	0.231	49.96	49.99	2001.4	93.54	0.000	-0.00032
3.020	0.003	0.766	0.231	49.97	50.13	2002.6	174.94	0.000	-0.00089
3.030	0.003	0.766	0.231	49.70	49.79	1825.3	201.27	0.000	-0.00043
3.040	0.003	0.766	0.231	49.96	49.99	1621.2	201.60	0.000	-0.00015

TABLE B-7

Basic Isobaric Data for Nominal 0.50 C_2H_6, 0.50 C_3H_8 Mixture

RUN NO.	COMPOSITION (MOLE FRACTION) CH4	C2H6	C3H8	INLET TEMP. (°F)	OUTLET TEMP. (°F)	INLET PRES. (PSIA)	PRES. DROP (PSID)	HEAT INPUT (BTU/LB)	MEAN HEAT CAPACITY (BTU/LB°F)
16.010	0.004	0.495	0.501	-246.28	-236.61	2000.1	0.49	4.670	0.48276
16.020	0.004	0.495	0.501	-246.41	-214.98	1999.3	0.49	15.723	0.50031
16.030	0.004	0.495	0.501	-246.19	-187.72	2015.3	0.49	29.439	0.50343
16.040	0.004	0.495	0.501	-246.30	-153.99	2004.7	0.49	47.178	0.51108
16.050	0.004	0.495	0.501	-246.30	-126.90	2003.9	0.49	61.428	0.51448
16.051	0.004	0.495	0.501	-246.30	-125.63	2003.9	0.49	61.486	0.50955
16.052	0.004	0.495	0.501	-246.30	-125.89	1996.3	0.49	62.011	0.51504
15.010	0.004	0.491	0.505	-125.95	-117.48	2000.7	0.17	4.471	0.52802
15.020	0.004	0.491	0.505	-125.93	-48.19	1999.8	0.17	41.761	0.53717
15.030	0.004	0.505	0.491	-125.92	27.52	2003.2	0.15	85.451	0.55690
12.010	0.004	0.495	0.501	37.15	46.25	2002.2	0.12	5.664	0.62223
12.020	0.004	0.495	0.501	37.18	60.53	2000.0	0.12	14.686	0.62908
12.030	0.004	0.495	0.501	37.13	91.31	2000.4	0.12	35.849	0.66161
12.040	0.004	0.495	0.501	37.09	122.40	2001.2	0.12	55.506	0.65068
12.050	0.004	0.495	0.501	37.09	149.01	2002.0	0.12	74.377	0.66459
1.010	0.004	0.481	0.515	150.80	158.22	2000.6	0.06	5.498	0.74132
1.011	0.004	0.481	0.515	150.81	158.31	2001.2	0.06	5.506	0.73453
1.020	0.004	0.485	0.511	150.50	175.26	2000.1	0.06	18.726	0.75801
1.030	0.004	0.491	0.505	150.50	201.76	1999.7	0.06	39.990	0.78016
1.040	0.004	0.489	0.507	150.57	225.81	1999.7	0.06	59.195	0.78672
1.110	0.004	0.494	0.502	149.91	157.51	2001.2	0.08	5.599	0.73707
1.120	0.004	0.494	0.502	150.06	174.71	2003.3	0.08	18.470	0.74942
1.121	0.004	0.494	0.502	150.01	175.30	2000.4	0.07	18.969	0.75010
1.130	0.004	0.494	0.502	150.23	202.63	2001.0	0.12	40.469	0.77231
1.140	0.004	0.494	0.502	149.95	224.85	2000.5	0.08	59.269	0.79129
1.150	0.004	0.494	0.502	149.97	249.96	2000.9	0.05	80.778	0.80786
17.010	0.004	0.497	0.500	250.27	258.13	2003.4	0.12	7.030	0.89472
17.011	0.004	0.497	0.500	250.27	258.00	2003.4	0.12	6.899	0.89279
17.020	0.004	0.497	0.500	250.13	272.20	2001.4	0.12	19.804	0.89728
17.030	0.004	0.497	0.500	250.27	293.73	2000.1	0.12	39.239	0.90293
11.010	0.004	0.502	0.494	37.11	45.86	1000.0	0.11	5.648	0.64542
11.020	0.004	0.502	0.494	37.10	59.62	999.7	0.11	14.717	0.65342
11.030	0.004	0.496	0.500	37.12	90.40	1001.1	0.11	35.999	0.67571
11.040	0.004	0.496	0.500	37.12	119.02	1000.0	0.11	57.752	0.70512
11.050	0.004	0.496	0.500	37.17	131.38	1002.4	0.11	67.804	0.71971
11.060	0.004	0.496	0.500	37.21	149.01	1002.1	0.12	83.704	0.74866
2.010	0.004	0.498	0.498	150.13	157.45	1001.1	0.07	7.431	1.01489
2.011	0.004	0.498	0.498	150.13	157.48	1001.3	0.07	7.426	1.01063
2.020	0.004	0.495	0.501	150.26	174.94	999.6	0.07	28.327	1.14796
2.030	0.004	0.495	0.501	150.30	198.60	1000.1	0.13	65.686	1.35983
2.040	0.004	0.496	0.500	150.20	223.01	1001.0	0.07	97.860	1.34388
2.050	0.004	0.496	0.500	150.28	251.32	999.6	0.07	123.413	1.22142
6.010	0.004	0.492	0.504	101.78	111.73	762.6	0.05	8.014	0.80473
6.020	0.004	0.492	0.504	101.66	130.72	762.2	0.02	24.890	0.85665
6.030	0.004	0.492	0.504	101.64	158.72	761.3	0.19	65.068	1.13993
6.040	0.004	0.495	0.501	101.72	179.24	759.1	0.07	119.098	1.53629
6.050	0.004	0.495	0.501	101.72	192.11	758.8	0.06	144.928	1.60335
10.010	0.004	0.495	0.501	37.03	44.69	500.9	0.15	5.153	0.67186
10.015	0.004	0.495	0.501	37.03	44.69	500.9	0.15	5.166	0.67359
10.016	0.004	0.495	0.501	37.03	44.69	500.9	0.15	5.139	0.67015
10.020	0.004	0.495	0.501	37.05	52.37	499.5	0.15	10.372	0.67681
10.025	0.004	0.495	0.501	37.05	52.37	499.5	0.15	10.398	0.67852
10.026	0.004	0.495	0.501	37.05	52.37	499.5	0.15	10.346	0.67511
10.030	0.004	0.495	0.501	37.10	81.89	499.4	0.15	31.509	0.70345
10.040	0.004	0.498	0.498	37.10	103.51	499.9	0.15	49.131	0.73983
10.050	0.004	0.498	0.498	37.08	115.13	501.8	0.22	68.688	0.88000
3.010	0.004	0.486	0.510	150.31	157.50	498.8	1.03	5.196	0.72330
3.020	0.004	0.486	0.510	150.35	175.13	498.9	0.58	17.582	0.70948
3.030	0.004	0.490	0.506	150.35	199.91	501.9	0.69	33.875	0.68347
3.040	0.004	0.490	0.506	150.38	226.33	498.5	0.75	50.340	0.66276
3.050	0.004	0.490	0.506	150.45	248.60	500.3	0.81	62.040	0.63209
7.010	0.004	0.488	0.508	101.71	104.95	501.4	0.05	2.855	0.88085
7.020	0.004	0.488	0.508	101.72	108.97	501.3	0.10	6.448	0.88969
7.030	0.004	0.488	0.508	101.67	112.28	501.3	0.13	10.262	0.96752
7.040	0.004	0.488	0.508	101.78	115.80	501.4	0.27	23.780	1.69626
7.050	0.004	0.498	0.498	101.56	114.28	501.4	0.14	17.698	1.39081
7.060	0.004	0.498	0.498	101.63	118.84	501.6	0.17	37.270	2.16497
7.070	0.004	0.498	0.498	101.66	123.14	500.8	0.22	59.176	2.75561
7.080	0.004	0.498	0.498	101.60	127.57	501.1	0.27	81.095	3.12308
7.090	0.004	0.494	0.502	101.61	130.84	501.1	0.27	98.628	3.37378
7.100	0.004	0.494	0.502	101.62	137.02	501.1	0.27	118.143	3.33674
7.110	0.004	0.494	0.502	101.60	141.25	501.1	0.28	121.573	3.06636
7.120	0.004	0.494	0.502	101.70	146.27	501.1	0.28	125.552	2.81667
7.130	0.004	0.494	0.502	101.72	157.26	501.1	0.28	133.671	2.40660

TABLE B-7
(CONTINUED)

RUN NO.	COMPOSITION CH4	C2H6	C3H8 (MOLE FRACTION)	INLET TEMP. (°F)	OUTLET TEMP. (°F)	INLET PRES. (PSIA)	PRES. DROP (PSID)	HEAT INPUT (BTU/LB)	MEAN HEAT CAPACITY (BTU/LB°F)
9.010	0.004	0.486	0.510	37.21	39.80	250.0	0.10	1.747	0.67551
9.020	0.004	0.486	0.510	37.22	42.56	250.2	0.10	3.610	0.67669
9.030	0.004	0.486	0.510	37.11	44.50	250.0	0.10	5.038	0.68205
9.040	0.004	0.489	0.507	37.20	47.60	250.3	0.12	7.136	0.68623
9.050	0.004	0.489	0.507	37.21	50.13	250.1	0.22	11.847	0.91661
9.060	0.004	0.494	0.502	37.10	51.46	249.9	0.32	16.239	1.13041
9.070	0.004	0.494	0.502	37.19	53.50	250.1	0.37	23.164	1.42036
9.080	0.004	0.495	0.501	37.08	57.93	250.2	0.39	43.291	2.07636
9.090	0.004	0.495	0.501	37.14	62.93	250.0	0.47	66.568	2.58077
9.100	0.004	0.495	0.501	37.20	68.45	250.3	0.54	92.685	2.96568
9.110	0.004	0.495	0.501	37.20	73.78	250.1	0.59	121.075	3.30945
9.120	0.004	0.487	0.509	37.11	97.90	250.3	0.59	171.256	2.81696
9.121	0.004	0.487	0.509	37.11	98.23	250.3	0.34	171.294	2.80263
9.130	0.004	0.487	0.509	37.06	94.95	250.1	0.37	169.760	2.93247
9.140	0.004	0.487	0.509	37.06	87.52	250.3	0.37	165.401	3.27778
9.150	0.004	0.487	0.509	37.06	85.03	250.2	0.38	164.096	3.42076
9.160	0.004	0.487	0.509	37.07	82.57	250.4	0.34	162.658	3.57461
9.170	0.004	0.487	0.509	37.07	79.53	249.6	0.37	156.269	3.68047
4.010	0.004	0.495	0.501	150.15	157.48	248.9	1.47	3.888	0.53065
4.020	0.004	0.495	0.501	150.13	174.56	250.7	1.47	12.747	0.52189
4.030	0.004	0.495	0.501	150.21	199.51	248.6	1.47	25.713	0.52154
4.040	0.004	0.495	0.501	150.24	225.65	252.1	1.57	39.653	0.52585
4.050	0.004	0.495	0.501	150.33	253.52	249.3	1.72	54.628	0.52940
5.010	0.004	0.466	0.530	101.72	112.46	250.5	1.42	5.844	0.54440
5.020	0.004	0.466	0.530	101.68	122.14	252.1	1.33	11.026	0.53875
5.030	0.004	0.466	0.530	101.70	130.40	251.2	1.40	15.260	0.53182
5.040	0.004	0.469	0.527	101.72	158.72	251.1	1.50	30.037	0.52694
5.050	0.004	0.469	0.527	101.65	178.69	250.1	1.55	40.434	0.52488

TABLE B-8

Basic Isothermal Data for Nominal 0.50 C_2H_6, 0.50 C_3H_8 Mixture

RUN NO.	COMPOSITION CH4	C2H6	C3H8 (MOLE FRACTION)	INLET TEMP. (°F)	OUTLET TEMP. (°F)	INLET PRES. (PSIA)	PRES. DROP (PSID)	HEAT INPUT (BTU/LB)	ISOTHERMAL J.T.COEFF. (BTU/LB PSIA)
19.010	0.004	0.506	0.490	151.03	151.00	2000.4	94.61	0.300	-0.00317
19.020	0.004	0.506	0.490	150.96	150.96	1795.3	101.11	0.452	-0.00447
19.035	0.004	0.506	0.490	150.98	150.98	1605.0	101.31	0.768	-0.00759
19.036	0.004	0.506	0.490	150.98	150.98	1605.0	101.31	0.621	-0.00613
19.040	0.004	0.506	0.490	150.99	150.96	1401.5	108.42	0.929	-0.00857
19.050	0.004	0.506	0.490	151.01	151.00	1204.3	111.04	1.459	-0.01314
19.060	0.004	0.506	0.490	151.00	150.99	968.9	115.13	3.076	-0.02672
19.080	0.004	0.506	0.490	151.00	151.05	650.6	226.79	55.628	-0.24528
19.090	0.004	0.506	0.490	150.94	150.98	819.7	137.82	20.228	-0.14676
19.100	0.004	0.506	0.490	150.94	150.96	395.9	287.14	21.730	-0.07568
19.110	0.004	0.506	0.490	150.98	151.04	397.3	287.73	21.481	-0.07466
18.010	0.004	0.492	0.504	250.92	250.92	2015.3	124.29	2.604	-0.02095
18.020	0.004	0.492	0.504	251.30	251.31	1817.6	109.83	3.233	-0.02944
18.030	0.004	0.492	0.504	251.07	251.07	1603.3	103.33	4.514	-0.04368
18.040	0.004	0.491	0.505	251.17	251.18	1521.3	104.55	5.466	-0.05228
18.050	0.004	0.491	0.505	250.93	250.97	1221.5	208.67	15.997	-0.07666
18.060	0.004	0.491	0.505	251.11	251.14	1021.6	220.60	15.950	-0.07230
18.070	0.004	0.493	0.503	251.11	251.11	822.5	251.32	15.462	-0.06152
18.080	0.004	0.493	0.503	251.10	251.07	620.8	225.20	12.174	-0.05406
18.090	0.004	0.497	0.499	251.13	251.11	617.8	425.34	21.528	-0.05061
18.100	0.004	0.497	0.499	251.19	251.19	358.7	255.14	11.610	-0.04551

TABLE B-9

Basic Isenthalpic Data for Nominal 0.50 C_2H_6, 0.50 C_3H_8 Mixture

RUN NO.	COMPOSITION CH4	C2H6	C3H8 (MOLE FRACTION)	INLET TEMP. (°F)	OUTLET TEMP. (°F)	INLET PRES. (PSIA)	PRES. DROP (PSID)	HEAT INPUT (BTU/LB)	J.THOMSON COEFF. (°F/PSIA)
14.010	0.004	0.495	0.501	-125.53	-124.69	2009.1	165.59	0.000	-0.00507
14.020	0.004	0.495	0.501	-125.48	-124.69	1619.4	167.36	0.000	-0.00472
14.030	0.004	0.495	0.501	-125.48	-124.70	1237.4	167.92	0.000	-0.00465
14.040	0.004	0.497	0.499	-125.49	-124.74	816.8	167.18	0.000	-0.00451
14.050	0.004	0.497	0.499	-125.51	-124.69	415.8	183.42	0.000	-0.00447
14.060	0.004	0.497	0.499	-125.51	-125.01	319.5	125.68	0.000	-0.00398
13.010	0.004	0.495	0.501	37.48	37.73	2014.0	93.11	0.000	-0.00266
13.015	0.004	0.495	0.501	37.48	37.74	2014.0	93.11	0.000	-0.00276
13.020	0.004	0.495	0.501	37.44	37.87	2011.5	158.03	0.000	-0.00272
13.030	0.004	0.495	0.501	37.51	37.92	1814.6	170.64	0.000	-0.00244
13.040	0.004	0.495	0.501	37.48	37.85	1614.9	168.08	0.000	-0.00224
13.050	0.004	0.495	0.501	37.52	37.84	1415.4	166.62	0.000	-0.00194
13.060	0.004	0.495	0.501	37.49	37.79	1217.4	180.74	0.000	-0.00165
13.070	0.004	0.495	0.501	37.52	37.72	915.3	181.55	0.000	-0.00110
13.080	0.004	0.495	0.501	37.39	37.47	618.6	186.05	0.000	-0.00043
13.090	0.004	0.495	0.501	37.52	37.51	402.3	156.67	0.000	-0.00007

TABLE B-10

Basic Isobaric Data for Nominal 0.27 C_2H_6, 0.73 C_3H_8 Mixture

RUN NO.	COMPOSITION (MOLE FRACTION) CH4	C2H6	C3H8	INLET TEMP. (°F)	OUTLET TEMP. (°F)	INLET PRES. (PSIA)	PRES. DROP (PSID)	HEAT INPUT (BTU/LB)	MEAN HEAT CAPACITY (BTU/LB°F)
8.010	0.001	0.274	0.725	200.82	211.37	2002.1	0.15	8.280	0.78484
8.020	0.001	0.274	0.725	200.92	225.48	1999.7	0.15	19.254	0.78392
8.021	0.001	0.274	0.725	200.92	225.51	1999.6	0.15	19.237	0.78235
8.030	0.001	0.274	0.725	200.81	251.54	2000.2	0.15	40.592	0.80020
8.031	0.001	0.274	0.725	200.81	251.49	1999.2	0.15	40.561	0.80047
8.040	0.001	0.274	0.725	200.81	274.88	2000.0	0.15	60.442	0.81602
8.050	0.001	0.274	0.725	200.81	294.97	1999.6	0.15	77.912	0.82748
8.051	0.001	0.274	0.725	200.82	294.77	1999.6	0.15	77.730	0.82736
1.010	0.001	0.282	0.717	-238.26	-228.18	1001.1	0.72	4.881	0.48416
1.020	0.001	0.282	0.717	-238.22	-214.40	1000.0	0.72	11.621	0.48793
1.030	0.001	0.281	0.718	-238.24	-186.34	1002.7	0.70	25.665	0.49450
1.040	0.001	0.281	0.718	-238.43	-159.84	999.9	0.72	38.774	0.49335
1.050	0.001	0.282	0.717	-237.96	-139.70	1001.2	0.70	48.743	0.49604
1.060	0.001	0.282	0.717	-238.03	-113.78	1002.5	0.70	62.507	0.50310
1.065	0.001	0.282	0.717	-238.03	-113.78	1002.5	0.70	61.821	0.49758
1.066	0.001	0.282	0.717	-238.03	-113.78	1002.5	0.70	63.225	0.50888
2.010	0.001	0.283	0.716	-153.70	-144.59	1000.5	0.55	4.605	0.50569
2.020	0.001	0.283	0.716	-153.70	-131.14	999.0	0.55	11.450	0.50754
2.030	0.001	0.283	0.716	-153.67	-101.90	1000.0	0.55	26.546	0.51279
2.040	0.001	0.283	0.716	-153.66	-78.54	1000.2	0.55	38.827	0.51689
2.050	0.001	0.282	0.717	-153.64	-55.91	1003.0	0.50	50.887	0.52069
2.060	0.001	0.282	0.717	-153.64	-36.88	1000.4	0.50	61.395	0.52582
2.070	0.001	0.290	0.709	-153.64	-11.56	1001.0	0.30	75.969	0.53469
2.071	0.001	0.290	0.709	-153.64	-11.47	1001.0	0.30	75.969	0.53433
2.072	0.001	0.290	0.709	-153.64	-11.37	1001.2	0.30	76.073	0.53472
3.010	0.001	0.279	0.720	0.82	10.59	1000.1	0.25	5.722	0.58573
3.020	0.001	0.279	0.720	0.85	30.81	1001.9	0.25	17.762	0.59287
3.030	0.001	0.282	0.717	0.88	64.88	1000.3	0.25	39.013	0.60953
3.040	0.001	0.282	0.717	0.89	102.01	1002.9	0.25	63.547	0.62842
3.040	0.001	0.277	0.722	0.82	129.42	999.7	0.25	83.191	0.64691
9.010	0.001	0.274	0.725	200.78	207.65	1000.3	0.35	9.214	1.34252
9.020	0.001	0.274	0.725	200.75	221.56	1000.3	0.35	30.228	1.45273
9.030	0.001	0.274	0.725	200.77	235.23	1000.3	0.35	49.773	1.44404
9.031	0.001	0.274	0.725	200.77	235.27	1000.5	0.35	49.814	1.44369
9.040	0.001	0.274	0.725	200.77	250.73	1001.1	0.35	67.872	1.35845
9.050	0.001	0.275	0.724	200.68	274.10	1001.3	0.35	90.492	1.23252
9.060	0.001	0.275	0.724	200.77	291.48	999.5	0.35	104.567	1.15274
9.061	0.001	0.275	0.724	200.77	291.67	1000.3	0.35	104.756	1.15241
7.010	0.001	0.271	0.728	124.64	134.84	1000.3	0.20	7.633	0.74891
7.011	0.001	0.271	0.728	124.64	134.87	1000.9	0.20	7.658	0.74863
7.020	0.001	0.271	0.728	124.67	159.28	1001.0	0.20	27.178	0.78525
7.030	0.001	0.274	0.725	124.75	175.05	1001.5	0.20	41.178	0.81864
7.040	0.001	0.274	0.725	124.71	194.63	998.7	0.20	61.583	0.88069
7.050	0.001	0.274	0.725	124.71	205.48	999.9	0.20	75.231	0.93141
6.010	0.001	0.277	0.722	125.21	134.87	498.9	0.45	8.560	0.88602
6.020	0.001	0.277	0.722	125.30	140.12	501.5	0.45	13.727	0.92599
6.030	0.001	0.277	0.722	125.09	141.75	501.1	0.70	19.816	1.18954
6.040	0.001	0.277	0.722	125.05	144.06	501.1	0.80	31.104	1.63581
6.050	0.001	0.277	0.722	125.09	130.76	501.3	0.40	4.881	0.86195
6.060	0.001	0.277	0.722	124.97	148.64	501.1	0.80	56.931	2.40513
6.065	0.001	0.277	0.722	124.97	148.64	501.1	0.80	56.409	2.38308
6.066	0.001	0.277	0.722	124.97	148.64	501.1	0.80	57.535	2.43066
6.067	0.001	0.277	0.722	124.97	148.64	501.1	0.80	56.352	2.38068
6.070	0.001	0.277	0.722	124.97	153.59	501.2	0.90	91.403	3.19370
6.080	0.001	0.277	0.722	124.88	155.33	501.0	0.90	106.542	3.49849
6.090	0.001	0.279	0.720	124.95	159.21	501.0	1.00	111.174	3.24552
6.100	0.001	0.279	0.720	124.95	165.80	501.1	1.00	117.432	2.87504
6.110	0.001	0.279	0.720	124.81	175.01	501.0	1.00	124.821	2.48658
6.120	0.001	0.274	0.725	124.73	199.12	501.0	1.00	141.680	1.90460
6.130	0.001	0.279	0.720	124.81	206.01	501.1	1.00	146.337	1.80236

TABLE B-11a

Basic Isothermal Data for Nominal 0.27 C_2H_6, 0.73 C_3H_8 Mixture
Using Absolute Pressure Transducers

RUN NO.	COMPOSITION CH4	C2H6	C3H8 (MOLE FRACTION)	INLET TEMP. (°F)	OUTLET TEMP. (°F)	INLET PRES. (PSIA)	PRES. DROP (PSID)	HEAT INPUT (BTU/LB)	ISOTHERMAL J.T.COEFF. (BTU/LB PSIA)
5.030	0.001	0.277	0.722	127.40	127.37	1616.1	93.04	0.062	-0.00066
5.040	0.001	0.277	0.722	127.51	127.50	1412.4	94.90	0.138	-0.00145
5.050	0.001	0.277	0.722	127.40	127.39	1221.7	91.99	0.212	-0.00230
5.055	0.001	0.277	0.722	127.40	127.39	1221.7	91.99	0.212	-0.00230
5.060	0.001	0.272	0.727	127.45	127.45	1015.7	94.89	0.335	-0.00353
5.070	0.001	0.272	0.727	127.55	127.57	825.2	101.02	0.529	-0.00523
5.080	0.001	0.272	0.727	127.20	127.19	606.9	105.86	0.872	-0.00824
5.090	0.001	0.275	0.724	127.41	127.39	519.9	79.13	0.783	-0.00990
10.010	0.001	0.275	0.724	202.99	203.00	1996.7	85.97	0.485	-0.00564
10.020	0.001	0.275	0.724	203.11	203.10	1810.9	91.36	0.669	-0.00732
10.030	0.001	0.275	0.724	203.06	203.04	1613.6	105.85	1.103	-0.01042
10.040	0.001	0.274	0.725	203.31	203.28	1404.8	115.22	1.870	-0.01623
10.050	0.001	0.274	0.725	203.23	203.22	1218.4	119.99	3.388	-0.02824
10.060	0.001	0.274	0.725	203.07	203.09	1006.8	138.87	13.821	-0.09952
10.070	0.001	0.273	0.726	203.17	203.19	884.0	208.09	47.806	-0.22973
10.075	0.001	0.273	0.726	203.17	203.19	884.0	208.09	47.730	-0.22937
10.076	0.001	0.273	0.726	203.17	203.19	884.0	208.09	47.899	-0.23018
10.080	0.001	0.273	0.726	202.99	203.03	686.0	133.93	17.445	-0.13025
10.090	0.001	0.278	0.721	203.08	203.10	565.0	179.61	16.012	-0.08915
10.100	0.001	0.278	0.721	202.96	202.99	387.5	277.36	17.754	-0.06401
11.010	0.001	0.274	0.725	268.99	268.98	2002.1	122.03	2.065	-0.01692
11.011	0.001	0.274	0.725	268.99	269.01	2010.1	120.40	2.086	-0.01733
11.016	0.001	0.274	0.725	268.99	269.01	2012.1	120.40	2.083	-0.01730
11.020	0.001	0.274	0.725	268.93	268.93	1799.0	125.38	3.134	-0.02499
11.030	0.001	0.274	0.725	268.82	268.80	1600.9	140.56	5.445	-0.03873
11.040	0.001	0.274	0.725	268.84	268.83	1398.0	161.53	10.235	-0.06336
11.050	0.001	0.274	0.725	269.31	269.36	1210.7	202.61	17.071	-0.08425
11.060	0.001	0.275	0.724	268.89	268.92	1003.8	321.70	24.820	-0.07715
11.070	0.001	0.275	0.724	268.86	268.87	800.9	476.33	28.953	-0.06078
11.080	0.001	0.275	0.724	268.86	268.84	599.2	302.06	16.637	-0.05508
11.090	0.001	0.275	0.724	268.71	268.73	465.3	345.41	17.270	-0.05000

* ΔH VALUES ARE SUSPECTED TO BE FROM 3 TO 10 PERCENT TOO HIGH DUE TO MASS LEAK

TABLE B-11b

Basic Isothermal Data for Nominal 0.27 C_2H_6, 0.73 C_3H_8 Mixture
Using Differential Pressure Transducer

RUN NO.	COMPOSITION CH4	C2H6	C3H8 (MOLE FRACTION)	INLET TEMP. (°F)	OUTLET TEMP. (°F)	INLET PRES. (PSIA)	PRES. DROP (PSID)	HEAT INPUT (BTU/LB)	ISOTHERMAL J.T.COEFF. (BTU/LB PSIA)
5.030	0.001	0.277	0.722	127.40	127.37	1616.1	92.70	0.062	-0.00067
5.040	0.001	0.277	0.722	127.51	127.50	1412.4	94.54	0.138	-0.00146
5.050	0.001	0.277	0.722	127.40	127.39	1221.7	95.00	0.212	-0.00223
5.055	0.001	0.277	0.722	127.40	127.39	1221.7	93.44	0.212	-0.00227
5.060	0.001	0.272	0.727	127.45	127.45	1015.7	95.35	0.335	-0.00351
5.070	0.001	0.272	0.727	127.55	127.57	825.2	101.17	0.529	-0.00523
5.080	0.001	0.272	0.727	127.20	127.19	606.9	106.70	0.872	-0.00817
5.090	0.001	0.275	0.724	127.41	127.39	519.9	79.79	0.783	-0.00982
10.010	0.001	0.275	0.724	202.99	203.00	1996.7	85.49	0.485	-0.00567
10.020	0.001	0.275	0.724	203.11	203.10	1810.9	90.56	0.669	-0.00739
10.030	0.001	0.275	0.724	203.06	203.04	1613.6	106.18	1.103	-0.01039
10.040	0.001	0.274	0.725	203.31	203.28	1404.8	115.38	1.870	-0.01621
10.050	0.001	0.274	0.725	203.23	203.22	1218.4	120.39	3.388	-0.02814
10.060	0.001	0.274	0.725	203.07	203.09	1006.8	139.62	13.821	-0.09898
10.070	0.001	0.273	0.726	203.17	203.19	884.0	208.78	47.806	-0.22898
10.075	0.001	0.273	0.726	203.17	203.19	884.0	208.78	47.730	-0.22862
10.076	0.001	0.273	0.726	203.17	203.19	884.0	208.78	47.899	-0.22943
10.080	0.001	0.273	0.726	202.99	203.03	686.0	134.51	17.445	-0.12969
10.090	0.001	0.278	0.721	203.08	203.10	565.0	181.00	16.012	-0.08846
10.100	0.001	0.278	0.721	202.96	202.99	387.5	279.69	17.754	-0.06348
11.010	0.001	0.274	0.725	268.99	268.98	2002.1	121.37	2.065	-0.01701
11.011	0.001	0.274	0.725	268.99	269.01	2010.1	118.97	2.086	-0.01754
11.016	0.001	0.274	0.725	268.99	269.01	2012.1	118.97	2.083	-0.01751
11.020	0.001	0.274	0.725	268.93	268.93	1799.0	125.88	3.134	-0.02490
11.030	0.001	0.274	0.725	268.82	268.80	1600.9	140.58	5.445	-0.03873
11.040	0.001	0.274	0.725	268.84	268.83	1398.0	162.20	10.235	-0.06310
11.050	0.001	0.274	0.725	269.31	269.36	1210.7	203.49	17.071	-0.08389
11.060	0.001	0.275	0.724	268.89	268.92	1003.8	322.89	24.820	-0.07687
11.070	0.001	0.275	0.724	268.86	268.87	800.9	477.48	28.953	-0.06064
11.080	0.001	0.275	0.724	268.86	268.84	599.2	303.62	16.637	-0.05479
11.090	0.001	0.275	0.724	268.71	268.73	465.3	348.42	17.270	-0.04957

* ΔH VALUES ARE SUSPECTED TO BE FROM 3 TO 10 PERCENT TOO HIGH DUE TO MASS LEAK

TABLE B-12

Basic Isenthalpic Data for Nominal 0.27 C_2H_6, 0.73 C_3H_8 Mixture Using Absolute Pressure Transducers

RUN NO.	COMPOSITION (MOLE FRACTION) CH4	C2H6	C3H8	INLET TEMP. (°F)	OUTLET TEMP. (°F)	INLET PRES. (PSIA)	PRES. DROP (PSID)	HEAT INPUT (BTU/LB)	J.THOMSON COEFF. (°F/PSIA)
12.010	0.001	0.272	0.727	-150.23	-149.66	1992.3	100.96	0.000	-0.00568
12.020	0.001	0.272	0.727	-150.23	-149.80	1194.3	118.94	0.000	-0.00367
12.030	0.001	0.272	0.727	-150.22	-149.75	805.7	115.45	0.000	-0.00410
12.040	0.001	0.272	0.727	-150.20	-149.86	317.9	125.71	0.000	-0.00269
4.010	0.001	0.275	0.724	1.61	2.03	2003.6	104.90	0.000	-0.00396
4.015	0.001	0.275	0.724	1.61	2.03	2003.5	104.90	0.000	-0.00396
4.030	0.001	0.275	0.724	1.68	2.09	1604.9	109.05	0.000	-0.00379
4.040	0.001	0.273	0.726	1.68	2.06	1431.0	103.52	0.000	-0.00367
4.050	0.001	0.273	0.726	1.68	2.07	1203.7	109.44	0.000	-0.00359
4.060	0.001	0.276	0.723	1.68	2.07	1006.6	117.67	0.000	-0.00336
4.070	0.001	0.276	0.723	1.61	1.98	711.2	116.39	0.000	-0.00318
4.080	0.001	0.276	0.723	1.58	1.90	416.1	111.19	0.000	-0.00291
4.090	0.001	0.276	0.723	1.58	1.83	248.8	93.19	0.000	-0.00273
4.100	0.001	0.276	0.723	1.58	1.85	1041.6	81.95	0.000	-0.00334
5.010	0.001	0.277	0.722	127.25	127.27	2018.7	102.91	0.000	-0.00012
5.020	0.001	0.277	0.722	127.35	127.30	1821.8	98.09	0.000	0.00045

TABLE B-13

Basic Isobaric Data for Nominal 0.78 CH_4, 0.22 C_2H_6 Mixture

RUN NO.	COMPOSITION (MOLE FRACTION) CH4	C2H6	C3H8	INLET TEMP. (°F)	OUTLET TEMP. (°F)	INLET PRES. (PSIA)	PRES. DROP (PSID)	HEAT INPUT (BTU/LB)	MEAN HEAT CAPACITY (BTU/LB°F)
8.010	0.778	0.221	0.001	-59.23	-38.57	2000.1	0.07	19.686	0.95240
8.020	0.778	0.221	0.001	-59.20	-19.20	1999.8	0.07	39.543	0.98570
8.030	0.778	0.221	0.001	-59.13	1.02	2001.0	0.07	61.709	1.02548
8.040	0.778	0.221	0.001	-59.21	26.01	2002.2	0.07	86.872	1.04284
8.050	0.778	0.221	0.001	-59.27	47.80	1999.8	0.07	101.557	1.04624
8.060	0.778	0.221	0.001	-59.28	42.93	2001.8	0.07	106.836	1.04530
8.070	0.778	0.221	0.001	-59.25	52.04	2000.6	0.07	114.794	1.03149
8.080	0.778	0.221	0.001	-59.23	75.73	2000.8	0.07	138.655	1.02745
2.010	0.777	0.222	0.001	78.06	88.37	2001.8	0.05	9.140	0.88683
2.020	0.777	0.222	0.001	78.12	108.64	2002.5	0.05	29.190	0.85831
2.030	0.777	0.222	0.001	78.02	137.38	2001.1	0.06	49.082	0.82684
2.040	0.775	0.224	0.001	78.02	168.68	2002.2	0.09	72.452	0.79915
2.050	0.775	0.224	0.001	78.02	202.04	1999.6	0.09	96.992	0.77885
4.010	0.778	0.221	0.001	202.09	212.68	1999.7	0.11	7.559	0.71395
4.020	0.778	0.221	0.001	202.14	226.74	2003.4	0.11	17.320	0.70433
4.030	0.777	0.222	0.001	202.16	252.35	2003.3	0.12	35.479	0.70691
4.040	0.777	0.222	0.001	202.31	277.43	2002.6	0.14	52.846	0.70349
4.050	0.777	0.222	0.001	202.24	301.15	2001.2	0.14	69.459	0.70020
9.010	0.776	0.223	0.001	-59.44	-40.36	1502.2	0.05	21.460	1.12491
9.020	0.776	0.223	0.001	-59.47	-19.66	1501.0	0.05	40.349	1.21457
9.030	0.776	0.223	0.001	-59.46	-29.25	1503.4	0.05	35.028	1.15965
9.040	0.776	0.223	0.001	-59.46	-24.67	1502.4	0.05	41.763	1.20055
9.050	0.777	0.222	0.001	-59.44	1.41	1500.7	0.05	77.449	1.27277
9.060	0.777	0.222	0.001	-59.37	25.36	1499.3	0.05	106.816	1.26073
9.070	0.777	0.222	0.001	-59.28	52.35	1497.5	0.05	132.760	1.18924
9.080	0.777	0.222	0.001	-59.37	77.28	1499.4	0.05	155.126	1.13517
18.010	0.770	0.229	0.001	-152.14	-127.12	1001.1	0.06	20.524	0.82026
18.015	0.770	0.229	0.001	-152.14	-127.12	1001.1	0.06	20.581	0.82252
18.020	0.770	0.229	0.001	-152.14	-102.44	999.7	0.06	42.56	0.8552
18.030	0.771	0.228	0.001	-152.13	-82.18	999.1	0.06	63.65	0.90446
18.040	0.771	0.228	0.001	-152.10	-60.85	1002.1	0.06	90.203	0.98850
10.010	0.778	0.221	0.001	-59.47	-54.92	998.7	0.06	8.127	1.78580
10.015	0.778	0.221	0.001	-59.47	-54.92	998.7	0.06	8.101	1.78009
10.016	0.778	0.221	0.001	-59.47	-54.92	998.7	0.06	8.152	1.79128
10.020	0.778	0.221	0.001	-59.45	-49.65	1001.4	0.06	19.048	1.94450
10.030	0.778	0.221	0.001	-59.47	-40.21	1000.1	0.06	41.634	2.16154
10.040	0.778	0.221	0.001	-59.47	-29.23	1001.8	0.06	64.717	2.14012
10.050	0.777	0.222	0.001	-59.43	-19.64	1003.1	0.06	80.461	2.02102
10.060	0.777	0.222	0.001	-59.42	0.24	999.1	0.06	104.676	1.75460
10.070	0.777	0.222	0.001	-59.46	26.53	1000.0	0.06	128.417	1.63082
10.080	0.778	0.221	0.001	-59.42	51.65	1000.5	0.06	147.511	1.52833
10.090	0.778	0.221	0.001	-59.49	75.58	1000.9	0.06	166.565	1.43824

TABLE B-13

(CONTINUED)

ISOBARIC DATA FOR NOMINAL 0.777 CH4, 0.223 C2H6 MIXTURE

RUN NO.	COMPOSITION (MOLE FRACTION) CH4	C2H6	C3H8	INLET TEMP. (°F)	OUTLET TEMP. (°F)	INLET PRES. (PSIA)	PRES. DROP (PSID)	HEAT INPUT (BTU/LB)	MEAN HEAT CAPACITY (BTU/LB°F)
14.010	0.777	0.222	0.001	-240.69	-221.28	999.1	0.05	14.179	0.73050
14.020	0.777	0.222	0.001	-240.76	-189.32	1000.4	0.05	37.998	0.73865
14.030	0.777	0.222	0.001	-240.73	-169.16	1002.2	0.05	53.421	0.74632
14.040	0.777	0.222	0.001	-240.76	-148.43	1002.8	0.05	69.734	0.75530
3.010	0.779	0.220	0.001	78.23	87.84	1001.9	0.14	6.460	0.67258
3.020	0.779	0.220	0.001	78.00	108.37	999.3	0.16	20.144	0.66325
3.030	0.779	0.220	0.001	78.00	138.47	999.8	0.19	39.768	0.65765
3.035	0.779	0.220	0.001	78.00	138.47	999.8	0.19	39.701	0.65654
3.040	0.778	0.221	0.001	78.01	167.57	1001.7	0.19	57.916	0.64667
3.050	0.778	0.221	0.001	77.92	202.95	1000.0	0.19	80.211	0.64152
5.010	0.778	0.221	0.001	202.28	212.81	998.4	0.18	5.862	0.55682
5.015	0.778	0.221	0.001	202.28	212.81	998.4	0.18	5.957	0.56581
5.020	0.778	0.221	0.001	202.21	227.11	1002.6	0.18	15.756	0.63258
5.030	0.778	0.221	0.001	202.25	251.74	1000.5	0.18	31.443	0.63535
5.040	0.778	0.221	0.001	202.20	276.66	1001.9	0.18	47.491	0.63777
5.050	0.778	0.221	0.001	202.17	300.70	1001.4	0.18	63.208	0.64150
17.010	0.771	0.228	0.001	-152.30	-130.83	498.8	0.07	18.797	0.87550
17.020	0.771	0.228	0.001	-152.29	-126.03	500.1	0.07	22.954	0.87423
17.030	0.771	0.228	0.001	-152.31	-116.34	499.4	0.07	32.267	0.89716
17.040	0.771	0.228	0.001	-152.30	-113.10	499.5	0.07	35.137	0.89647
17.050	0.771	0.228	0.001	-152.29	-102.79	501.9	0.17	78.641	1.58857
17.060	0.780	0.219	0.001	-152.28	-90.48	498.9	0.17	111.371	1.80200
17.070	0.780	0.219	0.001	-152.22	-66.00	501.8	0.17	163.664	1.89804
17.080	0.780	0.219	0.001	-152.16	-56.78	500.3	0.17	183.233	1.92109
17.090	0.769	0.230	0.001	-152.17	-51.26	499.5	0.17	193.828	1.92089
17.100	0.769	0.230	0.001	-152.20	-42.23	499.0	0.17	206.370	1.87650
15.010	0.778	0.221	0.001	-240.72	-214.98	249.7	0.10	18.990	0.73771
15.020	0.778	0.221	0.001	-240.71	-185.18	250.1	0.10	41.758	0.75199
15.025	0.778	0.221	0.001	-240.71	-185.18	250.1	0.10	41.853	0.75370
15.030	0.778	0.221	0.001	-240.70	-158.85	251.3	0.10	62.592	0.76470
16.010	0.771	0.228	0.001	-165.84	-161.30	250.1	0.10	3.756	0.82878
16.020	0.771	0.228	0.001	-165.81	-155.50	248.4	0.10	8.551	0.82965
16.030	0.771	0.228	0.001	-165.80	-153.97	250.4	0.34	14.197	1.14996
16.040	0.771	0.228	0.001	-165.81	-153.47	248.9	0.34	21.158	1.71408
16.045	0.771	0.228	0.001	-165.81	-153.47	248.9	0.34	21.214	1.71864
16.050	0.771	0.228	0.001	-165.81	-150.23	248.5	0.34	43.735	2.80600
16.060	0.771	0.228	0.001	-165.78	-137.35	249.7	0.34	92.025	3.23785
16.070	0.769	0.230	0.001	-165.78	-116.63	249.5	0.34	134.749	2.74196
16.080	0.769	0.230	0.001	-165.77	-92.31	249.3	0.34	182.357	2.48231
16.090	0.769	0.230	0.001	-165.77	-90.25	249.1	0.34	186.023	2.46306
16.100	0.769	0.230	0.001	-165.77	-86.45	249.7	0.34	194.764	2.45534
16.110	0.769	0.230	0.001	-165.76	-78.89	248.9	0.34	212.651	2.44794
16.120	0.769	0.230	0.001	-165.69	-75.14	249.5	0.34	218.055	2.40806
16.130	0.769	0.230	0.001	-165.75	-59.92	249.1	0.34	227.104	2.14592
11.010	0.777	0.222	0.001	-59.55	-36.41	251.5	0.38	12.736	0.55042
11.020	0.777	0.222	0.001	-59.56	-18.86	251.2	0.39	22.246	0.54650
11.030	0.777	0.222	0.001	-59.57	1.40	250.3	0.39	32.737	0.53693
11.040	0.778	0.221	0.001	-59.58	25.85	249.7	0.39	45.377	0.53118
11.050	0.778	0.221	0.001	-59.55	50.47	250.0	0.39	58.203	0.52900
11.060	0.778	0.221	0.001	-59.56	75.29	252.1	0.39	71.295	0.52868

TABLE B-14

Basic Isothermal Data for Nominal 0.78 CH_4, 0.22 C_2H_6 Mixture

RUN NO.	COMPOSITION (MOLE FRACTION) CH4	C2H6	C3H8	INLET TEMP. (°F)	OUTLET TEMP. (°F)	INLET PRES. (PSIA)	PRES. DROP (PSID)	HEAT INPUT (BTU/LB)	ISOTHERMAL J.T.COEFF. (BTU/LB PSIA)
7.010	0.778	0.221	0.001	-58.37	-58.31	1999.4	178.65	1.033	-0.00578
7.020	0.778	0.221	0.001	-58.46	-58.39	1799.6	70.62	1.595	-0.02258
7.030	0.778	0.221	0.001	-58.45	-58.37	1603.2	263.46	3.138	-0.01191
7.040	0.778	0.221	0.001	-58.44	-58.40	1600.8	432.04	6.312	-0.01461
7.050	0.778	0.221	0.001	-58.49	-58.45	1390.5	394.80	10.130	-0.02566
7.060	0.778	0.221	0.001	-58.60	-58.71	1405.1	517.47	14.667	-0.02834
7.065	0.778	0.221	0.001	-58.60	-58.71	1405.1	504.50	14.667	-0.02907
7.070	0.778	0.221	0.001	-58.47	-58.60	1202.1	243.42	9.285	-0.03814
7.080	0.778	0.221	0.001	-58.32	-58.17	998.8	155.75	20.113	-0.12913
7.090	0.778	0.221	0.001	-58.37	-58.30	984.7	288.02	45.239	-0.15707
7.095	0.778	0.221	0.001	-58.37	-58.30	984.7	275.99	45.232	-0.16389
1.010	0.777	0.222	0.001	79.28	79.31	1996.3	203.70	7.269	-0.03568
1.020	0.777	0.222	0.001	79.14	79.13	2000.0	415.98	15.711	-0.03777
1.025	0.777	0.222	0.001	79.14	79.13	2000.0	415.98	15.772	-0.03792
1.026	0.777	0.222	0.001	79.14	79.13	2000.0	415.98	15.656	-0.03764
1.030	0.777	0.222	0.001	79.16	79.12	1602.6	105.93	4.433	-0.04185
1.040	0.778	0.221	0.001	79.07	79.09	1601.2	339.09	14.464	-0.04266
1.050	0.778	0.221	0.001	79.12	79.06	1600.9	541.47	23.433	-0.04328
1.060	0.778	0.221	0.001	79.06	79.04	1045.8	220.67	9.421	-0.04269
1.070	0.777	0.222	0.001	78.97	78.90	1045.8	439.20	18.576	-0.04230
1.075	0.777	0.222	0.001	78.97	78.90	1045.8	439.20	18.643	-0.04245
1.076	0.777	0.222	0.001	78.97	78.90	1045.8	439.20	18.510	-0.04215
1.080	0.777	0.222	0.001	79.08	79.02	1048.4	636.18	26.555	-0.04174
1.090	0.777	0.222	0.001	79.07	79.09	1045.6	842.79	34.322	-0.04072
1.095	0.777	0.222	0.001	79.07	79.09	1045.6	842.79	34.415	-0.04083
1.096	0.777	0.222	0.001	79.07	79.09	1045.6	842.79	34.231	-0.04062
1.100	0.777	0.222	0.001	79.07	79.09	1045.2	918.97	37.292	-0.04058
6.010	0.778	0.221	0.001	254.86	254.88	1999.9	208.48	3.769	-0.01808
6.020	0.778	0.221	0.001	254.92	254.87	2001.5	424.86	7.876	-0.01854
6.030	0.778	0.221	0.001	254.93	254.93	2000.5	646.95	12.189	-0.01884
6.040	0.778	0.221	0.001	255.00	254.94	2004.1	857.01	16.394	-0.01913
6.050	0.778	0.221	0.001	255.04	255.04	1153.0	228.69	4.647	-0.02032
6.060	0.778	0.221	0.001	256.22	256.24	1148.2	455.62	9.398	-0.02063
6.070	0.778	0.221	0.001	255.81	255.81	1148.9	635.89	13.144	-0.02067
6.080	0.778	0.221	0.001	256.08	256.05	1148.5	846.91	17.570	-0.02075
6.090	0.778	0.221	0.001	256.13	256.11	1145.1	1038.00	21.489	-0.02073

* H VALUES ARE SUSPECTED TO BE FROM 3 TO 10 PERCENT TOO HIGH DUE TO MASS LEAK

TABLE B-15

Basic Isenthalpic Data for Nominal 0.78 CH_4, 0.22 C_2H_6 Mixture

RUN NO.	COMPOSITION (MOLE FRACTION) CH4	C2H6	C3H8	INLET TEMP. (°F)	OUTLET TEMP. (°F)	INLET PRES. (PSIA)	PRES. DROP (PSID)	HEAT INPUT (BTU/LB)	J.THOMSON COEFF. (°F/PSIA)
13.010	0.777	0.222	0.001	-253.21	-252.39	2008.2	142.38	0.000	-0.00580
13.020	0.777	0.222	0.001	-253.22	-252.29	1703.3	135.72	0.000	-0.00686
13.030	0.777	0.222	0.001	-253.23	-252.22	1393.9	132.89	0.000	-0.00757
13.040	0.777	0.222	0.001	-253.18	-252.09	1035.1	119.97	0.000	-0.00906
13.050	0.777	0.222	0.001	-253.23	-252.17	804.0	129.04	0.000	-0.00823
13.055	0.777	0.222	0.001	-253.23	-252.17	804.0	124.02	0.000	-0.00856
12.010	0.778	0.221	0.001	-150.55	-150.57	2000.6	161.29	0.000	0.00014
12.020	0.778	0.221	0.001	-150.64	-150.56	1701.1	154.23	0.000	-0.00051
12.030	0.778	0.221	0.001	-150.58	-150.47	1401.7	161.12	0.000	-0.00070
12.040	0.778	0.221	0.001	-150.57	-150.38	1099.8	161.50	0.000	-0.00114
12.050	0.778	0.221	0.001	-150.53	-150.27	804.0	171.13	0.000	-0.00151
12.060	0.778	0.221	0.001	-150.51	-150.22	603.9	180.39	0.000	-0.00156
12.070	0.778	0.221	0.001	-150.51	-150.14	499.5	160.69	0.000	-0.00230

TABLE B-16

Basic Isobaric Data for Nominal 0.48 CH_4, 0.52 C_2H_6 Mixture

RUN NO.	COMPOSITION (MOLE FRACTION) CH4	C2H6	C3H8	INLET TEMP. (°F)	OUTLET TEMP. (°F)	INLET PRES. (PSIA)	PRES. DROP (PSID)	HEAT INPUT (BTU/LB)	MEAN HEAT CAPACITY (BTU/LB°F)
17.010	0.480	0.517	0.003	0.40	28.69	1999.4	0.13	25.032	0.88469
17.020	0.480	0.517	0.003	0.25	51.97	1999.8	0.13	46.758	0.90408
17.030	0.480	0.517	0.003	0.28	75.92	1999.4	0.13	71.930	0.95090
17.040	0.477	0.520	0.003	0.32	81.41	2002.8	0.13	76.394	0.94198
17.045	0.477	0.520	0.003	0.32	81.41	2002.8	0.13	75.991	0.93701
17.046	0.477	0.520	0.003	0.32	81.41	2002.8	0.13	76.696	0.94570
17.050	0.477	0.520	0.003	0.28	87.18	2001.4	0.13	83.036	0.95582
3.010	0.479	0.518	0.003	-230.03	-204.41	1490.6	0.05	16.624	0.64877
3.020	0.479	0.518	0.003	-230.01	-176.32	1490.5	0.05	34.522	0.64300
3.030	0.480	0.517	0.003	-229.99	-151.58	1489.3	0.05	50.507	0.64412
3.040	0.480	0.517	0.003	-229.99	-127.44	1490.3	0.05	66.492	0.64839
3.050	0.480	0.517	0.003	-229.94	-99.68	1490.4	0.05	85.413	0.65570
8.010	0.479	0.518	0.003	-100.17	-69.83	1499.5	0.06	21.834	0.71972
8.020	0.479	0.518	0.003	-100.13	-30.16	1499.6	0.06	53.577	0.76564
8.030	0.479	0.518	0.003	-100.13	0.53	1501.3	0.06	80.001	0.79470
16.010	0.475	0.522	0.003	0.32	30.04	1499.8	0.10	31.314	1.05369
16.020	0.475	0.522	0.003	0.36	45.82	1502.0	0.10	49.846	1.09664
16.030	0.475	0.522	0.003	0.29	49.53	1503.1	0.10	54.226	1.10130
16.040	0.475	0.522	0.003	0.14	53.57	1501.0	0.10	59.847	1.12010
16.050	0.475	0.522	0.003	0.16	57.76	1499.7	0.10	65.432	1.13588
16.060	0.475	0.522	0.003	0.21	80.47	1499.1	0.10	93.322	1.16263
16.070	0.475	0.522	0.003	0.25	102.86	1500.0	0.10	117.013	1.14035
14.010	0.477	0.520	0.003	99.95	133.98	1499.0	0.15	31.293	0.91957
14.020	0.477	0.520	0.003	99.72	161.32	1499.8	0.15	53.159	0.86290
14.030	0.477	0.520	0.003	99.41	194.38	1499.3	0.15	77.120	0.81204
14.035	0.477	0.520	0.003	99.41	194.38	1499.3	0.15	75.099	0.79076
14.036	0.477	0.520	0.003	99.41	194.38	1499.3	0.15	76.726	0.80790
14.040	0.478	0.519	0.003	99.81	220.49	1502.1	0.15	96.753	0.80172
14.050	0.478	0.519	0.003	100.20	251.34	1499.9	0.15	117.742	0.77904
11.010	0.482	0.514	0.003	249.88	271.97	1500.2	0.10	15.013	0.67971
11.020	0.482	0.514	0.003	249.90	291.23	1500.8	0.10	28.198	0.68227
11.030	0.482	0.514	0.003	249.96	302.80	1500.9	0.10	36.337	0.68772
15.010	0.479	0.518	0.003	0.31	15.62	1253.6	0.10	17.901	1.16871
15.020	0.479	0.518	0.003	0.23	20.10	1253.7	0.10	23.715	1.19314
15.030	0.479	0.518	0.003	0.31	25.69	1253.9	0.10	31.432	1.23812
15.040	0.477	0.520	0.003	0.23	30.38	1251.0	0.10	38.224	1.26791
15.050	0.477	0.520	0.003	0.20	35.91	1249.6	0.10	46.906	1.31361
15.060	0.477	0.520	0.003	0.31	44.70	1248.6	0.10	60.039	1.35234
15.070	0.478	0.519	0.003	0.25	58.62	1251.9	0.10	80.495	1.37893
15.080	0.478	0.519	0.003	-0.44	108.37	1249.6	0.10	133.888	1.23051
7.010	0.479	0.518	0.003	-100.04	-65.41	975.3	0.08	25.935	0.74883
7.020	0.479	0.518	0.003	-100.04	-32.48	975.4	0.08	53.901	0.79787
7.030	0.479	0.518	0.003	-99.96	0.42	975.2	0.08	91.054	0.90714
7.040	0.479	0.518	0.003	-100.04	4.68	974.5	0.08	98.225	0.93796
7.050	0.479	0.518	0.003	-100.03	8.85	976.3	0.08	105.569	0.96956
10.010	0.480	0.517	0.003	0.90	5.87	979.3	0.07	8.041	1.62060
10.020	0.480	0.517	0.003	1.08	8.66	979.6	0.07	13.121	1.73031
10.030	0.480	0.517	0.003	0.95	11.17	978.8	0.07	18.381	1.79725
10.050	0.480	0.517	0.003	1.12	15.83	980.7	0.07	27.496	1.86920
10.060	0.479	0.518	0.003	0.98	20.76	979.8	0.07	38.661	1.95505
10.070	0.479	0.518	0.003	1.16	25.69	982.1	0.07	48.736	1.98622
10.080	0.479	0.518	0.003	0.94	32.55	982.7	0.07	62.617	1.98050
10.090	0.479	0.518	0.003	0.69	70.80	980.8	0.07	110.389	1.57443
10.100	0.479	0.518	0.003	1.38	103.07	980.1	0.07	135.513	1.33259
6.010	0.475	0.522	0.003	-101.11	-70.33	749.9	0.35	23.257	0.75561
6.020	0.475	0.522	0.003	-100.86	-35.97	751.4	0.22	53.394	0.82290
6.030	0.476	0.521	0.003	-101.49	-31.64	749.5	0.22	58.893	0.84311
6.040	0.476	0.521	0.003	-101.48	-26.18	749.1	0.22	69.119	0.91796
6.050	0.476	0.521	0.003	-101.45	-6.30	749.1	0.22	106.737	1.12178
6.060	0.474	0.523	0.003	-101.43	5.83	748.7	0.22	133.614	1.24579
6.070	0.474	0.523	0.003	-101.43	19.99	750.0	0.22	169.160	1.39322
6.080	0.474	0.523	0.003	-101.41	39.13	749.7	0.22	194.937	1.38704
5.010	0.477	0.520	0.003	-99.42	-78.40	499.7	0.14	16.353	0.77818
5.020	0.477	0.520	0.003	-99.35	-75.05	499.6	0.14	19.104	0.78612
5.030	0.477	0.520	0.003	-99.33	-69.80	500.7	0.14	28.842	0.97678
5.040	0.477	0.520	0.003	-99.33	-64.05	501.5	0.14	39.286	1.11329
5.050	0.483	0.514	0.003	-99.35	-59.64	501.6	0.14	47.317	1.10143
5.060	0.483	0.514	0.003	-99.26	-10.74	500.6	0.14	148.787	1.68077
5.070	0.483	0.514	0.003	-99.30	-3.95	499.7	0.14	169.551	1.77817
5.080	0.483	0.514	0.003	-99.33	1.13	500.0	0.14	186.991	1.86118
5.090	0.480	0.517	0.003	-99.33	9.43	500.7	0.14	195.934	1.80148
5.100	0.480	0.517	0.003	-99.20	19.70	500.4	0.14	202.654	1.70444
5.110	0.480	0.517	0.003	-99.35	50.14	501.2	0.14	222.354	1.48749
4.010	0.485	0.512	0.003	-136.77	-132.08	250.7	0.07	3.405	0.72732
4.020	0.485	0.512	0.003	-136.71	-128.23	250.9	0.07	7.054	0.83244
4.030	0.485	0.512	0.003	-136.75	-123.88	249.8	0.07	17.310	1.34503
4.040	0.485	0.512	0.003	-136.77	-125.33	248.8	0.07	14.661	1.28094
4.050	0.485	0.512	0.003	-136.75	-120.92	249.6	0.07	23.426	1.47929
4.060	0.485	0.512	0.003	-136.75	-115.20	249.2	0.07	34.406	1.59674
4.070	0.485	0.512	0.003	-136.81	-81.69	249.6	0.07	92.359	1.67540
4.080	0.485	0.512	0.003	-136.71	-46.55	250.7	0.07	176.913	1.96235
4.090	0.480	0.517	0.003	-136.71	-41.94	250.2	0.07	194.255	2.04988
4.100	0.480	0.517	0.003	-136.70	-37.41	251.3	0.07	213.092	2.14821
4.110	0.480	0.517	0.003	-136.75	-18.40	251.6	0.07	228.971	1.93467
4.120	0.480	0.517	0.003	-136.71	6.27	250.6	0.07	240.602	1.98270

TABLE B-17

Basic Isothermal Data for Nominal 0.48 CH_4, 0.52 C_2H_6 Mixture

RUN NO.	COMPOSITION (MOLE FRACTION) CH4	C2H6	C3H8	INLET TEMP. (°F)	OUTLET TEMP. (°F)	INLET PRES. (PSIA)	PRES. DROP (PSID)	HEAT INPUT (BTU/LB)	ISOTHERMAL J.T.COEFF. (BTU/LB PSIA)
9.045	0.486	0.511	0.003	-99.00	-98.91	395.5	272.23	83.494	-0.30671
18.010	0.479	0.518	0.003	1.71	1.65	2020.7	149.34	0.623	-0.00417
18.020	0.479	0.518	0.003	1.64	1.56	1803.8	152.24	0.940	-0.00618
18.030	0.479	0.518	0.003	1.53	1.47	1602.7	154.55	1.561	-0.01010
18.035	0.479	0.518	0.003	1.53	1.47	1602.7	154.55	1.399	-0.00905
18.040	0.479	0.518	0.003	1.77	1.65	1397.0	157.35	2.191	-0.01392
18.050	0.479	0.518	0.003	1.95	1.90	1202.1	163.50	4.060	-0.02483
18.055	0.479	0.518	0.003	1.95	1.90	1202.1	163.50	4.050	-0.02477
18.056	0.479	0.518	0.003	1.95	1.90	1202.1	163.50	4.068	-0.02488
18.060	0.479	0.518	0.003	1.66	1.86	977.3	134.63	15.876	-0.11792
18.070	0.479	0.518	0.003	2.00	2.04	978.3	270.76	38.601	-0.14257
18.080	0.479	0.518	0.003	1.37	1.34	691.5	293.53	71.912	-0.24499
18.090	0.479	0.518	0.003	0.69	0.55	447.9	341.39	27.609	-0.08087
13.010	0.480	0.517	0.003	101.43	101.31	1959.0	223.91	8.719	-0.03894
13.020	0.480	0.517	0.003	101.45	101.41	1604.8	258.55	15.119	-0.05848
13.030	0.480	0.517	0.003	101.32	101.33	1224.2	301.46	19.197	-0.06368
13.040	0.480	0.517	0.003	101.67	101.63	989.1	358.64	20.807	-0.05802
13.050	0.480	0.517	0.003	101.52	101.50	793.6	344.16	18.330	-0.05326
13.060	0.480	0.517	0.003	101.59	101.67	598.1	281.95	13.995	-0.04964
13.070	0.480	0.517	0.003	101.64	101.55	397.2	294.81	13.333	-0.04522
12.010	0.479	0.518	0.003	252.57	252.55	1996.8	189.09	4.592	-0.02428
12.020	0.479	0.518	0.003	252.23	252.23	1679.5	234.31	6.500	-0.02774
12.030	0.479	0.518	0.003	252.22	252.23	1511.7	282.75	7.721	-0.02731
12.035	0.479	0.518	0.003	252.22	252.23	1511.7	281.08	7.721	-0.02747
12.040	0.478	0.519	0.003	252.38	252.47	1133.9	377.75	10.521	-0.02785
12.050	0.478	0.519	0.003	252.36	252.27	829.7	300.20	8.287	-0.02761
12.055	0.478	0.519	0.003	252.36	252.27	829.7	300.20	8.327	-0.02774
12.056	0.478	0.519	0.003	252.36	252.27	827.7	300.20	8.248	-0.02747
12.060	0.478	0.519	0.003	252.67	252.77	535.9	296.55	8.131	-0.02742
12.070	0.478	0.519	0.003	252.78	252.76	335.4	242.22	3.200	-0.01321

* H VALUES ARE SUSPECTED TO BE FROM 3 TO 10 PERCENT TOO HIGH DUE TO MASS LEAK

TABLE B-18

Basic Isenthalpic Data for Nominal 0.48 CH_4, 0.52 C_2H_6 Mixture

RUN NO.	COMPOSITION (MOLE FRACTION) CH4	C2H6	C3H8	INLET TEMP. (°F)	OUTLET TEMP. (°F)	INLET PRES. (PSIA)	PRES. DROP (PSID)	HEAT INPUT (BTU/LB)	J.THOMSON COEFF. (°F/PSIA)
1.010	0.481	0.516	0.003	-228.45	-228.40	1961.0	191.09	0.000	-0.00024
1.020	0.481	0.516	0.003	-228.41	-228.32	1648.6	204.90	0.000	-0.00044
1.030	0.481	0.516	0.003	-228.46	-228.40	1331.1	197.28	0.000	-0.00031
1.040	0.481	0.516	0.003	-228.47	-227.91	1005.6	212.41	0.000	-0.00266
1.050	0.468	0.529	0.003	-228.45	-228.18	795.0	205.15	0.000	-0.00135
1.060	0.468	0.529	0.003	-228.42	-228.18	588.5	204.37	0.000	-0.00119
2.010	0.479	0.518	0.003	-99.14	-98.69	1980.7	208.76	0.000	-0.00211
2.020	0.477	0.520	0.003	-99.09	-98.17	1668.5	140.48	0.000	-0.00658
2.030	0.476	0.521	0.003	-99.12	-98.50	1354.5	353.17	0.000	-0.00176
9.010	0.479	0.518	0.003	-99.04	-98.63	1272.5	231.76	0.000	-0.00177
9.020	0.479	0.518	0.003	-99.09	-98.93	883.0	184.57	0.000	-0.00086
9.030	0.486	0.511	0.003	-99.01	-98.92	602.6	218.44	0.000	-0.00041

TABLE B-19

Basic Isobaric Data for Nominal 0.369 CH_4, 0.306 C_2H_6, 0.325 C_3H_8 Mixture

RUN NO.	COMPOSITION (MOLE FRACTION) CH4	C2H6	C3H8	INLET TEMP. (°F)	OUTLET TEMP. (°F)	INLET PRES. (PSIA)	PRES. DROP (PSID)	HEAT INPUT (BTU/LB)	MEAN HEAT CAPACITY (BTU/LB°F)
25.010	0.370	0.303	0.327	-236.16	-226.23	2001.3	0.21	5.508	0.55424
25.011	0.370	0.303	0.327	-236.16	-226.21	2004.0	0.21	5.515	0.55425
25.020	0.370	0.303	0.327	-236.16	-200.94	2001.3	0.16	19.649	0.55788
25.030	0.370	0.305	0.325	-236.32	-181.82	2001.6	0.15	30.445	0.55856
25.040	0.370	0.305	0.325	-236.14	-161.80	2001.5	0.13	41.621	0.55991
29.010	0.372	0.305	0.323	-161.91	-145.60	2003.0	0.12	9.343	0.57274
29.011	0.372	0.305	0.323	-161.90	-145.70	2000.6	0.12	9.280	0.57299
29.020	0.372	0.305	0.323	-161.87	-115.22	2002.7	0.12	27.658	0.59285
29.030	0.372	0.303	0.325	-161.89	-93.01	1999.4	0.10	40.183	0.58332
29.040	0.372	0.303	0.325	-161.91	-84.14	1999.9	0.10	45.574	0.58606
29.045	0.372	0.303	0.325	-161.91	-84.14	1999.9	0.10	45.467	0.58468
33.010	0.366	0.303	0.331	-88.09	-78.51	1999.8	0.05	5.792	0.60442
33.011	0.366	0.303	0.331	-88.12	-78.28	1999.5	0.05	5.952	0.60485
33.020	0.366	0.305	0.329	-88.14	-58.95	2000.1	0.05	17.790	0.60954
33.030	0.366	0.305	0.329	-88.14	-38.12	2001.3	0.05	30.849	0.61681
33.040	0.366	0.305	0.329	-88.14	-21.59	1999.7	0.05	41.278	0.62029
16.010	0.376	0.305	0.319	-22.57	-12.65	1999.7	0.07	6.609	0.66633
16.011	0.376	0.305	0.319	-23.02	-13.05	1999.7	0.07	6.657	0.66776
16.020	0.376	0.305	0.319	-22.69	2.61	2003.3	0.05	16.735	0.66157
16.021	0.376	0.305	0.319	-22.30	3.05	2002.3	0.06	16.816	0.66342
16.030	0.376	0.305	0.319	-22.44	19.46	2002.8	0.06	28.115	0.67101
16.031	0.376	0.305	0.319	-22.45	19.87	1999.9	0.06	28.488	0.67309
16.040	0.376	0.305	0.319	-22.62	52.69	1999.3	0.08	52.084	0.69167
9.010	0.369	0.306	0.326	51.75	61.70	2002.5	0.00	7.616	0.76534
9.020	0.369	0.306	0.326	51.69	76.50	1999.9	0.0	19.060	0.76809
9.030	0.369	0.306	0.326	51.69	91.78	2000.2	0.01	31.106	0.77583
9.040	0.369	0.306	0.326	51.76	110.18	2000.6	0.04	46.328	0.79298
9.050	0.369	0.306	0.326	51.77	126.46	2002.2	0.07	61.106	0.81806
42.010	0.367	0.305	0.328	146.42	149.54	1999.4	0.09	2.867	0.91932
42.011	0.367	0.305	0.328	146.42	149.56	2000.8	0.09	2.870	0.91408
42.021	0.367	0.305	0.328	145.37	151.31	2003.1	0.12	5.395	0.90802
42.030	0.367	0.305	0.328	145.41	155.83	2000.1	0.12	9.527	0.91505
42.040	0.370	0.304	0.327	145.50	159.12	1999.8	0.12	12.503	0.91793
42.050	0.370	0.304	0.327	141.30	170.57	1999.4	0.12	24.386	0.83303
42.055	0.370	0.304	0.327	141.30	170.57	1999.4	0.12	26.963	0.92105
42.060	0.370	0.304	0.327	140.52	185.57	1998.5	0.15	41.471	0.92065
35.010	0.367	0.303	0.330	193.61	198.97	2000.5	0.24	4.778	0.89064
35.020	0.367	0.303	0.330	193.69	203.18	1999.8	0.24	8.468	0.89242
35.030	0.367	0.303	0.330	193.64	208.85	1999.7	0.32	13.419	0.88266
35.040	0.367	0.304	0.330	193.67	213.72	1999.9	0.31	17.689	0.88245
35.050	0.367	0.304	0.330	193.72	234.26	2002.3	0.34	35.066	0.86509
39.010	0.369	0.303	0.328	227.92	237.63	2001.8	0.07	8.085	0.83221
39.011	0.369	0.303	0.328	227.90	237.55	2002.6	0.07	8.099	0.83924
39.020	0.369	0.303	0.328	227.90	248.07	2000.2	0.07	16.743	0.83028
39.030	0.369	0.303	0.328	227.93	258.21	1999.6	0.10	24.958	0.82424
39.040	0.369	0.303	0.328	227.59	267.61	2000.4	0.10	32.703	0.81717
10.010	0.370	0.306	0.325	51.78	62.36	1751.1	0.08	7.967	0.75275
10.012	0.370	0.306	0.325	51.78	62.36	1751.1	0.08	8.318	0.78596
10.015	0.370	0.306	0.325	51.78	62.36	1751.1	0.08	8.342	0.78819
10.020	0.370	0.306	0.325	51.80	76.76	1751.1	0.09	21.648	0.86712
10.026	0.370	0.306	0.325	51.80	76.76	1751.1	0.09	20.050	0.80314
10.025	0.370	0.306	0.325	51.80	76.76	1751.1	0.09	20.121	0.80596
10.030	0.370	0.306	0.325	51.77	91.92	1751.0	0.10	33.006	0.82214
10.040	0.370	0.307	0.324	51.79	109.91	1751.2	0.11	49.264	0.84756
10.050	0.370	0.306	0.324	51.79	126.62	1750.6	0.13	65.123	0.87023
41.010	0.371	0.303	0.326	138.44	141.43	1751.8	0.12	2.942	0.98392
41.020	0.371	0.303	0.326	138.39	144.37	1750.3	0.11	5.917	0.98983
41.025	0.371	0.303	0.326	138.39	144.37	1750.3	0.11	5.908	0.98843
41.030	0.371	0.303	0.326	138.41	148.76	1751.3	0.11	10.280	0.99255
41.040	0.371	0.303	0.326	138.39	151.67	1753.9	0.11	13.159	0.99128
2.010	0.369	0.306	0.325	127.21	137.22	1751.3	0.06	9.828	0.98179
2.020	0.369	0.306	0.325	127.21	147.33	1751.8	0.10	19.630	0.97569
2.030	0.369	0.306	0.325	127.17	152.06	1749.1	0.10	24.882	0.99968
2.035	0.369	0.306	0.325	127.17	152.06	1749.1	0.10	25.290	1.01608
2.036	0.369	0.306	0.325	127.17	152.06	1749.1	0.10	28.015	1.12556
2.040	0.370	0.307	0.323	127.28	167.26	1749.9	0.10	39.720	0.99338
2.050	0.370	0.307	0.323	127.19	202.18	1751.0	0.12	71.393	0.95206
17.010	0.375	0.306	0.319	-22.54	-12.40	1501.7	0.10	6.832	0.67416
17.011	0.375	0.306	0.319	-22.52	-12.29	1501.2	0.10	6.897	0.67381
17.020	0.375	0.306	0.319	-22.50	2.41	1499.9	0.10	16.986	0.68195
17.021	0.375	0.306	0.319	-22.52	2.42	1500.1	0.10	17.125	0.68660
17.030	0.374	0.305	0.320	-22.48	17.69	1500.8	0.10	28.066	0.69877
17.031	0.374	0.305	0.320	-22.49	17.80	1500.8	0.10	28.106	0.69752
17.040	0.374	0.305	0.320	-22.49	52.37	1500.8	0.10	54.718	0.73094

TABLE B-19
(CONTINUED)

RUN NO.	COMPOSITION (MOLE FRACTION) CH4	C2H6	C3H8	INLET TEMP. (°F)	OUTLET TEMP. (°F)	INLET PRES. (PSIA)	PRES. DROP (PSID)	HEAT INPUT (BTU/LB)	MEAN HEAT CAPACITY (BTU/LB°F)
11.010	0.370	0.305	0.325	51.88	61.74	1501.5	0.09	8.186	0.82999
11.020	0.370	0.305	0.325	51.87	76.76	1500.5	0.10	21.347	0.85751
11.030	0.369	0.306	0.326	51.99	91.93	1500.5	0.10	35.514	0.88908
11.040	0.369	0.306	0.326	51.85	110.04	1502.2	0.10	53.344	0.91666
11.050	0.369	0.306	0.326	51.89	126.64	1501.6	0.10	72.117	0.96479
40.010	0.370	0.304	0.325	121.97	124.97	1499.6	0.10	3.271	1.08876
40.020	0.370	0.304	0.325	122.13	128.15	1500.3	0.11	6.604	1.09599
40.040	0.370	0.304	0.325	122.18	134.18	1499.3	0.14	13.131	1.09416
40.045	0.370	0.304	0.325	122.18	134.18	1499.3	0.14	13.145	1.09536
3.010	0.370	0.305	0.325	127.12	132.09	1499.6	0.10	5.484	1.10368
3.015	0.370	0.305	0.325	127.12	132.09	1499.6	0.10	5.498	1.10664
3.020	0.370	0.305	0.325	127.09	137.22	1499.4	0.10	11.116	1.09708
3.030	0.370	0.305	0.325	127.27	152.22	1499.4	0.12	27.084	1.08526
3.040	0.370	0.306	0.324	127.34	167.32	1499.5	0.13	42.473	1.06221
3.050	0.370	0.306	0.324	127.26	202.05	1499.2	0.15	74.395	0.99461
36.010	0.372	0.300	0.328	191.70	201.57	1500.8	0.12	8.634	0.87469
36.011	0.372	0.300	0.328	191.78	201.74	1501.7	0.12	8.684	0.87127
36.020	0.372	0.300	0.328	191.75	218.00	1502.9	0.12	22.184	0.84518
36.030	0.368	0.303	0.328	191.79	237.11	1501.7	0.15	37.305	0.82304
36.040	0.368	0.303	0.328	191.28	264.10	1501.5	0.15	57.994	0.79630
12.010	0.370	0.306	0.325	51.83	61.93	1250.3	0.10	9.102	0.90141
12.020	0.370	0.306	0.325	51.84	76.77	1249.3	0.10	23.770	0.95338
12.030	0.368	0.307	0.326	51.84	91.88	1249.1	0.11	40.659	1.01545
12.040	0.368	0.307	0.326	51.85	111.61	1249.3	0.12	65.310	1.09274
12.050	0.370	0.307	0.324	51.85	122.41	1249.5	0.14	78.991	1.11946
12.060	0.370	0.307	0.324	51.87	126.76	1249.3	0.15	84.311	1.12575
12.065	0.370	0.307	0.324	51.87	126.76	1249.3	0.15	84.387	1.12676
44.010	0.369	0.305	0.326	107.50	110.63	1252.7	0.11	3.987	1.27384
44.020	0.369	0.305	0.326	107.47	114.06	1251.9	0.12	8.390	1.27327
44.030	0.369	0.305	0.326	107.38	117.13	1252.4	0.12	12.398	1.27143
44.040	0.369	0.305	0.326	107.46	120.66	1252.2	0.12	16.691	1.26434
4.010	0.369	0.305	0.326	127.35	137.25	1251.5	0.11	11.700	1.18120
4.020	0.369	0.305	0.326	127.30	152.19	1251.2	0.12	28.107	1.12920
4.030	0.369	0.306	0.324	127.29	167.30	1249.9	0.12	42.861	1.07121
4.040	0.369	0.306	0.324	127.37	202.16	1252.2	0.13	72.332	0.96715
13.010	0.370	0.306	0.324	51.90	61.79	1100.7	0.09	9.688	0.98002
13.020	0.370	0.306	0.324	51.92	76.78	1100.6	0.10	26.617	1.07093
13.030	0.370	0.306	0.324	51.89	91.77	1100.2	0.12	46.774	1.17286
13.040	0.370	0.306	0.325	51.87	101.71	1099.9	0.13	60.881	1.22139
13.050	0.370	0.306	0.325	51.89	106.76	1099.6	0.15	68.116	1.24142
13.060	0.370	0.306	0.324	51.93	127.06	1099.8	0.18	95.161	1.26663
43.010	0.369	0.304	0.327	94.52	96.91	1102.9	0.07	3.422	1.43303
43.011	0.369	0.304	0.327	94.90	97.31	1102.9	0.07	3.427	1.42368
43.020	0.369	0.304	0.327	94.48	99.28	1100.6	0.10	6.852	1.42657
43.030	0.369	0.304	0.327	94.60	102.18	1101.4	0.10	10.534	1.38827
43.035	0.369	0.304	0.327	94.60	102.18	1101.4	0.10	10.334	1.36182
43.036	0.369	0.304	0.327	94.60	102.18	1101.4	0.10	10.813	1.42501
43.040	0.369	0.304	0.327	94.48	104.64	1099.1	0.11	14.479	1.42407
30.010	0.373	0.305	0.323	-161.93	-146.51	1002.5	0.05	9.043	0.58661
30.011	0.373	0.305	0.323	-161.81	-146.29	1002.2	0.07	9.021	0.58125
30.020	0.373	0.305	0.323	-161.97	-116.01	1002.6	0.10	27.068	0.58894
30.030	0.374	0.305	0.321	-161.97	-93.26	1000.8	0.10	40.870	0.59481
30.040	0.374	0.305	0.321	-161.96	-82.65	1000.8	0.10	47.436	0.59814
30.041	0.374	0.305	0.321	-161.68	-82.32	1001.1	0.10	47.437	0.59778
34.010	0.365	0.304	0.331	-88.14	-78.55	999.4	0.0	5.946	0.62023
34.011	0.365	0.304	0.331	-88.14	-78.54	1000.0	0.0	5.946	0.61968
34.020	0.365	0.304	0.331	-88.13	-58.34	1002.1	0.10	18.718	0.62835
34.030	0.364	0.305	0.331	-88.08	-38.62	1000.5	0.11	31.592	0.63868
34.040	0.364	0.305	0.331	-88.07	-13.69	1002.1	0.25	48.537	0.65255
18.010	0.374	0.306	0.321	-22.51	-12.91	1002.2	0.10	6.740	0.70169
18.011	0.374	0.306	0.321	-22.70	-13.06	1002.2	0.10	6.745	0.69950
18.020	0.374	0.306	0.321	-22.66	1.85	1002.3	0.11	17.556	0.71611
18.021	0.374	0.306	0.321	-22.67	1.87	1001.5	0.11	17.578	0.71621
18.030	0.374	0.306	0.321	-22.52	17.49	1001.4	0.11	29.457	0.73624
18.031	0.374	0.306	0.321	-22.64	17.51	1001.6	0.11	29.510	0.73494
18.040	0.374	0.306	0.321	-22.62	52.63	999.8	0.13	61.160	0.81275
18.041	0.374	0.306	0.321	-22.67	52.68	1000.5	0.13	61.283	0.81328
14.010	0.370	0.306	0.324	51.88	61.84	1000.9	0.06	12.081	1.21380
14.020	0.370	0.306	0.324	51.84	64.00	1001.0	0.09	14.766	1.21399
14.030	0.370	0.306	0.324	51.86	65.91	1000.6	0.11	17.170	1.22248
14.040	0.368	0.309	0.324	51.85	69.62	1000.4	0.14	21.949	1.23476
14.050	0.368	0.309	0.324	51.85	74.45	1000.5	0.11	28.300	1.25173
14.070	0.369	0.307	0.323	51.82	67.03	999.8	0.09	18.685	1.22912
14.080	0.368	0.307	0.324	51.86	91.60	1000.1	0.13	52.194	1.31342
14.090	0.368	0.307	0.324	51.81	109.82	999.4	0.16	81.518	1.40518
14.100	0.368	0.307	0.324	51.83	111.86	1000.2	0.17	84.454	1.40685
14.110	0.368	0.307	0.324	51.84	113.98	999.9	0.16	87.671	1.41084
14.120	0.368	0.307	0.324	51.87	103.29	1000.8	0.16	70.237	1.36599
14.130	0.368	0.307	0.324	51.84	106.14	1000.6	0.17	75.269	1.38612

TABLE B-19
(CONTINUED)

RUN NO.	COMPOSITION (MOLE FRACTION) CH4	C2H6	C3H8	INLET TEMP. (°F)	OUTLET TEMP. (°F)	INLET PRES. (PSIA)	PRES. DROP (PSID)	HEAT INPUT (BTU/LB)	MEAN HEAT CAPACITY (BTU/LB°F)
20.010	0.367	0.306	0.327	52.11	65.05	1001.0	0.10	15.630	1.20802
20.011	0.367	0.306	0.327	52.11	64.95	1000.5	0.10	15.675	1.22085
20.020	0.367	0.306	0.327	52.10	67.55	1001.4	0.06	18.885	1.22239
20.030	0.367	0.306	0.327	52.07	70.22	999.5	0.02	22.363	1.23380
20.040	0.367	0.306	0.327	52.09	74.21	998.9	0.03	27.591	1.24734
20.050	0.367	0.306	0.327	52.19	103.54	1000.8	0.10	70.094	1.36515
20.060	0.367	0.305	0.327	52.30	107.36	1001.5	0.11	75.947	1.37932
20.070	0.367	0.305	0.327	52.14	109.32	1001.5	0.13	79.311	1.38715
20.080	0.367	0.305	0.327	52.13	112.62	1000.9	0.11	85.119	1.40697
20.090	0.367	0.305	0.327	52.12	99.72	1000.4	0.13	63.778	1.33974
20.100	0.367	0.305	0.327	52.36	93.18	1000.0	0.12	53.549	1.31183
20.110	0.367	0.305	0.327	52.12	119.15	1001.4	0.14	93.703	1.39786
20.120	0.367	0.305	0.327	52.09	115.87	1001.9	0.13	89.366	1.40125
45.010	0.366	0.304	0.331	52.03	110.06	1001.8	0.15	80.904	1.39412
45.011	0.366	0.304	0.331	52.07	109.70	998.8	0.15	80.169	1.39111
45.020	0.367	0.304	0.329	52.29	120.64	999.8	0.17	95.206	1.39280
45.030	0.367	0.304	0.329	52.20	131.51	1000.8	0.17	107.987	1.36153
37.010	0.369	0.304	0.327	191.74	202.01	1002.7	0.02	7.314	0.71258
37.011	0.369	0.304	0.327	191.71	202.04	1002.0	0.07	7.338	0.71037
37.020	0.369	0.304	0.327	191.75	217.77	1001.5	0.12	18.390	0.70668
37.030	0.369	0.304	0.327	191.78	236.97	1002.0	0.20	31.290	0.69248
37.040	0.369	0.304	0.327	191.74	264.48	1001.8	0.20	49.597	0.68181
5.010	0.369	0.306	0.325	127.28	137.05	1001.8	0.14	10.337	1.05820
5.020	0.369	0.306	0.325	127.31	152.29	1001.4	0.15	24.236	0.97009
5.030	0.369	0.306	0.326	127.32	167.38	1002.2	0.18	36.617	0.91394
5.040	0.369	0.306	0.326	127.35	202.00	1002.9	0.18	62.153	0.83252
46.010	0.364	0.305	0.331	-83.07	-72.76	748.9	0.18	6.495	0.62951
46.011	0.364	0.304	0.331	-83.08	-72.75	749.6	0.18	6.502	0.62947
46.020	0.364	0.304	0.331	-83.00	-63.51	751.0	0.25	12.332	0.63295
46.030	0.364	0.306	0.330	-83.01	-43.24	751.2	0.29	25.721	0.64679
46.040	0.364	0.306	0.330	-82.92	-34.60	751.1	0.30	31.459	0.65103
46.050	0.364	0.306	0.330	-82.94	-23.25	751.5	0.32	39.317	0.65877
19.010	0.374	0.307	0.319	-22.79	-12.76	751.7	0.07	7.255	0.72381
19.011	0.374	0.307	0.319	-22.69	-12.69	752.7	0.06	7.212	0.72109
19.020	0.374	0.307	0.319	-22.75	0.48	751.1	0.11	17.652	0.75994
19.021	0.374	0.307	0.319	-22.74	0.42	750.8	0.13	17.583	0.75899
19.030	0.374	0.307	0.319	-22.73	-18.50	751.1	0.07	3.014	0.71250
19.031	0.374	0.307	0.319	-22.77	-18.53	751.2	0.05	3.006	0.70862
19.040	0.374	0.307	0.319	-22.72	3.57	751.7	0.10	21.229	0.80768
19.050	0.374	0.307	0.319	-22.76	17.39	751.5	0.15	36.677	0.91358
19.051	0.374	0.307	0.319	-22.76	17.33	751.4	0.15	36.754	0.91687
19.060	0.374	0.307	0.319	-22.72	52.67	750.7	0.21	78.545	1.04192
19.061	0.374	0.307	0.319	-22.73	52.94	750.7	0.21	80.148	1.05926
19.065	0.374	0.307	0.319	-22.72	52.67	750.7	0.21	79.584	1.05571
22.010	0.373	0.304	0.324	52.03	61.97	748.0	0.07	13.662	1.37386
22.011	0.373	0.304	0.324	52.04	62.02	749.5	0.07	13.634	1.36622
22.020	0.373	0.304	0.324	52.10	77.02	750.4	0.12	36.040	1.44631
22.030	0.375	0.304	0.321	52.02	91.94	752.4	0.12	61.331	1.53628
22.040	0.375	0.304	0.321	52.09	106.84	752.4	0.15	90.258	1.64854
22.050	0.373	0.303	0.324	52.00	112.00	749.3	0.15	95.668	1.59434
22.060	0.373	0.303	0.324	51.98	118.81	751.8	0.15	101.862	1.52418
22.070	0.369	0.305	0.326	52.05	127.58	750.4	0.17	108.163	1.43208
22.080	0.372	0.305	0.323	52.03	99.95	750.3	0.13	76.547	1.59758
6.010	0.370	0.305	0.324	127.31	137.33	749.1	0.24	7.522	0.75072
6.020	0.370	0.305	0.324	127.39	152.22	750.0	0.24	17.910	0.72114
6.030	0.370	0.306	0.324	127.21	167.21	750.7	0.24	27.931	0.69820
6.040	0.370	0.306	0.324	127.27	202.05	750.8	0.27	50.542	0.67595
6.045	0.370	0.306	0.324	127.27	202.05	750.8	0.27	50.542	0.67595
26.010	0.371	0.305	0.324	-236.18	-226.87	501.2	0.13	5.193	0.55767
26.020	0.371	0.305	0.324	-236.17	-201.20	501.6	0.13	19.648	0.56183
26.030	0.371	0.305	0.324	-236.16	-181.50	499.9	0.10	30.878	0.56497
26.040	0.371	0.305	0.324	-236.14	-161.61	501.5	0.12	42.323	0.56788
31.010	0.375	0.305	0.321	-161.90	-147.41	501.3	0.12	8.487	0.58559
31.020	0.375	0.305	0.321	-161.92	-113.96	500.5	0.10	28.537	0.59503
31.030	0.373	0.304	0.323	-161.93	-90.84	499.3	0.08	42.761	0.60151
31.040	0.373	0.304	0.323	-161.94	-80.34	499.9	0.08	49.394	0.60530
32.010	0.358	0.305	0.338	-88.20	-78.73	500.0	0.06	5.971	0.63017
32.011	0.358	0.305	0.338	-88.14	-78.62	499.6	0.06	5.970	0.62684
32.020	0.359	0.307	0.333	-88.15	-58.43	499.0	0.08	19.118	0.64330
32.030	0.359	0.306	0.335	-88.14	-48.77	499.5	0.20	25.565	0.64932
32.040	0.363	0.305	0.332	-88.12	-38.65	500.1	0.24	36.466	0.73710
32.050	0.362	0.305	0.333	-88.11	-26.63	499.9	0.25	49.274	0.80142
32.060	0.363	0.308	0.330	-88.11	1.18	500.9	0.31	80.108	0.89714
32.070	0.361	0.306	0.332	-88.08	27.96	500.1	0.26	113.428	0.97751
32.080	0.361	0.306	0.332	-88.09	59.90	502.4	0.27	163.350	1.10378

TABLE B-19
(CONTINUED)

RUN NO.	COMPOSITION (MOLE FRACTION) CH4	C2H6	C3H8	INLET TEMP. (°F)	OUTLET TEMP. (°F)	INLET PRES. (PSIA)	PRES. DROP (PSID)	HEAT INPUT (BTU/LB)	MEAN HEAT CAPACITY (BTU/LB°F)
23.010	0.374	0.303	0.323	52.03	61.80	501.6	0.04	17.606	1.80153
23.011	0.374	0.303	0.323	52.01	61.84	502.0	0.04	17.576	1.78795
23.020	0.374	0.303	0.323	51.99	76.66	500.9	0.10	48.005	1.94634
23.030	0.374	0.303	0.323	51.95	82.68	501.2	0.17	62.130	2.02176
23.031	0.374	0.303	0.323	51.98	82.80	501.3	0.17	62.338	2.02260
23.040	0.374	0.303	0.323	52.03	91.64	502.5	0.09	73.242	1.84942
23.050	0.374	0.303	0.323	52.03	100.72	502.3	0.05	78.761	1.61739
23.060	0.374	0.303	0.323	52.02	114.06	499.0	0.04	86.758	1.39857
23.070	0.374	0.303	0.323	52.02	89.16	499.1	0.02	71.068	1.91358
23.080	0.374	0.303	0.323	52.05	127.50	498.8	0.15	95.670	1.26799
7.010	0.370	0.305	0.325	127.42	137.22	499.4	0.38	5.648	0.57649
7.015	0.370	0.305	0.325	127.42	137.22	499.4	0.38	5.655	0.57725
7.020	0.370	0.305	0.325	127.36	152.32	500.0	0.40	14.662	0.58740
7.030	0.369	0.305	0.325	127.48	167.45	499.9	0.42	23.097	0.57784
7.040	0.369	0.305	0.325	127.40	202.29	499.9	0.43	43.324	0.57858
38.010	0.369	0.304	0.327	191.69	201.03	500.0	0.33	5.341	0.57175
38.011	0.369	0.304	0.327	191.69	201.05	500.0	0.33	5.347	0.57158
38.020	0.369	0.304	0.327	191.79	218.14	502.6	0.34	15.111	0.57350
38.030	0.369	0.304	0.327	191.71	236.59	502.1	0.34	25.784	0.57442
38.040	0.369	0.304	0.327	191.68	265.67	501.9	0.39	42.849	0.57910
38.041	0.369	0.304	0.327	191.68	265.54	503.7	0.39	42.720	0.57841
27.010	0.369	0.305	0.326	-213.16	-204.25	251.2	0.15	5.081	0.56994
27.011	0.369	0.305	0.326	-213.16	-204.18	251.3	0.15	5.078	0.56575
27.020	0.369	0.305	0.326	-213.17	-180.80	250.0	0.15	18.406	0.56864
27.030	0.369	0.305	0.326	-213.14	-161.75	250.0	0.15	29.380	0.57168
27.040	0.369	0.305	0.326	-213.21	-135.07	249.6	0.15	44.977	0.57561
28.010	0.369	0.305	0.326	-133.87	-126.53	251.6	0.10	4.415	0.60135
28.020	0.369	0.305	0.326	-133.85	-109.69	251.7	0.27	18.209	0.75375
28.030	0.374	0.305	0.322	-133.84	-104.24	252.2	0.25	24.839	0.83921
28.040	0.374	0.305	0.322	-133.84	-98.26	251.8	0.29	31.921	0.89712
28.050	0.374	0.305	0.322	-133.89	-88.97	251.1	0.27	42.050	0.93611
28.060	0.371	0.302	0.326	-133.80	-53.95	249.9	0.29	78.784	0.98673
28.070	0.371	0.302	0.326	-133.84	-19.86	250.4	0.29	119.575	1.04910
24.010	0.378	0.302	0.320	-22.63	-12.82	252.5	0.29	13.882	1.41497
24.011	0.378	0.302	0.320	-22.69	-12.77	251.3	0.27	14.045	1.41492
24.020	0.381	0.301	0.318	-22.56	2.25	251.0	0.50	37.843	1.52531
24.030	0.379	0.303	0.318	-22.55	17.80	250.6	0.52	67.232	1.66600
24.040	0.379	0.303	0.318	-22.59	38.12	249.4	0.59	116.229	1.91447
24.041	0.379	0.303	0.318	-22.57	38.18	249.4	0.59	116.276	1.91411
24.050	0.379	0.303	0.318	-22.60	53.47	252.2	0.34	138.300	1.81822
21.010	0.368	0.307	0.325	51.97	61.94	252.2	1.23	5.185	0.52018
21.011	0.368	0.307	0.325	52.00	61.94	252.1	1.18	5.187	0.52154
21.020	0.368	0.307	0.325	52.03	77.05	250.1	1.18	12.794	0.51149
21.030	0.368	0.307	0.325	52.03	91.91	251.4	1.19	20.317	0.50939
21.040	0.369	0.307	0.325	52.05	110.77	251.3	1.23	29.741	0.50650
21.050	0.369	0.307	0.325	52.02	126.07	250.9	1.23	37.622	0.50802
21.060	0.369	0.307	0.325	52.05	55.29	250.2	0.98	1.735	0.53451
8.010	0.369	0.306	0.326	127.24	137.22	248.8	0.83	5.086	0.50964
8.020	0.368	0.305	0.327	127.46	152.33	249.4	0.83	12.725	0.51169
8.030	0.369	0.306	0.326	127.46	167.26	249.3	0.83	20.477	0.51446
8.040	0.369	0.306	0.326	127.48	202.35	249.3	0.89	38.871	0.51918

TABLE B-20

Basic Isothermal Data for Nominal 0.369 CH_4, 0.306 C_2H_6, 0.325 C_3H_8 Mixture

RUN NO.	COMPOSITION (MOLE FRACTION) CH4	C2H6	C3H8	INLET TEMP. (°F)	OUTLET TEMP. (°F)	INLET PRES. (PSIA)	PRES. DROP (PSID)	HEAT INPUT (BTU/LB)	ISOTHERMAL J.T.COEFF. (BTU/LB PSIA)
4.060	0.368	0.304	0.327	-16.04	-16.03	935.7	265.38	0.135	-0.00051
4.070	0.370	0.304	0.326	-16.16	-16.14	686.4	205.18	15.342	-0.07477
4.080	0.370	0.304	0.326	-16.13	-16.13	494.1	221.38	28.094	-0.12690
4.090	0.368	0.302	0.330	-16.04	-16.05	307.0	207.78	88.923	-0.42796
2.010	0.373	0.306	0.320	52.04	52.07	2020.5	122.59	0.341	-0.00278
2.011	0.373	0.306	0.320	52.01	52.03	2023.0	122.79	0.341	-0.00278
2.020	0.373	0.306	0.320	52.00	52.00	1913.6	123.39	0.383	-0.00310
2.021	0.373	0.306	0.320	51.96	51.96	1910.8	123.19	0.383	-0.00311
2.030	0.373	0.306	0.320	51.96	51.97	1794.0	118.89	0.439	-0.00369
2.031	0.373	0.306	0.320	52.11	52.11	1793.6	118.59	0.475	-0.00400
2.040	0.373	0.306	0.320	51.86	51.86	1679.1	117.99	0.517	-0.00438
2.041	0.374	0.305	0.321	52.09	52.09	1683.7	117.99	0.538	-0.00456
2.050	0.374	0.305	0.321	52.04	52.04	1569.1	118.39	0.679	-0.00574
2.051	0.374	0.305	0.321	51.87	51.89	1569.3	118.39	0.668	-0.00564
2.060	0.374	0.305	0.321	51.93	51.94	1457.6	116.59	0.780	-0.00669
2.061	0.372	0.306	0.321	51.85	51.86	1461.5	114.39	0.787	-0.00688
2.070	0.372	0.306	0.321	51.99	52.00	1348.7	118.59	1.001	-0.00844
2.071	0.372	0.306	0.321	51.99	52.00	1349.7	117.99	1.006	-0.00853
2.080	0.372	0.306	0.321	52.03	52.03	1232.8	137.19	1.534	-0.01118
2.081	0.372	0.306	0.321	52.02	52.03	1234.1	137.99	1.536	-0.01113
2.082	0.372	0.306	0.321	52.03	52.03	1232.8	137.19	1.543	-0.01125
2.090	0.371	0.306	0.322	52.00	52.00	1100.9	137.39	4.101	-0.02985
2.091	0.371	0.306	0.322	51.98	51.99	1101.2	135.79	3.889	-0.02864
2.110	0.371	0.306	0.322	52.04	52.07	987.0	131.39	8.866	-0.06748
2.111	0.371	0.306	0.322	52.08	52.10	986.7	131.39	8.882	-0.06760
2.120	0.373	0.306	0.321	52.05	52.06	997.8	58.59	3.643	-0.06217
2.121	0.373	0.306	0.321	52.12	52.13	997.8	58.19	3.657	-0.06284
7.010	0.366	0.304	0.330	52.33	52.34	1077.9	71.69	1.036	-0.01446
7.020	0.366	0.304	0.330	52.32	52.32	1077.0	104.79	2.669	-0.02547
7.030	0.366	0.304	0.330	52.30	52.31	1079.2	150.99	5.698	-0.03774
7.040	0.366	0.304	0.330	52.34	52.35	928.3	258.18	21.103	-0.08174
7.050	0.380	0.305	0.315	52.28	52.30	680.2	403.56	95.165	-0.23581
7.055	0.380	0.305	0.315	52.28	52.30	680.2	403.56	96.023	-0.23794
7.056	0.380	0.305	0.315	52.28	52.30	680.2	403.56	96.581	-0.23932
7.057	0.380	0.305	0.315	52.28	52.30	680.2	403.56	93.797	-0.23242
7.060	0.380	0.305	0.315	52.39	52.40	535.4	427.76	88.506	-0.20691
1.010	0.371	0.308	0.321	126.30	126.31	2000.0	158.99	2.732	-0.01719
1.011	0.371	0.308	0.321	126.27	126.28	2004.5	156.99	2.668	-0.01699
1.020	0.371	0.308	0.321	126.27	126.28	1837.3	160.69	3.746	-0.02331
1.030	0.371	0.308	0.321	126.26	126.28	1676.0	152.79	5.026	-0.03290
1.031	0.371	0.308	0.321	126.25	126.27	1675.9	152.39	5.008	-0.03286
1.040	0.371	0.308	0.321	126.24	126.26	1531.2	163.98	7.573	-0.04618
1.041	0.371	0.308	0.321	126.26	126.28	1531.1	166.58	7.727	-0.04638
1.050	0.372	0.306	0.323	126.25	126.28	1372.9	157.59	10.380	-0.06587
1.051	0.372	0.306	0.321	126.29	126.31	1371.4	158.39	10.563	-0.06669
1.060	0.372	0.306	0.323	126.27	126.31	1233.6	161.24	14.153	-0.08777
1.061	0.372	0.306	0.321	126.30	126.33	1232.6	164.38	14.323	-0.08713
1.070	0.372	0.306	0.323	126.23	126.26	1084.1	170.58	16.944	-0.09933
1.071	0.372	0.307	0.321	126.24	126.27	1085.2	171.78	17.148	-0.09982
1.080	0.372	0.307	0.321	126.21	126.24	922.3	158.49	14.683	-0.09265
1.081	0.372	0.307	0.321	126.24	126.27	921.7	158.59	14.683	-0.09259
1.090	0.372	0.307	0.321	126.24	126.26	771.1	178.18	14.057	-0.07889
1.091	0.372	0.307	0.321	126.23	126.25	771.1	177.88	13.949	-0.07842
1.100	0.374	0.303	0.323	126.22	126.24	605.7	167.68	11.245	-0.06706
1.110	0.374	0.303	0.323	126.26	126.27	448.2	172.38	10.018	-0.05811
1.120	0.374	0.303	0.323	126.50	126.50	278.7	165.78	8.585	-0.05178
6.010	0.368	0.305	0.327	191.67	191.72	2002.3	105.19	2.956	-0.02810
6.020	0.368	0.305	0.327	191.99	192.04	2005.0	196.58	6.256	-0.03183
6.030	0.368	0.305	0.327	191.96	191.97	1818.1	228.18	9.080	-0.03979
6.040	0.368	0.303	0.329	192.01	192.01	1593.2	270.77	13.232	-0.04887
6.050	0.368	0.303	0.329	192.01	192.02	1332.6	354.37	19.150	-0.05404
6.060	0.368	0.303	0.329	192.02	192.03	1008.7	255.78	13.268	-0.05187
6.070	0.367	0.304	0.329	192.01	192.03	765.4	256.38	12.325	-0.04807
6.080	0.367	0.304	0.329	192.05	192.06	521.2	277.77	12.067	-0.04344
6.090	0.367	0.304	0.329	192.05	192.06	339.7	234.98	9.711	-0.04047

TABLE B-21

Basic Isenthalpic Data for Nominal 0.369 CH_4, 0.306 C_2H_6, 0.325 C_3H_8 Mixture

RUN NO.	COMPOSITION (MOLE FRACTION) CH4	C2H6	C3H8	INLET TEMP. (°F)	OUTLET TEMP. (°F)	INLET PRES. (PSIA)	PRES. DROP (PSID)	HEAT INPUT (BTU/LB)	J.THOMSON COEFF. (°F/PSIA)
3.010	0.372	0.305	0.323	-236.48	-233.57	1999.4	436.96	0.000	-0.00666
3.011	0.372	0.305	0.323	-236.47	-233.55	1997.6	437.76	0.000	-0.00667
3.020	0.372	0.305	0.323	-236.57	-233.52	1586.4	455.96	0.000	-0.00669
3.030	0.365	0.303	0.332	-236.46	-233.88	1139.2	391.16	0.000	-0.00661
3.040	0.365	0.303	0.332	-236.40	-234.67	769.6	267.38	0.000	-0.00649
3.041	0.365	0.303	0.332	-236.46	-234.69	773.1	271.97	0.000	-0.00648
3.051	0.370	0.306	0.324	-236.51	-234.82	512.6	260.98	0.000	-0.00647
3.060	0.370	0.306	0.324	-236.40	-235.12	314.5	193.38	0.000	-0.00660
4.010	0.367	0.305	0.328	-16.03	-15.57	1981.5	230.98	0.000	-0.00199
4.020	0.367	0.305	0.328	-16.07	-15.68	1775.6	252.98	0.000	-0.00156
4.030	0.367	0.304	0.329	-16.09	-15.81	1529.9	271.37	0.000	-0.00104
4.040	0.367	0.304	0.329	-16.08	-15.98	1269.8	262.78	0.000	-0.00038
4.050	0.368	0.304	0.327	-16.11	-16.10	1022.1	107.59	0.000	-0.00008

APPENDIX C

Sample Results Involving the Smoothing of the Basic Data

TABLE C-1

Sample Results for PGC Corrections to the Basic Data as Applied to the Ternary Mixture

Isobaric

Run	Mole Fraction CH_4	C_2H_6	C_3H_8	T_i °F	T_o °F	P_i psia	ΔP psid	Q/F Btu/lb	Correction Factors For* Comp.	T_i to 127.40F	P_i to 500 psia	ΔP to 0 psid	ΔH Corrected Btu/lb	PGC Prediction Deviation Btu/lb	%
7.010	0.370	0.305	0.325	127.42	137.22	499.4	0.38	5.648	1.000	1.000	1.007	0.990	5.626	0.018	0.3
7.015	0.370	0.305	0.325	127.42	137.22	499.4	0.38	5.655	1.000	1.000	1.007	0.990	5.633	0.011	0.2
7.020	0.370	0.305	0.325	127.36	152.32	500.0	0.40	14.662	1.000	0.998	1.000	0.998	14.600	-0.321	-2.2
7.030	0.369	0.305	0.325	127.48	167.45	499.9	0.42	23.097	1.000	1.002	1.000	0.999	23.104	-0.184	-0.8
7.040	0.369	0.305	0.325	127.40	202.29	499.9	0.43	43.324	1.000	1.000	1.000	0.999	43.282	-0.511	-1.2

Isothermal

Run	Mole Fraction CH_4	C_2H_6	C_3H_8	T_i °F	T_o °F	P_i psia	ΔP psid	Q/F Btu/lb	Correction Factors For* Comp.	T_i to 192.00F	P_i unchanged	ΔT to 0°F	ΔH Corrected Btu/lb	PGC Prediction Deviation Btu/lb	%
6.010	0.368	0.305	0.327	191.67	191.72	2002.3	105.19	2.956	1.004	0.912	1.000	1.082	2.931	0.332	11.2
6.020	0.368	0.305	0.327	191.99	192.04	2005.0	196.58	6.256	1.004	1.000	1.000	0.993	6.234	0.157	2.5
6.030	0.368	0.305	0.327	191.96	191.97	1818.1	228.18	9.080	1.000	0.997	1.000	1.002	9.072	0.118	1.3
6.040	0.368	0.303	0.329	192.01	192.01	1593.2	270.77	13.232	0.996	1.001	1.000	0.999	13.181	0.402	3.0
6.050	0.368	0.303	0.329	192.01	192.02	1332.6	354.37	19.150	0.993	1.001	1.000	0.999	19.011	0.101	0.5
6.060	0.368	0.303	0.329	192.02	192.03	1008.7	255.78	13.268	0.994	1.002	1.000	0.998	13.183	0.008	0.1
6.070	0.367	0.304	0.329	192.01	192.03	765.4	256.38	12.325	0.992	1.001	1.000	0.998	12.213	-0.141	-1.1
6.080	0.367	0.304	0.329	192.05	192.06	521.2	277.77	12.067	0.995	1.003	1.000	0.997	12.008	-0.128	-1.1
6.090	0.367	0.304	0.329	192.05	192.06	339.7	239.98	9.711	0.997	1.003	1.000	0.996	9.675	-0.219	-2.3

* Corrected to the ternary composition of Table VI-3

TABLE C-2

a) The Results Obtained on Constructing an Equal Area $(\partial H/\partial P)_T$ Curve for the Ternary Mixture at 126.2°F Using a Non-Linear Least Squares Technique

Run No.	Inlet Pressure P_h (Psia)	Outlet Pressure P_l (Psia)	$\Delta H/\Delta P$ Expt. Btu/lb/°F	$\Delta H/\Delta P^*$ Calc. Btu/lb/psia	% Error
0.10100E 01	0.20000E 04	0.18410E 04	-0.17190E-01	-0.17207E-01	-0.98279E-01
0.10110E 01	0.20045E 04	0.18475E 04	-0.16990E-01	-0.16899E-01	0.53781E 00
0.10200E 01	0.18373E 04	0.16766E 04	-0.23310E-01	-0.24012E-01	-0.30134E 01
0.10300E 01	0.16760E 04	0.15232E 04	-0.32900E-01	-0.31519E-01	0.41979E 01
0.10310E 01	0.10000E 01	0.10000E 01	-0.46500E-01	-0.46121E-01	0.81605E 00
0.10400E 01	0.15312E 04	0.13672E 04	-0.46180E-01	-0.46078E-01	0.22176E 00
0.10410E 01	0.15311E 04	0.13645E 04	-0.46380E-01	-0.46264E-01	0.24970E 00
0.10500E 01	0.13729E 04	0.12153E 04	-0.65870E-01	-0.67876E-01	-0.30450E 01
0.10510E 01	0.13714E 04	0.12130E 04	-0.66690E-01	-0.68149E-01	-0.21877E 01
0.10600E 01	0.12336E 04	0.10724E 04	-0.87770E-01	-0.85215E-01	0.29110E 01
0.10610E 01	0.12326E 04	0.10682E 04	-0.87130E-01	-0.85419E-01	0.19639E 01
0.10700E 01	0.10841E 04	0.91352E 03	-0.99330E-01	-0.99743E-01	-0.41567E 00
0.10710E 01	0.10852E 04	0.91342E 03	-0.99820E-01	-0.99671E-01	0.14922E 00
0.10800E 01	0.92230E 03	0.76381E 03	-0.92650E-01	-0.94061E-01	-0.15230E 01
0.10810E 01	0.92170E 03	0.76311E 03	-0.92590E-01	-0.94012E-01	-0.15355E 01
0.10900E 01	0.77110E 03	0.59292E 03	-0.78890E-01	-0.78468E-01	0.53455E 00
0.10910E 01	0.77110E 03	0.59322E 03	-0.78420E-01	-0.78483E-01	-0.80339E-01
0.11000E 01	0.60570E 03	0.43802E 03	-0.67060E-01	-0.64885E-01	0.32435E 01
0.11100E 01	0.44820E 03	0.27582E 03	-0.58110E-01	-0.57745E-01	0.62896E 00
0.11200E 01	0.27870E 03	0.11292E 03	-0.51780E-01	-0.53329E-01	-0.29914E 01

b) Computer Aided Interpolation and Integration of Equal Area $(\partial H/\partial P)_T$ Curve for the Ternary Mixture at 126.2°F.

Pressure P, (Psia)	dH/dP Btu/lb/psia	$\int_o^P (\frac{dH}{dP})_T dP/P$ Btu/lb/psia	H - H° Btu/lb
0.	-0.46070E-01	-0.46070E-01	0.0
0.50000E 02	-0.48424E-01	-0.47278E-01	-0.23639E 01
0.10000E 03	-0.50418E-01	-0.48364E-01	-0.48364E 01
0.15000E 03	-0.52096E-01	-0.49336E-01	-0.74005E 01
0.20000E 03	-0.53520E-01	-0.50209E-01	-0.10042E 02
0.25000E 03	-0.54777E-01	-0.50999E-01	-0.12750E 02
0.30000E 03	-0.55980E-01	-0.51728E-01	-0.15519E 02
0.35000E 03	-0.57266E-01	-0.52426E-01	-0.18349E 02
0.40000E 03	-0.58794E-01	-0.53123E-01	-0.21249E 02
0.45000E 03	-0.60733E-01	-0.53856E-01	-0.24235E 02
0.50000E 03	-0.63240E-01	-0.54664E-01	-0.27332E 02
0.55000E 03	-0.66437E-01	-0.55583E-01	-0.30571E 02
0.60000E 03	-0.70380E-01	-0.56647E-01	-0.33988E 02
0.65000E 03	-0.75023E-01	-0.57878E-01	-0.37621E 02
0.70000E 03	-0.80196E-01	-0.59285E-01	-0.41499E 02
0.75000E 03	-0.85589E-01	-0.60858E-01	-0.45644E 02
0.80000E 03	-0.90758E-01	-0.62568E-01	-0.50054E 02
0.85000E 03	-0.95148E-01	-0.64361E-01	-0.54707E 02
0.90000E 03	-0.98148E-01	-0.66162E-01	-0.59546E 02
0.95000E 03	-0.99150E-01	-0.67882E-01	-0.64488E 02
0.10000E 04	-0.97631E-01	-0.69419E-01	-0.69419E 02
0.10500E 04	-0.93214E-01	-0.70669E-01	-0.74203E 02
0.11000E 04	-0.89861E-01	-0.71602E-01	-0.78762E 02
0.11500E 04	-0.86154E-01	-0.72321E-01	-0.83169E 02
0.12000E 04	-0.80886E-01	-0.72793E-01	-0.87351E 02
0.12500E 04	-0.74392E-01	-0.72990E-01	-0.91238E 02
0.13000E 04	-0.67130E-01	-0.72906E-01	-0.94778E 02
0.13500E 04	-0.59604E-01	-0.72553E-01	-0.97946E 02
0.14000E 04	-0.52292E-01	-0.71958E-01	-0.10074E 03
0.14500E 04	-0.45588E-01	-0.71163E-01	-0.10319E 03
0.15000E 04	-0.39765E-01	-0.70210E-01	-0.10532E 03
0.15500E 04	-0.34952E-01	-0.69148E-01	-0.10718E 03
0.16000E 04	-0.31147E-01	-0.68017E-01	-0.10883E 03
0.16500E 04	-0.28231E-01	-0.66854E-01	-0.11031E 03
0.17000E 04	-0.26000E-01	-0.65684E-01	-0.11166E 03
0.17500E 04	-0.24198E-01	-0.64523E-01	-0.11292E 03
0.18000E 04	-0.22544E-01	-0.63380E-01	-0.11408E 03
0.18500E 04	-0.20760E-01	-0.62253E-01	-0.11517E 03
0.19000E 04	-0.18579E-01	-0.61134E-01	-0.11615E 03
0.19500E 04	-0.15761E-01	-0.60008E-01	-0.11702E 03
0.20000E 04	-0.12091E-01	-0.58858E-01	-0.11772E 03

* Calculated using the equation

$$\left(\frac{dH}{dP}\right)_T = -0.0457 - 0.1742\times10^{-4}P - 0.8661\times10^{-7}P^2 + 0.1163\times10^{-9}P^3 - 0.3250\times10^{-3}P^4$$

$$-(0.1018\times10^{2})(0.3397\times10^{-2})e^{-0.003397(P - 1012.1)^2}$$

The equation is plotted as the dashed curve in Figure VIII-52

TABLE C-3a

Computer Aided Consistency Check Results for Graphically Determined Equal Area Cp Curve as Illustrated for Ethane at 819 psia.

T_i (°F)	T_f (°F)	$(\frac{\Delta H}{\Delta T})$ Fxpt* Btu/lb/°F	$(\frac{\Delta H}{\Delta T})$ Cal** Btu/lb/°F	Percent Error	$(C_p)_{T_i}$ Btu/lb/°F	$(C_p)_{T_f}$ Btu/lb/°F
0.9937D 02	0.1023D 03	0.4516D 01	0.4472E 01	0.957E 00	0.3456E 01	0.5453E 01
0.9937D 02	0.1044D 03	0.4857D 01	0.4839E 01	0.368E 00	0.3456E 01	0.4807E 01
0.9937D 02	0.1033D 03	0.4706D 01	0.4735E 01	-.617E 00	0.3456E 01	0.5531E 01
0.9937D 02	0.1003D 03	0.3747D 01	0.3760E 01	-.329E 00	0.3456E 01	0.4107E 01
0.9937D 02	0.1014D 03	0.4136D 01	0.4137E 01	-.234E-01	0.3456E 01	0.4893E 01
0.9937D 02	0.1023D 03	0.4485D 01	0.4479E 01	0.134E 00	0.3456E 01	0.5460E 01
0.9937D 02	0.1033D 03	0.4712D 01	0.4735E 01	-.487E 00	0.3456E 01	0.5531E 01
0.9937D 02	0.1044D 03	0.4864D 01	0.4839E 01	0.507E 00	0.3456E 01	0.4831E 01
0.9937D 02	0.1054D 03	0.4782D 01	0.4773E 01	0.185E 00	0.3456E 01	0.4130E 01
0.9937D 02	0.1054D 03	0.4792D 01	0.4771E 01	0.430E 00	0.3456E 01	0.4119E 01
0.1003D 03	0.1023D 03	0.4849D 01	0.4835E 01	0.305E 00	0.4107E 01	0.5460E 01
0.1023D 03	0.1044D 03	0.5415D 01	0.5363E 01	0.961E 00	0.5460E 01	0.4831E 01
0.1023D 03	0.1044D 03	0.5337D 01	0.5356E 01	-.354E 00	0.5453E 01	0.4807E 01
0.1023D 03	0.1054D 03	0.5067D 01	0.5055E 01	0.237E 00	0.5460E 01	0.4130E 01
0.1023D 03	0.1054D 03	0.5084D 01	0.5049E 01	0.685E 00	0.5460E 01	0.4119E 01
0.1003D 03	0.1033D 03	0.5032D 01	0.5059E 01	-.533E 00	0.4107E 01	0.5531E 01
0.1003D 03	0.1054D 03	0.4993D 01	0.4966E 01	0.542E 00	0.4107E 01	0.4119E 01
0.1033D 03	0.1044D 03	0.5424D 01	0.5224E 01	0.370E 01	0.5531E 01	0.4831E 01
0.1033D 03	0.1054D 03	0.4913D 01	0.4845E 01	0.139E 01	0.5531E 01	0.4130E 01
0.1033D 03	0.1054D 03	0.4939D 01	0.4838E 01	0.204E 01	0.5531E 01	0.4119E 01
0.1044D 03	0.1054D 03	0.4458D 01	0.4456E 01	0.523E-01	0.4831E 01	0.4119E 01

* These values differ from those for runs 40 and 51 in Table B-2 as they have been corrected for pressure level, pressure drop and variable inlet temperature as explained in section VII.

** Calculated from the results in Table C-3b.

TABLE C-3b

Computer Aided Interpolation and Integration of Equal Area Cp Curve as Illustrated for Ethane at 819 Psia.

T_i (°F)	T_f (°F)	$(C_p)_{T_i}$ Btu/lb/°F	$(C_p)_{T_f}$+ Btu/lb/°F	$[\int_{T_i}^{T_f} CpdT]_{Cal}$++ Btu/lb/°F	$[\int_{99°F}^{T_f} CpdT]_{Cal}$ Btu/lb/°F
0.9900D 02	0.9950D 02	0.3250D 01	0.3530D 01	0.1695D 01	0.1695E 01
0.9950D 02	0.1000D 03	0.3530D 01	0.3840D 01	0.1840D 01	0.3535E 01
0.1000D 03	0.1005D 03	0.3840D 01	0.4225D 01	0.2015D 01	0.5550E 01
0.1005D 03	0.1010D 03	0.4225D 01	0.4590D 01	0.2204D 01	0.7754E 01
0.1010D 03	0.1015D 03	0.4590D 01	0.4980D 01	0.2394D 01	0.1015E 02
0.1015D 03	0.1020D 03	0.4980D 01	0.5300D 01	0.2571D 01	0.1272E 02
0.1020D 03	0.1022D 03	0.5300D 01	0.5410D 01	0.1072D 01	0.1379E 02
0.1022D 03	0.1024D 03	0.5410D 01	0.5480D 01	0.1090D 01	0.1488E 02
0.1024D 03	0.1025D 03	0.5480D 01	0.5500D 01	0.5491D 00	0.1543E 02
0.1025D 03	0.1030D 03	0.5500D 01	0.5520D 01	0.2759D 01	0.1819E 02
0.1030D 03	0.1034D 03	0.5520D 01	0.5500D 01	0.2211D 01	0.2040E 02
0.1034D 03	0.1036D 03	0.5500D 01	0.5460D 01	0.1091D 01	0.2149E 02
0.1036D 03	0.1040D 03	0.5400D 01	0.5120D 01	0.2106D 01	0.2360E 02
0.1040D 03	0.1045D 03	0.5120D 01	0.4730D 01	0.2462D 01	0.2606E 02
0.1045D 03	0.1050D 03	0.4730D 01	0.4390D 01	0.2278D 01	0.2834E 02
0.1050D 03	0.1055D 03	0.4390D 01	0.4092D 01	0.2118D 01	0.3046E 02
0.1055D 03	0.1060D 03	0.4092D 01	0.3850D 01	0.1985D 01	0.3244E 02

\+ Cp values are obtained from graphical smoothing of the basic data as shown in Figure VIII-8.

++ The integral is estimated using the Gauss-Legendre Quadrature [40]. The Lagrange interpolating polynomial for the integration is generated using five contiguous points with T_i and T_f as the central points.

APPENDIX D

Equipment Summary

Item No.	Equipment or Material Specification	Function
1	Calorimeters and Accessories	
1a	Isobaric Calorimeter: Construction details in reference [79]. Modified heater capsule drawings in Appendix E of this work.	Basic apparatus for isobaric calorimetric measurements from -240°F to + 300°F and up to 2000 psi.
1b	Throttling Calorimeter: Construction details in reference [168]. Modifications described on page 147 of this work.	Basic apparatus for isothermal and isenthalpic measurements over the above range of conditions.
1c	AP 10-16 temperature compensated coupling using C1344A-TEF, hollow stainless steel double teflon coated gaskets. The D.S.D. Co., Hamden, Conn.	Pressure sealing device for throttling calorimeter.
1d	16-19 B&S gage hypodermic tubing, (0.008" wall), C.A. Roberts, Detroit, Michigan.	Element causing pressure drop in throttling calorimeter.
1e	GTC 100, thermocouple vacuum gauge, 0-1000 microns, Consolidated Vacuum Corp., Rochester, N.Y.	Original vacuum indicator for either calorimeter.
1f	Televac, thermocouple vacuum gauge 0-1000 microns, Huntingdon Valley, Penn.	Replacement vacuum indicator for either calorimeter.
1g	RPS-MTG-24-L, and MTG-24-A2L Sealing glands, Conax Corp., Buffalo, N.Y.	Pressure to vacuum sealing device for the throttling and isobaric calorimeter respectively.
1h	26 B &S gage, nichrome heater wire with double glass insulation and silicone binder 2.594 ohms/ft. Driver-Harris Co., Harrison, N.J.	Original heater wire supplying energy input to calorimeters.
1i	26 B &S gage, "Moleculoy" wire with 0.026 double glass insulation and Hi-Mol binder, 2.557 ohms/ft. Molecu-wire Co., Farmingdale, N.J.	Improved substitute for original heater wire.

1j	30 B &S gage, Constantan wire. Leeds and Northrup, Philadelphia, Penn.	Used in preparation of multijunction Cu/Constantan thermocouple wires for both calorimeters.
1k	36 B &S gage, (.005") Copper wire Consolidated Wire Co., Chicago, Illinois.	
1l	Apiezon N grease	Improvement of thermal contact between thermocouple and thermowell surface.
1m	CN-967, Beryllia epoxy thermally conductive resin, and CN-773 thermally conductive resin. Mereco Inc., Cranston, R.I.	Materials for binding heater wire to the isobaric calorimeter heater capsule.
1n	SS-4UK-SW-TEF Bellows stainless valve operating range from -300°F to +600°F, Nupro Inc., Cleveland, Ohio.	Shut off valves in calorimeter bath to permit switching of the flow stream from one calorimeter to the other.
2	A2CCV50/250, 2 stage Diaphragm Compressor with remote heads, Corblin, Paris, France.	Compression and recirculation of the system fluid in the gaseous state up to 2700 psia.
3	Electrical Measurement Equipment & Accessories	
3a	No. 7553, Type K-3 Universal Potentiometer Leeds and Northrup, Philadelphia, Penn.	Measurement of voltages: Power input, thermocouple output, pressure and differential pressure transducer input and output, Pt. resistance thermometer output.
3b	Unsaturated Cadmium Sulfate standard cell, Eppley Laboratories, Inc.	Reference voltage for potentiometer
3c	No. 9834, D.C. Null Detector (Maximum sensitivity of 0.1μv/scale div.), Leeds and Northrup, Philadelphia, Penn.	Null point indicator for K-3 potentiometer.
3d	Model 2500 A. Type R Reflecting Mirror Galvanometer. With a sensitivity of 0.47μv/mm at 1 meter, Leeds and Northrup, Philadelphia, Penn.	Indication of Emf of differential thermocouple between guard heater, and heater capsule.

4	SM 325-2A(M)X, D.C. Power Supply, 0.01% line and 0.05% load regulation respectively, Kepco Inc., Flushing, N.Y.	Power supply to either calorimeter, limited to 325 volts or 2 amps.
5	8163-B, Platinum Resistance Thermometer, Leeds and Northrup, Philadelphia, Penn.	Measurement of calorimeter bath temperature
5a	162C, Platinum Resistance Thermometer, -200°C to 500°C, Rosemount Engineering, Minneapolis, Minn.	
6	SY 152 113(W)-93-11(v) Temperature Controller, Honeywell Inc., Minneapolis, Minn. with Model 73N12 Pneumatic Controller, Conoflo Corp. Philidelphia, Penn.	Control of calorimeter bath temperature from -250°F to +300°F in conjunction with a variable Ni resistor.
7	Model 243, Electronic Temperature Controller, Bailey Instruments, Danville, Conn.	Control of preconditioning bath temperature.
8	Flow Measurement and Calibration	
8a	50MJ10-1/4, Laminar Flow Element, 0.4SCFM at 4" water differential, Meriam Instrument Co., Cleveland, Ohio.	Measurement of mass flow through calorimeter.
8b	Model M12, Water Manometer, 0-10" water. National Instrument Co., New York, N.Y.	Measurement of pressure drop at the flowmeter with an accuracy of 0.001".
8c	180 inch Mercury Manometer. King Eng. Co., Ann Arbor, Mich.	Measurement of pressure at the flowmeter.
8d	Model 15-180-15 Mercury Thermoregulator, and Model 130 Transitor Relay, Fisher Scientific, Detroit, Mich.	Control of flowmeter bath temperature to 27 $\pm$ 0.2°C.
8e	Model 6R-6M-50-SS, Relief venting valve, Nupro Inc., Cleveland, Ohio.	Relief of flowmeter pressure above 100 psig.
8f	Model 1014, 30" vacuum to 150 psig gages. Ashcroft Inc., Stratford, Conn.	Measurement of pressure in collection cylinders during flowmeter calibration.

8g	No. 83027 H.R., 3 way Solenoid Switch, American Switch Co., Florham Park, N.J.	Switch to transfer flow from reservoir cylinder to collection cylinder and vice versa
8h	Model 26-1521-24-067, 0-150 psig, hand loaded non-relieving stainless steel regulator. Tescom Inc., Minneapolis, Minn.	Control of flowmeter pressure during calibration.
9	Composition Measurement	
9a	Custom portable chromatograph with thermal conductivity detector. Phillips Petroleum, Bartlesville, Oklahoma	Measurement of system composition.
9b	No. 64101 Speedomax G, adjustable chart speed chromatographic recorder. Leeds and Northrup, Philadelphia, Penn.	Recording of chromatographic output.
9c	30% Hexa-methyl-phosphor amide (H.M.P.A.) on 60-80 mesh Columpak. Fisher Chemicals, Detroit, Michigan.	Materials for chromatographic column for separation of methane, ethane, and propane.
9d	No. A-540, Adsorption Alumina, Fisher Chemicals, Detroit, Michigan.	
10	Calorimeter Pressure and Differential Pressure Measurement	
10a	Model 260-W.G., Dead Weight Gauge. Mansfield and Green, Cleveland, Ohio.	Measurement of pressure at calorimeter inlet.
10b	Model 2416-2 Differential Pressure Null Indicator and Model 2413-5 Gas to Oil Pressure Transmitter. Ruska Instruments, Houston, Texas.	
10c	PT 119 HDC-2500 Temperature compensated (75°F-250°F) Strain Gage Pressure Transducers (3 millivolts/volt full scale). Dynisco, Cambridge, Mass.	Pressure measurement at calorimeter inlet and outlet upto a maximum of 2500 psia.
10d	PT-98D-2M ±1000 Temperature compensated Differential Pressure Transducer (2 millivolts/volt full scale). Dynisco, Cambridge, Mass.	Measurement of differential pressure across the throttling calorimeter with a maximum range of 1000 psid.

10e	Model 30-FA-200, high pressure well type 40" differential pressure manometer. Meriam Instrument Co., Cleveland, Ohio.	Measurement of differential pressure across isobaric calorimeter.
10f	KG 25-0 2-0.2(c) D.C. Power Supply, 0.005% load regulation, 0 to 25 volts, and upto 0.2 amps, Kepco Inc., Flushing, N.Y.	Exitation voltage source for all transducers.
10g	Model X500, 3" length, flat glass reflex liquid level gages, Penberthy Inc., Prophetstown, Illinois.	Sightglasses for visual examination of mercury level in gas to oil U leg connected to the calorimeter exit.
11	Model 156x62-P12, Brown Potentiometer Pyrometer. Honeywell Inc., Minneapolis, Minn.	Multipoint temperature indicator over the range -250°F to +150°F
12	Model 10-11-AF6 shut-off valves with Teflon O rings, and Model 30-11 HF4-cc- 316 calibrated control valves with viton O rings. High Pressure Equipment Co., Erie, Penn.	Shut off and throttling valves used in the control valve mainfold.
13	Model 6AVD-B Filter Dryers, with AC1, Activated charcoal dessicant. King Engineering, Ann Arbor, Mi. and Molecular Sieves 3a and 4a, Linde, Cleveland, Ohio.	Adsorption of oil and unsaturated hydrocarbon impurities at the flowmeter and bypass streams.
14	Calibration Manometer	
14a	OKS2 shutoff, and ORS2 regulating stainless steel valves. Whitey Research Tool Co., Emeryville, California.	Used to construct the calibration valve manifold which controls the calibration manometer.
14b	LC-621, 200-2300 psia outlet Relief venting regulator. Standard Pneumatic, Hemet, California.	Regulation of pressure at each leg of the differential manometer.
14c	SVR-3, 11 7/8" length, flat glass reflex liquid level gages. Strahman, Inc. Illinois.	Sight glasses for visual examination of mercury level at the manometer.
14d	Model M-911, Cathetometer. Gaertner Inc., Chicago, Illinois.	Measurement of mercury column levels with respect to a reference scale at the 200" Diff. Press. Manometer

14e	300 inch steel tape. Lufkin Rule Co., Saginaw, Michigan.	Reference scale for measuring the height of any mercury column.
14f	Model 1502-DGS-1. Filter-Fink Differential Pressure Indicator 0-1000 psid, upto 2000 psia with variable differential pressure setpoint for the activation of an electric contact. Orange Research, East Orange, N.J.	Indicates the approximate height of any given mercury column. (For the 200" Diff. Press. Manometer)
14g	No. 8267C79, stainless steel normally closed 2,3,4 way solenoid valve. American Switch Co., Florham Park, N.J.	Used in conjunction with the above device to prevent any mercury column height from exceeding 210".
15	Materials	
15a	Methane, 99.8%, Southern California Gas Co., Bowerbank Well, Taft, California.	Used in preparation of system mixtures containing methane.
15b	Methane, Ultra-High Purity, (less than 50 ppm impurity content). Matheson Co., Joliet, Ill.	Used in preparation of reference mixtures containing methane.
15c	Ethane, 99.5% min., Pure Grade, and Ethane, 99.99% min., Research Grade, Phillips Petroleum, Bartlesville, Oklahoma.	Used in preparation of system and reference mixtures respectively, that contain ethane.
15d	Propane, 28 gallons, Instrument Grade 99.9%, and Propane, 99.99% min., Research Grade, Phillips Petroleum, Bartlesville, Oklahoma.	Used in preparation of system and reference mixtures respectively, that contain propane.
15e	Isopentane, Technical Grade. Phillips Petroleum, Bartlesville, Oklahoma.	Calorimeter bath fluid in the range -240°F to -60°F.
15f	#200 Silicone Fluid. Dow-Corning Corp., Midland, Michigan.	Calorimeter bath fluid in the range -60°F to +300°F.
15g	Coating No. 756, Front surface mirrors. Libby Owens Ford, Detroit, Michigan.	To permit the observation of the calibration manometer sight glasses at the cathetometer by reflection.

APPENDIX E

Detailed Drawings for the Modified Heater Capsule
of the Isobaric Calorimeter

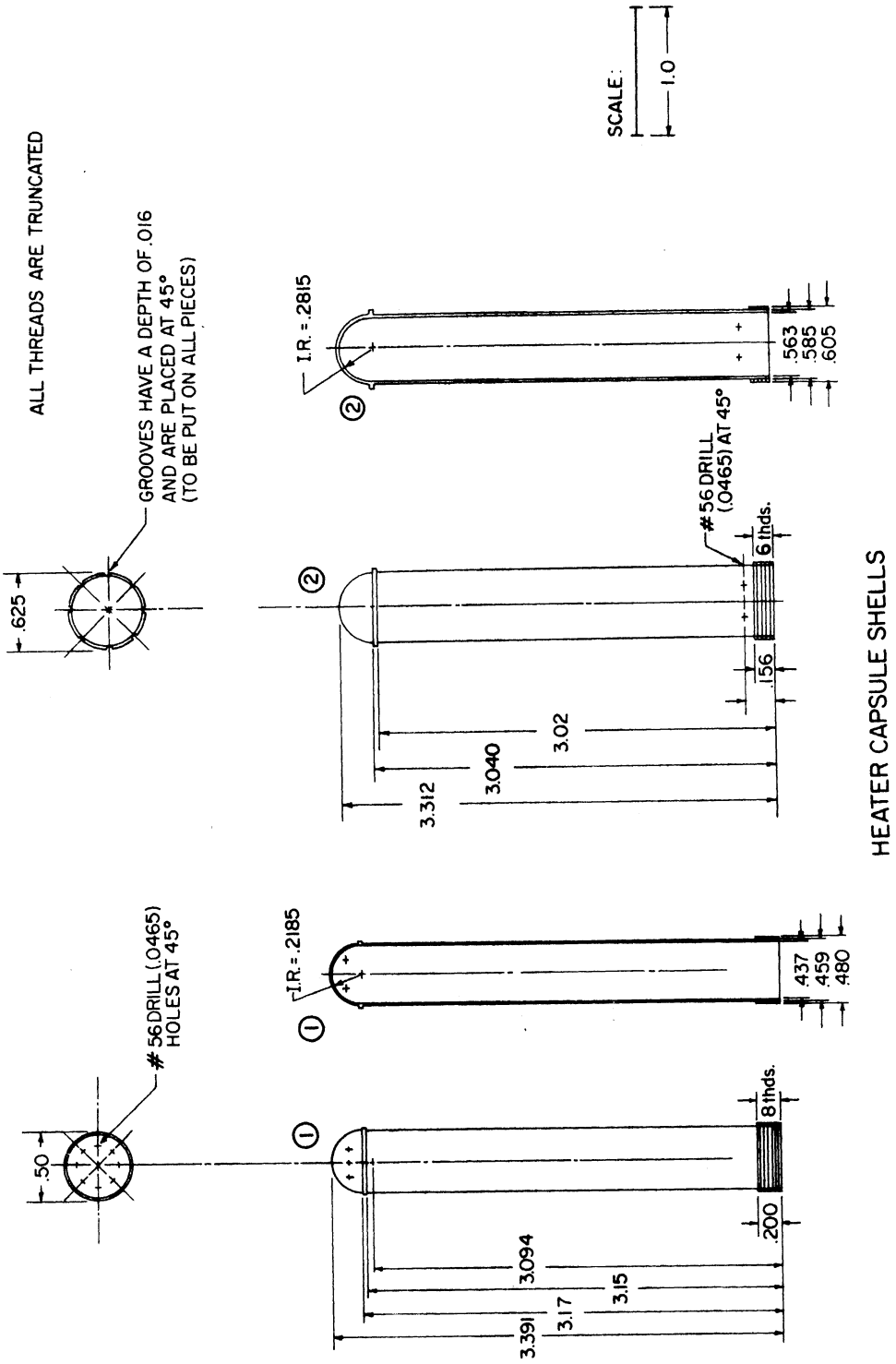

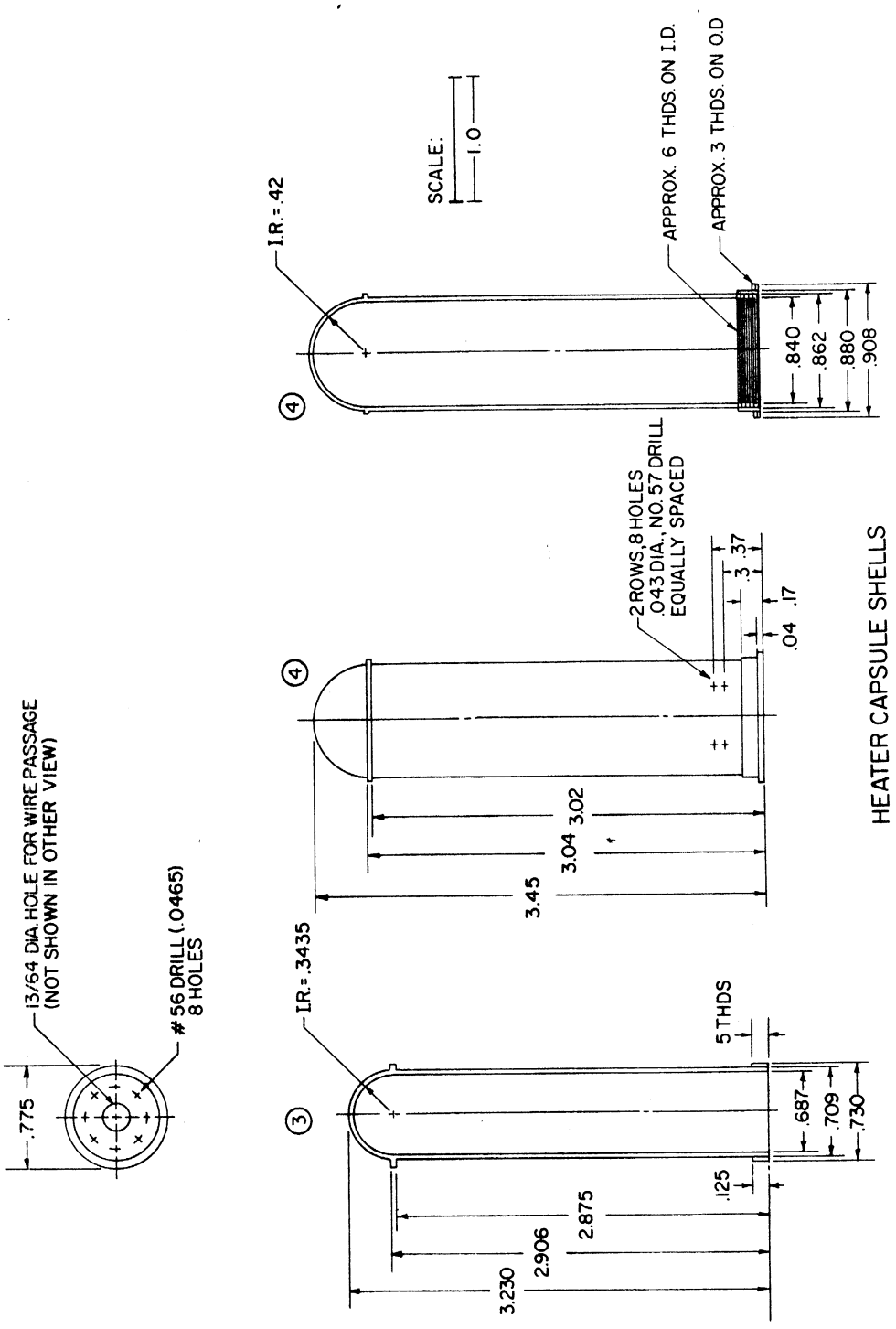

HEATER CAPSULE SHELLS

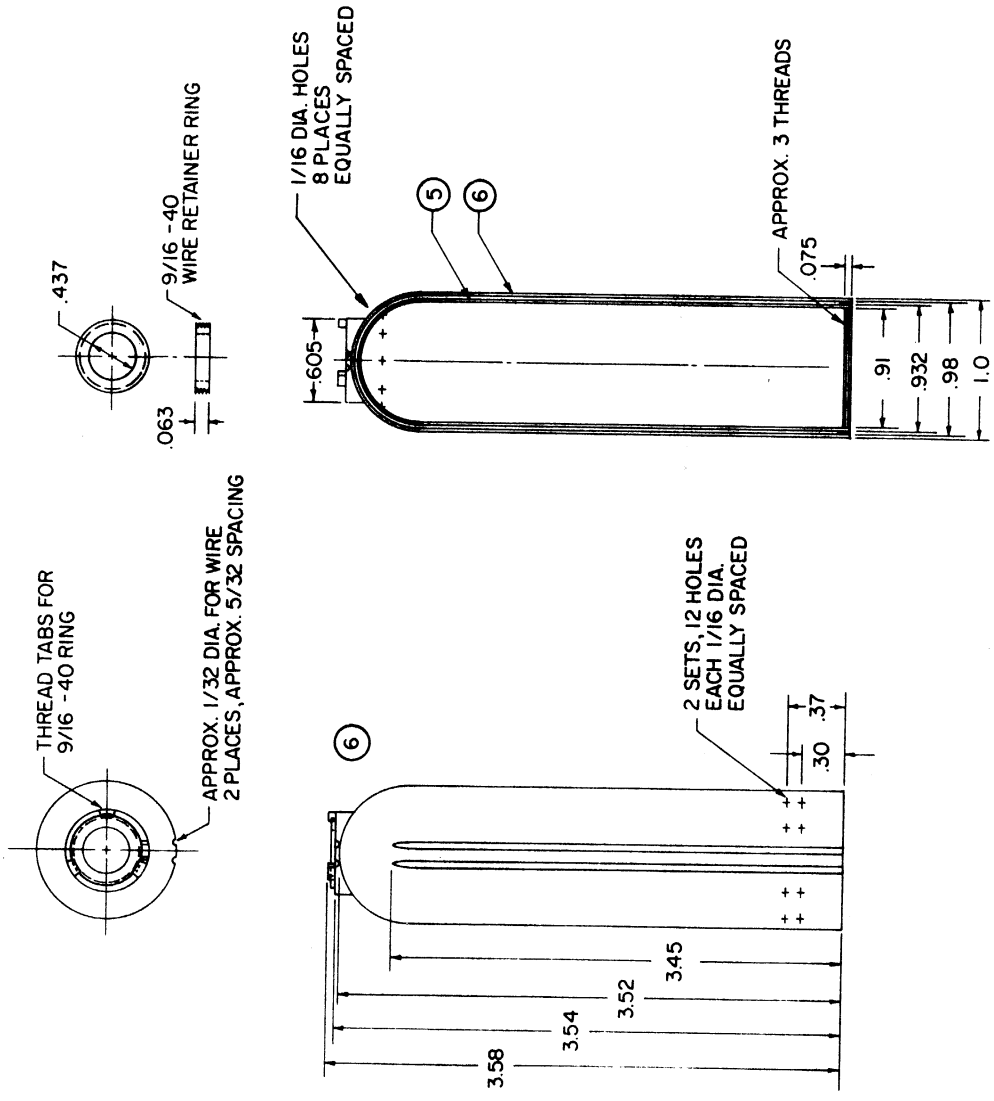

HEATER CAPSULE SHELLS

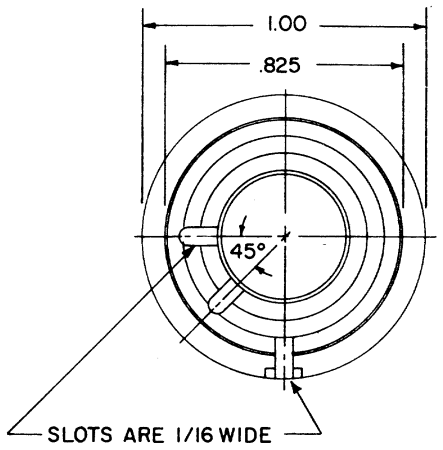

THREAD DIMENSIONS

① These threads must match those on shell one
② " " " " " " " two
③ " " " " " " " three
④ " " " " " " " on inside of shell five

(All threads shallow 40 threads / inch, NF)

SCALE:

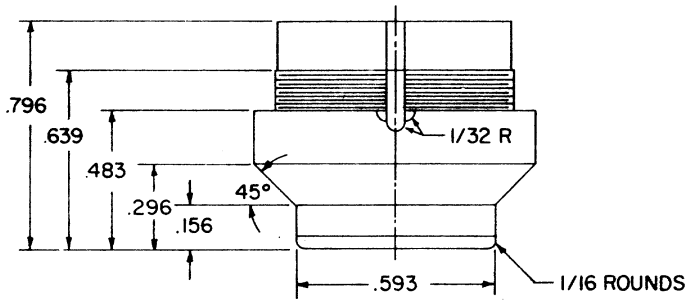

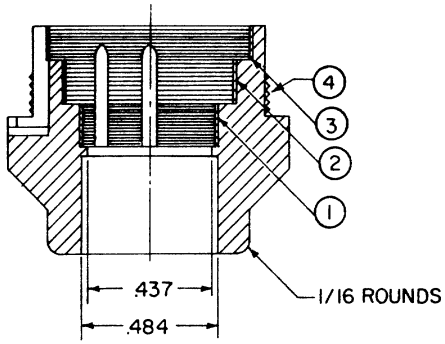

CAPSULE MOUNT

APPENDIX F

Sample Calculations

Appendix F-1

Calculation of Mass Flowrate

System: - 0.276 C_2H_6 - C_3H_8

Run: - 4.020

Relevant Data

Mercury manometer reading for flowmeter pressure,	P_{fg}	= 157.56 in. Hg
Temperature of scale on manometer,	T_{ps}	= 78.0°F
Temperature of mercury in manometer,	T_{pm}	= 78.0°F
Barometric pressure,	P_{bar}	= 29.20 in. Hg.
Barometric temperature,	T_{bar}	= 78.44°F
Flowmeter bath temperature,	T_f	= 27.08°C
Reading on left hand side of water manometer,	R_h	= 9.180 in. H_2O
Reading on right hand side of water manometer,	R_l	= 3.005 in. H_2O
Zero error correction for water manometer,	R_o	= + 0.006 in. H_2O
Molecular weight of mixture,	W_m	= 40.21

a) Calculation of gas density

The density of the fluid stream at the flowmeter is computed from the virial equation truncated at the second virial coefficient. The individual pure component and interaction second virial coefficients and their variation with temperature in the vicinity of 27°C are summarized in Table F-1 below

Table F-1

Virial Coefficient Data for Calculation of Gas Density at the Flowmeter

System	Reference	$B_{298.15K}$ $cm^3/mole$	$[dB/d(1/T)]\times10^{-5}_{298.15K}$ cc °K/mole	$B_{27.08°C}$ $cm^3/mole$
CH_4	[67]	-42.82	0.331	-42.05
C_2H_6	[174]	-185.6	1.12	-182.99

Table F-1. Continued

C_3H_8	[122,123]	-388.0	3.08	-380.84
CH_4-C_2H_6	[59]	-93.1	0.539	-91.84
CH_4-C_3H_8	[59]	-139.0	0.539	-136.94
C_2H_6-C_3H_8	[59]	-274.0	0.885	-270.07

The B values at the flowmeter bath temperature T_f are in each case calculated from the equation

$$(B)_{T_f} = B_{298.15} + \left[\frac{dB}{d(\frac{1}{T})}\right]_{298.15} \frac{(T_f - 298.15)}{(T_f)(298.15)} \qquad \text{(F1-1)}$$

These results are also reported in Table F-1. The mixture virial coefficient is then calculated using the relation:

$$(B_{mix})_{27.08°C} = \sum_{i=1}^{n} \sum_{j=1}^{n} x_i x_j B_{ij} \qquad \text{(F1-2)}$$

Thus

$$\begin{aligned} B_{mix} &= (0.001)^2(-42.05) + (0.2747)^2(-182.99) + (0.7248)^2(-380.84) \\ &+ (2)(0.001)(0.2747)(-93.1) + (2)(0.2747)(.7248)(-270.07) \\ &+ (2)(0.7248)(0.001)(-136.94) \\ &= -321.5 \text{ cm}^3/\text{mole} \end{aligned}$$

The pressure P_{fo} at the flowmeter outlet in psia is given by

$$P_{fo} = P_{fg} F_s G_{fg} + P_{bar} G_{bar} \qquad \text{(F1-3)}$$

where

$$F_s = 1. + 13.34\text{x}10^{-6}(T_{ps} - 68°F) \qquad \text{(F1-4)}$$

$$G_{fg} = 0.4894\ [1 - 99\text{x}10^{-5}(T_{pm} - 68°F)] \qquad \text{(F1-5)}$$

$$G_{bar} = 0.4912\ [1 - \frac{0.00275}{P_{bar}}(T_{bar} - 32°C)] \qquad \text{(F1-6)}$$

F_s is the temperature correction factor for the scale of the 180 inch mercury manometer. G_{fg} involves a conversion of the mercury column

height as a function of temperature into psi units. G_{bar} involves the conversion of the barometer reading in inches of mercury to psi and was developed by Jones [119] from the manufacturer's calibration included in his thesis. Thus:

$$P_{fo} = (157.56)(0.4894)[1 - 9.9\times10^{-5}(78.-68.)][1. + 13.34\times10^{-6}(78.-68.)] + (29.2)(0.49115)[1 - (\frac{0.00275}{29.20})(78.44 - 32.)]$$
$$= 91.32 \text{ psia}$$

The approximate pressure drop at the flowmeter is given by

$$\Delta P_{approx} = R_h - R_1 - R_o = 9.180 - 3.005 - 0.006$$
$$= 6.169 \text{ in. } H_2O \qquad \text{(F1-7)}$$

Average pressure at flowmeter, $P_f = P_{fo} + (\frac{\Delta P}{2} \text{ in. } H_2O)(\frac{0.03612 \text{ psia}}{\text{in. } H_2O})$

$$= 91.32 + (\frac{6.169}{2})(0.03612)$$
$$= 91.43 \text{ psia} \qquad \text{(F1-8)}$$

The compressibility factor z at the flowmeter conditions is approximated by:

$$z = 1 + BP_f/R(T_f + 273.15°K) \qquad \text{(F1-9)}$$
$$= 1. - \frac{321.5 \text{ cm}^3}{\text{gm•mole}} \quad \frac{1}{(14.696)(82.06)} \quad \frac{\text{gm mole K}}{\text{cm}^3 \text{ psia}} \quad \frac{91.43 \text{ psia}}{(300.23°K)}$$
$$= 0.91884$$

The mean density ρ_f at the flowmeter is given by:

$$\rho_f = \frac{(P_f)(W_m)}{R(T_f + 273.15)z} \qquad \text{(F1-10)}$$
$$= [(\frac{91.43 \text{ psia}}{300.23 \text{ K}})(\frac{1}{19.314} \frac{\text{lb. mole K}}{\text{psia ft}^3})(\frac{40.21 \text{ lbs}}{\text{lb mole}})$$
$$(\frac{1}{0.9188})] = 0.6900 \frac{\text{lbs}}{\text{ft}^3}$$

b) Calculation of pressure drop across flowmeter

The true pressure drop, ΔP, across the flowmeter in inches of water is given by:

$$\Delta P = (R_h - R_1 - R_o)(F'_{H_2O}) \frac{g}{g_c} \left(1 - \frac{\rho_g}{\rho_{H_2O}} \right) \qquad \text{(F1-11)}$$

where

$$F'_{H_2O} = 0.99823 - \frac{1.91}{1.8} \times 10^{-4} (T_{bar} - 68.) - \frac{5.3 \times 10^{-6}}{1.8} (T_{bar} - 68.)^2 \qquad \text{(F1-12)}$$

$$\rho_{H_2O} = 62.427(F'_{H_2O}) \quad lb_m/ft^3 \qquad \text{(F1-13)}$$

$$\frac{g}{g_c} = \frac{980.314}{980.665} = 0.99964$$

and ρ_{H_2O}, ρ_g are the densities of the water, and the system fluid above the water in the water manometer respectively. F'_{H_2O} corrects the height of water in inches to 68°F. The temperature at the water manometer is assumed to be the same as that of the barometer which is located nearby.

The compressibility factor z_g for the gas at the water manometer is calculated from Equation (F1-9) as:

$$z_g = 1. + \frac{(-324.9)\ cm^3}{gm.mole} \quad \frac{1}{14.696} \frac{gm\ mole}{cm^3\ atm.} \frac{91.43\ psia}{298.95°K} = 0.9176$$

where the B_m value of -324.9 $cm^3/gm \cdot mole$ was calculated using Equations (F1-1) and (F1-2) at a temperature of 78.44°F. Thus:

$$\rho_g = \left(\frac{91.43\ psia}{298.95°K} \right) \left(\frac{1}{19.314} \frac{lb.\ mole\ K}{psia\ fts.} \right) \left(40.21 \frac{lbs.}{lb.mole} \right) \left(\frac{1}{0.9176} \right) = 0.6939 \frac{lbs.}{ft^3}$$

$$F'_{H_2O}\ (78.44°F) = 0.99752$$

$$\rho_{H_2O}\ (68°F) = 62.232\ lbs./ft^3$$

Therefore:

$$\Delta P = (6.169 \text{ in. } H_2O)(0.9975)(0.99964)\left(1 - \frac{0.6939}{62.232}\right)$$

$$= 6.083 \text{ in. water at } 68°F \text{ or } 20°C$$

c) Calculation of the mixture viscosity at the flowmeter conditions

The relations used to calculate the viscosity at the flowmeter conditions are discussed in Section VI. The values of A and S in Equation (VI-10) for the individual pure components are presented in Table F-2.

Table F-2

Sutherland Constants for the Zero Pressure Viscosity

System	A_i (μ poise/°R$^{1/2}$)	S_i (°R)
CH_4	7.39	295.2
C_2H_6	7.461	466.2
C_3H_8	6.700	502.4

The A_i and S_i values in the above table were obtained from Lee and Eakin [143]. The A_i value for propane was, however, adjusted from 6.805 to 6.700. The adjustement was dictated by the desire to match the dimensionless flowmeter calibration curves for ethane and propane [284] as described by Equation (VI-1) by a suitable adjustment of their viscosities relative to each other. This adjustment is believed to be within the accuracy of the data used to generate the original A_i set by Lee and Eakin [142]. The mixture constants are calculated as:

$$A_m = \sum_{i=1} x_i A_i \sqrt{W_i} \Big/ \sum_{i=1} x_i \sqrt{W_i} \qquad \text{(F1-14)}$$

$$= (0.001)(7.39)(16.042)^{1/2} + (0.2746)(7.461)(30.070)^{1/2}$$

$$+ (0.7244)(0.670)(44.094)^{1/2} / [(0.001)(16.042)^{1/2}$$

$$+ 6.2746\ (30.070)^{1/2} + (0.7244)(44.094)^{1/2}\ ]$$

$$= 6.860$$

$$S_m = \sum_{i=1} x_i S_i$$

$$= (0.001)(295.2) + (0.2746)(466.2) + (0.7244)(502.4)$$

$$= 492.22 \qquad \text{(F1-15)}$$

$$\mu^\circ_m = \frac{A_m[(T_f + 273.15)1.8]^{1.5}}{[(T_f + 273.15)(1.8) + S_m]}$$

$$= \frac{6.86(540.4)^{1.5}}{(540.4 + 492.2)} = 83.47 \text{ micropoises} \qquad \text{(F1-16)}$$

The mixture viscosity μ_m at the flowmeter pressure is calculated from Equation (VI-7)

$$\mu_m = \mu^\circ_m \exp\ [X(T)\ \rho^{Y(T)}] \qquad \text{(F1-17)}$$

where:

$$X(T) = 2.57 + \frac{1914.5}{(T_f + 273.15)(1.8)} + 0.0095\ W_m \qquad \text{(F1-18)}$$

and: $Y(T) = 1.11 + 0.04X = 1.3697$ (F1-19)

and if ρ is in gms/cm^3.

$$\mu_m = 83.47 \exp\ [\ 6.435\{(0.6900\ \frac{lb_m}{ft^3})(0.01602\ \frac{gms}{cm^3}\ \frac{ft^3}{lb_m})\}^{1.3697}\ ]$$

$$= 85.73 \text{ micropoises}$$

d) Calculation of mass flowrate

The flowmeter calibration data for the system was fitted to the calibration equations:

$$\frac{10F}{(\rho_f \Delta P)^{1/2}} = 1.6587 + 0.3172\left[\ln\left(\frac{1000\ \rho_f\ \Delta P}{\mu^2_m}\right)\right] - 0.01793\left[\ln\left(\frac{1000\ \rho_f\ \Delta P}{\mu^2_m}\right)\right]^2 \qquad \text{(F1-20)}$$

$$\frac{\rho_f\ \Delta P}{\mu_m F} = 0.10351 + 15.2494\left(\frac{F}{\mu_m}\right) + 417.06187\left(\frac{F}{\mu_m}\right)^2 \qquad \text{(F1-21)}$$

where ρ_f is in lbs./ft^3, ΔP is in inches of water at 68°F, μ_m is in micropoises and the mass flowrate F is expressed in lbs/min. If Equation (F1-20) is solved for F we obtain the mass flowrate as 0.29382 lbs./min. A trial and error solution of Equation (F1-21) yields a value of F as 0.2936 lbs/min. In this particular case, the results of Equation (F1-20) were given priority over the results from Equation (F1-21) as the former equation was superior in the representation of the calibration data in the approximate range of the calculated flowrate.

Appendix F-2

Sample Calculations involving the Differential Pressure Calibration System.

The calculations in this section illustrate how the calibration data for the differential pressure transducer are obtained from measurements using the high pressure differential mercury manometer. The procedure for calculating the differential pressure from the transducer calibration equation is also discussed.

I Measurement of Mercury Density

The density of mercury used in the manometer is determined by weight using a cylindrical Lucite box of known volume

I.D. of Lucite box = 1.4997 in. @ 75°F

Depth of Lucite box = 1.4988 in. @ 75°F

Volume of box = $\pi \frac{(1.4997)^2}{4}$ 1.4988 = 7.06173 in.^{3} = 115.721 cm^3

Wt. of box with mercury = 1873.651 gms.

Wt. of mercury = 1565.583 gms.

Net calibration correction for weights = 0.006 gms.

Measured temperature = 75°F

Coefficient of cubical expansion of Lucite = 0.66×10^{-4} cm^3/°C cm^3

Corrected volume of Lucite box = $(0.66 \times 10^{-4})(75.-75.)(115.721) + 115.721$

= 115.721 cc.

Density of mercury = $\frac{1565.589 \text{ gms}}{115.721 \text{ cm}^3} = 13.528 \frac{\text{gms}}{\text{cm}^3}$ @ 75°F

II Calculation of Pressure and Differential Pressure at the Transducers for a Sample Set of Measurements Obtained with the High Pressure Differential Manometer

The sample set is confined to a measured pressure drop of about 100 psid, and consequently uses only legs I and II in Figure VI-13.

a) Elevation measurements with respect to Lufkin 300 in scale

Elevation of transducers,	h_o	= 34.16 in.
Elevation of mercury in leg I,	h_2	= 212.07 in.
Elevation of mercury in reservoir of leg I,	h_1	= 6.74 in.

b) Electrical measurements

Transducer excitation voltage (potentiometer scaled reading),	E_x	= 0.90854 volts
Differential pressure transducer output (scaled reading),	E_{DP}	= 2468 μv
High pressure transducer output (scaled reading),	E_h	= 11788 μv
Reference transducer excitation voltage (scaled reading),	E_{xo}	= 0.90650 μv

c) Additional data

Temperature at top of manometer	T_h	= 67°F
Temperature at bottom of manometer	T_1	= 69°F
Mean temperature of manometer	T_m	= 68°F
Density of mercury at 1 atm., and 32°F	ρs	= 13.595 gm/cm^3
Measured pressure at dead wt. gage at elevation h_o	Pg	= 985.6 psig
Barometric pressure	P_{bar}	= 28.16
Barometric temperature	T_{bar}	= 75°F
Standard gravity	gc	= 980.665 cm/sec^2
Latitude	L	= 42 deg. 16.6 min. N.
Elevation	z	= 876 ft. above sea level
Local gravity	g	= 980.314 cm/sec^2
Vertical tension on 300 in scale	W_v	= 10 lbs.
Coefficient of thermal expansion of tape	α	= 6.45x10^{-6} in./in.°F
Product of tape cross section A, and the Young's modulus of elasticity E, (Table A-11),	AE	= 88200 lbs

d) Corrections for scale marking errors

NBS Calibration correction at h_1 (Table A-11)	=	-0.004 in.
NBS Calibration correction at h_2 (Table A-11)	=	+0.003 in.
Measured height difference, $h_2 - h_1$	=	205.33 in.
Height difference corrected for scale marking errors	=	205.32 in.

e) Correction for tension on scale

The change in length δh for a horizontal tension of W_H lbs., is given by:

$$\delta h = \frac{(w_H - 10)(h_2 - h_1)}{A\ E} \qquad \text{(F2-1)}$$

where the calibration tension is 10 lbs. horizontally applied. The effect of applying a tension vertically instead of horizontally is to increase the length by 0.0005 in. over a span of 300 in. For a weight of 10 lbs. applied in this work, no correction was necessary.

f) Correction for temperature variation of scale length

The change in length $\delta 1$ corresponding to some fixed interval of length ΔL is given by:

$$\delta 1 = \alpha(T - T_s)\Delta L \qquad \text{(F2-2)}$$

where

α = Coefficient of linear thermal expansion

T_s = Temperature of calibration of the scale, °F

$\delta 1 = .45 \times 10^{-6} \frac{\text{in}}{\text{in.}\,^\circ\text{F}} (75. - 68.) (205.32) + 0.01$ in.

Corrected Height = 205.32 in - 0.01 in. = 205.31 in.

g) Absolute pressure at the high pressure transducer

From Table A-9, the corrected gage pressure P_{gc} using the M & G dead wt. gage is given by

$$P_{gc} = (985.6) + 0.1 + 0.49 \times 10^{-3} (985.6) = 986.1 \text{ psia}$$

The barometric pressure is corrected to psia using the empirical calibration equation of Jones [119]

$$(P_{bar})_c = [\, P_{bar} - 0.00275(T-32) \,] \text{ in Hg } (0.49116 \tfrac{\text{psia}}{\text{in Hg.}}) \qquad \text{(F2-3)}$$

$$= [\, 28.16 - 0.00275(75-32) \,]0.49116 = 13.98 \text{ psia}$$

Pressure at high pressure transducer, $P_{ho} = 986.1 + 13.98$

$\underline{\sim}$ 1000.1 psia

h) Pressure at bottom of mercury column

The pressure at the bottom of the mercury column at the reservoir, P_{h1}, is higher than the corresponding pressure at the transducers by an amount equivalent to the head of nitrogen gas corresponding to the elevation difference

$$P_{h1} = P_{ho} - g \int_{ho}^{h1} \rho_{N2}\, dh \qquad \text{(F2-4)}$$

where ρ_{N2} is the density of nitrogen. The minus sign indicates that the elevation convention increases negatively in going from ho to h1. If ρ_{N2} is independent of elevation we obtain:

$$P_{h1} = P_{ho} + g \frac{P_{ho}}{zRT} (h1 - ho) \qquad \text{(F2-5)}$$

where z = compressibility factor for N_2 at 1000.1 psia and 75°F

= 0.9994 (Reference [232])

$R = 2.9673 \times 10^6 \frac{cm^2}{sec^2}\,{}^\circ K$, (Reference [29])

Therefore:

$$P_{h1} = 1000.1 \text{ psia} - (980.314 \tfrac{cm}{sec^2})(\tfrac{1000.1 \text{ psia}}{0.9994})(6.74 - 34.16) \text{ in.}$$

$$(2.54 \tfrac{cm}{in.})(\tfrac{1}{2.9673 \times 10^6} \tfrac{sec^2 {}^\circ K}{cm^2})(\tfrac{1}{297.03 \text{ K}})$$

= 1000.176 psia

i) Conversion of mercury column height to psid

The relation

$$P_{h2} = P_{h1} - \frac{g}{gc} \int_{h1}^{h2} \rho_{Hg}(h)\, dh \qquad \text{(F2-6)}$$

is used to connect the actual mercury column height in inches to the desired units taking into account the variation of mercury density due to temperature and pressure. The density variation of mercury can be expressed as

$$\rho(P_h,T) = \rho(P_s,T_s) + \int_{Ps}^{P_{h1}} \left(\frac{d\rho}{dP}\right)_T dP + \int_{P_{h1}}^{P_h} \left(\frac{d\rho}{dT}\right)_P dP + \int_{Ts}^{T} \left(\frac{d\rho}{dT}\right)_P dT \qquad \text{(F2-7)}$$

where P_s, T_s are the conditions of the actual density measurement using the Lucite box. The pressure dependence of the density of mercury is given by the relation [29]

$$\rho = \rho(T_s, P_s)\ [\ 1 + 137\text{x}10^{-9}P] \qquad \text{(F2-8)}$$

where P is in inches of mercury. The temperature dependence relative to 32°F is expressed as [29].

$$\rho = \rho(32°F,P_s)\ [\ 1 - 0.000101\ (T-32)] \qquad \text{(F2-9)}$$

Therefore, expressing P in psia units, Equation (F2-7) yields the result

$$\rho_{Hg}(P_h, T) = \rho(T_s, P_s)[\ 1 + \frac{137\text{x}10^{-9}}{0.49916}(P_{h1} - P_s) + \frac{137\text{x}10^{-9}}{0.49916}(P_h + P_{h1}) - 0.000101\ (T - T_s)] \qquad \text{(F2-10)}$$

Expressing the term $(P_h - P_{h1})$ in terms of inches of mercury, and setting P_s = 14.0 psia, T = 68°F, T_s = 75°F, and $\rho(T_s,P_s)$ = 13.528 gms/cm^3 we obtain

$$\rho_{Hg}(P_h, T) = 13.528[1.0008 + 137x10^{-9}(h - h1) \qquad \text{(F2-11)}$$

Substituting this result into Equation (F2-7) we obtain

$$P_{h2} = P_{h1} - \frac{g}{gc} \int_{h1}^{h2} 13.528\ [1.0008 + 137x10^{-9}(h - h1)]\ dh \qquad \text{(F2-12)}$$

where the height h must now be expressed in terms of inches of mercury with h1 as the reference. Therefore:

$$P_{h2} = P_{h1} - 13.528\ [(1.0008)(h2 - h1) + 137x10^{-9}\left(\frac{h2^2 - h1^2}{2}\right)]\ \frac{g}{gc}$$

$$= 1000.176 \text{ psia} - \{13.528\ \frac{gm}{cm^3}\ [(1.0008)(205.31) +$$

$$137x10^{-9}\left(\frac{205.31}{2}\right)^2]\ \text{in.}\ 980.314\ \frac{cm}{sec^2}\ \frac{1}{980.665}\ \frac{gmf\ sec^2}{gm.cm.}$$

$$(2.54)^3\ \frac{cm}{in^3}^3\ \frac{lb_f}{453.59\ gms_f}\}$$

$$= 1000.076 - 100.313 = 899.863 \text{ psia.}$$

j) Pressure at the low pressure transducer

The pressure at the low pressure transducer P_{h3} is expressed in terms of the pressure at the top of the mercury column in leg I by the relation

$$P_{h3} = P_{h2} - g \int_{h2}^{h3} (\rho_{N2})\ dh \qquad \text{(F2-14)}$$

$$= P_{h2} - g\ \frac{P_{h2}}{zRT}\ (h3 - h2) \qquad \text{(F2-15)}$$

$z_{N2} = 0.9996$ at 900 psia and 75°F [232]

Therefore:

$$P_{h3} = 899.863 - 980.314\ \left(\frac{899.863}{0.9996}\right)(34.16 - 212.07)$$

$$(\frac{254}{297.03}\ \frac{1}{2.9673x10^6}) = 899.863 + 0.452 = 900.32 \text{ psia.}$$

$$= 899 + 863 + 0.452 = 900.32 \text{ psia}$$

True differential pressure at transducers = $P_{ho} - P_{h3} = \Delta P_{true}$

= 1000.18 - 900.32

= 99.76 psid

k) Adjustment of electrical output

Normalization factor for variation of supply voltage to transducers

$$= \frac{E_{xo}}{E_x} = \frac{0.90650}{0.90854} = 0.9977$$

Normalized value of high pressure transducer output = (11802μv)(0.9977)

= 11775 μv

Normalized value of Diff. pressure transducer output = (2468)(0.9977)

= 2462 μv

Normalized value of Diff. pressure tranducer null = (471)(0.9977)

= 470 μv

Normalized value of $E_{DP} - (E_{DP})_{Null}$ = (2462-470)μv

= 1992 μv

Having defined ΔP_{true}, $E_{DP} - (E_{DP})_{Null}$, and P_{ho}, we can from a series of such measurements obtain the calibration constant β', δ' and γ' in Equation VI-19.

1) Sample Calculation of Pressure and Differential Pressure from Transducer Outputs

System: - 28% C_2H_6 - C_3H_8

Run No. 4.020

Relevant Data

High pressure transducer reading at null,	$E_{hn} = 2135.6 \times 10^{-5}$ volts
Low pressure transducer reading at null,	$E_{ln} = 2148.9 \times 10^{-5}$ volts
Differential pressure transducer reading at null,	$E_{null} = 44.2 \times 10^{-5}$ volts
High pressure transducer reading,	$E_h = 2128.6 \times 10^{-5}$ volts
Low pressure transducer reading,	$E_l = 2019.2 \times 10^{-5}$ volts
Differential pressure transducer reading,	$E_{DP} = 249 \times 10^{-5}$ volts
Calibration reference scaled transducer excitation voltage,	$E_{xo} = 0.90650$ volts
Actual scaled transducer excitation voltage,	$E_x = 0.90751$ volts
Inlet pressure to calorimeter (M & G dead wt. gage),	$P_{hgr} = 1776.7$ psig
Barometric pressure,	$P_{bar} = 29.07$ in Hg.
Barometric temperature,	$T_{bar} = 75.8°F$

Transducer Calibration Equations

High Pressure: $E_h/10 = -3.989 + 1.1988\ P_{hg} - 0.3526 \times 10^{-6}\ P_{hg}^2$ (F2-16)

Low Pressure: $E_l/10 = 12.001 + 1.1999\ P_{lg} - 0.227 \times 10^{-5}\ P_{lg}^2$ (F2-17)

Diff. Pressure: $(E_{DP}-E_{null})/10 = \Delta P[1.9985 - 0.563 \times 10^{-5}(2P_h - \Delta P)$

$+ 0.217 \times 10^{-8}(3P_h^2 - 3P_h \Delta P + \Delta P^2)$ (F2-18)

where all voltages are expressed in microvolts. The subscript g implies

that gage rather than absolute pressure is utilized.

Corrected barometer pressure using Equation (F2-3)

$= [29.2 - 0.00275\ (75.8 - 32.0)]\ [0.49116]$

$= 14.26$ psia

Corrected M & G pressure using results of Table A-9

$= (1776.7) + 0.1 + 0.49 \times 10^{-3}(1776.7)$

$= 1777.6$ psid

Absolute pressure at calorimeter, $P_h = 1777.6 + 14.26$

$= 1791.9$ psia

Corrected value of $E_{hn} = 2135.6 \times 10^5 (\frac{E_{xo}}{E_x}) = 2133.2 \times 10^{-5}$ volts

The solution of Equation (F2-16) using the corrected value of E_{hn} yields

$$P_{hgn} = 1783.8 \text{ psig}$$

where P_{hgn} is the calculated gage pressure at null using the high pressure transducer. Similarly, the solution of Equation (F2-17) using the corrected value of E_{ln} yields

$$P_{lgn} = 1784.8 \text{ psig}$$

where P_{lgn} is the calculated gage pressure at null using the low pressure transducer. Now, as the true pressure is the same in both cases at null, the difference ΔP_{null} defined by

$$\Delta P_{null} = P_{hgn} - P_{lgn} = 1783.8 - 1784.8 = -1.0 \text{ psia}$$

serves as a check for relative calibration changes between the two transducers. For convenience, we adjust a_1 in Eqn. (VI-13) so that the low pressure transducer also yields 1784.8 psig. As a result a_1 is changed from 12.001 in Equation (F2-17) to 13.201.

Similarly, the values of E_h and E_l corrected for reference voltage changes and used in conjunction with Equations (F2-16) and (F2-17), respectively, yield

$$P_{hg} = 1777.5 \text{ psig}$$

P_{lg} = 1675.4 psig

where a_1 in Equation (F2-17) now has a value of 13.201.

Therefore, the pressure drop ΔP is calculated as

$$\Delta P = P_{hg} - P_{lg} = 1777.5 - 1675.4 = 102.1 \text{ psid.}$$

The values of E_{DP} and E_{null} corrected for reference voltage changes when used in conjunction with Equation (F2-17) yields the pressure drop ΔP as 103.1 psid. The discrepancy between the redundant measurements is 1 psi or approximately 1%. The absolute pressure transducers were found to be less susceptible to hysteresis than the differential pressure transducer, and consequently were preferred for specifying the differential pressure on the rare occasions when both of them were in service simultaneously.

Appendix F-3

The Preparation of Calibration Standard Mixtures for the Composition Measurement

Reference mixtures necessary for the calibration of the chromatograph are prepared by weight using 374 cc capacity steel cans. As the weight of the gas is only between 0.2% and 1.5% of the total weight of a can, calibration changes in the balance must be carefully monitored. Changes in the buoyancy contribution of the ambient air caused by variations in air density or in the can volume as a function of pressure must also be taken into account. To simplify the technique a dummy can, with dimensions similar to the sample can, is maintained at the balance location and weighed along with the sample can at all times. The contribution of such additional measurements is derived below:

a) Nomenclature

V_d = Volume of dummy can at atmospheric pressure
V_i = Initial evacuated volume of sample can at pressure P_i
V_2 = Volume of sample can at filling pressure P_2
W_1 = Observed initial weight of sample can at pressure P_1
W_2 = Observed weight of sample can at pressure P_2
D_1 = Observed weight of dummy can at initial weighing of sample can
D_2 = Observed weight of dummy can at final weighing of sample can
W_{iT}, D_{iT} = True weight of can with observed weight W_i or D_i
v_d = Volume of weights used to measure dummy can
v_1 = Volume of weights used to measure sample can initially
v_2 = Volume of weights used to measure sample can finally
ρ_1 = Density of air at initial conditions
ρ_2 = Density of air at final conditions
ρ_w = Density of weights

b) Derivation of the Technique

The difference between the true and the observed weight of a can is ascribed to the combined effects of air buoyancy and calibration changes in the weights. Thus:

$$D_{1T} - D_1 = \rho_1[V_d - v_d] + d_1 \quad \text{(F3-1)}$$

$$D_{2T} - D_2 = \rho_2[V_d - v_d] + d_2 \quad \text{(F3-2)}$$

$$W_{1T} - W_1 = \rho_1[V_1 - v_1] + d_1 + e_1 \quad \text{(F3-3)}$$

$$W_2T - W_2 = \rho_2[V_2 - v_2] + d_2 + e_2 \quad \text{(F3-4)}$$

where d_i is the calibration correction for the true weight D_{iT}, and e_i is the calibration correction involved in the true weight difference $(W_{iT} - D_{iT})$. The development assumes that the true weight and volume of the dummy can is unchanged over the time period covering both sample measurements, and that the change in v_d involved in the weight difference $(D_2 - D_1)$ is negligible. From equations (F3-1) and (F3-2) we obtain:

$$D_2 - D_1 = \rho_1[V_d - v_d] - \rho_2[V_d - v_d] + d_2 - d_1 \quad \text{(F3-5)}$$

Similarly,

$$W_{2T} - W_{1T} = (W_2 - W_1) + \rho_2[V_2 - v_2] - \rho_1[V_1 - v_1] + (d_2 - d_1) + (e_2 - e_1) \quad \text{(F3-6)}$$

The effect of pressure on the displacement volume of a can may be represented by the relation:

$$V_j = V_i + b(P_j - P_i) \quad \text{(F3-7)}$$

where V_j is the can volume at pressure P_j. Equation (F3-6) may now be represented in the form:

$$W_{2T} - W_{1T} = (W_2 - W_1) + (\rho_2 - \rho_1)(V_d - v_d) + \rho_2[(V_2 - V_d) - (v_2 - v_d)] - \rho_1[(V_1 - V_d) - (v_1 - v_d)] + (d_2 - d_1) + (e_2 - e_1) \quad \text{(F3-8)}$$

Using Equation (F3-5) in conjunction with Equation (F3-6) we obtain:

$$W_{2T} - W_{1T} = (W_2 - W_1) - (D_2 - D_1) + \rho_2[\Delta V_2 - \delta v_2] - \rho_1[\Delta V_1 - \delta v_1] + (e_2 - e_1) \quad \text{(F3-9)}$$

Now $$\Delta V_2 = \Delta V_1 + b(P_2 - P_1) \quad \text{(F3-10)}$$

and $$\delta v_2 = \delta v_1 + \frac{W_2 - W_1}{\rho_W} \quad \text{(F3-11)}$$

Thus, on substitution into Equation (F3-8) the result

$$W_{2T} - W_{1T} = (W_2 - W_1) - (D_2 - D_1) + (\rho_2 - \rho_1)(\Delta V_1 - \delta v_1) + \rho_2 b(P_2 - P_1) - \rho_2 \left(\frac{W_2 - W_1}{\rho_W} \right) + (e_2 - e_1) \quad \text{(F3-12)}$$

is obtained.

c) Sample calculation for an ethane-propane mixture

Set I	Relevant Data		
Wt. of empty can 8,	W_1	=	189.0208 gms.
Can 8 pressure,	P_1	=	< 10 microns Hg.
Observed wt. of reference can 12,	D_1	=	187.2046 gms.
Evacuated displacement of can 8,	V_1	=	374.22 cm^3
Evacuated displacement of can 12	V_d	=	372.3 cm^3
Wet bulb temperature,	T_{wb1}	=	67.0°F
Dry bulb temperature,	T_{db1}	=	76.9°F
Air temperature at balance,	T_1	=	26.1°C
Corrected Barometric pressure,	Pa_1	=	732.9 mm.Hg.
Molecular wt. of dry air	$(MW)_r$	=	29.00

Set II			
Wt. of can 8 + ethane,	W_2	=	190.3735 gms.
Can 8 pressure,	P_2	=	30.3 psig

Observed wt. of reference can, D_2 = 187.2076 gms.
Wet bulb temperature, T_{wb2} = 59.0°F
Dry bulb temperature, T_{db2} = 76.3°F
Air temperature at balance, T_2 = 25.2°C
Corrected barometric pressure, Pa_2 = 745.14 mm. Hg.

Set III
Observed wt. of can 8 + ethane + propane W_3 = 192.0214 gms.
Can 8 pressure, P_3 = 68.0 psig
Observed wt. of reference can, D_3 = 187.2044
Wet bulb temperature, T_{wb3} = 75.2°F
Dry bulb temperature, T_{db3} = 62.2°F
Air temperature at balance, T_3 = 24.4°C
Corrected barometric pressure, Pa_3 = 737.65 mm. Hg.

Miscellaneous Data:

Volume expansion coefficient for cans, $\frac{1}{V}\frac{dV}{dP}$ = 0.156×10^{-4} $psia^{-1}$
Specific gravity of weights, ρw = 8.7 gms/cm^3
Calibration correction to 2 gm. pan weight difference for $(W_1 - D_1)$, e_1 = + 0.0012 gms.
Calibration correction to 3 gm. pan weight difference for $(W_2 - D_2)$, e_2 = + 0.0014 gms.
Calibration correction to 5 gm. pan weight difference for $(W_3 - D_3)$, e_3 = + 0.0013 gms.

Calculations of air density for Set I

Density of dry air at 26.1°C and 760 mm. Hg.,

$$\rho_n = \frac{1}{13.575}\frac{lbs}{ft^3} = 0.001179\ \frac{gms}{cm^3}\ [192]$$

Saturation pressure of H_2O at 67.0°F wet bulb temperature,

= 17.04 mm Hg. [192]

Mole fraction of water in air at saturation = $\frac{17.04}{732.9}$ = 0.02325 mole %

The relative humidity was calculated as 60% from a chart of T_{db} vs. $(T_{db} - T_{wb})$ for the conditions of Set I.

Actual mole fraction of water in air = (0.02325)(0.6) = 0.01395 mole %.

If the compressibility factor of air is assumed to be unchanged by a variation in moisture content, then the change in moist air density may be ascribed entirely due to a change in molecular weight.

Molecular wt. of moist air, (MW), = (0.01395)(18.0) + (1.- 0.01395)(29.0) = 28.844.

Density of moist air for set I, $\rho_1 = (\rho_n) \frac{Pa_1}{760} \frac{(MW)_r}{(MW)_1}$

$$= [\ 0.001179 \frac{gms}{cm^3}][\ \frac{732.9}{760}\ ][\ \frac{29.00}{28.844}\ ]$$

$$= 0.0011431 \frac{gms}{cm^3} \qquad \text{(F3-13)}$$

Similarly, density of moist air for Set II, ρ_2 = 0.0011757 gms/cm^3

Application of Equation (F3-12) for Calculations $W_{2T} - W_{1T}$

$$\Delta V_1 = 374.22 - 372.30 = 1.92 \text{ cm}^3$$

$$\delta v_1 = \frac{W_1 - D_1}{8.7} = \frac{189.021 - 187.2046}{8.7} = 0.208 \text{ cm}^3 \qquad \text{(F3-14)}$$

$$b = (\frac{1}{V}\frac{dV}{dP})(V_1) = [0.156 \times 10^{-4}][374.22] = 0.0058 \frac{cm^3}{Psia} \qquad \text{(F3-15)}$$

$W_2 - W_1$ = 190.3735 - 189.0208 = 1.3527 gms

$D_2 - D_1$ = 187.2076 - 187.2046 = + 0.0030 gms

Substituting into Equation (F3-12) the true weight difference $W_{2T} - W_{1T}$ i.e., the weight of ethane added is calculated as:

$$W_{2T} - W_{1T} = 1.3527 - 0.0030 + (0.0011757 - 0.0011489)(1.92 - 0.208) + 0.0011757[0.0058 \frac{cm^3}{psia}(30.3 + 14.2)\ psia - \frac{1.352}{8.7} + (e_2 - e_1)$$

$$- 1.3525/8.7] + (e_2 - e_1)$$
$$= 1.3527 - 0.0030 + 0.00006 - 0.000125 + (0.0014 - 0.0012)$$
$$= 1.3494 \text{ gms}$$

Moles of ethane added $= (1.3494 \text{ gms}) \left(\frac{1 \text{ gm. mole}}{30.060 \text{ gms}}\right) = 0.04489$ gm.moles

The above results indicate that the major part of the correction to the weight difference between successive measurements on a given can is represented by the change in weight of the reference can. Furthermore, the contribution of the term $(\rho_2 - \rho_1)(\Delta V_1 - \delta V_1)$ is not very significant, and its omission may make the determination of the wet and dry bulb temperature, and the barometric pressure unnecessary.

Similarly,

Wt. of Ethane + Propane $= W_{3T} - W_{1T} = 3.006$ gms.

Wt. of Ethane $= W_{2T} - W_{1T} = 1.3494$ gms.

Wt. of Propane $= W_{3T} - W_{2T} = 1.6512$ gms.

Moles of propane added $= 1.6512/44.094 = 0.037447$ moles.

Mole fraction of ethane $= 0.04489/(0.04489 + 0.037447) = 0.5452$

Mole fraction of propane $= 1. - 0.5452 = 0.4547$

Appendix F-4

Calculation of System Composition

From the peak height vs. composition curve of Figure F-1 it is reasonable to assume a linear dependence in the relationship between the two quantities in the immediate vicinity ($\pm$ 5%) of any given composition. The constants a and b for the functional form

$$x_i = a + bh_i \tag{F4-1}$$

where the peak height h_i corresponding to the mole fraction x_i of the ith component can be determined from peak height measurements on two standard mixtures with compositons close to x_i, assuming that the measurement conditions are substantially unchanged in all three cases. Thus,

$$a = (x_i)_{S1} - [(x_i)_{S1} - (x_i)_{S2}](h_i)_{S1} \tag{F4-2}$$

$$b = \frac{(x_i)_{S1} - (x_i)_{S2}}{(h_i)_{S1} - (h_i)_{S2}} = \left(\frac{\Delta x_i}{\Delta h_i}\right) \tag{F4-3}$$

where S1 and S2 are the two reference mixtures.

In practice, only one reference S1 is used, and consequently a simpler assumption

$$x_i = b'h_i \tag{F4-4}$$

is necessary, where

$$b' = \frac{(x_i)_{S1}}{(h_i)_{S1}} \tag{F4-5}$$

The error in the computed value of x_i with respect to Equation (F4-1) is given by:

$$(x_i)_{(F4-1)} - x_{i(F4-4)} = (b' - b)\,[(h_i)_{S1} - h_i] \tag{F4-6}$$

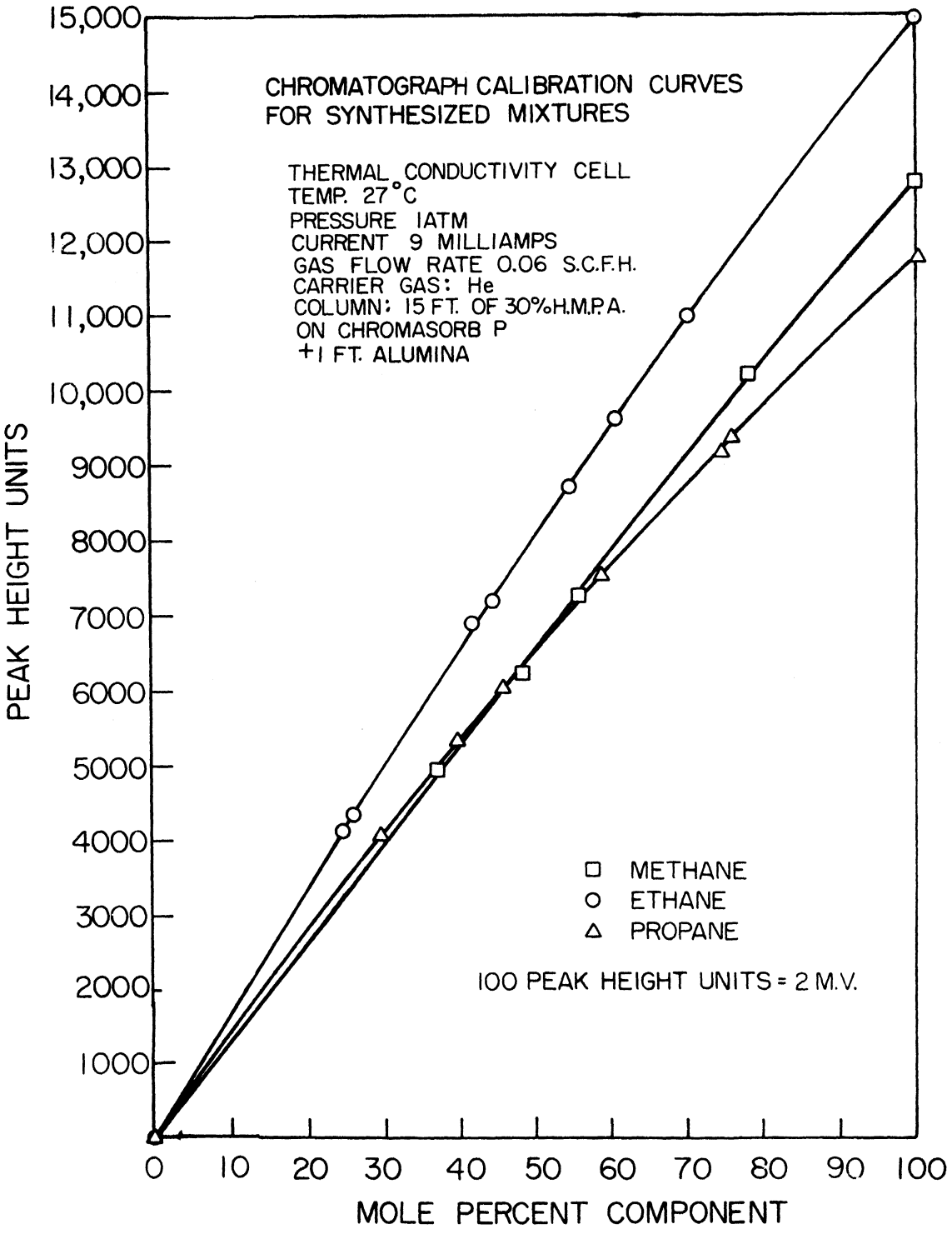

Figure F-1. Calibration Results for the Chromatograph Using Reference Mixtures of Methane, Ethane and Propane.

and is seen to be proportional to the difference in peak heights between the system and the standard mixture. From Figure F-1, the difference (b' - b) is seen to be a function of composition approaching zero at infinite dilution, and reaching a maximum in the pure component case. For the mixtures of this work, the maximum value of (b' - b) occurs for the propane concentration of the 0.27 C_2H_6 - C_3H_8 mixture, and corresponds to an error of 10% in the value of the composition difference between the system and the standard. As the standard tank composition differed by as much as 2% from the system composition for this particular system, the error introduced in the calculated composition by assuming (F4-4) was as high as 0.2%.

Relevant Data

System: - 0.27 C_2H_6 - C_3H_8

Run: - 4.020

Standard Mixture Properties

$(x_{CH_4})_{S_1}$ = 0.001

$(x_{C_2H_6})_{S_1}$ = 0.271, $(h_{C_2H_6})_{S_1}$ = 35.70 units

$(x_{C_3H_8})_{S_1}$ = 0.728, $(h_{C_3H_8})_{S_1}$ = 69.9 units

System Mixture Properties

$(h_{C_2H_6})$ = 36.20 units

$(h_{C_3H_8})$ = 70.20 units

The methane mole fraction is assumed to be the same for both the system and the standard. Analysis of some methane peaks indicated differences of less than 10% in the peak heights between the system and the standard which were ignored. The ethane and propane mole fractions are calculated using the assumption of Equations (F4-4) and (F4-5) respectively.

$$x_{C_2H_6} = \left(\frac{36.2}{35.7}\right)(0.271) = 0.2747$$

$$x_{C_3H_8} = \left(\frac{69.9}{70.2}\right)(0.7248) = 0.7248$$

$$\sum_{i=1} x_i = 0.001 + 0.2747 + 0.7248 = 1.0005$$

The mole fractions are then normalized to yield a unity sum.

Appendix F-5

Derivation of High Temperature Mixing Rule of Equation (V-41)

Described below are the calculations that were necessary to derive the high temperature mixing rule described by Equation (V-41) using the assumptions described on pages 131 and 132 in Chapter IV.

I. Calculations Illustrating the Modification of the Reduced Second Virial Coefficient Tabulation of Leland et al., [145].

The ratio of B_M/Vc to B/Vc at Tr values of 1.0 and 2.0 are respectively given by Leland et al. [145] as

$$\frac{(B_M/Vc)_{T=T_M}}{(B/Vc)_{T=Tc}} = \frac{0.420}{-1.275} = -0.3296 \qquad \text{(F5-1)}$$

$$\frac{(B_M/Vc)_{T=T_M}}{(B/Vc)_{T=2Tc}} = \frac{0.420}{-0.210} = 2.0 \qquad \text{(F5-2)}$$

If the above results are valid for methane, then the insertion of the appropriate B/Vc values obtained from precise experimental data into the denominators of Equations (F5-1) and (F5-2) should yield identical B_M/Vc values that are also in agreement with the results. of Leland et al.

Using Equation (F5-1), the precise data of Douslin [67] for methane at T = Tc, at T = 2Tc, and a Vc value of 99.0 cm^3/gm mole, we obtain

$$\left[\frac{B_M}{Vc}\right] = -0.3296 \left[\frac{-115.8}{99.0}\right]_{T=191.07K} = 0.389 \qquad \text{(F5-3)}$$

From Equation (F5-2)

$$\left[\frac{B_M}{Vc}\right] = -2. \left[\frac{-19.3}{99.0}\right]_{T=382.14K} = 0.387 \qquad \text{(F5-4)}$$

Also,

$$\left[\frac{B_M}{Vc}\right]_{\text{Leland et al.}} = 0.420 \qquad \text{(F5-5)}$$

Although there is close correspondence between the B_M/Vc values calculated in (F5-3) and (F5-4), their agreement with Leland's suggested value is somewhat poorer. The value of B_M for methane was adjusted from -41.5 cc/mole as given by the tabulation to -38.5 cc/mole to conform to (F5-3). The function B/Vc vs T/Tc of Leland et al. was then redefined in terms of the variables B/B_M and T/T_M using the modified value of B_M. The function is plotted as Figure V-2.

II. Determination of the Ratios T_M/Tc and $B_M/(RTc/Pc)$ as Functions of αc

The experimental data on CF_4 and CH_4 were used exclusively to derive these relationships. From the results of Leland et al. [145], T_M = 18.0 Tc for methane. From the data of Douslin et al. [67] Tb = 509.3K for methane.
Therefore,

$$\left(\frac{T_M}{Tb}\right)_{CH_4} = \frac{(18)(191.07)}{509.3} = 6.753 \qquad \text{(F5-6)}$$

From the data of Douslin et al., Vb = 54.34 for methane
Therefore,

$$\left(\frac{B_M}{Vb}\right)_{CH_4} = 0.7085 \qquad \text{(F5-7)}$$

The experimental second virial coefficient data for CF_4 [65] yields:

$$(Vb)_{CF_4} = 104.13 \text{ cm}^3/\text{gm.mole}$$

$$(Tb)_{CF_4} = 518.14°K$$

These results were used in combination with the critical properties for CF_4 in Table J-1 to specify the empirical linear relationships

$$\frac{Vb}{RTc/Pc} = 0.15903 + 0.05883\ (\alpha c - \alpha c_{oo}) \qquad \text{(F5-8)}$$

$$\frac{Tc}{Tb} = \frac{1 + 0.189(\alpha c - \alpha c_{oo})}{2.6656} \qquad \text{(F5-9)}$$

where

$$\alpha c_{oo} = \alpha c_{CH_4} = 5.82 \qquad \text{(F5-10)}$$

Therefore:

$$\frac{T_M}{Tc} = \left(\frac{T_M}{Tb}\right)\left(\frac{Tb}{Tc}\right) = \frac{18.}{1.0 + 0.189(\alpha c - 5.82)} \qquad \text{(F5-11)}$$

and

$$\frac{B_M}{RTc/Pc} = \left(\frac{B_M}{Vb}\right)\left(\frac{Vb}{RTc/Pc}\right) = [0.7085][0.15903 + 0.05883\ (\alpha c - \alpha c_{oo})] \qquad \text{(F5-12)}$$

if it is assumed that T_M/Tb and B_M/Vb are universal and independent of the αc value of a substance. If T_M and B_M in Equation (V-38) are expressed in terms of Equations (F5-11) and (F5-12) respectively, then we in fact obtain the generalized reduced correlation of Equation (V-39) valid at high reduced temperatures beyond the Boyle point. The mixing rule of Equation (V-41) may be derived by combining Equation (V-39) with Equation (V-1).

Apppendix F-6

Estimation of Errors in the Computation of the Second Interaction Virial Coefficients from the Correlation of This Work

Assumptions. 1) The second virial coefficient of methane is accurately known to as low as 198.15K.

2) The discrepancy $\delta_{C_3H_8}$ between the B_{C_3H} data of Brewer. (-579 cm^3/gm mole, [28]), and that of Kapallo, (-588.5 cm^3/mole, [123]) at 248.15K is taken to be a measure of the uncertainty of the data.

3) For temperatures other than 248.15K, the uncertainty $^{\delta}C_3H_8$ is assumed to be proportional to the value of the reduced second virial coefficient $Br_{C_3H_8}$

$$\delta r_{C_3H_8} = k[Br_{C_3H_8}] \qquad \text{(F6-1)}$$

4) As a consequence of the first two assumptions, the uncertainty in the propane data is concentrated in the slope function term of Equation (V-30). The uncertainty, δ, introduced by the correlation in the calculation of the B values for other substances at a given reduced temperature Tr_{CH_4}, can be expressed as

$$\delta r = \frac{\delta}{RTc/Pc} = \frac{k[\alpha c - \alpha c_{CH_4}]}{[\alpha c_{C_3H_8} - \alpha c_{CH_4}]} Br_{C_3H_8} \qquad \text{(F6-2)}$$

5) The uncertainty, δ_{ij}, involved in the calculation of the interaction virial coefficient B_{ij} from Equation (V-1) due to uncertainties in the B value for the pure components and for the mixture is given by

$$\delta_{ij} = \frac{\delta_m - x_i^2\delta_{ii} - x_j^2\delta_{jj}}{2x_ix_j} \qquad \text{(F6-3)}$$

Sample Calculation for 0.498 C_2H_6 – C_3H_8 Mixture

a) Determination of the value of k.

At 248.15K

$$Br_{C_3H_8} = \frac{-588.5 \text{ cm}^3/\text{gm mole}}{722.57 \text{ cm}^3/\text{gm mole}} = -0.8143, \text{ (Using the data of Kapallo et al.)}$$

$$\delta r_{C_3H_8} = \frac{B_{Kapallo} - B_{Brewer}}{RTc/Pc} = \frac{-588.5 + 579.0}{722.57} \text{ (By definition)}$$

$$= k[-0.8143] \quad \text{(From Equation F6-1)}$$

Therefore, $k = 1.617 \times 10^{-2}$ gm moles/cm^3

b) Calculation of error in δ_{ij} at 223.15K. For the given mixture, Equation (F6-3) reduces to

$$\delta_{ij} = (\delta_m - 0.248\ \delta_{C_2H_6} - 0.252\ \delta_{C_3H_8})/0.5 \qquad \text{(F6-4)}$$

Tc_m = 339.6K

RTc_m/Pc_m = 622.1 cc/mole

αc_m = 6.379

Tr_m = 223.15K/339.6K = 0.6572

$(Tr_{oo})_m$ = 0.6410 [Using Equations (III-36) through (III-36c)]

$Br_{C_3H_8}$ = -0.814 @ Tr_{CH_4} = 0.6410

From Equation (F6-3), we obtain:

$$\delta_{m\ 223.15K} = (622.1)(1.617 \times 10^{-2}) \frac{(6.379 - 5.82)}{(6.54 - 5.82)} (-0.814)$$

$$= -6.4 \text{ cm}^3/\text{mole}$$

Similarly, $\delta_{C_2H_6} = (519.98)(1.617 \times 10^{-2}) \frac{(6.275 - 5.82)}{(6.54 - 5.82)} (-0.662)$

$$= -3.5 \text{ cm}^3/\text{mole}$$

and $\delta_{C_3H_8} = (722.57)(1.617 \times 10^{-2})(1)(-1.028) = -12.0 \text{ cm}^3/\text{mole}$

Therefore from Equation (F6-4):

$$\delta_{ij} = [-6.4 - 0.248(-3.7) - 0.52(-12.0)]/0.5 = -5 \text{ cm}^3/\text{mole}$$

Table F-3 below contains a list of the calculated values of δ_{ij} for several methane-propane and ethane-propane mixtures at 223.15K and 398.15K. The results show that although there are some changes in the calculated values of B_{ij} for each system, the spread in the B_{ij} values as a function of composition remains relatively unchanged.

TABLE F-3

Estimated Change in the Calculated Value of the Interaction Second Virial Coefficient Using the Technique of Figure V-2 Due to a Modification of the Second Virial Coefficient Correlation of this Work

SYSTEM	TEMPERATURE 223.15 K δ_{ij} (CC/MOLE)	TEMPERATURE 398.15 K δ_{ij} (CC/MOLE)
.72 CH4, .28 C3H8	+1.1	+1.9
.49 CH4, .51 C3H8	-1.4	+1.6
.23 CH4, .77 C3H8	-2.0	+0.2
.76 C2H6, .24 C3H8	-4.7	-1.1
.50 C2H6, .50 C3H8	-5.0	-1.1
.28 C2H6, .72 C3H8	-6.2	-1.2

Appendix F-7

Outline of Calculation Procedure for Rules VII, IX and X

1) Calculation of Mixture Virial Coefficients as a Function of Temperature. This calculation is illustrated for the approximately equimolal ethane-propane mixture which, for the sake of simplicity, is treated as a two component system with the light impurities added to the methane mole fraction and the heavy impurities added to the propane content.

a) Relevant Data:

i) Composition

Mole fraction methane, $x_1 = 0.00$

Mole fraction ethane, $x_2 = 0.498$

Mole fraction propane, $x_3 = 0.502$

ii) Critical Parameters for pure components and mixtures

Methane	Ethane	Propane	Equimolal Mixture
$Tc_{11} = 190.7K$	$Tc_{22} = 305.4K$	$Tc_{33} = 369.9K$	$Tc_m = 339.55K$
$Pc_{11} = 45.8$ atm	$Pc_{22} = 48.2$ atm	$Pc_{33} = 42.01$ atm	$Pc_m = 44.8$ atm
$\alpha c_{11} = 5.82$	$\alpha c_{22} = 6.275$	$\alpha c_{33} = 6.540$	$\alpha c_m = 6.379$
$\frac{RTc_{11}}{Pc_{11}} = 341.69$ $cm^3/mole$	$\frac{RTc_{22}}{Pc_{22}} = 519.96$ $cm^3/mole$	$\frac{RTc_{33}}{Pc_{33}} = 722.57$ $cm^3/mole$	$\frac{RTc_m}{Pc_m} = 621.97$ $cm^3/mole$

The equimolar mixture pseudo-parameters were specified from Column I of Table IX-14 and were obtained by optimization of the enthalpy data for the given mixture within the framework of the PGC.

b) Calculation of B_m at T = 198.15K.

$$Tr_m = \frac{T}{Tc_m} = \frac{198.15K}{339.55K} = 0.5836$$

The modified reduced temperature (Tr_{oo}) for the mixture must be calculated from Tr_m and αc_m before Equation (V-30) can be used to calculate Br_m. The criterion:

$$\log Pr_s[Tr_m, \alpha c_m] = \log Pr_s[(Tr_{oo})_m, \alpha c_{CH_4}] \qquad (F7\text{-}1)$$

is used to specify $(Tr_{oo})_m$, where Pr_s is the reduced vapor pressure. If the Riedel vapor pressure equation is used to express Pr_s as a function of the reduced temperature, then we obtain

$$-\phi(0.5830) - [6.379 - 7.00]\Psi(0.5836) = -\phi((Tr_{oo})_m)$$

$$- [5.82 - 7.00]\Psi((Tr_{oo})_m)$$

where ϕ and Ψ are defined by Equations (IV-36 a and b). A trial and error calculation yields

$$(Tr_{oo})_m = 0.5544$$

The value of the reduced second virial coefficient Br_m at 198.15K is then computed using Equation (V-30). Thus

$$Br_m = 0.14416 + 0.49095(1 - e^{0.68511/0.5544}) + (6.379 - 5.82)$$

$$\left[0.0175 - \frac{0.220}{0.5544} - \frac{0.00614}{(0.5544)^2} + \frac{0.0281}{(0.5544)^3}\right]$$

$$= -1.0546 + (6.379 - 5.82)(-0.0256)$$

$$= -1.069$$

$$B_m(198.15K) = (Br_m)\left(\frac{RTc_m}{Pc_m}\right) = (-1.069)(621.97) = -664.86 \text{ cc/mole}$$

2) Calculation of the Interaction Second Virial Coefficient B_{23} at 198.15K. Using Equation (V-30) and the appropriate critical parameters, the second virial coefficients for ethane and propane at 198.15K are respectively calculated as:

$B_{22} = -435.75$ cc/gm mole

$B_{33} = -965.96$ cc/gm mole

Therefore, given B_{11}, B_{22}, B_{33} and B_m for a binary mixture, Equation (V-1) may be rearranged to permit the extraction of B_{23}. Thus:

$$B_{23} = \frac{B_m - x_2^2 B_{22} - x_3^2 B_{33}}{2\, x_2 x_3} \qquad \text{(F7-2)}$$

$$= \frac{-664.86 - (0.498)^2(-435.75) - (0.502)^2(-965.96)}{(2)(0.498)(0.502)}$$

$$= -626.74 \text{ cc/gm mole}$$

Using the optimum pseudo-parameters for the 0.498 C_2H_6 mixture, B_{23} values were calculated at fourteen selected temperatures. The results appear as part of Table IX-5 in the column appropriate to the equimolal mixture.

3) Calculation of pseudo-parameters αc_{23} and RTc_{23}/Pc_{23} for Rule VII of Table IX-10. The value of αc_{23} is obtained from the mixing rule

$$\alpha c_{23} = \frac{\alpha c_m - x_2^2 \alpha c_{22} - x_3^2 \alpha c_{33}}{2\, x_2 x_3} \qquad \text{(F7-3)}$$

$$= \frac{6.379 - (0.498)^2(6.275) - (0.502)^2(6.540)}{2(0.498)(0.502)}$$

$$= 6.351$$

The mixing rule for RTc_{23}/Pc_{23} is independantly obtained from Equation (V-41).

a) Calculation of h ratios, $h(\alpha c_{ii})/h(\alpha c_m)$:

$$h(\alpha c_m) = 0.7085[0.15903 + 0.0588(6.379 - 5.82)] = 0.13596$$

and $h(\alpha c_{22}) = 0.7085[0.15903 + 0.0588(6.275 - 5.82)] = 0.131625$

Therefore, $h_r(\alpha c_{22}) = \frac{h(\alpha_{22})}{h(\alpha c_m)} = 0.9675$

Similarly, $h_r(\alpha_{33}) = \quad = 1.049$

$h_r(\alpha_{23}) = \quad = 0.9914$

b) Calculation of g ratios, $g(Tr_{ii}, \alpha c_{ii})/g(Tr_m, \alpha c_m)$:

The first step in the evaluation of the terms $g(\alpha c, Tr)$ is the initial selection of some high temperature where Equation (V-41) is simultaneously applicable to all components, i.e., the reduced temperature for each component must lie in the range $8.0 \leq Tr \leq 30$. The ultimate application of the rule to the ternary methane-ethane-propane mixture requires the temperature limits to be set by Tc_{11} and Tc_{33}, respectively. Upper temperature limit = (30)(190.7K) = 5721K Lower temperature limit = (8)(369.9K) = 2959K. A value of 5000K was arbitrarily selected for the calculation.

Referring to Equation (V-40), we obtain

$$T_M/Tc = 18/[1.0 + 0.189(6.379 - 5.82)] = (18)/(1.10565)$$

Also, $Tr_m = 5000K/339.55K = 14.725$

$$\text{Therefore, } \frac{T}{T_M} = Tr_m\left(\frac{Tc}{T_M}\right) = \frac{(14.725)(1.10565)}{(18)} = 0.9046$$

$$g(Tr_m, \alpha c_m) = 0.3517 + 1.5068(0.9046) - 1.11379(0.9046)^2$$

$$+ 0.25874(0.9046)^3$$

$$= 0.99189$$

Similarly, $g(Tr_{22}, \alpha c_{22}) = 0.9991$

and $g(Tr_{33}, \alpha c_{33}) = 1.0072$

$g(Tr_{23}, \alpha c_{23})$ cannot be evaluated until Tc_{23} is known. An initial estimate is obtained from the Redlich-Kwong rule (III) in Table (IX-8)

Assume $Tc_{23} = 335.2K$

then $g(Tr_{23}, \alpha c_{23}) = 0.9927$

$$gr(Tr_{22}, \alpha c_{22}) = \frac{g(Tr_{22}, \alpha c_{22})}{g(Tr_m, \alpha c_m)} = 1.0072$$

$$gr(Tr_{33}, \alpha c_{33}) = 0.9918$$

$$gr(Tr_{23}, \alpha c_{23}) = 1.0008$$

The value of RTc_{23}/Pc_{23} is obtained from the solution of Equation (V-41) rewritten below in the form

$$\frac{RTc_m}{Pc_m} = x_2^2 \frac{RTc_{22}}{Pc_{22}} hr(\alpha c_{22})\ gr(Tr_{22}, \alpha c_{22}) + 2x_2x_3 \frac{RTc_{23}}{Pc_{23}}$$
$$hr(\alpha c_{23})\ gr(Tr_{23}, \alpha c_{23}) + x_3^2 \frac{RTc_{33}}{Pc_{33}} hr(\alpha c_{33})\ gr(Tr_{33}, \alpha c_{33}) \qquad (F7\text{-}4)$$

$$621.97 \frac{cc}{mole} = (0.498)^2(519.96)(0.9675)(1.0072) + 2(0.498)(0.502)$$
$$(\frac{RTc_{23}}{Pc_{23}})(0.991)(1.0008) + (0.502)^2(722.57)(1.049)(0.9911)$$

Therefore, $\frac{RTc_{23}}{Pc_{23}} = \frac{621.97 - 125.7 - 189.61}{0.496} = 618.2\ cm^3/gm\ mole$

As a matter of academic interest, the calculation was repeated for selected temperatures of 4000K and 6000K for application of Equation (V-41). The calculated values of RTc_{23}/Pc_{23} were 617.0 and 617.7 cm^3/mole respectively. These results confirm the relative insensitivity of the mixing recipe RTc_{23}/Pc_{23} in Rule VII to the precise temperature at which it is applied.

4) Calculation of Tc_{23} for Rule VII of Table IX-10. The calculated values of RTc_{23}/Pc_{23} and αc_{23} are then used in conjunction with Equation (V-30) to determine the best value of Tc_{23} that will yield a set of B_{23} values from the equation that are in closest agreement with the results in step 2 over the temperature range from 198.15K to 510K. At each stage in the trial, the value of Tc_{23} is revised using Newton's method. Thus,

$$(Tc_{23})_{New} = (Tc_{23})_{Old} + \left\{ \frac{\sum_{i=1}^{n} [Br_{23} - (Br_{23})_{cal}] \frac{d(Br_{23})}{dTc_{23}}_{cal}}{\sum_{i=1}^{n} [\frac{d(Br_{23})}{dTc_{23}}_{cal}]^2 - [Br_{23} - (Br_{23})_{cal}] \frac{d^2(Br_{23})}{dTc_{23}}_{cal}} \right\}_{Old}$$

if the function $\sum_{i=1}^{n} [Br_{23} - (Br_{23})_{cal}]^2$ is to be minimized. The calculation of the derivatives $\left(\frac{d(Br_{23})}{dTc_{23}}\right)_{cal}$ and $\left(\frac{d^2(Br_{23})}{dTr_{23}^2}\right)_{cal}$ from Equation (V-30) is tedious. At any given temperature T.

$$\left(\frac{d(Br_{23})}{dTc_{23}}\right)_{cal} = \left(\frac{d(Br_{23})}{dTr}\right)_{cal} \cdot \frac{dTr}{dTc_{23}} = -\left(\frac{d(Br_{23})}{dTr}\right)_{cal} \cdot \left(\frac{T}{Tc_{23}^2}\right) \quad \text{(F7-6)}$$

The quantity $\left(\frac{dBr}{dTr}\right)_{oo}$ is calculated analytically from Equation (V-30). $\frac{dBr}{dTr}$ can then be related to this derivative through the expressions developed in Appendix H-2. Similar considerations apply to the evaluation of

$$\frac{d^2Br_{23}}{dTc_{23}^2}$$

The initial estimate for Tc_{23} was set at 331.5K. The trials are all listed in Table F-6 along with the calculated increments for Tc_{23} at the end of each stage. The final value of Tc_{23} is 333.25K. This value of Tc_{23} is then used to recompute $g_r(Tr_{23}, \alpha c_{23})$. Its value was calculated as 1.0004 as opposed to the original estimate of 1.0008 obtained from the Redlich-Kwong rule. The change in the recomputed value of

$$\frac{RTc_{23}}{Pc_{23}}$$

lies in the fifth significant figure and can be ignored. The final values of the interaction parameters calculated from the given mixture are:

$$\frac{RTc_{23}}{Pc_{23}} = 618.2 \text{ cm}^3/\text{gm mole}$$

$$Tc_{23} = 333.25\text{K}$$

$$\alpha c_{23} = 6.351$$

5) Calculation of Smoothed Mixture Second Virial Coefficients as a Function of Temperature. The B_{23} values computed from the individual ethane-propane mixtures as a function of temperature are

listed in Table IX-5. The final selected values also indicated in the same table were obtained by averaging over all three mixtures in this particular case. The virial coefficients B_m for the 0.498 C_2H_6, 0.502 C_3H_8 mixture are now recalculated using the averaged B_{23} values.

At T = 198.15K, $(B_{23})_{\text{averaged}} = -614.0$ cm^3/gm mole

Using Equation (V-1),

$$B_m = (0.498)^2(-435.75) + 2(0.498)(0.502)(-614.0) + (0.502)(965.96)$$
$$= -658.49 \text{ cc/mole}$$

The calculated results covering the range from 198.15K to 510K are summarized in Table F-5.

6) Recalculation of Pseudo-Parameters for the 0.498 C_2H_6, 0.502 C_3H_8 Mixture Using Optimum Interaction Parameters for Rule VII of Table IX-10. The values of

$$\frac{RTc_{23}}{Pc_{23}}$$

Tc_{23} and αc_{23} as obtained from an analysis of the individual ethane-propane mixtures are indicated in Table IX-8. An

$$\frac{RTc_{23}}{Pc_{23}}$$

value of 612.2 cm^3/gm mole was finally selected for rule VII.

Similarly, the final value of αc_{23} was defined to be 6.380. Therefore, in order to determine how well the mixing rule encodes the enthalpy data for the entire binary system, it is first necessary to recalculate the pseudo-parameters for each mixture using the averaged interaction parameters. The calculations for the 0.498 C_2H_6 mixture are indicated below.

a) Calculation of αc_m. (See rule for αc_m for VII in Table IX-10)

$$\alpha c_m = (0.498)^2(6.275) + 2(0.498)(0.502)(6.380) + (6.502)^2(6.540)$$

= 6.394

b) Calculation of RTc_m/Pc_m: The value of RTc_m/Pc_m is computed from Equation (V-41) at T = 5000K in a fashion similar to that indicated for RTc_{23}/Pc_{23} in Step 3. The initial estimate of Tc_m necessary for the evaluation of $g(Tr_m, \alpha c_m)$ is again calculated from the Redlich-Kwong rule (IV) of Table IX-10 as 337.5K. The value of RTc_m/Pc_m is computed to be 618.9 cc/gm mole, as opposed to the optimum value of 621.97 cc/gm mole. This change is mainly attributed to a difference between the value of RTc_{23}/Pc_{23} used here and that calculated at the end of step 3.

c) Calculation of Tc_m: The calculated values of RTC_m/Pc_m and αc_m are used together with Equation (V-39) to determine the optimum value of Tc_m that will realize B_m values that are in best agreement with the results obtained in step 5. The calculation procedure is analogous to that indicated for Tc_{23} in step 4. The optimum value for Tc_m is calculated as 338.5K. The trials are indicated in Table F-4 using Newton's method to estimate the increment ΔTc_m. These parameters are then used to calculate the enthalpies for Rule VII in Table IX-14 using the PGC.

7) Calculation of Pseudo-parameters for the Ternary Mixture from Rule IX and X.

a) Calculation of Second Virial Coefficients for 0.369 CH_4, 0.308 C_2H_6 and 0.325 C_3H_8 Mixtures:

At 198.15K,

B_{11} = -107.35 cc/mole

B_{22} = -435.75 cc/mole

B_{33} = -965.96 cc/mole

B_{12} = -198.69 cc/mole

B_{23} = -614.0 cc/mole Obtained from Table F-5

B_{31} = -277.41 cc/mole

The pure component values are obtained from Equation (V-30) using the true critical parameters, and the interaction values are obtained by

TABLE F-4

Sample Results Illustrating The Calculation of The Pseudo-Critical Temperature Tc_m for the 0.498 Ethane-Propane Mixture Using Rule VII of Table IX-10

T	$B_{C_2H_6}$ ** cc/mole	$B_{C_3H_8}$ ** cc/mole	$B_{C_2H_6-C_3H_8}$ + cc/mole	B_m ++ cc/mole	Br_m +++	Estimation of Tc_m for Rule VII			
						First Guess Tc_m=334.5K		Second Guess Tc_m=338.5K	
						Tr_m	$Br_m-(Br_m)_{cal}$ *	Tr_m	$Br_m-(Br_m)_{cal}$
198.15	-435.75	-965.96	-614.00	-658.49	-1.0654	0.5925	-0.0308	0.5853	-0.0035
223.15	-341.14	-741.64	-478.00	-510.34	-0.8256	0.6672	-0.0217	0.6592	-0.0010
248.15	-274.47	-588.53	-387.00	-409.88	-0.6601	0.7420	-0.0162	0.7330	0.0003
273.16	-225.18	-479.27	-317.00	-335.12	-0.5399	0.8167	-0.0125	0.8069	0.0010
298.15	-187.42	-397.73	-263.50	-278.46	-0.4490	0.8915	-0.0100	0.8807	0.0013
310.90	-171.39	-363.68	-242.50	-255.40	-0.4108	0.9296	-0.0091	0.9184	0.0014
323.15	-157.62	-334.72	-223.00	-234.94	-0.3781	0.9662	-0.0083	0.9546	0.0015
348.15	-133.56	-284.70	-189.50	-199.62	-0.3213	1.0409	-0.0070	1.0284	0.0016
373.15	-113.75	-244.12	-163.00	-171.23	-0.2750	1.1157	-0.0059	1.1023	0.0016
398.15	-97.19	-210.63	-140.00	-147.18	-0.2365	1.1904	-0.0051	1.1761	0.0016
423.15	-83.15	-182.57	-120.00	-126.63	-0.2040	1.2652	-0.0045	1.2500	0.0016
444.36	-72.84	-162.17	-106.00	-111.93	-0.1803	1.3284	-0.0041	1.3124	0.0015
473.15	-60.65	-138.27	-90.00	-94.89	-0.1524	1.4147	-0.0036	1.3976	0.0015
510.90	-47.28	-112.34	-70.00	-75.04	-0.1220	1.5276	-0.0031	1.5092	0.0014
							ΔTc_m= 4.07K		ΔTc_m= 0.026K

\+ Weighted average values obtained from Table IX-5

++ Calculated values of the second virial coefficient for the 0.50 mole fraction ethane-propane mixture using Equation (V-1)

+++ $Br_m = B_m/(RTc_m/Pc_m)$, where RTc_m/Pc_m is obtained as 618.9 cm^3/gm mole by application of Equation (V-41)

* $(Br_m)_{cal}$ is obtained from Equation (V-30) from specified values of the mixture pseudo-parameter

** Obtained from Equation (V-30) using appropriate critical parameters

averaging the individual mixture results for each constituent binary system. The ternary mixture virial coefficient, B_m at 198.15K is now calculated from the rigorous relationship:

$$B_{mix} = x_1^2 B_{11} + x_2^2 B_{22} + x_3^2 B_{33} + 2\, x_1 x_2 B_{12} + 2x_2 x_3 B_{23}$$

$$+ 2x_3 x_1 B_{31}$$

$$= (0.369)^2(-107.35) + (0.308)^2(-435.75) + (0.325)^2(-965.96)$$

$$+ (2)(0.369)(0.308)(-198.69) + (2)(0.308)(0.325)(-614.0)$$

$$+ (2)(0.325)(0.369)(-277.41)$$

$$= -392.61 \text{ cc/gm mole}$$

The results for the temperature range from 198.15K to 510.9K are indicated in Table F-5.

b) Determination of αc_m: The optimum averaged values of αc_{ij} for each binary system as obtained from Tables IX-4 through IX-6 are:

$\alpha c_{12} = 6.08$

$\alpha c_{23} = 6.38$

$\alpha c_{31} = 6.35$

Therefore, using the quadratic mixing rule for αc_m as indicated in Table IX-10, we obtain

$$\alpha c_m = (0.369)^2(5.82) + (0.308)^2(6.275) + (0.325)^2(6.54)$$

$$+ (2)(0.369)(0.308)(6.08) + (2)(0.308)(0.325)(6.38)$$

$$+ (2)(0.325)(0.369)(6.35)$$

$$= 6.236$$

Rule IX only involves the prediction of Tc_m and RTc_m/Pc_m and

TABLE F-5

The Calculation of the Second Virial Coefficient[++] of the Ternary Mixture as a Function of Temperature Using the Technique of Figure V-2

$\left(\begin{smallmatrix}T\\ °K\end{smallmatrix}\right)$	B_{CH_4}	$B_{C_2H_6}$	$B_{C_3H_8}$	$B^{+}_{CH_4\text{-}C_2H_6}$	$B^{+}_{C_2H_6\text{-}C_3H_8}$	$B^{+}_{C_3H_8\text{-}CH_4}$	B^{*}_{m} (Ternary Mix)
198.150	-107.35	-435.75	-965.96	-198.69	-614.00	-277.41	-392.61
223.150	-84.25	-341.14	-741.04	-157.87	-478.00	-223.11	-307.20
248.150	-66.99	-274.47	-588.53	-127.69	-387.00	-182.20	-247.52
273.150	-53.63	-225.18	-479.27	-104.53	-317.00	-150.44	-202.59
298.150	-42.99	-187.42	-397.73	-86.27	-263.50	-125.18	-168.03
310.900	-38.36	-171.39	-363.68	-78.36	-242.50	-114.21	-153.65
323.150	-34.33	-157.62	-334.72	-71.50	-223.00	-104.66	-140.98
348.150	-27.13	-133.56	-284.70	-59.32	-189.50	-87.69	-118.89
373.150	-21.07	-113.75	-244.12	-49.12	-163.00	-73.44	-100.86
398.150	-15.09	-97.19	-210.63	-40.45	-140.00	-61.32	-85.45
423.150	-11.42	-83.15	-182.57	-33.00	-120.00	-50.90	-72.46
444.300	-8.09	-72.84	-162.17	-27.48	-106.00	-43.15	-62.96
473.150	-4.08	-60.65	-138.27	-20.87	-90.00	-33.88	-51.80
510.900	0.38	-47.28	-112.34	-13.53	-70.00	-23.59	-39.05

*Calculated from the Equation

$$B_m = \sum_i \sum_j x_i x_j B_{ij} .$$

+Values Obtained from the Interpretation of the Enthalpy Data of this Work.

++Values Obtained from Eqn.(V-30) Using Appropriate Critical Properties from Table J-1.

consequently an αc_m value of 6.245 obtained from the direct optimization of the ternary enthalpy data in the PGC framework (Rule I, Table (X-10)) is used.

c) Determination of RTc_m/Pc_m and Tc_m for Rules IX and X:

Given the value of αc_m, the two parameters RTc_m/Pc_m and Tc_m are adjusted by trial and error to yield the best agreement with the B_m values from 198.15K to 510.9K. The optimum value of Tc_m for each estimate of RTc_m/Pc_m is again obtained as indicated in Step 2. The direction and size of the increment for RTc_m/Pc_m is at each stage dictated by the goodness of fit. The trials for rules IX and X are summarized in Table F-6. The close agreement between the calculated B_m values in each case, inspite of the differences in αc_m, confirms the difficulty of extracting three unique parameters from second virial coefficient data.

For rule VII, the value of αc_m is the same as calculated in Step 7b, the value of RTc_m/Pc_m is obtained by repeating the procedure in Step 6b using all constituent binary parameters. Step 7c is repeated using the same set of B_m values, but only Tc_m is optimized.

TABLE F-6

Optimization Results on the Pseudoparameters RTc_m/Pc_m and Tc_m for the Ternary Mixture Using Estimated 2nd Virial Coefficients from Table F-5

ESTIMATED $(RTC/PC)_m$ (CC/GM MOL)	OPTIMIZED TC_m (°K)	PC_m (ATM)	ITERATIONS	% STD. DEV.	ALPHAC
541.	285.3	43.28	3	.17	6.245 *
545.	284.3	42.81	3	.23	
537.	286.3	43.75	3	.14	
541.	285.3	43.28	3	.17	
533.	287.3	44.23	3	.14	
529.	288.3	44.72	3	.16	
531.	287.8	44.48	3	.14	
530.	288.0	44.60	2	.15	
532.	287.5	44.35	3	.14	
533.	287.3	44.23	2	.14	
535.	286.8	43.99	2	.13 +	
541.	285.35	43.29	3	.17	6.236 **
549.	283.41	42.37	3	.24	
533.	287.34	44.23	3	.19	
541.	285.35	43.28	3	.17	
545.	284.38	42.82	3	.20	
537.	286.34	43.76	3	.163	
541.	285.35	43.29	2	.17	
533.	287.34	44.24	2	.19	
535.	286.84	44.00	2	.17	
534.	287.09	44.12	2	.18	
536.	286.59	43.88	3	.17	
537.	286.34	43.76	3	.163	
538.	286.09	43.64	3	.162	
539.	285.84	43.52	3	.162 ++	

++ OPTIMUM PSEUDO-PARAMETERS
* ALPHAC VALUE USED IN THE OPTIMIZATION FOR RULE IX
** ALPHAC VALUE USED IN THE OPTIMIZATION FOR RULE X

Appendix G

Derivation of a Modified Van der Waal Mixing Rule

The original Van der Waal Equation has the form

$$\left(P + \frac{a}{V^2} \right) \left(V - b \right) = RT \qquad \text{(G-1)}$$

where a and b are constants which can be chosen to satisfy certain characteristics of the PVT surface. If we apply the criterion

$$\left(\frac{\partial P}{\partial V} \right)_{T=Tc} = 0 \qquad \text{(G-1a)}$$

at the critical point, then Equation (G-1) yields

$$(Vc - b)^2 = \frac{R\ Tc\ Vc^3}{2a} \qquad \text{(G-2)}$$

As our second criterion, we set the slope of the critical isochore at the critical point to be equivalent to the slope of the vapor pressure curve at the critical point on a log P vs log T plot. The continuity of these two slopes at the critical point has already been established [202]. The condition is mathematically expressed as

$$\left(\frac{d \ln P}{d \ln T} \right)_{V=Vc} = \alpha c \qquad \text{(G-3)}$$

Substituting Equation (G-3) into Equation (G-1) we obtain

$$\alpha c = \frac{R\ Tc}{Pc} \frac{1}{(Vc - b)} \qquad \text{(G-4)}$$

Combining Equations (G-2) and (G-4) we obtain

$$a = \frac{\alpha c^2\ Pc^2\ Vc^3}{2\ R\ Tc} \qquad \text{(G-5)}$$

At the critical point Equation (G-1) becomes

$$\left(Pc + \frac{a}{Vc^2}\right) (Vc - b) = R\ Tc \qquad \text{(G-6)}$$

Substituting Equation (G-4) into Equation (G-6) we obtain

$$\alpha c = (Pc + \frac{a}{Vc^2})/Pc \qquad (G-7)$$

Resubstituting for a in Equation (G-7) using Equation (G-5), we obtain

$$\frac{Pc\ Vc}{R\ Tc} \equiv zc = \frac{2(\alpha c - 1)}{\alpha c^2} \qquad (G-8)$$

Rearranging Equation (G-4) we obtain

$$b = Vc - \frac{R\ Tc}{Pc}\ \frac{1}{\alpha c} \equiv \frac{R\ Tc}{Pc}\ [\ zc - \frac{1}{\alpha c}\ ] \qquad (G-9)$$

If we substitute for zc in Equation (G-9) using the right hand side of Equation (G-8) we obtain

$$b = \frac{R\ Tc}{Pc}\ [\ \frac{\alpha c - 2}{\alpha c^2}\ ] \qquad (G-10)$$

Combining Equations (G-5) and (G-8) we obtain

$$a = \frac{\alpha c^2\ zc^3\ R^2\ Tc^2}{2\ Pc} = 4\ \frac{(\alpha c - 1)^3}{\alpha c^4}\ \frac{R^2\ Tc^2}{Pc} \qquad (G-11)$$

The modified reduced Van der Waal Equation now has the form

$$[\ P + \frac{4(\alpha c - 1)^3}{\alpha c^4}\ \frac{R^2\ Tc^2}{Pc}\ \frac{1}{V^2}\ ]\ [\ V - \frac{R\ Tc}{Pc}\ (\ \frac{\alpha c - 2}{\alpha c^2})\ ] \qquad (G-12)$$

$$= RT$$

The second virial coefficient for the above equation can be written as

$$B = \lim_{V \to \infty} \frac{d(z - 1)}{d(1/V)} = b - \frac{a}{RT} \qquad (G-13)$$

$$= \frac{R\ Tc}{Pc}\ \frac{(\alpha c - 2)}{\alpha c^2} - 4\ \frac{(\alpha c - 1)^3}{\alpha c^4}\ \frac{R\ Tc^2}{T\ Pc} \qquad (G-14)$$

It is now assumed that Equation (G-14) can be applied to all the constituent pure components of a mixture, to all mixtures of such components, and to the interaction virial coefficients defined by appropriate pseudoconstants Tc_{ij} and Pc_{ij}. We also recall that the mixture second virial coefficients can be rigorously expressed in terms of like and unlike pair interaction second virials by the relation

$$B_m = \sum_{i=1}^{n} \sum_{j=1}^{n} x_i x_j B_{ij} \qquad \text{(G-15)}$$

Therefore, it is permissible to substitute Equation (G-14) with appropriate pseudoconstants for each of the B terms in Equation (G-15). Now since Equations (G-14) and (G-15) are presumed to be valid at all temperatures, they are presumed to hold for the special case as T approaches infinity. Therefore, we may substitute Equation (G-14) into Equation (G-15) as $T \to \infty$, which yields the result

$$\frac{R\,Tc_m}{Pc_m}\,\frac{(\alpha c_m - 2)}{\alpha c_m^{\,2}} = \sum_{i=1}^{n} \sum_{j=1}^{n} x_i x_j \frac{R\,Tc_{ij}}{Pc_{ij}} \left(\frac{\alpha c_{ij} - 2}{\alpha c_{ij}^{\,2}} \right) \qquad \text{(G-16)}$$

Now, if we substitute Equation (G-14) into Equation (G-15) at any finite temperature and take cognizance of the equality in Equation (G-16), we obtain the result

$$\frac{R\,Tc_m^{\,2}}{Pc_m}\,\frac{(\alpha c_m - 1)^3}{\alpha c_m^{\,4}} = \sum_{i=1}^{n} \sum_{j=1}^{n} x_i x_j \frac{R\,Tc_{ij}^2}{Pc_{ij}} \frac{(\alpha c_{ij} - 1)^3}{\alpha c_{ij}^4} \qquad \text{(G-17)}$$

Equations (G-16) and (G-17) now comprise the modified Van der Waal mixing rules. A host of other mixing rules may be similarly derived by either choosing a different two parameter equation of state or by selecting different characterizing conditions for the PVT surface.

APPENDIX H

Thermodynamic Property Calculations Using Selected Methods

Appendix H-1

Thermodynamic Properties from the Starling Modified Benedict-Webb-Rubin Equation of State

a) Volume [254]

$$P = RT\rho + \left(B_oRT - A_o - \frac{C_o}{T^2} + \frac{D_o}{T^3} - \frac{E_o}{T^4} \right) \rho^2 + \left(bRT - a - \frac{d}{T}\right) \rho^3 + \left(a + \frac{d}{T}\right) \alpha\rho^6 + \frac{c\rho^3}{T^2} \left[(1 + \gamma\rho^2)\, e^{-\gamma\rho^2}\right]$$

b) Second Virial Coefficient

$$B = \frac{1}{RT} \left(B_oRT - A_o - \frac{C_o}{T^2} + \frac{D_o}{T^3} - \frac{E_o}{T^4} \right)$$

c) Third Virial Coefficient

$$C = \frac{1}{RT} \left(bRT - a - \frac{d}{T} \right)$$

4) Enthalpy Departure

$$H - H^\circ = \left(B_oRT - 2A_o - \frac{4C_o}{T^2} + \frac{5D_o}{T^3} - \frac{6E_o}{T^4} \right) \rho + \left(bRT - \frac{3a}{2} - \frac{2d}{T}\right) \rho^2 + (6a+7d)\, \frac{\alpha\rho^5}{5} + \frac{c\rho^2}{T^2} \left[3 \left(\frac{1-e^{-\gamma^2}}{\gamma\rho^2}\right) - \frac{e^{-\gamma\rho^2}}{2} + \gamma\rho^2 e^{-\gamma\rho^2} \right]$$

5) Isothermal Throttling Coefficient

$$\phi = \frac{\left(B_oRT - A_o - \frac{4C_o}{T^2} + \frac{5D_o}{T^3} - \frac{6E_o}{T^4} \right) + \left(2bRT - 3a - \frac{4d}{T} \right) \rho + (6a+7d)\, \alpha\rho^4 + \frac{ce^{-\gamma\rho^2}}{T^2} \left[5\rho + 5\gamma\rho^3 - 2\gamma^2\rho^5 \right]}{RT + 2\rho \left(B_oRT - A_o - \frac{C_o}{T^2} - \frac{2D_o}{T^3} + \frac{2E_o}{T^4} \right) + 3\rho^2 \left(bRT - a - \frac{d}{T}\right) + 6\left(a + \frac{d}{T}\right) + 6\left(a + \frac{d}{T}\right) \alpha\rho^5 + \frac{ce^{-\gamma\rho^2}}{T^2} \left[3\rho^2(1 + \gamma\rho^2) - 2\gamma^2\rho^6\right]}$$

6) Heat Capacity

$$C_p - C_p^\circ = \frac{-R + 6C_o\rho}{T^3} - \frac{6c}{\gamma T^3} - \frac{12\, D_o\rho}{T^4} + \frac{20\, E_o\rho}{T^5} + \frac{d}{T^2}\, \rho^2 - \frac{2}{5}\, \alpha \frac{d}{T^2}\, \rho^5 + \left(\frac{6c}{\gamma T^3} + \frac{3c\rho^2}{T^3} \right) e^{-\gamma\rho^2} +$$

$$\frac{\left[R + \left(B_o + \frac{2C_o}{T^3} - \frac{3D_o}{T^4} + \frac{4E_o}{T^5}\right) \rho + \left(bR + \frac{d}{T}\right)\rho^2 - \frac{\alpha d\rho^5}{T^2} - \frac{2c\rho^2}{T^3} \left(1 + \gamma\rho^2 \right) e^{-\gamma\rho^2} \right]^2}{R + \left(2B_oR - \frac{2A_o}{T} - \frac{2C_o}{T^3} + \frac{2D_o}{T^4} - \frac{2E_o}{T^5} - \frac{3d}{T}\right) \rho + \left(3bR - \frac{3a}{T}\right) \rho^2 + \frac{6\alpha d\rho^4}{T^2} + \frac{6a\alpha\rho^5}{T} + \frac{\left(3c\rho^2 + 3c\gamma\rho^4 - 2c\gamma^2\rho^6\right) e^{-\gamma\rho^2}}{T^3}}$$

Appendix H-2

COMBINING RULES FOR CONSTANTS IN THE STARLING B-W-R EQUATION OF STATE

$$A_{o\ mix} = \left(\sum_i x_i A_{o_i}^{1/2}\right)^2$$

$$B_{o\ mix} = \sum_i x_i B_{o_i}$$

$$C_{o\ mix} = \left(\sum_i x_i C_{o_i}^{1/2}\right)^2$$

$$D_{o\ mix} = \left[\sum_i x_i D_{o_i}^{1/2}\right]^2 + \sum_{i=1}^{} \sum_{j=1}^{} x_i x_j h_{ij} \left[(D_{o_i} + D_{o_j})/2 - (D_{o_i} D_{o_j})^{1/2}\right]$$

$$E_{o\ mix} = \left[\sum_{i=1} x_i E_{o_i}^{1/2}\right]^2 + \sum_{i=1}^{} \sum_{j=1}^{} x_i x_j k_{ij} \left[(E_{o_i} + E_{o_j})/2 - (E_{o_i} E_{o_j})^{1/2}\right]$$

$$a_{mix} = \left(\sum_i x_i a_i^{1/3}\right)^3$$

$$b_{mix} = \left(\sum_i x_i b_i^{1/3}\right)^3$$

$$c_{mix} = \left(\sum_i x_i c_i^{1/3}\right)^3$$

$$d_{mix} = \left(\sum_i x_i d_i^{1/3}\right)^3$$

$$\alpha_{mix} = \left(\sum_i x_i \alpha_i^{1/3}\right)^3$$

$$\gamma_{mix} = \left(\sum_i x_i \gamma_i^{1/2}\right)^2$$

Appendix H-3

Thermodynamic Properties from the Reduced Virial Equation Truncated at the Third Virial Coefficient

1) Definitions

$Br = B/(RTc/Pc)$

$Cr = C/(RTc/Pc)^2$

$Tr = T/Tc$

$\tilde{V} = z\,Tr/Pr = ZcVr$

2) Thermodynamic Relations

$$z(z-1) = Br\frac{Pr}{Tr} + \frac{1}{z}Cr\frac{Pr^2}{Tr^2} \qquad \text{(H2-1)}$$

$$\phi r = \frac{(dH/dP)}{RTc/Pc}_T = \left(Br - Tr\frac{dBr}{dTr}\right) + \frac{1}{\tilde{V}}\left[\left(2Cr - Tr\frac{dCr}{dTr}\right)\frac{1}{\tilde{V}}\right]$$

$$\left[1 + 2Br - \frac{3Cr}{\tilde{V}}\right] \qquad \text{(H2-2)}$$

$$\frac{U - U^\circ}{RTc} = \frac{Tr^2}{\tilde{V}}\left(\frac{dBr}{dTr} + 0.5\frac{dCr}{dTr}\frac{1}{\tilde{V}}\right) \qquad \text{(H2-3)}$$

$$\frac{H - H^\circ}{RTc} = \frac{U - U^\circ}{RTc} + Tr(1 - z) \qquad \text{(H2-4)}$$

$$f/P = \exp\left\{\left[Br + 0.5\frac{Cr}{\tilde{V}}\right]\frac{1}{\tilde{V}} + (z-1)\right\}/z \qquad \text{(H2-5)}$$

$$\frac{Cv - Cv^\circ}{R} = -\frac{Tr}{\tilde{V}}\left\{2\frac{dBr}{dTr} + \frac{dCr}{dTr}\frac{1}{\tilde{V}} + Tr\left[\frac{d^2Br}{d\,Tr^2} + \frac{1}{z}\frac{d^2Cr}{d\,Tr^2}\frac{1}{\tilde{V}}\right]\right\} \qquad \text{(H2-6)}$$

$$\frac{Cp - Cp^\circ}{R} = \left(Br - Tr\frac{dBr}{dTr}\right)^2\frac{1}{\tilde{V}^2} - Tr^2\frac{d^2Br}{dTr^2}\frac{1}{\tilde{V}} + \left(Cr - Tr\frac{dCr}{dTr}\right)\left(\frac{1}{\tilde{V}^2}\right) \qquad \text{(H2-7)}$$

3) Determination of dBr/dTr and d^2Br/dTr^2 from the Second Virial Coefficient Correlation of this Work (Equation V-30)

If Equation (V-30) is used to represent the reduced second virial coefficient, then the derivatives dBr/dTr_{oo} and d^2Br/dTr_{oo} may be straight forwardly obtained in analytic form by differentiation. The extraction of the derivatives dBr/dTr and d^2Br/dTr^2 necessary for the calculation of thermodynamic properties is, however, more complicated. We recall from Chapter III that the Riedel reduced vapor pressure equation (III-36) may be used to obtain Tr_{oo} from Tr by requiring the reduced saturated vapor pressure Pr_s to be the same in both cases. Therefore, for methane as the reference fluid we obtain:

$$- \phi\ (Tr) - (\alpha c - 7)\ \Psi(Tr) = - \phi(\ Tr_{CH_4}) - (\alpha c_{CH_4} - 7.0)\ \Psi(Tr_{CH_4}) \qquad \text{(H2-8)}$$

where ϕ and Ψ are defined by Equations (III-36a) and (III-36b) respectively. On substituting the αc value for methane and differentiating the above equation, we obtain on rearrangement:

$$\frac{dTr_{CH_4}}{dTr} = [\ \dot{\phi}_{Tr_{CH_4}} - (\alpha c - 7.00)\ \dot{\Psi}_{Tr_{CH_4}}\ ]/[\ \dot{\phi}_{Tr} - (5.82-7.00)\ \dot{\Psi}_{Tr}] \qquad \text{(H2-9)}$$

On further differentiation, the result

$$\frac{d^2Tr_{CH_4}}{dTr^2} = \frac{d\ Tr_{CH_4}}{dTr}\ [\ \phi_{Tr_{CH_4}} - (5.82-7.0)\ \Psi_{Tr_{CH_4}}\ ]/$$

$$[\ \phi_{Tr} - (\alpha c - 7.0)\ \Psi_{Tr}\ ] \qquad \text{(H2-10)}$$

is obtained. The derivatives dBr/dTr, and d^2Br/dTr^2 required for the evaluation of the thermodynamic properties in 2) can now be

expressed in terms of the corresponding derivatives with Tr_{CH_4} as variable using the transformations:

$$\frac{dBr}{dTr} = \left(\frac{dBr}{dTr_{CH_4}}\right)\frac{dTr_{CH_4}}{dTr} \qquad \text{(H2-11)}$$

$$\frac{d^2Br}{dTr^2} = \left(\frac{dBr}{dTr_{CH_4}}\right)\left(\frac{d^2Tr_{CH_4}}{dTr^2}\right) + \left(\frac{dTr_{CH_4}}{dTr}\right)^2 \frac{d^2Br}{dTr_{CH_4}} \qquad \text{(H2-12)}$$

The value of dCr/dTr and d^2Cr/dTr^2 can also be directly obtained from Equation III.

Appendix H-4

Sample Output of Thermodynamic Property Calculations on the Ternary Mixture at 126.2°F by Several Techniques

T (°K)	P (psia)		B (cc/gm mole)	C (cc/gm mole)^2	PHI Btu/lb/psia	CP Btu/lb/°F	H* Btu/lb	HDEP Btu/lb	CPDEP Btu/lb/°F	Z
126.30	0.01	1	-0.1397E 03		-0.4558E-01	0.4570E 00	0.3875E 03	-0.0	0.0	0.1000E 01
		2	-0.1397E 03	0.9045E 04	-0.4558E-01	0.4570E 00	0.3875E 03	-0.0	0.0	0.1000E 01
		3	-0.1400E 03	0.9045E 04	-0.4558E-01	0.4570E 00	0.3875E 03	-0.0	0.0	0.1000E 01
		4	-0.1389E 03	0.9045E 04	-0.4396E-01	0.4570E 00	0.3875E 03	-0.0	0.0	0.1000E 01
		5	-0.1432E 03	-0.1113E 04	-0.4709E-01	0.4570E 00	0.3875E 03	-0.	0.0	0.1000E 01
		6					0.3875E 03	-0.		
126.30	250.00	1	-0.1397E 03		-0.5680E-01	0.5058E 00	0.3748E 03	-0.1264E 02	0.4876E-01	0.9013E 00
		2	-0.1397E 03	0.9045E 04	-0.5305E-01	0.5038E 00	0.3752E 03	-0.1227E 02	0.4637E-01	0.9063E 00
		3	-0.1400E 03	0.9045E 04	-0.5308E-01	0.5029E 00	0.3752E 03	-0.1227E 02	0.4586E-01	0.9061E 00
		4	-0.1389E 03	0.9045E 04	-0.5099E-01	0.5015E 00	0.3757E 03	-0.1181E 02	0.4445E-01	0.9070E 00
		5	-0.1432E 03	-0.1113E 04	-0.5439E-01	0.5101E 00	0.3749E 03	-0.1262E 02	0.5302E-01	0.9041E 00
		6					0.3756E 03	-0.1189E 02		
126.30	500.00	1	-0.1397E 03		-0.8491E-01	0.6220E 00	0.3578E 03	-0.2966E 02	0.1650E 00	0.7684E 00
		2	-0.1397E 03	0.9045E 04	-0.6492E-01	0.5860E 00	0.3606E 03	-0.2689E 02	0.1290E 00	0.8006E 00
		3	-0.1400E 03	0.9045E 04	-0.6503E-01	0.5850E 00	0.3606E 03	-0.2690E 02	0.1280E 00	0.8001E 00
		4	-0.1389E 03	0.9045E 04	-0.6201E-01	0.5790E 00	0.3617E 03	-0.2582E 02	0.1220E 00	0.8024E 00
		5	-0.1432E 03	-0.1113E 04	-0.6558E-01	0.5966E 00	0.3600E 03	-0.2750E 02	0.1396E 00	0.7967E 00
		6					0.3611E 03	-0.2635E 02		
126.30	750.00**	1	-0.1397E 03							0.1000E-01
		2	-0.1397E 03	0.9045E 04	-0.8552E-01	0.7646E 00	0.3420E 03	-0.4545E 02	0.3076E 00	0.6782E 00
		3	-0.1400E 03	0.9045E 04	-0.8593E-01	0.7640E 00	0.3419E 03	-0.4553E 02	0.3070E 00	0.6769E 00
		4	-0.1389E 03	0.9045E 04	-0.8058E-01	0.7408E 00	0.3440E 03	-0.4344E 02	0.2837E 00	0.6819E 00
		5	-0.1432E 03	-0.1113E 04	-0.8268E-01	0.7613E 00	0.3416E 03	-0.4591E 02	0.3043E 00	0.6751E 00
		6					0.3425E 03	-0.4496E 02		
126.30	1000.00	1	-0.1397E 03							0.1000E-01
		2	-0.1397E 03	0.9045E 04	-0.1071E 00	0.1153E 01	0.3174E 03	-0.7008E 02	0.6959E 00	0.5441E 00
		3	-0.1400E 03	0.9045E 04	-0.1080E 00	0.1158E 01	0.3171E 03	-0.7034E 02	0.7007E 00	0.5416E 00
		4	-0.1389E 03	0.9045E 04	-0.9884E-01	0.1073E 01	0.3211E 03	-0.6638E 02	0.6162E 00	0.5516E 00
		5	-0.1432E 03	-0.1113E 04	-0.9194E-01	0.1028E 01	0.3191E 03	-0.6837E 02	0.5705E 00	0.5522E 00
		6					0.3184E 03	-0.6909E 02		
126.30	1500.00	1	-0.1397E 03							0.1000E-01
		2	-0.1397E 03	0.9045E 04	-0.3563E-01	0.1084E 01	0.2823E 03	-0.1051E 03	0.6274E 00	0.4629E 00
		3	-0.1400E 03	0.9045E 04	-0.3534E-01	0.1077E 01	0.2821E 03	-0.1052E 03	0.6201E 00	0.4610E 00
		4	-0.1389E 03	0.9045E 04	-0.3349E-01	0.1022E 01	0.2883E 03	-0.9911E 02	0.5647E 00	0.4690E 00
		5	-0.1432E 03	-0.1113E 04	-0.4045E-01	0.1048E 01	0.2862E 03	-0.1013E 03	0.5910E 00	0.4675E 00
		6					0.2814E 03	-0.1061E 03		
126.30	2000.00	1	-0.1397E 03							0.1000E-01
		2	-0.1397E 03	0.9045E 04	-0.1478E-01	0.9354E 00	0.2709E 03	-0.1166E 03	0.4783E 00	0.5082E 00
		3	-0.1400E 03	0.9045E 04	-0.1464E-01	0.9267E 00	0.2707E 03	-0.1168E 03	0.4697E 00	0.5067E 00
		4	-0.1389E 03	0.9045E 04	-0.1345E-01	0.8894E 00	0.2777E 03	-0.1098E 03	0.4324E 00	0.5129E 00
		5	-0.1432E 03	-0.1113E 04	-0.1718E-01	0.9067E 00	0.2726E 03	-0.1149E 03	0.4497E 00	0.5044E 00
		6					0.2694E 03	-0.1181E 03		

* Assuming H=0 for the pure components methane, ethane and propane at -280°F.

** Method 1 diverges beyond 750 psia.

Code

1. Results obtained with the reduced virial equation using the B correlation of this work [Eqn.(V-30)].
2. Results obtained with the reduced virial equation using the B correlation of this work [Eqn.(V-30)] and the Chueh-Prausnitz C correlation [Eqn.(III-44)].
3. Results obtained with the B correlation of Pitzer et al. [Eqn.(III-40)] and the C correlation of [Eqn.(III-44)].
4. Results obtained with the B correlation of McGlashan and Potter [Eqn.(III-43)] and the C correlation of [Eqn.(III-44)].
5. Results obtained with the Starling modified BWR Equation [Eqn.(III-19)]
6. Enthalpy values generated by the Powers Generalized correlation

Methods 1 through 5 use the optimum pseudo-parameters in Table (IX-19).

APPENDIX I

Procedures

Appendix I-1

Procedure for Flowmeter Calibration

The procedure for calibrating the flowmeter has been described in detail by Jones [119]. The basic technique is outlined in Section VI. Further improvements in the procedure are discussed here using Figure VI-1 as a guide.

a) Initial preparation

Storage tanks 1, 2, 3 and 4 are equalized through valves 11, 12 and 13 in between tanks. By initially increasing the volume of gas involved in the calibration operation, the variation in the measured fluid properties at the flowmeter (including the flowrate) due to a fixed rate of decrease in the supply is kept to a minimum. The pressure in the equalized tanks should not exceed 1000 psia for the heavier hydrocarbons if the Joule-Thomson cooling effect is to be prevented from causing fractionation and subsequent composition upsets at throttle TR. The compressor is started up, and the total gas flow is initially directed through the bypass stream. The water manometer is levelled and pressurized to flowmeter conditions with both legs equalized. The manometer is then isolated at the pressure taps leading to the flowmeter, and the null height difference correction observed. The center tap is shut, isolating the individual legs, and the manometer null reading is observed as a function of time for at least ten minutes. A mass leak is indicated in a given leg if the water level continues to rise with time.

b) Leak test of solenoid valves

The solenoid valve S (Appendix D, Item 8g) switches the flow instantaneously from the reservoir to the sample cylinder and is normally open at the reservoir. A leaky valve seat can cause the system fluid to simultaneously condense in both cylinders causing serious measurement errors. As a precautionary measure, the line to the reservoir is pressurized to about 80 psig in the open position through valves 16 and 17. The solenoid valve is now electrically activated into the closed position, and the sample line evacuated. A change in pressure

at the reservoir line as monitored by an Ashcroft gage (Item 8f, Appendix D), during this operation indicates a leak across the valve in the closed position which must be rectified. Leakage tests in the open position may be similarly conducted. As a further precaution, valve 19 on the reservoir is shut just after the sample cylinder begins to fill. Similarly, valve 18 on the sample cylinder is closed during the reservoir filling period, until just before the solenoid is activated.

c) Simulation of calibration conditions.

To ensure that the calibration operation is smooth, the conditions are first simulated in recycle mode. The compressed gas is fed directly into tank 1 via valve 10 bypassing the high pressure side of the manifold. The gas to the flowmeter and bypass section is supplied by tank 4 through valve 4H. Valves 6 and 7 opened, and the Tescom regulator (Item 8h Appendix D) TR is adjusted until the desired flowmeter pressure is attained. The desired flow through the flowmeter section is obtained by suitable adjustment of the bypass throttle BT. Variacs supplying electrical energy to heating tapes located at throttling valves are adjusted until steady state temperature conditions are achieved.

d) Calibration

The compressor is shut down, the bypass valve closed, and the bypass throttle heat removed. The metering valve 17 is adjusted until the desired flowrate is noted at the water manometer. The regulator TR is also adjusted to provide the desired pressure at the flowmeter. The solenoid valve S is activated along with a timer that records the duration of flow into the sample cylinder B. The flowmeter pressure, and the water monometer readings are recorded approximately every 30 seconds. The time of calibration is a function of the flowrate and is chosen to condense equivalent amounts of gas in each sample cylinder. The maximum amount permitted in any sample cylinder is subject to a pressure limitation of 1200 psia at room temperature. Approximately 9 gram moles of gas may be safely condensed per cylinder. Any trend in the flowmeter pressure during calibration may be reversed by

adjusting the calibration line heat between valve 6 and TR. The pressure is decreased if the line temperature is increased and vice-versa.

e) Post calibration procedure

After the solenoid valve S is deactivated, and the calibration time noted, valve 4H is shut, cutting off the gas supply to the flowmeter section. Next, all variacs supplying heat at throttling points are turned off. Chromatographic analyses of the system fluid at the flowmeter and the standard mixture are then made. It is important to ensure that the chromatograph sampling valves located after the flowmeter are shut subsequent to each analysis to prevent the occurence of a leakage path parallel to the sampling cylinder B. The next set of calibration conditions are simulated as in step c.

f) Precautions for heavy hydrocarbons

In the case of the ethane-propane system, the valve mainfold temperature could not be raised significantly above the critical temperatures of the mixtures investigated. As a result, substantial cooling effects were obtained at all throttling locations. Condensation and subsequent composition upsets were known to occur for the 0.27 C_2H_6 - C_3H_8 mixture after the regulator TR. This was in part caused by the accumulation of carbon deposits that decreased the effective orifice size of the regulator around which an additional heating tape were wrapped. The use of such extra tapes before throttling processes are not without their disadvantages. Consequently, for this particular mixture, additional heating tapes were added to the lines after the throttling valves. In some cases, however, this technique overheated the gas entering the flowmeter bath to the extent that the heat transfer area in the bath was insufficient to bring the gas to the bath temperature, which it normally is assumed to have attained, and led to errors in the estimation of the viscosity and density of the fluid used in the calculation of the mass flowrate. To avoid such occurences, the cooling coil before the flowmeter bath should be placed in the path of the gas as it leaves the valve manifold.

Appendix I-2

Procedure for System Mixture Preparation

In every case, the mixture investigated at the recycle facility is prepared *in situ*. The general procedure is explained here using Figure VI-1 as a guide. The pressure is equalized in all the storage tanks prior to the introduction of the external feed gas. An approximate estimate of the total quantity of gas within the tanks can be made from a knowledge of the pressure, temperature, and volume of the tanks, and from the composition of the existing gas mixture. The optimum capacity of the system lies between 2.5 and 3 lb. moles. The amount of each component required to be fed to the system to achieve the desired capacity is then computed for the case where all components in the existing mixture are present in the desired case.

The required quantities of the individual pure components are successively fed to the system at between 40 and 120 psig via valve FL on the low side of the valve manifold from external tanks set on a weighing platform. The gas is compressed and distributed to all the storage tanks if valves 1 through 4, and 1H through 5H are kept open. The external pure component tanks are wrapped with heating tapes, either to prevent condensation during the throttling process in the case of a high pressure source, or to generate a steady vapor flowrate from a liquid source such as propane.

Valves 1 through 4, and 1H through 5H are shut, and the fluid is circulated successively through the tanks starting with tank 1, if valves 10, 11, 12, 13 and 14 in between succesive tanks are open. Extra heating tapes are utilized to heat the storage tanks during this operation. The fluid is recycled to the compressor from tanks through valve 5L on the low side of the manifold, and the operation continued for about 24 hours. Each tank from 1 to 5 is then emptied in sequence into the rest of the tanks, after which all five tanks are equilibrated. Thus, if tank 3 is to be emptied, all valves on the low side of the manifold are shut except 3L, which supplies the compressor feed. Valves 1H, 2H, 4H and 5H are opened together with valves 1, 2, 4 and 5, while valves 11 through 14 are shut. When tank 3 is empty, valve 3L is shut, and all the tanks are equilibrated by opening valve

3H. This technique was found to hasten the mixing process.

The composition in each tank is chromatographically monitored through the bypass stream about every 2 hours by temporarily switching to the appropriate tank to feed the compressor. Thus, in order to analyse tank 1, it is necessary to shut valve 5L and open 4L. The analysis is compared with those from independently and accurately prepared standards using 400 cc containers. If the composition upon complete mixing is not quite at the desired value, additional amounts of the appropriate components are then fed to the system and the mixing process continued. It was determined that complete homogeneity could be easily achieved within 64 hours using this technique.

APPENDIX J

Data and Results Relevant to the Development of the Second Virial Coefficient Coefficients Correlations [Equations (V-30) and (V-41)] of This Work

TABLE J-1

Summary of Characteristic Properties of Substances Used in the Development of the Second Virial Coefficient Correlation of This Work

	Tc (°K)	Pc (Atm)	αc	ω	Vc (cc/gm mole)	Mol. Wt.	RTc/Pc (cc/gm mole)	1/zc
METHANE	190.70	45.80	5.820	0.0130	100.30	16.042	341.69	3.4067
ARGON	150.70	48.00	5.760	-0.0020	75.30	39.944	257.64	3.4216
KRYPTON	209.40	54.30	5.940	-0.0020	92.10	83.700	316.46	3.4361
ETHANE	305.40	48.20	6.275	0.1050	148.00	30.068	519.96	3.5132
PROPANE	369.90	42.01	6.540	0.1520	200.00	44.094	722.57	3.6128
BUTANE	425.20	37.50	6.772	0.2020	255.10	58.120	930.48	3.6475
CF4	227.70	37.00	6.725	0.2100	153.00	88.010	505.02	3.3008
PENTANE	469.50	33.30	7.000	0.2520	311.00	72.250	1157.01	3.7203
OCTANE	568.60	24.60	7.760	0.4080	486.00	114.220	1896.79	3.9029
NITROGEN	126.20	33.50	5.980	0.0400	90.10	28.016	309.14	3.4311
CO2	304.20	72.90	6.916	0.2250	94.00	44.010	342.44	3.6429
OXYGEN	154.80	50.10	5.920	0.0210	74.40	32.050	253.56	3.4081
NEOPENTANE	433.80	31.60	6.780	0.1950	303.00	72.150	1126.55	3.7180
ISOPENTANE	460.40	32.90	6.870	0.2060	308.00	72.150	1148.38	3.7285

TABLE J-2

Least Squares Regression Results for the Reduced Second Virial Coefficient Tabulation of Leland et al. [145] at High Temperatures++

T/T_M	B/B_M	$(B/B_M)_{Cal}$	$(\frac{B}{B_M})-(\frac{B}{B_M})_{Cal}$	$(100)(Y-Y_{Est})/Y$
X VALUE	Y VALUE+	Y ESTIMATE*	RESIDUAL	PCERR
C.4444000	C.8280C	C.82336	0.00464	0.560
C.5000000	C.85942	C.85810	0.00132	0.153
C.5549999	0.87610	C.88803	-0.01193	-1.362
C.6944000	C.95000	C.94587	0.00413	0.434
C.8333000	C.98570	C.98114	0.00456	0.462
1.0000000	1.00000	C.99987	0.00013	0.013
1.1109991	C.99760	1.00137	-0.00377	-0.378
1.3879995	C.98330	C.98234	0.00096	0.097
1.6659994	C.95710	C.95711	-0.00001	-0.001

Absolute Average % Error = 0.38464

* Using the equation $\frac{B}{B_M} = 0.3517 + 1.5068(\frac{T}{T_M}) - 1.11739(\frac{T}{T_M})^2 + 0.25874(\frac{T}{T_M})^3$

\+ Obtained by modification of a tabulation by Leland et al. [145] as explained in Appendix F-5

++ The reduction parameters T_M and B_M were substituted for Tc and Vc as used in the original correlation

TABLE J-3

Comprehensive Results for The Generalized Second Virial Coefficient Correlation of Equation V-30

System	T (°K)	Tr	B*	Br_{oo}	Tr_{oo}	Br_{cal}	B cc/mole	B^{+}_{cal} cc/mole	Reference*
CH_4	110.83	0.5812	-0.9661	-0.9608	0.5812	-0.9608	-330.10	-328.28	[35]
	112.43	0.5896	-0.9362	-0.9342	0.5896	-0.9342	-319.90	-319.21	
	114.45	0.6002	-0.9008	-0.9024	0.6002	-0.9024	-307.80	-308.33	
	116.79	0.6124	-0.8648	-0.8676	0.6124	-0.8676	-295.50	-296.45	
	121.25	0.6358	-0.8034	-0.8070	0.6358	-0.8070	-274.50	-275.75	
	128.84	0.6756	-0.7150	-0.7183	0.6756	-0.7183	-244.30	-245.44	
	136.75	0.7171	-0.6406	-0.6412	0.7171	-0.6412	-218.90	-219.1[illegible]	
	148.28	0.7776	-0.5493	-0.5498	0.7776	-0.5498	-187.70	-187.87	
	162.29	0.8510	-0.4636	-0.4630	0.8510	-0.4630	-158.40	-158.22	
	178.41	0.9356	-0.3869	-0.3860	0.9356	-0.3860	-132.20	-131.89	
	202.49	1.0618	-0.3026	-0.3008	1.0618	-0.3008	-103.40	-102.79	
	221.10	1.1594	-0.2511	-0.2514	1.1594	-0.2514	-85.80	-85.89	
	243.80	1.2784	-0.2057	-0.2039	1.2784	-0.2039	-70.30	-69.67	
	273.17	1.4325	-0.1572	-0.1569	1.4325	-0.1569	-53.70	-53.62	
	191.06	1.0019	-0.3404	-0.3377	1.0019	-0.3377	-116.30	-115.38	[108]
	200.06	1.0491	-0.3123	-0.3082	1.0491	-0.3082	-106.70	-105.31	
	215.06	1.1277	-0.2710	-0.2662	1.1277	-0.2662	-92.59	-90.96	
	240.00	1.2585	-0.2128	-0.2111	1.2585	-0.2111	-72.72	-72.12	
	273.15	1.4324	-0.1559	-0.1570	1.4324	-0.1570	-53.28	-53.63	
	123.15	0.6458	-0.7735	-0.7832	0.6458	-0.7833	-264.30	-267.63	[28]
	148.15	0.7769	-0.5441	-0.5507	0.7769	-0.5507	-185.90	-188.19	
	173.15	0.9080	-0.4059	-0.4090	0.9080	-0.4090	-138.69	-139.74	
	198.15	1.0391	-0.3117	-0.3142	1.0391	-0.3142	-106.50	-107.35	
	223.15	1.1702	-0.2446	-0.2466	1.1702	-0.2466	-83.58	-84.25	
	273.15	1.4324	-0.1561	-0.1570	1.4324	-0.1570	-53.35	-53.63	[67]
	298.15	1.5634	-0.1231	-0.1258	1.5634	-0.1258	-42.06	-42.99	
	273.16	1.4324	-0.1561	-0.1569	1.4324	-0.1569	-53.35	-53.63	
	298.15	1.5634	-0.1253	-0.1258	1.5634	-0.1258	-42.82	-42.99	
	303.15	1.5897	-0.1197	-0.1203	1.5897	-0.1203	-40.91	-41.12	
	323.15	1.6945	-0.1002	-0.1005	1.6945	-0.1005	-34.23	-34.33	
	348.15	1.8256	-0.0792	-0.0794	1.8256	-0.0794	-27.06	-27.13	
	373.15	1.9568	-0.0616	-0.0617	1.9568	-0.0617	-21.06	-21.07	
	398.17	2.0879	-0.0464	-0.0465	2.0879	-0.0465	-15.87	-15.89	
	423.18	2.2191	-0.0336	-0.0334	2.2191	-0.0334	-11.47	-11.42	
	448.28	2.3507	-0.0221	-0.0220	2.3507	-0.0220	-7.57	-7.50	
	473.21	2.4814	-0.0122	-0.0119	2.4814	-0.0119	-4.16	-4.08	
	498.23	2.6126	0.0034	-0.0030	2.6126	-0.0030	1.16	-1.04	
	523.25	2.7438	0.0044	0.0049	2.7438	0.0049	1.49	1.68	
	548.26	2.8750	0.0114	0.0120	2.8750	0.0120	3.89	4.12	
	573.27	3.0061	0.0175	0.0185	3.0061	0.0185	5.98	6.32	
	598.29	3.1373	0.0231	0.0243	3.1373	0.0243	7.88	8.32	
	623.39	3.2690	0.0283	0.0297	3.2690	0.0297	9.66	10.14	
	126.60	0.6639	-0.6971	-0.7428	0.6639	-0.7428	-238.20	-253.81	[200]
	136.00	0.7132	-0.6304	-0.6480	0.7132	-0.6480	-215.40	-221.40	
	147.59	0.7739	-0.5414	-0.5547	0.7739	-0.5547	-185.00	-189.54	
	158.90	0.8332	-0.4727	-0.4821	0.8332	-0.4821	-161.50	-164.72	
	173.46	0.9096	-0.4027	-0.4076	0.9096	-0.4076	-137.60	-139.26	
	191.07	1.0019	-0.3369	-0.3376	1.0019	-0.3376	-115.10	-115.37	
C_2H_6	209.50	0.6860	-0.6991	-0.6977	0.6662	-0.7379	-363.50	-388.35	[200]
	238.75	0.7818	-0.5520	-0.5442	0.7670	-0.5643	-287.00	-297.06	
	254.80	0.8343	-0.4873	-0.4809	0.8227	-0.4940	-253.40	-259.96	
	273.15	0.8944	-0.4218	-0.4210	0.8867	-0.4281	-219.30	-225.2[illegible]	
	306.07	1.0022	-0.3385	-0.3375	1.0024	-0.3374	-176.00	-177.24	
	273.15	0.8944	-0.4258	-0.4210	0.8867	-0.4281	-221.40	-225.20	[174]
	298.14	0.9762	-0.3570	-0.3553	0.9744	-0.3566	-185.60	-187.44	
	322.75	1.0568	-0.3018	-0.3037	1.0614	-0.3011	-156.90	-158.34	
	347.65	1.1383	-0.2564	-0.2611	1.1499	-0.2557	-133.30	-133.99	
	372.55	1.2199	-0.2194	-0.2258	1.2390	-0.2184	-114.06	-114.19	
	397.44	1.3027	-0.1879	-0.1956	1.3299	-0.1867	-97.72	-97.38	
	422.74	1.3842	-0.1614	-0.1702	1.4199	-0.1603	-83.91	-83.36	
	273.15	0.8944	-0.4297	-0.4210	0.8867	-0.4281	-223.41	-225.20	[108]
	240.00	0.7859	-0.5318	-0.5389	0.7713	-0.5583	-276.51	-293.60	
	215.00	0.7040	-0.6551	-0.6641	0.6851	-0.6995	-340.63	-368.20	
	200.00	0.6549	-0.8757	-0.7625	0.6337	-0.8123	-455.31	-427.43	[61]
	225.00	0.7367	-0.6733	-0.6091	0.7195	-0.6372	-350.10	-335.42	
	250.00	0.8186	-0.5317	-0.4986	0.8060	-0.5136	-276.44	-270.32	
	275.00	0.9005	-0.4291	-0.4156	0.8931	-0.4221	-223.14	-222.06	
	300.00	0.9823	-0.3529	-0.3510	0.9809	-0.3520	-183.50	-184.98	
	325.00	1.0642	-0.2949	-0.2995	1.0694	-0.2966	-153.36	-155.66	
	350.00	1.1460	-0.2500	-0.2575	1.1583	-0.2519	-130.00	-131.96	
	375.00	1.2279	-0.2146	-0.2226	1.2478	-0.2150	-111.60	-112.43	
	400.00	1.3098	-0.1864	-0.1932	1.3377	-0.1842	-96.91	-96.07	
	425.00	1.3916	-0.1636	-0.1681	1.4280	-0.1581	-85.04	-82.19	
	450.00	1.4735	-0.1449	-0.1465	1.5188	-0.1357	-75.35	-70.27	
	475.00	1.5553	-0.1296	-0.1276	1.6100	-0.1162	-67.37	-59.93	
	500.00	1.6372	-0.1168	-0.1110	1.7015	-0.0992	-60.74	-50.89	
	377.60	1.2364	-0.2104	-0.2193	1.2571	-0.2116	-109.40	-110.59	[94]
	410.90	1.3454	-0.1724	-0.1818	1.3770	-0.1723	-89.64	-89.75	
	510.90	1.6729	-0.0990	-0.1043	1.7416	-0.0925	-51.46	-47.28	

\+ Using Equation (V-30)

* Indicated reference holds for all data until the next listed reference appears.

TABLE J-3

(CONTINUED)

	T (°K)	Tr	Br	Br_{oo}	Tr_{oo}	Br_{cal}	B cc/mole	B_{cal} cc/mole	Reference
C_3H_8	248.15	0.6709	-0.8013	-0.7281	0.6390	-0.7993	-579.00	-588.53	[28]
	273.15	0.7384	-0.6477	-0.6064	0.7116	-0.6506	-468.00	-479.31	
	298.15	0.8060	-0.5370	-0.5135	0.7850	-0.5399	-388.00	-397.73	
	295.40	0.7986	-0.5522	-0.5226	0.7769	-0.5507	-399.00	-405.67	[159]
	306.55	0.8286	-0.5107	-0.4872	0.8097	-0.5091	-369.00	-374.95	
	317.60	0.8586	-0.4692	-0.4553	0.8427	-0.4718	-339.00	-347.43	
	327.60	0.8856	-0.4484	-0.4290	0.8725	-0.4415	-324.00	-324.99	
	337.80	0.9132	-0.4138	-0.4045	0.9031	-0.4133	-299.00	-304.09	
	347.90	0.9405	-0.3792	-0.3821	0.9334	-0.3877	-274.00	-285.15	
	357.90	0.9676	-0.3667	-0.3616	0.9636	-0.3645	-265.00	-267.90	
	368.20	0.9954	-0.3377	-0.3420	0.9948	-0.3424	-244.00	-251.53	
	377.70	1.0211	-0.3169	-0.3252	1.0237	-0.3236	-229.00	-237.56	
	388.50	1.0503	-0.2948	-0.3075	1.0567	-0.3038	-213.00	-222.84	
	400.10	1.0816	-0.2782	-0.2898	1.0922	-0.2842	-201.00	-208.27	
	412.90	1.1162	-0.2519	-0.2719	1.1315	-0.2644	-182.00	-193.50	
	274.45	0.7420	-0.6606	-0.6010	0.7154	-0.6441	-477.30	-474.49	[136]
	297.20	0.8035	-0.5465	-0.5166	0.7822	-0.5436	-394.90	-400.45	
	315.95	0.8650	-0.4710	-0.4489	0.8497	-0.4644	-340.30	-341.96	
	193.00	0.5218	-1.4047	-1.1900	0.4820	-1.3986	-1015.00	-1025.83	[122,123]
	198.00	0.5353	-1.3314	-1.1305	0.4961	-1.3185	-962.00	-967.63	
	203.00	0.5488	-1.2622	-1.0757	0.5101	-1.2455	-912.00	-914.52	
	218.00	0.5893	-1.0767	-0.9349	0.5526	-1.0612	-778.00	-780.11	
	244.00	0.6596	-0.8442	-0.7520	0.6270	-0.8290	-610.00	-610.29	
	273.00	0.7380	-0.6601	-0.6071	0.7112	-0.6514	-477.00	-479.87	
	297.06	0.8031	-0.5453	-0.5171	0.7818	-0.5441	-394.00	-400.85	
	303.16	0.8196	-0.5314	-0.4975	0.7998	-0.5211	-384.00	-383.83	
	321.06	0.8680	-0.4705	-0.4459	0.8530	-0.4610	-340.00	-339.43	
	348.16	0.9412	-0.4055	-0.3815	0.9342	-0.3871	-293.00	-284.68	
	369.97	1.0002	-0.3598	-0.3388	1.0002	-0.3388	-260.00	-248.85	
	423.16	1.1440	-0.2533	-0.2585	1.1632	-0.2497	-183.00	-182.56	
	448.16	1.2116	-0.2214	-0.2291	1.2407	-0.2177	-160.00	-158.73	
	523.16	1.4143	-0.1509	-0.1618	1.4763	-0.1458	-109.00	-104.98	
	570.46	1.5422	-0.1232	-0.1304	1.6271	-0.1129	-89.00	-80.36	
	243.00	0.6569	-0.8681	-0.7579	0.6241	-0.8364	-627.27	-615.71	[240]
	258.00	0.6975	-0.7591	-0.6760	0.6675	-0.7351	-548.50	-541.39	
	273.00	0.7380	-0.6664	-0.6071	0.7112	-0.6514	-481.52	-479.87	
	288.00	0.7786	-0.5918	-0.5484	0.7551	-0.5812	-427.60	-428.20	
	323.00	0.8732	-0.4603	-0.4408	0.8588	-0.4551	-332.60	-335.05	
	348.00	0.9408	-0.3775	-0.3818	0.9337	-0.3875	-272.80	-284.97	
	369.16	0.9980	-0.3598	-0.3403	0.9977	-0.3404	-260.00	-250.07	[16]
	373.16	1.0088	-0.3418	-0.3331	1.0099	-0.3324	-247.00	-244.11	
	398.16	1.0764	-0.2920	-0.2927	1.0862	-0.2874	-211.00	-210.62	
	423.16	1.1440	-0.2533	-0.2585	1.1632	-0.2497	-183.00	-182.56	
	448.16	1.2116	-0.2214	-0.2291	1.2407	-0.2177	-160.00	-158.73	
	473.16	1.2792	-0.1924	-0.2037	1.3187	-0.1903	-139.00	-138.26	
	498.16	1.3467	-0.1675	-0.1814	1.3973	-0.1665	-121.00	-120.51	
	523.16	1.4143	-0.1509	-0.1618	1.4763	-0.1458	-109.00	-104.98	
	548.16	1.4819	-0.1329	-0.1444	1.5558	-0.1275	-96.00	-91.28	
	303.16	0.8196	-0.5314	-0.4975	0.7998	-0.5211	-384.00	-383.83	[60]
	348.16	0.9412	-0.4055	-0.3815	0.9342	-0.3871	-293.00	-284.68	
	398.16	1.0764	-0.3100	-0.2927	1.0862	-0.2874	-224.00	-210.62	
	423.16	1.1440	-0.2726	-0.2585	1.1632	-0.2497	-197.00	-182.56	
	473.16	1.2792	-0.2145	-0.2037	1.3187	-0.1903	-155.00	-138.26	
	570.46	1.5422	-0.1232	-0.1304	1.6271	-0.1129	-89.00	-80.36	
	250.00	0.6759	-0.8047	-0.7178	0.6443	-0.7866	-581.46	-579.22	[61]
	275.00	0.7434	-0.6522	-0.5987	0.7170	-0.6413	-471.23	-472.47	
	300.00	0.8110	-0.5395	-0.5075	0.7905	-0.5329	-389.85	-392.52	
	325.00	0.8786	-0.4537	-0.4356	0.8647	-0.4491	-327.81	-330.62	
	350.00	0.9462	-0.3865	-0.3776	0.9398	-0.3827	-279.24	-281.41	
	375.00	1.0138	-0.3326	-0.3299	1.0155	-0.3288	-240.33	-241.43	
	400.00	1.0814	-0.2887	-0.2900	1.0919	-0.2844	-208.57	-208.39	
	425.00	1.1490	-0.2521	-0.2561	1.1689	-0.2471	-182.19	-180.67	
	450.00	1.2165	-0.2214	-0.2271	1.2464	-0.2155	-159.98	-157.12	
	475.00	1.2841	-0.1952	-0.2019	1.3245	-0.1884	-141.03	-136.87	
	500.00	1.3517	-0.1726	-0.1799	1.4031	-0.1649	-124.69	-119.30	
	525.00	1.4193	-0.1529	-0.1605	1.4821	-0.1443	-110.45	-103.91	
	550.00	1.4869	-0.1355	-0.1432	1.5617	-0.1262	-97.94	-90.33	

TABLE J-3

(CONTINUED)

	T (°K)	Tr	Br	Br_{oo}	Tr_{oo}	Br_{cal}	B cc/mole	B_{cal} cc/mole	Reference
$n-C_4H_{10}$	273.05	0.6422	-0.9640	-0.7917	0.5983	-0.9077	-897.00	-865.16	[27]
	297.15	0.6988	-0.7899	-0.6735	0.6599	-0.7514	-735.00	-716.92	
	323.15	0.7600	-0.6513	-0.5742	0.7272	-0.6243	-606.00	-595.97	
	346.45	0.8148	-0.5610	-0.5031	0.7883	-0.5357	-522.00	-511.26	
	330.67	0.7777	-0.6395	-0.5497	0.7469	-0.5935	-595.00	-566.56	
	370.85	0.8722	-0.4825	-0.4418	0.8531	-0.4609	-449.00	-439.67	
	397.33	0.9345	-0.4181	-0.3869	0.9242	-0.3952	-389.00	-376.53	
	426.21	1.0024	-0.3557	-0.3374	1.0028	-0.3371	-331.00	-320.50	
	244.00	0.5738	-1.3219	-0.9850	0.5253	-1.1740	-1230.00	-1116.44	[122]
	273.40	0.6430	-0.9920	-0.7898	0.5992	-0.9051	-923.00	-862.69	
	282.30	0.6639	-0.9264	-0.7427	0.6219	-0.8423	-862.00	-803.20	
	297.30	0.6992	-0.8146	-0.6728	0.6603	-0.7505	-758.00	-716.12	
	321.30	0.7556	-0.6824	-0.5805	0.7224	-0.6323	-635.00	-603.54	
	423.16	0.9952	-0.3482	-0.3422	0.9944	-0.3427	-324.00	-325.89	
	296.40	0.6971	-0.7738	-0.6767	0.6580	-0.7556	-720.00	-720.94	[159]
	307.50	0.7232	-0.7168	-0.6310	0.6866	-0.6965	-667.00	-664.77	
	318.20	0.7484	-0.6652	-0.5913	0.7144	-0.6459	-619.00	-616.55	
	328.90	0.7735	-0.6104	-0.5553	0.7422	-0.6006	-568.00	-573.29	
	337.80	0.7944	-0.5728	-0.5278	0.7656	-0.5663	-533.00	-540.57	
	348.45	0.8194	-0.5384	-0.4977	0.7935	-0.5291	-501.00	-504.96	
	358.40	0.8429	-0.5008	-0.4716	0.8199	-0.4971	-466.00	-474.33	
	368.40	0.8664	-0.4729	-0.4474	0.8465	-0.4678	-440.00	-446.21	
	377.90	0.8888	-0.4406	-0.4261	0.8719	-0.4421	-410.00	-421.56	
	387.60	0.9116	-0.4116	-0.4059	0.8979	-0.4178	-383.00	-398.24	
	400.40	0.9417	-0.3794	-0.3812	0.9325	-0.3885	-353.00	-370.01	
	413.40	0.9722	-0.3461	-0.3582	0.9678	-0.3614	-322.00	-343.94	
$i-C_5H_{12}$	298.20	0.6351	-1.0320	-0.8087	0.5811	-0.9610	-1194.00	-1144.85	[159]
	306.10	0.6520	-0.9654	-0.7690	0.5995	-0.9043	-1117.00	-1077.88	
	318.10	0.6775	-0.8738	-0.7144	0.6276	-0.8274	-1011.00	-986.96	
	329.10	0.7010	-0.7977	-0.6696	0.6536	-0.7653	-923.00	-913.34	
	339.10	0.7223	-0.7459	-0.6325	0.6774	-0.7148	-863.00	-853.27	
	349.10	0.7436	-0.6914	-0.5985	0.7013	-0.6690	-800.00	-798.84	
	358.10	0.7627	-0.6551	-0.5703	0.7229	-0.6315	-758.00	-754.05	
	368.60	0.7851	-0.6059	-0.5399	0.7483	-0.5914	-701.00	-706.21	
	378.90	0.8070	-0.5635	-0.5123	0.7733	-0.5555	-652.00	-661.36	
	388.40	0.8273	-0.5289	-0.4887	0.7966	-0.5252	-612.00	-627.00	
	401.40	0.8550	-0.4996	-0.4590	0.8286	-0.4873	-578.00	-581.54	
	413.60	0.8809	-0.4468	-0.4334	0.8588	-0.4551	-517.00	-543.85	
	300.00	0.6390	-1.0181	-0.7993	0.5853	-0.9476	-1177.90	-1125.04	[61]
	325.00	0.6922	-0.8229	-0.6858	0.6439	-0.7876	-952.07	-939.80	
	350.00	0.7455	-0.6825	-0.5956	0.7034	-0.6651	-789.65	-794.18	
	375.00	0.7987	-0.5779	-0.5225	0.7638	-0.5687	-668.66	-679.15	
	400.00	0.8520	-0.4975	-0.4621	0.8251	-0.4912	-575.57	-586.22	
	425.00	0.9052	-0.4337	-0.4114	0.8872	-0.4275	-501.78	-509.72	
	450.00	0.9585	-0.3817	-0.3683	0.9503	-0.3745	-441.69	-445.76	
	475.00	1.0117	-0.3384	-0.3312	1.0141	-0.3297	-391.55	-391.61	
	500.00	1.0650	-0.3015	-0.2991	1.0786	-0.2915	-348.81	-345.30	
$n-C_5H_{12}$	273.15	0.5933	-1.1904	-0.9228	0.5415	-1.1047	-1367.00	-1300.26	[159]
	298.15	0.6476	-1.0014	-0.7790	0.6001	-0.9026	-1150.00	-1064.41	
	323.15	0.7019	-0.8238	-0.6679	0.6595	-0.7522	-946.00	-888.09	
	348.15	0.7562	-0.6722	-0.5797	0.7198	-0.6367	-772.00	-752.02	
	373.15	0.8105	-0.5643	-0.5082	0.7808	-0.5455	-648.00	-644.24	
	423.15	0.9191	-0.4319	-0.3995	0.9053	-0.4113	-496.00	-484.97	
	448.15	0.9734	-0.3738	-0.3573	0.9687	-0.3608	-435.00	-424.69	
	461.65	1.0027	-0.3509	-0.3371	1.0032	-0.3368	-403.00	-396.07	
C_8H_{18}	373.00	0.6560	-1.1187	-0.7600	0.5748	-0.9819	-2122.00	-1952.53	[241]
	378.20	0.6651	-1.0797	-0.7401	0.5852	-0.9479	-2048.00	-1885.96	
	383.20	0.6739	-1.0223	-0.7217	0.5953	-0.9169	-1939.00	-1825.08	
	384.30	0.6759	-1.0043	-0.7178	0.5975	-0.9102	-1905.00	-1812.07	
	388.10	0.6826	-0.9853	-0.7044	0.6052	-0.8879	-1869.00	-1768.16	
	389.20	0.6845	-0.9637	-0.7006	0.6074	-0.8816	-1828.00	-1755.74	
	393.50	0.6921	-0.9374	-0.6861	0.6162	-0.8575	-1778.00	-1709.38	
	394.20	0.6933	-0.9300	-0.6838	0.6176	-0.8536	-1764.00	-1702.84	
	403.50	0.7096	-0.8651	-0.6541	0.6366	-0.8051	-1641.00	-1605.15	
	413.50	0.7272	-0.8003	-0.6243	0.6573	-0.7572	-1518.00	-1510.61	
	375.00	0.6595	-1.0982	-0.7522	0.5788	-0.9686	-2082.96	-1926.51	
	401.00	0.7035	-0.8904	-0.6650	0.6294	-0.8229	-1688.81	-1640.23	
	425.00	0.7475	-0.7431	-0.5926	0.6812	-0.7071	-1409.59	-1411.38	
	450.00	0.7914	-0.6352	-0.5317	0.7340	-0.6134	-1204.91	-1224.07	
	475.00	0.8354	-0.5531	-0.4797	0.7880	-0.5361	-1049.10	-1070.26	
	500.00	0.8794	-0.4880	-0.4349	0.8430	-0.4714	-925.59	-940.21	
	525.00	0.9233	-0.4342	-0.3960	0.8993	-0.4166	-823.58	-829.43	
	550.00	0.9673	-0.3880	-0.3618	0.9566	-0.3697	-735.95	-734.11	

TABLE J-3

(CONTINUED)

	T (°K)	Tr	Br	Br_{oo}	Tr_{oo}	Br_{cal}	B cc/mole	B_{cal} cc/mole	Reference
CF_4	273.15	1.1996	-0.2198	-0.2340	1.2340	-0.2202	-111.00	-112.53	[66]
	298.15	1.3094	-0.1748	-0.1933	1.3654	-0.1757	-88.30	-89.11	
	323.15	1.4192	-0.1394	-0.1605	1.4986	-0.1404	-70.40	-70.47	
	348.15	1.5290	-0.1103	-0.1334	1.6333	-0.1117	-55.70	-55.31	
	373.15	1.6388	-0.0861	-0.1106	1.7696	-0.0880	-43.50	-42.76	
	423.15	1.8584	-0.0483	-0.0747	2.0464	-0.0511	-24.40	-23.22	
	448.15	1.9682	-0.0333	-0.0603	2.1867	-0.0365	-16.80	-15.49	
	473.15	2.0780	-0.0200	-0.0476	2.3282	-0.0238	-10.10	-8.76	
	623.15	2.7367	0.0338	0.0045	3.2005	0.0270	17.05	18.24	
	203.15	0.8922	-0.4292	-0.4230	0.8766	-0.4376	-216.75	-226.17	[137]
	223.15	0.9800	-0.3519	-0.3526	0.9769	-0.3548	-177.71	-183.02	
	243.15	1.0679	-0.2839	-0.2974	1.0788	-0.2914	-143.36	-149.85	
	273.15	1.1996	-0.2195	-0.2340	1.2340	-0.2202	-110.87	-112.53	
	313.15	1.3753	-0.1530	-0.1728	1.4451	-0.1536	-77.26	-77.45	
	368.15	1.6168	-0.0906	-0.1149	1.7422	-0.0924	-45.75	-45.09	
Ar	85.96	0.5704	-0.9711	-0.9967	0.5738	-0.9851	-250.20	-253.43	[35]
	88.94	0.5902	-0.9063	-0.9323	0.5935	-0.9222	-233.50	-237.25	
	89.57	0.5944	-0.8857	-0.9196	0.5976	-0.9098	-228.20	-234.04	
	93.59	0.6210	-0.8139	-0.8445	0.6242	-0.8363	-209.70	-215.14	
	97.69	0.6482	-0.7514	-0.7775	0.6512	-0.7708	-193.60	-198.27	
	102.79	0.6821	-0.6823	-0.7054	0.6848	-0.7000	-175.80	-180.06	
	107.93	0.7162	-0.6253	-0.6428	0.7187	-0.6385	-161.10	-164.24	
	113.97	0.7563	-0.5667	-0.5796	0.7585	-0.5764	-146.00	-148.27	
	122.78	0.8147	-0.4941	-0.5031	0.8165	-0.5011	-127.30	-128.90	
	124.70	0.8275	-0.4793	-0.4885	0.8291	-0.4867	-123.50	-125.19	
	130.96	0.8690	-0.4374	-0.4449	0.8703	-0.4437	-112.70	-114.13	
	140.44	0.9319	-0.3846	-0.3889	0.9326	-0.3884	-99.10	-99.91	
	159.72	1.0599	-0.2993	-0.3020	1.0592	-0.3023	-77.10	-77.79	
	179.85	1.1934	-0.2356	-0.2366	1.1913	-0.2375	-60.70	-61.13	
	209.94	1.3931	-0.1696	-0.1677	1.3883	-0.1691	-43.70	-43.55	
	241.04	1.5995	-0.1199	-0.1184	1.5917	-0.1199	-30.90	-30.93	
	271.39	1.8009	-0.0850	-0.0831	1.7900	-0.0848	-21.90	-21.90	
Kr	117.41	0.5607	-1.0330	-1.0310	0.5539	-1.0560	-326.90	-335.17	[35]
	120.19	0.5740	-0.9729	-0.9845	0.5673	-1.0073	-307.90	-319.73	
	124.01	0.5922	-0.9085	-0.9261	0.5858	-0.9461	-287.50	-300.32	
	129.15	0.6168	-0.8386	-0.8558	0.6106	-0.8727	-265.40	-277.04	
	134.69	0.6432	-0.7805	-0.7892	0.6373	-0.8033	-247.00	-255.03	
	142.45	0.6803	-0.6961	-0.7089	0.6749	-0.7199	-220.30	-228.54	
	150.98	0.7210	-0.6260	-0.6346	0.7161	-0.6428	-198.10	-204.09	
	161.12	0.7694	-0.5536	-0.5609	0.7653	-0.5667	-175.20	-179.92	
	172.29	0.8228	-0.4882	-0.4938	0.8195	-0.4976	-154.50	-157.98	
	186.86	0.8924	-0.4193	-0.4228	0.8903	-0.4248	-132.70	-134.83	
	209.16	0.9989	-0.3378	-0.3397	0.9988	-0.3397	-106.90	-107.80	
	251.94	1.2032	-0.2364	-0.2325	1.2077	-0.2306	-74.80	-73.12	
	123.15	0.5881	-0.9126	-0.9387	0.5816	-0.9594	-288.80	-304.52	[28]
	148.15	0.7075	-0.6453	-0.6579	0.7024	-0.6669	-204.20	-211.74	
	173.15	0.8269	-0.4847	-0.4892	0.8237	-0.4928	-153.40	-156.46	
	198.15	0.9463	-0.3766	-0.3776	0.9452	-0.3784	-119.17	-120.10	
	223.15	1.0657	-0.3000	-0.2987	1.0671	-0.2979	-94.95	-94.50	
	273.15	1.3044	-0.1989	-0.1950	1.3116	-0.1926	-62.96	-61.02	
	298.15	1.4238	-0.1656	-0.1592	1.4342	-0.1565	-52.40	-49.51	
	323.15	1.5432	-0.1352	-0.1302	1.5571	-0.1272	-42.80	-40.19	

APPENDIX K

Enthalpy Calculations[++] From the Powers Generalized Correlation (PGC)

++ Reference Enthalpy H=0 for Each Pure Component as a Saturated Liquid at -280°F

TABLE K-1

ENTHALPY OF METHANE IN B.T.U. PER POUND USING POWERS GENERALIZED CORRELATION

TEMPERATURE °F	PRESSURE (#/SQ.IN.)									
	0.0	100.0	250.0	300.0	400.0	500.0	600.0	750.0	800.0	900.0
-280.0	228.75	3.39	2.19	1.78	2.00	2.64	2.59	3.21	3.67	4.23
-260.0	238.67	19.12	18.27	18.24	17.98	17.68	18.16	19.16	19.45	19.87
-240.0	248.58	35.44	35.08	35.03	34.33	34.14	34.07	34.35	34.64	35.41
-220.0	258.49	51.30	52.07	52.16	51.44	51.34	51.38	51.70	51.95	52.40
-200.0	268.40	257.35	69.91	69.79	69.80	69.47	69.24	69.28	69.39	69.75
-180.0	278.30	267.99	88.67	88.68	88.32	88.22	87.67	87.77	87.70	87.69
-160.0	288.20	279.98	263.72	109.64	108.91	108.32	107.37	106.83	106.64	106.74
-140.0	298.10	290.74	276.30	272.01	258.19	132.58	130.47	128.57	128.23	127.48
-120.0	308.01	300.86	290.05	285.71	275.79	262.73	240.11	158.89	156.83	153.91
-100.0	317.96	311.68	301.93	298.37	290.37	280.85	269.99	244.29	230.91	198.59
-80.0	327.96	322.32	313.59	310.47	303.80	296.71	288.17	273.14	267.09	252.54
-60.0	338.02	332.87	324.99	322.23	316.49	310.46	303.95	292.62	288.38	279.09
-40.0	348.12	343.30	336.18	333.77	328.80	323.51	317.94	308.64	305.32	298.38
-20.0	358.29	353.93	347.47	345.28	340.78	336.09	331.41	323.48	320.69	315.01
0.0	368.51	364.63	358.67	356.64	352.52	348.27	344.23	337.55	335.18	330.37
20.0	378.79	375.21	369.70	367.84	364.07	360.22	356.50	350.70	348.65	344.52
40.0	389.15	385.84	380.62	378.91	375.56	372.05	368.57	363.45	361.72	358.06
60.0	399.61	396.53	391.53	389.97	387.01	383.81	380.55	375.95	374.50	371.20
80.0	410.18	407.28	402.55	401.12	398.45	395.49	392.45	388.27	386.99	384.07
100.0	420.90	418.13	413.76	412.44	409.94	407.14	404.36	400.52	399.33	396.81
120.0	431.77	429.10	425.10	423.87	421.51	418.84	416.33	412.72	411.59	409.41
140.0	442.78	440.25	436.57	435.43	433.22	430.68	428.49	424.97	423.90	421.91
160.0	453.95	451.55	448.17	447.11	445.03	442.60	440.75	437.28	436.28	434.40
180.0	465.30	463.02	459.91	458.94	456.97	454.65	453.12	449.68	448.75	446.94
200.0	476.84	474.67	471.81	470.90	469.06	466.83	465.59	462.18	461.32	459.56
220.0	488.55	486.49	483.85	483.00	481.26	479.13	478.13	474.78	473.98	472.25
240.0	500.43	498.47	496.00	495.20	493.55	491.54	490.59	487.44	486.70	485.06
260.0	512.49	510.61	508.28	507.53	505.95	504.07	503.09	500.19	499.51	497.98
280.0	524.66	522.87	520.66	519.94	518.44	516.69	515.64	513.00	512.38	510.96
300.0	537.10	535.29	533.19	532.51	531.08	529.45	528.31	525.93	525.36	524.05

TABLE K-1 (CONTINUED)

ENTHALPY OF METHANE IN B.T.U. PER POUND USING POWERS GENERALIZED CORRELATION

PRESSURE (#/SQ.IN.)										TEMPERATURE °F
1000.0	1100.0	1250.0	1300.0	1400.0	1500.0	1600.0	1750.0	1900.0	2000.0	
3.86	4.47	5.76	6.22	7.07	7.82	8.52	9.37	10.01	10.38	-280.0
20.07	20.78	22.05	22.48	23.28	23.97	24.58	25.23	25.58	25.75	-260.0
36.19	36.92	38.17	38.59	39.34	39.96	40.51	41.16	41.61	41.86	-240.0
52.72	53.44	54.64	55.04	55.72	56.29	56.80	57.51	58.16	58.55	-220.0
69.94	70.58	71.64	71.98	72.59	73.12	73.59	74.23	74.79	75.12	-200.0
88.14	88.60	89.22	89.41	89.82	90.27	90.70	91.24	91.66	91.89	-180.0
107.21	107.71	108.12	108.20	108.57	109.10	109.36	109.54	109.71	109.81	-160.0
127.20	127.37	127.55	127.61	127.77	127.94	128.05	128.14	128.21	128.26	-140.0
152.20	150.89	149.01	148.52	147.93	147.84	148.05	147.84	146.83	146.05	-120.0
185.27	178.92	175.15	174.22	172.70	171.52	170.47	168.81	167.42	166.61	-100.0
236.76	221.87	209.90	207.12	202.51	198.44	195.15	191.17	188.66	187.50	-80.0
269.28	259.60	246.12	242.10	234.75	228.24	222.65	216.51	212.52	210.66	-60.0
291.11	284.07	273.65	270.24	263.49	257.05	251.18	243.67	237.77	234.52	-40.0
309.23	303.58	295.31	292.60	287.02	281.38	276.08	268.70	262.05	258.08	-20.0
325.51	320.56	313.57	311.36	306.63	301.65	297.00	290.34	283.99	280.06	-0.0
340.32	336.04	330.05	328.15	323.99	319.48	315.27	309.32	303.75	300.30	20.0
354.13	350.48	345.11	343.30	339.60	335.85	332.22	327.05	322.27	319.31	40.0
367.41	364.28	359.32	357.50	354.19	351.24	348.18	343.73	339.66	337.11	60.0
380.69	377.92	373.32	371.60	368.58	366.02	363.27	359.30	355.77	353.55	80.0
394.08	391.51	387.30	385.79	382.99	380.43	377.76	374.02	370.85	368.87	100.0
407.29	404.85	400.98	399.69	397.08	394.46	391.82	388.26	385.35	383.55	120.0
420.02	417.73	414.15	412.98	410.58	408.13	405.70	402.44	399.76	398.09	140.0
432.61	430.47	427.15	426.07	423.85	421.60	419.39	416.43	413.94	412.38	160.0
445.15	443.15	440.06	439.05	437.00	434.96	432.97	430.29	427.97	426.50	180.0
457.73	455.85	452.96	452.00	450.11	448.27	446.50	444.07	441.90	440.51	200.0
470.35	468.59	465.90	464.98	463.21	461.57	459.99	457.79	455.76	454.44	220.0
483.22	481.57	479.04	478.18	476.52	474.98	473.50	471.47	469.62	468.43	240.0
496.24	494.69	492.33	491.51	489.95	488.48	487.06	485.14	483.47	482.42	260.0
509.32	507.86	505.65	504.88	503.40	501.98	500.60	498.77	497.28	496.36	280.0
522.51	521.14	519.06	518.34	516.92	515.56	514.20	512.44	511.11	510.31	300.0

TABLE K-2

ENTHALPY OF ETHANE IN B.T.U. PER POUND USING POWERS GENERALIZED CORRELATION

TEMPERATURE °F	PRESSURE (#/SQ.IN.)									
	0.0	100.0	250.0	300.0	400.0	500.0	600.0	677.0	713.0	750.0
-280.0	250.53	-0.11	-0.43	-0.37	0.20	0.33	0.44	0.66	0.82	1.05
-260.0	256.28	10.52	10.47	10.52	10.92	11.06	11.26	11.50	11.64	11.79
-240.0	260.19	17.90	17.87	17.86	18.01	18.15	18.43	18.70	18.84	18.97
-220.0	262.14	21.39	21.49	21.48	21.58	21.71	21.95	22.17	22.29	22.46
-200.0	266.12	32.08	32.53	32.58	32.60	32.71	32.75	32.76	32.84	33.10
-180.0	274.21	43.39	43.37	43.91	43.91	44.04	43.99	43.91	43.95	44.19
-160.0	280.41	55.22	55.04	54.88	54.94	55.38	55.31	55.10	55.09	55.32
-140.0	286.70	66.99	66.26	65.94	65.96	66.58	66.68	66.58	66.62	66.86
-120.0	293.12	77.83	77.60	77.49	77.39	77.46	77.94	78.50	78.77	79.00
-100.0	298.57	87.03	87.16	87.21	87.22	87.10	87.42	87.88	88.08	88.22
-80.0	299.66	88.88	89.06	89.14	89.18	89.06	89.32	89.69	89.86	89.98
-60.0	306.35	100.65	100.87	100.98	101.04	100.97	101.03	101.10	101.15	101.22
-40.0	313.18	112.95	112.90	112.98	113.00	112.97	113.13	113.25	113.35	113.52
-20.0	320.18	125.17	125.20	125.49	125.83	125.73	125.83	125.92	125.99	126.09
0.0	327.34	316.47	138.72	138.59	138.86	138.76	138.76	138.82	138.86	138.90
20.0	333.01	323.94	149.82	149.50	148.99	148.96	148.93	148.95	148.98	149.01
40.0	334.67	325.26	152.80	152.78	151.89	151.93	151.92	151.93	152.04	152.22
60.0	342.20	333.22	167.90	166.81	165.97	165.47	165.54	165.47	165.48	165.20
80.0	349.93	342.45	328.52	182.97	181.12	180.47	179.70	179.98	180.00	179.20
100.0	342.20	333.22	167.90	166.81	165.97	165.47	165.54	165.47	165.48	165.20
119.2	361.57	355.20	342.58	338.93	326.66	205.98	203.75	203.28	202.92	202.52
140.0	365.78	359.65	348.35	344.32	333.72	217.18	214.80	212.61	211.86	211.40
160.0	374.38	369.16	358.56	354.86	346.40	335.22	316.71	237.79	236.27	234.71
180.0	382.77	377.13	368.37	365.10	357.61	349.06	337.31	324.81	316.43	306.69
189.8	378.42	372.45	363.35	359.93	351.96	342.41	327.70	308.85	259.63	251.37
200.0	382.77	377.13	368.37	365.10	357.61	349.06	337.31	324.81	316.43	306.69
220.0	391.45	386.36	378.20	375.20	368.57	360.95	352.28	344.54	340.09	334.97
240.0	393.65	388.64	380.65	377.74	371.33	364.06	355.46	348.51	344.53	339.94
260.0	400.34	395.55	388.06	385.37	379.55	373.14	365.63	358.92	355.72	352.52
280.0	409.46	405.00	398.08	395.61	390.30	384.50	378.14	372.79	370.14	367.34
300.0	418.06	414.72	408.23	405.93	401.02	395.80	390.29	385.84	383.68	381.39
320.0	427.55	424.60	418.55	416.42	411.93	407.20	402.27	398.29	396.36	394.33
340.0	428.84	424.90	418.86	416.74	412.26	407.54	402.62	398.65	396.73	394.71
360.0	438.47	434.76	429.09	427.11	422.99	418.64	414.17	410.54	408.76	406.92
380.0	448.63	445.29	439.89	438.02	434.16	430.09	426.08	422.89	421.30	419.70
400.0	459.36	455.87	450.79	449.03	445.42	441.61	437.93	435.09	433.68	432.24
420.0	480.10	477.29	472.78	471.23	468.08	464.75	461.49	459.18	458.08	456.83

TABLE K-2 (CONTINUED)

ENTHALPY OF ETHANE IN B.T.U. PER POUND USING POWERS GENERALIZED CORRELATION

PRESSURE (#/SQ.IN.)										TEMPERATURE °F
819.6	1000.0	1250.0	1300.0	1400.0	1500.0	1600.0	1750.0	1900.0	2000.0	
1.55	1.92	2.74	3.04	3.62	4.07	4.45	4.99	5.57	5.97	-280.0
12.12	12.51	13.42	13.70	14.25	14.69	15.07	15.61	16.20	16.59	-260.0
19.25	19.57	20.46	20.72	21.22	21.66	22.07	22.65	23.24	23.64	-246.6
22.76	23.03	23.93	24.17	24.65	25.09	25.51	26.12	26.72	27.11	-240.0
33.62	33.81	34.71	34.93	35.37	35.82	36.27	36.93	37.53	37.92	-220.0
44.71	45.18	45.78	45.99	46.43	46.89	47.35	48.03	48.63	49.01	-200.0
55.38	56.55	57.04	57.28	57.76	58.22	58.68	59.35	59.93	60.30	-180.0
67.40	67.97	68.61	68.85	69.36	69.82	70.27	70.90	71.45	71.79	-160.0
79.33	79.48	80.25	80.49	80.97	81.42	81.85	82.43	82.91	83.20	-140.0
88.45	88.97	89.89	90.12	90.59	91.02	91.42	91.97	92.41	92.66	-123.3
90.15	90.35	91.81	92.04	92.50	92.93	93.33	93.87	94.30	94.54	-120.0
101.42	102.45	103.50	103.73	104.17	104.57	104.94	105.45	105.89	106.15	-100.0
113.37	114.42	115.37	115.58	116.00	116.37	116.71	117.20	117.65	117.93	-80.0
126.32	126.68	127.45	127.65	128.04	128.38	128.69	129.14	129.58	129.87	-60.0
139.02	139.24	139.81	139.98	140.32	140.62	140.91	141.32	141.71	141.96	-40.0
149.11	149.20	149.64	149.79	150.08	150.35	150.60	150.97	151.30	151.51	-24.5
152.52	152.61	152.51	152.65	152.92	153.17	153.42	153.77	154.09	154.29	-20.0
165.04	165.39	165.71	165.78	165.93	166.11	166.30	166.59	166.84	166.99	0.0
179.02	179.55	179.96	179.97	180.00	180.27	180.55	180.55	180.58	180.63	20.0
165.04	165.39	165.71	165.78	165.93	166.11	166.30	166.59	166.84	166.99	0.0
202.33	201.73	201.28	201.19	201.02	200.93	200.86	200.62	200.41	200.30	49.2
211.27	210.03	209.58	209.46	209.21	208.95	208.69	208.31	208.10	208.05	60.0
232.90	229.06	226.35	225.87	224.97	224.28	223.78	223.25	222.74	222.47	80.0
268.30	252.16	244.75	244.09	242.96	241.65	240.76	239.65	238.63	238.06	100.0
245.59	239.65	235.42	234.87	233.91	232.88	231.91	231.21	230.48	230.01	89.8
268.06	252.16	244.75	244.09	242.96	241.65	240.76	239.65	238.63	238.06	100.0
324.03	284.05	266.35	265.01	262.31	260.01	258.56	256.81	255.17	254.20	120.0
330.19	294.62	272.42	270.61	267.74	265.04	263.11	261.04	259.34	258.33	125.0
345.63	322.44	293.18	290.10	285.22	281.49	278.50	274.90	272.17	270.81	140.0
361.96	345.69	320.70	316.40	309.62	304.36	299.68	293.81	289.98	288.30	160.0
378.15	363.96	344.20	340.23	332.73	326.21	320.85	314.41	309.75	307.41	180.0
394.48	379.61	363.21	359.34	353.30	347.31	341.95	335.01	329.54	326.57	200.0
394.89	380.05	363.76	360.40	353.90	347.93	342.56	335.62	330.13	327.14	200.6
411.44	394.03	380.38	377.58	372.04	366.65	361.55	354.64	348.78	345.41	220.0
410.84	408.22	395.93	393.54	388.83	384.00	379.32	373.00	367.28	363.81	240.0
429.47	421.97	411.05	409.01	404.93	400.53	396.12	390.18	384.68	381.28	260.0
454.47	448.34	439.66	438.04	434.78	431.08	427.28	422.06	417.25	414.29	300.0

TABLE K-3

ENTHALPY OF PROPANE IN B.T.U. PER POUND USING POWERS GENERALIZED CORRELATION

TEMPERATURE °F	PRESSURE (#/SQ.IN.)									
	0.0	100.0	250.0	300.0	400.0	500.0	600.0	750.0	800.0	900.0
-280.0	234.45	0.26	0.25	0.73	0.61	0.68	1.22	1.46	1.48	0.88
-260.0	239.16	9.76	8.85	9.02	9.13	9.48	10.06	10.89	11.12	10.09
-240.0	244.15	18.26	17.80	18.03	18.25	18.59	19.04	19.81	20.05	19.34
-220.0	249.40	27.17	27.13	27.44	27.70	27.99	28.36	28.92	29.12	28.76
-200.0	254.86	37.00	36.87	37.07	37.30	37.61	38.01	38.50	38.67	38.44
-180.0	260.38	46.71	46.69	46.86	47.07	47.29	47.53	48.23	48.41	48.09
-160.0	265.87	56.17	56.42	56.60	56.82	56.88	56.86	57.90	58.12	57.69
-140.0	271.48	65.98	66.34	66.50	66.70	66.69	66.55	67.64	67.97	67.56
-120.0	277.21	76.12	76.25	76.29	76.59	76.63	76.39	77.45	77.88	77.51
-100.0	283.09	86.49	86.03	85.87	86.37	86.62	86.30	87.35	87.78	87.48
-80.0	289.24	96.48	95.98	95.82	96.15	96.52	96.71	97.66	97.94	97.65
-60.0	295.58	106.44	106.32	106.31	106.28	106.66	107.52	108.26	108.37	108.05
-40.0	302.12	116.78	116.87	117.03	117.03	117.25	117.79	118.18	118.32	118.60
-20.0	308.87	127.55	127.62	127.89	128.01	128.11	128.29	128.58	128.78	129.40
-0.0	315.83	138.78	138.60	138.91	139.07	139.22	139.44	140.02	140.19	140.42
20.0	323.01	150.13	150.02	150.51	150.69	150.81	151.05	151.63	151.77	151.74
40.0	330.41	162.81	162.03	162.62	162.76	162.82	163.01	163.36	163.48	163.39
60.0	338.05	327.59	174.82	174.96	174.94	175.06	175.19	175.45	175.56	175.32
80.0	345.92	336.99	188.46	187.68	187.25	187.54	187.66	187.95	187.69	187.52
100.0	354.05	345.13	201.83	201.12	200.08	200.34	200.51	200.53	200.34	200.15
120.0	362.43	354.58	216.90	215.42	214.24	213.59	214.03	213.75	213.64	213.55
140.0	371.06	364.32	350.53	344.27	229.65	228.46	228.60	227.74	227.72	227.42
160.0	379.93	373.53	361.98	356.41	247.20	244.39	243.35	242.86	242.72	241.98
180.0	389.05	382.87	372.19	368.23	356.56	263.72	260.72	258.51	258.33	257.53
200.0	398.40	392.52	383.00	379.29	370.54	356.48	286.25	278.46	276.93	275.06
220.0	408.00	402.65	393.81	390.39	382.39	372.62	357.54	306.31	301.31	295.61
240.0	417.85	412.94	404.70	401.53	394.40	386.03	376.02	352.37	340.15	321.23
260.0	427.94	423.25	415.71	412.90	406.69	399.36	390.61	375.06	368.55	354.05
280.0	438.27	433.88	426.87	424.28	418.58	412.06	404.68	392.87	388.21	377.53
300.0	448.83	444.75	438.16	435.71	430.41	424.60	418.39	408.27	404.58	396.85

TABLE K-3 (CONTINUED)

ENTHALPY OF PROPANE IN B.T.U. PER POUND USING POWERS GENERALIZED CORRELATION

PRESSURE (#/SQ.IN.)										TEMPERATURE °F
1000.0	1100.0	1250.0	1300.0	1400.0	1500.0	1600.0	1750.0	1900.0	2000.0	
1.06	1.44	1.99	2.18	2.55	2.92	3.29	3.85	4.40	4.77	-280.0
10.10	10.47	11.02	11.20	11.57	11.94	12.31	12.86	13.42	13.78	-260.0
19.42	19.78	20.33	20.51	20.88	21.25	21.61	22.16	22.71	23.08	-240.0
28.92	29.28	29.82	30.00	30.36	30.73	31.09	31.63	32.18	32.54	-220.0
38.63	38.99	39.52	39.70	40.06	40.42	40.78	41.32	41.85	42.21	-200.0
48.35	48.70	49.23	49.41	49.76	50.12	50.47	51.00	51.53	51.89	-180.0
58.03	58.38	58.90	59.07	59.42	59.77	60.12	60.64	61.17	61.52	-160.0
67.77	68.11	68.62	68.79	69.13	69.47	69.82	70. 3	70.84	71.19	-140.0
77.62	77.95	78.45	78.62	78.95	79.29	79.62	80 13	80.63	80.97	-120.0
87.60	87.93	88.41	88.58	88.90	89.23	89.56	90.05	90.54	90.87	-100.0
97.84	98.15	98.62	98.78	99.09	99.41	99.73	100.20	100.68	101.00	-80.0
108.27	108.57	109.02	109.17	109.48	109.78	110.09	110.55	111.01	111.32	-60.0
118.83	119.11	119.54	119.69	119.98	120.27	120.56	121.00	121.45	121.74	-40.0
129.64	129.91	130.32	130.45	130.73	131.00	131.28	131.70	132.12	132.40	-20.0
140.67	140.92	141.30	141.43	141.68	141.94	142.20	142.59	142.99	143.25	-0.0
151.94	152.16	152.51	152.62	152.86	153.09	153.33	153.69	154.06	154.30	20.0
163.50	163.69	163.99	164.09	164.30	164.51	164.72	165.05	165.38	165.60	40.0
175.34	175.50	175.75	175.83	176.01	176.19	176.37	176.65	176.94	177.14	60.0
187.51	187.62	187.81	187.87	188.01	188.15	188.30	188.53	188.77	188.94	80.0
200.11	200.17	200.28	200.32	200.40	200.50	200.60	200.78	200.96	201.09	100.0
213.64	213.66	213.67	213.79	213.99	213.92	213.84	213.89	213.97	213.99	120.0
227.29	227.26	227.05	227.06	227.05	226.88	226.71	226.60	226.61	226.71	140.0
241.76	241.51	241.01	240.88	240.61	240.30	240.03	239.78	239.73	239.83	160.0
257.13	256.42	255.60	255.29	254.67	254.14	253.76	253.52	253.47	253.43	180.0
273.76	272.60	271.06	270.44	269.41	268.70	268.21	267.85	267.65	267.42	200.0
291.98	289.53	287.38	286.65	285.53	284.59	283.73	282.88	282.21	281.80	220.0
313.79	309.65	305.23	304.13	302.71	301.60	300.43	298.83	297.48	296.74	240.0
339.62	332.34	325.29	323.61	320.89	318.78	317.03	314.96	313.37	312.28	260.0
366.55	356.29	346.91	344.51	340.27	336.72	334.11	331.44	329.69	328.51	280.0
388.10	379.28	367.61	364.68	359.47	355.40	352.34	349.11	346.80	345.25	300.0

TABLE K-4 (CONTINUED)

ENTHALPY OF .76 C2H6-C3H8 IN B.T.U. PER POUND USING POWERS GENERALIZED CORRELATION

TEMPERATURE °F	PRESSURE (#/SQ.IN.)									
	0.0	100.0	250.0	300.0	400.0	500.0	600.0	716.0	750.0	800.0
-280.0	244.97	2.44	1.77	1.76	2.09	2.24	2.50	3.05	3.29	4.38
-260.0	250.40	11.87	11.77	11.93	12.45	12.56	12.72	13.11	13.29	14.14
-240.0	255.99	22.31	22.23	22.27	22.51	22.67	22.95	23.36	23.49	24.11
-220.0	261.74	32.52	32.69	32.73	32.80	32.96	33.12	33.44	33.63	34.34
-200.0	267.64	42.91	43.36	43.43	43.46	43.59	43.55	43.73	43.98	44.94
-180.0	273.62	53.81	54.17	54.20	54.26	54.43	54.31	54.39	54.61	55.77
-160.0	279.67	65.11	64.76	64.57	64.70	65.21	65.05	64.96	65.20	66.47
-140.0	285.83	76.11	75.46	75.19	75.26	75.79	75.89	76.09	76.38	77.39
-120.0	292.13	86.47	86.31	86.24	86.15	86.19	86.77	87.65	87.85	88.41
-100.0	298.56	97.14	97.31	97.41	97.44	97.35	97.65	98.13	98.22	98.71
-80.0	305.19	108.49	108.65	108.78	108.84	108.81	108.88	109.04	109.11	109.68
-60.0	311.98	120.31	120.21	120.32	120.35	120.38	120.54	120.82	120.98	121.64
-50.1	315.40	125.99	126.01	126.22	126.37	126.37	126.52	126.78	126.92	127.51
-40.0	318.95	132.07	132.09	132.40	132.67	132.63	132.74	132.96	133.06	133.58
-20.0	326.10		144.83	144.99	145.25	145.18	145.21	145.34	145.39	145.74
0.0	333.45	324.66	158.78	158.42	157.91	157.92	157.90	157.97	158.01	158.20
20.0	341.01	332.02	172.28	172.04	171.08	170.94	170.99	170.92	171.01	170.93
40.0	348.77	341.04			185.49	184.78	184.65	184.37	184.24	184.43
50.0	352.72	345.71	332.24		193.26	192.61	191.70	191.46	191.24	191.42
60.0	356.74	350.31	337.27		201.78	200.45	199.53	198.63	198.52	198.72
80.0	364.91	358.68	346.69	343.22		218.40	216.01	214.82	214.51	213.95
100.0	373.28	367.20	357.28	353.37	344.29		237.41	234.09	233.20	231.11
102.4	374.29	368.24	358.48	354.65	345.79	333.16	240.28	236.99	236.01	233.53
120.0	381.86	376.08	367.22	363.87	356.06	346.61	331.91		261.47	252.78
140.0	390.66	385.50	377.21	374.11	367.13	358.92	349.51	333.16	327.04	284.87
151.6	395.90	390.97	383.04	380.11	373.63	366.17	357.70	345.16	340.54	313.69
160.0	399.70	394.89	387.23	384.44	378.31	371.39	363.07	352.46	348.57	327.11
180.0	409.01	404.49	397.43	394.89	389.40	383.35	376.40	367.18	364.42	350.12
200.0	418.59	414.38	407.80	405.44	400.38	394.88	388.95	381.43	379.09	367.89
220.0	428.41	424.48	418.29	416.08	411.39	406.43	401.24	394.87	392.90	383.41
240.0	438.47	434.68	428.90	426.87	422.58	418.05	413.34	407.48	405.70	397.58
250.7	443.96	440.30	434.70	432.75	428.64	424.30	419.82	414.22	412.53	404.90
260.0	448.75	445.23	439.77	437.86	433.89	429.69	425.44	420.11	418.52	411.28
280.0	459.18	455.99	450.78	448.97	445.24	441.30	437.48	432.75	431.34	424.83
300.0	469.82	466.81	461.90	460.19	456.70	453.00	449.48	445.26	443.97	438.08

TABLE K-4 (CONTINUED)

ENTHALPY OF .76 C2H6-C3H8 IN B.T.U. PER POUND USING POWERS GENERALIZED CORRELATION

PRESSURE (#/SQ.IN.)										TEMPERATURE °F
1000.0	1100.0	1250.0	1300.0	1400.0	1500.0	1600.0	1750.0	1900.0	2000.0	
3.71	3.77	4.54	4.80	5.28	5.70	6.11	6.69	7.27	7.66	-280.0
13.85	14.06	14.89	15.16	15.67	16.06	16.42	16.94	17.51	17.89	-260.0
23.96	24.19	24.95	25.19	25.67	26.07	26.44	26.99	27.57	27.95	-240.0
34.04	34.36	35.02	35.24	35.68	36.09	36.50	37.10	37.67	38.05	-220.0
44.54	44.87	45.47	45.68	46.09	46.52	46.95	47.58	48.15	48.52	-200.0
55.42	55.52	56.13	56.34	56.77	57.21	57.65	58.27	58.83	59.20	-180.0
66.15	66.22	66.86	67.09	67.54	67.97	68.40	69.01	69.55	69.90	-160.0
77.08	77.24	77.90	78.13	78.59	79.01	79.42	80.00	80.50	80.82	-140.0
88.10	88.34	88.98	89.21	89.65	90.06	90.45	90.98	91.42	91.70	-120.0
99.10	99.41	100.04	100.25	100.67	101.06	101.43	101.92	102.31	102.55	-100.0
110.33	110.68	111.29	111.49	111.89	112.26	112.60	113.07	113.48	113.73	-80.0
121.79	122.14	122.72	122.91	123.30	123.63	123.95	124.40	124.83	125.10	-60.0
127.57	127.88	128.43	128.62	128.99	129.31	129.62	130.06	130.49	130.76	-50.1
133.58	133.83	134.37	134.55	134.90	135.21	135.50	135.93	136.35	136.62	-40.0
145.68	145.83	146.30	146.46	146.78	147.05	147.32	147.70	148.08	148.32	-20.0
158.08	158.16	158.56	158.69	158.94	159.19	159.42	159.75	160.05	160.25	0.0
170.90	170.98	171.22	171.29	171.45	171.64	171.82	172.09	172.34	172.49	20.0
184.51	184.76	184.90	184.91	185.01	185.36	185.57	185.56	185.65	185.74	40.0
191.40	191.53	191.67	191.66	191.70	191.94	192.07	191.99	191.99	192.03	50.0
198.58	198.55	198.64	198.61	198.58	198.70	198.74	198.59	198.50	198.48	60.0
213.36	213.36	213.13	213.02	212.82	212.66	212.48	212.18	211.99	211.92	80.0
230.40	229.60	228.55	228.21	227.72	227.24	226.81	226.32	226.04	225.95	100.0
232.81	231.74	230.52	230.14	229.53	229.02	228.57	228.07	227.74	227.61	102.4
250.09	248.06	246.00	245.52	244.54	243.40	242.48	241.77	241.04	240.61	120.0
274.06	268.41	264.04	263.03	261.41	260.26	259.27	257.93	256.48	255.66	140.0
292.66	283.46	276.83	275.48	272.80	270.66	269.27	267.55	265.97	265.05	151.6
309.28	295.53	286.56	284.62	281.46	278.82	276.77	274.53	272.81	271.74	160.0
336.63	326.65	311.87	308.97	304.36	300.18	296.44	292.34	289.47	288.12	180.0
359.80	350.73	337.69	333.66	326.95	321.34	316.58	311.08	307.53	305.87	200.0
376.71	369.43	358.42	354.69	347.78	341.98	337.03	331.04	326.63	324.34	220.0
391.83	385.87	376.67	373.56	367.56	362.06	357.06	350.57	345.42	342.60	240.0
399.59	394.14	385.79	382.96	377.42	372.16	367.26	360.73	355.37	352.33	250.7
406.27	401.13	393.27	390.64	385.45	380.39	375.65	369.27	363.84	360.69	260.0
420.35	415.68	408.64	406.39	401.89	397.25	392.87	386.96	381.59	378.35	280.0
434.09	429.91	423.67	421.73	417.76	413.45	409.31	403.70	398.51	395.34	300.0

TABLE K-5

ENTHALPY OF .494 C2H6-C3H8 IN B.T.U. PER POUND USING POWERS GENERALIZED CORRELATION

TEMPERATURE °F	PRESSURE (#/SQ.IN.)									
	0.0	100.0	250.0	300.0	400.0	500.0	600.0	750.0	800.0	900.0
-280.0	240.50	2.16	1.24	1.25	1.34	1.57	2.02	2.97	3.31	3.25
-260.0	245.64	11.09	10.62	10.81	11.19	11.35	11.64	12.45	12.78	12.88
-240.0	250.98	20.52	20.41	20.64	21.00	21.16	21.44	22.05	22.29	22.44
-220.0	256.53	30.72	30.58	30.66	30.83	31.06	31.40	31.94	32.13	32.27
-200.0	262.25	40.59	40.76	40.85	40.96	41.14	41.24	41.92	42.20	42.23
-180.0	268.04	50.71	51.11	51.21	51.29	51.42	51.31	52.03	52.40	52.52
-160.0	273.87	61.20	61.50	61.55	61.67	61.83	61.63	62.25	62.67	63.01
-140.0	279.80	72.07	71.69	71.54	71.81	72.27	71.95	72.50	72.95	73.36
-125.5	284.19	79.77	79.06	78.81	79.10	79.68	79.48	80.08	80.50	80.87
-120.0	285.87	82.59	81.94	81.71	81.94	82.45	82.45	83.14	83.52	83.79
-100.0	292.08	92.69	92.48	92.42	92.37	92.54	93.24	94.21	94.42	94.40
-80.0	298.51	103.13	103.25	103.35	103.34	103.34	103.82	104.40	104.54	104.86
-60.0	305.12	114.11	114.25	114.43	114.49	114.51	114.62	114.88	115.04	115.64
-40.0	311.91	125.60	125.48	125.65	125.70	125.80	125.96	126.48	126.70	127.03
-20.0	318.90	137.06	137.06	137.41	137.57	137.63	137.79	138.26	138.45	138.62
0.0	326.09		149.29	149.67	149.88	149.87	149.97	150.23	150.35	150.48
20.0	333.49		162.85	162.34	162.26	162.31	162.34	162.52	162.61	162.67
37.5	340.14	331.06	174.36	174.17	173.11	173.40	173.41	173.92	173.68	173.35
40.0	341.11	331.95	176.09	175.90	174.69	175.02	175.03	175.49	175.26	174.94
60.0	348.94	340.47		189.41	188.55	188.17	188.14	188.20	188.10	187.83
80.0	357.00	349.85			203.34	202.45	201.96	201.82	201.74	201.60
100.0	365.27	358.82	346.60			218.06	217.27	216.30	216.51	216.48
120.0	373.77	367.51	356.34	352.49	340.77		234.30	232.15	231.81	231.12
140.0	382.50	376.47	366.81	363.02	354.28	341.01		252.15	250.95	249.27
151.1	387.45	381.61	372.49	368.99	360.88	350.03		266.35	263.63	260.59
160.0	391.47	385.89	377.06	373.70	365.79	356.38	342.30	283.76	276.72	270.95
180.0	400.70	395.66	387.39	384.27	377.26	369.01	359.64	337.63	326.74	301.05
200.0	410.19	405.42	397.82	395.03	388.92	381.96	373.54	358.88	352.51	339.14
220.0	419.93	415.45	408.42	405.86	400.32	394.12	387.05	375.23	371.10	360.80
240.0	429.90	425.73	419.14	416.74	411.60	406.01	400.02	390.13	385.57	378.92
251.1	435.53	431.51	425.14	422.82	417.89	412.63	407.08	398.09	394.97	387.92
260.0	440.10	436.17	429.98	427.73	422.98	417.93	412.68	404.21	401.19	394.73
280.0	450.49	446.72	440.91	438.34	434.47	429.86	425.05	417.26	414.69	408.03
300.0	461.10	457.61	452.09	450.15	446.09	441.80	437.48	430.42	428.21	423.07

TABLE K-5 (CONTINUED)

ENTHALPY OF .494 C2H6-C3H8 IN B.T.U. PER POUND USING POWERS GENERALIZED CORRELATION

PRESSURE (#/SQ.IN.)

1000.0	1100.0	1250.0	1300.0	1400.0	1500.0	1600.0	1750.0	1900.0	2000.0	TEMPERATURE °F
2.49	2.94	3.58	3.78	4.22	4.65	5.08	5.68	6.25	6.63	-260.0
12.41	12.91	13.65	13.89	14.31	14.68	15.05	15.61	16.18	16.56	-250.0
22.25	22.73	23.47	23.70	24.11	24.47	24.83	25.38	25.95	26.33	-240.0
32.19	32.63	33.31	33.53	33.93	34.31	34.68	35.25	35.81	36.20	-230.0
42.17	42.58	43.19	43.40	43.80	44.20	44.60	45.17	45.73	46.11	-220.0
52.39	52.78	53.36	53.55	53.96	54.37	54.78	55.35	55.90	56.27	-210.0
62.64	63.02	63.62	63.82	64.23	64.64	65.04	65.61	66.15	66.51	-200.0
72.99	73.37	73.99	74.20	74.61	75.01	75.41	75.96	76.47	76.82	-190.0
80.59	80.97	81.60	81.81	82.22	82.61	82.99	83.52	84.03	84.36	-185.5
83.55	83.93	84.56	84.77	85.17	85.56	85.93	86.46	86.94	87.26	-180.0
94.28	94.66	95.26	95.47	95.86	96.23	96.58	97.06	97.50	97.79	-170.0
105.09	105.46	106.04	106.24	106.60	106.96	107.29	107.73	108.13	108.39	-160.0
116.10	116.46	117.02	117.21	117.55	117.89	118.20	118.63	119.03	119.29	-150.0
127.30	127.64	128.17	128.35	128.67	128.98	129.28	129.70	130.11	130.38	-140.0
138.72	139.04	139.53	139.69	139.99	140.27	140.55	140.95	141.35	141.61	-130.0
150.44	150.72	151.16	151.31	151.57	151.83	152.08	152.45	152.82	153.06	-120.0
162.49	162.73	163.10	163.23	163.46	163.68	163.90	164.22	164.53	164.72	-110.0
173.33	173.52	173.79	173.88	174.07	174.26	174.44	174.71	174.96	175.12	-102.5
174.93	175.11	175.36	175.45	175.63	175.81	175.99	176.25	176.49	176.65	-100.0
186.25	188.37	188.45	188.49	188.80	189.09	189.13	189.23	189.41	189.52	-90.0
201.63	201.75	201.76	201.75	201.92	202.08	202.02	201.93	201.96	202.00	-80.0
215.81	215.77	215.60	215.51	215.45	215.39	215.22	214.98	214.85	214.83	-70.0
230.99	230.66	230.13	229.96	229.60	229.23	228.90	228.57	228.46	228.46	-60.0
247.99	247.06	245.57	245.12	244.35	243.74	243.27	242.73	242.41	242.26	-50.0
258.31	256.73	255.05	254.56	253.42	252.34	251.76	251.06	250.50	250.19	-41.1
267.34	264.82	262.75	262.09	260.74	259.72	258.91	257.99	257.26	256.81	-30.0
290.62	285.30	281.06	279.83	277.97	276.84	275.78	274.15	272.72	271.89	-20.0
322.11	310.97	302.49	300.65	297.43	294.89	292.88	290.57	288.78	287.79	-10.0
349.67	338.50	325.82	323.44	318.83	314.68	311.17	307.52	305.23	304.16	0.0
370.70	361.91	349.34	345.70	339.62	334.42	330.30	325.87	322.96	321.47	10.0
380.42	372.70	360.78	357.10	350.71	345.55	341.30	336.46	333.06	331.26	15.1
387.74	380.44	369.31	365.77	359.65	354.45	350.06	344.92	341.14	339.09	20.0
403.19	397.15	387.81	384.76	379.07	373.93	369.32	363.57	359.06	356.53	30.0
417.97	412.70	404.70	402.07	396.90	392.03	387.58	381.74	376.85	374.03	40.0

TABLE K-6

ENTHALPY OF .275 C2H6-C3H8 IN B.T.U. PER POUND USING POWERS GENERALIZED CORRELATION

TEMPERATURE °F	PRESSURE (#/SQ.IN.)									
	0.0	100.0	250.0	300.0	400.0	500.0	600.0	750.0	800.0	900.0
-280.0	237.61	1.84	1.22	1.44	1.48	1.67	2.20	2.92	3.11	2.49
-260.0	242.54	11.03	10.33	10.49	10.69	10.99	11.45	12.34	12.63	12.09
-240.0	247.71	19.83	19.73	20.06	20.38	20.60	20.92	21.58	21.81	21.59
-220.0	253.10	29.75	29.62	29.84	30.09	30.35	30.73	31.26	31.45	31.35
-200.0	258.70	39.81	39.76	39.89	40.08	40.32	40.59	41.23	41.42	41.26
-180.0	264.35	49.60	49.84	49.99	50.18	50.29	50.28	51.20	51.47	51.15
-160.0	270.01	59.67	60.05	60.18	60.35	60.39	60.24	61.19	61.56	61.34
-150.2	272.82	64.74	65.07	65.17	65.36	65.40	65.22	66.13	66.55	66.41
-140.0	275.78	70.12	70.23	70.25	70.52	70.64	70.38	71.28	71.72	71.63
-120.0	281.68	80.78	80.25	80.07	80.51	80.88	80.55	81.43	81.87	81.83
-100.0	287.72	90.87	90.36	90.20	90.44	90.84	91.09	91.99	92.28	92.13
-80.0	294.01	100.99	100.91	100.92	100.85	101.12	101.95	102.74	102.87	102.69
-60.0	300.49	111.51	111.64	111.80	111.83	111.94	112.35	112.73	112.88	113.33
-40.0	307.16	122.53	122.57	122.80	122.91	123.00	123.15	123.50	123.69	124.25
-20.0	314.02	133.99	133.75	134.02	134.15	134.31	134.52	135.16	135.36	135.49
0.0	321.10	145.57	145.42	145.91	146.10	146.18	146.37	146.86	147.01	147.02
1.6	321.67	146.55	146.38	146.88	147.07	147.14	147.33	147.80	147.95	147.96
20.0	328.39		157.78	158.19	158.32	158.37	158.50	158.79	158.91	158.87
40.0	335.90	326.13	171.32	170.80	170.64	170.77	170.85	171.07	171.17	171.00
60.0	343.63	334.55	184.59	184.22	183.03	183.43	183.53	183.80	183.54	183.36
80.0	351.59	343.18		197.80	196.82	196.53	196.67	196.61	196.49	196.18
100.0	359.79	352.66			211.76	210.72	210.48	210.26	210.22	210.05
120.0	368.23	361.72	349.54	343.64	228.72	226.25	225.56	224.96	225.16	224.63
127.4	371.41	365.00	353.28	348.27		232.77	231.46	230.67	230.57	229.84
140.0	376.91	370.63	359.44	355.54	343.22	245.06	241.97	240.28	240.22	239.42
160.0	385.83	379.81	370.05	366.21	357.21	342.84	265.43	259.82	258.66	257.10
180.0	395.00	389.46	380.51	377.07	369.03	359.12	343.27	286.60	282.61	277.47
200.0	404.42	399.40	391.05	387.85	380.62	372.24	361.97	337.64	324.06	303.86
203.0	405.85	400.88	392.63	389.49	382.42	374.10	364.46	341.82	331.02	308.84
220.0	414.08	409.32	401.67	398.83	392.57	385.28	376.66	360.83	354.10	339.10
240.0	423.99	419.53	412.45	409.85	404.17	397.70	390.32	378.37	373.76	362.94
260.0	434.13	429.98	423.36	421.91	415.63	409.86	403.66	393.51	389.84	382.09
280.0	444.48	440.59	434.36	433.05	427.16	422.01	416.62	407.96	404.85	398.18
300.0	455.07	451.33	445.49	443.37	438.88	434.16	429.22	421.31	418.59	412.89

TABLE K-6 (CONTINUED)

ENTHALPY OF .275 C2H6-C3H8 IN B.T.U. PER POUND USING POWERS GENERALIZED CORRELATION

PRESSURE (#/SQ.IN.)										TEMPERATURE °F
1000.0	1100.0	1250.0	1300.0	1400.0	1500.0	1600.0	1750.0	1900.0	2000.0	
3.35	2.73	3.32	3.51	3.91	4.31	4.70	5.27	5.83	6.21	-280.0
11.85	12.30	12.90	13.10	13.48	13.86	14.24	14.81	15.37	15.74	-260.0
21.60	22.02	22.64	22.84	23.21	23.57	23.93	24.49	25.05	25.42	-240.0
31.42	31.82	32.43	32.62	32.99	33.35	33.71	34.27	34.82	35.19	-220.0
41.41	41.79	42.37	42.56	42.93	43.30	43.66	44.21	44.76	45.13	-200.0
51.39	51.76	52.32	52.50	52.88	53.25	53.61	54.16	54.69	55.06	-180.0
61.41	61.77	62.31	62.50	62.87	63.24	63.60	64.14	64.66	65.02	-160.0
66.38	66.74	67.28	67.46	67.83	68.20	68.56	69.09	69.61	69.97	-150.2
71.55	71.90	72.45	72.63	73.00	73.36	73.72	74.24	74.75	75.10	-140.0
81.79	82.14	82.68	82.86	83.22	83.57	83.92	84.42	84.92	85.26	-120.0
92.19	92.54	93.07	93.24	93.59	93.93	94.26	94.74	95.21	95.54	-100.0
102.63	103.16	103.67	103.84	104.17	104.49	104.81	105.26	105.71	106.02	-80.0
113.58	113.90	114.38	114.54	114.85	115.16	115.46	115.89	116.31	116.60	-60.0
124.55	124.85	125.31	125.46	125.75	126.04	126.33	126.74	127.15	127.43	-40.0
135.74	136.02	136.45	136.59	136.86	137.13	137.40	137.79	138.19	138.45	-20.0
147.17	147.42	147.81	147.94	148.18	148.43	148.67	149.04	149.41	149.65	0.0
148.10	148.35	148.74	148.86	149.10	149.35	149.59	149.96	150.32	150.56	1.6
158.89	159.11	159.44	159.55	159.77	159.99	160.21	160.53	160.86	161.08	20.0
170.93	171.11	171.38	171.47	171.65	171.84	172.02	172.30	172.57	172.76	40.0
183.33	183.45	183.63	183.69	183.83	183.97	184.11	184.33	184.55	184.70	60.0
196.42	196.46	196.52	196.60	196.81	196.89	196.91	197.04	197.19	197.25	80.0
210.01	210.06	209.95	209.99	210.14	210.09	209.95	209.89	209.91	209.98	100.0
224.19	224.09	223.74	223.66	223.54	223.34	223.11	222.88	222.78	222.86	120.0
229.66	229.46	229.01	228.38	228.64	228.37	228.09	227.83	227.71	227.77	127.4
239.32	238.83	238.20	237.97	237.50	237.05	236.69	236.41	236.36	236.34	140.0
255.04	254.90	253.41	252.92	252.11	251.45	250.95	250.52	250.35	250.15	160.0
274.31	272.03	270.10	269.35	268.06	267.09	266.27	265.51	264.90	264.49	180.0
296.15	292.62	287.78	286.68	285.24	284.24	283.07	281.47	280.10	279.38	200.0
297.98	295.21	290.76	289.51	287.83	286.70	285.53	283.90	282.50	281.68	203.0
323.43	319.45	308.26	306.53	303.69	301.49	299.78	297.67	296.06	295.02	220.0
351.74	340.88	330.63	328.27	323.84	320.05	317.21	314.18	312.41	311.17	240.0
373.40	364.53	352.34	349.13	343.64	339.08	335.67	332.05	329.70	328.06	260.0
390.80	383.42	372.08	368.87	363.29	358.64	354.83	350.46	347.29	345.21	280.0
406.84	400.55	390.94	387.99	382.58	377.78	373.60	368.59	364.69	362.27	300.0

TABLE K-7

ENTHALPY OF TERNARY MIXTURE IN B.T.U. PER POUND USING POWERS GENERALIZED CORRELATION

TEMPERATURE °F	PRESSURE (#/SQ.IN.)									
	0.0	100.0	250.0	300.0	400.0	500.0	600.0	750.0	800.0	900.0
-280.0	237.84	0.98	0.83	1.11	1.54	1.60	1.79	2.54	2.87	3.06
-260.0	243.92	12.22	12.11	12.17	12.29	12.48	12.81	13.41	13.63	13.80
-240.0	250.16	23.13	23.45	23.49	23.46	23.64	23.71	24.46	24.76	24.76
-234.9	251.78	25.97	26.37	26.41	26.38	26.54	26.53	27.32	27.65	27.64
-220.0	256.57	34.58	35.09	35.10	35.04	35.19	35.07	35.80	36.18	36.34
-200.0	263.13	46.67	46.57	46.47	46.65	46.98	46.70	47.34	47.79	48.13
-180.0	269.73	58.89	58.02	57.73	58.08	58.67	58.44	59.10	59.54	59.86
-160.0	276.36		69.67	69.56	69.52	69.73	70.36	71.36	71.62	71.60
-140.0	283.08		81.40	81.49	81.41	81.36	81.81	82.41	82.59	82.99
-120.0	289.90		93.39	93.52	93.41	93.40	93.47	93.80	94.01	94.65
-100.0	296.85				105.52	105.62	105.77	106.36	106.61	106.88
-80.0	303.98				118.55	118.54	118.64	118.98	119.15	119.34
-60.0	311.27					131.69	131.70	131.88	131.99	132.12
-40.0	318.72						145.03	145.52	145.27	145.03
-20.0	326.33							158.83	158.77	158.64
-10.0	327.86							161.61	161.56	161.26
0.0	334.12	326.79								173.11
20.0	342.09	335.36								
40.0	350.25	343.73								
52.0	355.25	348.90	338.89							
60.0	358.59	352.40	342.85	339.17						
80.0	367.14	361.65	352.76	349.41	341.81					
100.0	375.90	370.79	362.67	359.69	353.18	345.78	336.89			
120.0	384.86	380.11	372.67	369.97	364.17	357.76	350.44	338.03	333.66	322.78
128.2	387.68	383.04	375.78	373.16	367.52	361.32	354.45	342.69	338.44	329.36
140.0	394.04	389.64	382.73	380.23	374.93	369.25	363.17	353.06	349.39	341.42
160.0	403.45	399.29	392.86	390.57	385.75	380.66	375.33	366.65	363.58	357.07
180.0	413.09	409.16	403.18	401.08	396.69	392.05	387.25	379.37	376.68	371.13
192.0	419.00	415.30	409.51	407.49	403.30	398.87	394.45	387.15	384.64	379.51
200.0	422.98	419.45	413.77	411.80	407.72	403.43	399.24	392.32	389.92	385.03
220.0	433.10	429.82	424.48	422.63	418.83	414.85	411.09	404.94	402.78	398.45
240.0	443.45	440.33	435.33	433.60	430.05	426.34	422.88	417.35	415.42	411.55
260.0	454.01	451.02	446.31	444.70	441.40	437.94	434.69	429.65	427.93	424.41
280.0	464.75	461.93	457.38	455.88	452.87	449.64	446.54	441.91	440.39	437.06
300.0	475.70	473.04	468.62	467.23	464.48	461.44	458.47	454.17	452.83	449.66

TABLE K-7 (CONTINUED)

ENTHALPY OF TERNARY MIXTURE IN B.T.U. PER POUND USING POWERS GENERALIZED CORRELATION

PRESSURE (#/SQ.IN.)										TEMPERATURE °F
1000.0	1100.0	1250.0	1300.0	1400.0	1500.0	1600.0	1750.0	1900.0	2000.0	
2.94	3.56	4.52	4.83	5.27	5.66	6.02	6.61	7.24	7.66	-280.0
13.81	14.36	15.19	15.46	15.91	16.33	16.74	17.36	17.99	18.41	-260.0
24.82	25.30	26.01	26.25	26.72	27.19	27.65	28.29	28.90	29.32	-240.0
27.72	28.19	28.88	29.11	29.59	30.07	30.54	31.18	31.79	32.21	-234.9
36.21	36.65	37.32	37.55	38.04	38.53	39.02	39.66	40.26	40.67	-220.0
47.78	48.23	48.97	49.23	49.73	50.22	50.69	51.33	51.90	52.29	-200.0
59.62	60.09	60.88	61.15	61.65	62.13	62.58	63.18	63.71	64.07	-180.0
71.53	72.00	72.78	73.04	73.52	73.97	74.39	74.91	75.35	75.65	-160.0
83.29	83.76	84.50	84.75	85.20	85.62	86.01	86.46	86.83	87.09	-140.0
95.14	95.60	96.32	96.56	96.98	97.37	97.74	98.20	98.60	98.87	-120.0
107.17	107.61	108.29	108.52	108.91	109.27	109.61	110.09	110.54	110.83	-100.0
119.46	119.86	120.49	120.70	121.05	121.39	121.70	122.17	122.62	122.90	-80.0
132.09	132.45	133.00	133.17	133.49	133.79	134.07	134.48	134.85	135.08	-60.0
145.13	145.40	145.80	145.93	146.19	146.44	146.68	147.01	147.30	147.48	-40.0
159.17	159.34	159.48	159.55	159.95	160.29	160.38	160.54	160.77	160.88	-20.0
161.54	161.67	161.80	161.85	162.07	162.28	162.44	162.65	162.85	162.97	-16.0
173.16	173.34	173.41	173.41	173.64	173.82	173.79	173.74	173.77	173.83	0.0
188.22	188.17	188.00	187.92	187.87	187.81	187.66	187.45	187.31	187.30	20.0
	204.31	203.45	203.26	202.84	202.46	202.15	201.87	201.78	201.74	40.0
	214.95	213.34	212.87	212.10	211.63	211.29	210.72	210.22	209.91	52.0
	222.85	221.11	220.60	219.53	218.60	218.15	217.39	216.62	216.14	60.0
	242.67	239.09	238.23	236.84	235.81	234.85	233.28	231.93	231.25	80.0
	269.55	261.70	259.97	256.79	254.27	252.29	250.09	248.34	247.34	100.0
311.96	299.66	286.80	284.29	279.49	275.08	271.34	267.52	265.26	264.11	120.0
318.51	308.17	294.97	291.77	286.37	281.55	277.45	273.27	270.83	269.56	126.2
333.02	324.37	311.70	307.97	301.41	295.99	291.64	286.87	283.67	281.95	140.0
350.15	343.00	332.25	328.85	322.61	317.13	312.38	306.69	302.39	299.98	160.0
365.41	359.64	350.81	347.91	342.25	336.97	332.14	325.93	320.86	317.96	180.0
374.24	368.87	360.84	358.20	352.90	347.88	343.27	337.12	331.84	328.78	192.0
379.98	374.78	367.21	364.74	359.68	354.86	350.45	344.41	339.07	335.94	200.0
394.01	389.38	382.85	380.72	376.11	371.60	367.48	361.70	356.46	353.34	220.0
407.60	403.50	397.81	395.93	391.69	387.47	383.60	378.18	373.24	370.28	240.0
420.82	417.21	412.09	410.38	406.53	402.67	399.09	394.09	389.56	386.82	260.0
433.65	430.51	425.68	424.03	420.70	417.41	414.20	409.69	405.55	403.01	280.0
446.39	443.64	438.93	437.38	434.54	431.78	428.94	424.90	421.15	418.80	300.0

BIBLIOBRAPHY

1. Adler, G. C., H. C. Ozkardesh, and W. C. Schreiner, Hydrocarbon Processing, 46, No. 10, 28 (1967).

2. Alder, B. J., J. Chem. Phys., 40, No. 9, 2724 (1964).

3. Alder, B. J., and T. E. Wainwright, J. Chem. Phys., 33, 1439 (1960).

4. Alkasab, K., Ph.D. Thesis, Illinois Inst. Tech. (1970).

5. American Petroleum Institute, Bibliography No. 1, "Bibliography of Vapor-Liquid Equilibrium Data for Hydrocarbon Systems," New York (1963).

6. American Petroleum Institute, Bibliography No. 3, "Bibliography of Volumetric and Thermodynamic Data for Pure Hydrocarbons and their Mixtures," New York (1964).

7. American Petroleum Institute, "Documentation of the Basis for Selection of the Contents of Chapter 7 - Thermal Properties," in "Technical Data Book - Petroleum Refining," Documentation Report No. 7-66, New York (1966).

8. Bailey, B. J., and K. Kellner, Thermodynamik Symp., Heidelberg, Section VI, Paper 4, Sept. 1967.

9. Balaban, S. M., "Effect of Pressure on the Constant Pressure Heat Capacities of the Nitrogen-Trifluoromethane System," Ph.D. Thesis, Lehigh University (1966).

10. Balaban, S. M., and L. M. Wenzel, Presented at 159th National Meeting of ACS, Houston, Texas, February 22-27, 1970.

11. Barieau, R.E., U. S. Bur. Mines Inform. Circ., No. 8245 (1965).

12. Barkelew, C. H., J. L. Valentine, and C. O. Hurd, Trans. Am. Inst. Chem. Eng., 43, 25 (1947).

13. Barker, J. A., and D. Henderson, J. Chem. Phys., 47, 2856 (1967).

14. Barker, J. A., and D. Henderson, J. Chem. Ed., 45, 2 (1968).

15. Barner, H. E., and C. W. Quinlan, Ind. Eng. Chem. Process Design Develop., 8, No. 3, 407 (1969).

16. Beattie, J. A., C. Hadlock, and N. Poffenberger, J. Chem. Phys., 3, 93 (1935).

17. Beattie, J. A., W. C. Kay, and J. Kaminsky, J. Am. Chem. Soc., 59, 1589 (1937).

18. Beattie, J. A., G. Su, and G. Simard, J. Am. Chem. Soc., 61, 924 (1939).

19. Bellemans, A., V. Mathot, and M. Simon, Adv. Chem. Phys., 11, 117 (1967).

20. Benedict, M., G. B. Webb, and L. C. Rubin, J. Chem. Phys., 8, 334 (1940).

21. Berry, V., and B. Sage, Ind. Eng. Chem., 3, No. 1, 52 (1958).

22. Bhirud, V. L. and J. E. Powers, Thermodynamic Properties of a 5 Mole Percent Propane in Methane Mixture, Univ. of Mich. Aug. (1969).

23. Bird, R. B., W. E. Stewart, and E. L. Lightfoot, Transport Phenomena, Wiley, New York (1960).

24. Bishnoi, P. R., Ph.D. Thesis, Univ. of Alberta (1970).

25. Bloomer, O. T., D. C. Gami, and J. D. Parent, "Physico-Chemical Properties of Methane-Ethane Mixtures," Inst. of Gas Tech. Res. Bull., No. 22 (1953).

26. Bottomley, G. A., D. S. Massie, and R. Whitlaw-Gray, Proc. Roy. Soc., A200, 201 (1950).

27. Bottomley, G. A., and T. H. Spurling, Austral. J. Chem., 17, 501 (1964).

28. Brewer, J., "Determination of Mixed Virial Coefficients," CFSTI, AD 663-448 (1967).

29. Brombacher, W. G., D. P. Johnson, and J. L. Cross, NBS Monograph, 8, May 20 (1960).

30. Brown, E. H. Bull. Inst. Int. De Froid, Annexe, 169 (1960-1961).

31. Brown, W. B., Phil. Trans. Roy. Soc., A250, 175 (1957).

32. Brown, W. B., Proc. Roy. Soc., A240, 651 (1957).

33. Brown, W. B., Comment in "Thermodyn. Transport Prop. Fluids," Inst. Mech. Engrs., London (1958), pg. 205.

34. Budenholzer, R. A., B. H. Sage, and W. N. Lacey, Ind. Eng. Chem. 31, 1288 (1939).

35. Byrne, M. A., M. R. Jones, and L. A. K. Staveley, Trans. Farad. Soc., 64, 1747 (1968).

36. Calado, J. C. G., and L. A. K. Staveley, Trans. Farad. Soc., 67, 289 (1971).

37. Calado, J. C. G., and L. A. K. Staveley, Trans. Farad. Soc., 67, 1261 (1971).

38. Canjar, L. N., Chem. Eng. Data, 3, No. 2, 185 (1958).

39. Canjar, L. N., and F. S. Manning, Thermodynamic Properties and Reduced Correlations for Gases, Gulf Publishing Co. (1967).

40. Carnahan B., Luther H. A., and J. O. Wilkes, Applied Numerical Methods, Wiley (1967).

41. Carnahan, N. F., and K. E. Starling, J. Chem. Phys., 51, 635 (1969).

42. Carruth, G. F., Ph.D. Thesis, Rice University (1970).

43. Chang, J., J. Chromatography, 37, 14 (1968).

44. Chiu, C. H., Special Problem, University of Oklahoma (1967).

45. Chueh, P. L., and J. M. Prausnitz, J. A.I.Ch.E., 13, 896 (1967).

46. Chueh, P. L., and J. M. Prausnitz, Ind. Eng. Chem. Fund., 6, 492 (1967).

47. Chueh, P. L., and J. M. Prausnitz, Ind. Eng. Chem., 60, No. 3, 35 (1968).

48. Clark, R. G., F. L. Hyman, and G. M. Wilson, Tech. Rept. AFML-TR-66-136, Wright-Patterson AFB, Ohio (1966).

49. Cook, D., and J. S. Rowlinson, Proc. Roy. Soc., A219, 405 (1953).

50. Cooper, H. W., and J. C. Goldfranck, Hydrocarbon Processing, 46, No. 12, 14 (1967).

51. Cryogenic Data Center, "Bibliography of References, Thermophysical Properties of Ethane," NBS, Boulder Colorado (1968).

52. Cryogenic Data Center, "The Thermophysical Properties of Methane and Deuteromethanes in the Solid, Liquid and Gaseous Phases," Rept. B 635, NBS, Boulder, Colorado (1970).

53. Cryogenic Data Center, "The Thermophysical Properties of Methane Mixtures," Rept. B 636, NBS, Boulder, Colorado (1970).

54. Curl, R. F., Jr. and K. S. Pitzer, Ind. Eng. Chem., 50, 265 (1958).

55. Cutler, A. J. B., and J. A. Morrison, Trans Farad. Soc., 61, 429 (1965).

56. Dailey, B. P., and W. A. Felsing, J. Am. Chem. Soc., 65, 42 (1943).

57. Dana, L. I., A. C. Jenkins, J. N. Burdick, and R. C. Timm, Refrig. Engineering, 12, 387 (1926).

58. Danon, F., and K. S. Pitzer, J. Phys. Chem., 66, 583 (1962).

59. Dantzler, E. M., C. M. Knobler, and M. L. Windsor, J. Phys. Chem., 72, 676 (1968).

60. Deschner W. W., and G. G. Brown, Ind. Eng. Chem., 32, 836 (1940).

61. Diaz-pena, M., Communication to J. E. Powers (1968).

62. Diaz-pena, M., and A. Cervera, Thermodynamik-Symposium, Kl. Schafer, Ed., Heidelberg, Germany, Section II, Paper 10, September (1967).

63. Djordjevich, L., Ph.D. Thesis, Illinois Inst. Tech. (1968).

64. Dixon, A., W. Campbell, and C. Parker, Proc. Roy. Soc., A100 1 (1921).

65. Douslin, D. R., and R. H. Harrison, Thermodynamik Symp., Heidelberg, Germany, Section III, Paper 11, September (1967).

66. Douslin, D. R., R. H. Harrison, and R. T. Moore, J. Phy. Chem. 71, 3477 (1967).

67. Douslin, D. R., R. H. Harrison, R. T. Moore, and J. P. McCullough, J. Chem. Eng. Data, 9, 358 (1964).

68. Edmister, W. C., "Enthalpies of Co-existing Equilibrium Vapor and Liquid Mixtures from Solubility Data and Equation of State Calculations," Monograph TD-6-68, Oklahoma State University, September (1968).

69. Ellington, R. T., and B. E. Eakin, Chem. Eng. Prog., 59, No. 11, 80 (1963).

70. Ellington, R. T., B. E. Eakin, J. D. Parent, D. C. Gami, and O. T. Bloomer, in "Thermodynamic and Transport Properties of Gases, Liquids and Solids," ASME (1959), pg. 180.

71. Ergun, S., Chem. Eng. Prog., 48, 89 (1952).

72. Ernst, G., D. Ing. Thesis, Univ. Karlsruhe, Germany (1967).

73. Ernst, G., and J. Busser, J. Chem. Thermodynamics, 2, 787 (1970).

74. Eubank, P. T., To be published in Adv. Cryg. Eng., 17.

75. Eubank, P. T., To be published in Adv. Cryg. Eng., 17.

76. Eubank, P. T., and B. F. Fort, Can. J. Chem. Eng., 47, 177 (1969).

77. Eucken, A., and F. Hauk, Z. Physik. Chem., (Leipzig) 134, 161 (1928).

78. Ewing, M. B., K. N. Marsh, R. H. Stokes, and C. W. Tuxford, J. Chem. Thermodynamics, 2, 751 (1970).

79. Faulkner, R. C., Jr., Ph.D. Thesis, University of Michigan (1959).

80. Fisher, G. D., P. S. Chappelear, and T. W. Leland, Proc. Ann. Conv., Nat. Gas. Process. Assoc., Tech. Papers, 47, 26 (1968).

81. Fisher, G. D., and T. W. Leland, Paper presented at 159th National ACS Meeting, February 22, 1970.

82. Fort, B. F., Ph.D. Thesis, Texas A & M University (1969).

83. Francis, P. G., M. L. McGlashan, and C. J. Wormald, J. Chem. Thermodynamics, 1, 441 (1969).

84. Frank, A., and K. Clusius, Z. Physik. Chem., B36, 291 (1937).

85. Gamson, B. W., and K. M. Watson, National Pet. News Tech. Sec., 36, R-556 (1944).

86. Garcia-Rangel, S., and L. C. Yen, Paper presented at 159th National Meeting, ACS, February 22, 1970.

87. Ginnings, D. C., and H. F. Stimson (See Ref. 158, pg. 399).

88. Goode, R. J., and C. J. Hope, J. Chem. Phys., 55, No. 1, 111 (1971).

89. Goodwin, S. R., and D. M. T. Newsham, J. Chem. Thermodynamics, 3, 325 (1971).

90. Gosman, A. L., R. D. McCarthy, and J. G. Hurst, National Standard Reference Data Series, NBS, No. 27, March (1969).

91. Greenkorn, R. A., and K. C. Chao, Proc. Ann. Conv., Nat. Gas. Process. Assoc., Tech. Papers, 50, 42 (1971).

92. Guggenheim, E. A., Mixtures Oxford (1952).

93. Guggenheim, E. A., and M. L. McGlashan, Proc. Roy. Soc., A206, 448 (1951).

94. Gunn, R. D., quoted in Ref 112.

95. Gunn, R. D., P. L. Chueh, and J. M. Prausnitz, Cryogenics, 324 (1966).

96. Gunn, R. D., P. A. Franks, and S. V. Mainkar, Proc. Ann. Conv., Nat. Gas Process. Assoc., Tech. Papers, 50, 51 (1971).

97. Harrison, R. H., and D. R. Douslin, J. Chem. Eng. Data, 11, 383 (1966).

98. Hauge, E. H., J. Chem. Phys., 44, 2249 (1966).

99. Hecht, G., and E. Donth, Z. Phys. Chem., Bd 239 (1968).

100. Hejmadi, Arun, Vasudev, Ph.D. Thesis, University of Michigan (1970).

101. Henderson, D., and P. J. Leonard, Proc. Nat. Acad. Sci., 67, No. 4, 1818 (1970).

102. Henderson, D., and P. J. Leonard, Proc. Nat. Acad. Sci., 68, No. 3, 632 (1971).

103. Herning, F., and L. Zipperer, Gas und Wasserfach, 79, 69 (1936).

104. Hildebrand, J. H., J. M. Prausnitz, and R. L. Scott, "Regular and Related Solutions," Van Nostrand-Reinhold, N.Y. (1970).

105. Hill, T. S., "An Introduction to Statistical Thermodynamics," Addison-Wesley, New York (1960).

106. Hirschfelder, J. O., Ed., "Intermolecular Forces," Adv. Chem. Phys., 12 (1967).

107. Hirschfelder, J. O., C. F. Curtiss, and R. B. Bird, "Molecular Theory of Gases and Liquids," Wiley, New York (1954).

108. Hoover, A. D., T. W. Leland, and R. Kobayashi, J. Chem. Phys., 45, 399 (1966).

109. Houser, C. G., and J. H. Weber, J. Chem. Eng. Data, 6, 510 (1961).

110. Huang, E. T. S., G. W. Swift, and F. Kurata, J. A.I.Ch.E., 13, 846 (1967).

111. Hudson, G. H., and J. C. McCoubrey, Trans. Farad. Soc., 57, 761 (1960).

112. Huff, J. A., and T. M. Reed, III, J. Chem. Eng. Data, 8, 306 (1963).

113. "Intermolecular Forces," Disc. Farad. Soc., 40 (1965).

114. Jacobsen, J. A., and R. E. Barieau, Presented at 159th National Meeting ACS, Houston, Texas, Feb. 22-27, 1970.

115. Jacobsen, R. T., Ph.D. Thesis, Washington State Univ. (1972).

116. Joffe, J., and E. C. Delaney, Chem. Eng., 65, No. 6, 138 (1958).

117. Joffe, J., and D. Zudkevitch, Chem. Eng. Symp. Ser., 63, No. 81, 433 (1967).

118. Johnson, D. W., and C. P. Colver. Proc. Ann. Conv., Nat. Gas Process. Assoc., Tech. Papers, 49, 19 (1970).

119. Jones, M. L., Jr., Ph.D. Thesis, University of Michigan (1961).

120. Kac, M., G. E. Uhlenbeck, and P. C. Hemmer, J. Math. Phys., 4, 216, 229 (1963).

121. Kant, R., A. W. Furtado, and J. E. Powers, Research Report, Nat. Gas. Process. Assoc., Tulsa, Oklahoma, March, 1973.

122. Kapallo, W., N. Lund, and K. Schafer, Z. Phys. Chem. [Frankfurt] 37, 196 (1963).

123. Kapallo, W., and K. Schafer, Z. Elektrochem., Ber. Bun. Phys. Chem., 66, 508 (1962).

124. Katz, D. L., and M. G. Rzasa, Bibliography for Physical Behavior of Hydrocarbons under Pressure and Related Phenomena, J. W. Edwards Inc., Ann Arbor, 1946.

125. Kay, W. B., Ind. Eng. Chem., 28, 1014 (1936).

126. Kay, W. B., Ind. Eng. Chem., 30, 459 (1938).

127. Kemp, J. D., and C. J. Egan, J. Am. Chem. Soc., 60, 1521 (1938).

128. Kim, D., D. Henderson, and J. A. Barker, Can. J. Phys., 47, 99 (1969).

129. Kistiakowsky, G. B., J. R. Lacher, and F. Stitt, J. Chem. Phys. 7, 289 (1939).

130. Kistiakowsky, G. B., and W. W. Rice, J. Chem. Phys., 8, 510 (1940).

131. Klaus, R., Ph.D. Thesis, Eeunslaer Polytechnic (1967).

132. Koeppe, W., Proc. 7th Int. Congr. Refrig., Copenhagen, 1, 156 (1959).

133. Kreglewski, A., J. Phys. Chem., 71, 2860 (1967).

134. Kreglewski, A., J. Phys. Chem., 72, 2280 (1968).

135. Kuloor, N. R., D. M. Newitt, and J. S. Bateman, "Thermodynamic Functions of Gases," Ed., F. Din. Vol. 2, 115 (1956).

136. Kunz, H., Dissertation, Heidelberg (1959).

137. Lange, H. B., and F. P. Stein, J. Chem. Eng. Data., 15, No. 1, 56 (1970).

138. Laverman, R. J., Communicated to J. E. Powers (1969).

139. Laverman, R. J., and Y. A. Selcukoglu, Paper presented at 11th Int. Inst. Refrig. Cong., Madrid (1967).

140. Leach, J. W., P. S. Chappelear, and T. W. Leland, J. A.I.Ch.E., 14, No. 4, 568 (1968).

141. Lebowitz, J. L., Phys. Rev., 133, 895 (1964).

142. Lee, A. L., and B. E. Eakin, J. Soc. Pet. Eng., 245-249 (1964).

143. Lee, A. L., K. E. Starling, J. P. Dolan, and R. T. Ellington, J. A.I.Ch.E., 10, No. 5, 694 (1964).

144. Leland, T. W., and P. S. Chappelear, Ind. Eng. Chem., 60, No. 7, 15 (1968).

145. Leland, T. W., R. Kobayashi, and W. H. Mueller, J. A.I.Ch.E., 1, 535 (1961).

146. Leland, T. W., and W. H. Mueller, Ind. Eng. Chem., 51, 597 (1959).

147. Leland, T. W., J. S. Rowlinson, and G. A. Sather, Trans. Farad. Soc., 64, 1447 (1968).

148. Leland, T. W., J. S. Rowlinson, G. A. Sather, and I. D. Watson, Trans. Farad. Soc., 65, 2034 (1969).

149. Lenoir, J. M., G. K. Kuravila, and H. G. Hipkin, Proc. 34th Mid Year Meeting, API Div. Refining, Philadelphia, May (1969).

150. Lenoir, J. M., D. G. Robinson, and H. G. Hipkin, Proc. 33rd Mid Year Meeting, API Div. Refining, Philadelphia, May (1968).

151. Leonard, P. J., D. Henderson, and J. A. Barker, Trans. Farad. Soc., 66, 2439 (1970).

152. Levitskaya, E. P., J. Tech. Phys., USSR 11, 197 (1941).

153. London, Fritz, Z. Phys. Chem., B 11, 235 (1930).

154. Longuet-Higgins, H. C., Proc. Roy. Soc., 205A, 247 (1951).

155. Longuet-Higgins, H. C., and B. Widom, Mat. Phys., 8, 549 (1964).

156. Natural Gas Processors Suppliers Association "Engineering Data Book," Tulsa, Oklahoma (1966).

157. Lydersen, A., and H. G. Ronne, Chem. Eng. Symp. Ser., 64, No. 88, 95-100 (1968).

158. McCullough, J. P., and D. W. Scott, Eds., "Experimental Thermodynamics," Vol. I, Butterworths, London (1968).

159. McGlashan, M. L., and D. J. B. Potter, Proc. Roy. Soc., A267, 478 (1962).

160. McGlashan, M. L., and H. F. Stoeckli, J. Chem. Thermodynamics, 1, 589 (1969).

161. Mage, D. T., Ph.D. Thesis, University of Michigan (1964).

162. Manker, E. A., Ph.D. Thesis, University of Michigan (1964).

163. Mansoori, G. A., and F. B. Canfield, Ind. Eng. Chem., 62, No. 8, 13 (1970).

164. Mansoori, G. A., and T. W. Leland, Rice University, Houston, Texas, To be published.

165. Martin, J. J., Ind. Eng. Chem., 59, No. 12, 34 (1967).

166. Masi, J. F., Trans. Amer. Soc. Mech. Eng., 76, 1067 (1954).

167. Mason, E. A., and T. H. Spurling, The Virial Equation of State, International Encyclopedia of Physical Chemistry and Chemical Physics, Vol. 2 of Topic 10, Pergamon Press, London (1969).

168. Mather, A. E., Ph.D. Thesis, University of Michigan (1967).

169. Matschke, D. E., and G. Thodos, J. Chem. Eng. Data, 7, No. 2, 232.

170. Maurer, G., D. Ing. Thesis, University Karlsruhe, Germany (1971).

171. Michels, A., and G. W. Nederbraght, Physica, 2, 1000 (1935).

172. Michels, A., and G. W. Nederbraght, Physica, 3, 569 (1936).

173. Michels, A., and G. W. Nederbraght, Physica, 6, No. 7, 656 (1939).

174. Michels, A., W. Van Stratten, and J. Dawson, Physica, 20, 17 (1954).

175. Michels, A., T. Wassenaar, P. Louwerse, R. J. Lunbeck, and J. G. Wolkers, Physica, 19, 287 (1953).

176. Mikolaj, P. G., and C. J. Pings, Phys. Rev. Letters, 15, 849 (1965).

177. Miller, R. C., J. Chem. Phys., 55, No. 4, 1613 (1971).

178. Miyazaki, T., Personal Communication (1973).

179. Miyazaki, T., A. W. Furtado, and J. E. Powers, Proc. 1st Intern. Conf. Calorimetry and Thermodynamics Warsaw, 1969, pg. 618.

180. Monk, P., and I. Wadso, Acta. Chem. Scand., 22, 1842 (1968).

181. Morlet, J., Revue Inst. Fran. Pet., 18, No. 1, 127 (1963).

182. Morsy, T., J. Chem. Eng. Data, 15, No. 2, 256 (1970).

183. Muckleroy, J. A., "Bibliography on Hydrocarbons, 1946-1960," Natural Gas Processors Association, Tulsa, Oklahoma, 1962.

184. National Bureau of Standards, "Reference Tables for Thermocouples," Circular 561, April 27, 1955.

185. Nicholson, G. A., and W. G. Schneider, Can. J. Chem., 33, 589 (1955).

186. Noury, J., Ph.D. Thesis, Universite´ Paris (1956).

187. Noury, J., A. Lacam, A. M'Hirsi, R. Bergeon, L. Galatry, and B. Vodar, Proc. Conf. Thermodyn. Transport Prop. Fluids, London, 48 (1957).

188. O'Connell, J. P., and J. M. Prausnitz, Ind. Eng. Chem., 60, No. 1, 37 (1968).

189. Orentlicher, M., and J. M. Prausnitz, Can. J. Chem. Eng., 45, 78 (1967).

190. Partington, J. R., and W. G. Shilling, The Specific Heat of Gases, Ernest Benn Ltd., London, 1924.

191. Percus, J. K., and G. J. Yevick, Phys. Rev., 110, 1 (1958).

192. Perry, John H., Ed., Chemical Engineers' Handbook, McGraw-Hill, New York, 1963.

193. Pitzer, K. S., J. Chem. Phys., 7, 583 (1939).

194. Pitzer, K. S., in "Adv. Chem. Phys.," Vol. I, I. Prigogine, Ed., Interscience, New York, 1959, pg. 59.

195. Pitzer, K. S., and R. F. Curl, Proc. Conf. Thermodyn. Transport Prop. Fluids, London, 1 (1957).

196. Pitzer, K. S., and R. F. Curl, J. Am. Chem. Soc., 79, 2369 (1957).

197. Pitzer, K. S., and G. O. Hultgren, J. Am. Chem. Soc., 80, 4793 (1958).

198. Pitzer, K. S., D. Z. Lippman, R. F. Curl, Jr., C. M. Huggins, D. E. Petersen, J. Am. Chem. Soc., 77, 3427 (1955).

199. Plank, Von R., and J. Kambeitz, Z. Gas. Kalte-Industrie, 43, 209 (1936).

200. Pope, G. A., Ph.D. Thesis, Rice University (1971).

201. Porter, Frank, J. Am. Chem. Soc., 48, 2055 (1926).

202. Powers, J. E., Personal Communications (1968-1973).

203. Powers, J. E., Proc. Ann. Conv. Nat. Gas Process. Assoc., Tech. Papers, 48, 12 (1969).

204. Powers, J. E., Presented at 64th Annual Meeting, AIChE, San Francisco, Cal., November 28, 1971.

205. Prausnitz, J. M., "Molecular Thermodynamics of Fluid Phase Equilibria," Prentice-Hall, N. J. (1969).

206. Prausnitz, J. M., and R. D. Gunn, J. A.I.Ch.E., 4, 430 (1958).

207. Price, A. R., and R. Kobayashi, J. Chem. Eng. Data, 4, 40 (1959).

208. Prigogine, I., and R. Defay, Treatise on Thermodynamics, Longmans, London (1954).

209. Reamer, H. H., R. H. Olds, B. H. Sage, and W. N. Lacey, Ind. Eng. Chem., 36, No. 10, 956 (1944).

210. Reamer, H. H., B. H. Sage, and W. N. Lacey, Ind. Eng. Chem., 41, 428 (1949).

211. Reamer, H. H., B. H. Sage, and W. N. Lacey, Ind. Eng. Chem., 42, 534 (1950).

212. Reed, T. M., and K. E. Gubbins, Applied Statistical Mechanics, McGraw-Hill, New York (1972).

213. Reid, R. C., and T. W. Leland, J. A.I.Ch.E., 11, 228 (1965).

214. Reid, R. C., and T. K. Sherwood, "The Properties of Gases and Liquids," (Pergamon Press, Oxford, 1967).

215. Rhee, F. H., and W. G. Hoover, J. Chem. Phys., 40, No. 4, 939 (1964).

216. Riedel, L., Chem. Ing. Tech., 26, 83 (1954).

217. Riedel, L., Chem. Ing. Tech., 27, 209 (1955).

218. Roebuck, J. R., Phys. Rev., 2, 99 (1913).

219. Rogers, B. L., and J. M. Prausnitz, Trans. Farad. Soc., 67, No. 588, 3474 (1971).

220. Rossini, F. D., et al., Selected Values of Physical and Thermodynamic Properties of Hydrocarbons and Related Compounds, Carnegie Press, Pittsburgh, Pennsylvania (1953).

221. Rowlinson, J. S., Trans. Farad. Soc., 50, 647 (1954).

222. Rowlinson, J. S., Trans. Farad. Soc., 51, 1317 (1955).

223. Rowlinson, J. S., "The Perfect Gas," International Encyclopedia of Physical Chemistry and Chemical Physics, Pergamon Press, London (1963).

224. Rowlinson, J. S., Rept. Progr. Phys., 28, 169 (1965).

225. Rowlinson, J. S., Liquids and Liquid Mixtures, Butterworths, London (1969).

226. Rowlinson, J. S., Disc. Farad. Soc., 49, 30 (1970).

227. Rowlinson, J. S., and I. D. Watson, Chem. Eng. Sci., 24, 1565 (1969).

228. Rotenberg, A., J. Chem. Phys., 43, 4377 (1965).

229. Ruhemann, M., Proc. Roy. Soc., 171A, 121 (1939).

230. Rutherford, W. M., J. Soc. Pet. Eng., 340 (1962).

231. Sage, B. H., and W. N. Lacey, Ind. Eng. Chem., 31, 1497 (1939).

232. Sage, B. H., and W. N. Lacey, "Thermodynamic Properties of the Lighter Paraffin Hydrocarbons and Nitrogen," American Petroleum Institute, New York (1950).

233. Sage, B. H., J. G. Schaafsma, and W. N. Lacey, Ind. Eng. Chem., 26, 214 (1934).

234. Sage, B. H., D. C. Webster, and W. N. Lacey, Ind. Eng. Chem., 29, No. 6, 658 (1937).

235. Salsburg., Z. W., P. J. Wojtowicz, and J. G. Kirkwood, J. Chem. Phys., 26, No. 6, 1533 (1957).

236. Scheele, K., and W. Heuse, Ann. Phys. Leipzeig, 40, 473 (1913).

237. Scott, C. G., J. Inst. Pet., 45, No. 424, 118 (1959).

238. Scott, R. L., and D. V. Fenby, Ann. Rev. of Phys. Chem., 20, 111 (1969).

239. Shana'a, M. Y., and R. B. Canfield, submitted to Trans. Farad. Soc.

240. Silberberg, I. H., P. K. Kuo, and J. J. McKetta, Pet. Eng., 24, C-9 (1952).

241. Silberberg, I. H., J. J. McKetta, and K. A. Kobe, J. Chem. Eng. Data., 4, 323 (1959).

242. Singer, J. V. L., and K. Singer, Mol. Phys., 19, 279 (1970).

243. Singer, K., Chem. Phys. Lett., 3, 164 (1969).

244. Sirota, A. M., V. K. Mal'tsev and A. Ya. Grishkov, Teploenergetika, 9, 57 (1963).

245. Sirota, A. M., and Z. K. Shrago, Teploenergetika, 15, No. 3, 24 (1968).

246. Sliwinski, P., Z. Physik Chem. N. F., 63, 263 (1969).

247. Smith, L. G., J. Chem. Phys., 17, 139 (1949).

248. Snider, N. S., and T. M. Herrington, J. Chem. Phys., 47, 2248 (1967).

249. Starling, K. E., Personal Communication, August, 1968.

250. Starling, K. E., NGPA Enthalpy Project Progress Report, September (1969).

251. Starling, K. E., Proc. Ann. Conv., Nat. Gas Process. Assoc., Tech. Papers, 49, 9 (1970).

252. Starling, K. E., and R. T. Ellington, J. A.I.Ch.E., 10, No. 1, 11 (1964).

253. Starling, K. E., D. W. Johnson, and C. P. Colver, Nat. Gas Process. Assoc., Research Rept., RR4, May, 1971.

254. Starling, K. E., and J. E. Powers, Ind. Eng. Chem. Fund., 9, 531 (1970).

255. Stockett, A. L., and L. A. Wenzel, J. A.I.Ch.E., 10, 557 (1964).

256. Stokes, R. H., K. N. Marsh, and R. P. Tomlins, J. Chem. Thermodynamics, 1, 211 (1969).

257. Strickland-Constable, R. F., Proc. Roy. Soc., A209, 14 (1951).

258. Sturtevant, J. M., "Calorimetry," Ch. XIV, in "Physical Methods of Organic Chemistry," Vol. I, Pt. 1, A. Weissberger, Ed., Interscience, New York (1949).

259. Subramanian, T. K., R. L. Kao, and A. L. Lee, Paper presented at American Gas Association Distribution Conference, Philadelphia, May 12, 1969.

260. Sutherland, W., Phil. Mag., 36, 507 (1893).

261. Tannenberger, H., Z. Physik, 153, 450 (1958-1959).

262. Tao, L. C., J. A.I.Ch.E., 14, No. 6, 988 (1968).

263. Tester, H. E., in "Thermodynamic Functions of Gases," F. Din, Ed., Vol. 1 (1956).

264. Tester, H. E., "Thermodynamic Functions of Gases," F. Din, Ed., Vol. 3 (1956), pg. 1.

265. Thayer, V. R., and G. Stegeman, J. Phys. Chem., 35, 1505 (1931).

266. Throop, G., and R. G. Bearman, J. Chem. Phys., 42, 2838 (1965).

267. Throop, G., and R. G. Bearman, J. Chem. Phys., 44, 1423 (1966).

268. Tiwari, K. K., Ph.D. Thesis, Univ. of Alberta (1968).

269. Tsaturyants, A. B., A. R. Mamedov, and R. G. Fivazova, Dokl. Akad. Nauk. Azerb. SSR 18, No. 11, 23 (1962).

270. Van Eijnsbergen, Bert, Ph.D. Thesis, Leiden (1966).

271. Van Eijnsbergen, Bert, and J. J. M. Beenakker, Physica, 39, 499 (1968).

272. Van Eijnsbergen, Bert, and J. J. M. Beenakker, Physica, 39, 510 (1968).

273. Vennix, A. J., Ph.D. Thesis, Rice University, 1966.

274. Vera, J. H., and J. M. Prausnitz, Can. J. Chem. Eng., 49, No. 12 (1971).

275. Watson, I. D., and J. S. Rowlinson, Chem. Eng. Science, 24, 1575 (1969).

276. Wichterle, I., and R. Kobayashi, Monograph, Dept. of Chem. Eng., Rice University, August 31, 1970.

277. Wiebe, R., K. H. Hubbard, and M. J. Brevoort, J. Am. Chem. Soc., 52, 611 (1930).

278. Wiener, L. D., Hydrocarbon Processing, 46, No. 4, 131 (1967).

279. Wilson, G. T., Paper 15C, Presented at the 65th National AIChE Meeting. Cleveland, Ohio (1970).

280. Witt, R. K., and J. D. Kemp, J. Am. Chem. Soc., 59, 273 (1937).

281. Wojtowicz, P. J., J. G. Kirkwood, and Z. W. Salsburg, J. Chem. Phys., 27, No. 2, 505 (1957).

282. Wolberg, A., Jr., Prediction Analysis, Van Nostrand, 1967.

283. Yarborough, L., in "Engineering Data Book," Natural Gas Processors Suppliers Assoc., Eight Edition (1966), p. 203.

284. Yesavage, V. F., Ph.D. Thesis, Univ. of Michigan (1968).

285. Yesavage, V. F., A. W. Furtado, and J. E. Powers, Proc. Ann. Conv. Nat. Gas Conv., Nat. Gas Process. Assoc., Tech. Papers, 47, 3 (1968).

286. Yesavage, V. F., A. E. Mather, D. L. Katz, and J. E. Powers, Ind. Eng. Chem., 56, 35 (1967).

287. Zwanzig, R. W., P. Chem. Phys., 22, 1420 (1954).

THE UNIVERSITY OF MICHIGAN